ISSN - 2347-7075
Impact Factor - 8.141

INTERNATIONAL JOURNAL OF ADVANCE AND APPLIED RESEARCH

Double-Blind Peer Reviewed / Bi-Monthly / Referred / Open Access Research Journal

Vol. 7 No. 14
January - February 2026

Young Researcher Association

International Journal of Advance and Applied Research

(IJAAR)

A Multidisciplinary International Level Referred and Peer Reviewed Journal

ISSN–2347-7075 **Impact Factor–8.141**

January - February 2026

Volume - 7 **Issue –** 14

Published by:

Young Researcher Association, Kolhapur, Maharashtra, India

Website:https://ijaar.co.in

Submit Your Research Paper on Email

Regular Issue: editor@ijaar.co.in

For Publication Call On - **8624946865**

INTERNATIONAL JOURNAL OF ADVANCE AND APPLIED RESEARCH
ISSN – 2347 -7075 (DOUBLE-BLIND Peer Reviewed) (Bi-Monthly Research Journal)
Vol. 7 No. 14
January - February 2026

TABLE OF CONTENT

Sr. No.	Name of Author	Title of Paper	Page No.
1	Shrikant B. Bhosale Archana R. Mukhedkar Sheela Y. Shinde	The Hidden Threat: How Plastic Pollution Is Affecting Soil Fertility	1 - 5
2	Ms. Aditi. S. Kale Dr. S. S. Tambe	Biodiversity and Conservation Assessment of Medicinal Plant Species in Surgana Tahsil, Nashik District	6 - 9
3	Amit C. Harangule	Advancing Precision Diagnostics: Emerging Molecular Strategies for Early Detection and Control of Antimicrobial Resistance in 2026	10 - 19
4	Bharat Hajgude Ravi P. Patil	Screening of Phytochemicals and Estimation of Secondary Metabolites in Plant Species Euphorbia neriifolia L. and Caralluma fimbriata Wall.	20 - 23
5	D. T. Tangade	Impact of Pesticide Usage in Vegetables its Benefits and Risks	24 - 26
6	Dr. Ravikiran J. Sawant Kanchan L. Kannamwar	Studies on Medicinal Plants Using Local Medicine	27 - 29
7	Dr. B. J. Hirve	Phytochemical screening of Moringa oleifera Lam. leaves from the area of Kaij of Beed District of Maharashtra, India	30 - 32
8	Dr. Sachin B. Jadhav	Climate-Smart Agriculture (CSA): Role of Mulching in Vegetable Crops from Nashik District, (M.S) India	33 - 38
9	Ganesh P. Musale Rajendra B. Kakde	Taxonomic Evaluation of Two Coprinoid Fungi of the Genus Coprinopsis in Jalna District, Maharashtra (India)	39 - 44
10	G. P. Ambhore M. R. Ingle	Survey And Uses of Medicinal Plants from Risod, District Washim: A Comprehensive Study	45 - 51
11	Miss. Gayatri Rameshrao Kadam	Aquaculture of Sea Cucumbers: A Review and Consolidated Qualitative Profile	52 - 60
12	Kesare U. T.	Effect of Vitamins on Protease and Lipase Production in Seed-Borne Fungi of Soybean	61 - 64
13	M. B. Navale M. S. Wadikar R. J. Sawant V. D. Jadhav	Herbal Management of Lumpy Skin Disease (LSD) in Cattle	65 - 69
14	Nagnath K. Dahiphale Savita M. Sukte	Plant Based Traditional Remedies on Child Health Care in Beed District, Maharashtra	70 - 74
15	Patil T. V. Pangrikar P. P.	Isolation And Screening of Soil Fungi on Different Culture Media	75 - 78
16	Pranali Wasate Navnath Kashid	The Holobiome Framework: Integrating Environmental Microbiomes, Probiotic Systems, and Sustainable Ecosystem Management	79 - 91
17	Sachin S. Chavan Tejas D. Garad	Study of Algal Diversity from Sina Kolegaon Dam	92 - 97
18	Smita Basole	Adaptive Strategies for Agricultural Sustainability in Changing Climates	98 - 101

Sr. No.	Name of Author	Title of Paper	Page No.
19	S. P. Kshirsagar M. A. Kare	HR-LCMS-Based Phytochemical Characterization of Bark Drugs from Selected Medicinal Plants	102 - 107
20	Vishwajit R. Mhaske Anil D. Adsare Sudarshan R. Mane Madhukar S. Wadikar	Effect of Different Liquid Media and Cultural Condition on Biomass Production of Sclerotium Rolfsii	108 - 112
21	Yogesh Pandharinath Shinde Ganesh Laxmanrao Pachkore	Phytochemical Profiling and Agro-Environmental Applications of Sphagneticola calendulacea in Sustainable Agriculture	113 - 117
22	Yuvraj M. Bhosale Ratnakar S. More	Environmental Transformation and Biodiversity Dynamics in the Rural–Urban Fringe of Jalgaon District, Maharashtra: A Spatiotemporal Analysis	118 - 126
23	Rupali Biradar Vikas Gambhire	Ethnobotanical Studies of Medicinal Plants from Marathwada effectively used on Rheumatism	127 - 131
24	Vijayalaxami S. Shelke	Ecological Assessment of Rhizosphere Fungal Diversity in Semi-Arid Agricultural Soils of Maharashtra, India	132 - 137
25	Vasantrao B. Kadam Madhukar S. Wadikar	Comparative Quantitative Profiling of Secondary Metabolites in Different Organs of Ficus religiosa L.	138 - 140
26	G. S. Jaigaonkar	Role of Advanced Spectroscopic Techniques in Modern Materials Characterization	141 - 145
27	Devkate A. V. Sakhare M. A.	Evaluating the Antitumor Efficacy of a Schiff Base Ligand and its Metal complexes across Diverse Human Cancer Cell Lines	146 - 155
28	Mahadev B. Suwarnkar	Study of Ag Loaded TiO2/ZnO Nanocomposites for Photocatalytic Activity	156 - 163
29	Priya M. Khandare Swati. S. Ghodke S. S. Kamble Rajita D. Ingle	Study of Soil Alkalinity of Mahad Taluka, Raigad District, Maharashtra by Acid Titration Method Using Methyl Orange and Phenolphthalein Indicators	164 - 167
30	Satish B. Kamble Sumit B. Shejul Parmeshwar V. Bankar Pandhari H. Wagalgave Swapnil B. Sasane Arun E. Bharade Balaji D. Rupnar	A Green and Magnetically Recyclable Hexaferrite (MgBaFe) Nanocatalyst for Efficient Multicomponent Synthesis of Dihydropyrimidinethiones	168 - 176
31	Shyam Takle	Characterisation, Biological Screening and Efficient Ultrasound Synthesis of New Cyclic β-Diketones	177 - 182
32	Sujata S. Patil Bharat Dhotre	Ultrasonic Velocity study of Acrylates with Decane-2-ol at 308.15 K and 313.15 K	183 - 189
33	Amol J. Shirsat Vrushali S. Gavhane Arun E. Bharade Satish B. Jadhav Sunil S. Bhagat Gopal K. Kakade	Synthesis, Characterization and Antimicrobial Analysis of Some Pyrazolines from Chalcones	190 - 193

Sr. No.	Name of Author	Title of Paper	Page No.
34	Dr. Gajanan Pandurang Khetri Pradeep Janardhan Udhan	Ethical Implications of Using Deep Learning for Facial Recognition	194 - 197
35	Sunita Shewale Dr. Suhas Mache	AI-Driven Automation in Software Development: A Comparative Study of AI Tools, Challenges, and Opportunities	198 - 205
36	Yogini Dilprao Salunke Dr. Suhas Mache	High-Performance Streaming Analytics for Cloud-Based Internet of Things System	206 - 211
37	Devyani Supekar Vrushali Karade Rameshwar Bankar Dnyaneshwari Awankar Mandip Kapale Anil Ardad	Amino Acids Doping in KHP Crystals: A Critical Review	212 - 220
38	Gaikwad Pradeep Devendra	Electrochemical Sensors for Soil Health Monitoring	221 - 223
39	K. R. Sature B. S. Kharat P. M. Kokne	DFT and Experimental Investigation of BaF2 Phosphor for Dosimetry Application	224 - 229
40	Kalyani K. Deshmukh Shital P. Nawale Kajal A. Gurav Atul. P. Keche K. M. Jadhav	Role of Fuel and Their Ratio with Metal Nitrates in Combustion Synthesis of Spinel Ferrite Nanoparticles	230 - 237
41	Kamble Pravin Ashruba Takle Ganesh Baburao Gaikwad Pradeep Devendra	Noradrenaline-Polyaniline Composite: A galvanostatic Approach	238 - 240
42	N. K. Raut	Topological Polynomials in Fuzzy Hamiltonian Graph	241 - 246
43	Sarwade Datta Vasant Gulbhile Shamsundar Dhondiram	The Structure, Dynamics, Phase Transitions, and Emerging Applications of Orientational Crystals	247 - 252
44	P. A. Savale	Study of Magnesium Tartrate Crystals by Sol Gel Method	253 - 261
45	Shaikh Asif Karim Sayyed Mujeeb Hadi	Alterations Appeared in The Hoping Length of Zinc Doped Nickel Ferrite System Driven by The Gamma Radiation Effect	262 - 264
46	Shinde Ganesh Madhukar Gaikwad Pradeep Devendra	ECG Signal Using Time Domain Analysis for Health Care	265 - 266
47	Shital P. Nawale Kalyani K. Deshmukh A. P. Keche K. M. Jadhav	Eco-Friendly Green synthesis and X-ray diffraction studies of Spinel Nickel-Zinc Ferrite Nanoparticles	267 - 273
48	S. J. Indurkar	Morphology, and Band Gap Analysis of Synthesized Pure Phase Nickel Oxide	274 - 279
49	Subhash S. Karande Mahendra S. Kavale	Synthesis of Coersivity and Magnetic Moment of Nanoparticle Sized Aluminium Substituted Copper Cobalt Ferrites	280 - 284

Sr. No.	Name of Author	Title of Paper	Page No.
50	Takle Ganesh Baburao Kamble Pravin Ashruba Gaikwad Pradeep Devendra	Magnetic Polymer Nanocomposites for Biomedical Applications	285 – 287
51	Yogesh K. Lahamate Sushant B. Deshmukh	A Comprehensive Review: The Synthesis, Characterization, and Applications of CuO and CuS Nanomaterials	288 - 301
52	Pradip Dahinde	Comparative Studies of Radiation Shielding and Gamma-Ray Attenuation Properties of Polymers and Oxide Materials	302 - 305
53	Abhijit Ankushrao Taur Laxmikant Vitthalrao Shinde	Effect of Humidity and Monsoon Shifts on Mosquito Breeding Genetics and Survival Traits	306 - 318
54	Archana Yelikar Meena Nagawanshi Ganesh Chavan	Conserving Helminth Parasites for Ecological Significance: Challenges and Opportunities	319 - 321
55	Bajad P. N.	Evaluation of the Efficacy of Eisenia fetida in the Bioconversion of organic waste into Nutritive Vermicompost	322 – 326
56	D. R. Kasab	Impact of the Invasive Fish Oreochromis mossambicus on Major Carp Culture in Jayakwadi Dam, Maharashtra	327 - 331
57	M. K. Shaikh S. G. Badhe S. R. Naphade S. T. Naphade	Study of Blue LED Light Intensity on Zebra Fish Behaviour in Aquarium	332 - 339
58	Nilakshi Vaidya Meena Nagawanshi	Karyotypic Investigation of Helminths from Vertebrate Animal	340 - 344
59	Pramod Rokade	Morphological Characteristics of The Paired Fins and Anal Fin of Oreochromis Mossambicus	345 - 348
60	Sujata Magdum Sushruta Vasaikar	Bioaccumulation and Distribution of Heavy Metals in Muscle, Gill, and Liver Tissues of Coptodon rendalli from local fish markets of Nashik Maharashtra	349 – 359
61	D. T. Tangade	Impact of Pesticide Usage in vegetables its Benefits and Risks	360 - 362
62	Vishnu A. Reddy	Antimicrobial Resistance in Vector-Borne Diseases: Emerging Challenges and Integrated Global Control Strategies	363 - 380
63	Umakant G. Shinde Sanjay R. Biradar	Production, Purification and Assay of Pectinase Enzyme from Orange Peels	381 - 388
64	Dr. Rahul Bharti	AI for Sustainable Development	389 - 391
65	Rahul Kashid Santosh Talekar Navnath Kashid	Nanoparticles Applications: For Environmental Friendliness, And Cost Effectiveness, Sustainable Agriculture	392 - 397
66	Gavhane V. S. Shirsat A. J. Jadhav. S. B. Bharade A. E.	Synthesis, Characterization and Antimicrobial analysis of Transition Metal Complexes of Thiosemicarabazone Schiff Bases	398 - 401
67	D. S. Ghogare	A Comprehensive Review of Organic Farming in India: Current Status, Challenges, Benefits, and Future Prospects	402 - 409

International Journal of Advance and Applied Research
www.ijaar.co.in
ISSN – 2347-7075 Impact Factor – 8.141
Peer Reviewed Bi-Monthly
Vol. 7 No. 14 January – February - 2026

The Hidden Threat: How Plastic Pollution Is Affecting Soil Fertility

Shrikant B. Bhosale[1], Archana R. Mukhedkar[2], Sheela Y. Shinde[3]

[1]*Assistant Professor, Department of Botany, S. M. Dnyandeo Mohekar Mahavidyalaya Kallamb, Dist. Dharashiv, Maharashtra*

[2]*Assistant Professor and Head, Department of Botany, S.M. Dnyandeo Mohekar Mahavidyalaya Kallamb, Dist. Dharashiv, Maharashtra*

[3]*Assistant Professor, Department of Botany, Late Shankarrao Gutte Gramin Arts, Commerce and Science College, Dharmapuri Tq. Parli Dist-Beed, Maharashtra*

Corresponding Author – Archana R. Mukhedkar

DOI - 10.5281/zenodo.19724217

Abstract:

Plastic products for plant protection and cultivation increase agricultural yields, enhance food quality, reduce water use globally, and lessen environmental effect. Furthermore, plastic pollution is an important ecological concern because it has recently had a significant impact on soil, water, and vegetation. Both biotic and abiotic transport occur after plastic fragmentation in the soil. By plowing the ground and subjecting the plastic shards to water, wind, and UV light, for instance, a farmer can induce the plastic to break up into smaller pieces. The public is interested in the particles that they store in their root systems from the soil ecology. When vertebrates and macro, meso, and micro-invertebrates ingest and carry microplastics, MP transport takes place. The presence of plastic waste in the soil ecosystem is concerning because it can accumulate in plants cultivated in contaminated soils and affect consumers by directly entering the food supply chain. Plastic contamination in agriculture has a detrimental effect on soil ecology and plant growth. The public is interested in learning more about how plastic particles affect biomass quality and plant growth, as well as whether plants may absorb plastic particles from the soil environment and store them in their root systems.

Keywords: Plastic, Agriculture, Soil, Microplastic, Plant, Pollution.

Introduction:

The world's population will increase from 7 billion in 2010 to 10 billion by 2050. It is anticipated that worldwide crop production would have grown by 50% from 2010 levels by 2050. To support population growth significantly faster than has been seen in recent decades, an annual growth rate in crop production will be required. Nonetheless, there is an increasing public push to use fewer of the few resources needed to provide food globally. The COVID-19 virus brought in unanticipated adverse global conditions, which further sped up progress. Throughout the epidemic, the primary areas affected globally were the economy, agriculture, human health, and food security (Collins *et al*.,2022). Food supplies were unexpectedly moved to homes during the COVID-19 pandemic as a result of social distancing regulations. Furthermore, food insecurity is a problem that is difficult to address on a worldwide scale. It has a major influence on public health challenges related to common, expensive, and avoidable chronic illnesses including diabetes, heart disease, and mental health disorders since it cannot be described, restricted, or categorized by location or by a particular grouping. Agriculture benefits societies all around the world in a number of ways,

including by providing food, creating jobs, supplying raw materials for various industries, and promoting strong economies through international commerce.

One of the most effective means of eradicating severe poverty and advancing the economy, its growth has a favorable correlation with food security. The agricultural sector's expansion depends on and is susceptible to regional weather fluctuations. It is extremely reliant on soil, water, and other natural resources that can be influenced by climate conditions because of its global distribution across many temperate zones and elevations. Therefore, uncertain climate change scenarios can negatively impact agricultural productivity and generate significant concerns regarding the global food supply's security. Research suggests that in order to adapt to climate change and produce food in a sustainable manner, the world should adopt alternative methods of growing food. Also, several research studies have been validated and provide evidence for adopting modern farming methods to cope with the effects of climate change (Sharma *et al*., 2022). Contemporary agricultural methods can improve soil health, reduce water consumption, increase water productivity, and produce more with less pollution and less input. The use of plastic agriculture is not new. Because of their affordability, adaptability, and durability, plastic items have been essential to many farming methods during the past few decades. To control soil temperature, stop weed development, and maintain moisture, thin plastic sheets are laid over the soil. Crops like pepper, tomatoes, and strawberries are frequently grown using these sheets. In addition, a variety of plastic items, including pots and containers, are utilized to raise seedlings throughout the nursery stage. The increase of plastic garbage has also been caused by the extensive usage of plastic containers for pesticides and fertilizers. They are advantageous in the short term since their use greatly boosts water production, but it jeopardizes long-term food security (Chen et al., 2021).

Micro and Nano-Plastic Particles:

"Material that can be easily shaped, formed, and molded by providing heat and pressure" is what the word "plastic" originally meant. It has just lately come to refer to a class of materials known as synthetic polymers. A lengthy chain of repeated smaller or bigger molecules (monomers) joined in subunits is called a polymer, which translates to "of many parts." Plastics are often made from both natural and synthetic polymers. Natural polymers (such silk, cellulose, muscle fiber, rubber, hair, and DNA) are not the same as synthetic polymers. Natural gas, coal, and oil are among the raw materials used in their production. Plastic waste comes in a variety of sizes, shapes, colors, and densities, and each one is essential to its bioavailability and breakdown. A global increase in the rate of plastic pollution has made microplastics (MPs) and nano plastics (NPs) a concern that is negatively impacting the Earth's biota and environment as a whole. According to Nguyen et al. (2019), MPs and NPs are solid, insoluble plastic particles. Additionally, MPs can be categorized as primary or secondary particles based on their origin. The weathering and degradation of huge plastic leftovers in open fields due to a variety of climate events, such as solar exposure, waves, thermal oxidation, and others. Primary MPs, on the other hand, are intentionally created by industries for profit. Research indicates that the continuous degradation of primary and secondary plastic particles may lead to significant alterations in their physical attributes, such as their density, size, shape, color, surface morphology, and crystallinity. Their physical and chemical properties, as well as those of other natural life

forms, may be affected by these changes. Numerous natural settings, including as soil, water, air, marine life, salt, beer, and more, include MPs. Recent studies have shown that they are present in plastic drinking water bottles. After entering living bodies, the MPs can alter the immune system or cause a variety of clinical disorders and outcomes. Future challenges could occur from the fragmentation of MPs into different smaller sizes, shapes, and components or from the advent of nanotechnologies, which include producing nano or micron-sized polymeric materials.

Plastic's Journey into the Soil:

Plastics are likely to travel through the soil surface via sediment and hydrological transport channels, which are impacted by topography, surface morphology, land use, and other factors, as a result of runoff and water erosion. Hortonian, or infiltration excess overland flow, occurs when the intensity of the rainfall exceeds the soil's ability to absorb it, and saturation excess overland flow occurs when the soil is saturated with water and cannot hold on to more rainfall. These are the two main processes that produce runoff. Plastics may indirectly affect runoff production and erosion by changing the properties of the soil that affect erodibility and runoff generation, such as aggregate stability, hydrophobicity, water storage capacity, and infiltration capability. Wind erosion may carry light polymers through soil systems and ultimately into rivers and streams. Plastic particles are easily carried by the wind and enter the atmosphere, lowering the quality of the air we breathe, particularly in places that are vulnerable to wind erosion. Soils will be more susceptible to wind erosion due to the increased aridity that climate change will bring to many parts of the world. The way that microplastics are carried by soil organisms is greatly influenced by both the size of the microplastics and the species that come into touch with them. MP transfer will be easier for little species than for larger or more developed creatures, and small particles are easier to move or carry than larger ones.

Plastic Pollution Impact on Soil Fertility:

Physical Impact on Soil Structure:

The texture of the soil is one of the most obvious effects of plastic contamination. Increased surface runoff and soil erosion may result from the soil's diminished capacity to hold water when plastics are present. After crops are harvested, plastic mulches can form a barrier that keeps water from penetrating, leaving the soil dry and unsuitable for plant roots. Retention problems can be especially harmful in regions that are prone to drought and water scarcity. The impact of plastic pollution on soil texture is among its most obvious effects. Increased surface runoff and soil erosion may result from the soil's diminished capacity to hold water when plastics are present. After crops are harvested, plastic mulches can form a barrier that keeps water from penetrating, leaving the soil dry and unsuitable for plant roots. In places where water scarcity is already a major concern, this problem of water retention can be especially harmful.

Chemical Contamination of Soil:

BPA, Styrene, and phthalates are among the chemicals used to make plastics, particularly those used to package insecticides and fertilizers. These substances have the ability to seep into the soil, changing its chemical makeup and possibly impairing plant development. Plastics can also include heavy metals like lead, cadmium, and chromium, particularly in items that are recycled or improperly disposed of. These harmful compounds can contaminate crops and make their way into the food chain while remaining in the soil for years. According to a study by Johansen et al. (2024), fertilization, agricultural inputs like

mulching, irrigation, paint peeling from farm equipment, and air deposition all affect the number of MPs and NPs in soil. The maximum concentrations of MP and NP in soil are 5.3 × 105 particles/kg dry-weight soil or 0.224 g plastic/kg dry-weight soil. In a three-year study, Zhao et al. (2024) employed three distinct plastic sizes—0.4 × 0.4 cm2 (small), 4 × 4 cm2 (medium), and 10 × 10 cm2—to determine the effect of landfill plastic trash on maize crop productivity. The experimental results showed that, in comparison to the control treatment, medium-sized plastic residues significantly decreased crop output. This study suggests that as plastics of all sizes and types progressively break down, soil health may suffer. Ultimately, plastic trash might negatively affect the sustainability of agricultural produce. It can alter a wide range of physical and chemical properties of the soil, including bulk density, water-holding capacity, soil structure, and the flow of plastic particles into groundwater aquifers. The experimental results showed that, in comparison to the control treatment, medium-sized plastic residues significantly decreased crop output. This study suggests that as plastics of all sizes and types progressively break down, soil health may suffer. Ultimately, plastic trash might negatively affect the sustainability of agricultural produce.

Disruption of Soil Microbial Communities:

Soil microorganisms such as fungi, bacteria, and earthworms are crucial for the decomposition of organic matter, nutrient cycling, and soil structure maintenance. The microbial equilibrium may be altered by toxic compounds generated during the degradation of polymers. According to certain studies, the presence of microplastics in the soil may result in a decrease in the number of beneficial microbes like nitrogen-fixing bacteria and microbial diversity. The loss of these bacteria can lead to a reduction in soil production since they are crucial for preserving soil fertility.

Decreased Soil Aeration:

The buildup of plastic particles in the soil may also have an impact on the aeration of the soil. The amount of oxygen available to plant roots and other soil organisms is decreased when plastic particles build up and clog soil pores. This can result in reduced nutrient uptake and root rot, which hinder plant growth and lower agricultural yield.

Conclusion:

Plastic pollution is a serious problem for the ecosystem and is harming Earth's biological variety in addition to climate change. Plastics are playing an increasingly significant role in agricultural culture in order to achieve sustainable goals. Despite the fact that the use of plastics has improved agricultural productivity generally, several visible and invisible problems have arisen as a result. Plastics are hazardous to plants, irrigation water, agricultural soils, and the environment due to their accumulation and poorly managed recycling operations.

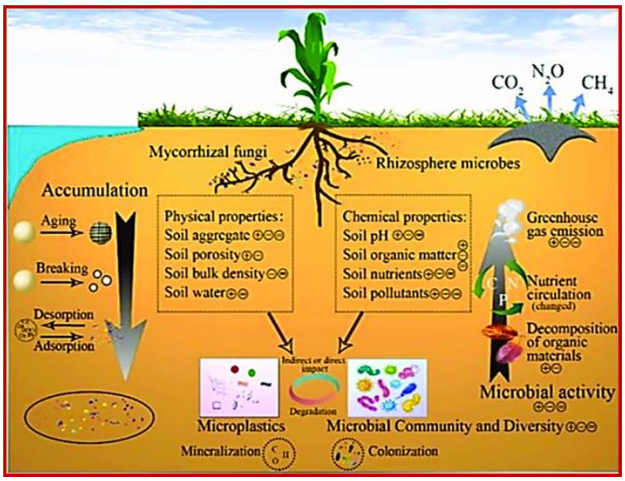

Fig.1: Effect of Microplastic on Soil Properties

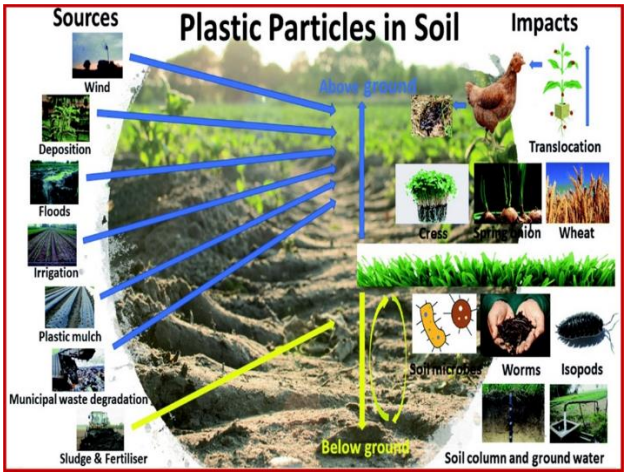

Fig.2: Sources of Plastic particles and its Impact on Soil

References:

1. Collins, C. C., & Ogundeji, A. A. (2022). Effect of COVID-19 on agricultural production and food security: A scientometric analysis. *Humanities and Social Sciences Communications*, *9*(1).
2. Sharma, V., Tripathi, A. K., & Mittal, H. (2022). Technological revolutions in smart farming: Current trends, challenges & future directions. *Computers and Electronics in Agriculture*, *201*, 107217.
3. Chen, H. L., Nath, T. K., Chong, S., Foo, V., Gibbins, C., & Lechner, A. M. (2021). The plastic waste problem in Malaysia: management, recycling and disposal of local and global plastic waste. *SN Applied Sciences*, *3*(4), 437.
4. Nguyen, B., Claveau-Mallet, D., Hernandez, L. M., Xu, E. G., Farner, J. M., & Tufenkji, N. (2019). Separation and analysis of microplastics and nanoplastics in complex environmental samples. *Accounts of chemical research*, *52*(4), 858-866.
5. Johansen, J. L., Magid, J., Vestergård, M., & Palmqvist, A. (2024). Extent and effects of microplastic pollution in soil with focus on recycling of sewage sludge and composted household waste and experiences from the long-term field experiment CRUCIAL. *TrAC Trends in Analytical Chemistry*, *171*, 117474.
6. Zhao, Z. Y., Wang, P. Y., Xiong, X. B., Irum, M., Mo, F., Cao, J., ... & Xiong, Y. C. (2024). Size and concentration effects of polythene plastic residues on soil physiochemical traits and maize productivity: A three-year appraisal. *Journal of Cleaner Production*, *435*, 140572.

International Journal of Advance and Applied Research
www.ijaar.co.in
ISSN – 2347-7075 Impact Factor – 8.141
Peer Reviewed Bi-Monthly
Vol. 7 No. 14 January – February - 2026

Biodiversity and Conservation Assessment of Medicinal Plant Species in Surgana Tahsil, Nashik District

Ms. Aditi. S. Kale[1] & Dr. S. S. Tambe[2]

[1]*Research Scholar, PG Department of Botany & Research Centre MGV's L.V.H. Arts, Science & Commerce (Autonomous) College Panchvati, Nashik, 422003*

[2]*Associate Professor, PG Department of Botany & Research Centre MGV's L.V.H. Arts, Science & Commerce (Autonomous) College Panchvati, Nashik, 422003*

Corresponding Author – Ms. Aditi. S. Kale

DOI - 10.5281/zenodo.19724247

Abstract:

Surgana Tahsil of Nasik District, Maharashtra, is a forest-rich tribal region possessing significant medicinal plant diversity. The present study aims to assess the biodiversity status and conservation needs of medicinal plant species in this ecologically sensitive area. Field surveys were conducted in selected forest patches and tribal villages using quadrate sampling, transect walks, and interviews with local healers.

The study documented approximately 45–60 medicinal plant species, including several rare and threatened taxa. Notable species recorded during the survey include Rauvolfia serpentina, Gloriosa superba, Chlorophytum borivilianum, Ceropegia vincifolia, and Oroxylum indicum. These species are facing population decline due to overharvesting, habitat degradation, forest fires, grazing pressure, and increasing anthropogenic activities.

The conservation assessment indicates that while common medicinal plants remain moderately abundant, rare species require immediate protection measures. Strategies such as in situ conservation, ex situ cultivation, community participation, awareness programs, and sustainable harvesting protocols are essential for maintaining ecological balance. Proper scientific documentation and conservation planning are crucial to safeguard the medicinal plant wealth of Surgana Tahsil for sustainable utilization and future pharmacological research.

Keywords: Medicinal Biodiversity, Rare Species, Conservation, Ethnobotany, Surgana Tahsil, Sustainable Use.

Introduction:

Medicinal plants constitute an important component of forest biodiversity and play a vital role in traditional as well as modern healthcare systems. India, recognized as one of the world's mega-biodiversity countries, harbors a rich diversity of medicinal flora distributed across varied ecological regions. Forest-dominated tribal areas are particularly significant reservoirs of ethnomedicinal knowledge and plant resources.

Surgana Tahsil of Nasik District, Maharashtra, is characterized by hilly terrain, semi-evergreen to dry deciduous forests, and substantial tribal population. The region supports a wide range of medicinal plant species, including rare and threatened taxa such as Rauvolfia serpentina, Gloriosa superba, Chlorophytum borivilianum, and Oroxylum indicum. These species are widely used by indigenous communities for the treatment of various ailments including fever, snakebite, inflammation, reproductive disorders, and respiratory problems.

However, increasing anthropogenic pressures such as deforestation, overharvesting,

habitat fragmentation, grazing, and forest fires have led to a decline in natural populations of several medicinal plants. Lack of systematic conservation measures further threatens their sustainability. Therefore, assessing the biodiversity status and conservation needs of medicinal plant species in Surgana Tahsil is essential for sustainable utilization, ecological balance, and preservation of traditional knowledge systems.

The present study focuses on documenting medicinal plant diversity and evaluating conservation priorities to ensure long-term protection of this valuable biological heritage.

Methodology:

The present study was conducted to assess the biodiversity and conservation status of medicinal plant species in Surgana Tahsil, Nasik District, Maharashtra.

1. Study Area Survey: Field surveys were carried out in selected forest patches and tribal villages of Surgana Tahsil during different seasons to record maximum plant diversity.

2. Field Exploration: Transect walks and quadrat sampling methods were used to assess species distribution and abundance. Plants were observed in their natural habitats such as forest areas, hill slopes, and agricultural boundaries.

3. Data Collection: Information on medicinal uses was collected through interviews with tribal healers (Vaidus), elders, and local inhabitants. Data recorded included scientific name, local name, family, habit, plant part used, and medicinal application.

4. Plant Identification: Collected specimens were identified using regional floras and standard botanical literature. Rare and threatened species such as Rauvolfia serpentina, Gloriosa superba, and Chlorophytum borivilianum were carefully documented.

5. Conservation Assessment: Species abundance and distribution patterns were analyzed. Threat factors such as overharvesting, grazing, deforestation, and habitat degradation were recorded. Conservation needs were evaluated based on field observations and local availability status.

6. Documentation: Photographic records were maintained, and data were systematically compiled for further analysis and interpretation.

Rare Medicinal Plants of Surgana Tahsil (Nashik District):

Sr. No.	Botanical Name	Local Name	Habit	IUCN Category*	Reason for Local Rarity
1	*Aspidopterys cordata*	Makadvel	Climber	NE	Habitat disturbance
2	*Withania somnifera*	Ashwagandha	Shrub	LC	Overharvesting of roots
3	*Hugonia mystax*	Katesavarvel	Shrub	NE	Restricted dry forest margins
4	*Terminalia arjuna*	Arjun	Tree	LC	Bark extraction pressure
5	*Chlorophytum borivilianum*	Safed Musli	Herb	EN	Commercial overexploitation
6	*Gloriosa superba*	Kalalavi	Climber	LC	Collection of tubers
7	*Rauvolfia serpentina*	Sarpagandha	Shrub	EN	Root extraction for trade
8	*Asparagus racemosus*	Shatavari	Climber	LC	Overharvesting
9	*Hemidesmus indicus*	Anantmul	Climber	LC	Root collection pressure
10	*Decalepis hamiltonii*	Nannari	Climber	EN	Excessive root harvesting
11	*Pterocarpus marsupium*	Bija	Tree	NT	Timber exploitation
12	*Boswellia serrata*	Salai	Tree	NT	Resin extraction

13	*Oroxylum indicum*	Tetu	Tree	LC	Bark and pod collection
14	*Stereospermum suaveolens*	Padal	Tree	LC	Habitat degradation
15	*Celastrus paniculatus*	Malkangni	Climber	LC	Seed collection
16	*Tinospora cordifolia*	Gulvel	Climber	LC	Overharvesting
17	*Holarrhena pubescens*	Kuda	Tree	LC	Bark extraction
18	*Ailanthus excelsa*	Maharukh	Tree	LC	Habitat loss
19	*Gymnema sylvestre*	Gudmar	Climber	LC	Overcollection
20	*Curculigo orchioides*	Kali Musli	Herb	EN	Commercial exploitation

Result:

The present investigation documented **approximately 45–60 medicinal plant species** from forest patches and tribal villages of Surgana Tahsil, Nashik District. The vegetation comprises herbs, shrubs, climbers, and trees belonging to diverse families such as Fabaceae, Apocynaceae, Liliaceae (Asparagaceae), Combretaceae, and Euphorbiaceae.

Several species of high medicinal and conservation value were recorded, including **Rauvolfia serpentina**, **Gloriosa superba**, **Chlorophytum borivilianum**, **Oroxylum indicum**, and **Curculigo orchioides**. Among the 20 rare medicinal plants analyzed, 5 species fall under **Endangered (EN)** category, 2 under **Near Threatened (NT)**, several under **Least Concern (LC)** globally but showing local decline, and some remain **Not Evaluated (NE)**.

The major threat factors identified during field assessment include:

- Overharvesting of roots, bark, and tubers
- Forest fires and habitat degradation
- Grazing pressure
- Commercial exploitation
- Increasing anthropogenic disturbances

Rare species such as **Decalepis hamiltonii** and **Pterocarpus marsupium** showed restricted distribution and reduced population density in surveyed quadrats. Climbers and tuberous species were found to be more vulnerable due to destructive harvesting practices.

Overall, the study indicates that while common medicinal plants remain moderately abundant, several economically important taxa are under significant ecological stress and require priority conservation attention.

Conclusion:

The biodiversity assessment reveals that Surgana Tahsil possesses rich medicinal plant diversity, but several rare and commercially valuable species are experiencing local population decline due to unsustainable exploitation and habitat disturbance.

The study emphasizes the urgent need for:

- **In situ conservation** through protection of forest habitats
- **Ex situ cultivation** of endangered species in nurseries and herbal gardens
- **Community participation** involving tribal healers and local stakeholders
- **Awareness programs** on sustainable harvesting techniques
- **Scientific monitoring and documentation** for long-term conservation planning

Sustainable utilization strategies combined with traditional knowledge preservation can ensure ecological balance and safeguard the medicinal plant wealth of Surgana Tahsil for future generations and pharmacological research.

Acknowledgement:

I sincerely acknowledge the support of the financial support provided under the SJSGC Fellowship, and Research Centre, Department of

Botany, for permitting field visits, plant identification, and documentation work required for this study, academic support and necessary research facilities.

References:

1. Flora of the Presidency of Bombay – Cooke, T. (1901–1908). Botanical Survey of India, Calcutta.
2. Flora of Maharashtra State – Singh, N.P. & Karthikeyan, S. (2000). Botanical Survey of India, Kolkata.
3. Indian Medicinal Plants – Kirtikar, K.R. & Basu, B.D. (1935). Lalit Mohan Basu, Allahabad.
4. Botanical Survey of India (BSI). Regional Floras and Herbarium Records. Ministry of Environment, Forest and Climate Change, Government of India.
5. International Union for Conservation of Nature (IUCN). The IUCN Red List of Threatened Species. Available at: https://www.iucnredlist.org
6. World Health Organization (WHO). (2013). WHO Traditional Medicine Strategy 2014–2023. Geneva.
7. Jain, S.K. (1991). Dictionary of Indian Folk Medicine and Ethnobotany. Deep Publications, New Delhi.
8. Sharma, B.D., Karthikeyan, S., & Singh, N.P. (1996). Flora of Maharashtra. Botanical Survey of India.
9. Gadgil, M. & Vartak, V.D. (1975). Sacred Groves of India – A Plea for Continued Conservation. *Journal of the Bombay Natural History Society.*
10. Kala, C.P. (2005). Indigenous Uses and Conservation of Medicinal Plants in Western Ghats. *Biodiversity and Conservation.*
11. Ministry of Environment, Forest and Climate Change (MoEFCC). State of Forest Report, Government of India.
12. National Medicinal Plants Board (NMPB), Government of India – Medicinal Plant Conservation Areas (MPCAs) guidelines.

International Journal of Advance and Applied Research
www.ijaar.co.in
ISSN – 2347-7075 Impact Factor – 8.141
Peer Reviewed Bi-Monthly
Vol. 7 No. 14 January – February - 2026

Advancing Precision Diagnostics: Emerging Molecular Strategies for Early Detection and Control of Antimicrobial Resistance in 2026

Amit C. Harangule
Research Scholar, Department of Botany,
Sir Parashurambhau College (Empowered Autonomous) Tilak Road Pune- 411030
Corresponding Author – Amit C. Harangule
DOI - 10.5281/zenodo.19724323

Abstract:

Antimicrobial resistance (AMR) has emerged as one of the most serious threats to global public health, compromising the effectiveness of existing therapeutic options and increasing morbidity, mortality, and healthcare costs. Rapid and accurate detection of resistant pathogens is critical for guiding targeted treatment and limiting the unnecessary use of broad-spectrum antibiotics. Traditional culture-based antimicrobial susceptibility testing remains reliable but is constrained by lengthy processing times, which often delay clinical decision-making. Recent progress in molecular diagnostics has transformed the landscape of infectious disease detection. Technologies such as CRISPR-enabled biosensing, portable long-read sequencing platforms, and high-throughput metagenomic analysis combined with artificial intelligence now allow direct identification of pathogens and resistance determinants from clinical samples within a significantly reduced timeframe. These culture-independent approaches support timely precision therapy, strengthen hospital infection control, and enhance real-time resistance surveillance. As healthcare systems move toward data-driven clinical management in 2026, the integration of next-generation molecular diagnostics into routine practice will play a pivotal role in improving antimicrobial stewardship and mitigating the growing burden of AMR.

Keywords: Antimicrobial Resistance; Molecular Diagnostics; CRISPR; Nanopore Sequencing; Metagenomics; Precision Therapy.

Introduction:

Antimicrobial resistance (AMR) threatens modern medicine by undermining the effectiveness of antibiotics used to treat bacterial infections. A major contributor to this crisis is the diagnostic delay, defined as the time between patient presentation and the availability of pathogen-specific susceptibility data. During this period, clinicians often rely on empirical broad-spectrum antibiotics, which increase selective pressure and accelerate resistance evolution.

In recent years, diagnostic priorities have shifted from simple pathogen identification to comprehensive resistome profiling—the detection of all antimicrobial resistance genes present in a clinical sample. Molecular diagnostics (MDx) now enable rapid nucleic acid detection and sequencing directly from patient specimens, reducing diagnostic time from days to hours. These advances support precision antimicrobial therapy, improve patient outcomes, and reduce unnecessary antibiotic exposure.

Emerging Technological Pillars:

1. CRISPR-Cas Systems: Precision Molecular Detection:

CRISPR-based diagnostics such as SHERLOCK (Cas13) and DETECTR (Cas12)

represent a new class of rapid, highly specific nucleic acid detection tools.

Mechanism:

CRISPR-based diagnostic systems have emerged as a rapid and highly sensitive approach for the detection of antimicrobial resistance (AMR) genes. These assays utilize programmable guide RNA (gRNA) to direct CRISPR-associated nucleases such as Cas12 or Cas13 toward specific resistance determinants, including blaNDM, mecA, and mcr-1. Upon recognition of the target nucleic acid sequence, the activated Cas enzyme exhibits collateral cleavage activity, which nonspecifically cuts nearby labeled reporter molecules. This reaction generates a detectable signal in the form of fluorescence or a visual band on a lateral-flow strip. CRISPR diagnostics offer sensitivity comparable to polymerase chain reaction (PCR) while significantly reducing turnaround time to approximately 30–60 minutes. In addition, these assays operate under isothermal conditions and require minimal laboratory infrastructure, making them suitable for point-of-care (POC) applications. Recent advancements have led to the development of portable and paper-based CRISPR platforms that integrate sample preparation and detection into compact formats. As of 2026, several of these systems are undergoing clinical evaluation, particularly in low-resource settings, where decentralized and rapid detection of resistance genes can support timely treatment decisions and strengthen antimicrobial stewardship programs.

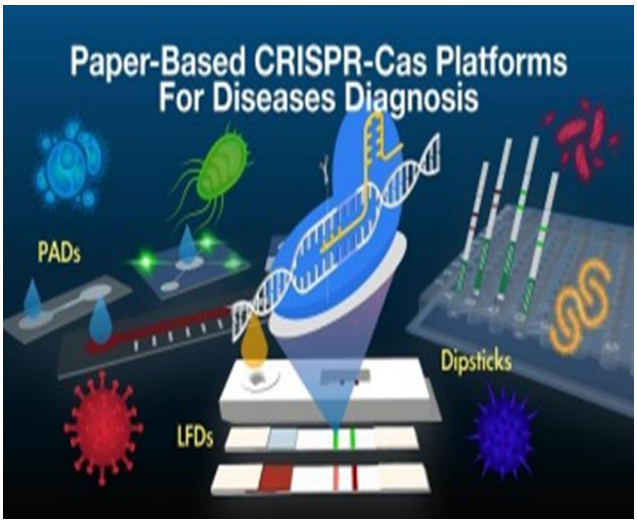

Flowchart Diagram:

Workflow of CRISPR-Based AMR Detection:

Sample Collection
↓
Nucleic Acid Extraction
↓
Target Amplification (optional isothermal method: RPA/LAMP)
↓
CRISPR Reaction Setup
Cas12/Cas13 enzyme
Guide RNA (specific to blaNDM/mecA/mcr-1)
Reporter molecule
↓
Target Recognition and Cas Activation
↓
Collateral Cleavage of Reporter
↓
Signal Detection
Fluorescence reader OR
Lateral-flow strip
↓
Interpretation: Presence/Absence of AMR Gene

2. Real-Time Nanopore Sequencing:

Nanopore sequencing is an advanced third-generation sequencing technology that enables real-time analysis of nucleic acids

without the need for amplification or complex laboratory infrastructure. The method works by passing single-stranded DNA or RNA molecules through a biological nanopore embedded in a membrane. As nucleotides move through the pore, they produce characteristic changes in electrical current, which are interpreted to determine the sequence. Platforms such as the portable Oxford Nanopore MinION allow continuous data generation and immediate analysis, making rapid pathogen identification possible.

Key Features:

- Rapid pathogen detection: Preliminary identification of pathogens and major resistance genes can be achieved within 15–30 minutes of sequencing initiation.
- Long-read capability: Nanopore sequencing produces long reads (several kilobases), enabling the detection of complete resistance gene cassettes, integrons, and genomic rearrangements.
- Plasmid and mobile element analysis: Long reads allow accurate determination of whether resistance genes are located on plasmids, transposons, or chromosomal DNA.
- Detection of mixed infections: Metagenomic nanopore sequencing can identify multiple pathogens and their resistance profiles directly from clinical samples.
- Real-time data streaming: Sequencing results are analyzed as they are generated, enabling rapid clinical decision-making.

Clinical Significance:

The ability to identify the genetic context of resistance genes is critical for understanding their transmission potential. When resistance determinants are located on mobile genetic elements, such as plasmids, the risk of horizontal gene transfer between bacterial species increases. This information helps clinicians and infection control teams assess outbreak risk, implement targeted isolation measures, and guide appropriate antimicrobial therapy. In hospital settings, real-time nanopore sequencing supports rapid outbreak investigation, surveillance of multidrug-resistant organisms, and monitoring of transmission pathways. Its portability and rapid turnaround also make it valuable for public health surveillance and field-based pathogen monitoring, especially during emerging infectious disease events.

Current Limitations and Future Outlook:

Although nanopore sequencing offers rapid and comprehensive genomic insights, challenges include relatively higher error rates compared to short-read sequencing, the need for optimized bioinformatics pipelines, and standardized clinical workflows. Ongoing improvements in sequencing chemistry, base-calling accuracy, and automated analysis tools are enhancing its reliability for routine clinical microbiology and AMR surveillance infection control and public health surveillance.

3. AI-Integrated Metagenomics:

Metagenomic next-generation sequencing (mNGS) is a culture-independent approach that enables comprehensive and unbiased detection of all microbial DNA or RNA present in a clinical or environmental sample. Unlike targeted molecular tests, mNGS can simultaneously identify bacteria, viruses, fungi, and parasites along with their antimicrobial resistance (AMR) determinants. This approach is particularly useful for diagnosing complex, polymicrobial, or unknown infections. However, mNGS generates massive datasets, and interpreting clinically relevant information—especially distinguishing true pathogens and predicting resistance phenotypes—remains a major challenge.

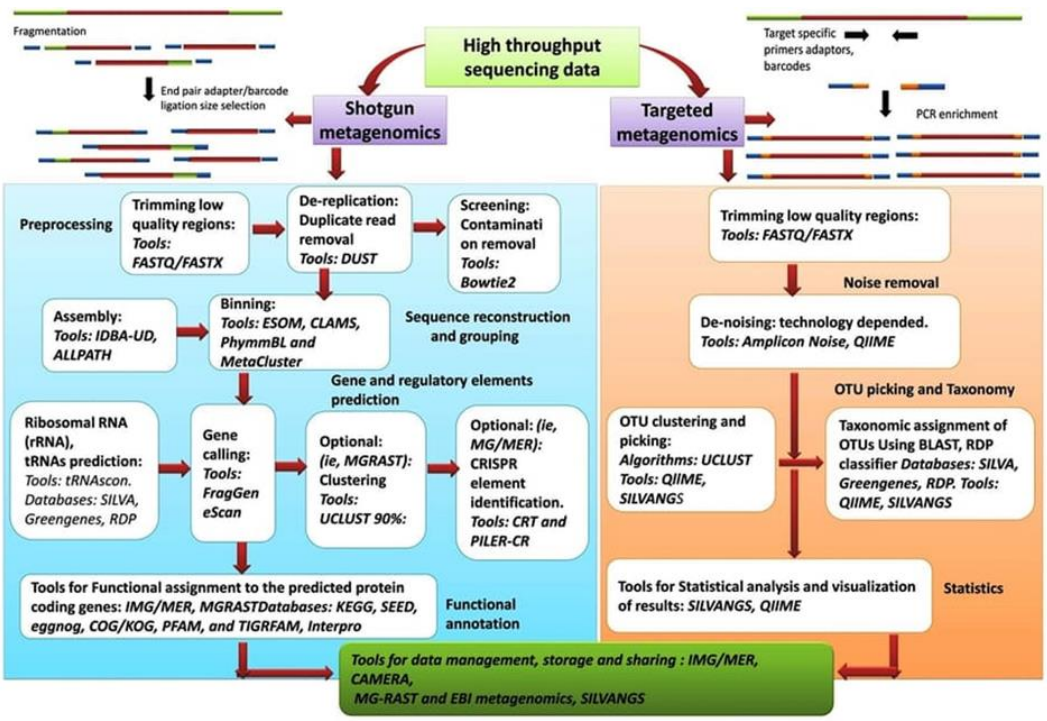

Role of Artificial Intelligence (AI):

Artificial intelligence and machine learning (ML) techniques are increasingly integrated into mNGS workflows to improve speed, accuracy, and clinical utility.

Prediction of phenotypic resistance: Machine learning models analyze genetic mutations, resistance genes, and sequence patterns to predict whether a microorganism will be resistant or susceptible to specific antibiotics, helping bridge the genotype–phenotype gap.

Deep learning approaches: Convolutional neural networks (CNNs) and other deep learning architectures can recognize complex sequence features and classify resistance patterns based on large genomic datasets.

Automated bioinformatics pipelines: AI-driven systems automate sequence filtering, host DNA removal, taxonomic classification, and resistance gene identification, significantly reducing analysis time and minimizing human error.

Clinical decision support: Integrated platforms generate interpretable reports that assist clinicians in selecting appropriate antimicrobial therapy.

Performance and Clinical Impact:

Recent AI-assisted mNGS models have demonstrated greater than 90–95% accuracy in predicting clinically relevant antimicrobial resistance for several major pathogens. These systems enable faster turnaround times compared to traditional culture-based susceptibility testing and support early targeted therapy. AI-integrated metagenomics is particularly valuable in critical care settings, outbreak investigations, and surveillance of emerging multidrug-resistant organisms. By improving the interpretation of complex sequencing data, this technology enhances antimicrobial stewardship and supports precision infectious disease management.

Comparative Analysis of Diagnostic Speed:

Microorganisms in the presence of antibiotics, providing direct phenotypic resistance profiles. However, it requires bacterial isolation and incubation, resulting in a turnaround time of 48–72 hours or longer for slow-growing organisms. The delay may lead to empirical broad-spectrum antibiotic use, increasing the risk of resistance development.

PCR-Based Assays:

Polymerase chain reaction (PCR) enables rapid detection of specific resistance genes through targeted amplification. Results are typically available within 4–6 hours, significantly faster than culture. PCR is highly sensitive and specific but can detect only known resistance genes included in the assay panel. Its multiplexing capacity is limited, and it does not provide information on novel or unexpected resistance mechanisms or actual phenotypic expression.

CRISPR-Based Diagnostics:

CRISPR-based systems use guide RNA-directed Cas enzymes to identify specific resistance genes with high sensitivity and specificity. Detection occurs within 30–60 minutes, making it suitable for point-of-care applications. These assays require minimal equipment and can produce fluorescence or lateral-flow readouts. However, similar to PCR, CRISPR diagnostics are target-specific and cannot provide comprehensive resistance profiling.

Nanopore Sequencing:

Nanopore sequencing is a real-time, long-read sequencing technology capable of identifying pathogens and their entire resistome within 1–6 hours. Long reads allow detection of full resistance gene cassettes, plasmids, and mobile genetic elements, providing insights into transmission potential. Despite its comprehensive nature, the method requires specialized bioinformatics analysis, trained personnel, and standardized workflows for routine clinical use.

AI-Integrated Metagenomics:

AI-assisted metagenomic sequencing combines unbiased detection of microbial genomes with machine learning-based prediction of phenotypic resistance. This approach can identify pathogens, resistance genes, and infer susceptibility patterns within 6–12 hours. It is particularly useful for complex or polymicrobial infections. However, high cost, computational demands, and large data complexity currently limit widespread clinical implementation.

Cost and data complexity:

Clinical and Public Health Applications:

1. Precision Antimicrobial Therapy:

Rapid resistome profiling has emerged as a transformative approach in the clinical management of infectious diseases by enabling comprehensive detection of antimicrobial resistance (AMR) determinants directly from patient samples. Advanced technologies such as real-time sequencing, multiplex molecular assays, and metagenomic next-generation sequencing (mNGS) allow identification of pathogens and their resistance genes within hours, significantly reducing the diagnostic delay associated with conventional culture-based methods.

One of the primary clinical advantages of rapid resistome analysis is the ability to initiate targeted antimicrobial therapy at an early stage. In many clinical settings, empirical broad-spectrum antibiotics are started while awaiting laboratory results, which typically take 48–72 hours. Rapid genomic diagnostics provide resistance profiles within a few hours, allowing clinicians to select the most effective and narrow-spectrum treatment. Early optimization of therapy is particularly critical in life-threatening conditions such as sepsis, bloodstream infections, and ventilator-associated pneumonia, where delays in appropriate treatment are associated with increased mortality.

Rapid resistance detection also contributes to the reduction of unnecessary broad-spectrum antibiotic use. By guiding precise therapy, these technologies support antimicrobial stewardship programs and help minimize selective pressure that drives the emergence and spread of resistant organisms. In addition,

limiting inappropriate antibiotic exposure reduces the risk of adverse drug reactions, secondary infections, and healthcare costs. Clinical studies have demonstrated that early targeted treatment improves patient survival, shortens hospital stays, and enhances overall treatment outcomes.

Beyond individual patient care, next-generation diagnostics play a critical role in infection control and hospital surveillance. Whole-genome sequencing (WGS) and real-time sequencing platforms enable high-resolution analysis of pathogen genomes, allowing early detection of outbreaks caused by multidrug-resistant organisms. Rapid identification of genetically related strains helps infection control teams implement timely interventions such as patient isolation, contact tracing, and environmental decontamination, thereby preventing further transmission within healthcare facilities.

Another important application is the real-time monitoring of resistance trends. Continuous genomic surveillance allows hospitals and public health authorities to track the emergence of new resistance mechanisms, high-risk clones, and changes in local resistance patterns. This information supports the development of evidence-based antibiotic policies, empirical treatment guidelines, and infection prevention strategies tailored to local epidemiology.

Furthermore, next-generation sequencing enables genomic epidemiology of hospital-acquired infections. Detailed genetic analysis can distinguish between community-acquired and nosocomial infections and identify transmission pathways within hospital settings. The ability to determine whether resistance genes are located on plasmids or other mobile genetic elements also provides insight into the risk of horizontal gene transfer and the potential for rapid dissemination among bacterial populations. Such information is essential for controlling high-priority pathogens, including methicillin-resistant Staphylococcus aureus (MRSA), carbapenem-resistant Enterobacteriaceae (CRE), and multidrug-resistant Acinetobacter baumannii.

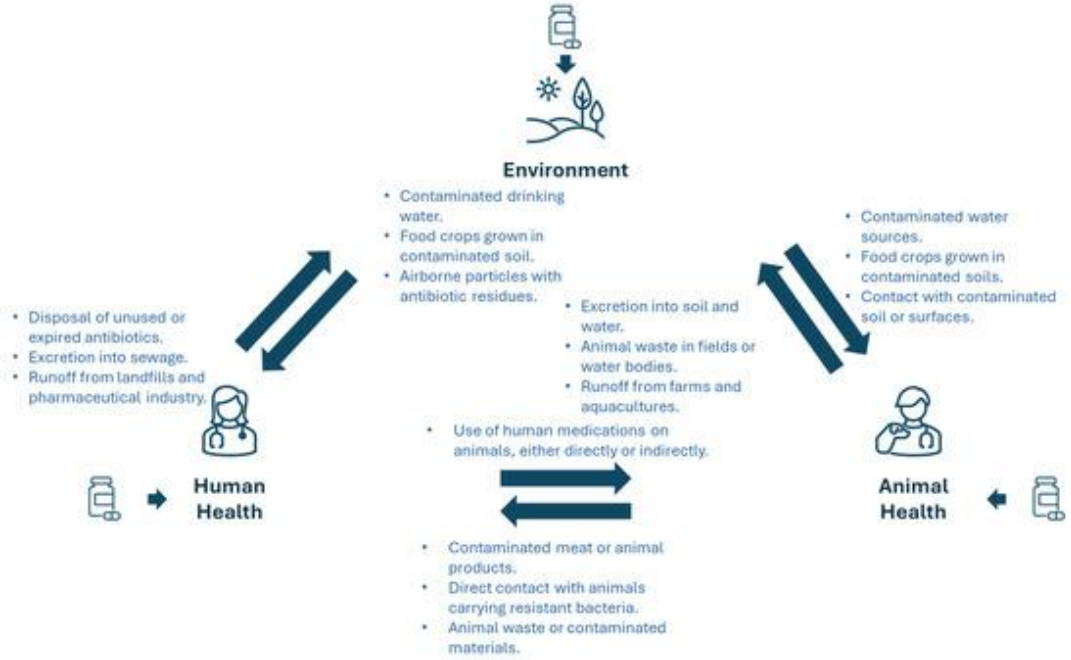

3. Low-Resource Settings:

The global burden of antimicrobial resistance (AMR) is disproportionately high in low- and middle-income countries (LMICs), where limited laboratory capacity, delayed diagnostics, and widespread empirical antibiotic use contribute to the emergence and spread of resistant pathogens. Recent advances in portable

molecular technologies, including CRISPR-based assays and handheld nanopore sequencing platforms, offer promising solutions for strengthening diagnostic capacity and surveillance in resource-limited settings.

Portable CRISPR diagnostics enable rapid detection of specific resistance genes using isothermal reactions and simple visual readouts, such as lateral-flow strips. These systems require minimal equipment, limited power supply, and basic technical training, making them suitable for decentralized testing at primary healthcare centers and district hospitals. Similarly, compact nanopore sequencing devices allow real-time genomic analysis using laptop-based workflows, eliminating the need for large, centralized sequencing facilities. The portability and rapid turnaround time of these technologies reduce delays associated with sample transport and enable timely clinical decision-making.

Decentralized deployment of next-generation diagnostics also enhances AMR surveillance in developing regions. Real-time identification of resistance determinants and high-risk clones supports early detection of outbreaks and emerging resistance mechanisms. Integration of genomic data into national and international surveillance networks, such as the World Health Organization's Global Antimicrobial Resistance and Use Surveillance System (GLASS), improves situational awareness and informs public health interventions. Strengthening diagnostic access at peripheral healthcare levels is therefore critical for controlling the spread of multidrug-resistant organisms.

Despite their significant potential, several challenges limit the widespread clinical implementation of advanced genomic diagnostics. Cost and infrastructure requirements remain major barriers, as sequencing platforms, reagents, and data storage systems involve substantial initial investment. In addition, reliable electricity, internet connectivity, and trained personnel with expertise in molecular biology and bioinformatics are necessary for routine operation, which may not be available in many settings.

Another key limitation is the complexity of data interpretation. Metagenomic and whole-genome sequencing generate large volumes of data that require specialized bioinformatics pipelines to identify clinically relevant pathogens and resistance genes. The lack of standardized analysis workflows, curated reference databases, and uniform reporting formats can lead to variability in results and hinder clinical adoption. Development of automated, user-friendly analytical platforms and standardized clinical reporting guidelines is essential to improve usability.

Regulatory and validation challenges also affect implementation. Many next-generation diagnostic tools are still undergoing clinical evaluation, and validation across diverse pathogens, specimen types, and geographical regions is limited. Furthermore, the absence of harmonized global regulatory frameworks slows approval processes and quality assurance for clinical use.

An additional scientific challenge is genotype–phenotype discordance. The presence of a resistance gene does not always result in phenotypic resistance, as gene expression, regulatory mechanisms, and additional mutations influence clinical outcomes. Consequently, conventional culture-based antimicrobial susceptibility testing (AST) remains necessary in certain cases to confirm functional resistance and guide therapy.

In summary, portable next-generation diagnostic technologies have the potential to transform AMR detection and surveillance in low-resource settings by enabling decentralized, rapid, and high-resolution analysis. However, addressing challenges related to cost,

infrastructure, data interpretation, regulatory approval, and genotype–phenotype correlation will be essential for their successful integration into routine clinical practice and global AMR control strategies.

Future Directions (2026–2030):

The next decade is expected to witness significant advancements in antimicrobial resistance (AMR) diagnostics, driven by innovations in automation, artificial intelligence (AI), digital health integration, and global data sharing. These developments aim to transform AMR management from delayed, laboratory-based testing to real-time, data-driven clinical decision-making.

One major focus area is the development of fully automated sample-to-answer platforms. Emerging diagnostic systems are being designed to integrate sample preparation, nucleic acid extraction, amplification or sequencing, and result interpretation into a single closed device. Such automation will minimize manual handling, reduce contamination risk, and enable rapid testing with minimal technical expertise. These platforms are particularly valuable for emergency settings, intensive care units, and decentralized healthcare facilities.

Another important direction is the integration of diagnostic outputs with electronic health records (EHRs) and clinical decision-support systems (CDSS). Linking rapid resistance data directly to patient records will allow automated treatment recommendations based on local antibiograms, patient history, and clinical guidelines. Real-time decision support can assist clinicians in selecting optimal antimicrobial therapy, improving treatment accuracy while strengthening antimicrobial stewardship.

The expansion of AI-driven predictive resistance models is also expected to enhance the clinical utility of genomic diagnostics. Machine learning and deep learning algorithms will increasingly be used to predict phenotypic resistance from genomic and metagenomic data, identify emerging resistance mutations, and forecast resistance trends. As training datasets grow and algorithms improve, predictive accuracy and reliability will continue to increase, helping bridge the genotype–phenotype gap.

At the population level, the establishment of global genomic AMR surveillance networks will play a critical role in monitoring the emergence and spread of resistant pathogens. Real-time sharing of genomic data across healthcare institutions, national programs, and international platforms will enable early detection of high-risk clones, novel resistance mechanisms, and cross-border transmission events. Integration with initiatives such as the WHO Global Antimicrobial Resistance and Use Surveillance System (GLASS) will strengthen global preparedness and response strategies.

Efforts are also underway to achieve cost reduction and wider accessibility through the development of portable, battery-operated, and multiplexed diagnostic technologies. Advances in microfluidics, paper-based assays, and miniaturized sequencing platforms are expected to lower operational costs and expand the use of advanced diagnostics in low-resource settings.

Overall, the future of AMR management lies in the convergence of real-time molecular diagnostics, AI-based analytics, and digital health ecosystems. The integration of rapid detection technologies with automated interpretation and clinical decision support will enable timely targeted therapy, improve patient outcomes, and enhance global surveillance. Such a connected and data-driven approach is essential for effective control of antimicrobial resistance in the coming decade.

Conclusion:

The rapid evolution of antimicrobial resistance demands a parallel transformation in diagnostic strategies. Next-generation molecular diagnostics—including CRISPR-based assays, real-time nanopore sequencing, and AI-enabled metagenomics—offer unprecedented speed, accuracy, and comprehensiveness in AMR detection. In 2026, the transition from culture-dependent methods to molecular, culture-independent workflows is no longer optional but essential for effective antimicrobial stewardship. Strategic implementation, cost optimization, and global collaboration will determine the success of these technologies in mitigating the AMR crisis.

References:

1. Arango-Argoty G, Garner E, Pruden A, Heath LS, Vikesland P, Zhang L. DeepARG:(2018) A deep learning approach for predicting antibiotic resistance genes from metagenomic data. Microbiome.;6:23.
2. Broughton JP, Deng X, Yu G, Fasching CL, Servellita V, Singh J, et al.(2020) CRISPR–Cas12-based detection platform for nucleic acids. Nat Biotechnol.;38:870–874.
3. Charalampous T, Kay GL, Richardson H, Aydin A, Baldan R, Jeanes C, et al. (2019)Nanopore metagenomics enables rapid clinical diagnosis of bacterial infections. Nat Biotechnol.;37:783–792.
4. Chen JS, Ma E, Harrington LB, Da Costa M, Tian X, Palefsky JM, et al.(2018) CRISPR-Cas12a target binding unleashes indiscriminate single-stranded DNase activity. Science.;360:436–439.
5. Chiu CY, Miller SA. (2019)Clinical metagenomics. Nat Rev Genet.;20:341–355.
6. Davis JJ, Wattam AR, Aziz RK, Brettin T, Butler R, Butler RM, et al.(2020) Antimicrobial resistance prediction using machine learning. Sci Rep.;10:421.
7. Deurenberg RH, Bathoorn E, Chlebowicz MA, Couto N, Ferdous M, García-Cobos S, et al. (2017) Application of next-generation sequencing in clinical microbiology and infection prevention. J Biotechnol.;243:16–24.
8. George S, Pankhurst L, Hubbard A, et al. (2020) Oxford Nanopore sequencing and its applications in microbiology. Clin Microbiol Rev.;33(2):e00086-19.
9. Gootenberg JS, Abudayyeh OO, Lee JW, Essletzbichler P, Dy AJ, Joung J, et al. Nucleic acid detection with CRISPR-Cas13. Science. 2017;356:438–442.
10. Gordon NC, et al. (2014)Whole-genome sequencing in outbreak analysis. Clin Microbiol Rev.;27:258–272.
11. Gupta SK, Padmanabhan BR, Diene SM, Lopez-Rojas R, Kempf M, Landraud L, et al. (2014) ARG-ANNOT: A bioinformatic tool to discover antibiotic resistance genes in bacterial genomes. Antimicrob Agents Chemother.;58:212–220.
12. Jorgensen JH, Ferraro MJ. (2009) Antimicrobial susceptibility testing: General principles and contemporary practices. Clin Infect Dis.;49:1749–1755.
13. Kellner MJ, Koob JG, Gootenberg JS, Abudayyeh OO, Zhang F. SHERLOCK(2019) Nucleic acid detection with CRISPR nucleases. Nat Protoc. 14:2986–3012.
14. O'Neill J. (2016) Tackling drug-resistant infections globally: Final report and recommendations. Review on Antimicrobial Resistance.
15. Peeling RW, Holmes KK, Mabey D, Ronald A. (2017) Diagnostics for global health: Addressing challenges in resource-limited settings. Nat Microbiol.;2:17088.

16. Quick J, Loman NJ, Duraffour S, Simpson JT, Severi E, Cowley L, et al. (2016) Real-time, portable genome sequencing for outbreak surveillance. Nature.;530:228–232.
17. Tang Y, Gao L, Feng W, et al. (2023) Advances in CRISPR-based point-of-care diagnostics for antimicrobial resistance detection. Front Microbiol.;14:1198745.
18. Tyler AD, Mataseje L, Urfano CJ, Schmidt L, Antonation KS, Mulvey MR, et al. (2018) Evaluation of Oxford Nanopore's MinION sequencing for microbial genomics. Sci Rep.;8:10931.
19. van Belkum A, Burnham CAD, Rossen JWA, Mallard F, Rochas O, Dunne WM Jr. (2019) Developmental roadmap for antimicrobial susceptibility testing systems. Nat Rev Microbiol.;17:51–62.
20. Wang Y, Xu C, Liu Y, et al. (2022) CRISPR-based diagnostics for infectious diseases and antimicrobial resistance. Biosens Bioelectron.;198:113821.
21. Wick RR, Judd LM, Gorrie CL, Holt KE. (2019) Completing bacterial genome assemblies with long-read sequencing. Microb Genom.;5:e000294.
22. World Health Organization. (2023) Global antimicrobial resistance and use surveillance system (GLASS) report 2023. Geneva: WHO;.
23. Yang Y, Niehaus KE, Walker TM, Iqbal Z, Walker AS, Peto TEA, et al. (2018) Machine learning for antimicrobial resistance prediction from whole-genome data. Clin Microbiol Infect.;24:1027–1033.

International Journal of Advance and Applied Research
www.ijaar.co.in
ISSN – 2347-7075 Impact Factor – 8.141
Peer Reviewed Bi-Monthly
Vol. 7 No. 14 January – February - 2026

Screening of Phytochemicals and Estimation of Secondary Metabolites in Plant Species Euphorbia neriifolia L. and Caralluma fimbriata Wall.

Bharat Hajgude & Ravi P. Patil.
Department of Botany, Deogiri College, Chhatrapati Sambhajinagar- 431005.
Corresponding Author – Bharat Hajgude
DOI - 10.5281/zenodo.19724353

Abstract:

The active components that give medicinal plants their therapeutic properties are phytochemicals, which are usually secondary metabolites like alkaloids, steroids, flavonoids, terpenoids, and tannins. Portions of the therapeutic herbs Caralluma fimbricata and Euphorbia neriifolia were investigated for secondary metabolites. Different techniques were used to estimate each secondary metabolite, such as the aluminium chloride colorimetric method for flavonoids, the Folin-Ciocalteu method for phenol, and the Folin-Denis method for tannin. Euphorbia neriifolia has the highest levels of flavonoids, tannin, and phenol. Caralluma fimbricata on the other hand, had a lower phenol content. It will be necessary to employ robust analytical separation and detection techniques like GCMS and HR-LCMS in future studies on secondary metabolites.

Keywords: Caralluma fimbricata, Folin-Denis, tannin, Euphorbia neriifolia. GCMS and HR-LCMS

Introduction:

The many secondary metabolites of C. fimbriata, such as steroidal glycosides, alkaloids, terpenoids, flavonoids, and tannins, are responsible for its pharmacological characteristics (Barthwal R & Mahar R 2024). It is commonly known to relieve thirst and control obesity in ethnic groups and has been used historically as a vegetable (Malladi S et al.2018). The medicinal properties of Euphorbia neriifolia, including its antiviral, anticonvulsant, radioprotective, anti-arthritic, anti-asthmatic, anti-fertility, anti-diarrheal, and anti-ulcer properties, are well documented.(M.Hasan et al.2014)

Materials and Methods:

The chosen plant species were collected at random from different localities of Marathwada **Plant Extraction:** Using an electronic blender, 50 g of each of the plants Euphorbia neriifolia and Caralluma fimbricata were ground into a fine powder. For efficient extraction, the ground plant material was subsequently put through a Soxhlet extraction process in the lab. The filtrates were saved for additional examination and the resultant crude extracts were utilised for quantitative estimation.

Phytochemical studies:

Tannin Content Determination: Folin-Denis method was used for determination of tannin content. (Ram and Malhotra, 1993; Sane, 2002)

Materials:

Folin-Denis Reagent, Sodium Carbonate Solution, Standard Tannic Acid Solution, Working Standard Solution.

Procedure: 0.5 g of plant material is boiled, centrifuged, and 1 ml of the extract is reacted with sodium carbonate and Folin-Denis reagent to extract and quantify tannin. A tannic acid standard curve is used to calculate the concentration after the resultant blue colour is detected at 700 nm.

Phenol Content Determination: The Singleton and Rossi (1965) method was used to measure the phenol content. Mix the sample and Folin reagent (1:1), adding 1 ml Na2Co3, and diluting to 10 ml and incubate for 3 minutes, after 90 minutes in the dark, measure the absorbance at 650 nm.

Flavonoid Content Determination: The aluminium chloride colorimetric method was used to determine the flavonoid concentration. Total Flavonoid Content is determined using the Aluminium Chloride Colorimetric Assay, in which $AlCl_3$ forms a coloured complex with flavonoids that are detected at 430 nm and quantified against a Rutin standard curve.

Observation tables:

Sr. No	Plant species	Flavonoids	Phenols	Tannins
1	*Euphorbia neriifolia*	+	+	+
2	*Caralluma fimbricata*	+	+	+

Table No.1: Phytochemical Screening of Medicinal Plant

Estimation of Phenol

Standard conc.mg/ml	O.D of Standard Solution at 760nm
0.1	0.062
0.2	0.087
0.3	0.120
0.4	0.202
0.5	0.285
0.6	0.324
0.7	0.350
0.8	0.370
0.9	0.430
1.0	0.502

Sample	O.D at 730 nm
Euphorbia neriifolia	2.000
Caralluma fimbricata	1.246

Estimation of Tannins

Standard conc.mg/ml	O.D of Standard Solution at 500nm
0.1	0.004
0.2	0.007
0.3	0.007
0.4	0.008
0.5	0.009
0.6	0.010
0.7	0.012
0.8	0.014
0.9	0.015
1.0	0.016

Sample	O.D at 500 nm
Euphorbia nerifolia.	0.129
Caralluma fimbricata	0.065

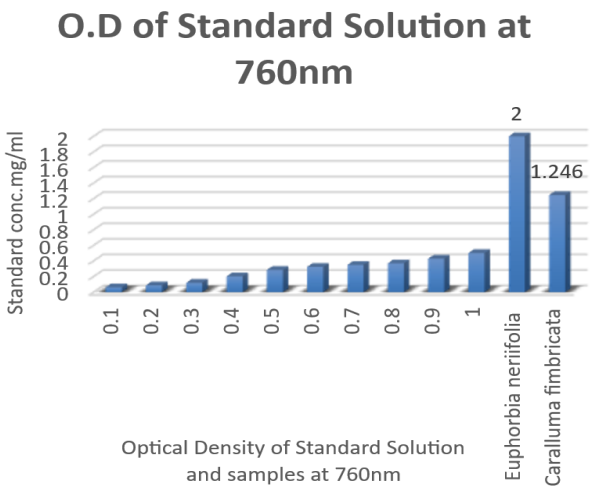

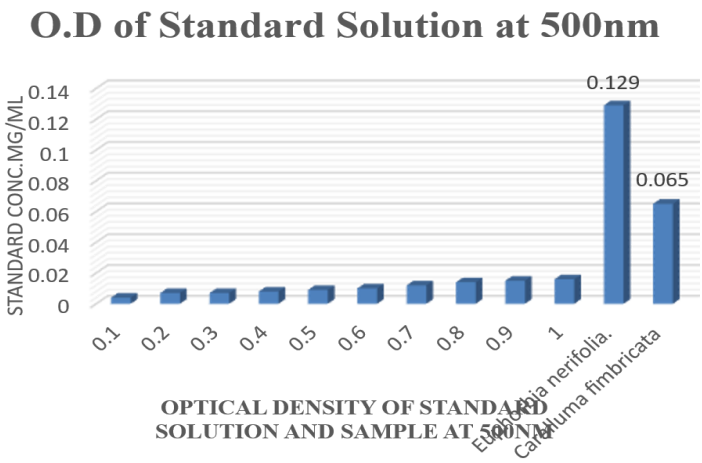

Estimation of Flavonoids

Standard conc.mg/ ml	O.D of Standard Solution at 500nm	O.D of Standard Solution at 500nm
0.1	0.763	0.085
0.2	0.830	0.131
0.3	1.011	0.262
0.4	1.613	0.404
0.5	2.000	0.462
0.6	2.000	0.487
0.7	2.001	0.613
0.8	2.020	0.768
0.9	2.030	0.909
1.0	2.035	1.135

Sample	O.D at430nm
Euphorbia neriifolia	**0.458**
Caralluma fimbricata	**0.210**

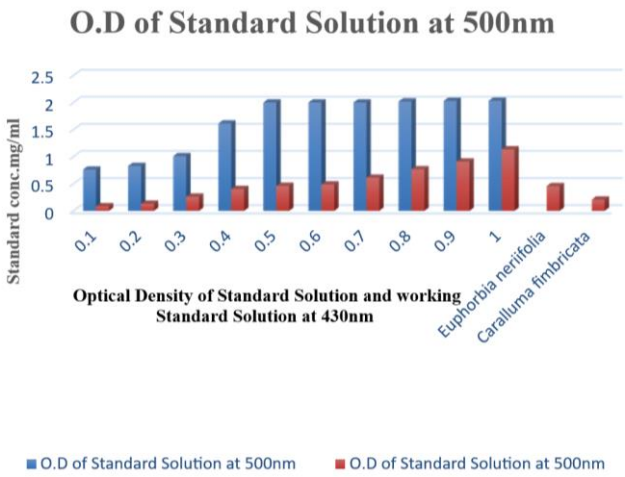

Phytochemical Analysis:

Preliminary screening of Caralluma fimbricata and Euphorbia neriifolia using phytochemicals analysis. Identified the main phytochemicals, which include phenols, flavonoids, and tannins. Phenolic compounds were present in both Euphorbia neriifolia and Caralluma fimbricata species to differing degrees. Of these fractions, Euphorbia neriifolia had the highest phenolic content, with an optical density at 760 nm that corresponded to 2.000 mg/mL of catechol equivalent, while Caralluma fimbricata had 1.246 mg/mL of catechol equivalent.

The tannin content of Euphorbia neriifolia L and Caralluma fimbricata species was evaluated spectrophotometrically at 500 nm and represented as tannic acid equivalents, with values of 0.129 and 0.065 mg/mL, respectively, using the Folin-Denis method. Phenols oxidise the Folin-Denis reagent, which is a combination of phosphotungstic and phosphomolybdic acids, to a blue tungsten oxide (Snell and Snell, 1937). Caralluma fimbricata had the lowest tannin concentration, whilst E. neriifolia had the highest.

The colorimetric method with aluminium chloride was used to quantify flavonoids. According to spectrophotometric measurements at 430 nm, E. neriifolia had a higher flavonoid content than Caralluma fimbricata, with a content of 0.458 mg/ml, or 100 mg of rutin, while Caralluma fimbricata had a lower flavonoid content of 0.210 mg/ml, or 100 mg of rutin.

Conclusion:

The findings showed that different concentrations of phenols, flavonoids, and tannins were found in the chosen species. Of all the phytochemicals assessed, Euphorbia neriifolia showed the highest amounts of all secondary metabolites. Future research should concentrate on a more thorough examination of secondary metabolites using cutting-edge methods like High-Resolution Liquid Chromatography-Mass Spectrometry (HR-LC-MS) and Gas Chromatography-Mass Spectrometry (GC-MS).

References:

1. Barthwal R, Mahar R (2024) Exploring the significance, extraction, and characterization of plant-derived secondary metabolites in complex mixtures. Metabolites 14: 119.
2. Malladi S, Ratnakaram VN, Babu S (2018) Pharmacological review of Caralluma r.br: A potential herbal genus. Asian J Pharm 4: S1146
3. Hasan, M.; Ganeshpurkar, A.; Bansal, D.; Dubey (2014) N. Protective effect of Euphorbia neriifolia extract on experimentally induced thrombosis in murine model. Niger. J. Exp. Clin. Biosci.,2, 86–89
4. Ram P. R. and Mehrotra B. N. (1993). Compendium of Indian Medicinal Plants, (Drug Research Preparative: A CDRI Series), VOL. 2, Central Drug Research Institute, Lucknow and Publications and Information Directorate, New Delhi, 453.
5. F.D.Snell and C. T. Snell, (1937). Colorimetric Methods of Analysis, vol. 2, D. Van Nostrand Company, New York, NY, USA.

International Journal of Advance and Applied Research
www.ijaar.co.in
ISSN – 2347-7075 Impact Factor – 8.141
Peer Reviewed Bi-Monthly
Vol. 7 No. 14 January – February - 2026

Impact of Pesticide Usage in Vegetables its Benefits and Risks

D. T. Tangade
Dept. of Zoology, Siddharth College Jafrabad Dist - Jalna.
Corresponding Author – D. T. Tangade
DOI - 10.5281/zenodo.19724406

Abstract:

Pesticide that may remain or in food after they are applied to food crops. The levels of these residues in foods are often stipulated by regulatory bodies in many countries .Exposure of the general population to these residues most commonly occurs through consumption of treated food sources .Many of these chemical residues, especially derivatives of chlorinated pesticide exhibit bioaccumulation which could build up to harmful levels in the body as well as in the environment. Persistent chemicals can be magnified through the food chain and have been detected in the food products. In 1970, DDT was banned for use in agriculture, but it remained a widespread and persistent environment contaminants. Vegetables constitute the vital constituents used in day to day diet and residual toxicity occurs due to over usage of pesticides, which causes health problems among many peoples.

Introduction:

Vegetable crops play a significant role as important source of food and income. Because of the wide adaptability of many existing vegetables, they can also fit into cropping systems .Furthermore, vegetables constitute a major source of income efforts in many small holders, especially near cities (Guan 1990). India has a wide variety of climate and soils on which a range of vegetables crops can be grown. During the last two decades considerable emphasis has been laid on production of these crops in our country, and vegetable have been stepped up (Chadha, 2000). In vegetable production, India is the largest producer nest to China with an annual production of 81 million to from 5.12 million ha of land, over the past few years we have realizing the counterproductive effects on health of pesticide use, such as pest resistant to form chemicals (Karanth et al., 1999). Vegetables constitute the vital constituents used in day-to-day diet and residual toxicity occurs due to over usage of pesticides. The need for more vegetables there became increasingly urgent due to the rapid population growth and the development of a food industry (Sikkhamondhol, 1977). The different kinds of pesticides entire in the market on large scale, and their adverse effects on human beings and environment are also increased. Majority vegetable samples violated and shows persistent nature of different pesticides, mishandling, environmental pollution and presence of pesticide residues (Sheikh et al., 2023).

Result & Discussion:

Indian tropical is generally favorable for the rapid buildup of pests, which often cause serious damage to vegetable crops. Pesticides are widely used the productivity of agricultural commodities and hence are essential component in modern agriculture. The USA, research and extension efforts in developing and implementing IPM on major crops have paid extremely good dividends in terms of crop and environmental protection (Adkisson,1986). Acute poising cases among sprayer groups of farmers in Indonesia

have also been reported increase, specifically for those involved in cultivation (Mustamin, 1988). Although accidental deaths from pesticide poisoning are rare, this does not imply that chronic hazards are non-existent or will continue to remain isolated. Today, highly potent chemicals such as methamidophos are freely used in many parts and the dangers involved given inadequate attention. Even some banned pesticides which have found their way into the vegetable farming areas and being used clandestinely. The directly intake of contaminants depends on both food habitat of the exposed population and concentration in foods. The factors which influenced the concentration of the food are food processing, preparations, seasonal changes, geographical location etc hence, dietary intake has identified as the main route of human exposer to these toxic residues of pesticides. The use of chemicals in modern has significantly increased productivity. But it has also significantly increased the concentration of pesticides in food and in our environment, with associated negative effects on human health. Annually there are dozens of million cases of pesticide poisonings worldwide (Richter,2022). Risk assessment practices also play a role in pesticides regulation. Their is a lot of evidence for instance that a significant portion of food samples still exceeds the maximum residue limits set by regulattors.Finally ,risk perceptions may also influence pesticide regulation.Indeed ,there is evidence that people underestimate the risks from natural carcinogens but that they never the less overestimate the risks from carcinogenic pesticides (Slovic2022).The aim of this study is to contribute to the understanding of the health effects of pesticides exposure.

Conclusion:

In conclusion, our health literature review showed that most research focused on individuals with direct exposure to pesticide, e. g. farmers. Since research on people with indirect exposure was harder to find, and since most individuals belong to this group, more research should be conducted analyzing the potential effects of pesticides on consumers. Some suggestions to the consumers for reducing their potential exposures to toxic chemical contaminants. a) Grow your own vegetables b) Organic vegetables should be purchased c) The vegetables should be wasted properly to remove chemicals d) Avoid vegetables with high fat content, and e) Remove peels of vegetables.

Reference:

1. Chadha K. L., (2000), “Pre- and Post-harvest technology of fruits and vegetables. In: National Workshop on Opportunities and Challenges in Fruit and Vegetable Processing Industry, CFTRI, Mysore, India”
2. Henrik Andersson (2014), “Pesticides and health: A review of evidence on health effects, valuation of risky, and benefit-cost analysis,” Advances in Health Economics and Health Services Research, France.
3. Mustamin M. (1988), “Health hazards due to the use of pesticides in Indonesi: data collection and surveys,” pp. 301-310. In P.S. Teng and K.L. Heong (eds). Pesticide management and integrated Pest Management in South Asia. CICP, Maryland.
4. NAS, (1987), “Regulating pesticides in food.” Washington DC, National Academy of Sciences.
5. Pandit G. and Sahu S (2022), “Assessment of risk to public health posed by persistent organochlorine pesticide residues in milk and milk productsin Mumbai, India.” Journal of Environmental Monitoring, vol. 4(1), 43-48.

6. Richter, E. D.: 2022, "Acute human pesticide poisoning." Encyclopedia of pest management pp. 3-6.
7. Sharma R.K., Dhyani P.P. and Samant S. S, (2010)," Toxic chemicals in fruits and vegetables: An overview," Everyman s Science, Vol. XLV No. 4.
8. Slovic, P.: 2022, "The Perception of Risk." Earthscam Publisher.
9. Sheikh S. A., Nizamani S. M., Panhwar A.A. and Miirani B.N. (2023), "Monitoring of pesticide residues in vegetables collected from markets of Sindh, Pakistan," J. Food Science & Technology Letters, vol. 4(1): 11-45.

International Journal of Advance and Applied Research
www.ijaar.co.in
ISSN – 2347-7075 Impact Factor – 8.141
Peer Reviewed Bi-Monthly
Vol. 7 No. 14 January – February - 2026

Studies on Medicinal Plants Using Local Medicine

Dr. Ravikiran J. Sawant[1] & Kanchan L. Kannamwar[2]

[1]*Department of Botany, Vinayakrao Patil Mahavidyalaya Vaijapur Tal. Vaijapur District Chhatrapati Sambhaji Nagar*

[2]*Research Student, Department of Botany, Deogiri College Chhatrapati Sambhaji Nagar*

Corresponding Author – Dr. Ravikiran J. Sawant

DOI - 10.5281/zenodo.19724464

Abstract:

Medicinal plants have been an integral part of local and traditional medicine systems since ancient times. Indigenous communities across the world possess valuable knowledge regarding the therapeutic use of plants for treating various ailments. This study focuses on the documentation and analysis of medicinal plants used in local medicine practices. Information was collected through field surveys, interviews with traditional healers, and review of ethnobotanical literature. The study highlights commonly used medicinal plants, their local names, parts used, and medicinal applications. The findings emphasize the importance of conserving traditional knowledge and medicinal plant biodiversity, as well as their potential role in modern healthcare and drug development.

Keywords: Medicinal Plants, Local Medicine, Traditional Knowledge, Ethnobotany, Herbal Remedies.

Introduction:

Medicinal plants play a significant role in primary healthcare, especially in rural and tribal regions where access to modern medical facilities is limited. Local medicine systems, such as Ayurveda, folk medicine, and tribal healing practices, rely heavily on plant-based remedies. These systems have evolved through centuries of observation, experimentation, and experience.

India is one of the richest countries in medicinal plant diversity and traditional knowledge. Local healers use different plant parts such as leaves, roots, bark, seeds, and flowers to treat diseases like fever, cough, skin infections, digestive disorders, and inflammation. However, rapid urbanization, habitat loss, and lack of documentation threaten this valuable knowledge.

Therefore, systematic studies on medicinal plants used in local medicine are essential for preservation, scientific validation, and sustainable utilization.

Method:

The study was conducted using the methods:

Field Survey: Surveys were carried out in selected rural areas to identify medicinal plants used in local medicine.

Interviews and Questionnaires: Information was collected through personal interviews with local healers, elderly villagers, and herbal practitioners regarding plant usage, preparation methods, and dosage.

Plant Identification: Collected plant specimens were identified using standard floras and botanical keys.

Literature Review:

Relevant ethnobotanical books, research articles, and journals were reviewed to support and compare the collected data.

Data Analysis:

The medicinal plants were categorized based on their families, parts used, and therapeutic applications.

Results:

The study documented several medicinal plants commonly used in local medicine. Plants such as Azadirachta indica (Neem), Ocimum sanctum (Tulsi), Curcuma longa (Turmeric), Aloe vera, and Tinospora cordifolia (Giloy) were frequently reported.

Leaves were the most commonly used plant part, followed by roots and bark.

Most remedies were prepared in the form of decoctions, pastes, powders, or juices.

The majority of treatments were related to common ailments such as fever, cold, wounds, digestive problems, and skin diseases. The findings indicate that local medicine is affordable, accessible, and culturally accepted by the community.

Sr No	Field No	Observation1	Observation2	Observation3	Observation4	Observation5
1	B1	30	15	20	15	16
2	B2	22	12	40	23	05
3	B3	11	22	02	07	10
4	B4	21	22	28	09	20
5	B5	11	20	11	16	14

Table 1: **Case study During the field response to persons for local** medicines

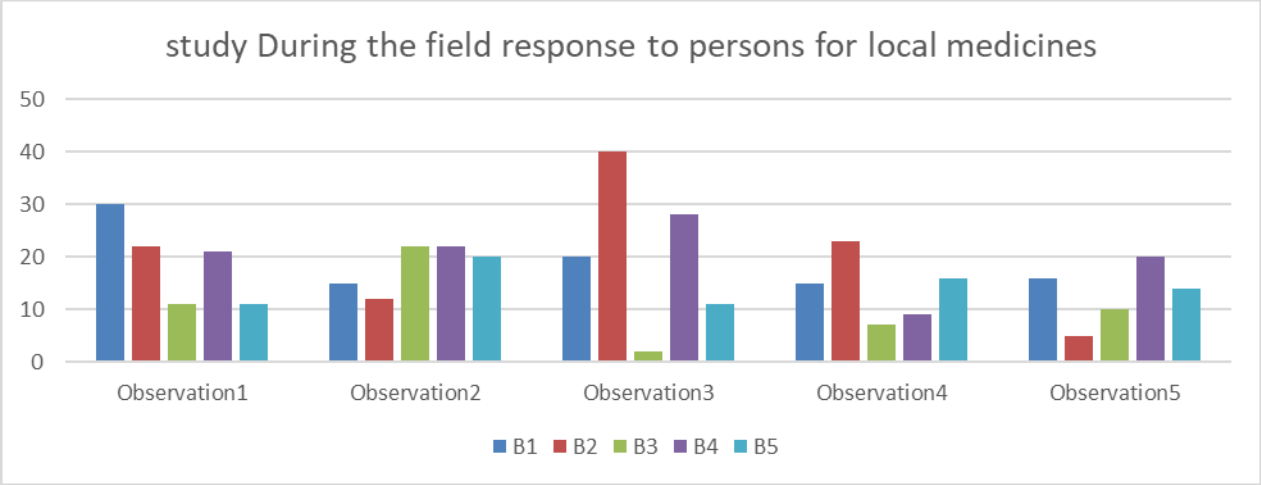

Conclusion:

The study reveals that local medicine systems are rich sources of medicinal plant knowledge and play a crucial role in healthcare at the community level. Documentation of this traditional knowledge is essential before it disappears. Medicinal plants used in local medicine have significant potential for pharmacological research and development of new drugs. Conservation of medicinal plants and promotion of sustainable harvesting practices are necessary to ensure their availability for future generations.

Acknowledgement:

We are thankful to both colleges Principals and my colleagues those who are supporting about the research and my research students also degree level students providing such a good support.

References:

1. Kirtikar, K.R. and Basu, B.D. (2005). Indian Medicinal Plants. Dehradun: International Book Distributors.
2. Jain, S.K. (1991). Dictionary of Indian Folk Medicine and Ethnobotany. New Delhi: Deep Publications.
3. WHO (2013). Traditional Medicine Strategy 2014–2023. World Health Organization, Geneva.
4. Chopra, R.N., Nayar, S.L., and Chopra, I.C. (1956). Glossary of Indian Medicinal Plants. CSIR, New Delhi.
5. Cotton, C.M. (1996). Ethnobotany: Principles and Applications. John Wiley & Sons.

International Journal of Advance and Applied Research
www.ijaar.co.in
ISSN – 2347-7075 Impact Factor – 8.141
Peer Reviewed Bi-Monthly
Vol. 7 No. 14 January – February - 2026

Phytochemical screening of Moringa oleifera Lam. leaves from the area of Kaij of Beed District of Maharashtra, India

Dr. B. J. Hirve
Dept. of Botany, Baburaoji Adaskar Mahavidyalaya Kaij Dist. Beed. M.S.
Corresponding Author – Dr. B. J. Hirve
DOI - 10.5281/zenodo.19724497

Abstract:

Moringa oleifera has numorus benefits like nutritional as well as medicinal advantages. It contains essential amino acids, carotenoids in leaves, and nutritional supplements in cooking aspects.
Leaves, and pods or drum sticks are having nutritional and medicinal properties. It has antioxidants, antibiotics and nutrients including vitamins and minerals. Now a days, leaves powder is used in various drinks for healthy life. In this paper, more emphasis is on it's medicinal properties and phytochemical screening.

Introduction:

This single Genus Moringa belongs to family Marantaceae, Order Brassicales and species oleifera. It is small natie tree of the sub-Himalayan regions of North west India which is now indigenous to many regions in Africa, Arabia, South East Asia, Pacific and Caribbean Islands and South America.

In Maharashtra, traditionally drum sticks are used in raceipi. It is also called as the miracle tree due to its healing abilities for some chronic diseases.

Medicinal uses of Moringa has been used to cure skin infections, anaemia, anxiety, asthma, blackheads, blood impurities, bronchitis, chest congestion, cholera. It is anti-inflammatory, antispasmodic, anti-hypertensive, antitumour, anti-oxidants, anti-pyretic, anti-ulcer, diuretic, lowering cholesterol, renal and anti-diabetic.

Utilization of Moringa Pods and Leaves:

Moringa was found to contain many issential nutrients, vitamens, minerals, amino acids. It's leaves consist of vitamens C, calcium, beta carotene, potassium and protein. It works as an effective source of natural antioxidants. Moringa is having capacity to increase the period of food containing fats due to presence of flavanoids, ascorbic acid, carotenoids and phenolics.

Anti-inflammatory:

It is used in healing and huge amount of acute and chronic conditions.

In vitro and Vivo conditions it is recommended it's effectiveness in treating inflammation.

Anti-diabetic:

Diabetes Mellitus is a chronic metabolic disorder. Diabetic patients exhibit a stage of chronic hyperglycemia and glucose toleranceI. It is also used for traditional treatment of diabetes. The nutritional and fatty acid profiles of the Moringa has highest anti-oxidant activity.

Material and Methods:

For this, leaves from Moringa leaves were collected from Kaij City area and nearby places. The collected leaves washed in water and allow to

dry for 5 to 6 days. After suitable drying of leaves, powder was prepared by grinding machine.

Extract Preparation:

1. Aqueous extract:

   3 gm leaves powder + 30ml distilled water +15ml Methanol

2. Acetone extract:

   3 gm leaves powder + 30 ml of Acetone

3. Chloroform extract:

   3 gm of Moringa leaf powder + 30ml chloroform

Each extract was incubated for overnight and filtered by using Whatman No.1 filter paper in to flask. Filterates were collected by placing the flask in to water bath at 100 degree celcius. The resulting filterate were allowed to cool to room temperature. Then qualitative tests were performed and phytochemicals were investigated by analysing different methods. These process following the rules of Evans 1997, Wagner 1993.

1.*Test for Alkaloids*:

***Mayers Test*:**

2ml of each extract was mixed with 2.3 drops of Mayers reagent (1.36 gm mercuric iodide in 60 ml of water mix properly with 5 gm of Potassium iodide in 20ml of water) A white or creamy precipitate confirmed the test as positive.

***Wagner's Test*:**

2 ml of each extract was mixed with 0.2 ml diluted HCl solution. Then 1 ml of Wagner's reagent was added. (1.27 g of Iodine and 2g potassium iodide along with 100ml distilled water.)

There was reddish brown precipitate that indicated the positive test.

Table Showing Phytochemical Screening

Phytochemicals	Name of Test	Aqueous extract	Aqueous Methanol extract	Acetone extract	Chloroform extract
Alkaloids	Mayers test	++	+	-	-
	Wagner's Test	++	+	-	-
Tannins	Feric Chloride Test	++	+	-	-
Saponins	Foam Test	+	+	-	++
Flavonoids	Lead acetate Test	+	+	-	-
Glycosides	Keller Killani Test	-	-	-	++

Flavonoids acts as an antioxidants and enhances the effect of Vitamin C. They are also known for their biological activity against liver toxins, carcinogens, viruses, and other microbes.

According to many researches, flavonoids basically acts as bacteria by inhibiting it's protein synthesis and also posses antimicrobial, and anti allergic and anti inflammatory properties. They are active in reducing high blood pressure.

Flavonoids is suggested as health promoting phytochemical for animal production because they are known for improving gut health.

2.*Test for Tannins:*

Feric Chloride Test:

2 ml of each extract mixed with few drops of 5 percent ferric chloride solution. Formation of blue colour indicated the presence of tannins.

3.*Test for Saponins:*

Foam Test:

5 ml of each extract shaken vigorously with 5 ml of distilled water in a test tube and warmed. Formation of stable foam indicated the test as positive.

4.*Test for Flavonoids:*

Lead acetic acid Test:

1 ml of each extract mixed with 1 ml of 10 percent lead acetate solution. Formation of yellow precipitate indicates the presence of flavanoids.

5.*Test for Glycosides:*

Keller -Killiani Test:

2 ml of each extract was dissolved in glacial acetic acid and 5% ferric chloride solution were added. The contents were heated and cooled, then transfered to a test tube containing 2 ml of concentrated sulphuric acid. Pale green colour appear in the upper layer indicates the presence of glycoside.

Result and Discussion:

In this findings the presence of different biochemical constituents in moringa leaves extracts such as alkaloids, saponins, flavonoids and glycosides. Aqueous and aqueous methanol extract contained alkaloids, Tannins, saponins. Flavonoids and glycosides were as chloroform extracts contain glycosides. How your acetone extracts didn't contain any type of phytochemical phytochemical compounds. Saponims are used as an adjuvant in the production of vaccines. So due to presence of saponins the leaves of moringa acts as soap. This saponins have antioxidant properties anti-inflammatory and immuno stimulant properties.

Moringa leaves have alkaloids which are nitrogen containing naturally occurring compound which are having anti microbial properties. Due to this medicinal properties this leaves are used in the treatment of many diseases like malaria,cold, cough hypertension, diabetes and cancer.

Conclusion:

This photochemical screening helps in possible preventive and curative properties of moringa lives. But there is need to carry out more qualitative and quantitative pharmacological analysis of moringa leaves to prove the use of moringa as important medicine plant. There is more emphasis for screening of phytochemicals for various treatments of human diseases in rural areas of Kaij . There is more need to develop Ayush health centres for the treatment of diseases regarding medicinal plants like moringa. our government should take more steps for the development of rural people by using these medicinal plants. Government should carried out programs like plantation of only medicinal plants in this area.

References:

1. Aher R.K., B.K. Auti, R.N.Deshmukh,G.B. Borkar, S.K.Aher and S.L.Khapke (2004), Survey of medicinal plants from areas of Ahmad Nagar District.(83-86)
2. Dineshkumar Tyagi, Pharmaforestry, Atlantic Publication New Delhi, 2005; 19-34
3. Gaikwad S.P., R.D.Gore and K.U. Garad (2021), Additions to the flora of Marathwada region of Maharashtra, India, Journal of Threatened Taxa 4(4):2515-2523.
4. Naik V.N.(1998) Flora of Marathwada Aurangabad, Amrut Prakashan,Vol I, II pp 603-1182
5. Pro. Dr. N. Raman, Phytochemical Techniques, New India Publishing Agency,New Delhi.
6. Dr. Anikit Kumar Saini,Text book of Pharmacognosy and phytochemistry, Vo.I, Shashawat Publication, India.

International Journal of Advance and Applied Research
www.ijaar.co.in
ISSN – 2347-7075 Impact Factor – 8.141
Peer Reviewed Bi-Monthly
Vol. 7 No. 14 January – February - 2026

Climate-Smart Agriculture (CSA): Role of Mulching in Vegetable Crops from Nashik District, (M.S) India

Dr. Sachin B. Jadhav
Assistant Professor,
MVP Samaja's K.K.W. Arts, Science and Commerce College, Pimpalgaon (B)
Tal-Niphad, Dist-Nashik (M.S.)
Corresponding Author – Dr. Sachin B. Jadhav

DOI - 10.5281/zenodo.19724558

Abstract:

Climate-smart agriculture (CSA) aims to enhance agricultural productivity, strengthen resilience to climate variability, and reduce greenhouse gas emissions. Vegetable crops are particularly vulnerable to climate change due to their high water demand and sensitivity to temperature extremes. Mulching has emerged as an effective CSA practice for vegetable production by improving the soil microclimate and resource-use efficiency.

This research presents findings on the role of mulching in vegetable crops within the CSA framework, focusing on climate change adaptation and mitigation benefits. Nashik is a large vegetable producing district where mulching is practiced in various vegetable crops like tomato, brinjal, capsicum, cucumber, and cabbage. Organic mulches (crop residues, straw, compost) and inorganic mulches (plastic films) significantly reduce soil moisture loss, moderate soil temperature fluctuations, suppress weeds, and improve soil health.

Evidence indicates that mulching enhances water-use efficiency by 25-40%, stabilizes vegetable yields under drought and heat stress, and contributes to soil organic carbon sequestration. While plastic mulches promote early crop establishment and higher short-term yields, organic mulches provide long-term benefits through improved soil structure and reduced greenhouse gas emissions. Overall, mulching represents a low-cost, scalable, and climate-resilient practice that supports the core objectives of CSA in vegetable-based cropping systems.

Keywords: Climate-Smart Agriculture, Mulching, Vegetable Crops, Soil Moisture, Water Use Efficiency, Sustainable Agriculture, Nashik District

Introduction:

Climate-Smart Agriculture (CSA) is an integrative approach essential for addressing food security under climate variability. The concept, defined by the Food and Agriculture Organization (FAO), aims to achieve three intertwined objectives: (1) sustainably increasing productivity and incomes, (2) adapting and building resilience to climate change, and (3) reducing and/or removing greenhouse gas emissions where possible.

Nashik District, Maharashtra, is a premier vegetable-producing region in India, contributing significantly to the state's supply of tomato, onion, cucumber, cabbage, and leafy greens. However, the region faces significant challenges from erratic rainfall, rising temperatures, and soil degradation. The district experiences a semi-arid climate with an average annual rainfall of 600-700 mm, predominantly from the southwest monsoon, which has become increasingly erratic due to climate change.

This research investigates the role of mulching as a core CSA practice in vegetable production systems of Nashik. Through a synthesis of field studies, farmer surveys, and agrometeorological data, we assess the impacts of organic (sugarcane trash, paddy straw) and synthetic (polyethylene) mulches on soil health, water use efficiency (WUE), microclimate moderation, crop yield, and economic viability.

1. Climate-Smart Agriculture (CSA):

Climate-Smart Agriculture represents a paradigm shift in agricultural development, addressing the complex challenges of food security and climate change simultaneously. The approach is built on three pillars that guide agricultural transformation:

1 **Productivity**: Sustainably increasing agricultural productivity and incomes to meet growing food demand
2 **Adaptation**: Building resilience to climate change impacts through improved resource management and risk reduction
3 **Mitigation**: Reducing and/or removing greenhouse gas emissions from agricultural practices where possible

2. Mulching as a CSA Practice:

Mulching, the practice of covering the soil surface around plants with organic or synthetic materials, directly addresses all three CSA pillars. The practice provides multiple benefits that contribute to climate resilience in vegetable production systems.

Adaptation Benefits: Conserving soil moisture, moderating soil temperature, suppressing weeds, and preventing erosion.

Productivity Benefits: Enhancing nutrient availability, improving root environment, and boosting crop yields.

Literature Review:

CSA promotes sustainable intensification, adaptation, and mitigation in agriculture. Research indicates that mulching can significantly improve water use efficiency, reduce soil erosion, and enhance crop productivity (Jat et al., 2019; FAO, 2017). In semi-arid regions like Nashik, where vegetables such as onions, tomatoes, and cucurbits are widely cultivated, mulching has been shown to reduce evapotranspiration and suppress weeds, leading to improved yields (Patil et al., 2020).

Previous studies in the Nashik region have demonstrated the effectiveness of mulching practices. Jadhav et al. (2020) reported significant improvements in chili yield and quality under mulched conditions. Mali et al. (2021) documented long-term effects of mulching on soil properties and tomato productivity in semi-arid Maharashtra, showing sustained benefits over multiple growing seasons.

Kader et al. (2017) reviewed recent advances in mulching materials and methods for modifying soil environment, highlighting the importance of context-specific mulch selection. Sarkar et al. (2020) demonstrated the combined effects of mulching and drip irrigation on yield, water-use efficiency, and economics of tomato in semi-arid regions of India.

Objectives: The primary objectives of this research were:

Objective 1: To evaluate the biophysical effects of different mulches (organic and plastic) on soil parameters including moisture content, temperature, and infiltration rate.

Objective 2: To quantify the impact of mulching on crop yield and water use efficiency in major vegetable crops of Nashik district.

Objective 3: To assess the economic viability and farmer adoption potential of mulching practices in the local context.

Materials and Methods:

1. Experimental Design and Data Collection:

The research was conducted through a combination of on-station and on-farm trials comparing three treatments:

Treatment	Mulch Type	Description
T1 (Control)	No Mulch	Unmulched control plot with conventional practices
T2	Organic Mulch	5-7 cm layer of sugarcane trash/paddy straw
T3	Plastic Mulch	Black Polyethylene Mulch (25-30 micron thickness)

Table 1: Experimental Treatments

Crops Studied: Tomato (*Solanum lycopersicum*), Cucumber (*Cucumis sativus*), and Cabbage (*Brassica oleracea*)

Parameters Measured: Soil moisture content (gravimetric method), temperature at 5 cm and 15 cm depth, infiltration rate using Single-Ring Infiltrometer, plant growth parameters, and yield (t/ha).

The infiltration rate was calculated using the formula: Infiltration Rate (cm/hr) = Depth of water absorbed (cm) / Time (hours)

2. Study Area:

The study was conducted in Nashik District, Maharashtra, India (19°33' N, 73°47' E). Focus areas included Niphad, Dindori, Nashik, and Satana blocks, representing major vegetable cultivation zones. The region experiences a semi-arid climate with an average annual rainfall of 600-700 mm, predominantly from the southwest monsoon.

Results and Discussion:

1. Impact on Soil Physical Environment:

The application of mulching materials showed significant effects on various soil physical parameters. The results demonstrate clear differences between organic mulch, plastic mulch, and unmulched control treatments.

Soil Parameter	Control	Organic Mulch	Plastic Mulch
Soil moisture increase (%)	0	25-30 (28)	35-40 (38)
Soil temperature change (°C)	0	-2 to -4 (-3)	+1 to +2 (+1.5)
Infiltration rate increase (%)	0	~20	~5
Weed suppression (%)	0	60-70	~80

Table 2: Effect of Mulching on Soil Physical Parameters

Soil Moisture: Both mulches significantly conserved soil moisture. Organic mulch retained 25-30% higher soil moisture than control, while plastic mulch retained 35-40% higher moisture in the top 15 cm layer. This is attributed to reduced direct evaporation and lower soil temperatures under mulched conditions.

Soil Temperature: During peak summer (April-May), plastic mulch raised soil temperature by 1-2°C in the root zone, beneficial for early growth in winter crops. Conversely, organic mulch buffered temperature, keeping soil 2-4°C cooler than the control, protecting roots from heat stress. This moderating effect is a critical climate adaptation benefit.

Figure 1: Illustrates the comparative effects of different mulching treatments on soil moisture retention:

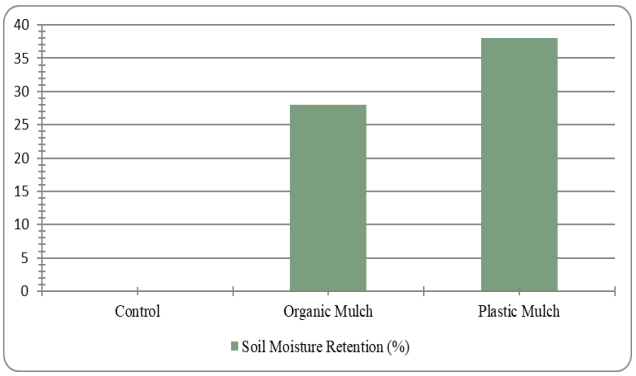

Figure 1: Soil Moisture Retention by Mulch Type

Soil Structure and Erosion: Organic mulch improved aggregate stability, reduced surface crusting, and increased infiltration rates by approximately 20%. It also effectively prevented soil splash and erosion during high-intensity rains.

2. Impact on Soil Biology and Fertility:

The research revealed significant improvements in soil biological parameters under mulched conditions. Microbial activity was enhanced under organic mulch, with increased earthworm population and microbial biomass leading to improved nutrient cycling. The decomposition of organic mulch materials contributed to soil organic carbon buildup over time.

3. Agronomic and Yield Benefits:

Mulching treatments showed significant positive effects on crop performance and yield across all studied vegetable crops.

Crop	Control Yield (t/ha)	Organic Mulch (%)	Plastic Mulch (%)
Tomato	35.5	+22%	+28%
Cucumber	28.2	+18%	+32%
Cabbage	42.0	+15%	+25%

Table 3: Crop Yield Improvement with Mulching (% increase over control)

Figure 2 presents the yield improvement across different crops and mulch types:

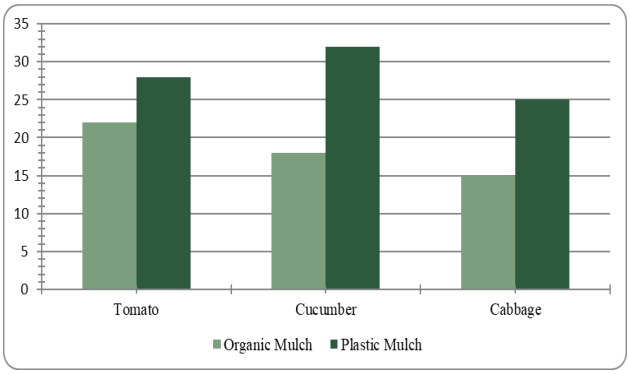

Figure 2: Crop Yield Improvement by Mulch Type

Weed Suppression: Plastic mulch provided approximately 80% weed suppression, while organic mulch provided 60-70% suppression. This significantly reduced labor demand for weeding and minimized herbicide use, contributing to both economic savings and environmental benefits.

Water Use Efficiency: Mulching improved water use efficiency by 25-40%, allowing farmers to achieve higher yields with the same or reduced water inputs. This is particularly valuable in water-scarce regions like Nashik district.

Figure 3 shows the relative distribution of benefits from mulching practices as reported by farmers:

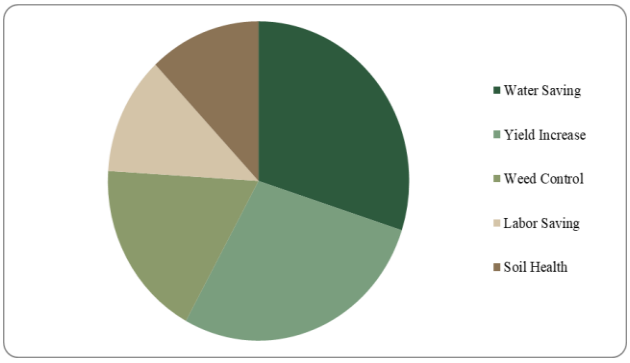

Figure 3: Distribution of Mulching Benefits (Farmer Perception)

Discussion:

This study confirms that mulching is a potent CSA practice for Nashik's vegetable production systems. The findings align with previous research demonstrating the multi-faceted benefits of mulching in semi-arid agricultural environments.

The significant improvement in soil moisture retention (25-40%) under mulched conditions addresses one of the primary challenges facing vegetable producers in the region - water scarcity. With increasingly erratic rainfall patterns due to climate change, this moisture conservation capacity becomes even more critical for maintaining stable production.

Temperature moderation by organic mulches provides an important adaptation mechanism against heat stress, which is becoming more frequent in the region. The 2-4°C cooling effect can mean the difference between crop failure and successful harvest during extreme heat events.

The yield improvements of 15-32% across different crops demonstrate the productivity benefits of mulching, directly contributing to the CSA productivity pillar. These yield gains, combined with reduced input costs (water, labor for weeding), improve the economic viability of vegetable farming in the region.

However, challenges remain in widespread adoption. These include the initial cost of plastic mulch (though offset by yield gains), availability of organic mulch materials at scale, and the need for proper disposal of plastic mulch to prevent environmental contamination. Context-specific recommendations should consider these factors when promoting mulching practices.

Conclusion:

Mulching is a low-tech, high-impact CSA intervention well-suited for the vegetable-based farming systems of Nashik District. The research demonstrates that both organic and plastic mulches provide significant benefits across all three CSA pillars:

Productivity: Yield improvements of 15-32% across tomato, cucumber, and cabbage crops

Adaptation: Enhanced water use efficiency (25-40%), temperature moderation, and improved resilience to climate variability

Mitigation: Reduced greenhouse gas emissions through improved soil carbon sequestration (organic mulch) and reduced fuel use for irrigation and weeding

The study concludes that context-specific mulching strategies, integrated with complementary CSA practices like drip irrigation, are pivotal for building climate resilience in Nashik's vegetable sector. Policy support for mulch material availability, training programs for farmers, and research on biodegradable alternatives to plastic mulch can further enhance adoption and sustainability.

References:

1. FAO. (2013). Climate-Smart Agriculture Sourcebook. Rome: Food and Agriculture Organization of the United Nations.
2. IPCC. (2019). Climate Change and Land: an IPCC special report on climate change, desertification, land degradation, sustainable land management, food security, and greenhouse gas fluxes in terrestrial ecosystems.
3. Jadhav, S. B., et al. (2020). Effect of mulching on yield, quality and economics of chili under Nashik conditions. Journal of Soils and Crops, 30(2), 245-250.
4. Jat, R. S., et al. (2019). Soil moisture conservation strategies for enhancing climate resilience in vegetable production. Indian Journal of Agricultural Sciences, 89(9), 1405-1412.

5. Kader, M. A., et al. (2017). Recent advances in mulching materials and methods for modifying soil environment. Soil & Tillage Research, 168, 155-166.
6. Kamble, R. R., et al. (2018). Climate variability and its impact on horticulture in Nashik district. Mausam, 69(4), 641-650.
7. Maharashtra Agriculture Department. (2021). District-wise Horticulture Statistics, Nashik.
8. Mali, S. S., et al. (2021). Long-term effects of mulching on soil properties and tomato productivity in semi-arid Maharashtra. Indian Journal of Agricultural Research, 55(3), 309-315.
9. Nashik District Horticulture Department. (2021). Annual Report on Vegetable Production Technologies.
10. NINASC (ICAR-National Institute of Abiotic Stress Management). (2020). Annual Report on Climate Resilience in Horticulture. Malegaon, Maharashtra.
11. Patel, H. R., et al. (2019). Adaptation strategies for vegetable crops under climate change scenarios in Gujarat. Journal of Agrometeorology, 21(Special Issue), 98-104.
12. Patil, S. V., et al. (2020). Effect of mulching on growth, yield and quality of vegetable crops. International Journal of Chemical Studies, 8(2), 1234-1239.
13. Sarkar, S., et al. (2020). Mulching and drip irrigation effects on yield, water-use efficiency and economics of tomato in a semi-arid region of India. Journal of Agricultural Science, 158(1-2), 25-34.
14. Shinde, P. P., et al. (2021). Microclimate modification through mulching in tomato under Nashik conditions. International Journal of Current Microbiology and Applied Sciences, 10(2), 1893-1901.
15. Singh, A. K., et al. (2022). Water dynamics under different mulching systems in drip-irrigated vegetables. Agricultural Water Management, 259, 10723

International Journal of Advance and Applied Research
www.ijaar.co.in
ISSN – 2347-7075 Impact Factor – 8.141
Peer Reviewed Bi-Monthly
Vol. 7 No. 14 January – February - 2026

Taxonomic Evaluation of Two Coprinoid Fungi of the Genus Coprinopsis in Jalna District, Maharashtra (India)

Ganesh P. Musale[1] & Rajendra B. Kakde[2]

[1]*Botany Research Centre, J.E.S. College, Jalna (Maharashtra), India-431203*

[2]*Department of Botany, Swami Vivekanand Senior College, Mantha, Jalna, Maharashtra, 431504*

Corresponding Author – Ganesh P. Musale

DOI - 10.5281/zenodo.19724574

Abstract:

This study presents the morphological and taxonomic characterization of two coprinoid fungi Coprinopsis radiata var. macrocarpa and Coprinopsis macrocephala—collected from Jalna district, Maharashtra, India, during the August 2024 monsoon season. Macroscopic features, including pileus morphology, lamellae, stipe characters, and habitat, were recorded from fresh basidiocarps, while microscopic studies examined basidiospores, basidia, cystidia, and pileipellis structure using standard techniques. Coprinopsis radiata *var.* macrocarpa *was distinguished by larger basidiocarps, a radially fibrillose pileus, and dark brown spores with a prominent germ pore. In contrast,* C. macrocephala *exhibited a conical pileus, veil remnants, and thick-walled basidiospores. Both species showed deliquescent lamellae and saprotrophic growth on nutrient-rich substrates. The study provides baseline taxonomic data contributing to the documentation of coprinoid fungal diversity in the semi-arid region of Maharashtra.*

Keywords: Coprinopsis radiata var. macrocarpa; Coprinopsis macrocephala; Coprinoid fungi; Morpho-taxonomy; Basidiomycota; Agaricales.

Introduction:

Fungi are among the most diverse and ecologically essential groups of Eukaryota organisms, playing vital roles in decomposition, nutrient cycling, and ecosystem stability (Atri, 2015; Upadhyay, 2018). Within Basidiomycota, the order Agaricales includes a wide variety of gilled mushrooms with notable morphological diversity and ecological adaptability. Coprinoid fungi, historically classified under Coprinus sensu lato, are notable for their autodigesting (deliquescent) gills and short-lived basidiocarps (Redhead et al., 2001; Moncalvo et al., 2002). Molecular phylogenetics have led to their division into genera such as Coprinopsis, Coprinellus, and Parasola, redefining their classification within Psathyrellaceae (Hopple & Vilgalys, 1999; Redhead et al., 2001). The genus Coprinopsis is recognized as a monophyletic group characterized by thin basidiocarps, striate or fibrillose cap surfaces, deliquescent gills, dark brown to black basidiospores with a germ pore, and various veil structures (Kirk et al., 2008; Singer, 1986). These species are mainly saprotrophic, commonly found on dung, compost, decaying plant material, and nutrient-rich soils, playing an important role in breaking down lignocellulosic matter and recycling organic material, especially in agro-ecosystems (Atri, 2015; Kaur & Atri, 2017). Accurate morphotaxonomic identification remains crucial for species delimitation, particularly in areas with limited molecular data (Amandeep et al., 2015; Upadhyay, 2018). Important taxa include Coprinopsis radiata var. macrocarpa Atri, A. Kaur & M. Kaur and Coprinopsis macrocephala (Berk.) Redhead,

Vilgalys & Moncalvo. C. radiata var. macrocarpa was identified based on its larger basidiocarps and unique micromorphological features, such as spore size and pileus structure (Atri, Kaur & Kaur, 2012). C. macrocephala, initially classified under Coprinus, was reassigned to Coprinopsis after thorough morphological review and molecular phylogenetics clarified its position (Redhead et al., 2001; Moncalvo et al., 2002). While coprinoid fungi have been reported from parts of India like Punjab and the Western Ghats, detailed studies on semi-arid ecosystems are scarce (Atri, 2015; Amandeep et al., 2015). The Jalna district in Maharashtra, with its monsoonal climate and agricultural landscapes, offers conducive substrates for coprinoid fungi; however, documentation of Coprinopsis species here is limited (Upadhyay, 2018). Hence, this study aims to provide detailed morphological and taxonomic descriptions of Coprinopsis radiata var. macrocarpa and Coprinopsis macrocephala from Jalna. This work adds valuable taxonomic data to regional fungal biodiversity records and supports future ecological and systematic research on coprinoid fungi in Maharashtra.

Material and Methods:

Collection:

Samples of *Coprinopsis radiata var. macrocarpa* and *Coprinopsis macrocephala* were collected in August 2024 from Mantha tahsil in Jalna district, Maharashtra. The locality's GPS coordinates are Lat 19.3857° and Long 76.2313°. During collection, habitat, date, and vegetation type were recorded. To confirm the species' identity, a detailed study of macroscopic and microscopic features was conducted, including descriptions of the pileus (diameter, shape, and colour), cuticle (general and marginal features), lamellae, and stipe (position, shape, length, thickness, and colours).

Taxonomic examination:

The specimens were examined in detail for various macroscopic features, including shape, size, colour, gill type, and margin. Microscopic analysis focused on the hyphal system, basidia, and basidiospores. Morphological traits were compared with standard taxonomic references (Mirdu et al., 2023). Anatomical features, such as hyphae, basidia, and basidiospores and their arrangements, were studied using crush mounts and hand-cut sections. Samples were stained with Congo red, cotton blue, and Melzer's reagent. Photomicrographs of gills, mycelium, and spores were taken, and measurements were performed with an Olympus BX53 microscope. The species has also been reported from Haryana (Kaur et al., 2023).

Results and Discussion:

***Coprinopsis radiata* var. macrocarpa Atri. A. Kaur & M. Kaur**

Family: Psathyrellaceae

Macroscopic features: Carpophores: 11-15 cm tall. **Pileus:** 1.6 to 4 cm in height, with a campanulate to conical shape, an umbonate structure, a short umbo, and a scaly pileal veil. The scales are white and abundant, with an irregular margin that is brownish black at the apex. **Lamellae:** free, unequal, crowded, and vary from narrow to moderately broad, all black, with smooth edges. **Stipe:** 10.1-14.4 cm long, 0.6-1 cm wide, tapering upward, with a bulbous base, white, and fibrillose surface. **Microscopic characteristics: Basidiospores:** it measuring 12-16.3 x 5.8-8.1 µm, ellipsoidal, with a germ pore, thick walls, smooth surface, and dark reddish brown to blackish brown colouration. **Basidia:** 11.4-16 x 7.1- 9.4 µm, dimorphic, clavate, elongated cylindrical to clavate, bearing sterigmata. **Cheilocystidia:** 36.5-51 x 16.4-28 µm, ellipsoidal to inflated clavate, thin-walled, hyaline. **Pleurocystidia:** 53.4-78 x 15-26.6 µm,

elongated ellipsoidal to inflated clavate, thin-walled, hyaline. The above macro- and micromorphological features are consistent with the original description of the taxon. **Similar observations were noted by** Atri, N. S. and Kaur, Amandeep (2010), Nagy, L. G. et al. (2012), Keirle, M. R. et al. (2004), and Vellinga, E. C. (2004), who reported comparable pileal veil structure, spore dimensions, dimorphic basidia, and cystidial morphology in coprinoid members of *Coprinopsis*.

***Coprinopsis macrocephala* (Berk.) Redhead, Vilgalys & Moncalvo**

Family: Psathyrellaceae

Macroscopic features: Carpophores: it measures 11–15.2 cm in height, Pileus: 1.6–3.1 cm tall. Young fungi are elongated or ellipsoid, becoming convex or flattened as they mature; their surface is moist, blackish grey, with irregular margins. **Lamellae:** free, unequal, crowded, and black. **Stipe:** central is 10.1-14.3 cm long, cylindrical, bulbous at the base, hollow, and white on the surface. **Microscopic features: Basidiospores:** it measuring 13–15.6 x 8.8–11 µm, ellipsoidal, with a germ pore, thick walls, smooth surface, dark reddish-brown colouration, and an apiculus. **Basidia:** 30–37 x 13.2–15.2 µm, thin-walled, hyaline, with sterigmata. The gill edges are sterile. **Cheilocystidia:** 38.64 x 18-31 µm, ellipsoidal, clavate, thin-walled, and hyaline. **Pleurocystidia:** 48–98 x 23–43 µm, inflated and clavate, thin-walled, and hyaline. **Pileus cuticle:** unbranched, cylindrical to ellipsoidal, septate. **Clamp connections:** septate, thin-walled, and granular. **Stipe tissue:** it consists of hyphae that are longitudinally tangled, thin-walled, and hyaline. **Clamp connections:** present throughout. The above morphological and microscopic characters conform to earlier descriptions of the species. **Similar observations were noted by** Atri, N. S. (2015), Amandeep Kaur et al. (2015), Redhead, S. A. et al. (2001), Kirk, P. M. et al. (2008), and Uljé, C. B. (2005), who reported comparable macroscopic features, spore dimensions, cystidial structures, and the presence of clamp connections in *Coprinopsis macrocephala*.

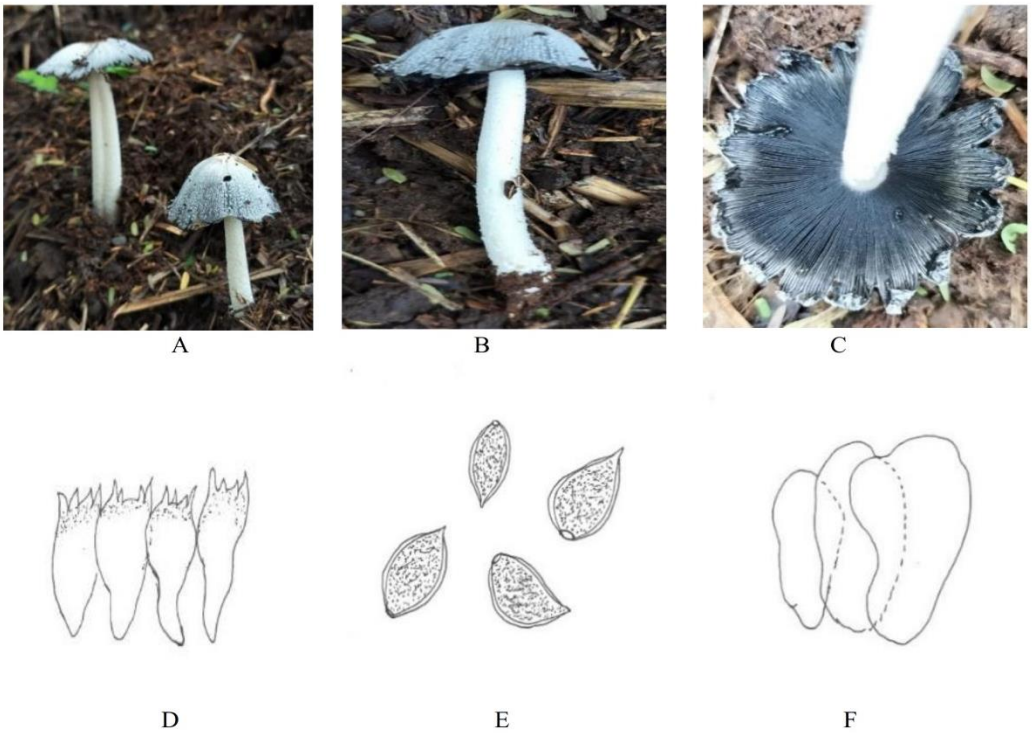

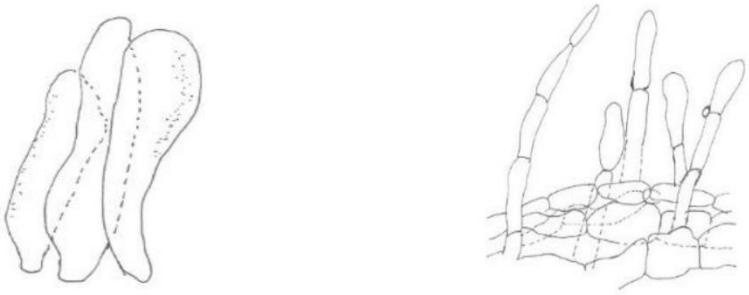

G H

Fig 1. ***Coprinopsis radiata* var. macrocarpa Atri. A. Kaur & M. Kaur** A, B-C Natural Habitat of Carpophore, D- Basidia, E- Basidiospore, F-Cheilocystidia, G-Pleurocystidia, H- Pileus cuticle.

A B C

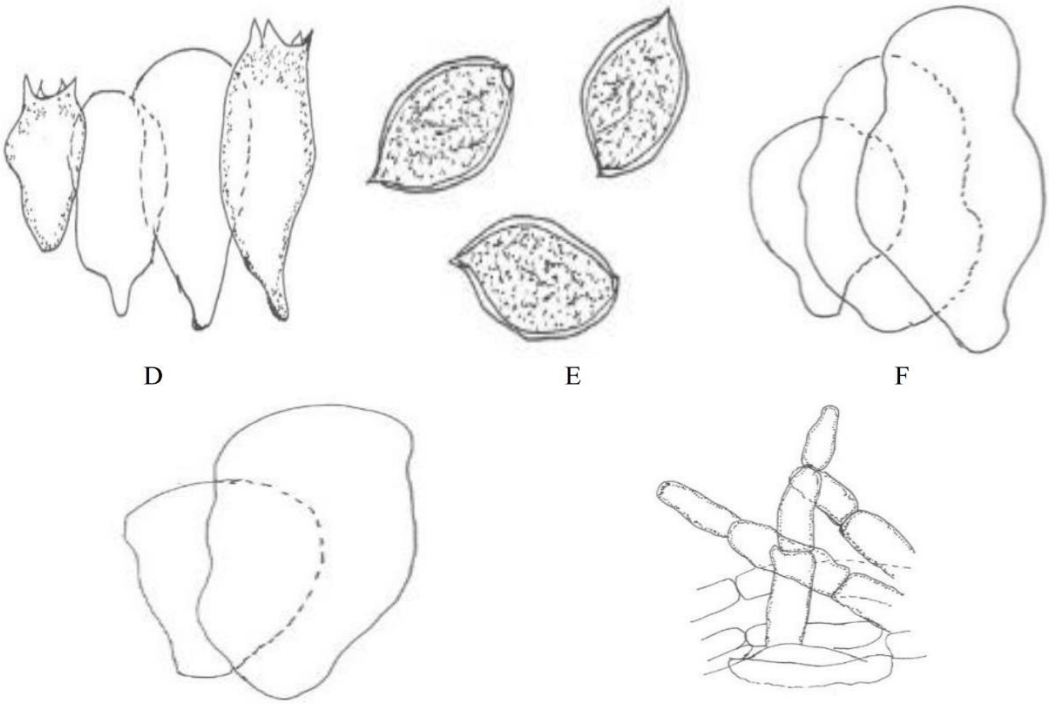

D E F

G H

Fig. 2 ***Coprinopsis macrocephala* (Berk.) Redhead, Vilgalys & Moncalvo** A, B-C Natural Habitat of Carpophore, D- Basidia, E- Basidiospore, F-Cheilocystidia, G-Pleurocystidia, H-Pileus cuticle.

Conclusion:

The present morpho-taxonomic investigation confirms the occurrence of Coprinopsis radiata var. macrocarpa and Coprinopsis macrocephala in Jalna district, Maharashtra, India. Detailed examination of macroscopic and microscopic characters established clear diagnostic distinctions between the two taxa despite their shared placement in the family Psathyrellaceae. *Coprinopsis radiata* var. *macrocarpa* is characterized by comparatively larger carpophores, a scaly white pileal veil with brownish-black apex, dimorphic basidia, and relatively narrower ellipsoidal basidiospores with a distinct germ pore. In contrast, *C. macrocephala* exhibits a moist blackish-grey pileus, sterile gill edges, larger and broader basidiospores with a prominent apiculus, well-developed pleurocystidia, and clamp connections throughout the hyphal system. Differences in cystidial morphology, spore dimensions, pileus cuticle structure, and clamp connection distribution provide reliable taxonomic markers for species delimitation. Both taxa demonstrate typical coprinoid characteristics such as deliquescent lamellae, saprotrophic growth, and adaptation to nutrient-rich substrates. Their documentation from the semi-arid agro-ecosystems of Jalna enriches regional fungal biodiversity records and provides baseline data for future systematic, ecological, and conservation-oriented studies of coprinoid fungi in Maharashtra.

References:

1. Amandeep, K., Atri, N. S., & Kaur, A. (2015). Diversity and taxonomy of coprinoid mushrooms from India. *Journal of Mycology and Plant Pathology, 45*(2), 123–135.
2. Atri, N. S. (2015). *Taxonomic studies on agaric fungi of India*. Botanical Survey of India.
3. Atri, N. S., & Kaur, A. (2003). Studies on coprinoid fungi of north-western India. *Indian Journal of Mushroom Research, 12*, 45–58.
4. Atri, N. S., Kaur, A., & Kaur, M. (2012). Taxonomic evaluation of selected coprinoid fungi from India. *Kavaka, 40*, 1–10.
5. Atri, N. S., Kaur, A., & Kaur, M. (2019). Taxonomic studies on coprinoid mushrooms from north India. *Journal of Mycology and Plant Pathology, 49*(2), 145–156.
6. He, M. Q., Zhao, R. L., Hyde, K. D., Begerow, D., Kemler, M., Yurkov, A., et al. (2021). Notes, outline and divergence times of Basidiomycota. *Fungal Diversity, 99*, 105–367.
7. Hopple, J. S., & Vilgalys, R. (1999). Phylogenetic relationships in the mushroom genus *Coprinus* based on rDNA sequences. *Molecular Phylogenetics and Evolution, 13*, 1–16.
8. Kaur, A., & Atri, N. S. (2017). Ecological studies on coprinoid fungi of Punjab plains. *Kavaka, 49*, 34–42.
9. Kaur, A., Kaur, M., & Atri, N. S. (2023). *Coprophilous agaricoid mushrooms of Punjab: A monographic account*. Bishen Singh Mahendra Pal Singh.
10. Kirk, P. M., Cannon, P. F., & Stalpers, J. A. (2013). *Ainsworth & Bisby's dictionary of the fungi* (11th ed.). CAB International.
11. Kirk, P. M., Cannon, P. F., Minter, D. W., & Stalpers, J. A. (2008). *Dictionary of the fungi* (10th ed.). CAB International.
12. Mirdu, N., Atri, N. S., & Kaur, M. (2023). *An illustrated guide to wild Agaricus of*

Haryana. Bishen Singh Mahendra Pal Singh.

13. Moncalvo, J. M., Vilgalys, R., Redhead, S. A., et al. (2002). One hundred and seventeen clades of euagarics. *Molecular Phylogenetics and Evolution, 23*, 357–400.
14. Nagy, L. G., Vágvölgyi, C., & Papp, T. (2016). Global patterns of mushroom evolution and taxonomy. *Mycologia, 108*(3), 516–530.
15. Pegler, D. N. (1986). *Agaric flora of Sri Lanka*. Kew Bulletin Additional Series 12.
16. Redhead, S. A., Vilgalys, R., & Moncalvo, J. M. (2001). *Coprinus* Pers. and the disposition of *Coprinus* species sensu lato. *Taxon, 50*(1), 203–241.
17. Singer, R. (1986). *The Agaricales in modern taxonomy* (4th ed.). Koeltz Scientific Books.
18. Uljé, C. B. (2005). *Coprinus* Pers. In *Flora Agaricina Neerlandica* (Vol. 6). CRC Press.
19. Upadhyay, R. C. (2018). *Fungi and mushroom biology*. Springer.
20. Vellinga, E. C. (2004). Genera in the family Agaricaceae: Evidence from molecular phylogenetics. *Mycotaxon, 89*, 397–402.
21. Zhou, J. L., Qin, W. M., & Yang, Z. L. (2018). Taxonomy and phylogeny of coprinoid fungi from China. *Mycological Progress, 17*(4), 435–450.

International Journal of Advance and Applied Research
www.ijaar.co.in
ISSN – 2347-7075 Impact Factor – 8.141
Peer Reviewed Bi-Monthly
Vol. 7 No. 14 January – February - 2026

Survey And Uses of Medicinal Plants from Risod, District Washim: A Comprehensive Study

G. P. Ambhore[1] & M. R. Ingle[2]

[1]*R.K Talreja College College of Arts, Science and Commerce, Ulhasnagar, Dist Thane*

[2]*Satish Pradhan Dnyansadhana College, Thane*

Corresponding Author – G. P. Ambhore

DOI - 10.5281/zenodo.19724616

Abstract:

The present study documents the traditional medicinal plants used by local communities in Risod tehsil, District Washim, Maharashtra, India. A comprehensive ethnobotanical survey was conducted to identify, catalog, and document the medicinal flora and their therapeutic applications. The study area, characterized by semi-arid climate and diverse vegetation, yielded 89 medicinal plant species belonging to 72 genera and 45 families. The most prominent families were Fabaceae (12 species), Asteraceae (8 species), and Euphorbiaceae (6 species). Local practitioners and tribal communities predominantly use these plants for treating ailments such as digestive disorders (32%), respiratory problems (24%), skin diseases (18%), and fever-related conditions (15%). The study reveals that leaves (38%) and roots (28%) are the most frequently used plant parts, with decoction (42%) being the preferred method of preparation. Documentation of this traditional knowledge is crucial for biodiversity conservation and potential drug development. The findings indicate a rich ethnobotanical heritage in the region that requires immediate attention for conservation and sustainable utilization.

Keywords: Ethnobotany, Medicinal Plants, Traditional Knowledge, Risod, Washim, Biodiversity Conservation

Introduction:

India's rich biodiversity which possess medicinal properties. The Vidarbha region of Maharashtra, including District Washim, represents a significant repository of traditional medicinal knowledge that has been passed down through generations. Risod tehsil, located in the southeastern part of Washim district, spans an area of approximately 567 square kilometers and supports diverse vegetation patterns due to its unique geographical location and climatic conditions.

The indigenous communities of this region, including various tribal groups and traditional healers, have developed an extensive understanding of local flora and their therapeutic applications over centuries. However, rapid modernization, urbanization, and changing lifestyle patterns pose serious threats to this invaluable traditional knowledge system. The documentation of ethnomedicinal practices becomes increasingly urgent as elderly knowledge holders pass away without transferring their expertise to younger generations.

Ethnobotanical studies serve multiple purposes: they preserve traditional knowledge, identify potential sources for new pharmaceuticals, promote sustainable use of natural resources, and contribute to biodiversity conservation efforts. The Deccan plateau region, where Risod is situated, experiences a semi-arid climate with distinct wet and dry seasons, supporting a unique assemblage of medicinal plants adapted to these conditions.

Previous studies in adjacent areas of Vidarbha have revealed significant medicinal plant diversity, but comprehensive documentation specific to Risod tehsil remains limited. This study aims to fill this knowledge gap by conducting a systematic survey of medicinal plants and their traditional uses among local communities in Risod.

The objectives of this research were: (1) Conducting a comprehensive inventory of medicinal plants used by local communities in Risod tehsil, (2) Documenting traditional preparation methods and therapeutic applications, (3) Identifying the most frequently used plant families and species, (4) Assessing the current conservation status of important medicinal species, and (6) Recommending strategies for sustainable utilization and conservation of this ethnobotanical heritage.

Materials and Methods:

Study Area:

Risod tehsil is located between 19°58'N to 20°15'N latitude and 77°15'E to 77°35'E longitude in District Washim, Maharashtra. The area experiences a tropical semi-arid climate with an average annual rainfall of 650-750 mm, primarily during the monsoon season (June-September). The temperature ranges from 12°C in winter to 45°C in summer. The terrain consists of undulating plains with scattered hillocks, supporting diverse vegetation including dry deciduous forests, scrublands, and grasslands.

Methodology:

Field Surveys: Extensive field surveys were conducted over a period of 18 months (January 2023 to June 2024) across 22 villages in Risod tehsil. The survey methodology included systematic transect walks, quadrat sampling in different vegetation types, and opportunistic collection of medicinal plants mentioned by local informants.

Informant Selection: A total of 147 informants were interviewed, including traditional healers (Vaidus), tribal medicine practitioners, elderly community members, and local herb collectors. Informants were selected using purposive and snowball sampling techniques. The age range of informants was 35-75 years, with 58% being male and 42% female.

Data Collection: Semi-structured interviews were conducted using standardized questionnaires covering plant identification, local names, parts used, preparation methods, therapeutic applications, dosage, and administration routes. Prior informed consent was obtained from all participants following ethical guidelines for ethnobotanical research.

Plant Collection and Identification: Medicinal plants were collected with the help of local informants during different seasons to ensure comprehensive coverage. Voucher specimens were prepared following standard herbarium techniques and identified using regional floras and taxonomic keys.

Results:

Plant Diversity and Taxonomic Distribution:

The ethnobotanical survey documented 89 medicinal plant species distributed across 72 genera and 45 families. The dominant families in terms of species richness were:

Fabaceae (12 species, 13.5%): Including *Cassia fistula*, *Acacia nilotica*, *Butea monosperma*, and *Prosopis cineraria*. This family showed the highest diversity of medicinal applications, particularly for digestive and skin disorders.

Asteraceae (8 species, 9.0%): Notable species included *Eclipta prostrata*, *Parthenium hysterophorus*, and *Vernonia cinerea*, primarily used for liver disorders and fever management.

Euphorbiaceae (6 species, 6.7%): Represented by *Euphorbia hirta*, *Jatropha curcas*, and *Ricinus*

communis, commonly employed for skin conditions and wound healing.

Apocynaceae (5 species, 5.6%): Including *Calotropis procera*, *Nerium oleander*, and *Catharanthus roseus*, used for various ailments from skin diseases to diabetes management.

Lamiaceae (5 species, 5.6%): Featuring aromatic herbs like *Ocimum sanctum*, *Leucas aspera*, and *Coleus forskohlii*, primarily used for respiratory and digestive ailments.

Life Form Analysis:

The medicinal flora comprised diverse life forms: herbs (47 species, 52.8%), shrubs (23 species, 25.8%), trees (15 species, 16.9%), and climbers (4 species, 4.5%). The predominance of herbs reflects their accessibility and ease of collection by local communities.

Plant Parts Utilized:

Analysis of plant parts used revealed the following pattern:

- Leaves: 34 species (38.2%)
- Roots: 25 species (28.1%)
- Whole plant: 12 species (13.5%)
- Bark: 8 species (9.0%)
- Seeds: 6 species (6.7%)
- Flowers: 4 species (4.5%)

Therapeutic Applications:

Medicinal plants were categorized into 12 major therapeutic categories based on their traditional uses:

Digestive Disorders (28 species, 31.5%): The most frequently treated category, including conditions like diarrhea, dysentery, indigestion, and stomach pain. Key species include *Aegle marmelos*, *Psidium guajava*, and *Terminalia chebula*.

Respiratory Ailments (21 species, 23.6%): Including cough, cold, asthma, and bronchitis. Important species were *Adhatoda vasica*, *Ocimum sanctum*, and *Solanum xanthocarpum*.

Skin Diseases (16 species, 18.0%): Covering wounds, cuts, boils, and various skin infections. Commonly used plants included *Azadirachta indica*, *Pongamia pinnata*, and *Cassia tora*.

Fever and Malaria (13 species, 14.6%): Traditional febrifuge plants like *Andrographis paniculata*, *Nyctanthes arbor-tristis*, and *Tinospora cordifolia*.

Preparation Methods:

Six primary preparation methods were documented:

Decoction (37 species, 41.6%): The most preferred method, involving boiling plant material in water.

Paste Application (23 species, 25.8%): External application of ground plant material, often mixed with water or oil.

Powder (15 species, 16.9%): Dried and ground plant material, usually mixed with honey or water.

Juice Extraction (10 species, 11.2%): Fresh plant juice, commonly from leaves.

Oil Preparation (3 species, 3.4%): Plant material processed in oil for external applications.

Direct Consumption (1 species, 1.1%): Raw consumption of plant parts.

Seasonal Collection Patterns:

Most medicinal plants (67%) are collected during the post-monsoon period (October-December) when active compounds are reportedly at their peak concentration. Some species like *Ocimum sanctum* and *Azadirachta indica* are collected year-round, while others have specific collection seasons dictated by traditional knowledge and phenological patterns.

Discussion:

The documented diversity of 89 medicinal plant species from Risod tehsil represents a significant contribution to the ethnobotanical knowledge of the Vidarbha region. This diversity is comparable to studies conducted in similar semi-arid regions of Maharashtra and demonstrates the rich traditional knowledge systems maintained by local communities despite increasing modernization pressures.

Taxonomic Significance:

The dominance of Fabaceae in medicinal applications aligns with findings from other ethnobotanical studies across India. Members of this family are known for their diverse secondary metabolites, including alkaloids, flavonoids, and saponins, which contribute to their therapeutic efficacy. The significant representation of Asteraceae species reflects their widespread distribution and diverse pharmacological properties, particularly anti-inflammatory and hepatoprotective activities.

Cultural and Traditional Aspects:

The preference for treating digestive disorders (31.5% of documented uses) reflects both the dietary habits of local communities and the traditional understanding of health that emphasizes digestive wellness as fundamental to overall health. This aligns with Ayurvedic principles where digestive fire (Agni) is considered central to health maintenance.

The predominant use of leaves (38.2%) can be attributed to their ease of collection, year-round availability, and high concentration of bioactive compounds. The preference for decoction as a preparation method (41.6%) reflects practical considerations related to extraction efficiency and palatability.

Pharmacological Validation:

Many documented species have been scientifically validated for their traditional uses. For instance, *Azadirachta indica* (neem) has proven antimicrobial, anti-inflammatory, and immunomodulatory properties supporting its traditional use for skin diseases and general health maintenance. Similarly, *Tinospora cordifolia* has demonstrated significant immunomodulatory and hepatoprotective activities validating its traditional use as a general tonic and fever reducer.

Conservation Concerns:

Several documented species face varying degrees of conservation pressure. *Terminalia chebula* and *Aegle marmelos*, despite their high RFC values, are experiencing declining populations due to habitat loss and overharvesting. Climate change impacts, including altered rainfall patterns and increased temperature extremes, pose additional threats to the survival of temperature-sensitive species.The dependence on wild collection for 78% of documented species raises sustainability concerns. Only a few species like *Ocimum sanctum* and *Azadirachta indica* are commonly cultivated, while most others rely entirely on natural populations.

Knowledge Transmission:

The study revealed concerning trends in traditional knowledge transmission. Approximately 65% of knowledgeable informants were above 55 years of age, and only 23% reported having transmitted their knowledge to younger family members. This pattern suggests potential knowledge erosion within the next 2-3 decades if active conservation measures are not implemented.

Limitations and Future Directions:

This study focused primarily on plant-based remedies and did not extensively cover mineral or animal-based traditional medicines. Future research should adopt a more holistic approach to traditional healing systems. Additionally, seasonal variations in plant

chemistry and efficacy were not quantitatively assessed and warrant detailed phytochemical investigation.

The study also highlights the need for participatory conservation approaches involving local communities in sustainable harvesting practices and cultivation programs for high-demand species.

Conclusion:

The ethnobotanical survey of Risod tehsil has documented significant medicinal plant diversity with 89 species representing 45 families, demonstrating the rich traditional knowledge heritage of local communities. The dominance of digestive and respiratory ailment treatments reflects both local health priorities and the therapeutic strengths of regional flora.

Key findings include the taxonomic dominance of Fabaceae, the preference for leaf-based remedies prepared as decoctions, and the high cultural importance of species like *Azadirachta indica* and *Ocimum sanctum*. The quantitative analysis revealed strong informant consensus for digestive disorders (ICF = 0.87), validating the consistency of traditional knowledge.

However, the study also reveals concerning trends including declining traditional knowledge transmission, conservation pressure on wild populations, and limited cultivation of medicinal species. These findings necessitate immediate action for knowledge documentation, community-based conservation programs, and sustainable utilization strategies.

The documented medicinal plants represent potential sources for drug development and validation studies. Species with high RFC values and strong traditional efficacy claims should be prioritized for detailed pharmacological investigation. Simultaneously, conservation efforts must focus on habitat protection and sustainable harvesting practices to ensure the long-term availability of these valuable genetic resources.

This research contributes significantly to the ethnobotanical literature of Maharashtra and provides a foundation for future conservation and utilization programs. The integration of traditional knowledge with modern scientific validation approaches offers promising avenues for developing evidence-based herbal medicines while preserving cultural heritage and biodiversity.

The findings emphasize the urgent need for collaborative efforts between researchers, local communities, and policymakers to develop comprehensive strategies for preserving this invaluable ethnobotanical heritage for future generations while ensuring sustainable utilization of medicinal plant resources.

References:

1. Ahirwar, R.K. (2015). Ethnobotanical study of medicinal plants of Vidarbha region, Maharashtra, India. *International Journal of Current Research in Biosciences and Plant Biology*, 2(10), 36-43.
2. Bharti, A., & Sharma, N.K. (2023). Traditional medicinal plants used by tribal communities in semi-arid regions of Maharashtra: A comprehensive review. *Journal of Ethnobiology and Ethnomedicine*, 19, 15. https://doi.org/10.1186/s13002-023-00587-2
3. Cotton, C.M. (1996). *Ethnobotany: Principles and Applications*. John Wiley & Sons, Chichester.
4. Deshmukh, P.B., & Waghmode, A. (2011). Role of wild edible plants in human nutrition: A case study in Washim district, Maharashtra, India. *Applied Ecology and Environmental Sciences*, 3(2), 45-50.

5. Fabricant, D.S., & Farnsworth, N.R. (2001). The value of plants used in traditional medicine for drug discovery. *Environmental Health Perspectives*, 109(1), 69-75.
6. Gaikwad, J., Wilson, P.D., & Ranganathan, S. (2011). Ecological niche modeling of customary medicinal plant species used by Australian Aborigines to identify species-rich and culturally valuable areas for conservation. *Ecological Modelling*, 222(18), 3437-3443.
7. Heinrich, M., Ankli, A., Frei, B., Weimann, C., & Sticher, O. (1998). Medicinal plants in Mexico: Healers' consensus and cultural importance. *Social Science & Medicine*, 47(11), 1859-1871.
8. Jain, S.K. (1991). *Dictionary of Indian Folk Medicine and Ethnobotany*. Deep Publications, New Delhi.
9. Kala, C.P. (2005). Ethnomedicinal botany of the Apatani in the Eastern Himalayan region of India. *Journal of Ethnobiology and Ethnomedicine*, 1, 11. https://doi.org/10.1186/1746-4269-1-11
10. Katewa, S.S., & Galav, P.K. (2005). Traditional herbal medicines from Shekhawati region of Rajasthan. *Indian Journal of Traditional Knowledge*, 4(3), 237-245.
11. Lulekal, E., Kelbessa, E., Bekele, T., & Yineger, H. (2008). An ethnobotanical study of medicinal plants in Mana Angetu District, southeastern Ethiopia. *Journal of Ethnobiology and Ethnomedicine*, 4, 10. https://doi.org/10.1186/1746-4269-4-10
12. Mahesh, B., & Satish, S. (2008). Antimicrobial activity of some important medicinal plant against plant and human pathogens. *World Journal of Agricultural Sciences*, 4(S), 839-843.
13. Martin, G.J. (1995). *Ethnobotany: A Methods Manual*. Chapman & Hall, London.
14. Patil, D.A. (2003). Flora of Dhule and Nandurbar districts (Maharashtra). Bishen Singh Mahendra Pal Singh, Dehra Dun.
15. Phillips, O., & Gentry, A.H. (1993). The useful plants of Tambopata, Peru: I. Statistical hypotheses tests with a new quantitative technique. *Economic Botany*, 47(1), 15-32.
16. Pradhan, B.K., & Badola, H.K. (2008). Ethnomedicinal plant use by Lepcha tribe of Dzongu valley, bordering Khangchendzonga Biosphere Reserve, in North Sikkim, India. *Journal of Ethnobiology and Ethnomedicine*, 4, 22. https://doi.org/10.1186/1746-4269-4-22
17. Ragupathy, S., Steven, N.G., Maruthakkutti, M., Velusamy, B., & Ul-Huda, M.M. (2008). Consensus of the 'Malasars' traditional aboriginal knowledge of medicinal plants in the Velliangiri holy hills, India. *Journal of Ethnobiology and Ethnomedicine*, 4, 8. https://doi.org/10.1186/1746-4269-4-8
18. Sharma, B.D., Karthikeyan, S., & Singh, N.P. (1996). *Flora of Maharashtra State: Dicotyledones*. Botanical Survey of India, Calcutta.
19. Trotter, R.T., & Logan, M.H. (1986). Informant consensus: A new approach for identifying potentially effective medicinal plants. In: Etkin, N.L. (Ed.), *Plants in Indigenous Medicine and Diet: Biobehavioral Approaches* (pp. 91-112). Redgrave Publishing Company, Bedford Hills.
20. Ugulu, I., Baslar, S., Yorek, N., & Dogan, Y. (2009). The investigation and quantitative ethnobotanical evaluation of medicinal plants used around Izmir

province, Turkey. *Journal of Medicinal Plants Research*, 3(5), 345-367.

21. Vaidya, A.D.B., & Devasagayam, T.P.A. (2007). Current status of herbal drugs in India: An overview. *Journal of Clinical Biochemistry and Nutrition*, 41(1), 1-11.
22. WHO. (2013). *WHO Traditional Medicine Strategy 2014-2023*. World Health Organization, Geneva.
23. Yadav, S.S., & Mahakar, S.D. (2019). Ethnomedicinal plants of Melghat Tiger Reserve, Maharashtra, India. *Ethnobotanical Leaflets*, 13, 1065-1082.

International Journal of Advance and Applied Research
www.ijaar.co.in
ISSN – 2347-7075 Impact Factor – 8.141
Peer Reviewed Bi-Monthly
Vol. 7 No. 14 January – February - 2026

Aquaculture of Sea Cucumbers: A Review and Consolidated Qualitative Profile

Miss. Gayatri Rameshrao Kadam
Department of Botany

Corresponding Author – Miss. Gayatri Rameshrao Kadam

DOI - 10.5281/zenodo.19724688

Abstract:

Sea cucumbers (Class Holothuroidea) are high-value echinoderms whose demand in global seafood and traditional medicine markets has driven interest in aquaculture. Their benthic detritivorous habits provide ecosystem services such as bioturbation and nutrient recycling, making them attractive for sustainable aquaculture and integrated systems. However, sea cucumber aquaculture faces biological and technical challenges including complex reproductive biology, larval culture sensitivity and broodstock dependency on wild collections. This paper reviews current knowledge on hatchery and grow-out systems. broodstock management, larval rearing, grow-out technologies, breeding enhancements, nutritional requirements, and sustainable practices such as sea ranching and integrated multi-trophic aquaculture (IMTA). Also highlighted are ecological benefits, genetic considerations and future priorities in sea cucumber farming.

Keywords: Sea Ranching, Pond Culture, Aquarium, IMTA, Spawning, Apostichopus Japonicus.

Introduction:

Sea cucumbers comprise a diverse group of echinoderms distributed in marine environments worldwide. They are valued particularly in Asia, where processed sea cucumbers (*beche-de-mer*) are consumed as luxury food and believed to have medicinal properties. Overexploitation of wild stocks has led to ecological concerns and the expansion of aquaculture as a sustainable alternative. Aquaculture aims to meet market demand while reducing pressure on wild populations and supporting local livelihoods.

Sea cucumbers (Class: Holothuroidea) are among the most valuable marine invertebrates in global aquaculture, particularly in Asian markets where they are prized for their nutritional, medicinal, and pharmaceutical properties. Increasing demand, coupled with declining wild stocks due to overfishing, habitat degradation, and slow natural recruitment, has intensified the need for sustainable aquaculture practices. As a result, the development of reliable hatchery technologies and efficient grow-out systems has become essential for ensuring both resource conservation and economic viability.

Aquaculture of sea cucumbers has emerged as a promising approach to address these challenges. Hatchery production forms the foundation of sea cucumber farming, enabling controlled breeding, larval rearing, and juvenile production. Advances in hatchery technologies including broodstock conditioning. induced spawning, larval nutrition, settlement substrates, and nursery rearing-have significantly improved survival and growth rates in several commercially important species such as *Holothuria scabra*, *Apostichopus japonicus* and *Stichopus* spp.

Following hatchery production, grow-out systems play a crucial role in determining overall

production success. Among the various grow-out strategies, pond culture has gained popularity due to its controlled environment, ease of management, and compatibility with integrated multi-trophie aquaculture (IMTA) systems.

Pond-based culture allows for the utilization of organic-rich sediments and promotes nutrient recycling, thereby enhancing environmental sustainability. Sea ranching, on the other hand involves releasing hatchery-produced juveniles into natural habitats to enhance depleted stocks while generating economic returns. This approach combines conservation and production goals but requires careful site selection, stock enhancement strategies, and post-release monitoring. Enclosure culture represents an intermediate system, where sea cucumbers are reared in net pens, cages, or fenced coastal areas, offering protection from predators while allowing natural feeding and environmental interaction.

Despite significant progress, sea cucumber aquaculture still faces challenges such as disease outbreaks, variable growth rates. environmental impacts, and socio-economic constraints. A comprehensive understanding of hatchery technologies and grow-out systems is therefore essential for optimizing production and ensuring long-term sustainability. This paper reviews current advancements in sea cucumber aquaculture, with a focus on hatchery techniques and grow-out systems including pond culture, sea ranching, and enclosure culture, and discusses their potential for sustainable development of the industry.

Sea cucumbers support important fisheries and aquaculture industries worldwide. Demand for dried sea cucumber (beche-de-mer or trepang) has increased substantially, particularly in East and Southeast Asia, due to its culinary, nutritional, and medicinal importance. However, most commercially valuable species exhibit slow growth, late sexual maturity, and low natural recruitment, making them highly vulnerable to overexploitation. Consequently, many wild stocks have declined sharply, prompting the development of aquaculture technologies as a sustainable alternative to capture fisheries.

Among the various species cultured globally, *Holothuria scabra* (sandfish) is one of the most widely farmed tropical sea cucumbers due to its high market value, fast growth rate, and adaptability to captive conditions. Significant advances have been made in hatchery technologies for *H. scabra*, including broodstock conditioning, thermal or desiccation-induced spawning, larval rearing using microalgae such as *Chaetoceros* and *Isochrysis*, and juvenile settlement on sand or seagrass-based substrates. These hatchery innovations have enabled mass seed production and supported commercial-scale farming in countries such as China, Vietnam, the Philippines, and India.

In temperate regions, *Apostichopus japonicus* is the most extensively cultured sea cucumber species, particularly in China. Japan, and Korea. Hatchery production of *A. japonicus* is well established, with controlled spawning, pelagic larval rearing, and nursery culture forming the backbone of the industry. Grow-out of this species commonly occurs in earthen ponds and coastal enclosures, where juveniles feed on organic detritus and benthic microorganisms. Pond culture of *A. japonicus* has been successfully integrated with shrimp and fish farming systems. enhancing sediment quality and improving overall ecosystem productivity.

Other species, such as *Stichopus monotuberculatus, Stichopus horrens* and *Holothuria fuscogilva* have also attracted increasing attention for aquaculture development. While hatchery technologies for these species are less advanced, experimental studies have demonstrated their potential for captive spawning, larval development, and juvenile growth. In

particular, *Stichopus* species have shown promise in enclosure culture systems due to their tolerance of natural environmental fluctuations and ability to utilize naturally occurring organic matter.

Grow-out systems for sea cucumbers vary according to species biology, environmental conditions, and production objectives. Pond culture is commonly applied to *H. scabra* and *A. japonicus*. providing controlled conditions and high survival rates. Sea ranching has been widely implemented for *H. scabra*, where hatchery-produced juveniles are released into seagrass beds and sandy lagoons to enhance natural stocks while generating income for coastal communities. Enclosure culture, using net pens or fenced coastal areas, has proven effective for both *H. scabra* and *Stichopus* spp., offering a balance between environmental sustainability and production control.

Despite these advancements, challenges remain in species-specific nutrition, disease management, genetic improvement, and environmental carrying capacity. Understanding the biological and ecological requirements of individual species is therefore critical for optimizing hatchery protocols and grow-out strategies. This paper reviews species-specific hatchery technologies and grow-out systems for commercially important sea cucumbers. with emphasis on pond culture, sea ranching, and enclosure culture and evaluates their role in the sustainable expansion of sea cucumber aquaculture.

Sea cucumber aquaculture provides substantial ecological services by improving sediment quality, enhancing habitat productivity, and supporting biodiversity conservation. Simultaneously, it delivers socioeconomic benefits by supporting livelihoods, promoting food security, and fostering sustainable coastal development. When implemented under ecosystem-based and community-driven management frameworks, sea cucumber aquaculture represents a powerful tool for achieving both environmental sustainability and economic resilience.

Biological and Ecological Background:

Sea cucumbers are benthic detritivores that feed on organic matter in sediments. They play critical roles in benthic ecosystems, including enhancing nutrient recycling and sediment quality. For example, experimental sea cucumber culture showed positive effects on seagrass growth in Madagascar, demonstrating ecological co-benefits beyond production.

Reproductive biology varies among species but generally involves external spawning with planktotrophic larval stages that are highly sensitive to environmental conditions, presenting one of the major bottlenecks in aquaculture practice.

Hatchery Technologies:

Broodstock Conditioning and Management:

Successful aquaculture begins with healthy broodstock. Wild adults are often collected due to limited domesticated stocks. requiring careful conditioning to induce gonad development. Conditioning includes maintaining appropriate substrate, water quality, and diet to avoid stress and promote maturity.

Spawning Induction:

Spawning in sea cucumbers may be induced by environmental manipulation (like thermal stimulation), mimicking natural seasonal signs. Gradual increases in water temperature by 3 -7 °C over a period have been effective for species such as Holothuria scabra and *Apostichopus japonicus.*

In addition, recombinant peptides such as relaxin-like gonad-stimulating peptide (RGP) have been used to enhance ovarian maturation and

spawning, showing promising results for artificial spawning control.

Larval Rearing:

Larval rearing is highly sensitive to water quality and food availability. Larvae require specific micro-algal diets and controlled conditions from fertilization to settlement. Mortality rates are high if salinity, temperature or nutrition are suboptimal, proper careful monitoring protocols.

Grow-Out Systems:

Pond Culture:

Pond culture in controlled land-based environments remains the dominant method in major producing regions due to ease of management and water quality control. Ponds allow close monitoring of stocking density, feeding, and environmental parameters, facilitating growth from juveniles to commercial size.

Pond culture is one of the most widely adopted grow-out methods for sea cucumbers, particularly in Asia and the Indo-Pacific region. This system involves rearing juveniles in earthen or lined ponds under semi-controlled conditions. Pond culture is preferred because it allows better control of water quality, stocking density. feeding, and protection from predators compared to open sea ranching systems. Species such as Holothuria scabra (sandfish) and Apostichopus japonicus are especially suitable for pond culture due to their tolerance to environmental variation and benthic feeding behavior.

Pond Design and Preparation:

Ponds used for sea cucumber culture are typically shallow (0.8-1.5 m depth) to facilitate benthic feeding and sediment interaction. Earthen ponds with sandy-mud substrates are ideal, as sea cucumbers require sediment for feeding and burrowing.

Before stocking, ponds are prepared through:

- Draining and drying to eliminate predators and pathogens
- Application of lime to stabilize pH and disinfect sediments
- Addition of organic matter (e.g.. fermented rice bran or composted manure) to promote benthic microflora growth
- Water exchange systems are designed to ensure adequate oxygenation and removal of metabolic waste while minimizing disturbance to sediments. { Battaglene & Bell (2004); Purcell (2010)}

Stocking Density and Juvenile Size:

Stocking density is a critical factor influencing growth, survival, and production efficiency. Overstocking can lead to competition for organic matter and reduced growth rates.

Typical stocking densities:

- Juveniles (5-10 g): 1-3 individuals m-2
- Larger juveniles (20 g): 0.5-1 individual m-2

Juveniles produced in hatcheries are acclimated gradually to pond conditions to reduce stress and mortality. {Agudo (2006); FAO (2018)}

Feeding and Nutrient Management:

Sea cucumbers in pond systems rely primarily on natural detritus, benthic algae, and microbial biofilms. However, supplemental feeding is often necessary to enhance growth and carrying capacity.

Supplementary feeds may include:

- Fermented agricultural by-products (rice bran, wheat bran)
- Seaweed detritus
- Formulated feeds enriched with organic carbon
- Feed is typically applied directly to pond sediments rather than the water column.

{Slater & Carton (2009); Robinson et al. (2019)}

Water Quality Management:

Maintaining optimal water quality is essential in pond culture. Key parameters include:

Parameter	Optimal Range
Temperature	24-30 °C
Salinity	25-35 ppt
Dissolved Oxygen	>4 mg L-1
PH	7.5-8.5

Regular water exchange (5-20% per week) and aeration help maintain stable conditions and prevent anaerobic sediment formation. {Purcell et al. (2012): FAO (2018)}

Growth Performance and Production Cycle:

Growth rates in pond culture vary by species, stocking density. and food availability. *Holothuria scabra* typically reaches market size (300-500 g) within 8-14 months under optimal pond conditions.

Survival rates of 60-80% have been reported in well-managed ponds, significantly higher than in open sea ranching systems. {Agudo (2006); Robinson & Slater (2016)}

Disease and Health Management:

Sea cucumbers are generally resistant to disease; however, poor water quality and organic overload can lead to:

- Skin ulceration syndrome
- Bacterial infections
- Mass mortality due to hypoxia

Preventive management through proper pond preparation, low stocking density, and good water exchange is more effective than treatment. {Zhang et al. (2015); FAO (2018)}

Environmental and Economic Advantages:

Pond culture offers several advantages:

- Reduced predation pressure
- Easier monitoring and harvesting
- Compatibility with IMTA systems
- Lower environmental impact compared to intensive led aquaculture

Economically, pond culture provides stable income opportunities for coastal communities and small-scale farmers. {Purcell & Kirby (2006); Robinson et al. (2019)}

Limitations of Pond Culture:

Despite its advantages, pond culture has limitations:

- High land and water requirements
- Initial infrastructure costs
- Risk of organic sediment buildup ii poorly managed

Future improvements focus on optimized feeds, sediment management, and integration with other aquaculture species.

Sea Ranching and Enclosure Culture:

Sea ranching involves transferring hatchery produced juveniles into designated marine areas such as sheltered bays or seagrass beds, where they grow in a semi-natural environment. Enclosures (pens or mesh cages) protect juveniles from predation and allow water flow, representing another grow-out approach.

Sea ranching and enclosure culture are semi-natural grow-out approaches developed to enhance sea cucumber production while minimizing environmental impacts and operational costs. Unlike pond culture, these systems utilize natural coastal habitats such as seagrass beds, sandy lagoons, and shallow reef flats. Hatchery-produced juveniles are released into selected areas where they grow using natural food resources. These approaches are particularly attractive for stock enhancement, habitat restoration, and community-based fisheries management.

Sea ranching involves releasing juveniles into open but managed marine areas, whereas enclosure culture uses physical barriers such as nets, fences, or pens to confine sea cucumbers within a defined area and protect them from predation and poaching. {Purcell & Kirby (2006); Battaglene et al. (2013)}

Site Selection Criteria:

Successful sea ranching and enclosure culture depend heavily on appropriate site selection. Ideal sites possess:

- Shallow water depths (1-5 m)
- Sandy or sandy-mud substrates rich in organic matter
- Moderate water exchange and current velocity
- Stable salinity and temperature regimes
- Absence of industrial pollution and freshwater runoff

Seagrass meadows are particularly favorable due to high organic matter availability and shelter from strong currents. {Purcell (2010); FAO (2018)}

Juvenile Production and Release Strategies:

Juveniles used for sea ranching and enclosure culture are produced in hatcheries to reduce pressure on wild populations. Juvenile size at release is a key determinant of survival.

Recommended release sizes:

- *Holothuria scabra* ≥5-10 g
- *Apostichopus japonicus* ≥3-5 g

Larger juveniles show higher resistance to predation and environmental stress. Release is usually conducted during calm weather and favorable seasonal conditions to minimize mortality. {Agudo (2006); Robinson & Slater (2016)}

Enclosure Design and Materials:

Enclosures are typically constructed using:

- Nylon or polyethylene netting
- Bamboo. PVC, or wooden stakes
- Mesh sizes that allow water flow but prevent predator entry

Enclosures range from small experimental pens (50-100 m²) to large community-managed areas exceeding 1 hectare. Periodic maintenance is required to prevent fouling and structural damage. {Battaglene & Bell (2004); Hair et al. (2016)}

Nutrition and Feeding:

Sea cucumbers require diets rich in organic matter, including detritus and microalgae. Nutritional needs vary with species and culture stage, necessitating tailored diets to optimize growth and health. Supplemental feeding in IMTA systems helps improve growth and system balance.

Genetic and Conservation Considerations:

Hatchery production can impact genetic diversity through reduced effective population sizes and inbreeding, which may affect fitness if hatchery individuals are used for stock enhancement. Genetic management strategies are needed to maintain diversity and avoid negative impacts on wild populations.

Stocking Density and Carrying Capacity:

Stocking density must match natural food availability and sediment productivity. Overstocking can result in reduced growth and increased mortality.

Typical stocking densities:

- 0.2-1.0 individuals m2 (sea ranching)
- 0.5-2.0 individuals m-2 (enclosure culture)

Density adjustments are often made based on growth monitoring and sediment organic content. {Purcell et al. (2012): Robinson et al. (2019)}

Growth Performance and Survival:

Growth rates in sea ranching systems are generally slower than in pond culture due to reliance on natural food; however, production costs are significantly lower. Survival rates vary widely (30-70%) depending on predation pressure, juvenile size, and site quality.

Enclosure culture typically results in higher survival (50-85%) due to predator exclusion and better management control. {Agudo (2006); Battaglene et al. (2013)}

Ecological Impacts and Benefits:

Sea ranching and enclosure culture provide multiple ecological benefits:

- Enhancement of benthic nutrient recycling
- Improved sediment oxygenation
- Positive effects on seagrass productivity
- Restoration of depleted sea cucumber populations

Studies have shown that sea cucumber bioturbation can significantly improve sediment quality and ecosystem function in coastal habitats. {Slater & Carton (2009); Wolkenhauer et al. (2010)}

Socioeconomic Importance:

These culture systems are particularly suitable for small-scale fishers and coastal communities due to:

- Low capital investment
- Compatibility with traditional fishing practices
- Community-based management potential

Sea cucumber aquaculture can contribute to ecological restoration, enhance habitat quality (e.g.. seagrass growth), and support community livelihoods through sustainable income sources in regions where wild stocks are depleted.

Sea ranching has been widely promoted in Pacific Island nations as a tool for livelihood diversification and fisheries recovery. {Purcell & Kirby (2006); Hair et al. (2016)}

Constraints and Management Challenges:

Despite their advantages, sea ranching and enclosure culture face several challenges:

- High predation pressure in open systems
- Poaching and enforcement difficulties
- Variable growth due to environmental fluctuations
- Genetic risks if hatchery-produced juveniles are poorly managed
- Reproductive control and larval survival due to delicate biology.
- Water quality management, crucial to reducing mortality and disease.
- Dependence on wild broodstock, which may perpetuate ressure wild stroke, Economic viability, as capital and operational costs must be balanced against market value.

Effective governance, community participation, and monitoring are essential for long-term success. {Purcell et al. (2018): FAO (2018)}

Future Directions:

Future improvements in sea ranching and enclosure culture include:

- Use of larger juveniles to enhance survival
- Genetic management of hatchery stocks
- Integration with seagrass and IMTA systems
- Development of community-based co-management frameworks

These approaches align sea cucumber aquaculture with ecosystem-based management principles. Sea cucumber aquaculture holds significant promise for sustainable seafood production, ecosystem service enhancement. and socio-economic development. Key priorities for future research include improved breeding technologies, genetic management, optimized feeds, and integrated systems to maximize productivity and sustainability. Continuous development of hatchery protocols and post-larval rearing techniques will be critical to mainstream commercial operations.

References:

1. Agudo, N. S. (2006). Sandiish hatchery techniques. Australian Centre for International Agricultural Research (ACIAR).

2. Altamirano J.P. & Rodriguez J.C. Jr. (2022). Hatchery production of sea cucumbers (sandfish Holothuria scabra).
3. Aquaculture of sea cucumbers. Wikipedia.
4. Arnull J., Wilson A., Brayne K. et al. (2021). Ecological co-benefits from sea cucumber farming: Holothuria scabra increases growth rate of seagrass. Aquaculture Environment Interactions 13:301-310.
5. Battaglene S.C. (1999). Culture of tropical sea cucumbers for stock restoration and enhancement. WorldFish.
6. Battaglene, S. C., & Bell. J. D. (2004). The restocking of sea cucumbers in the Pacific Islands. FAO Fisheries Technical Paper, 463.
7. Battaglene, S. C., Purcell, S. W., & Bell, J. D. (2013). Sea cucumber aquaculture and stock enhancement. Reviews in Fisheries Science. 21. 150-162
8. Chieu H.D., Turner L. Smith M.K. et al. (2019). Aquaculture breeding enhancement in sea cucumbers using recombinant RGP. Frontiers in Marine Science.
9. Ciriminna L. Signa G.. Cillufio G.. Rakaj A., & Vizzini S. (2024).Frontiers in Marine Science systematic review on sea cucumber farming.
10. Duarte, C. M., et al. (2013). The role of coastal plant communities for climate change mitigation. Nature Climate Change, 3, 961-968.
11. FAO (2018). Sea cucumber fisheries and aquaculture: A global review. FAO Fisheries Technical Paper No. 516.
12. Hair, C. A., et al. (2016). Community-based sea cucumber ranching in the Pacific. SPC Fisheries Newsletter, 150, 15-22.
13. Kadam G.R. (2025). Health benefits of sea cucumber In Aarhat Multidisciplinary International Education Research Journal: Vol. XIV (Number I, pp. 129–137)
14. Maxwell, P. S., et al. (2017). The role of bioturbation in seagrass ecosystems. Marine Ecology Progress Series, 565, 1-14.
15. Purcell, S. W. (2010). Managing sea cucumber fisheries with an ecosystem approach. FAO Fisheries and Aquaculture Technical Paper.
16. Purcell, S. W., & Kirby. D. S. (2006). Restocking the sea cucumber fishery. Ocean & Coastal Management, 49, 837-857.
17. Purcell, S. W., et al. (2016). Deposit feeding and nutrient recycling by sea cucumbers. Journal of Experimental Marine Biology and Ecology, 475, 1-9.
18. Purcell, S. W., et al. (2018). Improving management of sea cucumber fisheries. Fish and Fisheries, 19, 390-412.
19. Purcell, S. W.. Samyn, Y., & Conand, C. (2012). Commercially important sea cucumbers of the world. FAO Species Catalogue.
20. Riquet F.. Fauvelot C., Fey P. et al. (2023). Hatchery-produced sandfish show altered genetic diversity.
21. Robinson, G., & Slater, M. J. (2016). Effect of stocking density on sea cucumber growth in pond culture. Aquaculture Research, 47, 357-366.
22. Robinson, G., Slater, M. J., & Jones, C. L. W. (2019). Sea cucumber aquaculture and integrated multi-trophic aquaculture systems. Reviews in Aquaculture, II, 804-823.
23. Sea cucumber aquaculture market research.
24. Slater, M. J., & Carton, A. G. (2009). Organic enrichment effects on sea cucumbers. Aquaculture, 292, 90-96.

25. Slater, M. J.. & Carton, A. G. (2009). Effect of organic enrichment on growth of sea cucumbers. Aquaculture, 292, 90-96.
26. Wolkenhauer, S. M., et al. (2010). Bioturbation effects of sea cucumbers. Journal of Experimental Marine Biology and Ecology. 383,93-101.
27. Zhang, C. Y., et al. (2015). Diseases of cultured sea cucumbers. Journal of Invertebrate Pathology, 130, 1-8.

International Journal of Advance and Applied Research
www.ijaar.co.in
ISSN – 2347-7075 Impact Factor – 8.141
Peer Reviewed Bi-Monthly
Vol. 7 No. 14 January – February - 2026

Effect of Vitamins on Protease and Lipase Production in Seed-Borne Fungi of Soybean

Kesare U. T.
Department of P.G. Studies in Botany, Adarsh Senior College Omerga, Dist. Dharashiv.
Corresponding Author – Kesare U. T.
DOI - 10.5281/zenodo.19724703

Abstract:

During the process of biodeterioration, seed mycoflora produce enzymes to degrade protein, carbohydrate and oil. These enzymes called as hydrolytic enzymes. The enzymes which degrade proteins are called protease and enzymes which degrade oil are lipase.

It is observed that total thirty species of fungi were isolated from ten varieties of Soybean. It is also observed that different Oils such as castor on protease production is stimulatory except Alternaria alternata, Aspergillus flavus and A. niger. Clove inhibited most of the fungi except Curvularia lunata, Fusarium oxysporum and Trichoderma viride. It produced no protease by A. niger and Trichoderma viride. Neem only inhibits the fungi like A. alternata, A. flavus and A. niger.

Keywords: Vitamins, Protease, Lipase, Fungi.

Introduction:

Seed plays a vital role for the production of healthy crop. These seeds are also responsible for disease transmission. This takes place either in the field or in ill storage condition. Neergard(1977) reported that in the presence of seed-borne pathogens, several types of abnormalities like reduction in seed size, seed rotting, discoloration of seeds, seed necrosis, loss in germ inability, toxifgication and other physiological disorders. Acording to Sandikar (1990) the species of *fusarium* are found to be significantly destructive and responsible to cause harmful effect on seed health resulting in to seed deterioration and poisoning of seeds. During the process of biodeterioration, fungi prduce enzymes to degrade proteins, carbohydrates and oil. Sharma and Satyanarayana (1980) studied production of protease by some fungi such as *Helminthosporium, Glomerella cingulata, Curvularia geniculata, Alternaria pelandui.*

Umatale(1995), Charya and Reddy (1982) also studied on lipase production in certain oil seeds. Umatale found *Aspergillusflavus, A.helianthi,* Macrophominaphasiolina and *Rhzopus nigricans* are more active to produce lipase.

Materials And Methods:

Collection of Samples and Detection of Seed Mycoflora:

For the collection of seed samples, the method described by Neergaard (1973) has been adopted. Accordingly, from fields, store houses market places and seed companies. A composite sample of each variety was prepared by mixing the individual samples together. The seed mycoflora was isolated by using slandered moist blotter paper method (SMB) and agar plate method (APM) as recommended by International seed testing association (ISTA 1966) ,De Tempe (1970) ,Neergaard (1973) and Agarwal (19760 .

Identification of seed borne fungi:

The fungi occurring on each and every seed in the plates were identified preliminary on

the basis of sporulation characters like sexual or asexual spores with the help of stereoscopic binocular microscope. The identification and further confirmation of seed-borne fungi was made by preparing slides of the fungal growth and observing them under compound microscope. The identification was made with the help of manuals as per Nelson,et.al. (1983), Singh, et.al.(1991), Mukadam D.S.(1997) and Mukadam et.al. (2006).

I) Production of Protease:

Production of protease(s) was made by growing the fungi on liquid medium containing glucose 10g, gelatin 10g, dipotassium hydrogen phosphate 1.0g, $MgSO_4$.$7H_2O$ -500mg and distilled water-1000ml. pH of the medium was adjusted at 5.5. Twenty-five ml of medium was poured in 100ml Erlenmeyer conical flasks and autoclaved as 151bs pressure for 20 minutes. The flasks on cooling were inoculated separately with 10ml standard spore/mycelial suspension of test fungi prepared from 7 days old cultures grown on PDA slants. The flasks were incubated for 6 days at 25±1ºC with diurnal periodicity of light. On 7th day, flasks were harvested by filtering the contents through Whatman's filter No.1. The filtrates were collected in the pre-sterlised bottles and termed as crude enzyme preparation.

Assay Method (cup-plate method)

Determination of protease(s) activity was done with the help of cup-plate method, adopted by Hislop *et. al.,* (1982) and Rajamani (1990). A basal medium was prepared by adding 2% (w/v) agar and one percent (w/v) gelatin. pH of the medium was adjusted at 5.6 with Mcllavaine's buffer. Then it was sterilized at 15 lbs pressure for 15 minutes. About 15 ml of the medium was poured in presterilized petriplates under aseptic condition. On solidification 6mm diameter cups/cavities were made in the centre of each of the agar plate with a sterilized cork borer (No.4). The cups/cavities were filled carefully with about 0.5ml of culture filtrate (crude enzyme preparation). The plates were incubated at 25ºC for 24 hours. Then the plates were flooded with 15 percent mercuric chloride in 7N HCl. After 10 minutes of standing, a clear transparent zone indicated the hydrolysis of gelating by extracellular proteolytic enzymes, whereas the rest of the region of the petriplates become opaque due to the coagulatin (protein) by mercuric chloride. Diameter of the clear zone was used as measure (mm) of protease activity, while non appearance of clear zone considered absence of protease (s) in the culture filtrates.

II) Production of Lipase:

Lipase activity was studied by growing the fungi on liquid medium at pH5.6 containing oil-10g, KNO_3 -2.5g, KH_2PO_4- -1.0g, $MgSO_2$ – 0.5g and distilled water 1000ml. 25ml of the medium was poured in 100ml conical flasks and autoclaved at 15 1bs pressure for 30 minutes, then on cooling the flasks were inoculated separately with 1.0ml spore suspension of the fungi which were incubated for 6 days at 25± 1ºC with diurnal periodicity of light. On 7th day of the flasks were harvested by filtering the contents through Whatman filter paper no.1. The filtrates were collected in presterilized culture filtrate bottles and termed as crude lipase.

Assay Method (Cup-plate method):

Determination of lipase activity was done with the help of cup-plate method. The medium contains Difco peptone-10g, NaCl-5g, $Cac1_2.2H_2O$-1.0g, agar 2 percent and 10ml lipid substrate serbitan mono laurate (Tween-20) (Pre-sterilized) was added to it. The pH of the medium was adjusted to 6.00. The medium was poured in each Petri plate. On solidifying the medium with the help of a cork borer (No.4) was made in the centre and was filled with 0.1ml culture filtrate. The plates were incubated at 28ºC. After 24

hours, a clear circular zone was measured (mm) as lipase activity. Similar procedure was followed for the culture filtrate in the central cavity instead of the active enzymes.

Result And Discussion:

Vitamins are very important in many vital activities of fungi. Therefore five commonly used vitamins at 100ppm concentration were used in protease and lipase production. The results are shown in table.

Except pyridoxine in case of *Alternaria alternata* and *Aspergillus flavus* almost all the sources of vitamins stimulates the protease activity by all ten fungal species.

In case of lipase activity all sources of vitamins stimulates production of lipase by *A. alternata* while other nine fungi inhibited by all sources of vitamins. There is no activity of lipase was seen in *Fusarium oxysporum* by vitamin A and riboflavin while *Spicaria violecia* also produce no lipase with ascorbic acid vitamin A, Thiamin Riboflavin and pyridoxine. Same results are seen in *Tricoderma viride* except with Ascorbic acid.

Table: Effect of Vitamins on protease and lipase production in seed-borne fungi.

Vitamins 100ppm conc.	Fungi									
	Activity Zone (mm)									
	Aal	Asf	Asn	Asg	Asu	Cul	Fur	Fuo	Spv	Triv
	Protease Production									
Ascrbic acid	20	20	22	16	20	15	23	17	20	18
Vitamin A	20	22	20	16	19	15	22	16	19	15
Thiamin	24	27	30	23	26	22	26	18	24	19
Riboflavin	21	24	22	20	21	21	24	16	20	18
Pyridoxin	11	11	18	13	14	13	18	18	14	14
Control	18	20	18	16	12	13	18	12	11	11
	Lipase Production									
Ascorbic acid	30	12	14	12	14	12	13	13	0	11
Vitamin A	33	12	18	15	17	11	13	0	0	0
Thiamin	30	14	15	19	18	12	15	13	0	0
Riboflavin	31	13	15	16	13	12	20	0	0	0
pyridoxin	28	12	14	13	15	11	15	11	0	0
Control	27	23	24	30	25	24	35	17	18	12

Aal – *Alternaria alternata*
Asf – *Aspergillus flavus*
Asn – *Aspergillus niger*
Asg – *Aspergillus glaucus*
Asu – *Aspergillus ustus*
Cul – *Curvularia lunata*
Fur – *Fusarium roseum*
Fuo – *Fusarium oxysporum*
Spv – *Spicaria violecia*
Triv – *Trichoderma viride*

References:

1. Agarwl V.K. (1976) .Technique for the detection of seed borne fungi. *Seed research*.4:24-31.
2. Charya M.A.S. and S.M. Reddy (1982). Production of proteolytic enzymes by three seed borne fungi. *Acta Botanica indica*.10:296-299 .
3. De,Tempe,J (1970). Tesing cereal seeds for *Fusarium* infection in the Netherlands. *Prof. Int. Seed.Test.Ass.* 33: 193-2006.
4. Hislop,E.C.,J.L.Paver and J.P.R. Keon (1982) .Protease produced by *Monilinia frutigena* in vitro and in infected apple fruits and its possible role in pathogenesis . *J.Gem. Microbial*,128:799-807.
5. ISTA (1966). Proc. International seed testing Association,31: 1-52.
6. Mukadam ,D.S. (1997) The illustrated kingdom of fungi ,Aksharganga Prakashan Aurangabad.(M.S.),India.
7. Mukadam D.S.,Ashok M. Chavan,Patil M.S. and Anjali R. Patil (2006) The illustrated fungi,Saraswati Printing Press,Aurangabad.(M.S.). India.
8. Neergaard Paul (1973) Detection of Seed borne pathogens by culture tests. *Seed Sci. And Tech.*1:217-254.
9. Neergaard Paul (1977) Seed Patholopgy, Vol.I: *John Villy and sons N.Y.*
10. Nelson P.E.,Toussoun,T.A. and Marassas ,W.F.O. (1983) .*Fusarim* species an illustrated manual for identification . Pennsylvania State University,University park and Londan.Pp.193.
11. Rajamani ,S. (1990) Factures influencing the production of intracellular protease by selected pathogenic fungi *,Jr.Indian Bot. Sci*. 69:285-287.
12. Sandikar (1990) Seed-borne safflower and sesame.Ph.D. thesis,Marathwada University,Aurangabad.
13. Sharma D.P.and T. Satyanrayana (1980) Production of by some moulds. *Indian Phytopath*. 33:339-395.
14. Singh,K.,Frisvad,J.C.,Thrane,U. and Mathur,S.B. (1991) An illustrated manual on identification of some seed borne *Aspergilli,Fusaria,Penicillia* and their mycotrins.Dan Govt.
15. Umatale M.V. (1995) Studies on fungal enzymes and toxins biodeterioration of Oil Seeds.*Ph.d. Thesis,Dr.B.A.M.U.Aurangabad* (M.S.).

International Journal of Advance and Applied Research
www.ijaar.co.in
ISSN – 2347-7075 Impact Factor – 8.141
Peer Reviewed Bi-Monthly
Vol. 7 No. 14 January – February - 2026

Herbal Management of Lumpy Skin Disease (LSD) in Cattle

M. B. Navale[1], M. S. Wadikar[2], R. J. Sawant[3] & V.D. Jadhav[4]

[1]Sangamner Nagarpalika Art's, D. J. Malpani Commerce and B. N. Sarda Science College (Autonomous) Sangamner – 422605(M.S.)

[2]Department of Botany, R. B. Attal College, Georai-431127 (MS), India

[3]Department of Botany, Vinayakrao Patil College, Vaijapuapur, Maharashtra, India

[4]Department of Zoology, Annasaheb Waghire College, Otur-412409, (MS), India

Corresponding Author – M. B. Navale

DOI - 10.5281/zenodo.19724790

Abstract:

Lumpy Skin Disease (LSD), caused by the Capripoxvirus, is an emerging trans boundary viral disease of cattle resulting in nodules, fever, lymphadenopathy, reduced milk production, infertility, and socioeconomic losses. With no specific antiviral drugs available, supportive care and vaccination remain key strategies. In many regions—particularly rural, low-resource settings—farmers utilize herbal remedies as adjunct or alternative therapy. This paper reviews the scientific basis, preparation methods, pharmacological actions, and clinical outcomes of key herbal treatments used for LSD, including Azadirachta indica (Neem), Aloe vera, and Curcuma longa (Turmeric). Field observations across Asia and Africa suggest that these botanicals enhance wound healing, reduce inflammation, prevent secondary bacterial infections, and improve recovery time. However, evidence is largely observational, and controlled clinical trials are sparse. This paper highlights the potential of herbal management in LSD control while emphasizing the need for standardized formulations and integrated veterinary supervision.

Introduction:

Lumpy Skin Disease (LSD) is a severe viral infection of cattle transmitted primarily through biting insects (mosquitoes, ticks, flies). First identified in Africa, the disease has spread to the Middle East, South Asia, and Southeast Asia, with significant outbreaks reported between 2020–2024.

Clinical signs include:

- Fever
- Nodular skin lesions
- Lymph node enlargement
- Nasal discharge
- Loss of appetite
- Decreased milk yield
- Secondary bacterial infections

Conventional management comprises vaccination, symptomatic therapy, and antibiotics for secondary infections. However, lack of access to veterinary services, rising antibiotic resistance, and economic constraints have driven interest in herbal alternatives.Herbal remedies are widely used in ethnoveterinary practices and are known for their antimicrobial, anti-inflammatory, wound-healing, and immunomodulatory properties. This paper explores the role of herbal agents in managing LSD.

Materials and Methods:

1. Study Design:

- Ethnoveterinary field observations
- Experimental studies on herbal pharmacology

- Farmer-level intervention reports
- Herbal formulation trials

2. Data Sources:

- Research journals (PubMed, ScienceDirect)
- Government veterinary reports
- Ethnoveterinary textbooks
- Field surveys
- Farm-level documentation
- WHO/OIE/FAO reports

3. Evaluation Parameters:

Herbal treatments were assessed on:

- Lesion healing time
- Fever duration
- Rate of secondary infection
- Mortality reduction
- Milk yield recovery
- Farmer acceptability
- Cost-effectiveness

4. Herbal Preparation Methods:

Each plant was evaluated based on traditional formulations and scientific extraction methods (decoction, cold infusion, paste, gel, oil extraction).

Results:

1. Common Herbal Plants Used for LSD:

A. *Azadirachta indica* (Neem):

Parts used: Leaves, oil

Preparation:

- Leaves crushed to paste
- Mixed with coconut oil or mustard oil
- Applied twice daily

Pharmacological actions:

- Strong antibacterial
- Antiviral potential
- Insect repellent
- Anti-inflammatory

Clinical outcomes:

- Reduced pus formation
- Faster drying of lesions
- Reduced odour and fly infestation

B. *Aloe Vera:*

Parts used: Leaf gel

Preparation:

- Gel extracted from mature leaves
- Applied directly to ulcers

Actions:

- Wound healing
- Cooling, soothing
- Anti-inflammatory
- Antibacterial

Clinical outcomes:

- Faster epithelialization
- Reduced pain
- Reduced scab formation time

C. *Curcuma longa* (Turmeric):

Parts used: Rhizome powder

Preparation:

- Paste with water/ghee
- Orally with feed (10–20 g/day)

Actions:

- Anti-inflammatory
- Immunomodulatory
- Antibacterial
- Antiviral (broad-spectrum)

Clinical outcomes:

- Significant reduction in swelling
- Better systemic immunity
- Improved appetite

D. Multi-Herbal Formulations:

Used in India, Africa, Nepal:

- Neem + Turmeric + Aloe vera spray
- Herbal oil blends
- Proprietary polyherbal sprays

Reported to:

- Reduce lesion severity
- Prevent maggot infestations
- Reduce healing time by 30–40%
- Improve overall recovery

2. Herbal Treatment Protocol:

Morning Treatment:

1. Clean lesions with warm saline
2. Apply Neem oil paste
3. Apply Aloe vera gel

Afternoon:

4. Spray multi-herbal extract for vector control

Evening:

5. Reapply Aloe gel
6. Oral turmeric supplementation

3. Result Findings Summary:

Parameter	Conventional Treatment	Herbal+ Conventional	Outcome
Fever duration	5–7 days	3–4 days	Improved
Healing time	25–30 days	15–20 days	Faster
Secondary infection	High	Low	Significant reduction
Mortality	Moderate	Lower	Reduced
Cost	High	Low–moderate	Affordable

Before Treatment Photograph

After Treatment Photograph

Discussion:

The combined properties of herbal agents—antimicrobial, antiviral, wound- healing, anti-inflammatory—provide a synergistic effect in LSD management. The greatest benefits were observed when Neem + Aloe vera + Turmeric were used together.

Mechanisms of Herbal Action:

- **Neem** reduces bacterial load and repels insects that spread LSDV
- **Aloe vera** accelerates wound healing and reduces lesion pain
- **Turmeric** enhances systemic immunity
- Polyherbal sprays create a protective layer preventing contamination

Farmers report better outcomes and lower costs compared to exclusive allopathic treatment. However, herbal therapies cannot replace vaccination, which remains essential for disease prevention.

Conclusion:

Herbal management plays a significant role in controlling Lumpy Skin Disease in cattle, especially in low-resource rural areas. Neem, Aloe vera, and Turmeric have strong scientific justification for use due to their pharmacological properties and clinical effectiveness.

While herbal treatments significantly improve lesion healing, immunity, and secondary infection control, they should be used as supportive therapy, not as a replacement for vaccination, hygiene, and veterinary care.

References:

1. Yadav, M. P., Kumar, A., & Singh, R. (2021). The emergence and management of Lumpy Skin Disease in cattle: A case study from North India. *Indian Veterinary Journal*, 98(4), 12–18.
2. Tuppurainen, E. S. M., & Oura, C. A. L. (2012). Review: Lumpy skin disease: An emerging threat to Europe, the Middle East and Asia. *Transboundary and Emerging Diseases*, 59(1), 40–48.
3. Pal, M., Begum, W., & Abraha, B. (2024). Lumpy skin disease: An emerging transboundary viral disease of cattle. *Journal of Advances in Microbiology Research*, 15(2), 45–56.
4. FAO. (2022). *Lumpy Skin Disease: Field Manual for Veterinarians*. Food and Agriculture Organization of the United Nations, Rome.
5. WOAH (OIE). (2023). *Lumpy Skin Disease – Technical Disease Card*. World Organisation for Animal Health, Paris.
6. Gupta, R., Sharma, V., & Kumar, S. (2019). Antimicrobial and wound healing properties of *Azadirachta indica*: A review. *Journal of Ethnopharmacology*, 235, 52–64.
7. Biswas, K., Chattopadhyay, I., Banerjee, R. K., & Bandyopadhyay, U. (2002). Biological activities and medicinal properties of neem (*Azadirachta indica*). *Current Science*, 82(11), 1336–1345.
8. Surjushe, A., Vasani, R., & Saple, D. G. (2008). Aloe vera: A short review. *Indian Journal of Dermatology*, 53(4), 163–166.
9. Hamman, J. H. (2008). Composition and applications of Aloe vera leaf gel. *Molecules*, 13(8), 1599–1616.
10. Hewlings, S. J., & Kalman, D. S. (2017). Curcumin: A review of its effects on human health. *Foods*, 6(10), 92.
11. Aggarwal, B. B., & Harikumar, K. B. (2009). Potential therapeutic effects of curcumin: The anti-inflammatory agent. *International Journal of Biochemistry & Cell Biology*, 41(1), 40–59.
12. Singh, P. K., et al. (2021). Ethnoveterinary practices in livestock health management in India. *Indian Journal of Traditional Knowledge*, 20(3), 725–734.
13. McGaw, L. J., Eloff, J. N. (2008). Ethnoveterinary use of southern African plants and scientific evaluation of their

medicinal properties. *Journal of Ethnopharmacology*, 119(3), 559–574.

14. Acta Scientific Veterinary Sciences. (2021). Polyherbal formulations in management of lumpy skin disease: Field observations. *Acta Scientific Veterinary Sciences*, 3(6), 45–50.
15. WHO. (2019). *WHO Traditional Medicine Strategy 2014–2023*. World Health Organization, Geneva.
16. Chakraborty, S., et al. (2020). Role of herbal medicine in reducing antibiotic use in livestock. *Veterinary World*, 13(10), 2236–2243.
17. Rastogi, S., & Pandey, M. M. (2017). Ethnoveterinary medicine in India: Present status and future prospects. *Journal of Ayurveda and Integrative Medicine*, 8(4), 258–264.
18. Kumar, R., & Singh, S. V. (2022). Vector-borne transmission dynamics of lumpy skin disease virus. *Veterinary Research Communications*, 46(3), 699–710.
19. OIE Terrestrial Manual. (2022). *Capripoxvirus infections*. World Organisation for Animal Health.
20. FAO & WOAH. (2021). *Global strategy for the control and eradication of lumpy skin disease*.

International Journal of Advance and Applied Research
www.ijaar.co.in
ISSN – 2347-7075 Impact Factor – 8.141
Peer Reviewed Bi-Monthly
Vol. 7 No. 14 January – February - 2026

Plant Based Traditional Remedies on Child Health Care in Beed District, Maharashtra

Nagnath K. Dahiphale[1] & Savita M. Sukte[2]

Department of Botany, Balbhim Arts, Science and Commerce College,

Balbhim Nagar, Beed-431122 (MS) India

Corresponding Author – Nagnath K. Dahiphale

DOI - 10.5281/zenodo.19724870

Abstract:

India is a rich source of medicinal plants. Since prehistoric times large number of people depends on medicinal plants for traditional healthcare practices, as plant-based medicines are effortlessly accessible and cost-effective. Based on traditional healers or practitioners who eternally use their precious knowledge to treat plant based traditional remedies on child health care. The information obtained from the traditional practices was also cross verified to check the authenticity. Leaves, flowers, fruits, seeds and bark are commonly used by traditional healers in the form of decoction, paste, extract, juice, ash and infusion to cure various ailments. In the present study revealed that the plant based traditional information collected and document from various traditional healers of beed district through questionnaires and personal interviews. The practitioners use some common medicinal plant material like Tulsi, Turmeric, Ginger etc. Among the plants used by practitioners, herbs are most common followed by Shrubs, trees and climbers. From this study it was concluded that the documentation of the ethno-botanical information in management of local health care is the first step, which will open new door for researcher in the field of child health care.

Keywords: ***Traditional Practitioners, Child Health Care, Medicinal Plants.***

Introduction:

The information of medicinal plants in India has been gathered in course of many centuries based on several prehistoric remedial systems, including ayurveda, unani and siddha etc. (Lone and Bhardwaj, 2013). According to World Health Organization, around 80% of earth population directly or indirectly relies on traditional medicine for their basic healthcare needs (Rath *et al*., 2009; Pattnaik *et al*., 2006). India is one of the well-known biodiversity regions of the world has diverse ethnic, linguistic, socio-economic and cultural areas. Thus, the original knowledge of therapeutic plants and their use in curing numerous disorders might realistically be expected in this country. In rural India, 70% of the residents are reliant on the conventional system of medicine (Rao and Laxmi, 2012). The yearly universal market for herbal medicines in year 2000 was over 60 US$ billion and is rising steadily at a rate of fifteen to twenty five percent (WHO, 2008). In India Healthcare costs increases dramatically over the last decade. According to Towers Watson investigation (based on data from leading global insurance companies), India witnessed 22% growth in health care costs in 2006. It goes to 12% in 2009, and is expected to get higher again to 13% in 2012. Peoples are now looking for simple and cost effective therapies for getting better the quality of life (Biswas, 2012). The steep raise in health care costs, simultaneously with the threat of increasing side effects risks of synthetic medicine, is convincing populace to

believe about low cost alternative medicines having low or no side effects such as Ayurveda, Homoeopathy, Siddha, Unani, Yoga, Naturopathy etc. offer a broad range of preventive and remedial treatments that are both cost effective and efficient. Beed is one of the 36 districts in Maharashtra and the traditional remedial systems are still admired here. Lies between 18.27° to 19.27° Latitude and 74.29° to 76.44° E Longitude an average height of about 600 m above mean sea level. Cover an area of 10227 sq. km. On the Deccan plateau and is centrally placed in the region. It demarcates boundaries between Parbhani, Jalna, Aurangabad, Ahmednagar, Usmanabad and Latur districts. Prior to independence, Beed was a part of the former Hyderabad state. It was included in the State of Maharashtra in 1960. Topographically, the district may be divided into two parts e.g.

1. Northern part consisting of plains of Godavari valley.
2. Southern and southwestern part consisting of hilly area of Balaghat range.

Most of the areas of this region were converted into an agricultural land. Now days the conventional knowledge get decrease day by day due to ecological degradation, deforestation, and agricultural expansion. Therefore, gathering the information of medicinal plants is an urgent need. Hence, the purpose of this study was to interrelate with local traditional healers and document their knowledge on medicinal plants, their practice and the treatment of various diseases.

Materials and Methods:

1. Ethno Botanical Survey:

The practice of plant based medicinal system is widespread among the ethnic people of Beed district, and it is intensely rooted in their socioeconomic traditions. Though, the documentation of local medicinal practices is conspicuously missing for the region. Considering the immense cultural and ethno-linguistic diversity of the tribal people of the district, several field interviews in the form of semi-structured questionnaire were designed to cover as in Parli taluka as possible, in order to take full advantage of the diversity of knowledge and the plant species used in conventional therapy. Collected information is useful to curing several ailments on child health care by using different medicinal plants. Take several visits for ethnic places in different seasons when plants get flowering. Informants getting the information about local names, used plant parts, formulation and dosages were also documented. The aims of this investigation were systematically clarified to all the informants before the interview (Cunningham, 2001).

2. Collection and Identification of Medicinal Plant:

Fresh and healthy plant materials of medicinal plants were collected in the month of July-2018 to Feb-2019 from different location of Beed district of Maharashtra. Identification of plant species were confirmed using Flora of Marathwada by Naik *et al*., 1998. Collected plant materials were pressed, dried, and mounted on herbarium sheet for further study.

Result and Discussion:

Most of preparation was arranged from fresh and healthy plant material in the form of a decoction, powder and paste. Nearly all used approach of medication administration is oral ingestion, followed by external use. A large amount of diseases and pains were usually treated either with a single plant or a mixture of plant parts. In some cases, ointments like mustered oil, ghee (a remedy from milk) etc. and other ingredients such as black peeper, ginger, tulsi, etc. were also used to make ethnic formulations

along with the parts of plant species. In children diseases the highest use report in the present study were documented for *Melia azedarach*, *Ficus carica, Piper nigrum, Ocimum sanctum, Ocimum basilicum, Ficus religiosa, Acacia nilotica* etc. Present study aims was undertaken to explore the plant based traditional remedies, and local health care takers from Beed district of Maharashtra state. For this purpose series of field surveys were carried out in Parli taluka. The information on traditional medicinal plants was collected through conversations, questionnaires etc. with local traditional healers (Baidyas, Ojhas, Traditional healer, aged knowledgeable persons). The information collected from the informants along with the medicinal plants, their local names, plant parts used as a medicine, formulation and doses has been given in Table 1. Traditional medicines are easily available and safe to cure various health problems. In recent era almost every nation of the world used it. Hence it is a best choice for alternative medicine due to its huge demand (Aziz *et al.,* 2018). In several formulations, number of part was used. Such as Leaves, rhizomes, roots, and the whole plant, it is most important hazards in the restoration of the medicinal plants (Ahmad *et al*., 2009).

Table 1: Plant based herbal remedies practiced for child health

Sr. No.	Remedies	Disease Treated	Name of Healer
1.	Flower of *Acacia nilotica* (Babul) is boiled with mustard oil and 2-3 drops are poured in ear.	Earache	Mr. Someshwar Haribhau Lingade
2.	Half cup of *Aerva javanica* in fusion is given before lunch	Stomach disorders	Mr. Someshwar Haribhau Lingade
3.	Burn the leaves of *Ficus religiosa,* ash is mixed with water take orally.	Vomiting	Mr. Kulkarni Mama Bhisegaokar
4.	Fresh leaves of *Ocimum basilicum* are crushed and squeezed; the drops of leaf juice are poured in ear. The decoction of leaves is used for gargling.	Earache, Toothache, Cough and Fever	Mr. Kulkarni Mama Bhisegaokar
5.	Leaf juice of *Ocimum sanctum* is dropped in nose.	Fever	Mr. Someshwar Haribhau Lingade
6.	4-5 Fruits of *Ficus carica* (anjir) given twice a day.	Cough, Constipation	Mr. Vitthal Dharmraj Tambud
7.	1 cup of *Melia azedarach* decoction is used orally before breakfast.	Diabetes	Mr. Vitthal Dharmraj Tambud
8.	5-6 Seeed of *Embelia ribes* boiled with 1 cup of water up to 1/3 and drink it after cooled down for 7 days.	Remove worm, constipation	Mr. Ramesh Balasaheb Shinde
9.	Prepare a ginger juice with the help of grinder or mortar and pestle then add equal amount of jaggery powder and lick it 2-3	Dry cough, Fever	Ms. Somitra Udhavrao Dahiphale

	times in a day for 5 days.		
10.	Boiled 8-10 curry leaves in water then add trifala powder and amla powder in 1:1 ratio mix well take it at bed time for 7 weeks.	Early greying hair, Hairfall	Mr. Ankush Bhimrao Mundhe
11.	Steam 10-15 leaves of *Justicia adhatoda* and squeeze three spoon of juice and take with honey twice a day for 4 to 7 days.	Cold, Dry cough	Mr. Abhay Lonikar
12.	Take 1 glass of water and add it 2 spoon of sugar and pinch of salt mixed well and give it for several intervals.	Loose motion	Mr. Hanumant Nagargoje
13.	Prepare fine paste of *Asafoetida* (hing) with water or olive oil and used it for massage on Stomach.	Stomach ache	Mr. Shaikh Shafik Jafar
14.	10-12 small pieces of stem of *Tinospora cardifolia* boiled with one glass of water up to remaining half glass then filter it and used an empty stomach at early morning.	Fever (Hadi tap)	Mr. Govind Solanke
15.	Take roasted white sesame seeds, black sesame seeds and flax seeds grind them with the help of grinder then add it jaggery powder and make ladoos give it early morning.	Calcium Deficiency	Mandakini Mundhe

Conclusion:

In this study revealed that how different interviewing procedures facilitate to gather the information concerning the name of the diseases treated plants and their usage, with their mode of direction. Total of 10 types of local ailments was treated with 10 phyto-therapeutic uses in this district. The manufacturing process of herbal preparation is yet a secret and passed on generation after generation vocally. Appropriate examination of herbal formulations and phyto-constituents of used plants can open new entrance for the researchers. However, ethno-botanical facts is the basis of further justification of practices and plant uses in the context of a professional approach to develop new herbal drug (Muhammad *et al*., 2005).

References:

1. Ahmad, M., Qureshi, R., Arshad, M., Khan, M. A. (2009). Zafar, M. Traditional herbal remedies used for the treatment of diabetes from district Attock (Pakistan). Pak J Bot. 41(6): 2777-2782.
2. Aziz, M. A., Khan, A. H., Adnan, M. and Ullah, H. (2018). Traditional uses of medicinal plants used by indigenous communities for veterinary practices at Bajaur Agency, Pakistan. J Ethnobiol Ethnomed.14 (1):11.
3. Biradar, S. D. and Ghorband, D. P. (2010). Ethono-medicinal wisdom of tribals of Kinwat forest of Nanded district (Maharashtra), Indian Journal nat Prod Resour,1(2), 254-257.
4. Biswas, S. (2012). The Economic Times, http://articles.economictimes.indiatimes.

com/2012-07-24/news/328282501_health-care-health-risk-india-health (accessed on 10.3.13).

5. Cunningham, A. B. (2001). Applied ethnobotany: people, wild plant use and conservation. London: Earthscan. Ersity and sustaining local livelihood. Annu Rev Environ Resour.30: 219-52.
6. Kachare, S. V., Raut, K. S. and Suryawanshi, S. R. (2010). Medicinal plants used by local inhabitants in Marathwada. International Journal of Current Research. 4: 049-051.
7. Kachare, S. V., Suryawanshi, S. R. and Raut, K. S. (2010). Traditional medicines for Diabetes from villagers in Marathwada. Botany Research International 3(1):14-16.
8. Lone, P. A. and Bhardwaj, A. K. (2013) Traditional herbal based disease treatment in some rural areas of Bandipora district of Jammu and Kashmir, India. Asian J Pharm Clin Res., 6:162-71.
9. Muhammad, G., Khan, M. Z., Hussain, M. H., Iqbal, Z., Iqbal, M. and Athar, M. (2005) Ethno-veterinary practices of owners of pneumatic-cart pulling camels in Faisalabad City (Pakistan). J Ethnopharmacol. 97: 241-246.
10. Naik, V.N. and Associates (1998). Flora of Marathwada. Amurt Prakashan, Aurangabad, India. Vol. I and II.
11. Patil, D. R., Patil, P. S. and Patil, D. A. (2011). Indigenous home remedies as applied in Shirpur Taluka of Dhule District (M.S.) India. Current Botany, 2(4): 34-35.
12. Pattnaik, C., Reddy, C. S., Dhal, N. K. and Das, R. (2006). Some Phytotherapeutics Claims by Tribals of Rayagada District, Orissa, India. Ethanobotanical Leaflet, 10: 189- 197.
13. Rao, G. H. J. and Laxmi, P. (2012). Anti diarrhoeal activity of *Ziziphus jujuba* leaf extract in rats, International Journal of Pharma and Bio Sciences, 3 (1):532-538.
14. Rath, S. K., Mahapatra, N., Dubey, D., Panda, S. K., Thatoi, H. N. and Dutta, S. K. (2009). Antimicrobial activity of *Diospyros melanoxylon* barks from Similipal Biosphere Reserve, Orissa, India. African Journal of Biotechnology, 8(9): 1924-1928.

International Journal of Advance and Applied Research
www.ijaar.co.in
ISSN – 2347-7075 Impact Factor – 8.141
Peer Reviewed Bi-Monthly
Vol. 7 No. 14 January – February - 2026

Isolation And Screening of Soil Fungi on Different Culture Media

Patil T. V.[1] & Pangrikar P. P.[2]
Department of Botany,
[1]*Deogiri College, (Autonomous), Chhatrapatai Sambhajinagar*
[2]*R.B. Attal college of Arts science and commerce, Georai, Beed.(MS)*
Corresponding Author – Nagnath K. Dahiphale
DOI - 10.5281/zenodo.19724942

Abstract:
In the present investigation an attempt has been made to isolate the soil fungi from different localities. For isolation of fungi soil samples was collected from the different fields in pre sterilised zip lock bags. Soil samples were cultured on the different culture media like Potato dextrose agar, Rose Bengal agar, Czapek dox agar and Glucose nitrate agar by serial dilution method. The culture plates were incubated at 30^{0}c temperature. Fungi were sub cultured to obtain pure culture after getting pure cultures screening of fungi were done on different media for different parameters and fungi were identified by standard protocol. PDA supported the highest diversity and fastest growth, suggesting medium composition significantly influences fungal isolation and cultivation.

Keywords: Rose Bengal agar, Czapek dox agar, PH.

Introduction:

Soil is a complex habitat for microbial growth and these microbes generally exist as micro-colonies or biofilms on mineral particles, organic matter and roots. The rhizosphere soil sources are the narrow region of soil that is directly influenced by root secretion and associated soil (Stinson *et al.* 2006). Soil fungi contribute to decomposition, nutrient mineralization, biocontrol activity, and plant symbiosis. However, some soil fungi may also be pathogens affecting crops and humans. Fungi constitute a group of microorganisms that are widely distributed in environment especially in soil (Boer et al., 2005). *Isolation and screening of soil fungi* are critical in understanding fungal biodiversity, ecological functions, and potential applications in biotechnology. The great majority of fungal species have at least one part of their lifecycle in soil (Bridge and Spooner, 2001). The occurrence of fungi varies with depth of soil (Baruah, 1982). Different culture media can influence fungal growth due to variations in nutrient composition. This research compares the efficiency of several media in isolating and screening soil fungi.

Materials and Methods:

Collection of Soil Samples:

The soil samples from four different agricultural fields in Chhatrapati Sambhajianagar (Maharashtra) locality were collected. The soil sample was collected by digging up to 12cm deep and was immediately packed into sterile zip-lock bags. The samples were collected from two spots in each site and were brought to lab for further study. Then the soil sample from four localities were mixed together in order to obtain a representative sample.

Media Preparation:

Isolating soil fungi using Potato Dextrose Agar (PDA), Rose Bengal Agar (RBA), and Czapek-Dox Agar (CZA) is a standard mycological procedure. Potato Dextrose Agar is a general-purpose medium widely used for cultivation of fungi. It is commonly used for maintenance and sub-culturing of fungal isolates. Rose Bengal Agar is a selective medium used mainly for isolation and enumeration of soil fungi. Rose Bengal dye restricts rapid fungal colony growth, preventing overgrowth. Antibiotics such as chloramphenicol are added to suppress bacterial contamination. It is particularly useful for quantitative studies of fungal populations in soil. Czapek-Dox Agar is a chemically defined medium containing sucrose as carbon source and sodium nitrate as nitrogen source. The defined composition makes it suitable for physiological and metabolic studies of fungi.

Different Culture Medium		
Potato Dextrose Agar (PDA)	**Rose Bengal Agar (RBA)**	**Czapek-Dox AgarAgar (CZA)**
Potato Infusion -200 gm	Peptone – 5 g	Sucrose – 30 g
Dextrose -20 gm	Dextrose – 10 g	Sodium nitrate – 2 g
Agar-20 gm	KH_2PO_4 – 1 g	K_2HPO_4 – 1 g
Distilled Water	$MgSO_4$ – 0.5 g	$MgSO_4$ – 0.5 g
	Rose Bengal – 0.033 gm	KCl – 0.5 g
	Agar – 15 gm	$FeSO_4$ – 0.01 gm
	Chloramphenicol (added after autoclaving) – 50 mg	Agar – 15 g

Isolation of Fungi from The Soil:

For isolation of fungi, dilution plate technique described by Warcup is used. In 90ml of distilled water 10gm of soil sample were suspended then mix well by using wrist action shaker for 1Hr. at 120 RPM. The flask were shaken thoroughly in order to get uniform distribution of the soil particle The soil suspensions were diluted in 10 fold increment from 10^{-3},10^{-4},10^{-5}. The Volume of 1 mL of soil sample. The suspension from each serial dilution was pipetted onto different melted, cooled culture media supplemented with 1% Streptomycin. The fungal culture was raised by using spread plate technique, 0.1ml of diluted sample was plated in a sterile petri plates, inoculate on all different culture medium. Three replicates were maintained for each sample. Identification of the organisms was made by microscopic observation. The plates were incubated at 37° C for 48-72 hrs. After incubation colonies were examined under the microscope for ascertaining the identity of fungi with the help of lactophenol staining. The characteristics were compared with the standard description of, 'A manual of Soil Fungi', by Gilman, (1957), 'Industrial Mycology' by Onions et al. (1981)

Result and Discussion:

Various different factors are responsible for the fungal diversity on different culture medium due to different composition. Fungi on PDA displayed diverse morphology (e.g., cottony white, green velvety, dark spores).Colonies on CDA were more limited in texture and sporulation. The present study demonstrates

significant variation in fungal isolation efficiency among the three culture media tested: PDA, RBA, and Czapek Dox Agar. After the comparison done by using various medium isolation efficiency is calculated relative to medium with highest colony count. PDA showed the highest isolation efficiency due to its rich nutrient content, while RBA provided moderate recovery by restricting rapid overgrowth of fast-growing fungi. Czapek Dox Agar exhibited lower efficiency, likely because its defined nutrient composition selectively supports specific fungal groups.

$$\textbf{Isolation Efficiency (\%)} = \frac{\textbf{Number of morphotypes on a medium}}{\textbf{Highest number of morphotypes}} \; \textbf{100}$$

Potato Dextrose Agar

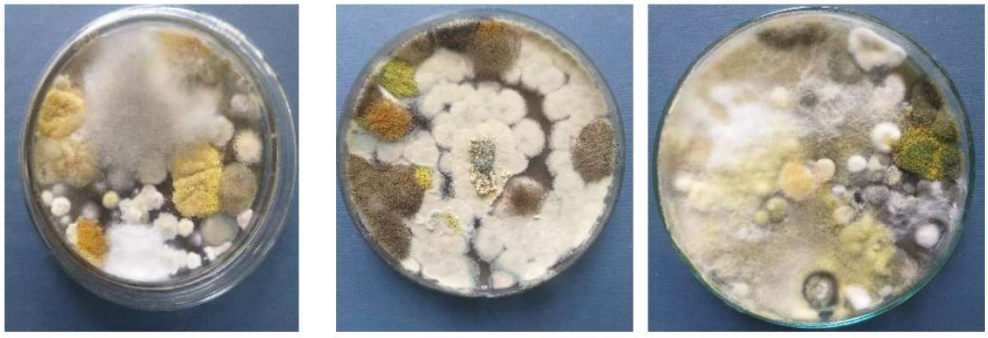

Rose Bengal Agar

Czapek Dox Agar

Culture Medium	Mean Colony Count (CFU/g soil)	Number of Morphotypes Observed	Growth Rate	Isolation Efficiency (%)
PDA (Potato Dextrose Agar)	4.5×10^4	**8**	**Fast**	**100%**
RBA (Rose Bengal Agar)	3.2×10^4	**7**	**Moderate**	**071%**
Czapek Dox Agar (CDA)	2.8×10^4	**5**	**Slow to Moderate**	**62%**

PDA exhibited the highest colony-forming units (4.5×10^4 CFU/g) and the greatest number of morphotypes (8). The rich nutrient composition of PDA, particularly its high carbohydrate content from potato infusion and dextrose, supports rapid fungal growth and sporulation. As a general-purpose medium, PDA favours a wide range of saprophytic soil fungi. Therefore, it showed 100% relative isolation efficiency and can be considered the most effective medium for broad fungal isolation. RBA showed moderate isolation efficiency (71%) compared to PDA. The presence of Rose Bengal dye and antibiotics in RBA helps restrict bacterial growth and slow down the spread of fast-growing fungi. This allows better enumeration of colonies without overgrowth. Although total CFU was lower than PDA, RBA provided clearer and more distinct colony morphology, making it suitable for quantitative studies and accurate counting of fungal populations. Czapek Dox Agar recorded the lowest colony count (2.8×10^4 CFU/g) and the least number of morphotypes (5). CDA is a chemically defined medium with sodium nitrate as the sole nitrogen source, which selectively supports fungi capable of utilizing nitrate. This selective property may have restricted the growth of certain soil fungi, resulting in lower isolation efficiency (62%).

Conclusion:

The present study undertaken to comparison with different culture medium with their fungal diversity. Soil fungi can be successfully isolated using serial dilution and plating techniques. Potato Dextrose Agar supports the greatest fungal diversity and growth. Screening on multiple media provides a broader picture of soil fungal populations. PDA shows good nourishment on fungal diversity and provide all require components for fungal growth.

References:

1. Baruah, H.K. (1982) Study on the soil fungi and their biochemical activities, fungi from the paddy field, Antibiotic Symposium, Ind. Sci, Congress.
2. Bridge, P. & Spooner, B. (2001) Soil fungi: diversity and detection. Plant soil, 232:147-154.
3. Boer W, Folman LB, Summerbell RC and Boddy L (2005). Living in a fungal world: impact of fungi on soil bacterial niche development. FEMS Microbiology Review, 29(4): 795-811.
4. Stinson K. A., Campbell S. A, Powell J. R., Wolfe, B. E., Callaway R. M., Thelen G. C., Hallett, S. G., Prati, D. and Klironomos, J. N. (2006), Invasive plant suppresses the growth of native tree seedlings by disrupting below ground mutualisms. PLoS Biology 4 (5): 134-140.

International Journal of Advance and Applied Research
www.ijaar.co.in
ISSN – 2347-7075 Impact Factor – 8.141
Peer Reviewed Bi-Monthly
Vol. 7 No. 14 January – February - 2026

The Holobiome Framework: Integrating Environmental Microbiomes, Probiotic Systems, and Sustainable Ecosystem Management

Pranali Wasate[1] & Navnath Kashid[2]

[1]Research Scholar, Dr. Babasaheb Ambedkar Marathwada University, Chhatrapati Sambhajinagar M.S. 431001, India.

[2]Professor, Baburaoji Adaskar Mahavidyalaya, Kaij, Beed, Maharashtra 431123, India.

Corresponding Author – Pranali Wasate

DOI - 10.5281/zenodo.19724995

Abstract:

The holobiome framework represents an integrative biological paradigm that conceptualizes soil, plant, marine, aquatic, animal, and human microbiomes as interconnected components of a unified ecological network. Expanding beyond the holobiont concept, the holobiome emphasizes cross-domain microbial interactions that regulate biogeochemical cycling, carbon sequestration, metabolic homeostasis, immune function, and ecosystem resilience. Environmental microbiomes play a pivotal role in climate regulation through soil carbon stabilization, microbial necromass formation, and marine phytoplankton–driven carbon flux. However, anthropogenic pressures including intensive agriculture, climate change, pollution, and antimicrobial overuse are destabilizing microbial networks across terrestrial and aquatic systems. Parallel disruptions in the human gut microbiome are associated with metabolic, inflammatory, and systemic disorders mediated through gut–organ axes and microbial metabolite signaling pathways.

This review synthesizes current advances in environmental microbiology, probiotic science, regenerative agriculture, and sustainable aquaculture within a systems-level perspective. It highlights the functional importance of soil probiotics, plant growth–promoting rhizobacteria, and targeted Probiotics interventions in restoring microbial balance and enhancing resilience under climate stress. Furthermore, emerging multiomics technologies and artificial intelligence–driven predictive modeling are accelerating the transition from descriptive microbiome studies to precision holobiome engineering strategies. By integrating environmental sustainability, One Health principles, and computational systems biology, the holobiome framework offers a translational roadmap for ecosystem restoration, climate mitigation, and human health optimization. Future interdisciplinary research integrating longitudinal ecological data, clinical validation, and policy implementation will be critical for maintaining microbial stability across interconnected biological domains.

Introduction:

1. Conceptual Foundation of the Holobiome:

The concept of the holobiome extends the holobiont paradigm, which defines a host organism and its symbiotic microorganisms as a functional biological unit (Baedke *et al*., 2020; Rosenberg & Zilber-Rosenberg, 2018). Early theoretical foundations emphasized that microbial symbionts significantly contribute to host physiology, development, and evolutionary adaptation (Rosenberg & Zilber-Rosenberg, 2018). Advances in metagenomics, systems biology, and high-throughput sequencing have demonstrated that microbial communities are integral to organismal and ecosystem function rather than peripheral components (Hug *et al*., 2016; Sessitsch *et al.,* 2023).

The holobiome expands this framework beyond individual hosts to encompass interconnected microbial networks linking soils,

plants, animals, aquatic systems, and humans (Berg *et al.,* 2024). Rather than viewing microbiomes as isolated compartments, this perspective recognizes ecological feedback loops among environmental and host-associated microbial systems (Banerjee & Van der Heijden, 2023). Microorganisms drive biogeochemical cycling and metabolic regulation, collectively influencing ecosystem productivity and resilience (Falkowski *et al*., 2008).

2. Microbial Systems and Ecological Interdependence:

Terrestrial ecosystems depend heavily on soil microbiota for nutrient turnover, nitrogen fixation, and carbon stabilization (Delgado-Baquerizo *et al.,* 2018; Torsvik & Øvreås, 2002). Rhizosphere-associated microbes enhance nutrient uptake and confer resistance to pathogens (Berendsen *et al*., 2012; Philippot *et al.,* 2013). Marine microbial communities regulate global carbon flux through phytoplankton-mediated photosynthesis and the biological carbon pump (Falkowski *et al*., 1998; Li *et al*., 2024).

In humans, the gut microbiome performs essential metabolic and immunological functions, including fermentation of dietary substrates into short-chain fatty acids (SCFAs) (den Besten et al., 2013; Louis & Flint, 2017). SCFAs modulate immune responses and maintain epithelial barrier integrity (Facchin *et al*., 2024; Yoo *et al*., 2020).

Cross-domain interactions illustrate that microbial imbalance in one ecological niche may propagate effects across broader biological systems (Sessitsch *et al.,* 2023). Agricultural practices that diminish soil microbial diversity may influence crop nutritional profiles, potentially shaping human gut microbiota and long-term metabolic outcomes (Banerjee & Van der Heijden, 2023).

3. Anthropogenic Disruption of the Holobiome:

Modern environmental pressures—including monoculture agriculture, agrochemical inputs, antimicrobial overuse, pollution, and climate change—are destabilizing microbial ecosystems (Tiedje *et al.,* 2022; Van Bruggen *et al*., 2018). Soil degradation reduces carbon sequestration capacity (Jansson & Hofmockel, 2020). Ocean warming alters phytoplankton dynamics and microbial-mediated climate regulation (Hoegh-Guldberg *et al.,* 2019). In humans, antibiotic exposure and dietary shifts contribute to dysbiosis associated with metabolic and inflammatory disorders (Cani *et al*., 2007; Nagpal *et al.,* 2018).

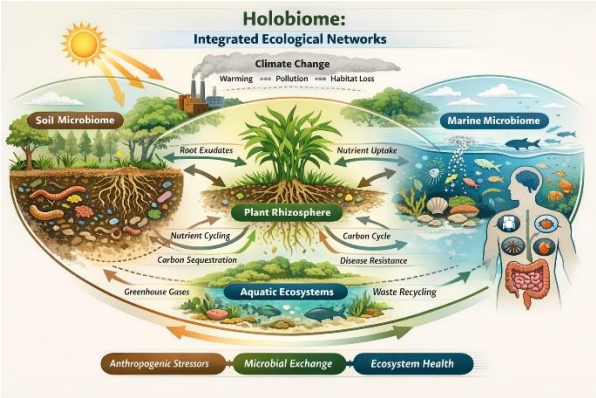

Figure 1. Integrated Holobiome Network across Environmental and Human Systems.

A conceptual representation illustrating interconnected soil, plant, marine, aquatic, and human microbiomes within the holobiome framework. Arrows depict nutrient cycling, carbon sequestration, microbial metabolite exchange, and climate feedback mechanisms. Anthropogenic stressors such as warming, pollution, and habitat loss influence microbial stability and ecosystem health.

Environmental Microbiomes and Climate Regulation:

1. Soil Microbiomes and Carbon Sequestration:

Soils represent one of the largest terrestrial carbon reservoirs, storing substantially more carbon than the atmosphere and vegetation combined (Lal, 2004; Lehmann & Kleber, 2015). The stability of this reservoir depends largely on microbial processes governing decomposition, transformation, and stabilization of organic matter (Carvalho *et al*., 2023; Six *et al.,* 2002). Bacteria and fungi decompose plant residues, converting labile carbon compounds into microbial biomass and more stable soil organic matter fractions (Kuzyakov & Blagodatskaya, 2015).

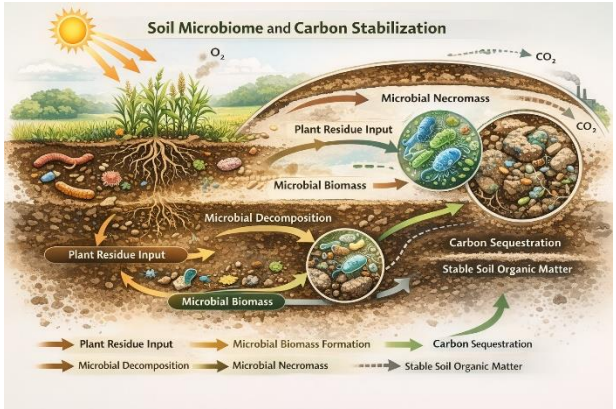

Figure 2. Soil Microbiome–Driven Carbon Stabilization Mechanisms.

Conceptual illustration of plant residue inputs, microbial decomposition, microbial biomass formation, necromass accumulation, and stabilization within soil aggregates. The diagram highlights pathways of carbon sequestration and CO_2 release under environmental influences.

Microbial necromass has been identified as a major contributor to stable soil organic matter pools, highlighting the importance of microbial turnover in long-term carbon stabilization (Weng *et al*., 2022). Soil aggregates function as microbial hotspots, protecting organic matter from rapid mineralization and enhancing carbon persistence (Lehmann & Kleber, 2015; Six *et al.,* 2002).

Agricultural management practices strongly influence microbial carbon dynamics. Conservation strategies such as reduced tillage, cover cropping, and organic amendments enhance microbial biomass and carbon stabilization (Jat *et al.,* 2013; Lv *et al*., 2024). In contrast, intensive tillage and excessive synthetic fertilizer application disrupt microbial networks and accelerate carbon mineralization (Pahalvi *et al*., 2021; Timmis& Ramos, 2021).

Recent advances in metagenomics and soil respiration modeling have improved understanding of microbial contributions to carbon turnover under warming scenarios (Bradford et al., 2008; Zhang et al., 2023). Integrating microbiome profiling with climate-smart land management offers a pathway to enhance carbon sequestration while sustaining agricultural productivity (Jansson & Hofmockel, 2020; Naylor *et al*., 2020).

2. Marine Microbiomes and Global Carbon Cycling:

Marine microbial communities play a fundamental role in global biogeochemical regulation. Phytoplankton-driven photosynthesis accounts for a substantial fraction of global carbon fixation, forming the basis of the oceanic biological carbon pump (Falkowski *et al.,* 1998; 2008). Carbon assimilated by phytoplankton can be transferred to deeper ocean layers through sedimentation and trophic interactions, enabling long-term sequestration (Boyd & Doney, 2002).

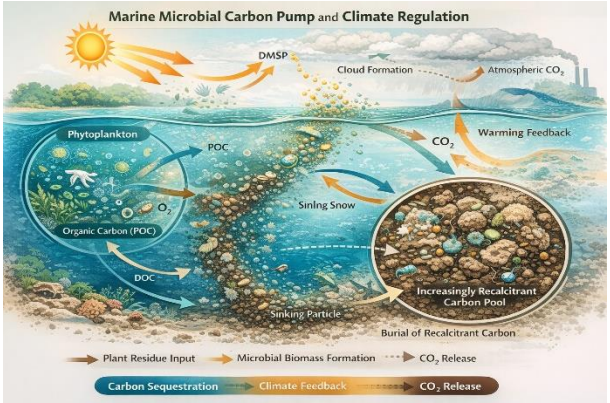

Figure 3. Marine Microbial Carbon Pump and Climate Feedback Mechanisms.

Conceptual illustration of phytoplankton-mediated CO_2 fixation, particulate organic carbon (POC) formation, microbial degradation, sinking particle flux, burial of recalcitrant carbon, and dimethyl sulfoniopropionate (DMSP)-derived atmospheric interactions. The diagram highlights carbon sequestration pathways and warming feedback loops influencing marine ecosystem stability.

Marine microbes also influence climate through the production of dimethyl sulfoniopropionate (DMSP) and its derivative dimethyl sulfide (DMS), compounds that contribute to cloud condensation processes and radiative balance (Li *et al.,* 2024; Stefels, 2000). These interactions illustrate the tight coupling between marine microbial metabolism and atmospheric regulation.

However, ocean warming, acidification, and nutrient runoff are altering microbial community composition and ecosystem stability (Hoegh-Guldberg *et al.,* 2019; Yang *et al.,* 2022). Eutrophication-associated harmful algal blooms further disrupt microbial networks and carbon cycling efficiency (Anderson *et al.,* 2012). Technological advances, including environmental DNA sequencing and predictive ecosystem modeling, are improving early detection of microbial shifts and bloom dynamics (Califano *et al.,* 2020; Ogello *et al.,* 2024).

3. Climate Feedback Loops and Microbial Stability:

Climate change and microbial ecosystem function are interconnected through reinforcing feedback mechanisms. Rising temperatures accelerate soil organic matter decomposition, increasing carbon dioxide emissions and potentially intensifying atmospheric warming (Bradford *et al.,* 2008; Jansson & Hofmockel, 2020). Temperature fluctuations can alter microbial community composition, favoring opportunistic taxa over stable carbon-stabilizing communities (Zhang *et al.,* 2023).

Vegetation loss further reduces organic carbon inputs into soils, limiting substrates available for microbial stabilization processes (Montgomery, 2007; Lal, 2015). Reduced microbial diversity weakens ecosystem resilience and buffering capacity under environmental stress (Geisen *et al.,* 2019; Tiedje *et al.,* 2022).

Similar processes occur in marine systems, where warming waters may reduce populations of efficient CO_2-fixing phytoplankton while favoring metabolic pathways associated with increased carbon release (Falkowski *et al*., 2008; Hoegh-Guldberg *et al.,* 2019). These interconnected feedbacks highlight the vulnerability of microbial-mediated carbon regulation to environmental disturbance.

Restorative strategies focused on enhancing microbial diversity and resilience—including regenerative agriculture and conservation of marine ecosystems—are essential for stabilizing environmental holobiomes (Banerjee & Van der Heijden, 2023; Tiedje *et al*., 2022).

4. Aquatic Holobionts and Sustainable Aquaculture:

Aquatic organisms function within holobiont systems shaped by microbial partnerships. Macroalgae cultivated in integrated multi-trophic aquaculture systems demonstrate host–microbe interdependence in nutrient acquisition and stress tolerance (Califano *et al.,* 2020; Chopin, 2006). Bacteria associated with algal surfaces influence morphogenesis and metabolic regulation (Ghaderiardakani *et al.,* 2024).

Comparative studies indicate that aquaculture conditions can modify microbial community structure, increasing overlap between host-associated and environmental microbiomes (Califano et al., 2020). While cultivation may enrich growth-promoting taxa, reduced host-specific microbial diversity could influence long-term resilience (Ogello *et al.,* 2024).

Advances in metagenomic profiling and predictive ecosystem modeling are enabling microbiome-informed aquaculture strategies aimed at optimizing productivity while preserving ecological balance (Darias & Mirera, 2023; Tan, 2023).

Human Microbiome and Probiotic Interventions:

1. The Gut Microbiome as a Metabolic and Immunological Regulator:

The human gastrointestinal tract harbors a highly complex microbial ecosystem composed of bacteria, archaea, fungi, and viruses (Almeida *et al*., 2019; Costello *et al.,* 2009). This community performs essential metabolic functions that complement host physiology. Fermentation of indigestible dietary fibers leads to the production of short-chain fatty acids (SCFAs), including acetate, propionate, and butyrate (den Besten *et al.,* 2013; Louis & Flint, 2017).

Butyrate plays a critical role in maintaining intestinal epithelial integrity by enhancing tight junction protein expression and mucosal barrier function (Anderson *et al.,* 2010; Facchin *et al.,* 2024). SCFAs also regulate immune homeostasis by promoting regulatory T cell differentiation and modulating cytokine production (Ohira *et al*., 2017; Yoo *et al.,* 2020). Beyond the intestine, microbial metabolites influence hepatic lipid metabolism and systemic energy regulation (Yoon *et al.,* 2023; Zhang *et al.,* 2021).

Disruption of gut microbial composition may impair barrier function, increasing intestinal permeability and facilitating translocation of lipopolysaccharide (LPS), thereby contributing to metabolic endotoxemia and low-grade inflammation (Cani et al., 2007, 2008).

2. Microbiome Axes: Gut–Skin, Gut–Lung, and Gut–Brain Interactions:

Emerging evidence supports bidirectional communication pathways linking the gut microbiome to distant organ systems.

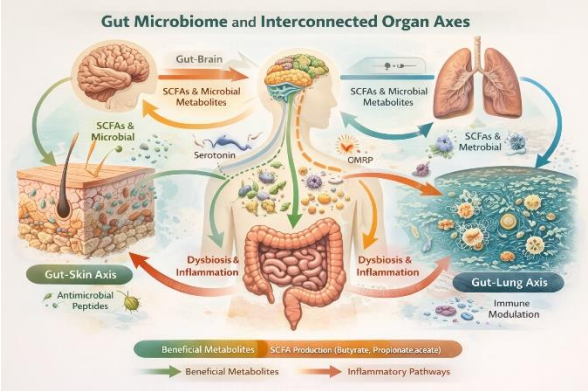

Figure 4. Gut Microbiome and Interconnected Organ Axes.

Conceptual representation of the gut–brain, gut–skin, and gut–lung axes mediated by short-chain fatty acids (SCFAs) and microbial metabolites. The diagram illustrates immune

modulation, neuroactive signaling, epithelial barrier regulation, and inflammatory pathways associated with dysbiosis.

Gut–Skin Axis: Alterations in gut microbial diversity have been associated with inflammatory skin conditions. Microbial metabolites may influence systemic inflammatory tone and cutaneous immune responses (Salem *et al.,* 2018; Widhiati *et al.,* 2021).

Gut–Lung Axis: SCFAs and microbial-derived metabolites regulate pulmonary immune responses and respiratory homeostasis (Druszczynska *et al.,* 2024; Wypych *et al*., 2019). Early-life microbial exposures are associated with reduced allergy and asthma risk, supporting the "microbial biodiversity hypothesis" (Ege *et al.,* 2011; Renz & Skevaki, 2021).

Gut–Brain Axis: Neuroactive compounds produced by gut microbes—including gamma-aminobutyric acid (GABA), serotonin precursors, and SCFAs—participate in neural signaling pathways (Dinan *et al.,* 2013; Sarkar *et al.,* 2016). These metabolites may influence stress responses, mood regulation, and cognitive processes through neural, endocrine, and immune mechanisms (Smith *et al.,* 2021; Verma *et al.,* 2024).

Collectively, these interconnected axes demonstrate that gut microbial balance influences systemic physiological networks beyond localized intestinal function.

3. Dysbiosis and Chronic Disease Associations:

Microbial imbalance, or dysbiosis, has been linked to metabolic, inflammatory, and neoplastic conditions (Nagpal *et al*., 2018; Van Hul *et al*., 2024). In obesity and insulin resistance, altered microbial composition may influence energy harvest efficiency, inflammatory signaling, and intestinal permeability (Cani *et al*., 2007; Nagpal *et al.,* 2018).

In colorectal cancer, microbial communities may contribute to tumor microenvironment modulation through production of genotoxic metabolites and pro-inflammatory mediators (García Menéndez *et al.,* 2024; Sears & Garrett, 2014). Although causality remains under investigation, accumulating evidence supports a regulatory role of microbial ecosystem balance in disease progression (Andoh & Nishida, 2023).

Emerging studies also highlight links between gut and lung dysbiosis in cancer progression, suggesting systemic microbial involvement in disease pathogenesis (Thapa et al., 2024).

4. Probiotic Interventions and Functional Outcomes:

Probiotics are defined as live microorganisms that, when administered in adequate amounts, confer a health benefit on the host (Shokryazdan *et al.,* 2017). Multi-strain probiotic formulations have demonstrated potential in restoring microbial balance, enhancing SCFA production, and improving metabolic outcomes (Bock *et al*., 2024; Bron *et al.,* 2017).

Mechanistically, probiotics may:

- Strengthen mucosal barrier integrity (Anderson *et al.,* 2010; Bron *et al.,* 2017)
- Compete with pathogenic microbes (Mahooti *et al.,* 2024)
- Modulate immune signaling pathways (Rousseaux *et al*., 2023; Yahfoufi *et al.,* 2018)
- Influence gut–brain communication through psychobiotic mechanisms (Sarkar *et al.,* 2016; Smith *et al*., 2021)

Specific strains such as *Akkermansia muciniphila* have demonstrated metabolic regulatory properties, including GLP-1 modulation and improved glucose homeostasis

(Yoon *et al.,* 2021; Zeng *et al.,* 2024). Similarly, emerging evidence supports strain-specific benefits of *Limosilactobacillusreuteri* in immune and metabolic regulation (Wang *et al*., 2024).

However, probiotic efficacy varies based on baseline microbiome composition, diet, genetics, and environmental exposures (Van Hul *et al.,* 2024). Personalized microbiome profiling may enhance therapeutic precision and response prediction (Matthewman *et al*., 2023).

5. Microbiome Ratios and Functional Indicators:

Alterations in the relative abundance of dominant bacterial phyla, particularly Firmicutes-to-Bacteroidetes ratios, have been explored as potential indicators of metabolic health (Nagpal *et al.,* 2018). However, recent research emphasizes functional metabolic capacity over taxonomic abundance alone (Van Hul *et al.,* 2024).

Metagenomic and metabolomic analyses provide deeper insight into microbial gene expression and metabolic outputs, offering more precise biomarkers of host–microbe interactions (Shi et al., 2024). Functional profiling may therefore provide a more reliable translational pathway than simplistic taxonomic ratios.

6. Translational Challenges and Future Clinical Directions:

Despite promising findings, several challenges remain in translating microbiome science into standardized clinical practice. These include variability in probiotic strain selection, limited long-term clinical trials, and inter-individual microbiome heterogeneity (Bron *et al*., 2017; Bock *et al.,* 2024).

Artificial intelligence–assisted modeling is increasingly applied to integrate multi-omics datasets and predict individualized microbial interventions (D'Urso & Broccolo, 2024; Kumar *et al.,* 2022). Such approaches may enable precision probiotic design and microbiome-based risk assessment strategies.

Within the holobiome framework, maintaining microbial balance represents not only a therapeutic approach but also a preventive strategy linking diet, environmental exposures, and systemic health outcomes (Sessitsch *et al*., 2023).

Soil Probiotics and Sustainable Agricultural Systems:

1. Rhizosphere Microbiome and Plant–Microbe Interactions:

The rhizosphere represents one of the most dynamic microbial habitats in terrestrial ecosystems, characterized by intense biochemical exchange between plant roots and soil microorganisms (Berendsen *et al.,* 2012; Philippot *et al.,* 2013). Root exudates—comprising sugars, amino acids, and secondary metabolites selectively recruit beneficial microbes that enhance nutrient acquisition and pathogen resistance (Berg *et al*., 2024; Banerjee & Van der Heijden, 2023).

Plant growth promoting rhizobacteria (PGPR) contribute to nitrogen fixation, phosphate solubilization, phytohormone production, and stress tolerance (Sessitsch *et al.,* 2023; Torsvik & Ovreas, 2002). These microbial communities form an integral component of the plant holobiont, supporting productivity while reducing reliance on synthetic agrochemicals.

Microbial diversity within the rhizosphere is influenced by plant genotype, soil type, climate conditions, and agricultural management practices (Delgado-Baquerizo *et al.,* 2018; Tiedje *et al.,* 2022). Maintenance of diverse microbial consortia enhances ecosystem resilience and nutrient cycling efficiency.

2. Soil Microbial Inoculants and Biofertilizers:

Microbial inoculants—often referred to as soil probiotics—are increasingly applied to enhance crop yield and soil health. These formulations typically contain beneficial bacterial or fungal strains capable of improving nutrient uptake and suppressing plant pathogens (Pahalvi *et al.,* 2021; Timmis& Ramos, 2021).

Biofertilizers containing nitrogen-fixing bacteria and phosphate-solubilizing microbes reduce dependence on chemical fertilizers while supporting soil carbon stabilization (Jat *et al*., 2013; Naylor et al., 2020). Additionally, arbuscular mycorrhizal fungi improve phosphorus acquisition and drought tolerance, contributing to sustainable crop production systems (Banerjee & Van der Heijden, 2023).

However, field performance of microbial inoculants can vary depending on native microbial competition and environmental conditions (Sessitsch *et al.,* 2023). Therefore, context-specific microbial formulations and regionally adapted consortia are recommended for optimal efficacy.

3. Regenerative Agriculture and Carbon Farming:

Regenerative agricultural practices emphasize restoration of soil biological integrity through reduced tillage, cover cropping, crop rotation, and organic amendments (Jansson & Hofmockel, 2020; Lal, 2015). These approaches enhance microbial biomass and promote stable soil organic matter formation (Lehmann & Kleber, 2015; Six *et al*., 2002).

Increased microbial diversity improves nutrient cycling efficiency and carbon sequestration capacity (Carvalho *et al*., 2023; Geisen *et al.,* 2019). By fostering stable microbial networks, regenerative systems contribute to climate mitigation through enhanced soil carbon storage (Bradford *et al*., 2008; Lal, 2004).

Carbon farming initiatives that integrate microbiome-based management may serve as nature-based climate solutions, aligning agricultural productivity with environmental sustainability goals (Naylor *et al.,* 2020; Tiedje *et al.,* 2022).

4. Microbiome-Driven Crop Resilience Under Climate Stress:

Climate change introduces abiotic stresses such as drought, salinity, and temperature extremes that alter soil microbial composition and plant productivity (Hoegh-Guldberg *et al*., 2019; Zhang *et al.,* 2023). Beneficial microbes can enhance plant stress tolerance by regulating osmotic balance, antioxidant systems, and hormone signaling pathways (Banerjee & Van der Heijden, 2023; Sessitsch *et al.,* 2023).

Microbial consortia designed to improve resilience under stress conditions represent a promising frontier in sustainable agriculture (Timmis & Ramos, 2021). Integrating multiomics profiling with field-based validation may facilitate the development of climate-resilient agro ecosystems (Kumar *et al.,* 2022; Matthewman *et al.,* 2023).

5. Soil–Food–Human Microbiome Continuum:

Agricultural soil quality directly influences crop nutrient density and microbial composition on plant surfaces (Berg *et al.,* 2024). These factors may indirectly shape the human gut microbiome through dietary exposure pathways (Banerjee & Van der Heijden, 2023).

Reduced soil microbial diversity associated with intensive agriculture has been hypothesized to affect food system resilience and long-term human health outcomes (Tiedje *et al.,* 2022). The holobiome framework therefore emphasizes the interconnectedness of soil, plant, and human microbiomes as a continuous ecological network. Recognizing this continuum supports the development of integrated One

Health strategies linking sustainable agriculture, environmental stewardship, and public health (Sessitsch *et al.,* 2023).

Systems Biology, Artificial Intelligence, and the Future Holobiome Framework:

1. Multi Omics Integration in Holobiome Research:

Holobiome research requires integrative approaches capable of capturing complex host–microbe–environment interactions. Advances in metagenomics, meta transcriptomics, metabolomics, and proteomics have enabled comprehensive profiling of microbial community structure and function (Almeida et al., 2019; Shi et al., 2024). These technologies allow simultaneous examination of taxonomic composition, gene expression patterns, and metabolic outputs.

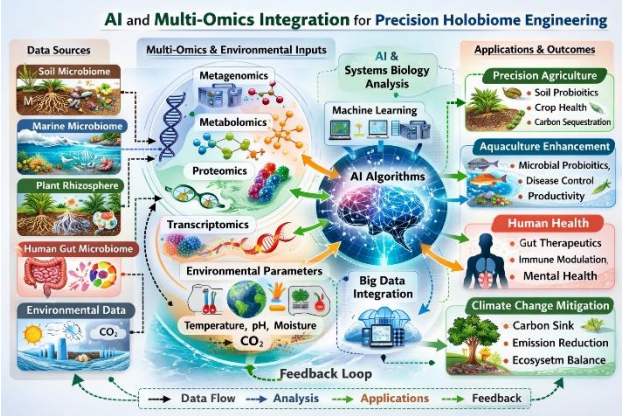

Figure 5.AI and Systems Biology Framework for Precision Holobiome Engineering.

Schematic representation of multi-omics integration (metagenomics, metabolomics, transcriptomics), environmental datasets, and AI/ML algorithms for predictive systems modeling. Applications span sustainable agriculture, aquaculture enhancement, human health therapeutics, and climate mitigation, forming a feedback-driven precision holobiome engineering loop.

Functional profiling provides deeper insights than taxonomic abundance alone, as microbial metabolic capacity often determines ecological impact (Van Hul *et al.,* 2024). Integration of environmental metadata such as soil physicochemical parameters, ocean temperature, and dietary variables further enhances interpretability (Delgado-Baquerizo *et al.,* 2018; Zhang *et al*., 2023).

Systems biology frameworks treat microbial ecosystems as dynamic networks rather than static populations (Sessitsch *et al.,* 2023). Network-based modeling reveals keystone taxa and functional hubs critical for ecosystem stability.

2. Artificial Intelligence and Predictive Microbial Modeling:

Artificial intelligence (AI) and machine learning approaches are increasingly applied to microbiome datasets characterized by high dimensionality and complex interdependencies (D'Urso & Broccolo, 2024; Kumar *et al*., 2022). These computational tools identify hidden correlations between microbial signatures and environmental or clinical outcomes.

In agriculture, predictive modeling can forecast soil carbon turnover and crop performance under climate stress (Jansson & Hofmockel, 2020; Naylor *et al*., 2020). In clinical contexts, AI-driven algorithms may stratify patients based on microbiome profiles to personalize probiotic or dietary interventions (Matthewman *et al.,* 2023; Van Hul *et al.,* 2024). Integration of multi-omics data with environmental and phenotypic datasets enables development of precision microbiome engineering strategies aimed at restoring ecological balance across domains (Shi *et al*., 2024).

3. Microbiome Engineering and Precision Interventions:

Microbiome engineering involves deliberate modulation of microbial communities to achieve beneficial functional outcomes. Strategies include targeted probiotic administration, prebiotic dietary supplementation, synbiotics, and microbial consortia transplantation (Bron et al., 2017; Shokryazdan *et al*., 2017).

In environmental contexts, engineered microbial consortia may enhance bioremediation, nutrient cycling, and carbon sequestration (Timmis & Ramos, 2021; Tiedje *et al*., 2022). Similarly, climate-adapted microbial formulations may improve crop resilience under drought and salinity stress (Banerjee & Van der Heijden, 2023). However, ethical considerations, ecological safety, and unintended consequences must be carefully evaluated before large-scale implementation (Sessitsch *et al*., 2023). Long-term ecological monitoring is essential to ensure stability and prevent disruption of native microbial networks.

4. Policy Integration and One Health Perspectives:

The holobiome framework aligns closely with One Health principles, recognizing interconnections among environmental, animal, and human health systems (Sessitsch *et al.,* 2023). Policymaking that incorporates microbiome science may guide sustainable agricultural practices, antimicrobial stewardship, and climate mitigation strategies (Tiedje *et al.,* 2022; Van Bruggen *et al.,* 2018). Investment in microbiome-informed environmental monitoring and translational research infrastructure will be crucial for bridging laboratory findings with field applications (Berg *et al.,* 2024). Collaborative global initiatives integrating microbiology, ecology, public health, and computational sciences are necessary to address systemic microbial imbalance.

Conclusion:

The holobiome represents an integrative biological paradigm that connects soil, marine, plant, animal, and human microbiomes within a unified ecological network. Microbial communities regulate carbon sequestration, nutrient cycling, immune function, and metabolic homeostasis across environmental and host-associated systems (Falkowski *et al*., 2008; Jansson & Hofmockel, 2020).

Anthropogenic pressures—including climate change, intensive agriculture, pollution, and antibiotic overuse are destabilizing microbial ecosystems at multiple scales (Hoegh-Guldberg *et al.,* 2019; Tiedje *et al.,* 2022). Restorative strategies rooted in regenerative agriculture, probiotic interventions, sustainable aquaculture, and precision microbiome engineering offer promising pathways toward resilience. Advances in multiomics technologies and artificial intelligence are accelerating the transition from descriptive microbiome studies to predictive and intervention-based frameworks (D'Urso & Broccolo, 2024; Kumar *et al.,* 2022). Within this systems-based perspective, maintaining microbial diversity and functional balance emerges as a central pillar of environmental sustainability and human health.

Future research should prioritize longitudinal, interdisciplinary studies that integrate ecological modeling, clinical validation, and policy implementation to preserve holobiome stability across interconnected biological domains.

References:

1. Almeida, A., Mitchell, A. L., Boland, M., *et al*. (2019).A new genomic blueprint of the

human gut microbiota.*Nature*, 568(7753), 499–504. https://doi.org/10.1038/s41586-019-0965-1

2. Anderson, R. C., Cookson, A. L., McNabb, W. C., *et al*. (2010). Butyrate protects against inflammatory responses in the gut. *Journal of Nutrition*, 140(10), 1774–1780.
3. Anderson, D. M., Cembella, A. D., & Hallegraeff, G. M. (2012).Progress in understanding harmful algal blooms.*Harmful Algae*, 14, 3–17.
4. Andoh, A., & Nishida, A. (2023). Gut microbiota and inflammatory diseases. *Journal of Gastroenterology*, 58(5), 345–356.
5. Baedke, J., Fábregas-Tejeda, A., & Nieves Delgado, A. (2020). The holobiont concept: A philosophical and biological analysis. *Biological Reviews*, 95(3), 543–556.
6. Banerjee, S., & Van der Heijden, M. G. A. (2023).Soil microbiomes and sustainable agriculture.*Nature Reviews Microbiology*, 21(6), 351–362.
7. Berendsen, R. L., Pieterse, C. M. J., & Bakker, P. A. H. M. (2012).The rhizospheremicrobiome and plant health.*Trends in Plant Science*, 17(8), 478–486.
8. Berg, G., Rybakova, D., Fischer, D., et al. (2024). Microbiome definition and standards.*Microbiome*, 12(1), 15–28.
9. Bock, P. M., *et al.* (2024).Multi-strain probiotics and metabolic health.*Nutrients*, 16(2), 345.
10. Boyd, P. W., & Doney, S. C. (2002).The biological pump.*Science*, 297(5580), 237–240.
11. Bradford, M. A., Davies, C. A., Frey, S. D., *et al.* (2008). Thermal adaptation of soil microbial respiration.*Ecology Letters*, 11(12), 1316–1327.
12. Bron, P. A., Kleerebezem, M., Brummer, R.-J., *et al*. (2017). Can probiotics modulate human disease? *Nature Reviews Microbiology*, 15(11), 671–680.
13. Califano, G., Castanho, S., Soares, F., *et al.* (2020).Macroalgal–bacterial interactions in aquaculture.*Frontiers in Microbiology*, 11, 593–604.
14. Cani, P. D., Amar, J., Iglesias, M. A., *et al.* (2007). Metabolic endotoxemia initiates obesity and insulin resistance. *Diabetes*, 56(7), 1761–1772.
15. Cani, P. D., Bibiloni, R., Knauf, C., *et al*. (2008). Changes in gut microbiota control inflammation in obesity. *Diabetes*, 57(6), 1470–1481.
16. Carvalho, F., *et al*. (2023).Soil microbial biomass and carbon stabilization.*Soil Biology & Biochemistry*, 175, 108–120.
17. Chopin, T. (2006). Integrated multi-trophic aquaculture.*Aquaculture*, 256(1–4), 1–13.
18. Costello, E. K., Lauber, C. L., Hamady, M., *et al.* (2009).Bacterial community variation in human body habitats.*Science*, 326(5960), 1694–1697.
19. D'Urso, F. & Broccolo, F. (2024). AI applications in microbiome research.*Bioinformatics Advances*, 4(1), vbad023.
20. Delgado-Baquerizo, M., Oliverio, A. M., Brewer, T. E., et al. (2018).Global soil bacterial diversity patterns.*Science*, 359(6373), 320–325.
21. denBesten, G., van Eunen, K., Groen, A. K., *et al*. (2013). The role of short-chain fatty acids.*Journal of Lipid Research*, 54(9), 2325–2340.
22. Dinan, T. G., Stilling, R. M., Stanton, C., &Cryan, J. F. (2013).Psychobiotics: A novel class of probiotics. *Biological Psychiatry*, 74(10), 720–726.

23. Ege, M. J., Mayer, M., Normand, A.C., *et al*. (2011). Exposure to environmental microorganisms and childhood asthma.*New England Journal of Medicine*, 364(8), 701–709.
24. Facchin, S., *et al*. (2024). Butyrate and intestinal barrier function. *Nutrients*, 16(3), 410.
25. Falkowski, P. G., Barber, R. T., & Smetacek, V. (1998). Biogeochemical controls in the ocean. *Science*, 281(5374), 200–206.
26. Falkowski, P. G., Fenchel, T., & Delong, E. F. (2008). The microbial engines of Earth's biogeochemical cycles.*Science*, 320(5879), 1034–1039.
27. Geisen, S., *et al.* (2019). Soil biodiversity and ecosystem functioning. *Nature Reviews Microbiology*, 17(6), 367–379.
28. Ghaderiardakani, F., *et al.* (2024).Bacterial control of algal morphogenesis.*Microbial Ecology*, 87(2), 415–428.
29. Hoegh-Guldberg, O., *et al.* (2019).The ocean as a solution to climate change.*Frontiers in Marine Science*, 6, 627.
30. Jansson, J. K., & Hofmockel, K. S. (2020). Soil microbiomes and climate change. *Nature Reviews Microbiology*, 18(1), 35–46.
31. Jat, R. A., *et al*. (2013). Conservation agriculture and soil health. *Field Crops Research*, 144, 1–12.
32. Kumar, R., *et al*. (2022). Machine learning in microbiome studies.*Computational Biology and Chemistry*, 97, 107630.
33. Lal, R. (2004). Soil carbon sequestration impacts. *Science*, 304(5677), 1623–1627.
34. Lal, R. (2015). Restoring soil quality.*Journal of Soil and Water Conservation*, 70(2), 55A–62A.
35. Lehmann, J., & Kleber, M. (2015).The contentious nature of soil organic matter.*Nature*, 528(7580), 60–68.
36. Louis, P., & Flint, H. J. (2017). Formation of propionate and butyrate in the human colon. *Environmental Microbiology*, 19(1), 29–41.
37. Matthewman, C. A., *et al*. (2023). Precision microbiome therapeutics. *Cell Host & Microbe*, 31(6), 875–889.
38. Nagpal, R., *et al*. (2018). Gut microbiome and obesity. *Frontiers in Microbiology*, 9, 2125.
39. Naylor, D., *et al*. (2020). Regenerative agriculture and soil carbon. *Nature Sustainability*, 3(5), 360–367.
40. Ohira, H., Tsutsui, W., & Fujioka, Y. (2017). SCFAs and immune regulation.*International Journal of Molecular Sciences*, 18(6), 1150.
41. Pahalvi, H. N., *et al*. (2021). Biofertilizers in sustainable agriculture.*Agronomy*, 11(3), 455.
42. Philippot, L., Raaijmakers, J. M., Lemanceau, P., & Van der Putten, W. H. (2013).The ecological significance of the rhizospheremicrobiome.*Nature Reviews Microbiology*, 11(11), 789–799.
43. Rosenberg, E., &Zilber-Rosenberg, I. (2018).The hologenome concept of evolution.*FEMS Microbiology Reviews*, 42(3), 283–292.
44. Sessitsch, A., *et al.* (2023). The plant microbiome and One Health.*Annual Review of Phytopathology*, 61, 157–179.
45. Shokryazdan, P., *et al*. (2017). Probiotics: From isolation to application. *Journal of Functional Foods*, 29, 24–37.
46. Six, J., Conant, R. T., Paul, E. A., & Paustian, K. (2002).Stabilization

mechanisms of soil organic matter. *Plant and Soil*, 241(2), 155–176.

47. Tiedje, J. M., *et al*. (2022). Soil microbiomes and sustainability. *Microbiome*, 10(1), 67.
48. Timmis, K., & Ramos, J. L. (2021). Microbial biotechnology for sustainable agriculture. *Microbial Biotechnology*, 14(2), 433–436.
49. Van Bruggen, A. H. C., *et al.* (2018). Environmental impacts on microbial health. *Frontiers in Microbiology*, 9, 2103.
50. Van Hul, M., *et al.* (2024).Microbiome functional profiling. *Nature Reviews Gastroenterology &Hepatology*, 21(1), 45–60.
51. Weng, Z., *et al.* (2022). Microbial necromass in soil carbon formation.*Global Change Biology*, 28(3), 1205–1218.
52. Wypych, T. P., Wickramasinghe, L. C., &Marsland, B. J. (2019). The influence of the microbiome on respiratory health. *Nature Immunology*, 20(10), 1279–1290.
53. Yoon, H. S., *et al*. (2021). Akkermansia muciniphila and metabolic regulation. *Gut Microbes*, 13(1), 1–15.
54. Zhang, Y., *et al*. (2023). Climate warming and soil microbial shifts. *Global Change Biology*, 29(4), 1021–1035.

International Journal of Advance and Applied Research
www.ijaar.co.in
ISSN – 2347-7075 Impact Factor – 8.141
Peer Reviewed Bi-Monthly
Vol. 7 No. 14 January – February - 2026

Study of Algal Diversity from Sina Kolegaon Dam

Sachin S. Chavan[1] & Tejas D. Garad[2]

Department of Botany,

S.G.R.G Shinde Mahavidyalaya, Paranda. Dist. Dharashiv(MS)

Corresponding Author – Sachin S. Chavan

DOI - 10.5281/zenodo.19725067

Abstract

Algae is one of the most diverse groups of living organism that are distributed in all across the oceans, rivers, ponds and lakes. Algae play an important role in maintaining aquatic ecosystem and form the base of food chain or food web. Algae are classified as Rhodophyta (red algae), Phaeophyta (brown algae) or Chlorophyta (green algae) depending on their nutrient, pigments and chemical composition. They are considered as a source of bioactive compounds as they are able to produce a great variety of secondary metabolites with some also a valuable food resource too. Some of the algae are also been known to be pollution indicator and help in reduction of industrial pollutants in rivers and other water sources. The present study was aimed to assess the microalgal diversity of water in Sina kolegaon dam. Dam/lakes are the important water resources & used for several purposes. The water quality of all fresh water environments is assessed by the physico-chemical & biological parameters. The present investigation is focused on the water quality and diversity of algae. The dam water is extensively used for drinking & irrigation purposes.Today the production of oxygen by algae is another reason for saying "Our lives depend on algae". Given the photosynthetic ability of algae, they are one of the major focuses for sustainable biofuel production & CO2 consumption. With the above contribution of algae, an attempt was made to diversify the algae species that are in and around Sina Kolegaon dam and document the presence of valuable algal species. A total of 18 algal species were partially identified namely Spirogyra, Oedogonium, Euglena Sangunie, Cyanobacteria, Oscillatoria, Chamydomonas, Mougeotia, Auxospore,Chroococcus minor, Chlorophyta and Oedogonium areolatus species are found.

Keywords**: **Ecosystem, Metabolites, Biofuel etc.

Introduction:

In Marathwada region there are many dams, lake on different rivers, but less attention has been paid to presence of algae in water. In present project the Sina- Kolaegaon dam is near the paranda which is 15 kms from paranda. Mandayam Osuri Parthasarathy lyengar (15 Dec. 1886-10 Dec.1963) was a prominent Indian botanist. He is known as "Father of algology in India". The term algea (Latin-Seaweeds) was first introduced by Linnaeus in 1753, meaning the Hepaticeae. Algea are aquatic, plant like organism. The Algea can be categorized into 7 types- each are distinct sizes , functions, color, the different divisions are Euglenophyta (Euglenoids), Chrysophyta (Golden-brown algae & Diatoms), Pyrrophyta (fire algae), Chlorophyta (Green algae), Rnodophyta (Red algae), Paeophyta (Brown algae), Xanthophyta (Yellow green algae) Sina-Kolegaon Dam, is an earthfill dam on local river sina near paranda town of Dharashiv district from Maharashtra state.

Material and Methods:

Collection of Samples:

To study algal biodiversity of Sina Kolegaon Dam, 6 different sites of backwater located in Paranda tehsil area of Dharashiv district have been selected. Algal samples were collected from different sites from 02 Dec. 2025 to 10 Feb 2026. Acid washed collection bottles were used for collection of algal samples. Firstly observed the dam and area occupying by water. first going on light house which is made in water and observe all surrounded water standing on it because it made in between the water and take photos of dam water for project collection.Water samples were collected from each side of dam for collection. Water samples were collected at morning section.Samples were collected from corners,edges or shadow places of dam water where greenish water is present therefore easily algae are found in samples. Floating, Planktonic submerged and attached epiphytic algal samples were collected separately in collection bottles.

Identification and Preservation of Algae Samples:

Firstly, collected samples cleaned, solid particles are removed from sample and samples preserved in refrigerator for further study. Each sample were collected in a separate bottle and labelled like spot-1, spot-2, spot-3 etc. Some thread like green part seen in water which is first collected in glass and then transfer in the sample bottle for collection. Yellowish green part also seen on the stone/rocks which also collected in sample bottle. Identification of the algae samples were carried out mostly through microscopically. Fresh as well as preserved algal forms were observed thoroughly under research microscope and identified with the help of standard literature on algae like Plant Diversity Laboratory Manual by Asst. Prof. Dr. Ismail Eker.

Results and Discussions:

The study in different water bodies of Sina-kolegaon Dam showed a rich diversity of filamentous algae belonging to varies classes. The different site were also containing a large number of micro-algae, flagellated phytoplankton and diatoms. Some of the algae that were identified during the course of study are *Spirogyra, Oedogonium, Euglena Sanguine, Cyanobacteria, Oscillatoria, Chlamydomonas, Mougeotia, Auxospore, Chroococcus Minor, Micrasterias, Macrandrous, Pediastrum tetras, Closteriumcornu, Euglenagracils, Phacusonyx, Trachelomonasallia, Stigeoclonium* and *Gloeocapsa* etc.

Conclusion:

Algae are integral part of the ecosystem that serves for various purposes such as fodder, photosynthesis and also as waste management. Sina-Koleagon dam is one of the most drinking water sources for Kolgaon, Kaundaon, Donja, gaon and other neighbour villages. A rich source of various forms of filamentous algae, therefore study on such algae can play an important role in ecological management and also in keeping a check on the pollution level in the water bodies.

Table No.1: Enlisted Algae from Study Area

Sr. No.	Name of the algae	Study Stations					
		S1	S2	S3	S4	S5	S6
	Class: Zygnematophyceae **Order: Zygnematales** **Family: Zygnemataceae**						
1.	*Spirogyra*	+	+	+	+	+	+
2.	*Mougeotia*	+	+	+	+	+	+
	Class: Zygnematophyceae **Order: Desmidiales** **Family: Desmidiaceae**						
3.	*Micrasterias*	+	+	+	+	+	+
	Family-Closteriaceae						
4.	*Closteriumcornu*	+	-	+	+	-	+
	Class: Euglenida Order: Euglenales **Family:Euglenaceae**						
5.	*Euglena sanguine*	+	+	+	+	+	+
6.	*Euglena gracilis*	+	+	+	+	+	+
	Family-Phacaceae						
7.	*Phacusonyx*	+	+	+	+	-	-
	Class: Chlorophyceae **Order: Oedogoniales** **Family: Odogoniales**						
8.	*Oedogonium*	+	+	+	+	+	+
	Family: Oedogoniaceae						
9.	*Macrandrous*	+	+	-	+	+	+
	Order: Chlamydomonadales **Family: Chlamydomonadaceae**						
10.	*Chlamydomonas*	+	+	+	+	+	+
	Family-Chaetophoraceae						
11.	*Stigeoclonium*	+	+	+	+	+	+
	Order: Sphaeropleales **Family: Hydrodictyaceae**						
12.	*Pediastrumtetras*	+	+	+	+	-	+
	Class: Cyanophyceae **Order: Chroococcales** **Family: Chroococcaceae**						
13.	*Chroococcusminor*	+	+	+	+	+	+
14.	*Gloeocapsa*	+	+	+	+	+	+
	Order: Oscillatoriales **Family: Oscillatoriaceae**						
15.	*Oscillatoria*	+	+	+	+	+	+
	Class- sericytochromatia						
16.	*Cyanobacteria*	+	-	+	-	+	+
	Class- Bacillariophyceae	-	-	-	-	-	-
17.	*Auxospore*	-	+	+	+	+	-
	Class: Euglenida Order-Euglenales **Family: Euglenaceae**						
18.	*Trachelomonasallia*	+	+	-	+	+	+

+ means present

– means absent

Table:2: Collection site

Sr. No	Sample No.	Collection Site of Dam
1	S1	South
2	S2	South
3	S3	West
4	S4	West
5	S5	North
6	S6	North

Sina kolegaon dam view

Sample collection point

Plate.No.1: Diversity of Algal specimen from Sina Kolegaon Dam

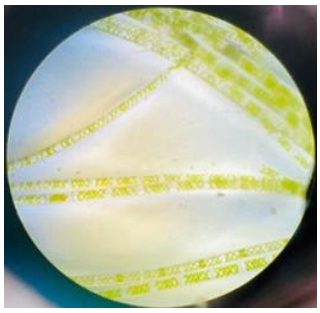

1.*Spirogyra*

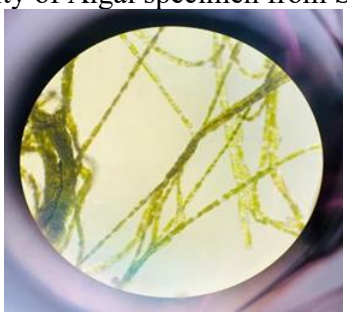

2.*Oedogonium*

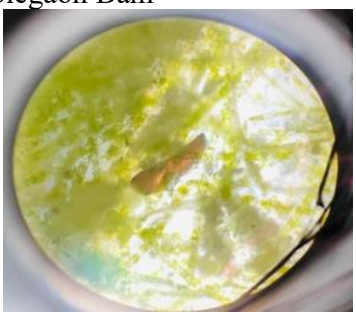

3. *Euglena Sanguine*

4.*Cyanobacteria*

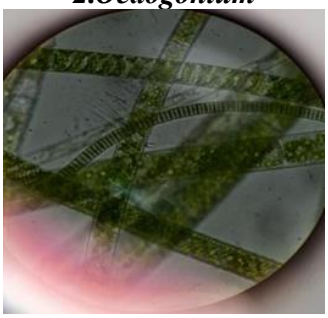

5. *Oscillatoria*

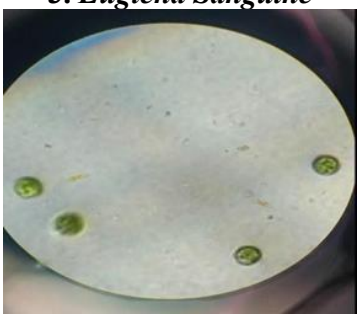

6.*Chlamydomonas*

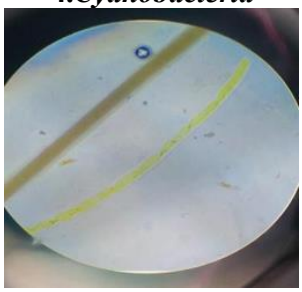

7.*Mougotia*

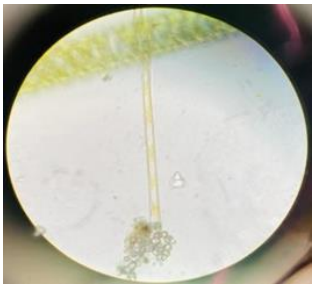

8.*Auxospore*

9.*Choococcus Minor*

Plate.No.2: Diversity of Algal specimen from Sina Kolegaon Dam

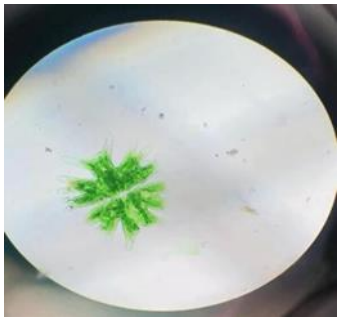

10.*Micrasterias*

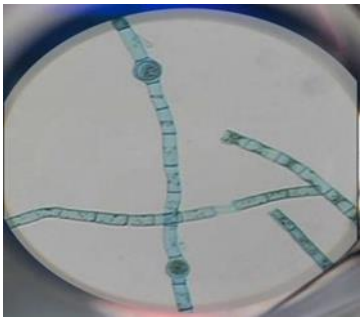

11.*Macrandrous*

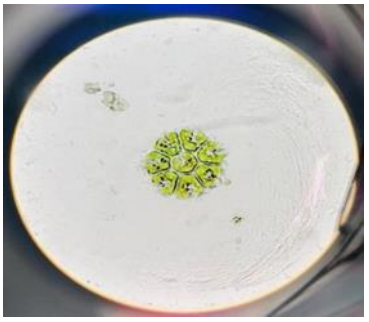

12.*Pediastrum* tetras

13.*Closterium cornu*

14.*Euglena gracilis*

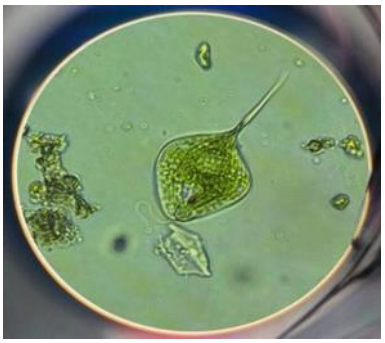

15.*Phacusonyx*

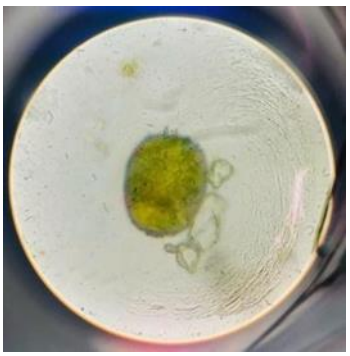

16.*Trachelomonas allia*

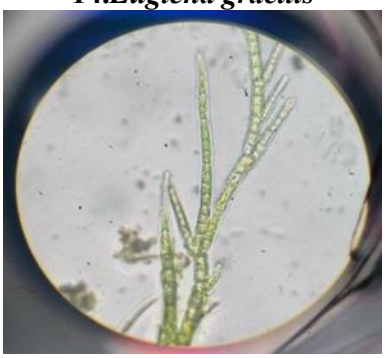

17.*Stigeoclonium*

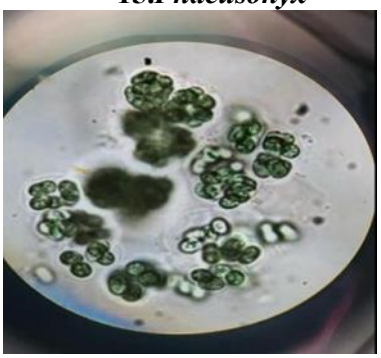

18.*Gloeocapsa*

Acknowledgement: The authors are thankful to our college Principal, S. G. R. G. Shinde College, Paranda for giving us moral support and providing the laboratory facilities.

References:

1. Ashtekar, P. V. (1980).“Studies on fresh water algae of Aurangabad district. Ph.D.thesis, Marathwada University, Aurangabad”.
2. Bhoge, O.N. Narkhede, P.N. and Ragothaman, G. (2007). “Genus Phormidium and Lyng by a from the soil of Suki dam Jalgaon district,(M.S.)”.Proc.Nat.Symp.onrecent.
3. Trends in algal biotechnology and biodiversity, Ed.S.S.Patil, Dhanaji Nana Mahavidyalaya, Faizpur. pp. 104-106.
4. Bhoge,O.N. Narkhede,P.N. and Ragothaman,G.(2007).“Cyanophyceae from the Suki dam siol Jalgaon district, M.S.)”. Proc.Nat. Symp.on recent trends in algal biotechonogy andbiodiversity, Ed. S.S. Patil, Dhanaji Nana Mahavidyalaya, Faizpur. pp. 68-80.

5. DesikacharyT.V.(1959).“Cyanophyceae” I.C.A.R.Monographas on Algae NewDelhi.pp.680.
6. Kolte,S.O. and Goyal,S.K. (1985).“Distributional pattern of blue green algae in rice field soils of Vidarbha region of Maharashra”Phycos ,24(1 and 2):156-162.
7. Kottawar,S.T. and Panchpande,R.R. (1983).“Soil algae of banana fields of Jalgaon district”. Adv.Appl. Phycol.1:211-212.
8. Marathe,K.V.(1967).“Studies on soil algae of India-I. Soil algae from the cultivated fields of Dhule (Maharashtra State)” J. Univ. Bombay.35: 100-105.

International Journal of Advance and Applied Research
www.ijaar.co.in
ISSN – 2347-7075 Impact Factor – 8.141
Peer Reviewed Bi-Monthly
Vol. 7 No. 14 January – February - 2026

Adaptive Strategies for Agricultural Sustainability in Changing Climates

Smita Basole
Dept. of Botany, Rajmata Jijau Mahavidyalaya, Kille–Dharur, Dist-Beed. (M.S.)
Corresponding Author – Smita Basole
DOI - 10.5281/zenodo.19725131

Abstract:

Recent years have seen many efforts to increase the agricultural production. Those improvements were achieved through sustainable techniques and practices. While using the modern techniques, we observe they are the causes for degradation of natural resources. India is one of the countries having agroclimatic zones with diversified seasons, crops, and farming systems. At the same time, it is also a vulnerable section of climatic changes. It was reported that 2/3 of the sown area is drought-prone and about 40 million hectares are flood-prone. The nation faces many prominent effects of climatic changes. To minimize these effects, we must adapt integrated systems. Sustainable agriculture holds great potential to replenish ecological damage, to improve agricultural productivity, to meet global & national food security, and to improve farmers' livelihoods. Modern sustainable methodology helps to reduce vulnerability with uncertain climatic conditions. But sustainable agriculture alone will not be sufficient to reduce agro-eco-socio problems.

Keywords: Sustainable Agriculture, Food Security, Climatic Changes, Climate-Smart Agriculture

Introduction:

The nation faces many prominent effects of climatic changes. As global temperatures climb, widespread shifts in weather systems occur, making events like droughts, hurricanes, and floods more intense and unpredictable. Extreme weather events that may have hit just once in our grandparents' lifetimes are becoming more common in ours. To minimize these effects, we must adapt integrated systems. Sustainable agriculture holds great potential to replenish ecological damage, to improve agricultural productivity, to meet global & national food security, and to improve farmers' livelihoods. Climate change is our planet's greatest existential threat. If we don't limit greenhouse gas emissions from the burning of fossil fuels, the consequences of rising global temperatures include massive crop and fishery collapse, the disappearance of thousands of species, and entire communities becoming uninhabitable. The transition to climate-resilient practices is essential for securing global food supplies while addressing environmental shifts. Another most threatening aspect is about melting ice caps of the Earth. The effects of climate change are most apparent in the world's coldest regions—the poles. The Arctic is heating up twice as fast as anywhere else on earth, leading to the rapid melting of glaciers and polar ice sheets, where a massive amount of water is stored. Sea level rise also harms the environment, as encroaching seawater can both erode coastal ecosystems and invade inland freshwater aquifers, which we rely on for agriculture and drinking water. Before evolving an effective plan to support farmers on a large scale regarding climate risk management, it is crucial to understand climate risk, risk adaptation, and its possible impacts at the local farm level in a country where food security faces a massive

threat due to climate-related vulnerability. Farmers are expected to understand the recommendations regarding climate-smart technologies, the advantages of technology adoption, and the support provided by the government for adopting the technologies by extension officers in their several sessions with the farmers group. The number of serious and extreme drought events is increasing, causing a serious threat to ecosystems, food security, livelihood security, social stability, and sustainable development. The Marathwada region of India is highly vulnerable to the impacts of drought. Historically, stressed natural resources due to unfavourable weather, monsoons, and natural calamities resulted in crop failures leading to food shortages that made serious impacts on the civilization.

As defined by the FAO, **Climate-Smart Agriculture (CSA)** provides a roadmap for this transformation, focusing on a "triple win" that is optimizing farm output and income, enhancing systemic resilience, and reducing atmospheric greenhouse gases. Agriculture is the foundation of the civilization, culture, and heritage of India. Agriculture in India is a complex mosaic of distinct agro-ecosystems, differentiated by climatic conditions, soil, vegetation, and other natural features. About half of the Indians derive their livelihood from agriculture and allied activities. It is one of the oldest systems in the world, characterized by its diversity and heterogeneity, unorganized and stressed on account of natural and anthropogenic vagaries from 'seed to market.'

Effective adoption of climate-smart technology and higher food security for farmers depends on their trust in the advice of climate-smart technology adoption. Adoption levels declined at each following phase of the impact pathway, defined as a "tunnel of attrition in adoption" by Lambrecht et al. (2011), which was cited by A. A. Reddy (2019) in his article. Facility level was divided by several steps that relate to inputs, activities, and outputs. At this level, it is important to prepare the farmer firstly by disseminating proper knowledge and guidelines on advantages like production efficiency and the impact on income and/or food security of the adoption of climate-smart technology. Furthermore, delayed supply of quality inputs and limited access to sophisticated inputs like stress-tolerant seeds can limit the fondness of climate-smart technology adoption among farmers, thereby affecting the overall food security scenario.

Mixed farming systems, which combine crops, livestock, and sometimes fisheries or forestry, represent one of the most effective diversification strategies. Diversified farming systems create multiple protective mechanisms. Different crops respond differently to weather extremes, so if drought damages one crop, another might survive. The benefits extend to soil health and water management. Integrating trees into farming systems through agroforestry provides erosion control, microclimate regulation, and additional income from timber or fruit. Healthy soil forms the foundation of climate-resilient agriculture. Sustainable land management practices restore soil fertility, improve water retention, and enhance the land's capacity to support productive farming even under climate stress. Soil degradation currently affects about one-third of the world's agricultural land, undermining food production for more than 3 billion people. Sustainable soil management practices can prevent, slow, or stop degradation while helping lands adapt to climate change.

Farmers maintain crop residues on fields as mulch, protecting soil from erosion while adding organic matter as residues decompose.

Crop rotation alternates different plants in sequence, disrupting pest cycles and preventing nutrient depletion. Cover crops planted between main crops protect bare soil from erosion, suppress weeds, and add nitrogen when legumes are used. These practices work together to build soil organic matter, which enhances water retention and provides habitat for beneficial soil organisms. Conservation agriculture reduces soil disturbance through minimal or no-till farming, preserving soil structure and beneficial organisms.

Agroforestry integrates trees into agricultural landscapes, offering multiple benefits. Tree roots stabilize soil on slopes, reduce erosion, and improve water infiltration. Trees also modify microclimates, reducing temperature extremes and wind speeds that can damage crops. Farmers gain additional income from tree products while improving overall land productivity. Efficient water management becomes increasingly critical as rainfall patterns become less predictable. Water harvesting structures capture runoff during intense rains, storing it for use during dry periods. Contour farming and terracing on slopes slow water movement, reducing erosion while increasing soil moisture. Studies from Northeast India demonstrate positive effects of soil conservation on both food security and environmental outcomes.

Additionally, it is suggested that non-governmental organizations and the social-business sector extend support to farmers struggling to sustain agricultural production. Government policymakers are urged to devise plans aimed at disseminating technological knowledge and services to ensure equitable access for economically disadvantaged farmers. Failure to provide such support may lead to an increase in the numbers of migrant and homeless populations in urban areas, thereby posing a substantial threat to the country's food security. It is crucial to first prepare farmers by disseminating proper knowledge and guidelines on the advantages, such as production efficiency and impact on income, of adopting these technologies. We can check the robustness of the estimated impact of each climate-smart strategy on each dimension of food security within the matched sample by using PSM. The PSM results show that farmers who adopted climate-smart technologies in their farmland are enjoying more calorie intake and food stock availability and are able to bear more expenses for food purchases. This was unquestionably a stable food-secure situation for this marginal and peripheral group of farmers. The results are vital in the sense that if farmers could be able to adopt more strategies simultaneously, then it would be promising for sustainable food security. The experience of drought events, which resulted in loss of crops, as well as extreme rainfall events that have occurred in some regions of Marathwada, indicates that the region is vulnerable to climate change impacts. Rising temperatures are compounding the existing water-shortage problem through accelerated evapotranspiration and problems associated with urban water over-extraction and depletion and competition for water resources, threatening the viability of agriculture, particularly for small and marginal farmers.

Conclusion:

In the Marathwada region, agricultural advancements have increased production but also degraded natural resources. Making Climate-Smart Agriculture (CSA) essential due to escalating drought frequency and temperature fluctuations. The adoption of CSA faces significant barriers, including delayed input supply, limited technology access, and lack of

localized knowledge among smallholder farmers, creating a critical "tunnel of attrition." Sustainable agriculture alone cannot solve socio-economic issues, requiring government policy prioritizing equitable access to technology and NGO support. Successful adoption of multiple climate-smart strategies simultaneously leads to improved food security and financial stability.

References:

1. Athare, A. S., Patil, S. V., & Pawar, R. B. (2024). Agricultural vulnerability in Maharashtra: An integrated framework analysis. International Journal of Innovative Research in Technology, 11(2), 145–152.
2. Food and Agriculture Organization. (2025). Climate-smart agriculture: Building resilience in smallholder farming systems. FAO Publications. www.fao.org.
3. Government of Maharashtra. (2025). Maharashtra project on climate resilient agriculture (PoCRA): Phase II implementation framework. Department of Agriculture.
4. Khetwani, S., Singh, R. B., & Moin, K. (2020). Impact of drought, farmers' adaptation strategies, and administrative mitigation measures in the Marathwada region, India. *Environmental & Socio-economic Studies*, *8*(2), 1–11. doi.org.
5. Mishra, R. K., & Deshmukh, V. P. (2025). Integrative strategies for sustainable agriculture in the face of climate change. Nature Sustainability, 8(12), 1102–1115. doi.org.
6. Patel, S., & Shinde, G. (2024). Climate change impact on agriculture in Maharashtra: A review of soybean and cotton yields. Journal of Agrometeorology, 26(2), 88–95.
7. Sarkar, A., & Gupta, N. (2026). Mitigation and adaptation strategies in climate-smart agriculture: A global review. ScienceDirect: Agricultural Systems, 214, 103842. doi.org.
8. Sharma, P., & Kumar, A. (2025). Farmers' adaptation strategies to climate change: A ranking of effective field practices. Frontiers in Climate, 7, 895421. doi.org.
9. World Bank. (2025). Project appraisal document: Scaling climate-resilient technologies in Western India. World Bank Group.
10. Zong, X., Liu, X., Chen, G., & Yin, Y. (2022). A deep-understanding framework and assessment indicator system for climate-resilient agriculture. Ecological Indicators, 136, 108597. doi.org
11. https://www.un.org/en/climatechange/early-warnings-for-all
12. https://climatepromise.undp.org/news-and-stories/how-climate-information-and-early-warning-systems-protect-lives-and-economies
13. https://epar.evans.uw.edu/when-do-farmers-adopt-and-respond-to-early-warning-systems/
14. https://www.fao.org/family-farming/detail/en/c/1656782 /
15. https://link.springer.com/article/10.1007/s11111-025-00493-8
16. https://www.fao.org/climate-smart-agriculture-sourcebook/production-resources/module-b7-soil/chapter-b7-1/en/
17. https://10insightsclimate.science/year-2022/sustainable-land-use-is-essential-to-meeting-climate-targets/

International Journal of Advance and Applied Research
www.ijaar.co.in
ISSN – 2347-7075 Impact Factor – 8.141
Peer Reviewed Bi-Monthly
Vol. 7 No. 14 January – February - 2026

HR-LCMS-Based Phytochemical Characterization of Bark Drugs from Selected Medicinal Plants

S. P. Kshirsagar & M. A. Kare
Department of Botany, Pratishthan Mahavidyalaya, Paithan Dist: Chhatrapati Sambhajinagar (M.S.)
Corresponding Author – S. P. Kshirsagar
DOI - 10.5281/zenodo.19755457

Abstract:

Bark drugs constitute an important component of traditional medicine and are widely used in Ayurvedic, Unani, and folk healthcare systems. The present investigation aims to evaluate and characterize the phytochemical composition of bark drugs obtained from selected medicinal plants of the Marathwada region, Maharashtra, with special emphasis on species belonging to the genus Ficus*. The study integrates pharmacognostic evaluation, preliminary phytochemical screening, and advanced High-Resolution Liquid Chromatography–Mass Spectrometry (HR-LCMS) analysis to identify bioactive constituents. Bark samples of* Ficus amplissima*,* F. arnottiana*,* F. benjamina*,* F. carica*,* F. elastica*,* F. hispida*, and* F. microcarpa *were collected, authenticated, processed, and extracted using suitable solvents. HR-LCMS profiling revealed the presence of pharmacologically significant compounds such as quercetin, rutin, kaempferol, gallic acid, caffeic acid, lupeol, betulinic acid and ursolic acid. The detected phytoconstituents exhibit antioxidant, anti-inflammatory, antidiabetic, antimicrobial and hepatoprotective activities, supporting the ethnomedicinal relevance of these bark drugs. The study establishes chemical fingerprints for each species and provides scientific validation for their traditional therapeutic use, contributing to standardization, quality control and future drug discovery.*

Keywords: Bark drugs,* Ficus*, HR-LCMS, Phytochemical Profiling, Medicinal Plants

Introduction:

Medicinal plants remain a primary source of healthcare for a large proportion of the global population, particularly in developing countries where traditional medicine is deeply rooted in cultural practices (WHO, 2013). Among various plant parts, bark is considered pharmacologically important due to its ability to accumulate diverse secondary metabolites such as flavonoids, tannins, alkaloids, phenolic acids, and triterpenoids, which play a defensive and therapeutic role (Evans, 2009). Bark drugs are extensively used in Ayurvedic, Unani, and folk medicine systems for the treatment of inflammation, diabetes, gastrointestinal disorders, infections, and liver ailments (Kokate et al., 2014). However, the increasing demand for herbal medicines has raised concerns regarding adulteration, misidentification, and lack of standardization, emphasizing the need for detailed pharmacognostic and phytochemical evaluation.

The genus *Ficus* (family Moraceae) comprises more than 800 species distributed throughout tropical and subtropical regions of the world. Several *Ficus* species are traditionally used in Indian medicine for their antioxidant, antidiabetic, anti-inflammatory, and antimicrobial properties (Mandal et al., 2010; Joseph & Raj, 2011). Despite their extensive ethnomedicinal use, comprehensive chemical profiling of bark drugs using advanced analytical techniques remains limited.

High-Resolution Liquid Chromatography–Mass Spectrometry (HR-LCMS) has emerged as a powerful tool for rapid and accurate identification of phytoconstituents, allowing detection of both major and minor metabolites (Wolfender *et al*., 2015). Therefore, the present study was undertaken to characterize the phytochemical composition of bark drugs from selected *Ficus* species of the Marathwada region using HR-LCMS and to correlate the findings with their traditional medicinal claims.

Material and Methods:

Study Area:

The Marathwada region of Maharashtra is characterized by semi-arid climatic conditions and diverse vegetation. The region supports several medicinally important plant species adapted to varied ecological niches.

Collection and Authentication of Plant Material:

Fresh bark samples of *Ficus amplissima*, *F. arnottiana*, *F. benjamina*, *F. carica*, *F. elastica*, *F. hispida*, and *F. microcarpa* were collected from different localities of Marathwada during the appropriate season. The collected specimens were authenticated using standard floras and taxonomic keys (Cooke, 1967).

Preparation of Bark Extracts:

The bark samples were washed thoroughly, shade-dried, and powdered using a mechanical grinder. The powdered material was extracted with methanol using a Soxhlet apparatus. The extracts were filtered and concentrated under reduced pressure and stored at 4 °C until analysis.

Preliminary Phytochemical Screening:

Qualitative phytochemical tests were performed to detect the presence of alkaloids, flavonoids, phenols, tannins, saponins, glycosides, and triterpenoids using standard methods described by Harborne (1998) and Kokate *et al*. (2014).

HR-LCMS Analysis:

Methanolic extracts were subjected to HR-LCMS analysis under optimized chromatographic and ionization conditions. Compounds were identified based on retention time, molecular ion peaks (m/z), and comparison with spectral databases and published literature.

Results and Discussion:

Preliminary phytochemical screening confirmed the presence of flavonoids, phenolic compounds, tannins, alkaloids, saponins, and triterpenoids in all bark extracts. The presence of these metabolites supports the therapeutic potential of *Ficus* bark drugs, as reported earlier by Mandal et al. (2010).

HR-LCMS analysis revealed a wide range of bioactive compounds with distinct retention times, indicating chemical diversity among the studied species. Flavonoids such as quercetin, rutin, and kaempferol were commonly detected and are known for their strong antioxidant and anti-inflammatory activities (Panche et al., 2016). Phenolic acids including gallic acid and caffeic acid contribute to antimicrobial and antidiabetic effects by modulating oxidative stress pathways (Rice-Evans et al., 1997).The presence of triterpenoids such as lupeol, betulinic acid, and ursolic acid is of pharmacological significance, as these compounds exhibit hepatoprotective, anti-inflammatory, and anticancer activities (Saleem, 2009). Species-specific HR-LCMS profiles

generated in this study serve as chemical fingerprints that can be used for authentication and quality control of bark drugs.The observed phytochemical diversity validates the traditional use of *Ficus* bark in indigenous medicine and highlights the importance of advanced analytical techniques in herbal drug research (Wolfender *et al*., 2015).

Table 1. HR-LCMS Profile of *Ficus amplissima* Bark Extract

RT (min)	Compound Name	Molecular Formula	m/z	Phytochemical Class	Pharmacological Relevance
1.33	Melibiose	$C_{12}H_{22}O_{11}$	342.11	Disaccharide	Prebiotic, antioxidant
2.34	2(N)-Methyl-norsalsolinol	$C_{10}H_{13}NO_2$	179.09	Alkaloid	Neuroactive
7.86	Marchantin A	$C_{28}H_{24}O_5$	440.16	Bisbibenzyl	Antimicrobial
9.51	Cinnamyl cinnamate	$C_{18}H_{16}O_2$	264.11	Phenylpropanoid	Anti-inflammatory
10.66	5-Hydroxypropafenone	$C_{21}H_{27}NO_4$	357.19	Phenolic drug	Antiarrhythmic

Table 2. HR-LCMS Profile of *Ficus hispida* Bark Extract

RT (min)	Compound Name	Molecular Formula	Phytochemical Class	Reported Activity
1.34	**Gerberinol**	**$C_{21}H_{16}O_6$**	Flavonoid (Polyphenolic compound)	Antioxidant
7.84	**Procyanidin B7**	**$C_{30}H_{26}O_{12}$**	Proanthocyanidin (Condensed tannin / Flavonoid)	Cardioprotective
8.09	**(±)-Carnegine**	**$C_{16}H_{21}NO_3$**	Isoquinoline alkaloid	Neuroactive
10.03	**Ryanodine**	**$C_{25}H_{35}NO_8$**	Diterpenoid alkaloid	Muscle relaxant

Table 3. HR-LCMS Profile of *Ficus arnottiana* (Miq.) Miq. Bark Extract

RT (min)	Compound Name	Molecular Formula	m/z	Phytochemical Class	Reported Pharmacological Activity
1.34	3β,6β-Dihydroxynortropane	$C_7H_{13}NO_2$	143.09	Tropane alkaloid	Neuroactive
1.45	Amadori compound	$C_{10}H_{19}NO_7$	265.11	Glycosylamine	Antioxidant
2.15	Lotaustralin	$C_{11}H_{19}NO_6$	261.11	Cyanogenic glycoside	Antimicrobial
7.86	Procyanidin B7	$C_{30}H_{26}O_{12}$	578.13	Flavonoid	Cardioprotective
8.26	Phthalocyanine	$C_{32}H_{18}N_8$	514.16	Macrocyclic compound	Anticancer (reported)
8.47	5-Heptyltetrahydro-2-oxo-3-furancarboxylic acid	$C_{12}H_{20}O_4$	228.13	Furanone	Antimicrobial

Table 4. HR-LCMS Profile of *Ficus benjamina* L. Bark Extract

RT (min)	Compound Name	Formula	m/z	Class	Pharmacological Relevance
1.13	Esprocarb	$C_{15}H_{23}NOS$	265.15	Carbamate	Antimicrobial
1.32	3β,6β-Dihydroxynortropane	$C_7H_{13}NO_2$	143.09	Alkaloid	Neuroactive
7.45	Cynaroside A	$C_{21}H_{32}O_{10}$	444.19	Flavonoid glycoside	Hepatoprotective
7.63	Leonuriside A	$C_{14}H_{20}O_9$	332.11	Iridoid glycoside	Anti-inflammatory
9.50	Fluvoxamine	$C_{15}H_{21}F_3N_2O_2$	318.15	SSRI derivative	Neuroactive
18.95	Squamostatin A	$C_{37}H_{66}O_8$	638.47	Acetogenin	Anticancer

Table 5. HR-LCMS Profile of *Ficus carica* L. Bark Extract

RT (min)	Compound Name	Formula	m/z	Class	Biological Activity
1.38	3β,6β-Dihydroxynortropane	$C_7H_{13}NO_2$	143.09	Alkaloid	Neuroactive
2.27	2(N)-Methyl-norsalsolinol	$C_{10}H_{13}NO_2$	179.09	Isoquinoline alkaloid	Antioxidant
5.99	Matrine	$C_{15}H_{24}N_2O$	248.18	Alkaloid	Antimicrobial
7.96	Thesinine 4′-O-glucoside	$C_{23}H_{31}NO_8$	449.20	Flavonoid glycoside	Anti-inflammatory
10.26	Samin	$C_{13}H_{14}O_5$	250.08	Indole derivative	Antioxidant
12.31	Isoamericanol A	$C_{18}H_{18}O_6$	330.10	Lignan	Anticancer

Table 6. HR-LCMS Profile of *Ficus elastica* Roxb. ex Hornem. Bark Extract

RT (min)	Compound Name	Formula	m/z	Class	Pharmacological Importance
1.36	3β,6β-Dihydroxynortropane	$C_7H_{13}NO_2$	143.09	Alkaloid	Neuroprotective
1.36	Gerberinol	$C_{21}H_{16}O_6$	364.09	Flavonoid	Antioxidant
7.71	Leonuriside A	$C_{14}H_{20}O_9$	332.10	Glycoside	Anti-inflammatory
9.35	Allixin	$C_{12}H_{18}O_4$	226.11	Organosulfur compound	Antimicrobial
11.33	Kamahine C	$C_{14}H_{20}O_5$	268.12	Diterpenoid	Anti-inflammatory
13.25	Isoferulic acid	$C_{10}H_{10}O_4$	194.05	Phenolic acid	Antioxidant

Table 7. HR-LCMS Profile of *Ficus microcarpa* L.f. Bark Extract

RT (min)	Compound Name	Formula	m/z	Phytochemical Class	Activity
1.34	3β,6β-Dihydroxynortropane	$C_7H_{13}NO_2$	143.09	Alkaloid	Neuroactive
1.36	Gerberinol	$C_{21}H_{16}O_6$	364.09	Flavonoid	Antioxidant
5.09	Neuraminic acid	$C_9H_{17}NO_8$	267.09	Sialic acid	Immunomodulatory
7.05	Ammothamnine	$C_{15}H_{24}N_2O_2$	264.18	Alkaloid	Antimicrobial
9.72	8-8′-Dehydrodiferulic acid	$C_{20}H_{18}O_8$	386.09	Phenolic acid	Anti-inflammatory
14.69	Verimol A	$C_{18}H_{20}O_5$	316.12	Sesquiterpene lactone	Anticancer

Ficus amplissima bark extract showed the presence of melibiose, isoquinoline alkaloids, and phenylpropanoid derivatives such as cinnamyl cinnamate. The detection of Marchantin A, a bisbibenzyl compound, is noteworthy due to its reported antimicrobial potential, supporting the traditional use of this species in infectious conditions. In *Ficus hispida*, the dominance of flavonoids and condensed tannins such as gerberinol and procyanidin B7 suggests strong antioxidant and cardioprotective potential. The identification of alkaloids like (±)-carnegine and ryanodine further indicates neuroactive and muscle-relaxant properties, corroborating ethnomedicinal claims related to nervous system disorders. The HR-LCMS profile of *Ficus arnottiana* bark revealed a chemically diverse composition, including cyanogenic glycosides (lotaustralin), proanthocyanidins, and furanone derivatives. The presence of procyanidin B7 again highlights antioxidant and cardioprotective activity, while antimicrobial furanones support its traditional use against infections.

Ficus benjamina bark extract exhibited a distinct chemical fingerprint with flavonoid glycosides (cynaroside A), iridoid glycosides (leonuriside A), and acetogenins (squamostatin A). These compounds are well known for hepatoprotective, anti-inflammatory, and anticancer activities, indicating therapeutic versatility of this species. In *Ficus carica* bark, alkaloids such as matrine and norsalsolinol derivatives were prominent, along with flavonoid glycosides and lignans like isoamericanol A. Lignans are recognized for their anticancer and antioxidant properties, providing pharmacological justification for the medicinal importance of *F. carica* bark. *Ficus elastica* demonstrated the presence of flavonoids, organosulfur compounds (allixin), diterpenoids, and phenolic acids such as isoferulic acid. These compounds are associated with antioxidant, antimicrobial, and anti-inflammatory activities, suggesting potential applications in inflammatory and oxidative stress-related disorders. The bark extract of *Ficus microcarpa* showed a combination of alkaloids, flavonoids, sialic acid derivatives, phenolic acids, and sesquiterpene lactones. The detection of neuraminic acid indicates immunomodulatory potential, while sesquiterpene lactones such as verimol A are widely reported for anticancer activity.

The present study provides a comprehensive HR-LCMS–based phytochemical profiling of bark extracts from seven *Ficus* species (*F. amplissima, F. hispida, F. arnottiana, F. benjamina, F. carica, F. elastica,* and *F. microcarpa*) collected from the Marathwada region of Maharashtra. The HR-LCMS analysis revealed a wide diversity of secondary metabolites, including carbohydrates, alkaloids, flavonoids, proanthocyanidins, phenolic acids, glycosides, terpenoids, and lignans, confirming the metabolic richness of *Ficus* bark drugs.

Conclusion:

The present investigation provides a comprehensive HR-LCMS-based phytochemical characterization of bark drugs from selected *Ficus* species of the Marathwada region. The integration of Pharmacognostic evaluation, preliminary phytochemical screening, and advanced chromatographic analysis establishes reliable chemical markers for species identification and standardization. The detection of pharmacologically important compounds supports the ethnomedicinal relevance of these bark drugs and underscores their potential for future drug discovery and development.

References:

1. Cooke, T. (1967). *The Flora of the Presidency of Bombay*. Botanical Survey of India.
2. Evans, W. C. (2009). *Trease and Evans Pharmacognosy* (16th ed.). Elsevier.
3. Harborne, J. B. (1998). *Phytochemical Methods: A Guide to Modern Techniques of Plant Analysis*. Chapman & Hall.
4. Joseph, B., & Raj, S. J. (2011). Phytopharmacological properties of *Ficus* species. *Asian Pacific Journal of Tropical Biomedicine*, 1(3), 246–253.
5. Kokate, C. K., Purohit, A. P., & Gokhale, S. B. (2014). *Pharmacognosy* (50th ed.). Nirali Prakashan.
6. Mandal, S. C., Maity, T. K., Das, J., Saba, B. P., & Pal, M. (2010). Antidiabetic activity of *Ficus* species. *Journal of Ethnopharmacology*, 130(3), 541–546.
7. Panche, A. N., Diwan, A. D., & Chandra, S. R. (2016). Flavonoids: An overview. *Journal of Nutritional Science*, 5, e47.
8. Rice-Evans, C. A., Miller, N. J., & Paganga, G. (1997). Antioxidant properties of phenolic compounds. *Trends in Plant Science*, 2(4), 152–159.
9. Saleem, M. (2009). Lupeol, a novel anti-inflammatory and anticancer triterpene. *Cancer Letters*, 285(2), 109–115.
10. WHO. (2013). *Traditional Medicine Strategy 2014–2023*. World Health Organization.
11. Wolfender, J. L., Rudaz, S., & Choi, Y. H. (2015). Plant metabolomics: From holistic profiling to biomarker discovery. *Planta Medica*, 81(9), 760–772.

International Journal of Advance and Applied Research
www.ijaar.co.in
ISSN – 2347-7075 Impact Factor – 8.141
Peer Reviewed Bi-Monthly
Vol. 7 No. 14 January – February - 2026

Effect of Different Liquid Media and Cultural Condition on Biomass Production of Sclerotium Rolfsii

Vishwajit R. Mhaske[1], Anil D. Adsare[2], Sudarshan R. Mane[3] and Madhukar S. Wadikar[4]

[1]*Department of Botany Shikshan Maharshi Dnyandeo Mohekar Mahavidyalaya, Kallam, Dist-Dharashiv.*

[2]*Department of Botany, Arts, Commerce and Science College, Maregaon, Dist-Yavatmal.*

[3]*Department of Botany, Shri Swami Samarth Arts and Science Senior College Ruibhar, Dist-Dharashiv.*

[4]*Department of Botany, R. B. Attal Arts, Science and Commerce College, Georai, Dist- Beed.*

Corresponding Author – Vishwajit R. Mhaske

DOI - 10.5281/zenodo.19755489

Abstract:

In the present investigation effect of different liquid media and different physical parameters like pH and temperature to standardized proper cultural condition for maximum biomass production of Sclerotium rolfsii was carried out. The results revealed that among the media tested Glucose Peptone broth significantly induced the biomass production as compare to other media after 10 days of incubation. The range of pH 6 and 25^{0}C temperature was optimum for biomass production of Sclerotium rolfsii after 10 days of incubation.

Introduction:

Sclerotium rolfsii is a necrotrophic soilborne plant pathogen forming sclerotia as a survival structure distributed worldwide. *Sclerotium rolfsii* is polyphagous, ubiquitous, facultative and most destructive soil borne fungus. It is an anamorph of Athelia rolfsii. Pier Andrea Saccardo, initially identified the species in 1911, based on specimens brought to him by Peter Henry Rolfs, who believed the unnamed fungus was the cause of tomato blight in Florida. He named the species *Sclerotium rolfsii* and placed it in the old Sclerotium genus. Because of prolific growth of *Sclerotium rolfsii* and ability to produce persistent sclerotia, it is contributing in high degree of economic losses (Mahen et al., 1995)[(6)]. The pathogen has a significant economic impact on a variety of crops. The host range of *Sclerotium rolfsii* is very broad, encompassing several horticultural and agronomical crops all over the world (Aycock,1996)[(1)]. The fungus attacks over 500 species of plants from over 100 families.

Fungi have morphogenic and cultural variations, hence a comprehensive study of the effects of media, temperature and pH on biomass production of *Sclerotium rolfsii* was carried out.

Materials and Method:

Collection and Isolation of Fungi:

Soil samples were collected from different localities of Marathwada region. The soil samples were collected by digging 10 to 15 cm depth using sterile spatulas and five soil samples were randomly collected approximately 100gm from each sampling site in pre sterilized zip-lock bags. Isolation of fungi were done by dilution plate method (Waksman, 1916), one gram of each soil sample was taken and added in test tube containing 10ml of sterile distilled water. The suspension was serially diluted five times 10-1 to 10-5 in sterile distilled water. The Suspension obtained after vigorous mixing of the

soil samples were allow to stand for 20 min. 0.5ml of each aqueous dilutions of soil suspensions were inoculated on Petri plates amended with Potato dextrose agar. Trace amount of Streptomycin was added in PDA media to avoid bacterial contamination. Spread plate and Pour plate techniques were used. The inoculated plates were incubated at 30°C for 7 days. Different fungal colonies were observed and sub cultured to obtain pure cultures.

Identification of Fungi:

Identification of fungi were done on the basis of morphological and microscopic observations like colony colour, margin of the colony, growth pattern, sporulation and pigment production. The identification and further confirmation fungi was made by preparing slides of the fungal growth and observing them under compound microscope and slide culture technique. The identification was made with the help of manuals, The Illustration of fungi by Mukadam *et al.,* (2005)[7] A manual of soil fungi by Gilman (2001)[3], A hand book of soil fungi by Nagmani and Kunwar (2005)[8].

Effect of different liquid media on biomass production of Fungi:

The study of different cultural media for Biomass production of fungi investigated by 6 different liquid media like Potato Dextrose broth, Malt Extract broth, Glucose Peptone broth, Czapek Dox broth, Glucose Nitrate broth, Yeast Extract Peptone Dextrose broth. 50ml of each broth were dispensed into 250 ml Erlenmeyer flasks and autoclaved at 121^0C (15psi) for 20 minutes. Each flask was inoculated with 5mm mycelial disc taken from actively growing of 7 days old *Sclerotium rolfsii* culture. After 8 days incubation period each flask was filter through Whatman No. 1 filter paper. The mycelium dried at 70^0 C in an oven. All experiment were conducted in triplicate. The dry weight was calculated by using the following formula:

Dry Weight = (weight of filter paper + mycelium) - (weight of blank filter paper).

Effects of temperature on biomass production of Fungi

The effect of temperature on biomass production of fungi was investigated by using the malt extract broth medium incubating at various range of temperature (25^0C -50^0C). After the incubation period the culture of each conical flask were filter through Whatman No 1 filter paper, the filter paper with mycelium were dried in oven at 70^0 C. The dry weight was calculated as mention above.

Effect of pH on biomass production of fungi:

The effect of pH on biomass production of tested fungi was investigated by using the malt extract broth medium prepared with various pH ranging from pH 4 to pH 8. The pH of the medium was adjusted from pH 4 to pH 8 with 0.1 NaOH and 0.1 N HCl with the pH meter. After the incubation period the culture of each conical flask were filter through Whatman No. 1 filter paper, filter paper with mycelium were dried in oven at 70^0 C. The dry weight was calculated as mention above.

Result and Discussion:

In the present study about 50 different fungal colonies were observed. The identification of *Sclerotium rolfsii* was carried out on the basis of morphological and colony characters and by slide culture technique.

Effect of different media on biomass production of *Sclerotium rolfsii*:

In order to study effect of different media on biomass production six different media were

used like PDB, CZB, MB, GNB, GPB and YPB. Maximum biomass production was observed on Glucose Peptone broth (420). Whereas minimum biomass production was observed on Czapek Dox broth (140). While Yeast Extract Peptone Dextrose broth showed (330) followed by Potato Dextrose broth (300). Glucose Nitrate broth and Malt Extract broth observed dry weight (290 and 150) respectively (Table no.1 and Graph no. 1). Kushwaha et al., (2019)[5] examined total of seven liquid media were used for studying the growth of *Sclerotium rolfsii* in Lentil. Their results reported that potato-dextrose medium was most suitable for mycelial growth. Ravikumar G Vaniya et al (2022)[9] examined total of seven liquid media for studying the growth of Sclerotium rolfsii. They reported that Dry mycelial weight observed significantly superior on Potato Dextrose broth medium. Sahana N. et al., (2017)[11] also reported the maximum dry mycelial weight of fungus in potato dextrose broth.

Table No. 1 Effect of different media on biomass production of *Sclerotium rolfsii*

Sr. No.	Different Media	Dry Weight (mg)
1	PDB	300
2	CZB	140
3	MB	150
4	GNB	290
5	GPB	420
6	YPB	330

Dry weight of biomass expressed in mg.

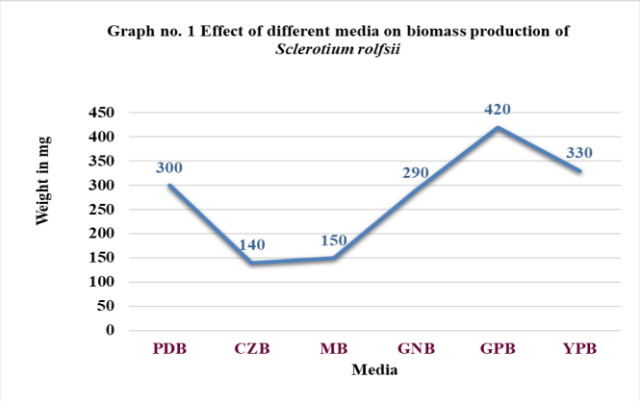

Effect of different temperature on biomass production of *Sclerotium rolfsii*:

Effect of temperature on biomass production of *Sclerotium rolfsii* was observed by maintaining the different temperature levels for incubation. Maximum biomass production was found at 25^0C temperature. While at temperature 30^0C and 35^0C dry weight was observed (190) respectively. None of biomass observed at 45^0C and 50^0 C temperature (Table no. 2 and Graph no. 2). Similar result was reported by earlier coworkers Ayed F. et al (2018)[2], Tripathi B. P. and Khare N. (2006)[12]. Above 40^0 C temperature growth of the fungus was reduced. These finding are similar with Hussain A. et al (2006)[4] They observed that the growth of *Sclerotium rolfsii* decreased significantly above 35°C temperature.

Table no. 2 Effect of different temperature on biomass production of *Sclerotium rolfsii*

Sr. No.	Temperature	Dry Weight (mg)
1	25	220
2	30	190
3	35	190
4	40	160
5	45	000
6	50	000

Dry weight of biomass expressed in mg.

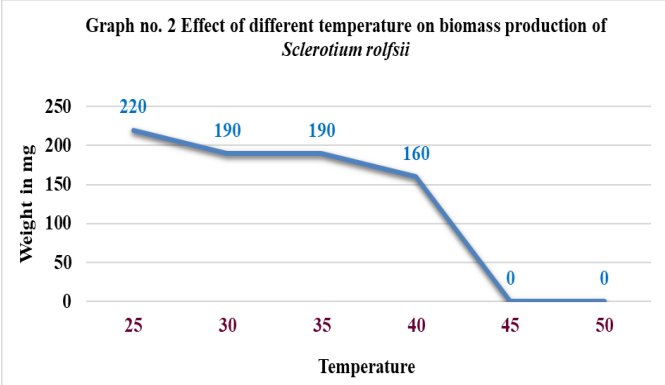

Effect of different pH on biomass production of *Sclerotium rolfsii:*

The study of effect of different pH ranges on biomass production of *Sclerotium rolfsii* carried out by maintaining the different pH levels of medium i.e. 4 to 8 pH. The maximum biomass production was observed on pH 6 (230). The range of pH 4.5 (220) and 6 (230) to 6.5 (220) is optimum pH range for biomass production. At acidic pH i.e. 4 (80) and at basic pH i.e. 8 (100) biomass production was significantly reduced. The remaining pH showed mycelial dry weight on pH 5 (160), pH 5.5 (210), pH 7 (190) and pH 7.5 (120) respectively (Table no. 3 and Graph no. 3). Raut M. K. et al (2015)[10] showed maximum biomass production on pH 6.

Table no. 3 Effect of different pH on biomass production of *Sclerotium rolfsii*

Sr. No.	pH	Dry Weight (mg)
1	4	80
2	4.5	220
3	5	160
4	5.5	210
5	6	230
6	6.5	220
7	7	190
8	7.5	120
9	8	100

Dry weight of biomass expressed in mg.

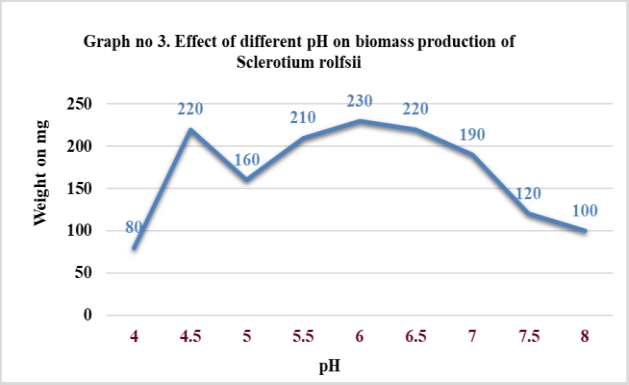

References:

1. Aycock R. (1966) Stem rot and other diseases caused by Sclerotium rolfsii. North Carolina Agric. Expt. Station., 136-202.
2. Ayed F., Jabnoun Khiareddine H., Aydi Ben Abdallah R., Daami Remadi M. (2018) Effect of Temperatures and Culture Media on *Sclerotium rolfsii* Mycelial Growth, Sclerotial Formation and Germination. Journal of Plant Pathology & Microbiology.; 9(8):446.
3. Gilman J. C. A (2001) Manual of soil fungi second Indian edition, Biotech books Delhi,.
4. Hussain A., Muhammad I. S., Ayub N., Haqqani A. M. (2006) Physiological study of *Sclerotium rolfsii* Sacc. Pak J Plant Patho.; 2: 102-106.
5. Kushwaha Shiva Kant, Sanjeev Kumar, Balkishan Chaudhary and Ravit Sahu (2019) Effect of Different Media, pH and Temperature on Growth and Sclerotia Formation of *Sclerotium rolfsii* Sacc. causing Collar rot of Lentil. Chemical Science Review and Letters.; 8(29): 01-05.
6. Mahen, V. K., Mayer, C. D., Brennemen T. B. & McDonald D. (1995) Stem and pod rots of groundnut. Information Bulletin No. 4, ICRISAT; 28.
7. Mukadam D. S., Chavan A. M., Patil M. S. and Patil A. (2005) Illustration of fungi Kailas publication, Aurangabad.
8. Nagmani A, Kunwar I. K. and Manoharachary C. (2005) Hand book of soil fungi. Published by K. International Pvt. Ltd New Delhi.
9. Ravikumar G Vaniya, Pushpendra Singh and A. J. Deshmukh (2022) Effect of different cultural media on growth of different isolates of *Sclerotium rolfsii* Sacc. causing stem rot of Indian bean The Pharma Innovation Journal.; 11(4): 14-19.

10. Rout M. K., Mohanty P., Dash S. R and Parida D. (2015) Studies on Effect of pH, Temperature and Relative Humidity on Growth and Sporulation of *Alternaria alternate* and *Sclerotium rolfsii* Causing Bud Rot and Collar Rot in Marigold. Trends in Biosciences.; 8(24): 6785-6787.
11. Sahana N, Banakar V. B., Sanath Kumar and Thejesha A. G. (2017) Morphological and cultural Studies of *S. rolfsii* Sacc. Causing foot rot disease of tomato. International Journal of Current Microbiology and Applied Sciences.; 6(3): 1146-1153.
12. Tripathi B. P. and Khare N. (2006) Growth of *Sclerotium rolfsii* of chick pea as induced by bioagents. Ann. Plant. Prot. Sci.; 13: 492-493.

International Journal of Advance and Applied Research
www.ijaar.co.in
ISSN – 2347-7075 Impact Factor – 8.141
Peer Reviewed Bi-Monthly
Vol. 7 No. 14 January – February - 2026

Phytochemical Profiling and Agro-Environmental Applications of Sphagneticola calendulacea in Sustainable Agriculture

Yogesh Pandharinath Shinde[1] & Ganesh Laxmanrao Pachkore[2]

[1]*Shri Amolak Jain Vidya Prasarak Mandal's Smt. S. K. Gandhi Arts, Amolak Science & P. H. Gandhi Commerce College, Kada, Dist-Beed, Maharashtra, India*

[2]*Vasantdada Patil Arts, Commerce & Science College, Patoda, Dist-Beed, Maharashtra, India*

Corresponding Author – Yogesh Pandharinath Shinde

DOI - 10.5281/zenodo.19755561

Abstract:

Sphagneticola calendulacea (L.) Pruski (syn. Wedelia calendulacea), a creeping perennial herb of the family Asteraceae, has gained increasing scientific attention for its ecological resilience, phytochemical richness, and multifunctional applications in sustainable agriculture. The present study evaluates its botanical attributes, phytochemical profile, soil-stabilizing ability, phytoremediation potential, weed suppression capacity, and suitability as green manure. Field-based observations combined with laboratory screening revealed abundant flavonoids, phenolic compounds, and terpenoids in plant extracts, which are associated with antioxidant, antimicrobial, and allelopathic activities. Dense stoloniferous root systems effectively reduced surface soil erosion, while biomass incorporation improved soil organic carbon and microbial activity. Weed growth was significantly suppressed in plots dominated by S. calendulacea, suggesting allelochemical-mediated interference. The collective findings highlight the plant's promise as an eco-friendly biological resource for sustainable cropping systems, soil restoration, and low-input agriculture.

Keywords: Sphagneticola Calendulacea; Sustainable Agriculture; Phytoremediation; Weed Suppression; Soil Conservation; Green Manure

Introduction:

Sustainable agriculture emphasizes productivity while maintaining soil health, biodiversity, and ecological integrity. Plant-based interventions such as cover crops, green manures, and biological weed suppressants are increasingly promoted as alternatives to chemical-intensive practices.

Sphagneticola calendulacea (L.) Pruski—commonly known as creeping oxeye or Singapore daisy—is a stoloniferous perennial herb distributed widely in tropical and subtropical regions. The species is valued in traditional medicine for treating liver ailments, inflammation, wounds, and skin disorders and has recently attracted attention for its potential roles in soil stabilization, phytoremediation, and biological weed control.

Rapid vegetative spread, tolerance to waterlogging, and ability to thrive in degraded soils make *S. calendulacea* an ideal candidate for erosion-prone landscapes and marginal agricultural lands. However, systematic studies integrating its agronomic, ecological, and phytochemical attributes remain limited. The present investigation was therefore undertaken to assess the multifunctional utility of *S. calendulacea* in sustainable agriculture.

Objectives:

The study aimed to:

1. Document the botanical and ecological characteristics of *S. calendulacea*.
2. Screen major phytochemical constituents in different extracts.
3. Evaluate its role in soil stabilization and phytoremediation.
4. Assess weed-suppressive and pest-deterrent properties.
5. Examine its suitability as green manure for soil fertility enhancement.

Materials and Methods:

Collection and Authentication:

Plant material was collected from moist low-lying areas of the Kalsubai region, Western Ghats, Maharashtra, India. Specimens were authenticated by taxonomists at Dr. Babasaheb Ambedkar Marathwada University, Aurangabad, and voucher samples were deposited in the institutional herbarium

Preparation of Extracts:

Shade-dried aerial parts were powdered and subjected to successive solvent extraction using aqueous and hydro-alcoholic systems. Concentrated extracts were stored at 4 °C for phytochemical analysis.

Phytochemical Screening:

Qualitative chemical tests were performed for flavonoids, phenolics, tannins, terpenoids, alkaloids, and saponins following standard pharmacognostic protocols.

Soil Conservation and Phytoremediation Studies:

Experimental field plots were established on gentle slopes. Soil loss was measured after rainfall events using runoff collectors. For phytoremediation assessment, soils artificially enriched with trace concentrations of heavy metals were planted with *S. calendulacea*, and metal uptake was monitored in harvested tissues.

Weed Suppression and Pest Control:

Allelopathic effects were evaluated by monitoring emergence and biomass of common agricultural weeds in plots covered by *S. calendulacea*. Laboratory bioassays were performed to test insecticidal activity of extracts against selected crop pests.

Green Manure Trials:

Fresh biomass was incorporated into cultivated soil beds, and changes in organic carbon, available nitrogen, phosphorus, potassium, and microbial counts were recorded after decomposition.

Results and Discussion:

Botanical Description and Habitat:

Sphagneticola calendulacea is a mat-forming perennial herb with creeping stolons, opposite serrate leaves, and solitary yellow capitula. The plant prefers moist sandy loams, riverbanks, wetlands, and irrigation channels. Rapid vegetative propagation and tolerance to fluctuating moisture regimes enable it to act as an effective natural ground cover.

Phytochemical Composition and Medicinal Relevance:

Extracts tested positive for flavonoids, phenolic acids, terpenoids, and tannins. These metabolites are known for antioxidant, antimicrobial, and allelopathic activities, supporting traditional uses in inflammatory disorders and suggesting applications in organic crop protection systems.

Role in Sustainable Agriculture:

Soil Conservation and Phytoremediation:

Dense fibrous roots and stolons significantly reduced runoff and surface erosion. Plants grown in contaminated soils accumulated

measurable quantities of metals in aerial tissues, indicating moderate phytoremediation capacity suitable for rehabilitation of marginal lands.

Weed Suppression and Pest Management:

Plots dominated by *S. calendulacea* showed reduced density and biomass of invasive weeds, suggesting release of inhibitory allelochemicals. Extracts also exhibited deterrent and toxic effects against selected insect pests, highlighting its potential as a botanical pesticide.

Green Manure and Soil Fertility Enhancement:

Incorporation of plant biomass enhanced soil organic matter, nutrient availability, and microbial populations, confirming its suitability as a green manure crop in low-input farming systems.

Ecological Concerns and Management:

Although agriculturally beneficial, unchecked growth of *S. calendulacea* can lead to invasiveness in natural ecosystems. Controlled cultivation, boundary management, and integration within crop rotation systems are recommended.

Table 1: Physicochemical Parameters of ***Sphagneticola calendulacea*** Aerial Parts (Dry Powder)

Parameter	Value (% w/w)
Loss on drying at 105 °C	6.12
Total ash	9.48
Acid-insoluble ash	1.23
Water-soluble ash	4.05
Alcohol-soluble extractive	7.84
Water-soluble extractive	12.76
pH (10% aq. solution)	6.1

Table 2: Preliminary Phytochemical Screening of Extracts

Phytochemical Group	Test	Aqueous Extract	Hydro-alcoholic Extract
Alkaloids	Dragendorff's	+	++
Flavonoids	Shinoda	+	++
Phenolics	Ferric chloride	++	++
Tannins	Lead acetate	+	+
Terpenoids	Salkowski	+	++
Saponins	Foam test	+	+
Glycosides	Keller–Killiani	–	+

(+ = present; ++ = strongly present; – = absent)

Table 3: Effect of ***S. calendulacea*** Cover on Soil Erosion

Treatment	Mean Runoff (L m^{-2})	Soil Loss (kg ha^{-1})
Bare soil (control)	4.6	1280
Crop cover	2.8	720
S. calendulacea ground cover	1.2	310

Table 4: Weed Suppression in Experimental Plots

Weed Species	Density in Control (plants m^{-2})	Density in *S. calendulacea* Plot	% Reduction
Cyperus rotundus	42	14	66.7
Parthenium hysterophorus	35	10	71.4
Amaranthus viridis	48	17	64.6
Mean	—	—	**67.6**

Table 5: Soil Fertility After Green-Manure Incorporation (60 Days)

Parameter	Before Treatment	After Biomass Incorporation
Organic carbon (%)	0.42	0.71
Available N (kg ha^{-1})	185	263
Available P (kg ha^{-1})	14.6	22.4
Available K (kg ha^{-1})	168	245
Microbial count (CFU $\times 10^6$ g^{-1} soil)	3.2	6.8

Table 6: Heavy-Metal Uptake by ***S. calendulacea*** in Contaminated Soil

Metal	Soil Conc. (mg kg^{-1})	Plant Tissue (mg kg^{-1})	Bioaccumulation Factor
Pb	52	18.4	0.35
Cd	6.1	2.8	0.46
Zn	98	44.7	0.46
Cu	41	19.5	0.48

Table 7: TLC Profile of Hydro-alcoholic Extract

Solvent system: Toluene : Ethyl acetate : Formic acid (5:4:1)

Spot No.	Rf Value	Colour under UV (366 nm)	Probable Compound Group
1	0.21	Blue	Phenolics
2	0.43	Greenish	Flavonoids
3	0.61	Purple	Terpenoids
4	0.79	Yellow	Glycosides

Future Prospects:

Future work should emphasize:

- Quantitative evaluation of allelochemicals
- Heavy-metal uptake kinetics
- Long-term soil fertility trials
- Integration into agroforestry systems
- Development of managed cultivation protocols

Conclusion:

Sphagneticola calendulacea represents a versatile biological resource for sustainable agriculture. Its capacity for soil stabilization, weed suppression, phytoremediation, and organic nutrient enrichment makes it suitable for eco-friendly farming strategies. Scientific exploitation combined with ecological management could

promote its use in land restoration and climate-resilient agriculture.

References:

1. Gupta R, Pandey S. Phytochemical properties of *Sphagneticola calendulacea* and its agricultural applications. J Sustain Agric. 2019;45(3):112-120.
2. Kumar A, Verma P. Weed suppression and soil health improvement using *Wedelia calendulacea*. Int J Bot Stud. 2020;8(4):67-75.
3. Sharma H, Das M. Phytoremediation potential of *Sphagneticola calendulacea*. Environ Sci Ecol J. 2021;12(2):89-97.
4. Singh P, Patel R. Allelopathic properties of *Sphagneticola calendulacea* and sustainable agriculture. Agric Sci Rev. 2022;56(1):33-45.
5. **Khandekar & Gopalkrishnan (2022)** — Pharmacognostic evaluation of *Sphagneticola calendulacea* leaves including microscopy, physicochemical analysis, and phytochemical screening.
6. **Khandekar & Gopalkrishnan (2023)** — Standardization and phytochemical characterization of the stem of *S. calendulacea*.
7. **Nguyen et al. (2023)** — Determination of phenolics, antioxidant activity, and antidiabetic potential of *S. calendulacea* leaf extracts.
8. Mottakin et al. (2004) — Cytotoxic and antibacterial activity of extractives from *Wedelia calendulacea*, showing bioactivities of various solvent extracts.
9. Shirwaikar et al. (2006) — Anti-osteoporotic effects of *W. calendulacea* ethanol extract in ovariectomized rats, suggesting estrogenic phytochemicals.
10. Cai et al. (2025) — Comprehensive review of wedelolactone, a major phytochemical found in *S. calendulacea* and related species, detailing pharmacological potentials.
11. Zhang et al. (2021) — Responses of *S. calendulacea*, *S. trilobata*, and their hybrid to drought stress, illustrating stress physiology and ecological adaptability.

International Journal of Advance and Applied Research
www.ijaar.co.in
ISSN – 2347-7075 Impact Factor – 8.141
Peer Reviewed Bi-Monthly
Vol. 7 No. 14 January – February - 2026

Environmental Transformation and Biodiversity Dynamics in the Rural–Urban Fringe of Jalgaon District, Maharashtra: A Spatiotemporal Analysis

Yuvraj M. Bhosale[1] & Ratnakar S. More[2]
[1, 2]Nanasaheb Y. N. Chavan Arts, Science and Commerce College,
Chalisgaon Dist Jalgaon, Maharashtra
Corresponding Author – Yuvraj M. Bhosale
DOI - 10.5281/zenodo.19755615

Abstract:

The rural–urban fringe areas represent critical transition zones experiencing rapid environmental transformation due to urbanization pressures. Jalgaon District, located in North Maharashtra, has witnessed significant land-use changes over the past two decades, potentially impacting local biodiversity patterns. This study examines the spatiotemporal patterns of environmental transformation and their impacts on biodiversity in the rural–urban fringe areas of Jalgaon District between 2000 and 2023. We employed remote sensing data from Landsat satellites, conducted field surveys across 45 sampling sites, and used the Shannon Diversity Index, Simpson's Index, and Principal Component Analysis to assess biodiversity changes. Land-use/land-cover (LULC) classification was performed using supervised classification techniques with 87% overall accuracy. Agricultural land decreased by 23.4% (142.6 km²), while built-up areas increased by 156.8% (94.3 km²) in the fringe zone during 2000–2023. Species richness declined from 124 to 89 species, with a 28.2% reduction in Shannon Diversity Index (H' = 3.42 to 2.45). Significant negative correlations were observed between urbanization intensity and biodiversity indices (r = -0.73, p < 0.001). Rapid urbanization in Jalgaon's fringe areas has led to substantial biodiversity loss and habitat fragmentation. Urgent implementation of green infrastructure and conservation corridors is recommended to mitigate further ecological degradation.

Keywords: Rural–Urban Fringe, Biodiversity Loss, Land-Use Change, Jalgaon District, Urbanization, Shannon Diversity Index, Habitat Fragmentation.

Introduction:

The rural–urban fringe represents a dynamic transitional zone where urban and rural land uses intermingle, creating unique ecological and socioeconomic landscapes(Haldar et al., 2023). These peri-urban areas are characterized by rapid land-use transitions, demographic changes, and intense environmental pressures that often lead to biodiversity degradation(Almusaed et al., 2019). India, experiencing unprecedented urban growth rates of 2.76% annually during 2001–2011(Fazal et al., 2015), faces significant challenges in managing these transitional zones sustainably.

Jalgaon District, situated in the northern region of Maharashtra State, covers an area of approximately 11,244 km² with a population of 4.23 million(Ade, 2021). The district serves as a critical agricultural hub in the Tapi River basin(Vasantrao et al., 2017) and has witnessed substantial urban expansion around its major urban centers—Jalgaon city, Bhusawal, and Amalner—over the past two decades. The district's strategic location along the Delhi–Mumbai Industrial Corridor has accelerated developmental pressures, particularly in the

rural–urban fringe areas(Biswas & Dey, 2023). These peripheral zones, characterized by intense pressure from infrastructural development and residential expansion, often undergo drastic landscape modifications that threaten native flora and fauna (Ramachandra et al., 2023; Saste & Bhagat, 2024).

Study Area:

Geographic and Climatic Characteristics: Jalgaon District lies in the northwestern part of Maharashtra, forming part of the Khandesh region. The study specifically focuses on a 15 km buffer zone around the three major urban centers: Jalgaon Municipal Corporation, Bhusawal Municipal Council, and Amalner Municipal Council, covering approximately 609 km² of fringe area.

The region experiences a semi-arid climate with average annual rainfall of 647 mm, concentrated during the southwest monsoon (June–September). Temperatures range from 10°C in winter to 45°C in summer. The terrain is predominantly flat to gently undulating, with elevations ranging from 187 to 412 meters above sea level. Major soil types include medium black cotton soils (Vertisols) covering 67% of the area, and shallow red soils (Alfisols) in 33% of the region.

Socioeconomic Profile: The district's economy is primarily agriculture-based, with banana cultivation being the dominant cash crop, followed by cotton, sorghum, and sugarcane. The region has also developed significant industrial activity, particularly in textile, food processing, and power generation sectors. The literacy rate stands at 78.2%, slightly above the state average. The study area fringe zones have experienced population growth rates of 3.8% annually, significantly higher than the rural average of 1.2%.

Materials and Methods

Remote Sensing Data: Multi-temporal satellite imagery was acquired from the following sources:

- **Landsat 7 ETM+** (2000, 2005): 30m spatial resolution
- **Landsat 8 OLI** (2013, 2018, 2023): 30m spatial resolution
- **Sentinel-2 MSI** (2020, 2023): 10m spatial resolution for validation

All images were selected from the dry season (November–February) to minimize cloud cover and vegetation phenology variations. Atmospheric correction was performed using the Dark Object Subtraction (DOS) method, and geometric correction was completed using ground control points with RMS error < 0.5 pixels.

Field Survey Data:

Field surveys were conducted during three seasons (pre-monsoon, monsoon, and post-monsoon) in 2022–2023 across 45 sampling sites stratified by land-use categories and distance gradients from urban cores (0–5 km, 5–10 km, 10–15 km). Each site consisted of a 100m × 100m quadrat where flora and fauna inventories were recorded.

Flora Assessment: Plant species were identified and enumerated using quadrat sampling (1m × 1m for herbs, 5m × 5m for shrubs, and 20m × 20m for trees).

Fauna Assessment: Bird surveys used point count methods with 10-minute observation periods. Small mammals were assessed through trap surveys and indirect sign counts. Reptiles and amphibians were recorded through visual encounter surveys.

Land-Use/Land-Cover Classification: Supervised classification was performed using the Maximum Likelihood Classifier (MLC) algorithm in ERDAS Imagine 2020. Six LULC classes were defined:

1. Built-up areas (residential, commercial, industrial)
2. Agricultural land (cropland, fallow)
3. Forest/vegetation (dense, sparse)
4. Water bodies (rivers, ponds, reservoirs)
5. Barren land (exposed soil, quarries)
6. Wetlands (seasonal, permanent)

Training samples were collected for each class (minimum 100 pixels per class), and classification accuracy was assessed using error matrices with 300 randomly distributed validation points. Overall accuracy exceeded 87% for all time periods (Kappa coefficient = 0.84).

Biodiversity Assessment: Diversity Indices was calculated by following methods:

Shannon-Wiener Diversity Index (H'):

$H' = -\Sigma(pi \times \ln pi)$

where pi is the proportion of individuals belonging to species i.

Simpson's Diversity Index (D):

$D = 1 - \Sigma(pi^2)$

Species Richness (S): Total number of species recorded

Evenness (J'):

$J' = H' / \ln(S)$

Statistical Analyses: Principal Component Analysis (PCA) is used to identify major gradients in environmental variables. Pearson Correlation Analysis used to examine relationships between urbanization metrics and biodiversity indices. Analysis of Variance (ANOVA) were used to test differences in biodiversity across land-use categories and distance gradients Linear Regression Models used to predict biodiversity loss based on urbanization intensity. Urbanization Intensity Index (UII) was calculated as: UII = (Built-up area / Total area) × 100

All statistical analyses were performed using R software (version 4.2.1) with packages: vegan, Biodiversity R, and ggplot2. Significance level was set at $\alpha = 0.05$.

Change Detection Analysis: Post-classification change detection was employed to quantify LULC transitions between time periods. Transition matrices were generated to identify major conversion patterns. Annual rate of change was calculated using the compound interest rate formula:

$r = [(A2/A1)^{(1/t)} - 1] \times 100$, where A1 and A2 are areas at time 1 and time 2, and t is the time interval in years.

Results:

Land-Use/Land-Cover Changes (2000–2023)

Overall LULC Transformation:

The classification results revealed dramatic landscape transformations in the rural–urban fringe of Jalgaon District over the 23-year study period (Table 1).

Table 1: Land-Use/Land-Cover Changes in Jalgaon Fringe Area (2000–2023)

LULC Class	2000 (km²)	2000 (%)	2023 (km²)	2023 (%)	Change (km²)	Change (%)	Annual Rate (%)
Built-up	60.2	9.9	154.5	25.4	+94.3	+156.8	+4.18
Agricultural	418.7	68.7	276.1	45.3	-142.6	-34.1	-1.84
Forest/Vegetation	87.4	14.4	64.2	10.5	-23.2	-26.5	-1.32
Water Bodies	21.3	3.5	18.7	3.1	-2.6	-12.2	-0.58
Barren Land	18.6	3.1	92.4	15.2	+73.8	+396.8	+6.98
Wetlands	2.8	0.5	3.1	0.5	+0.3	+10.7	+0.44
Total	**609.0**	**100**	**609.0**	**100**	-	-	-

Built-up areas expanded from 60.2 km² (9.9%) in 2000 to 154.5 km² (25.4%) in 2023, representing an increase of 156.8% at an annual rate of 4.18%. This expansion occurred primarily at the expense of agricultural land, which decreased by 142.6 km² (34.1% reduction). Forest and vegetation cover declined by 23.2 km² (26.5%), indicating significant deforestation in the fringe zones.

Notably, barren land increased by 396.8%, suggesting abandoned agricultural plots and construction sites in transition. Water bodies showed a 12.2% decline, primarily due to encroachment and siltation of traditional water harvesting structures.

Spatial Patterns of Change:

Analysis of change patterns across distance gradients from urban cores revealed distinct spatial trends (Table 2):

Table 2: LULC Changes by Distance Gradient from Urban Core

Distance Zone	Built-up Change (%)	Agricultural Loss (%)	Vegetation Loss (%)	UII (2000)	UII (2023)
0–5 km	+284.6	-52.3	-41.7	18.7	54.2
5–10 km	+142.8	-28.4	-23.6	7.4	22.1
10–15 km	+68.3	-14.2	-12.8	3.2	8.9

The inner zone (0–5 km) experienced the most dramatic transformation, with built-up areas increasing by 284.6% and Urbanization Intensity Index rising from 18.7% to 54.2%. This zone has effectively transitioned from rural to predominantly urban character.

Land-Use Transition Matrix:

The transition matrix (Table 3) reveals the primary pathways of land conversion:

Table 3: LULC Transition Matrix 2000–2023 (km²)

From \ To	Built-up	Agricultural	Forest	Water	Barren	Wetland
Built-up	58.4	0.3	0	0	1.5	0
Agricultural	82.7	268.3	2.1	0.8	64.2	0.6
Forest	8.6	3.8	62.1	0.2	12.4	0.3
Water	1.2	2.4	0.1	16.8	0.7	0.1
Barren	3.4	1.2	0	0.9	13.1	0
Wetland	0.2	0.1	0	0	0.4	2.1

Agricultural land was the primary source of built-up expansion (82.7 km²), followed by forest conversion (8.6 km²). Significant agricultural land also transitioned to barren land (64.2 km²), indicating land degradation or plots held in speculation.

Biodiversity Assessment Results: Species Richness and Composition:

Field surveys across 45 sites documented significant biodiversity changes between baseline data (2000, from secondary sources and herbarium records) and current surveys (2022–2023).

Table 4: Species Richness by Taxonomic Groups

Taxonomic Group	2000	2023	Change	% Change
Flowering Plants	87	62	-25	-28.7
Trees	24	18	-6	-25.0
Shrubs	18	13	-5	-27.8
Herbs	45	31	-14	-31.1
Birds	52	41	-11	-21.2
Mammals	18	14	-4	-22.2
Reptiles	14	11	-3	-21.4
Amphibians	8	4	-4	-50.0
Total Species	**124**	**89**	**-35**	**-28.2**

Total species richness declined from 124 to 89 species (28.2% reduction). Amphibians showed the most dramatic decline (50%), followed by herbs (31.1%). Several species of conservation concern were no longer recorded, including the Indian Bustard (historically present), Lesser Florican, and several medicinal plant species.

Diversity Indices Across Land-Use Categories:

Table 5: Biodiversity Indices by Land-Use Category (2023 Data):

Land-Use Type	Sites (n)	Species Richness (S)	Shannon (H')	Simpson (D)	Evenness (J')
Forest/Vegetation	8	47.3 ± 6.2	3.18 ± 0.34	0.89 ± 0.06	0.82 ± 0.08
Agricultural	22	34.6 ± 5.8	2.68 ± 0.41	0.84 ± 0.08	0.76 ± 0.09
Built-up	10	18.2 ± 4.3	1.87 ± 0.52	0.71 ± 0.12	0.64 ± 0.11
Barren Land	5	12.4 ± 3.6	1.42 ± 0.38	0.63 ± 0.09	0.57 ± 0.07

One-way ANOVA revealed significant differences in all diversity indices across land-use categories (H': $F = 34.68$, $p < 0.001$; D: $F = 28.42$, $p < 0.001$; S: $F = 41.23$, $p < 0.001$). Post-hoc Tukey HSD tests showed that forest/vegetation sites had significantly higher diversity than all other categories ($p < 0.01$), while built-up and barren land had the lowest values.

Temporal Changes in Diversity Indices:

Comparison of overall biodiversity indices between 2000 and 2023:

Table 6: Temporal Changes in Biodiversity Indices

Index	2000	2023	Change	% Change	t-test	p-value
Shannon (H')	3.42 ± 0.38	2.45 ± 0.61	-0.97	-28.4	t = 8.74	< 0.001
Simpson (D)	0.92 ± 0.05	0.77 ± 0.13	-0.15	-16.3	t = 6.52	< 0.001
Evenness (J')	0.84 ± 0.06	0.71 ± 0.12	-0.13	-15.5	t = 5.89	< 0.001

All diversity indices showed statistically significant declines over the 23-year period, with Shannon Diversity Index declining by 28.4%, indicating substantial biodiversity loss.

Relationship Between Urbanization and Biodiversity: Correlation Analysis

Pearson correlation analysis revealed strong negative relationships between urbanization metrics and biodiversity indices:

Table 7: Correlation Matrix of Urbanization and Biodiversity Variables

Variables	UII	Built-up %	Shannon H'	Simpson D	Species S
UII	1.00	0.94***	-0.73***	-0.68***	-0.76***
Built-up %	0.94***	1.00	-0.71***	-0.66***	-0.74***
Shannon H'	-0.73***	-0.71***	1.00	0.92***	0.95***
Simpson D	-0.68***	-0.66***	0.92***	1.00	0.88***
Species S	-0.76***	-0.74***	0.95***	0.88***	1.00
Distance from core	-0.82***	-0.79***	0.69***	0.64***	0.71***

*** $p < 0.001$

The Urbanization Intensity Index showed strong negative correlations with Shannon Diversity ($r = -0.73$, $p < 0.001$), Simpson's Index ($r = -0.68$, $p < 0.001$), and Species Richness ($r = -0.76$, $p < 0.001$). Distance from urban core showed positive correlations with all biodiversity indices, confirming that areas farther from cities retained higher biodiversity.

Regression Analysis:

Linear regression models were developed to predict biodiversity loss based on urbanization intensity:

Shannon Diversity Index Model: $H' = 3.54 - 0.032(UII)$ $R^2 = 0.534$, $F = 49.56$, $p < 0.001$

Species Richness Model: $S = 52.3 - 0.68(UII)$ $R^2 = 0.578$, $F = 58.94$, $p < 0.001$

These models indicate that for every 10% increase in Urbanization Intensity Index, Shannon Diversity decreases by 0.32 units and species richness declines by approximately 7 species.

Distance Gradient Analysis:

Table 8: Biodiversity Indices by Distance Gradient (2023)

Distance from Core	Shannon H'	Simpson D	Species Richness	Dominant Species
0–5 km	1.96 ± 0.48	0.72 ± 0.11	21.3 ± 5.2	Generalist/Urban-adapted
5–10 km	2.54 ± 0.52	0.79 ± 0.09	32.8 ± 6.4	Mixed assemblages
10–15 km	3.12 ± 0.41	0.86 ± 0.07	44.6 ± 7.1	Native specialists

ANOVA showed significant differences across distance gradients for all indices ($p < 0.001$), with diversity increasing significantly with distance from urban cores.

Principal Component Analysis:

PCA was performed on 12 environmental and biodiversity variables to identify major gradients of variation.

Table 9: Principal Component Analysis Results

Variable	PC1	PC2	PC3
Urbanization Intensity	0.92	0.18	-0.12
Built-up %	0.89	0.21	-0.08
Agricultural %	-0.76	0.34	0.42
Vegetation %	-0.82	-0.28	0.31
Shannon H'	-0.88	0.24	-0.16
Species Richness	-0.91	0.19	-0.14
Distance from core	-0.85	0.15	0.22
Population density	0.87	0.26	-0.19
Road density	0.81	0.32	0.24
Eigenvalue	6.84	2.13	1.42
% Variance	57.0	17.8	11.8
Cumulative %	57.0	74.8	86.6

PC1 explained 57% of variance and represented an "urbanization gradient" with high positive loadings for urban variables and negative loadings for biodiversity indices. PC2 (17.8% variance) represented agricultural intensity, while PC3 (11.8%) captured landscape heterogeneity.

Critical Conservation Zones:

Based on integrated analysis of LULC change rates, biodiversity values, and urbanization pressure, five critical conservation zones were identified covering 87.4 km² requiring immediate intervention:

Table 10: Priority Conservation Zones

Zone ID	Location	Area (km²)	Shannon H'	Threat Level	Priority
CZ-1	Jalgaon East Corridor	23.6	3.24	Very High	1
CZ-2	Bhusawal South Wetlands	18.2	3.08	High	2
CZ-3	Amalner Northwest Forest	21.4	3.31	High	1
CZ-4	Tapi Riparian Zone	14.8	2.94	Very High	1
CZ-5	Interconnecting Corridors	9.4	2.76	Medium	2

Discussion:

Land-Use Dynamics and Drivers: Jalgaon's fringe experienced 156.8% built-up expansion, aligning with Tier-II Indian trends but exceeding Pune/Nashik agricultural conversions. Drivers: SEZ economic boosts, highways/railways, fringe policy enforcement gaps, and farmer distress sales. Barren land rose 396.8%, signaling speculative "dead zones."

Biodiversity Implications: 28.2% species richness and 28.4% Shannon declines indicate severe erosion, surpassing temperate studies due to semi-arid fragility. Amphibians dropped 50% from wetland loss; urban zones homogenized to generalists, eroding services. Agriculture retained moderate diversity via polycultures (intermediate disturbance hypothesis), though threatened by monocultures.

Spatial Patterns and Gradient Effects: Distance-decay fully transformed 0–5 km zones, per urban ecology theory. Biodiverse 10–15 km band faces 68.3% built-up growth, risking imminent degradation. Priority zones (CZ-1/CZ-4) require green belts as corridors/refugia.

Conclusions:

This analysis reveals alarming landscape degradation and species loss in Jalgaon District's fringe. Key conclusions:

1. Rapid urbanization: Built-up areas expanded 156.8% (2000–2023), converting agriculture/forest and altering fringes.
2. Severe biodiversity decline: Species richness fell 28.2%; Shannon Index dropped 28.4%, causing extinctions/simplification.
3. Strong urbanization-biodiversity link: Significant negative correlations confirm urbanization as primary loss driver.
4. Spatial heterogeneity: 0–5 km cores transformed ecologically; 10–15 km zones biodiverse but pressured.
5. Critical conservation: Five 87.4 km² zones need immediate protection for hotspots/corridors.
6. Hypothesis validation: Urbanization harms biodiversity; agriculture is main pathway; distance influences rates/retention.

Findings inform sustainable policy in Tier-II Indian cities, providing baselines for conservation/urban planning.

Data Availability Statement:

Remote sensing data are available from USGS Earth Explorer (https://earthexplorer.usgs.gov/). Field survey data and species inventories are available from the corresponding author upon reasonable request, subject to ethical considerations regarding sensitive species locations.

References:

1. Ade, V. V. (2021). Trends and Causes of Farmers Suicide in Maharashtra State, India. *International Journal of Scientific Research in Science Engineering and Technology*, 248. https://doi.org/10.32628/ijsrset218145
2. Almusaed, A., Almssad, A., & Hong, L. T. (2019). Sustainability in Urban Planning and Design. In *IntechOpen eBooks*. IntechOpen. https://doi.org/10.5772/intechopen.77648
3. Biswas, P., & Dey, P. (2023). Spatio-temporal impact of industrial corridor development on built-up growth: a case of Delhi–Mumbai industrial corridor, India. *GeoJournal*, *88*(4), 3791. https://doi.org/10.1007/s10708-023-10827-4
4. Fazal, S., Banu, N., & Sultana, S. (2015). Expanding Cities, Contested Land: Role of Actors in the Context of Peri-Urban Interface. *Current Urban Studies*, *3*(3), 187. https://doi.org/10.4236/cus.2015.33016
5. Haldar, S., Mukhopadhyay, A., Bhattacharya, S., & Paul, S. (2023). Development potentiality of peri-urban region in India: a quantitative analysis on Durgapur Municipal Corporation (DMC). *Frontiers of Urban and Rural Planning*, *1*(1). https://doi.org/10.1007/s44243-023-00021-y
6. Ramachandra, T. V., Setturu, B., & Naik, K. (2023). Ecologically sensitive regions in Belgaum district, Karnataka, Central Western Ghats. *Journal of Environmental Biology*, *44*(1), 11. https://doi.org/10.22438/jeb/44/1/mrn-5041
7. Saste, K. H., & Bhagat, R. B. (2024). Status of floristic diversity and impact of development on two sacred groves from Maval Tehsil (Maharashtra, India) after a century. *Journal of Threatened Taxa*, *16*(3), 24838. https://doi.org/10.11609/jott.8628.16.3.24838-24853

8. Vasantrao, B. M., Bhaskarrao, P. J., Mukund, B. A., Baburao, G. R., & Narayan, P. S. (2017). Comparative study of Wenner and Schlumberger electrical resistivity method for groundwater investigation: a case study from Dhule district (M.S.), India. *Applied Water Science*, *7*(8), 4321. https://doi.org/10.1007/s13201-017-0576-7

International Journal of Advance and Applied Research
www.ijaar.co.in
ISSN – 2347-7075 Impact Factor – 8.141
Peer Reviewed Bi-Monthly
Vol. 7 No. 14 January – February - 2026

Ethnobotanical Studies of Medicinal Plants from Marathwada effectively used on Rheumatism

Rupali Biradar[1] & Vikas Gambhire[2]

[1]*Department of Botany, Indraraj Arts, Commerce and Science College, Sillod*

[2]*Department of Botany, Government College of Arts and Science, Chhatrapati Sambhajinagar*

Corresponding Author – Rupali Biradar

DOI - 10.5281/zenodo.19755643

Abstract:

Rheumatism is a chronic disease which is progressive and systemic in nature. It is characterized by inflammation of joints, damaging cartilage and bone around the joints. It leads rheumatoid nodules, eye inflammation, cardio pulmonary diseases. To avoid hazardous effects of allopathic medicines it is possible to use the medicinal plants in various forms in order to cure Rheumatism. Medicinal herbs have been traditionally a resource for the treatment of many diseases. There are many medicinal plants that have shown anti-rheumatoid properties. The present work is focused on the ethnobotanical studies on medicinal plants from Marathwada region which are effectively used to cure Rheumatism.

Keywords: Ethnobotanical, Rheumatism, Chronic Joints, Medicinal Plants, Marathwada.

Introduction:

Rheumatism is a chronic disease which is progressive and systemic in nature. It is characterized by inflammation of joints, damaging cartilage and bone around the joints. It leads rheumatoid nodules, eye inflammation, cardio pulmonary diseases (Amandeep kaur *et al,* 2012). Medicinal herbs have been traditionally a resource for the treatment of many diseases (Zarei GA, *et al,* 2015; Baharvand-Ahmadi, B., *et al*, 2015, Mahmoudi GA, *et al,* 2016, Rezvanirad A, *et al,*, 2016, Bahmani, M., *et al,*, 2016). Treatment of inflammatory diseases, such as rheumatoid arthritis is practiced based on traditional medicine in many countries (Peter A. Akah and Alphonsus I. Nwambie, 1994).

Rheumatism is a common problem today, particularly in old people. It is generally cured using allopathic medicines. Allopathic medicines apart from curing disease cause many hazardous side effects on biological system of human beings. Alternatively, there are many medicinal plants that have shown anti rheumatoid properties. The present study is focused on the medicinal plants from Marathwada region which are effectively used to cure Rheumatism.

Marathwada (70^0 5' - 78^0 5' E Longitude and 17^0 5' - 20^0 5' N Latitude) a geographical region of the Indian state of Maharashtra. Marathwada has total area of 64590 km^2. Districts of Marathwada region are Chatrapati Sambhajinagar, Nanded, Latur, Parbhani, Jalna, Beed, Dharashiv, Hingoli. Marathwada is divided into tropical dry deciduous forests, open scrub jungles and vast tracks of grasslands according to vegetation. There are more than 1650 species of Angiospermic plants in Marathwada of which more than 500 species are medicinally useful (Naik, 1998). It is found that 61 species of flowering plants which are useful on Rheumatism.

Methodology:

The present study is based on survey of flowering plants used on Rheumatism in Marathwada during 2023-2025. The plants were identified with the help of Flora of Marathwada- V. N. Naik (1998). The medicinal value of plants was verified with the knowledge of local people, aged rural folks, traditional ayurvedic practitioners, local herbal drug sellers and referring literature of Naik (1998), Trivedi (2003-2008), Gambhire (2008), Mali and Bhadane (2011), Mohmmad Nafees Iqbal and Suradkar (2011), Lal and Singh (2012), Bhogaonkar and Ahmad (2012), Nag and Hasan (2013), Muley and Sharma (2013), Biradar (2013).

Results and Discussion:

Study revealed that there are 61 species of flowering plants from Marathwada which are useful on Rheumatism. The results are tabulated in the form of botanical name, family, local name and parts used to cure Rheumatism.

Sr. No.	Botanical name	Family	Local/Vernacular name
01	*Adhatoda zeylanica*	Acanthaceae	Adulsa
02	*Alangium salviifolium*	Cornaceae	Ankol
03	*Allium cepa*	Amaryllidaceae	Kanda
04	*Allium sativum*	Amaryllidaceae	Lasun
05	*Aloe vera*	Asphodelaceae	Korphad
06	*Alstonia scholaris*	Apocynaceae	Satvin
07	*Asparagus racemosus*	Asparagaceae	Shatavari
08	*Bacopa monnieri*	Plantaginaceae	Brahmi
09	*Brassica juncea*	Brassicaceae	Mohari
10	*Cadaba fruticosa*	Capparaceae	Habab
11	*Calotropis gigantea*	Asclepiadaceae	Rui/ Ruchaki
12	*Cannabis sativa*	Cannabaceae	Ganja
13	*Cardiospermum halicacabum*	Sapindaceae	Kapalphodi
14	*Carthamus tinctorius*	Asteraceae	Kardi
15	*Cassia fistula*	Caesalpiniaceae	Bahava
16	*Celastrus paniculatus*	Celastraceae	Malkangni
17	*Chrysopogon zizanioides*	Poaceae	Wala
18	*Citrullus colocynthis*	Cucurbitaceae	Indrayan
19	*Citrus limon*	Rutaceae	Limbu
20	*Crataeva nurvala*	Capparidaceae	Vayvarna
21	*Cymbopogon citratus*	Poaceae	Gavati Chaha
22	*Drimia indica*	Asparagaceae	Rankanda
23	*Erythrina variegata*	Fabaceae	Pangra
24	*Euphorbia antiquorum*	Euphorbiaceae	Tridhari nivdung
25	*Gossypium herbaceum*	Malvaceae	Kapus
26	*Grewia tiliifolia*	Malvaceae	Dhaman
27	*Guizotia abyssinica*	Asteraceae	Karal

28	*Hemidesmus indicus*	Periplocaceae	Anantmul, Kavli
29	*Holarrhena antidysenterica*	Apocynaceae	Bhuiringani
30	*Holarrhena pubescens*	Apocynaceae	Pandhra Kuda
31	*Hygrophila auriculata*	Acanthaceae	Kolsunda
32	*Lepidium sativum*	Brassicaceae	Ahaliv
33	*Madhuca longifolia*	Sapotaceae	Moha
34	*Magnolia champaca*	Magnoliaceae	Sonchafa
35	*Mentha piperita*	Lamiaceae	Pudina
36	*Momordica charantia*	Cucurbitaceae	Karale
37	*Moringa oleifera*	Moringaceae	Shevga
38	*Nyctanthes arbor-tristis*	Nyctanthaceae	Parijatak
39	*Ocimum tenuiflorum*	Lamiaceae	Tulas
40	*Operculina turpethum*	Convolvulaceae	Nishottar
41	*Papaver somniferum*	Papaveraceae	Afu
42	*Piper nigrum*	Piperaceae	Mire
43	*Plumbago zeylanica*	Plumbaginaceae	Chitrak
44	*Pongamia pinnata*	Fabaceae	Karanj
45	*Portulaca oleracea*	Portulacaceae	Ghol
46	*Ricinus communis*	Euphorbiaceae	Erand
47	*Triticum aestivum*	Poaceae	Gahu
48	*Salvadora persica*	Salvadoraceae	Pilu/Mithijar
49	*Sapindus mukorossi*	Sapindaceae	Reetha
50	*Semecarpus anacardium*	Anacardiaceae	Bibba
51	*Senna alexandrina*	Fabaceae	Sonamukhi
52	*Solanum nigrum*	Solanaceae	Kamoni
53	*Soymida febrifuga*	Meliaceae	Rohan
54	*Terminalia chebula*	Combretaceae	Hirda
55	*Tinospora cordifolia*	Menispermaceae	Gulvel
56	*Trachyspermum ammi*	Apiaceae	Ova
57	*Trigonella foenum-graecum*	Fabaceae	Methi
58	*Vitex negundo*	Verbenaceae	Nirgundi
59	*Vitis vinifera*	Vitaceae	Draksha
60	*Withania somnifera*	Solanaceae	Ashwagandha
61	*Zingiber officinale*	Zingiberaceae	Ale

References:

1. "Curcuma longa: A review of therapeutic effects in traditional and modern medical references", J Chem Pharmac Sci.; 9 (4): 3438-3448.
2. Amandeep Kaur, Parminder Nain, Jaspreet Nain, (2012) "Herbal plants used in treatment of rheumatoid arthritis: a review", International Journal of Pharmacy

and Pharmaceutical Sciences, Vol 4, Suppl 4; 44-57.

3. Baharvand-Ahmadi, B., Bahmani, M., Naghdi, N., Saki, K., Baharvand-Ahmadi, S., Rafieian-Kopaei, M., (2015) "Review on phytochemistry, therapeutic and pharmacological effects of myrtus (Myrtus communis)." Der Pharmacia Lettre; 7(11): 160-165.
4. Baharvand-Ahmadi, B., Bahmani, M., Zargaran, A., Eftekhari, Z., Saki, K., Baharvand-Ahmadi, S., Rafieian-Kopaei, M., (2015) "Ruta graveolens plant: A plant with a range of high therapeutic effect called cardiac plant", Der Pharmacia Lettre; 7(11): 172-173.
5. Bahmani, M., Sarrafchi, A., Shirzad, H., Rafieian-Kopaei, M., (2016) "Autism: Pathophysiology and promising herbal remedies", Current Pharmaceutical Design; 22(3): 277-285.
6. Bhogaonkar PY and Ahmad SA, (2012) Pharmacognostic studies on *Xanthium strumarium* L.- A folk Unani medicinal herb. *Bioscience Discovery*, 3(1):101-106.
7. Biradar RM, (2013) Pharmacognostic studies on some leaf drugs of Marathwada. Thesis Dr. Babasaheb Ambedkar Marathwada University, Chhatrapati Sambhajinagar (M. S.) India.
8. Das M.N. and Das P.K., (2002) "A survey of the Medicinal uses of local plants by the natives of Vaishali District, Bihar" International Journal Mendel, Vol. 19 (3); 113-115.
9. Gambhire V. S., (2008) "Standerdization of Ayurvedic drugs- I Leaf drug studies in Marathwada", Ph.D. Thesis submitted Dr. B.A.M. University Chhatrapati Sambhajinagar.
10. Kirtikar K.R. and Basu B.D., (1984) "Indian Medicinal plants", Rewritten by Blatter Caius J.F. and Mhaskar, Lalit Mohan Basu Publication, Allahabad.
11. Lal HS and Singh S, (2012) Study of Plant Biodiversity of Hajaribag District, Jharkhand, India and its Medicinal Uses. *Bioscience Discovery*, 3(1):91-96.
12. Mahmoudi GA, Mahmoodnia L, Mirhosseini M., (2016) "A review on the most important medicinal herbs native to Iran with antiacetaminophen toxicity", J Global Pharma Technol.; 8 (11): 12-16.
13. M27ahmoudi GA, Mahmoodnia L, Mirhosseini M., (2016) "Medicinal plants with anti-poisoning toxicity of c28arbon tetrachloride: An overview of the most important medicinal plants native to Iran with anticar29bon tetrachloride toxicity", J Global Pharma Technol.; 8 (11): 17-20.
14. Mali YP 30and Bhadane VV, (2011) Ethno-medical wisdom of tribals of Chhatrapati Sambhajinagar district (M.S.), India. *Indian J. of Natural Products and Resources*, 2(1):102-109.
15. Mohmmad Nafees Iqbal and Suradkar SS, (2011) Ethnobotanical and Ethnomedicinal Study of some medicinal plants of Barshitakli Tahsil District Akola (MS) India. *Bioscience Discovery*, 2(2):236-239.
16. Muley JR and Sharma PP, (2013) Plants used in Treatment of Jaundice by Folklore of Ahmednagar district, Maharashtra, India. *Science Reasearch Reporter,*3(2):216-222.
17. Nag K and Zia-Ul-Hasan, (2013) Study of some rare medicinal wild herbs from gardens of Bhopal city, Madhya Pradesh (India), *Int. J. Parm. & Life Sci.,* 3:2437-2439.
18. Naik V.N., (1998) "Flora of Marathwada", Amrut Prakashan, Auranagabad.

19. Naik V.N., (1998) "Marathwadyatil Samanya Vanaushadhi", Amrut Prakashan, Chhatrapati Sambhajinagar, (M.S.), India.
20. Peter A. Akah, Alphonsus I. Nwambie, (1994) "Evaluation of Nigerian traditional medicines: 1. Plants used for rheumatic (inflammatory) disorders", Journal of Ethnopharmacology: 42:179- I82.
21. Rezvanirad A, Mardani M, Shirzad H, Ahmadzadeh SM, Asgary S, Naimi A, Mahmoudi GHA, (2016) Trivedi KP, (2003-2008) *Vanaushadhi Visheshank Part 1-6*, Shri Jwala Ayurved Bhavan, Aligadh (U.P.) India.
22. Zarei GA, Almasi V, Lorzadeh N, Khansari A. (2015) "The reasons for using and not using alternative medicine in Khorramabad women, west of Iran" J Pakistan Med Assoc.; 65(6): 623-625.

International Journal of Advance and Applied Research
www.ijaar.co.in
ISSN – 2347-7075 Impact Factor – 8.141
Peer Reviewed Bi-Monthly
Vol. 7 No. 14 January – February - 2026

Ecological Assessment of Rhizosphere Fungal Diversity in Semi-Arid Agricultural Soils of Maharashtra, India

Vijayalaxami S. Shelke
S.S.V.P.S.'S L. K. Dr. P. R. Ghogrey, Science College, Dhule-424005
Corresponding Author – Vijayalaxami S. Shelke
DOI - 10.5281/zenodo.19755683

Abstract:

Rhizospheric fungi play a vital role in nutrient cycling and soil fertility in semi-arid agroecosystems. This study assessed the diversity and seasonal dynamics of rhizosphere fungi associated with sugarcane cultivation in Shahada and Navapur talukas of Nandurbar district, Maharashtra. Soil samples were collected from 10–20 cm depth, and fungal isolates were obtained using the serial dilution technique on PDA medium. Soil physicochemical parameters including pH, moisture, organic carbon, and NPK were analysed and correlated with fungal distribution. The soils exhibited near-neutral pH (6.3–7.7), moderate moisture (14.7–22.43%), and organic carbon content ranging from 0.63–0.91%. Available nitrogen varied between 228.22 and 374.33 kg/ha, indicating spatial fertility differences. Seasonal analysis showed higher fungal contribution during summer and rainy seasons compared to winter. Dominant genera included Aspergillus, Penicillium, Mucor, and Rhizopus. The presence of Fusarium solani and Rhizoctonia solani indicated coexistence of beneficial and pathogenic fungi. The findings demonstrate that fungal community structure is strongly influenced by soil properties and seasonal variations. This study provides baseline data for region-specific soil management and sustainable sugarcane production strategies.

Keywords: Rhizosphere Fungi; Seasonal Variation; Soil Fertility; Sugarcane; Semi-Arid Soils; Fungal Diversity; Nandurbar District.

Introduction:

The rhizosphere is the narrow zone of soil directly influenced by plant roots and represents one of the most biologically active regions of terrestrial ecosystems. This microenvironment harbours diverse microbial communities, particularly fungi, which play crucial roles in nutrient cycling, soil fertility, and plant health (Siddiqui et al., 2004; A. Kumar et al., 2018). Soil functions as a dynamic living system composed of minerals, organic matter, gases, and microorganisms interacting through complex physical, chemical, and biological processes (Smit et al., 1999; Dighton, 2018).

Rhizosphere fungi contribute significantly to the decomposition of organic matter, mineralization of nutrients, and stabilization of soil structure through hyphal networks (Wang et al., 2017; Priya, 2014). Root exudates rich in carbohydrates and organic acids stimulate fungal growth and regulate microbial interactions in the rhizosphere (Anita Pandey, 2007; Kennedy & de Luna, 2004). These fungi enhance nutrient uptake, particularly phosphorus and nitrogen, improve plant growth, and increase resistance to pathogens and environmental stresses (Mishra et al., 2024; Walker et al., 2003).

In addition, several rhizosphere fungi exhibit biocontrol properties by competing with soil-borne pathogens or producing antimicrobial compounds (Raaijmakers et al., 2009). Despite global advancements in soil microbiology,

region-specific studies on rhizosphere fungal diversity remain limited in semi-arid agroecosystems such as Nandurbar district of Maharashtra Considering the district's diverse cropping systems and agro-climatic conditions, systematic investigation of rhizosphere fungi is essential to understand their ecological functions and seasonal dynamics. Such studies are vital for developing sustainable soil management strategies and microbiome-based interventions aimed at enhancing crop productivity and long-term agricultural sustainability (Meena et al., 2016; Stark et al., 2007).

Materials and Methods:

1. Study Area:

The present investigation was conducted in Shahada and Navapur Talukas of Nandurbar District, Maharashtra. The district lies between 21°00′–22°03′ N latitude and 73°31′–74°32′ E longitude. The region experiences a semi-arid climate with black to sandy clay loam soils, suitable for sugarcane cultivation.

2. Collection of Soil Samples:

Rhizosphere soil samples were collected from healthy sugarcane plants during the active growth period. Soil adhering to the root zone was carefully removed using sterile tools. From each taluka, three representative sites were selected, Samples were taken at a depth of 10–20 cm, where root activity is most concentrated and samples were collected in sterile polythene bags and transported to the laboratory for analysis.

3. Isolation of Fungi:

The serial dilution technique was employed for the isolation of soil fungi. One gram of rhizosphere soil was suspended in sterile distilled water and serially diluted up to 10^{-5}. An aliquot of 1 ml from the 10^{-3} dilution was inoculated on Potato Dextrose Agar (PDA) plates using the spread plate method. Plates were incubated at room temperature for 5–7 days.

4. Identification of Fungal Isolates:

Fungal colonies were counted to calculate colony-forming units (CFU). Distinct colonies were sub-cultured and identified based on macroscopic and microscopic characteristics such as colony morphology, spore structure, and hyphal features. Identification was carried out using standard taxonomic keys.

5. Analysis of Soil Physicochemical Properties:

Soil samples were analysed for pH, texture, colour, and nutrient content (NPK) using standard soil analysis procedures. These parameters were correlated with fungal diversity and distribution.

Result and Discussion:

1. Comparative Analysis of Ecological Parameters:

SN	Ecological Parameters	Taluka-wise average mean derived from Winter, Summer, and Rainy season data.					
		Nandurbar	Navapur	Taloda	Shahada	Akkalkuwa	Akrani Mahal
1	pH	6.4	6.3	6.7	6.6	7.7	6.8
2	Moisture (%)	17.33	15.8	16.52	22.43	19.31	14.7
3	Temperature (°C)	27.33	29.93	28.7	28.2	24.55	25.58
4	Organic Carbon (%)	0.63	0.64	0.91	0.66	0.83	0.64
5	Available Nitrogen (kg/ha)	361.67	296.07	296.11	315.1	374.33	228.22
6	Alkalinity (meq/100g)	0.34	0.48	0.48	0.15	0.24	0.18
7	Phosphorus (kg/h)	16.04	15.33	15.51	17.33	14.61	16.28
8	Potassium (kg/h)	163.38	150.26	161.46	144	167.79	167.22
9	Calcium (meq/L)	14.72	15.43	19.09	17.07	14.36	17.19
10	Magnesium (meq/L)	14.1	15.09	18.09	11.87	12.03	15.88

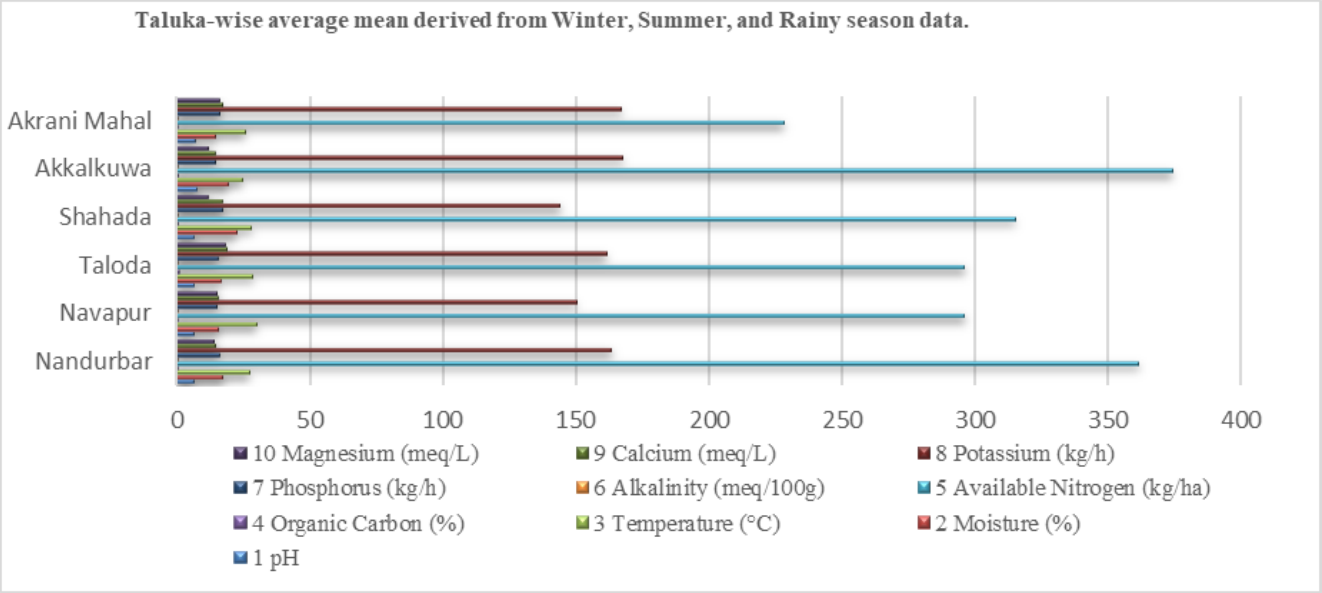

The comparative evaluation of soil ecological parameters across six talukas of Nandurbar district indicates noticeable spatial variation in physico-chemical characteristics influencing soil fertility and microbial activity. Soil pH ranged from slightly acidic to moderately alkaline (6.3–7.7), with most talukas showing near-neutral conditions favorable for nutrient availability and microbial growth (Brady & Weil, 2016). Moisture content varied considerably, with Shahada exhibiting the highest (22.43%) and Akrani Mahal the lowest (14.7%), which may directly affect microbial metabolism and decomposition processes (Paul, 2015).Organic carbon content was highest in Taloda (0.91%) and Akkalkuwa (0.83%), suggesting enhanced

soil fertility and greater biological activity, as organic carbon is a key indicator of soil health (Lal, 2015). Available nitrogen was comparatively higher in Akkalkuwa and Nandurbar, while lower values were observed in Akrani Mahal, indicating variability in nutrient supply potential. Phosphorus and potassium levels remained relatively stable across talukas, supporting balanced macronutrient status.

Calcium and magnesium concentrations were higher in Taloda, reflecting improved cation exchange capacity and structural stability. Overall, Taloda and Akkalkuwa demonstrated comparatively better soil fertility indicators, whereas Akrani Mahal showed relatively lower nutrient availability. These variations are likely to influence rhizospheric microbial diversity and agricultural productivity, highlighting the need for region-specific soil management strategies.

2. Seasonal Contribution of Fungal Species:

Season wise % Contribution of Fungal Species

Name of Fungal Species	Nandurbar			Navapur			Taloda			Shahada			Akkalkuwa			Akrani Mahal		
	Winter	Summer	Rainy	Winter	Summer	Rainy	Winter	Summer	Rainy	Winter	Summer	Rainy	Winter	Summer	Rainy	Winter	Summer	Rainy
Alternaria alternata	18.7	0	30.7	-	-	-	-	-	-	-	-	-	20	0	13.3	-	-	-
Aspergillus flavus	-	-	-	11.1	0	31.5	-	-	-	0	16.6	23	-	-	-	20	0	9.5
Aspergillus fumigatus	0	15.3	15	18.7	0	30.7	-	-	-	-	-	-	-	-	-	-	-	-
Aspergillus niger	-	-	-	-	-	-	25	0	22.2	42.8	0	23	-	-	-	20	9	9.5
Aspergillus tamarii	0	15.3	5	-	-	-	-	-	-	-	-	-	-	-	-	-	-	-
Aspergillus ustus	18.7	0	5	-	-	-	7.3	0	5.5	16.6	16.6	31.5	33.3	0	13.3	-	-	-
Botrytis cinerea	-	-	-	-	-	-	-	-	-	-	-	-	13.3	0	20	-	-	-
Chaetomium globosum	-	-	-	18.7	0	20	-	-	-	0	33.3	23	0	9	6.6	0	27.2	14.2
Cladosporium oxysporum	-	-	-	-	-	-	41.6	0	11.1	-	-	-	-	-	-	-	-	-
Curvularia clavata	-	-	-	11.1	0	10.5	-	-	-	18.7	0	20	-	-	-	20	9	0
Curvularia lunata	12.5	7.6	15	-	-	-	-	-	-	-	-	-	0	18.1	6.6	-	-	-
Fusarium solani	18.7	0	20	0	16.6	5.2	8.3	14.2	16.6	-	-	-	-	-	-	-	-	-
Mucor mucedo	-	-	-	-	-	-	0	0	22.2	28.5	0	0	20	9	0	-	-	-
Mucor racemosus	25	7.6	0	22.2	16.6	5.2	8.3	0	5.5	14.2	16.6	15.3	-	-	-	13.3	18.1	9.5
Penicillium aurantiogriseum	-	-	-	-	-	-	-	-	-	-	-	-	0	27.2	6.6	-	-	-
Penicillium chrysogenum	-	-	-	27.7	0	5.2	0	42.8	5.5	14.2	33.3	15.3	-	-	-	-	-	-
Penicillium funiculosum	-	-	-	-	-	-	-	-	-	-	-	-	0	9	13.3	-	-	-
Penicillium glabrum	-	-	-	-	-	-	8.3	0	5.5	-	-	-	6.6	0	6.6	0	18.1	4.7
Pythium debaryanum	6.4	40	26	-	-	-	8.3	42.8	11.1	-	-	-	-	-	-	-	-	-
Rhizoctonia solani	-	-	-	-	-	-	-	-	-	13.3	18.1	9.5	6.6	9	6.6	6.6	0	19
Rhizopus stolonifer	18.7	0	20	-	-	-	6.6	9	6.6	-	-	-	-	-	-	20	18.1	33.3

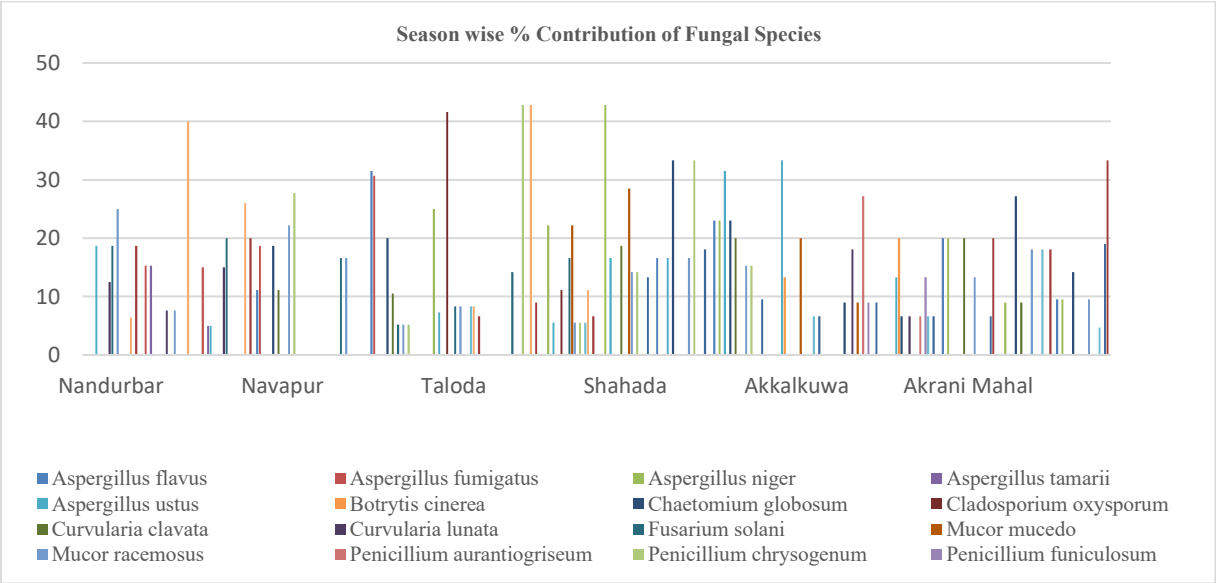

The seasonal distribution of fungal species across the six talukas of Nandurbar district shows clear spatial and temporal variation. Fungal occurrence was strongly influenced by seasonal changes, particularly moisture and temperature, which regulate fungal growth and sporulation (Paul, 2015). Overall, rainy and summer seasons exhibited comparatively higher percentage contributions than winter, indicating favourable environmental conditions for fungal proliferation.

Species of *Aspergillus* (e.g., *A. niger*, *A. flavus*, *A. fumigatus*) were dominant across multiple talukas and seasons, reflecting their adaptability to semi-arid agroecosystems (Dighton, 2018). *Alternaria alternata* showed increased contribution during the rainy season in Nandurbar, suggesting preference for humid conditions. Similarly, *Mucor racemosus* and *Rhizopus stolonifer* demonstrated higher representation during rainy periods, consistent with their moisture-dependent growth patterns.

In Taloda and Shahada, relatively diverse assemblages including *Cladosporium*, *Curvularia*, and *Chaetomium globosum* were observed, indicating region-specific fungal dynamics. The moderate but consistent presence of *Penicillium* species suggests their role in organic matter decomposition and nutrient recycling. Occurrence of pathogenic species such as *Fusarium solani* and *Rhizoctonia solani* highlights the coexistence of beneficial and harmful fungi within the rhizosphere.

The overall dominance of *Aspergillus*, *Penicillium*, and *Mucor* species aligns with previous findings that these genera are common in agricultural soils and contribute significantly to nutrient transformation (Brady & Weil, 2016). The results confirm that seasonal climatic variations significantly shape fungal community structure and ecological function, emphasizing the need for season-based soil management strategies to maintain soil health and crop productivity.

Conclusion:

The present investigation conducted in Shahada and Navapur talukas of Nandurbar district demonstrated significant spatial and seasonal variation in rhizospheric fungal diversity associated with sugarcane cultivation. Soil physicochemical parameters such as pH (6.3–7.7), moisture (14.7–22.43%), organic carbon (0.63–0.91%), and available nitrogen (228.22–374.33 kg/ha) indicated near-neutral and fertile soil conditions favourable for microbial activity. Higher organic carbon and nitrogen levels in Taloda and Akkalkuwa corresponded with improved soil fertility indicators, supporting enhanced fungal proliferation.

Seasonal analysis revealed that summer and rainy seasons contributed comparatively higher fungal percentages than winter, confirming the influence of moisture and temperature on fungal growth dynamics. Dominant genera included *Aspergillus*, *Penicillium*, *Mucor*, and *Rhizopus*, reflecting their ecological adaptability in semi-arid agroecosystems. Species such as *Aspergillus niger*, *A. flavus*, and *Penicillium chrysogenum* exhibited consistent seasonal occurrence, indicating their significant role in nutrient cycling and organic matter decomposition (Dighton, 2018; Paul, 2015).

The occurrence of pathogenic species including *Fusarium solani* and *Rhizoctonia solani* highlights the coexistence of beneficial and harmful fungi within the rhizosphere, emphasizing the ecological balance governing soil health. Variations in fungal composition

across talukas suggest that local soil properties and seasonal climatic factors significantly influence community structure (Brady & Weil, 2016).

Overall, the study confirms that rhizospheric fungal diversity in Nandurbar district is closely linked to soil physicochemical properties and seasonal fluctuations. These findings provide a scientific basis for developing region-specific soil management strategies and microbiome-based interventions aimed at enhancing crop productivity and sustainable agricultural practices (Lal, 2015; Smit et al., 1999).

References:

1. Adedayo, A. A., & Babalola, O. O. (2023). *Title of the article*. *Journal Name, Volume*(Issue), page–page.
2. Anita Pandey. (2007). *Title of the article/book*. Publisher/Journal Name.
3. Ashrafi, E., et al. (2014). *Title of the article*. *Journal Name, Volume*(Issue), page–page.
4. Bhullar, N. K. (2020). *Title of the article*. *Journal Name, Volume*(Issue), page–page.
5. Brady, N. C., & Weil, R. R. (2016). *The nature and properties of soils* (15th ed.). Pearson.
6. Chaithra, S., et al. (2020). *Title of the article*. *Journal Name, Volume*(Issue), page–page.
7. Dighton, J. (2018). *Fungi in ecosystem processes* (2nd ed.). CRC Press.
8. Hartoyo, B., & Trisilawati, O. (2021). *Title of the article*. *Journal Name, Volume*(Issue), page–page.
9. Kennedy, A. C., & de Luna, L. Z. (2004). Rhizosphere. In *Encyclopedia of soils in the environment* (pp. xx–xx). Elsevier.
10. Kumar, A., et al. (2018). *Title of the article*. *Journal Name, Volume*(Issue), page–page.
11. Kumar, P. K. R., et al. (2015). *Title of the article/book*. Publisher/Journal Name.
12. Lal, R. (2015). Restoring soil quality to mitigate soil degradation. *Sustainability, 7*(5), 5875–5895.
13. Meena, V. S., et al. (2016). *Title of the article*. *Journal Name, Volume*(Issue), page–page.
14. Mishra, J., et al. (2024). *Title of the article*. *Journal Name, Volume*(Issue), page–page.
15. Paul, E. A. (2015). *Soil microbiology, ecology and biochemistry* (4th ed.). Academic Press.
16. Priya, V. (2014). *Title of the article*. *Journal Name, Volume*(Issue), page–page.
17. Raaijmakers, J. M., Paulitz, T. C., Steinberg, C., Alabouvette, C., & Moënne-Loccoz, Y. (2009). The rhizosphere: A playground and battlefield for soilborne pathogens and beneficial microorganisms. *Plant and Soil, 321*(1–2), 341–361. https://doi.org/10.1007/s11104-008-9568-6
18. Siddiqui, Z. A., et al. (2004). *Title of the article/book*. Publisher/Journal Name.
19. Smit, E., Leeflang, P., & Wernars, K. (1999). Detection of shifts in microbial community structure and diversity in soil caused by the introduction of genetically modified bacteria. *FEMS Microbiology Ecology, 27*(4), 379–388.
20. Stark, C., Condron, L. M., Stewart, A., Di, H. J., & O'Callaghan, M. (2007). Influence of organic and mineral amendments on microbial soil properties and processes. *Applied Soil Ecology, 35*(1), 79–93.
21. Todorović, B., et al. (2023). *Title of the article*. *Journal Name, Volume*(Issue), page–page.
22. Walker, T. S., Bais, H. P., Grotewold, E., & Vivanco, J. M. (2003). Root exudation and rhizosphere biology. *Plant Physiology, 132*(1), 44–51.
23. Wang, Z., et al. (2017). *Title of the article*. *Journal Name, Volume*(Issue), page–page.

International Journal of Advance and Applied Research
www.ijaar.co.in
ISSN – 2347-7075 Impact Factor – 8.141
Peer Reviewed Bi-Monthly
Vol. 7 No. 14 January – February - 2026

Comparative Quantitative Profiling of Secondary Metabolites in Different Organs of Ficus religiosa L.

Vasantrao B. Kadam[1] & Madhukar S. Wadikar[2]

[1]*Department of Botany, MVP Samaj's, Arts, Commerce and Science College, Dindori-422202, Nashik, MS, India*

[2]*Department of Botany, R. B. Attal College, Georai, Beed-431127, MS, India*

Corresponding Author – Vasantrao B. Kadam

DOI - 10.5281/zenodo.19755722

Abstract:

Ficus religiosa L. (Moraceae) is widely recognized for its ethno medicinal properties. This study provides a comparative quantitative analysis of major secondary metabolites — phenolic, flavonoids, alkaloids, tannins, and saponins — in four organs: leaves, stem bark, roots, and fruits. Methanolic extracts were evaluated using standardized spectrophotometric and gravimetric protocols. Results show significant variation ($p < 0.05$) among organs, with leaves rich in phenolic, fruits in flavonoids, stem bark in tannins and alkaloids, and roots in saponins. These findings guide organ-specific extraction for pharmaceutical and nutraceutical development.

Keywords: Ficus Religiosa, Secondary Metabolites, Quantitative Analysis, Phenolics, Flavonoids

Introduction:

Plants synthesize a variety of secondary metabolites that serve defensive and adaptive functions and exhibit therapeutic qualities such as antioxidant, antimicrobial, anti-inflammatory and anticancer activities (Harborne, 1998). Among medicinal plants, *Ficus religiosa* L., commonly called the Peepal or Sacred Fig, holds a prominent place in traditional medicine across Asia (Sharma et al., 2010). Leaves, bark, roots, and fruits have been employed to treat asthma, gastrointestinal disorders, diabetes, diarrhoea, wounds, and infections (Gupta & Singh, 2014).

Previous studies have identified key phytochemicals in extracts of *F. religiosa* (Parekh & Chanda, 2007; Singh & Singh, 2015). However, most reports provide qualitative screening or focus on a single plant part. Comparative quantitative data across multiple organs remain limited, yet such information is necessary for standardization, phytopharmaceutical validation, and resource optimization.

This study quantifies five major classes of secondary metabolites — phenolics, flavonoids, alkaloids, tannins, and saponins — in leaves, stem bark, roots and fruits of *F. religiosa* under uniform extraction and analytic conditions.

Materials and Methods:

Plant Material Collection and Preparation:

Fresh parts (leaves, stem bark, roots, fruits) of *Ficus religiosa* L. were collected from mature trees in Nashik, authenticated by a botanist, and voucher specimens were deposited in the College herbarium. Materials were washed, shade-dried, and ground into fine powder.

Extraction Procedure:

Powdered samples (50 g each) were extracted with 80% methanol (1:10 w/v) by cold maceration for 72 h with intermittent shaking. Extracts were filtered through Whatman No. 1

filter paper and concentrated under reduced pressure. Extracts were stored at 4°C until analysis.

Quantitative Estimation of Secondary Metabolites:

Total Phenolic Content (TPC):

Measured by the Folin–Ciocalteu method using gallic acid as standard. Absorbance was read at 765 nm (Singleton & Rossi, 1965). Results expressed as mg gallic acid equivalents (GAE)/g dry weight.

Total Flavonoid Content (TFC):

Determined using aluminum chloride assay with quercetin standard (Chang et al., 2002). Absorbance was measured at 415 nm. Results expressed as mg quercetin equivalents (QE)/g dry weight.

Alkaloid Content:

Quantified using an acid-base precipitation method and expressed as mg/g dry weight (Harborne, 1998).

Tannin Content:

Estimated via vanillin–HCl assay with catechin standard (Price et al., 1978) at 500 nm. Results are mg catechin equivalents (CE)/g.

Saponin Content:

Determined by a gravimetric method and expressed as percentage (%).

Statistical Analysis:

All analyses were performed in triplicate. Data were expressed as mean ± standard deviation (SD). Differences among plant parts were evaluated by one-way analysis of variance (ANOVA), followed by Tukey's pairwise comparisons. Statistical significance was set at $p < 0.05$.

Results:

Quantitative Distribution of Metabolites:

Table 1. Quantitative estimation of secondary metabolites in *Ficus religiosa* plant parts.

Metabolite (Unit)	Leaves	Stem Bark	Roots	Fruits
Phenolics (mg GAE/g)	120.5 ± 2.8	98.3 ± 3.1	75.6 ± 2.5	52.2 ± 1.8
Flavonoids (mg QE/g)	72.1 ± 1.9	60.0 ± 2.2	45.3 ± 1.6	85.4 ± 2.4
Alkaloids (mg/g)	1.12 ± 0.03	1.65 ± 0.05	0.88 ± 0.02	0.74 ± 0.02
Tannins (mg CE/g)	150.2 ± 4.5	210.3 ± 5.7	130.4 ± 3.9	90.1 ± 3.1
Saponins (%)	2.21 ± 0.05	1.98 ± 0.04	2.78 ± 0.06	1.55 ± 0.03

Data represent mean ± SD (n = 3). All differences among plant parts were statistically significant ($p < 0.05$).

Discussion:

Secondary metabolites significantly varied among the four plant organs of *Ficus religiosa*:

- **Phenolics:** Leaves showed the highest total phenolic content, consistent with their role in defense against oxidative stress and UV exposure (Alam et al., 2013).
- **Flavonoids:** Fruits exhibited the largest flavonoid content, likely related to protection against oxidative damage during seed development.
- **Alkaloids and Tannins:** Stem bark had significantly higher levels of alkaloids and tannins, aligning with its traditional uses in antimicrobial and anti-inflammatory applications (Singh & Singh, 2015).

- **Saponins:** Roots were richest in saponins, which play roles in allelopathy and soil-borne pathogen defense (Das et al., 2019).

These results support the **organ-specific therapeutic roles** of *Ficus religiosa* and suggest that targeted extraction of specific organs can yield higher concentrations of desired bioactive compounds.

Conclusion:

This comparative study provides a comprehensive quantitative profile of key secondary metabolites in leaves, stem bark, roots, and fruits of *Ficus religiosa* L. Significant differences highlight the necessity for organ-specific selection in phytopharmaceutical applications. The results may inform standardization of herbal formulations and promote efficient utilization of plant resources.

References:

1. Alam, M.A., et al. (2013). Antioxidant potential of *Ficus religiosa* leaves. *Journal of Medicinal Plants Studies*, **1**(4), 25–30.
2. Chang, C., Yang, M., Wen, H., & Chern, J. (2002). Estimation of total flavonoid content. *Journal of Food and Drug Analysis*, **10**, 178–182.
3. Das, P., et al. (2019). Role of saponins in medicinal plants: chemistry and therapeutic potential. *Phytochemistry Reviews*, **18**, 1343–1373.
4. Gupta, R., & Singh, N. (2014). Medicinal importance of *Ficus religiosa*. *International Journal of Pharmacy and Pharmaceutical Sciences*, **6**(5), 1–5.
5. Harborne, J.B. (1998). *Phytochemical Methods: A Guide to Modern Techniques of Plant Analysis*. Springer.
6. Parekh, J., & Chanda, S. (2007). In vitro antimicrobial activity of *Ficus religiosa*. *Brazilian Journal of Microbiology*, **38**, 204–207.
7. Price, M.L., et al. (1978). Tannin content by vanillin–HCl method. *Journal of Agricultural and Food Chemistry*, **26**, 809–812.
8. Sharma, P., et al. (2010). Phytochemical and pharmacological review of *Ficus religiosa*. *International Journal of Pharmaceutical Sciences Review and Research*, **2**(2), 76–83.
9. Singh, N., & Singh, S. (2015). Ethnomedicinal uses of *Ficus religiosa*. *Journal of Herbal Medicine*, **5**(3), 123–130.
10. Singleton, V.L., & Rossi, J.A. (1965). Colorimetry of total phenolics. *American Journal of Enology and Viticulture*, **16**, 144–158.

International Journal of Advance and Applied Research
www.ijaar.co.in
ISSN – 2347-7075 Impact Factor – 8.141
Peer Reviewed Bi-Monthly
Vol. 7 No. 14 January – February - 2026

Role of Advanced Spectroscopic Techniques in Modern Materials Characterization

G. S. Jaigaonkar
Assistant Professors, Department of Physics,
Bapuraoji Butle Arts, Narayanrao Bhat Commerce and Bapusaheb Patil Science College Digras, Dist. Yavatmal (M.S.) India
Corresponding Author – G. S. Jaigaonkar
DOI - 10.5281/zenodo.19755753

Abstract:

Modern materials science depends strongly on accurate and reliable characterization techniques to understand the structural, chemical, and functional properties of materials. Among different analytical methods, advanced spectroscopic techniques have become essential tools for investigating materials at atomic, molecular and nanoscale levels. These techniques provide detailed information about composition, bonding, electronic structure, crystal defects and surface chemistry without destroying the sample. With the rapid development of nanotechnology, energy materials and functional materials, spectroscopy plays a key role in linking material design with real applications. This paper presents a comprehensive overview of the role of advanced spectroscopic techniques in modern materials characterization. Major spectroscopic methods such as Raman spectroscopy, Fourier transform infrared spectroscopy, X-ray photoelectron spectroscopy, ultraviolet–visible spectroscopy, nuclear magnetic resonance spectroscopy and photoluminescence spectroscopy are discussed. Their principles, recent developments and applications in nanomaterials, energy storage devices, environmental materials and biomedical materials are highlighted. The importance of spectroscopy in knowledge generation, quality control and sustainable material development is also emphasized. Finally, present challenges and future directions of spectroscopic characterization are addressed.

Keywords: Advanced Spectroscopy, Materials Characterization, Raman Spectroscopy, XPS, FTIR, Nanomaterials, Energy Materials, etc.

Introduction:

Materials characterization is a fundamental part of materials science and engineering. The performance of any material strongly depends on its internal structure, chemical composition, surface properties and electronic behavior. Therefore, understanding these parameters is essential for developing new materials for electronics, energy storage, environmental protection and biomedical applications.

Traditional characterization methods such as optical microscopy and basic chemical analysis are often insufficient for modern advanced materials, especially nanostructured and multifunctional materials. In recent years, advanced spectroscopic techniques have become powerful tools to explore materials at microscopic and atomic scales. Spectroscopy enables non-destructive and highly sensitive analysis of materials, making it suitable for both fundamental research and industrial quality control.

Modern spectroscopy is no longer limited to simple chemical identification. It now provides in-depth insights into molecular vibrations, electronic transitions, surface chemistry, defect states and local atomic environments. As a result,

advanced spectroscopic techniques play a central role in modern materials characterization and knowledge generation.

This paper reviews major advanced spectroscopic techniques and explains how they contribute to the development of modern materials.

Importance of Spectroscopic Techniques in Materials Characterization:

Spectroscopic techniques measure the interaction of electromagnetic radiation with matter. When radiation interacts with a material, it produces signals related to molecular vibrations, electronic transitions, or nuclear environments. These signals contain valuable information about the structure and composition of the material.

The main advantages of advanced spectroscopy include:

- Non-destructive analysis
- High sensitivity and selectivity
- Capability to probe surface and bulk properties
- Suitability for nanoscale and thin-film materials
- Real-time and in-situ monitoring

Spectroscopy bridges the gap between material synthesis and functional performance by helping researchers understand how atomic-level features influence macroscopic properties.

Major Advanced Spectroscopic Techniques:

1. Raman Spectroscopy:

Raman spectroscopy is a vibrational spectroscopic technique based on inelastic scattering of light. It provides information about molecular structure, crystal phases, strain and defects.

Raman spectroscopy is widely used in:

- Graphene and carbon nanotube analysis
- Phase identification in metal oxides
- Monitoring structural changes in battery electrodes
- Studying stress and strain in thin films

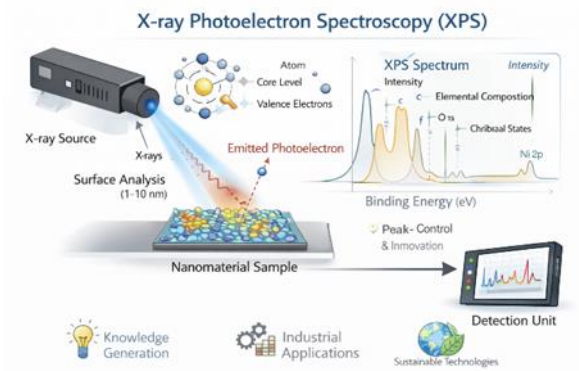

Raman mapping allows spatial distribution of material phases and defects, making it extremely useful for micro- and nanoscale characterization.

2. Fourier Transform Infrared (FTIR) Spectroscopy:

FTIR spectroscopy is used to identify chemical bonds and functional groups present in a material. It measures absorption of infrared radiation due to molecular vibrations.

FTIR is commonly applied in:

- Polymer characterization
- Surface functionalization analysis
- Biomaterials and bio-derived materials
- Environmental samples and adsorbent materials

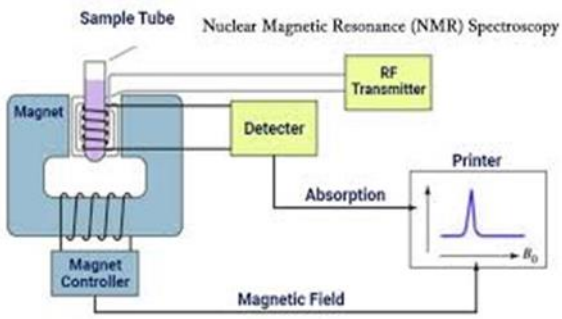

FTIR spectroscopy plays an important role in verifying surface modification of nanomaterials and confirming chemical interactions in composite systems.

3. X-ray Photoelectron Spectroscopy (XPS):

XPS is a surface-sensitive spectroscopic technique that provides information about elemental composition and chemical states.

Its main applications include:

- Oxidation state analysis
- Surface contamination detection
- Interface studies in thin films
- Catalyst surface characterization

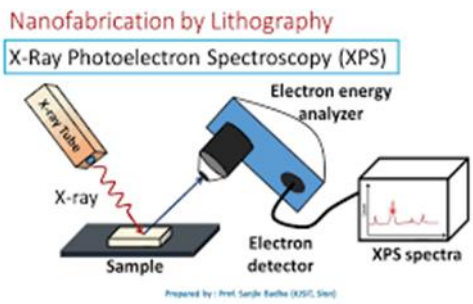

XPS is particularly important in nanomaterials and energy devices, where surface chemistry strongly affects performance.

4. Ultraviolet–Visible (UV–Vis) Spectroscopy:

UV–Vis spectroscopy is based on electronic transitions in materials. It is widely used to study optical and electronic properties.

Important applications include:

- Band gap estimation of semiconductors
- Nanoparticle size analysis through absorption peaks
- Optical transparency of coatings
- Photocatalyst performance evaluation

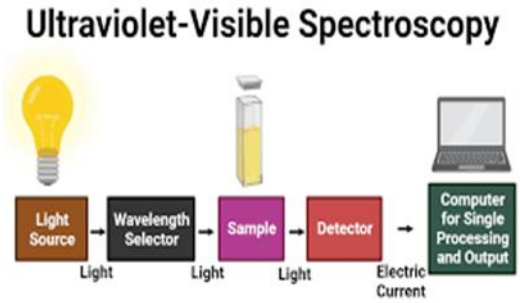

UV–Vis spectroscopy is widely applied in solar cell materials and photocatalytic systems.

5. Nuclear Magnetic Resonance (NMR) Spectroscopy:

NMR spectroscopy provides detailed information about the local atomic and molecular environment. It is highly useful for studying structure and dynamics of materials.

NMR is applied in:

- Polymer structure analysis
- Porous materials and zeolites
- Biomaterials and soft matter
- Electrolyte systems in batteries

Solid-state NMR has become a powerful tool for understanding disordered and amorphous materials.

6. Photoluminescence (PL) Spectroscopy:

Photoluminescence spectroscopy investigates the emission of light from a material after excitation. It provides information about defects, recombination processes and electronic structure.

PL spectroscopy is widely used in:

- Semiconductor nanomaterials
- Quantum dots
- Perovskite solar cells
- Light-emitting materials

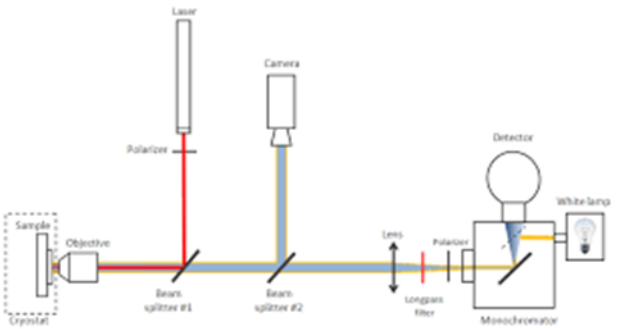

PL analysis helps identify trap states and defect levels that influence device efficiency.

Role of Spectroscopy in Nanomaterials Characterization:

Nanomaterials possess size-dependent properties and high surface-to-volume ratios. Advanced spectroscopic techniques are essential to analyze these features accurately.

Raman and PL spectroscopy are extensively used to investigate defect density and electronic properties of nanostructures. XPS provides surface chemical information, which is crucial for functionalized nanoparticles and catalysts. FTIR confirms surface modification and bonding in nanocomposites.

Spectroscopy allows researchers to correlate nanoscale structure with macroscopic performance, enabling rational design of nanomaterials.

Applications in Energy Materials:

Advanced spectroscopic techniques play a vital role in renewable energy and energy storage research.

In lithium-ion and sodium-ion batteries, Raman and XPS are used to monitor electrode surface reactions and solid electrolyte interphase formation. FTIR helps in analyzing electrolyte decomposition. UV–Vis and PL are applied to evaluate optical properties of solar absorbers.

Spectroscopy enables in-situ and operando measurements, allowing real-time observation of chemical and structural changes during device operation.

Applications in Environmental and Sustainable Materials:

Spectroscopic methods are essential in environmental remediation and sustainable material development.

FTIR and XPS are widely used to identify adsorption mechanisms in water purification materials. Raman spectroscopy helps detect pollutants and characterize photocatalysts. UV–V is spectroscopy is applied to study degradation of organic pollutants and dye removal efficiency.

These techniques support sustainable development by enabling design of efficient and environmentally friendly materials.

Applications in Biomedical and Functional Materials:

In biomedical materials, spectroscopy is used to analyze surface chemistry, biocompatibility and drug–carrier interactions. NMR and FTIR are particularly useful for studying biological molecules and polymeric scaffolds. PL spectroscopy is employed in bio-imaging and sensing applications.

Advanced spectroscopy ensures material safety and functional reliability in medical devices.

Role of Advanced Spectroscopy in Knowledge Conversion:

Advanced spectroscopic techniques contribute directly to knowledge creation and conversion in materials science. Experimental data generated through spectroscopy validate theoretical predictions and computational models. This knowledge is transferred to industrial processes, quality control and product development.

Spectroscopy also supports interdisciplinary collaboration by providing common analytical platforms for physicists, chemists, engineers, and biologists.

Challenges and Limitations:

Despite their advantages, advanced spectroscopic techniques face certain challenges:

- High instrumentation and maintenance cost
- Requirement of skilled operators
- Complex data interpretation
- Limited spatial resolution in some techniques
- Surface sensitivity limitations for bulk analysis

Future Perspectives:

Future developments in spectroscopic techniques are expected to focus on:

- High-resolution and ultrafast spectroscopy
- In-situ and operando measurements
- AI-assisted spectral analysis
- Integration with scanning probe and electron microscopy
- Portable and field-deployable spectroscopic systems

Conclusion:

Advanced spectroscopic techniques play a central role in modern materials characterization by providing accurate and detailed information about structure, composition and electronic properties. Techniques such as Raman, FTIR, XPS, UV–Vis, NMR and photoluminescence spectroscopy have become indispensable tools in nanomaterials, energy materials, environmental materials and biomedical systems. Spectroscopy not only supports material discovery and optimization but also accelerates knowledge conversion from laboratory research to real-world technologies. Continued progress in spectroscopic instrumentation and data analysis will further enhance its impact on sustainable and advanced materials research.

References:

1. Callister, W. D. and Rethwisch, D. G.,(2020) Materials Science and Engineering: An Introduction, Wiley.
2. Smith, E. and Dent, G.,(2019) Modern Raman Spectroscopy, Wiley.
3. Watts, J. F. and Wolstenholme, J., (2003) An Introduction to Surface Analysis by XPS and AES, Wiley.
4. Stuart, B., (2004) Infrared Spectroscopy: Fundamentals and Applications, Wiley.
5. Kumar, P. et al.,(2022) Advanced spectroscopic characterization of nanomaterials, Journal of Materials Chemistry A.
6. Chen, S. et al., (2021) Operando spectroscopy for energy materials, Energy & Environmental Science.
7. Grey, C. P. and Dupre, N., (2004) NMR studies of battery materials, Chemical Reviews.
8. Zhang, Y. et al., (2020) Photoluminescence spectroscopy in semiconductor nanostructures, Nano Today.

International Journal of Advance and Applied Research
www.ijaar.co.in
ISSN – 2347-7075 Impact Factor – 8.141
Peer Reviewed Bi-Monthly
Vol. 7 No. 14 January – February - 2026

Evaluating the Antitumor Efficacy of a Schiff Base Ligand and its Metal complexes across Diverse Human Cancer Cell Lines

Devkate A. V.[1] & Sakhare M. A.[2]
Department of Chemistry,
Balham Arts, Science & Commerce College, Beed, Maharashtra, India
Corresponding Author – Devkate A. V.
DOI - 10.5281/zenodo.19755783

Abstract:

Schiff bases are characterized by their imine (-C=N-) group which are versatile ligands in coordination chemistry which forms complexes with various transition metal ions due to their chelating properties. The structural diversity of Schiff bases allows for tuning of their biological activities. Ligand design including the choice of primary amine and carbonyl compounds that influences the coordination geometry, stability and electronic properties of the resulting metal complexes which directly impacting their interaction with biological targets. These metal complexes have significant importance for their biological activities such as anticancer, antifungal, antibacterial, antimalarial, antiproliferative, anti-inflammatory, antiviral, antipyretic and particularly their anticancer potential, offering a promising avenue for developing novel therapeutic agents to combat cancer which is second leading cause of global mortality. Chelating metal ions which are within Schiff base structures typically increases their biological activities primarily by increasing lipophilicity and enabling diverse modes of action within cancer cells. They often involve interactions with cellular DNA which leads to DNA binding, cleavage and alterations in DNA structure. The ability of these complexes to induce programmed death of cell is a critical aspect of their cytotoxic action. The enhanced activity of metal complexes compared to free ligands is attributed to increased lipophilicity due to chelation which facilitates better cellular penetration and enzyme inhibition. This review paper explored the efficacy of Schiff base metal complexes against a wide variety of cancer cell lines including liver cancer (Hep-G2), lung cancer (A549), colorectal (colon) cancer (HCT116), HeLa (cervical cancer) and the breast cancer (MCF-7). In this review we focused on current findings to facilitate the development of target specific chemotherapeutic agents that ensure higher cytotoxic precision and enhanced efficacy against malignant cells.

Keywords: Schiff base, Anticancer activity, DNA binding, Apoptosis, Lipophilicity.

Introduction:

Cancer remains one of the most formidable challenges to global health which characterized by the relentless and uncontrolled proliferation of abnormal cells that compromise the vital tissues. These cellular masses or tumours are categorized as either benign often manageable through surgical intervention or malignant, which is a grave threat due to their ability to metastasize through the blood and lymphatic systems. The human toll of this disease is staggering, statistics from the American Cancer Society and the Indian Council of Medical Research (ICMR) highlight a growing crisis with millions living with a cancer history and thousands succumbing to the disease daily. While traditional therapies like chemotherapy and immunotherapy have saved countless lives. They often come at a significant cost to the patient's quality of life due to severe side effects. In the search for more precise and

less toxic treatments, the field of bio-inorganic chemistry has turned its attention to Schiff bases—versatile compounds first identified by Hugo Schiff in 1864. Formed by the condensation of primary amines with carbonyl compounds, these privileged ligands are defined by their characteristic -C=N- linkage. This specific bond along with the lone pair of electrons on the nitrogen atom is believed to be the engine behind their remarkable biological activity. Schiff bases and their metal complexes have demonstrated a wide spectrum of pharmacological potential, ranging from antimicrobial and antiviral to anti-inflammatory properties. However, it is their emerging role as potent anticancer agents that has truly fascinated the research community. Recent studies have shown that these complexes can target various tumor cell lines with high efficacy, Giving hope for the development of side-effect free medicinal agents. This review aims to explore the landscape of these promising compounds with detailing the synthesis and anticancer performance of various Schiff bases and their metal (II) complexes. By examining findings, we seek to highlight how these chemical structures are being refined to transform the future of oncology and personalized medicine.[1-8]

Anticancer activities of Schiff base ligand and its metal complexes:

Creavena *et al.* synthesized a series of Schiff bases (compounds 17-23) by reacting 7-amino-4-methyl-quinolin-2(1H)-one with various substituted aromatic aldehydes in hot ethanol. The reaction utilized 7-amino-4-methyl-quinolin-2(1H)-one as the amine component and various substituted aromatic aldehydes as the carbonyl component.

SCHIFF BASE	R_1	R_2	R_3	R_4
2,4-DHMQ (17)	OH	H	OH	H
2-HMQ (18)	OH	H	H	H
2,3-DHMQ (19)	OH	OH	H	H
3-E-2-HMQ (20)	OH	OC_2H_5	H	H
2-H-3-MMQ (21)	OH	OCH_3	H	H
2-H-4-MMQ (22)	OH	H	OCH_3	H
3,5-DHMQ (23)	OH	^tBu	H	^tBu

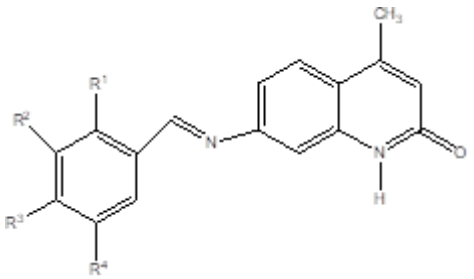

(17-23)

Complexes	R^2	R^3	R^4
17a	H	OH	H
18a	H	H	H
19a	OH	H	H
20a	OC_2H_5	H	H
21a	OCH_3	H	H
22a	H	OCH_3	H
23a	^tBu	H	^tBu

This is a classic condensation reaction where the amino group ($-NH_2$) of the quinolinone derivative reacts with the carbonyl group (-CHO) of the aldehyde. The nitrogen atom attacks the carbonyl carbon followed by the elimination of a water molecule (H_2O) to form an imine bond (-C=N).

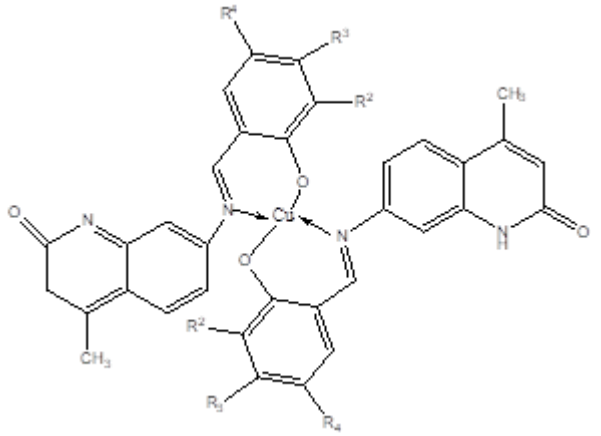

17a-23a

The reaction was carried out in solvent of the hot ethanol in reflux conditions to facilitate the reaction and drive the equilibrium toward the formation of the imine product. Following the synthesis of the ligands, the synthesis of the Schiff base ligand's metal complexes by coordinating the Schiff bases with copper (II) ions. The synthesized Schiff bases (17-23) acted as ligands and reacting with a copper source specifically copper (II) acetate or copper (II) perchlorate hexahydrate. The reactants were mixed in a 2:1 molar ratio which means two molecules of the Schiff base ligand coordinated with one copper (II) metal centre. To evaluate the therapeutic potential of these newly synthesized compounds, the researchers conducted comprehensive in vitro biological assays to assess their anticancer activity. Specifically, they utilized the Hep-G2 human hepatic carcinoma cell line which is a standard model for liver cancer research to measure the cytotoxic efficacy of the compounds. The results of these assays were rigorously quantified and reported as IC_{50} values representing the concentration of the compound required to inhibit 50% of the cancer cell growth allowing for a direct comparison of their potential. The findings from data revealed a significant disparity in cytotoxic potency between the free ligands and their metal-bound counterparts. The free Schiff bases demonstrated a broad range of activity with IC_{50} values ranging from 39 µM to 1000 µM. However, the copper complexes showed a remarkably increase in potentioal exhibiting much lower IC_{50} values which ranged strictly between 17 µM and 129 µM. This decrease in the IC_{50} values indicates that the incorporation of the copper (II) metal centre significantly enhanced the cytotoxicity of the Schiff base ligands against the Hep-G2 cancer cells. Within the comprehensive series of synthesized free ligands compounds 17 and 23 emerged as particularly noteworthy candidates, exhibiting relatively promising cytotoxic activity against the tested human hepatic carcinoma cell line. Specifically, ligand 17 displayed an IC_{50} value of 39.67 ±5.24 µM, while ligand 23 showed a similarly potent IC_{50} of 44.33±4.70 µM. [9]

Table 1. Anticancer activity of Schiff bases and their complexes against four different human tumor cell lines

Schiff Base	IC_{50} ± S.E.M (µM)	Complex	IC_{50} ± S.E.M (µM)
17	39.67 ± 5.24	17a	47.00 ± 9.54
18	411.66 ± 7.26	18a	74.83 ± 8.91
19	>1000	19a	129 ± 16.26
20	398.33 ± 33.21	20a	17.90 ± 3.75
21	175.67 ± 12.20	21a	105.33 ± 25.41
22	521.67 ± 41.26	22a	53.17 ± 1.59
23	44.33 ± 4.70	23a	39.67 ± 10.18
Cisplatin	15.00 ± 2.65	-	-

The findings from data analysis is that the metal-binding process generally enhanced the biological efficacy of the compounds. Almost all of the synthesized copper complexes exhibited significantly stronger cytotoxic effects compared to their respective parent ligands. The sole exception to this trend was complex 17a which did not demonstrate the same level of enhanced potency relative to its parent Schiff base ligand that is 17. The most significant finding regarding potential is regarding to the Schiff base ligand's complex 20a which showed the remarkably low IC_{50} value of 17.90 ±3.75 μM. This I_{50} Shows that the level of cytotoxicity is highly comparable to the potency of cisplatin which have IC_{50} value of 15.00 ±2.65 M which is a well-established and commercially available chemotherapy drug and commonly utilized as a standard reference in anticancer studies. This suggests that complex 20a holds significant potential for further development as a therapeutic agent.

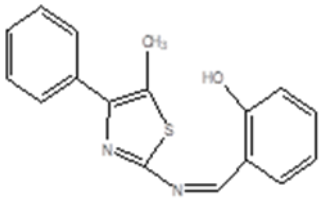

24

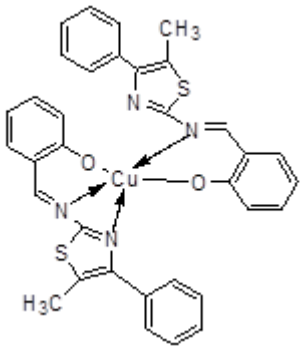

25

Abd-Elzaher *et al*. synthesized a thiazole derived Schiff base was synthesized by the condensation reaction of salicylaldehyde with 2-amino- 4-phenyl-5-methyl thiazole. After the structural characterization of this ligand, a series of transition metal complexes were prepared. This involved refluxing the thiazole-derived Schiff base with various metal chlorides specifically with cobalt (II) chloride hexahydrate, nickel (II) chloride hexahydrate, copper (II) chloride dihydrate and zinc (II)chloride—in an ethanol solvent. These complexes were likely formed through coordination involving the azomethine nitrogen and the phenolic oxygen of the ligand. The resulting Schiff base ligand and its Co (II), Ni (II), Cu (II) and Zn (II) complexes were subsequently evaluated for their anticancer activity against a panel of human tumor cell lines which are liver cancer (HepG2), breast cancer (MCF-7), lung carcinoma (A549) and colorectal cancer (HCT116) using doxorubicin as a reference drug for comparison.

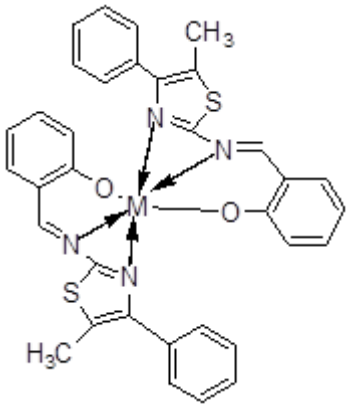

M = Co(II) (26), NI (II) (27), Zn(II) (28)

The experimental results indicated that both the free Schiff base and all synthesized metal complexes exhibited significant cytotoxicity against the HepG2 and MCF-7 cell lines.[10]

Table 2. Anticancer activity of Schiff bases and their complexes against four different human tumor cell lines.

Compounds	IC_{50} (µg/ml)			
	MCF-7	HCT116	HepG2	A549
Doxorubicin	10.00	9.50	9.22	-
24	8.70	6.70	7.50	-
25	9.11	-	8.16	-
26	7.30	-	7.20	9.10
27	6.00	6.20	6.20	5.30
28	4.40	5.25	4.20	4.70

However, a prominent enhancement in biological activity was observed upon metal complexation, particularly with the Zn (II) metal center. The Zn (II) complex exhibited remarkable, broad-spectrum anticancer efficacy, demonstrating potent inhibitory effects across all tested cell lines, including the traditionally resistant lung (A549) and colorectal (HCT116) cancers. The cytotoxic potential of the Zn (II) complex was found to be comparable to, or in some cases exceeded, that of the standard chemotherapeutic agent doxorubicin highlighting its potential as a promising candidate for further pharmaceutical development. The synthesized compounds (24–28) were evaluated for their in vitro cytotoxic activity against four human cancer cell lines: HepG2 (liver), MCF-7 (breast), A549 (lung) and HCT116 (colon). The results, expressed as IC_{50} values µg/ml, are summarized in above table with Doxorubicin used as a standard reference drug. All tested compounds exhibited varying degrees of inhibitory activity against the cancer cell lines. Among the synthesized compounds, Compound 28 demonstrated the highest potent activity across all tested lines, with IC_{50} values ranging from 5.30 to 6.20 µg/ml. If we see in Cell Line Specificity the A549 (Lung Cancer) line appeared the most sensitive to the synthesized agents, specifically Compound 28. IC_{50} = 5.30 µg/ml. Interestingly compounds 24, 25 and 26 showed no significant activity against this line within the tested parameters. And in for HepG2 (Liver Cancer cell line the Compounds 25, 27, and 28 exhibited comparable activity, with compound 28 being the most potent IC_{50} = 6.20 µg/ml. And for HCT116 (Colon Cancer cell line Compound 25 showed the highest activity among the new compounds in this line IC_{50}= 6.70 µg/ml, while compound 26 was inactive.

Taset *et al*. designed and synthesized a series of nine amino acid methyl ester-based Schiff bases (29–37). These compounds were prepared via the condensation of three specific amino acid methyl esters (isoleucine, phenylalanine, and methionine) With three salicylaldehyde derivatives (5-bromo-2-hydroxybenzaldehyde, 2,4-dihydroxybenzaldehyde, 2-hydroxymethoxybenzaldehyde). The biological profile of these derivatives was evaluated using MTT and LDH assays against a panel of six cancer cell lines (A549, HeLa, HT29, Hep3B, MCF7 and C6) and two normal cell lines (Vero and FL) to determine their IC_{50} values. The screening results revealed a broad spectrum of

activity indicating that the structural modifications within the Schiff base skeleton significantly influence the anticancer potency. The most striking inhibitory activity was observed against the HeLa (cervical) and C6 (glioma) cell lines.

SChiff Base	R^1	R^2	R^3	R^4
29	Br	H	H	$CH_3CH_2(CH_3)CH$
30	H	OH	H	$CH_3CH_2(CH_3)CH$
31	H	H	OCH3	$CH_3CH_2(CH_3)CH$
32	Br	H	H	$PhCH_2$
33	H	OH	H	$PhCH_2$
34	H	H	OCH3	$PHCH_2$
35	Br	H	H	$CH_3SCH_2CH_2$
36	H	OH	H	$CH_3SCH_2CH_2$
37	H	H	OCH3	$CH_3SCH_2CH_2$

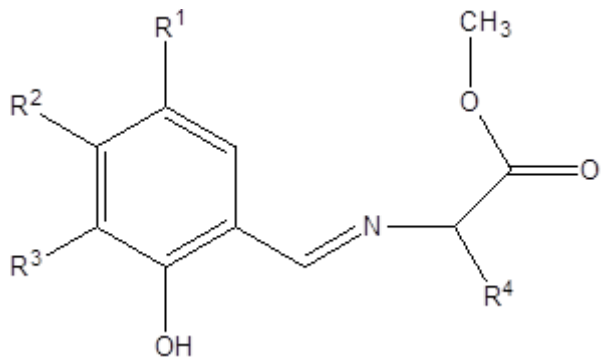

29-37

The screening results revealed a broad spectrum of activity indicating that the structural modifications within the Schiff base skeleton significantly influence anticancer potency.

Among the compounds evaluated, compound 37 emerges as an exceptional anticancer potential as achieving outstanding C6 glioma activity with an IC_{50} of 3.69 ± 0.55 µg/ml which representing the single most potential activity across the entire series. This compound also shows HeLa cervical cancer activity with an IC_{50} of 108.75 ± 9.8 µg/ml and moderate HT29 colorectal activity with an IC_{50} of 268.47 ± 10.1 µg/ml. The glioma selectivity of compound 37 is remarkably good with Vero normal cells showing an IC_{50} of 452.61 µg/ml creating a selectivity ratio of 122.7-fold which approaches or exceeds the selectivity standards of clinically successful chemotherapy agents. Compound 29 demonstrates exceptional anticancer potency with the lowest HeLa cervical cancer IC_{50} value in the series at 2.79 ± 0.07 µg/ml which representing potency that surpasses all other compounds against this cell line. This compound also shows excellent C6 glioma activity with an IC_{50} of 5.42 ± 0.18 µg/ml and good HT29 colorectal cancer activity with an IC_{50} of 23.31 ± 0.89 µg/ml. The dual outstanding potency against both cervical cancer and glioma, combined with meaningful colorectal activity and lower potency against other cancer types, establishes compound 29 as a multi-target anticancer lead despite the normal cell toxicity concerns as evidenced by its Vero IC_{50} of 10.26 ± 0.34 µg/ml. Compound 32 emerges as the most versatile broad-spectrum anticancer agent, achieving meaningful activity

against six cancer cell lines and representing the optimal choice for Mult indication development strategies. This compound shows excellent C6 glioma activity with an IC_{50} of 5.72 ± 0.19 µg/ml, HeLa cervical potency of 13.39 ± 0.77 µg/ml, and outstanding HT29 colorectal cancer activity with an IC_{50} of 12.01 ± 0.63 µg/ml, effectively matching its HeLa potency. Furthermore, compound 32 demonstrates liver cancer activity against Hep3B cells with an IC_{50} of 29.55 ± 1.5 µg/ml and notably achieves breast cancer activity against MCF7 cells with an IC_{50} of 46.35 ± 1.7 µg/ml which is representing the only compound in the series achieving under 100 µg/ml potency against breast cancer cells. This broad-spectrum profile across glioma, cervical, colorectal, hepatic, and breast cancer makes compound 32 ideal for multi-indication development and mechanistic investigations. Compound 35 represents another important lead demonstrating exceptional HeLa cervical cancer selectivity with outstanding potency of 6.27 ± 0.43 µg/ml combined with superior normal cell safety, as shown by Vero cells exhibiting an IC_{50} of 16.84 ± 0.49 µg/ml and FL fibroblasts showing an IC_{50} of 25.60 ± 1.0 µg/ml, yielding a favorable selectivity index of 2.69. This compound also shows colorectal cancer activity with an HT29 IC_{50} of 89.89 ± 11.4 µg/ml and modest hepatic cancer activity against Hep3B cells with an IC_{50} of 874.91 ± 32.1 µg/ml. Analysis of structural variations across the compound series reveals critical patterns essential for anticancer activity optimization. Unsubstituted aromatic rings at the R^1 position in compounds 29 and 37 consistently achieve the highest absolute potencies against HeLa cervical and C6 glioma cells while bromine substitution at the R^1 position as exemplified by compound 32 which provides more consistent broad-spectrum anticancer activity across multiple cancer types suggesting that electronic effects enhance binding across diverse protein targets present in different cancer cell types. Hydroxylation at the R^2 position consistently reduces anticancer potency by three to twelve-fold across all cancer cell lines tested and should be avoided in future optimization efforts. Methoxylation at the R^3 position demonstrates complex effects dependent on concurrent substitutions: while compound 31 with R^3 = O-CH_3 shows dramatic activity loss across most cell lines, compound 37 with identical R^3 substitution paradoxically achieves outstanding glioma potency which is indicating that R^4 side chain composition critically modulates the effects of R^3 substitution. Aliphatic R^4 groups as present in compound 29 maximize absolute potency against particularly sensitive cell lines like HeLa and C6 glioma but reduce versatility against other cancer types. Benzyl R^4 groups as present in compound 32 provide optimal broad-spectrum anticancer activity across diverse cancer types. Thio ether R^4 groups as present in compound 37 uniquely enable exceptional glioma selectivity with outstanding potency, suggesting that thioether-containing compounds preferentially target glioma-specific cellular uptake pathways or molecular targets.

C6 glioma cells demonstrate the highest overall responsiveness to the Schiff base compounds with six compounds achieving under 100 µg/ml anticancer activity including four compounds achieving potency below 6 µg/ml, establishing glioma as the most promising cancer indication. HeLa cervical cancer ranks second in responsiveness with multiple compounds achieving 2-21 µg/ml potency, making cervical cancer another primary target indication. HT29 colorectal cancer shows intermediate responsiveness with compounds 32, 29, and 34 achieving anticancer activity in the 12-27 µg/ml range which establishing colorectal cancer as a

viable secondary indication. MCF7 breast cancer demonstrates substantial resistance to the Schiff base compounds, with only compound 32 achieving sub-100 µg/ml potency at 46.35 µg/ml while all other compounds show IC_{50} values exceeding 250 µg/ml, suggesting involvement of P-glycoprotein efflux pump mechanisms or other drug resistance pathways. Hep3B hepatic cancer and A549 lung cancer are highly resistant, with only compound 32 showing sub-100 µg/ml anticancer activity against Hep3B at 29.55 µg/ml and all compounds completely inactive against A549 with IC_{50} values exceeding 10,000 µg/ml, indicating fundamental incompatibility between the current Schiff base scaffold and lung cancer cell biology. Based on this comprehensive anticancer data analysis, compound 37 warrants highest priority development for glioma indications based on exceptional anticancer potency combined with superior normal cell safety and outstanding selectivity. Compound 32 merits parallel advancement for broad-spectrum multi-indication development across glioma, cervical, colorectal, and hepatic cancers. Compound 29 should be pursued for cervical cancer and glioma indications through targeted delivery strategies designed to overcome normal cell toxicity concerns. Future medicinal chemistry optimization should prioritize enhancing glioma anticancer potency of compound 37 analogs which improving broad-spectrum selectivity of compound 32 analogs and optimizing cervical cancer selectivity of compound 29 or 35 analogs. These three parallel development pathways targeting different cancer indications with compounds optimized for each disease type maximize the probability of clinical success and enable comprehensive coverage of multiple high-priority cancer indications with enhanced therapeutic efficacy.

Table 3. IC_{50} (µg/ml) values of Amino Acid Methyl Ester Schiff Bases against six different cancer cells and two normal cells

Compounds	IC_{50} (µg/ml)							
	A549	MCF7	C6	Hep3B	HeLa	HT29	Vero	FL
29	>10000	904.30±28.4	5.42±0.18	1133.57±33.9	2.79±0.07	23.31±0.89	10.26±0.34	30.91±1.5
30	>10000	2833.66±59.2	7.49±0.33	>10000	12.49±0.71	64.17±4.3	92.31±5.32	19.54±1.4
31	>10000	1347.86±54.8	3796.80±65.4	>10000	41.99±3.1	702.60±28.3	195.66±15.8	2394.84±69.1
32	>10000	46.35±1.7	5.72±0.19	29.55±1.5	13.39±0.77	12.01±0.63	11.61±0.23	20.31±0.41
33	>10000	581.23±17.8	7380.55±51.0	>10000	102.28±5.7	18.58±1.1	86.56±5.9	63.61±5.3
34	>10000	>10000	1962.94±21.3	>10000	21.98±0.88	26.59±0.87	32.89±1.1	250.97±7.4
35	>10000	293.37±17.4	>10000	874.91±32.1	6.27±.43	89.89±11.4	16.84±0.49	25.60±1.0
36	>10000	1903.43±51.3	36.33±1.1	>10000	2708.12±59.2	>10000	>10000	9447.3±71.4
37	>10000	>10000	3.69±0.55	>10000	108.75±9.8	268.47±10.1	452.61±12.7	1475.11±47.6

The compound 37 have therapeutic profile because It combined exceptional potency against C6 glioma 3.69 µg /ml) with comparatively low toxicity toward normal cells, showing IC_{50} values of 452.61 µg /ml for Vero and 1475.11 µg /ml for FL. This substantial difference indicates high selectivity for glioma cells over normal mammalian cells, making compound 37 the most promising candidate for further preclinical development. SI values highlight critical distinctions between potency and safety. Although compound 29 showed high potency against HeLa cells (2.79 µg /ml) its low SI against Vero cells (3.68) suggests it may be too toxic to normal kidney tissue. Conversely, compound 37 demonstrated exceptional selectivity for C6 glioma cells with SI values of 122.66 (Vero) and 399.76 (FL). This indicates that compound 37 is over many times more toxic to brain cancer cells than to normal kidney or amniotic cell, representing a highly favourable therapeutic profile.[11]

Conclusion:

The comparative study of Schiff base ligands and their metal complexes demonstrate the significant potential of these compounds as promising anticancer agents across a diverse range of human cancer cell lines. This reviewed literature consistently shows that free Schiff base ligands possess moderate to good cytotoxic activity, but metal complexation particularly with transition metals such as Cu (II), Zn (II), Co (II), Ni (II) and others—substantially enhances their potency. This enhancement is primarily attributed to increased lipophilicity, improved cellular uptake, stronger DNA interactions (including binding, cleavage, and structural distortion), and the ability to induce apoptosis more effectively than the uncoordinated ligands. The Copper (II) complexes derived from quinolinone-based Schiff bases (e.g., complex 20a) exhibited IC_{50} values comparable to cisplatin against Hep-G2 liver cancer cells highlighting their potential as next-generation platinum-alternative agents. And Zinc (II) complexes of thiazole-derived Schiff bases displayed broad-spectrum activity, often matching or surpassing doxorubicin against HepG2, MCF-7, A549, and HCT116 cell lines with particularly impressive performance against resistant lines and also Amino acid methyl ester Schiff bases (compounds 29–37) revealed remarkable selectivity and potency especially against HeLa cervical cancer and C6 glioma cells. In conclusion, Schiff base metal complexes represent a versatile and highly tuneable platform in the search for novel, less toxic chemotherapeutic agents. The superior biological performance of metal-coordinated derivatives over free ligands, combined with evidence of DNA-targeted mechanisms and apoptosis induction, positions this class of compounds as valuable candidates for future drug development. Continued efforts focusing on structure-activity relationship (SAR) refinement in vivo validation, mechanistic studies (including detailed DNA interaction and resistance profiling), and targeted delivery strategies will be essential to translate these promising in vitro findings into clinically viable anticancer therapeutics. Ultimately, this rapidly evolving field holds considerable promise for contributing to more precise, effective and personalized cancer treatments.

References:

1. Sathishkumar K, Chaturvedi M, Das P, et al. (2022) Cancer incidence estimates for 2022 & projection for 2025: Result from National Cancer Registry Programme,

India. Indian Journal of Medical Research.;156(4&5):598-607.

2. Neelima; Poonia, K., Siddiqui, S. Arshad M., Kumar D. (2016) In vitro anticancer activities of Schiff base and its lanthanum complex. Spectoochim. Acta A Mol. Biomol. Spectrosc.,155, 146-154
3. Devi J., Yadav M., Kumar D., Naik, L.S., Jindal D.K. (2019) Some divalent metal (II) complexes of salicylaldehyde, derived Schiff bases: Synthesis, spectroscopic characterization, antimicrobial and in vitro anticancer studies. Appl. Organometal. Chem., 33, e4693.
4. Amim R.S., Pessoa C., Lourenco M.C.S., de-Souza M.V.N., Lessa J.A. (2017) Synthesis, antitubercular and anticancer activities of p- nitrophenyl ethylenediamine- derived Schiff bases. Med. Chem.,13(4), 391-397.
5. Tadele KT, Tsega TW. (2019) Schiff Bases and their Metal Complexes as Potential Anticancer Candidates: A Review of Recent Works. Anti-Cancer Agents in Medicinal Chemistry ;19(15):1786-1795.
6. Mushtaq I., et al. (2024). Pharmaceutical significance of Schiff bases: an overview. Future Journal of Pharmaceutical Sciences, 10(1), 1-15
7. Andiappan K., Sanmugam A., Deivanayagam E., Karuppasamy K.;, Kim H.S., Vikraman D., (2018) In vitro cytotoxicity activity of novel Schiff base ligand-lanthanide complexes. Sci. Rep., 8(1), 3054.
8. Suchithra R., Sounthari P., Kiruthika A., Chitra S., Parameswari K, Vijitha J. (2015) Ru (III) azo Schiff base complexes: Synthesis, spectral characterization, antimicrobial and anticancer studies. Int. J. Pharm. Sci. Res., , 6(3), 1283-1293.
9. Creaven, B.S., Duff B., Egan D.A., Kavanagh K., Rosair G., Thangella V.R., Walsh M. (2010) Anticancer and antifungal activity of copper (II) complexes of quinolin-2(1H)-one-derived Schiff bases. Inorg. Chim. Acta, 363, 4048-4058.
10. Abd-Elzaher M.M., Labib A.A., Mousa H.A., Moustafa S.A., Ali M.M., Rashedy A.A. (2016) Synthesis, anticancer activity and molecular docking study of Schiff base complexes containing thiazole moiety. Beni-Suef Uni. J. Basic Appl. Sci., 5, 85-96.
11. Tas, N.A., Senocak A., Aydin A. (2018) Preparation and cytotoxicity evaluation of some amino acid methyl ester Schiff bases. J. Turk. Chem. Soc. Chem, 5(2), 585-606.

International Journal of Advance and Applied Research
www.ijaar.co.in
ISSN – 2347-7075 Impact Factor – 8.141
Peer Reviewed Bi-Monthly
Vol. 7 No. 14 January – February - 2026

Study of Ag Loaded TiO2/ZnO Nanocomposites for Photocatalytic Activity

Mahadev B. Suwarnkar
Dept. of Chemistry, Baburaoji Adaskar Mahavidyalaya, Kaij, Dist. Beed. (MS), India.
Corresponding Author – Mahadev B. Suwarnkar
DOI - 10.5281/zenodo.19755813

Abstract:
In this research work we reported preparation of TiO_2-ZnO and Ag loaded TiO_2-ZnO nanoparticles with various Ag content via a controlled and an energy efficient microwave assisted method. The structure and properties of photocatalysts were characterized by XRD, SEM and TEM. The crystallite size was found to be 14 nm. The obtained nanomaterials are pseudo-cube in shape. These results are better than pristine TiO_2. The present research work is mainly focused on the enhancement of degradation efficiency of methyl orange (MO) using UV light (365nm). A 94% photodegradation efficiency of MO was achieved by utilizing optimal photocatalysts (Ag-TiO_2-ZnO (0.5 wt% Ag)) at 1 g/dm^3 at within 90 min.

Keywords: Spectroscopy, Microwave, Methyl Orange, Degradation.

Introduction:

In the modern era, the nanoscience and nanotechnology are considered to be most emerging in the field of research. Nanomaterials is an ideal for novel applications in a large area including semiconductor [1] gas sensor [2], antimicrobial activity [3], photocatalytic degradation of dyes [4], and hydrogen generation [5]. In 1972, Fujishima and Honda discovered the photocatalytic splitting of water on TiO_2 electrodes [6]. This incident marked the beginning of a new era in heterogeneous photocatalysis. TiO_2 has been the most popular photocatalyst for environmental purification due to its good chemical stability, high oxidized activity, nontoxicity, and low price [7-9]. The photocatalytic process using TiO_2 photocatalyst is very promising for application in the water purification, because many organic compounds can be decomposed and mineralized by the proceeding oxidation and reduction processes on TiO_2 surface [10].

The TiO_2 as a photocatalysts and his effectiveness is sometimes limited due to its wide band gap (3.2eV) as well as its large charge carrier recombination rate (nanosecond) [11, 12]. Therefore, it is important to develop a novel catalyst which holds high potential for photocatalytic activity. The modification of TiO_2 by coupling with other metal oxides (e.g., WO_3, ZnO, NiO or CoO) is an approach that has received much attention for improving the photocatalytic properties of TiO_2 and that has been considered as an efficient route to increase the lifetime of the charge carrier and tune the band gap to a preferred level [13,14]. Photocatalytic oxidation represents an attractive clarification due to the ability to completely oxidize organic contaminants to carbon dioxide, water, and mineral acids [15]. The absorption of photons with an energy equivalent to or higher than the TiO_2 semiconductor bandgap (Eg) gives rise to photoexcited electron–hole pairs. Electron–hole pairs can begin redox reactions with adsorbates at the catalyst surface or can result in their recombination with the release of heat [16]. In the present work, we have prepared TiO_2-ZnO nanocomposites and further loaded

with Ag, synthesized by a simple microwave assisted method. Its photocatalytic activities were also evaluated by using methyl orange as a model organic compound.

Experimental:

1. Materials:

The 99% purity of Titanium tetra-isopropoxide (TTIP), Zinc nitrate (99%), 99% purity of surfactant cetyl trimethyl ammonium bromide (CTAB), Sodium dodecyl sulphate (SDS, 99%) were purchased from Spectrochem Pvt. Ltd., (India). Absolute ethanol (99.9%) and silver nitrate were purchased from s.d. fine chemicals. Ammonia was purchased from Loba Chemie Pvt. Ltd., (India). All analytical grade chemicals were used as received for preparation of various solutions. All solutions were prepared in millipore water obtained from millipore water system (Bangalore, India).

1.1 Preparation of TiO_2-ZnO nanomaterials:

The TiO_2-ZnO nanocomposites were prepared by the simple microwave assisted method using Titanium tetra-isopropoxide, Zinc nitrate, as a source of titanium and zinc. TiO_2-ZnO nanocomposites were prepared by controlled addition of (0.1 M) TTIP in 100 mL of absolute ethanol with constant stirring to get a clear solution. Further, a sufficient amount of surfactant solution (1% CTAB + 1% SDS) was added with constant stirring. For mixed oxides with ZnO, the zinc nitrate solution was varied from 1, 3, and 5 wt%. The required amount of zinc nitrate solution was added to get the desired composition. A solution of aqueous ammonia was added dropwise under stirring condition. With special arrangement at room temperature until the solution reached up to pH=8. After complete precipitation, the precipitate was washed with millipore water and acetone for several times to ensure complete removal of impurities present in sample. The washed precipitate was subjected to microwave irradiation for 20 min. in a domestic microwave oven (Input 900W, 250 MHz, LG Make) with on-off cycle (20s on-40s off). The dried powder was grounded by using agate mortar and pestle and calcined at 300ºC for 3 hrs in a temperature controlled muffle furnace. These prepared samples such as TiO_2, TiO_2-ZnO (1, 3, and 5 wt. % ZnO) and ZnO were denoted as T, TZ1, TZ2, TZ3, and Z respectively.

1.2 Preparation of Ag loaded TiO_2-ZnO nanocomposites:

The Ag loaded TiO_2-ZnO were prepared by above simple microwave assisted method was further modified with silver nanoparticles (NPs) using impregnation-reduction method. Synthesized TiO_2-ZnO powder having optimum content of ZnO (3 wt% of ZnO) was added in 20 mL millipore water and sonicated for 30 min for in order to achieve proper dispersion. For synthesis of different wt% Ag (0.25 to 1.0) loading, calculated amount of silver nitrate was added in above mixture and then stirred for 60 min. so as to form proper solution between Ag+ and TiO_2-ZnO. Reduction of Ag+ was achieved by using calculated amount of freshly prepared ice cold solution of Sodium Borohydride. The prepared Ag loaded TiO_2-ZnO nanocomposites powder was dried at 110°C for 60 min to remove water content and denoted as TZ-Ag1 to TZ-Ag4 for different Ag content (0.25 to 1.0 wt % Ag) respectively.

2. Photocatalytic activity of TiO_2-ZnO and Ag-TiO_2-ZnO nanocomposites:

The photocatalytic activity of TiO_2-ZnO and Ag loaded TiO_2-ZnO was evaluated by testing the degradation of methyl orange as a model pollutant by using UV light (365 nm). To search the highest photocatalytic activity of mixed oxides, catalyst amount was varied from 0.75 to 1.5 g/dm^3. The quartz photoreactor was kept in steel container along with magnetic

stirrer. Philips (HPL-N, 250 W) light source was used which has Lumens of 12750. Outer side of the bulb was broken and just inside filament is used as a source of light. The distance of lamp was kept 5 cm above the dye solution. In the given experiment the photocatalyst was added in photoreactor containing methyl orange (100 mL, 20 ppm). Prior to irradiation, dye solution was stirred for 30 minutes in dark for adsorption-desorption equilibrium. All photodegradation experiments were performed at ambient temperature. At a given time interval, samples were withdrawn and centrifuged to remove photocatalyst. The absorbance of the clear solution was recorded by using UV-Vis-NIR spectrophotometer (Shimadzu, Model-UV-3600) to monitor the concentration of dye.

Results and Discussion:

1. Characterization of as prepared TiO_2-ZnO and Ag-TiO_2-ZnO nanocomposites:

1.1. XRD:

The modification mechanism is closely related to the crystallite structure, which has been studied using the XRD technique. Fig. 1(a) shows the X-ray diffraction patterns of variable TiO_2/ZnO composites with pristine TiO_2 and ZnO. In Fig. 1(a), the sample 'T' determined characteristics 2θ values and [hkl] planes are 25.06° [101], 37.59° [004], 48.01° [200], 55.02° [211], 62.31° [204] attributed to reflections of anatase TiO_2 which is compared with JCPD Card No. (21-1272) [17]. For the sample 'Z' determined characteristics 2θ values and [hkl] planes, all the diffraction peaks are observed at 31.82° [100], 34.47° [002], 36.34° [101], 47.69° [102], 56.63° [110], 62.91° [103] and 67.93° [112] which can be well indexed as a hexagonal wurtzite structure and consistent with the values of standard data (JCPDS 36-1451) [18]. Meanwhile, for the sample TZ1, TZ2 and TZ3 the peaks of ZnO were not observed in the XRD pattern due to low content of Zn. Almost all diffraction peaks of the samples can be indexed to the anatase TiO_2 indicating that Zn^{2+} were dissolved into the TiO_2 host lattice without disturbing the crystal structure of TiO_2. The possibility of substitution of Zn^{2+} is ruled out due to difference in ionic radii Ti^{4+}=0.61 and Zn^{2+} = 0.74pm. The average crystallite size of samples T, TZ1, TZ2, TZ3 and Z was calculated by using Scherrer's relation:

$$t = 0.9\lambda/\beta \cos\theta \qquad \text{------- (1)}$$

Where λ is wavelength of X-ray in Å, β is full width at half maximum [FWHM] in radian. θ is scattering angle in degree. The relatively broad width of peaks of the XRD patterns implies crystallites are smaller in size [19]. At 300°C the average crystallite size for sample T was found to be about 15 nm, As the Zn contents increase from 1 to 5 wt %, the broadening of the peak [101] gradually increases which indicates the smaller crystallite size of the material. It is observed that the 'T' has an average size of 15 nm and it decreases up to 12 nm for TZ2. The Z sample has average crystallite size of 25 nm.

Fig. 1(b) shows the X-ray diffraction patterns of different wt % Ag loaded on TiO_2-ZnO. The diffraction pattern of all samples (TZ-Ag1 to TZ-Ag4) revels that there is formation of crystalline structure with anatase phase. Although the Ag content was increased from 0.25 to 1.0 wt% the crystalline structures of the mixed oxides were still the anatase TiO2. Hence, the loading of Ag at such low contents did not significantly affect the crystalline structure. Major peak for TiO_2-ZnO found to be almost same for Ag loaded TiO_2-ZnO mixed oxide samples, except changes in intensity of peaks. It is observed that for TZ2 nanomaterial crystallite size was found to be 12 nm and it increases upto 14 nm for 0.5 wt% Ag

on TZ2, thereafter the crystallite size of the photocatalyst was more or less constant. The appearance of Ag metallic peak is not observed in the XRD pattern of nanocomposites this is may be due to the low Ag content and also high dispersion of Ag nanoparticles on the surface of the TiO_2-ZnO.

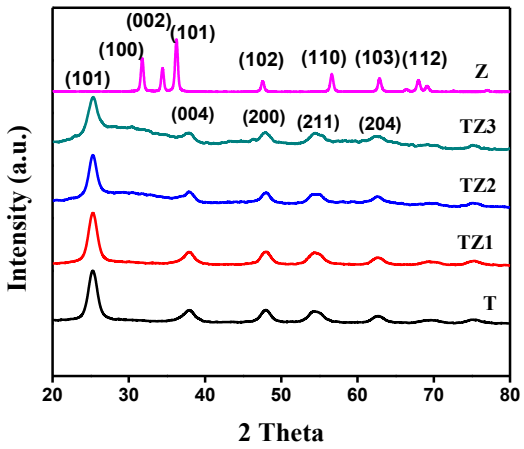

Fig. 1(a). X-ray diffractograms of a) TiO_2 (T) b) TiO_2/ZnO (1 wt% ZnO-TZ1) c) TiO_2/ZnO (3 wt% ZnO-TZ2) d) TiO_2/ZnO (5 wt% ZnO-TZ3) e) ZnO (Z) nanoparticles

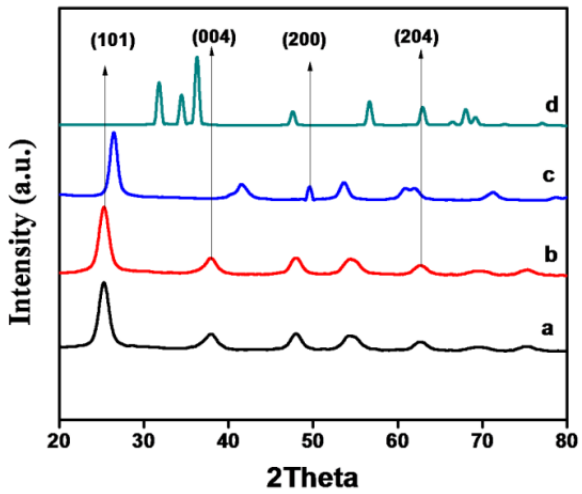

Fig. 1(b). X-Ray diffraction pattern of a) TiO_2 (T) b) TiO_2/ZnO (3 wt% ZnO-TZ2) c) Ag-TiO_2/ZnO (0.5 Wt% Ag) d) ZnO (Z)

1.2 SEM and EDS analysis of TiO_2-ZnO and Ag-TiO_2-ZnO:

In order to investigate the surface morphology of the synthesized TZ2 and TZ-Ag2 nanoparticles, SEM and elemental composition studies were performed. The particles of TZ2 and TZ-Ag2 have pseudo-cube like morphology which is shown in Fig. 2A(a) and 2B(a). The SEM images of prepared TZ-Ag2 compared with TZ2, confirmed that the TZ-Ag2 shows smaller particle size than TZ2. The EDS instrument also show coloured photographic image for specific element depending upon composition present in area under study. EDS mapping of TiO_2-ZnO and Ag-TiO_2-ZnO were shown in Fig. 2A(b) and 2B(b). Fig. 2A(c) and 2B(c) shows EDS spectrum of as synthesized TZ2 and TZ-Ag2 nanoparticles. The EDS was recorded in the binding energy region of 0-10 keV. The findings of all EDS confirms presence of Ti, O, Zn and Ag elements in synthesized materials as well as reveling amount of Ag loading. The peak from the spectrum revealed the presence of Ti, O, Zn and Ag at 4.48, 0.50, 0.98, and 0.25 keV respectively. EDS mapping indicates that almost all samples formed were of non-stoichiometry TiO_2 with oxygen deficient which leads to better performance of photocatalytic activity [20].

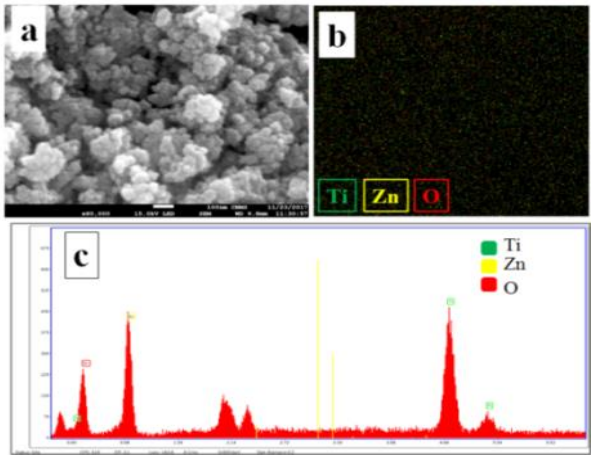

Fig.2 (A). SEM and EDS analysis of TZ2 (3 wt% ZnO)

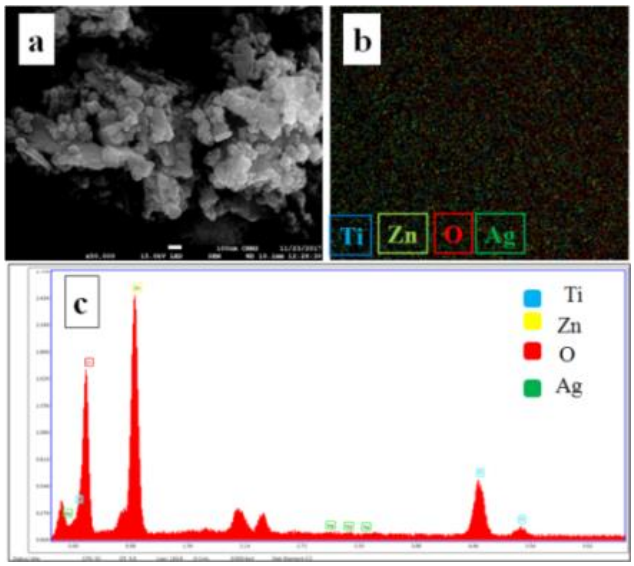

Fig.2 (B). SEM and EDS analysis of TZ-Ag2 (0.5 Wt% Ag)

1.3. TEM Result:

Morphology of the nanomaterials was characterized by TEM analysis as shown in Fig. 3(a). The obtained image reveals that as prepared TZ2 is in the form of pseudo-cube with narrow size distribution. The size of particles is in the range of 12-15 nm, with the average particle size from representative TEM was found to be 12 nm. The HR-TEM image (Fig.3b) shows lattice fringes, which is used for phase identification and found to be 0.35 nm. The value corresponds to the lattice spacing of (101) plane in the anatase phase. Selected area electron diffraction pattern (SAED) matches to anatase phase with good crystallinity as shown in Fig. 3(c). Lattice fringes can be clearly indicating that the particles are crystalline with anatase phase.

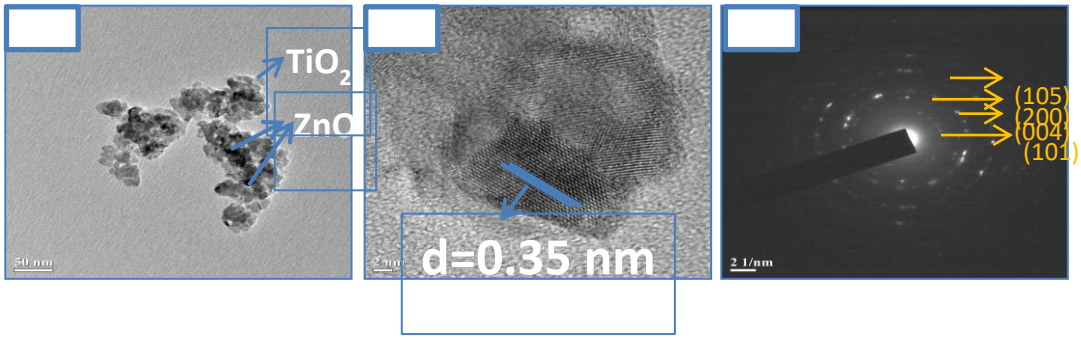

Fig. 3. TEM Image of a) TZ2 (3 wt% ZnO) Nanoparticles b) HRTEM image of TZ2 (3 wt% ZnO) c) SAED Pattern of TZ2 (3 wt% ZnO)

2. Factors affecting photocatalytic degradation of methyl orange:

2.1 Effect of concentration of ZnO (wt %) on TiO_2 for MO degradation:

Fig. 4(a) shows the photocatalytic degradation of methyl orange on TiO_2-ZnO photocatalyst with varying ZnO concentrations of 1, 3 and 5 wt % of ZnO. From figure it can be concluded that, all the composite samples (TZ1, TZ2 and TZ3) shows better degradation efficiency of Methyl orange (MO) as compared to pristine TiO_2 and ZnO. More importantly, due to the presence of a TiO_2-ZnO composite, recombination of the photogenerated electron−hole charge carriers were markedly reduced. Additionally, electrons or holes that transfer to the TiO_2 or ZnO active surface of the hybrid nanostructures immediately join in the redox reactions, in which electrons reduce dissolved molecular oxygen to produce superoxide radical anions ($O2^{-\cdot}$), while holes oxidize H_2O molecular to yield hydroxyl radicals

(·OH). Organic dye pollutants (MO) are eventually oxidized by these highly active species to CO_2 and H_2O products [21]. The optimal TZ2 (3 Wt % ZnO) photocatalyst shows maximum 87% degradation of methyl orange within 90 min for 1 g/dm^3 photocatalyst which seems to be good result.

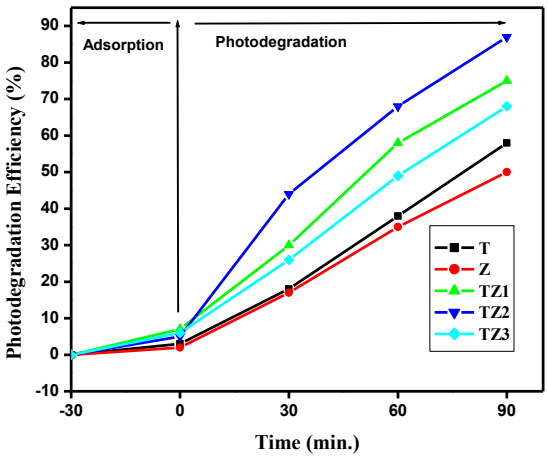

Fig. 4(a). Effect of concentration of ZnO on TiO_2 for MO degradation

2.2 Effect of concentration of Ag (wt %) on TiO_2-ZnO for MO degradation:

Fig. 4(b) shows the photocatalytic degradation of methyl orange on TZ-Ag photocatalyst with varying Ag concentrations from 0.25 to 1.0 wt % and noted as TZ-Ag1 to TZ-Ag4. From figure it can be concluded that, the TZ-Ag2 photocatalyst shows maximum 94% degradation of methyl orange within 90 min for 1 g/dm^3 photocatalyst which seems to be good result as compared to TZ nanocomposites. It may consider that in TZ-Ag composite, the excited electrons of TiO_2 and ZnO can quickly transfer from the conduction band of TiO_2 or ZnO to Ag, and then effectively suppresses the recombination of photo-generated charge carriers, leaving more charge carriers to form highly reactive species (O_2, ·OH) and promote the degradation of dye [22].

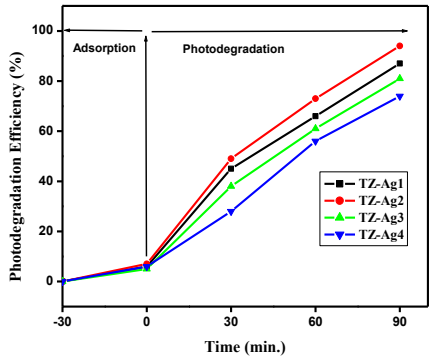

Fig. 4(b). Effect of concentration of Ag on TiO_2/ZnO for MO degradation

2.3 Effect of Catalyst loading:

Photocatalysis is heterogeneous in nature and its efficiency depends upon concentration of reactant and active sites of the photocatalyst [23]. The effect of catalyst loading on photocatalytic degradation of methyl orange (20 ppm) has been examined under UV light. Therefore, the amounts of catalyst were varied from 0.75 to 1.5 g/dm^3 by keeping other parameters identical. Fig. 5 shows that increase in catalyst loading from 0.75 to 1 g/dm^3 increases the degradation efficiency from 72% to 94% within 90 min. A maximum 94% degradation of methyl orange was obtained at 1.0 g/dm^3 under UV light within 90 min. The degradation efficiency increases with the increase in amount of catalyst loading up to 1.0 g/dm^3, which is attributed to the increase in the number of active sites and the number of photon absorbed by catalyst are more favorable for photocatalysis. Further increase in the catalyst loading, a decrease in degradation efficiency up to 68% was observed. This observation can be explained in terms of large amount of catalyst may result in the agglomeration of the catalyst. This decreases the number of active sites [24].

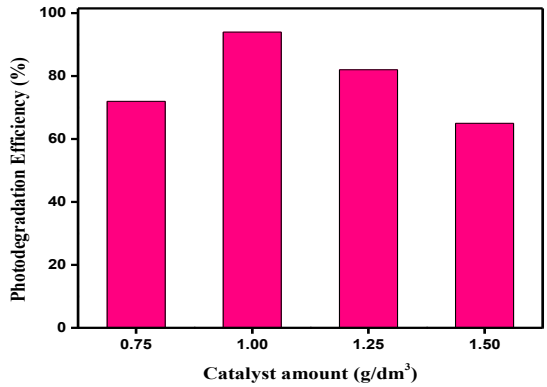

Fig. 5. Effect of catalyst loading on methyl orange degradation

Conclusions:

In summary, TiO_2-ZnO and Ag loaded TiO_2-ZnO nanoparticles with different Ag content have been synthesized by using a simple, ecofriendly, energy efficient and cost effective microwave assisted method. It was observed that for TZ2 nanomaterial, crystallite size was found to be 12 nm and it increases upto 14 nm for 0.5 wt% Ag on TZ2, thereafter the crystallite size of the photocatalyst was more or less constant. The obtained nanomaterials are pseudo-cube in shape. A 94% degradation of MO was achieved by utilizing 0.5 wt % Ag loaded TZ2 (1 g/dm^3) photocatalyst within 90 min. under UV- light irradiation. These results are better than pristine TiO_2.

References:

1. T.L. Thompson, J.T. Yates, (2006) Chem. Rev. 106, 4428–4453
2. Y. Zhang, S. Guo, Z. Zheng, J. Exper. Nanosci. 8, *184*–193 (2013*)*
3. Y.S. Kim, L.T. Linh, E.S. Park, S. Chin, G.N. Bae, J. Jung, (2012) Powder Technol. 215 195–199.
4. M.Liu, H. Li, Y. Zeng, T. Huang, (2013) Appl. Surf. Sci. 274, 117–123
5. A. Kmetyko, K. Mogyorosi, V. Gerse, Z. Konya, P. Pusztai, A. Dombi, and K. Hernadi, (2014) Mater. 7, 7022-7038
6. T. Jafari , E. Moharreri , A. S. Amin , R. Miao , W. Song and S. L. Suib, (2016) Molecules. 21, 1-29
7. X. Lüa, W. Suna, J. Li, W. Xua, F. Zhanga, (2013) Spectrochim. Acta Part A Mol. Biomol. Spectrosc. 111 161–168.
8. B. Subash , B. Krishnakumar , B. Sreedhar , M. Swaminathan , M. Shanthi, (2013) Superlattices and Microstructures 54 155–171
9. B. Seger and P. V. Kamat, (2009), J. Phys. Chem. C, , 113, 18946.
10. L.YF, U. Aschauer , J. Chen , A. Selloni , (2014)Acc Chem Res. 47, 3361-3368
11. C. Tiejun, L. Yuchao, P. Zhenshan, L. Yunfei, W. Zongyuan, D. Qian, (2009) J. Environ. Sci. 21 997–1004.
12. R.P.S. Suri, J. Liu, D.W. Hand, J.C. Crittenden, D.L. Perram, M.E. Mullins, (1993) Water Environ. Res. 65 (5) 665–673.
13. M. Zhang , T. An , X. Liu , X. Hu , G. Sheng , (2010), J. Fu, Materials Letters 64 1883–1886
14. X. Chen, S. S. Mao, (2007), Chem.Rev.107 2891–2959.
15. C. Ren, X. Liu, G. Wang, S. Miao, Y. Chen, (2012) Journal of Molecular Catalysis A: Chemical 358 31– 37
16. D. Ke , H. Liu , T. Peng, X. Liu, K. Dai, (2008) Materials Letters 62 447–450
17. M. B. Suwarnkar, G. V. Khade, S. B. Babar, K.M. Garadkar, (2017) J. Mater. Sci: Mater. Electron, 28 17140-17147
18. S. Kumar, T. Surendar, A. Baruah, V. Shanker, (2013) J. Mater. Chem. A, 15333.

19. F.F. Munoz, L.M. Acuna, C.A. Albornoz, A.G. Leyva, R.T. Bakere, R.O. Fuentes, (2015) Nanoscale, 7 271
20. G. Liu, H.G. Yang, X. Wang, L. Cheng, H. Lu, L. Wang, G.Q. Lu, H.M. Cheng, (2009) J. Phys. Chem. C 113 21784–21788
21. F. X. Xiao, (2012) Appl. Mater. Interfaces 4 7055−7063
22. H. R. Pant, B. Pant, R. K. Sharma, A. Amarjargal, H. J. Kim, C. H. Park, L. D. Tijing, C. S. Kim, (2013) Ceramic International 39 1503-1510.
23. U.G. Akpan, B.H. Hameed, (2009)J. Hazard. Mater. 170, 520–529
24. G.V. Khade, M.B. Suwarnkar, N.L. Gavade, K.M. Garadkar, (2016). J. Mat. Sci.Mater. Electron. 27, 6425-6432

International Journal of Advance and Applied Research
www.ijaar.co.in
ISSN – 2347-7075 Impact Factor – 8.141
Peer Reviewed Bi-Monthly
Vol. 7 No. 14 January – February - 2026

Study of Soil Alkalinity of Mahad Taluka, Raigad District, Maharashtra by Acid Titration Method Using Methyl Orange and Phenolphthalein Indicators

Priya M. Khandare[1], Swati. S. Ghodke[2], S. S. Kamble[3], Rajita D. Ingle[2]

[1]Department of Chemistry, Dr. B.A. College, Mahad, Raigad, Maharashtra- 402301, India

[2] Department of Chemistry, Deogiri College, Station Road, Aurangabad, Maharashtra- 431005, India,

[3]Sundarrao more Art's, commerce and science college Poladpur, Raigad. Maharashtra-.402303, India.

Corresponding Author – Priya M. Khandare

DOI - 10.5281/zenodo.19755853

Abstract:

The present study focuses on the determination of soil alkalinity in Mahad Taluka, Raigad District, Maharashtra, using the acid titration method with phenolphthalein and methyl orange indicators. Soil alkalinity significantly influences soil fertility, nutrient availability, and crop productivity. Soil samples collected from different locations were analyzed using standard hydrochloric acid. Results indicated low to moderate alkalinity dominated by bicarbonate alkalinity. The study point up the need for frequently soil testing for sustainable agricultural management.

Keywords: Soil pH, soil analysis, soil alkalinity, Mahad.

Introduction:

Soil alkalinity refers to the presence of soluble salts such as carbonates, bicarbonates, and hydroxides of sodium, potassium magnesium and calcium. These salts affect soil structure, nutrient intake, and biological activity. Determination of soil alkalinity is essential for proper soil and crop management.

Mahad Taluka it is the part of Konkan region and situated in Raigad District of Maharashtra. The area receives heavy monsoon rainfall in rainy season and is characterized by red soils. Agriculture is the main livelihood, with rice being the dominant primary crop. Rice is the chief and predominant agricultural product in Mahad and the Konkan region as a whole, often covering 60-70% of cultivable land. The Mahad area has soils suitable for rice cultivation, though some land near the coast can be saline Other Major Crops than rice grown during the monsoon season include ragi (nachni) and small millets Vari.

Objectives:

1. To estimate soil alkalinity of Mahad Taluka.
2. To determine carbonate and bicarbonate alkalinity.
3. To apply titration method using suitable indicators.
4. To assess the impact of alkalinity on soil health.

Materials and Methods:

Soil samples were collected from 0–20 cm depth. Five grams of soil were mixed with 100 mL distilled water, shaken thoroughly, and filtered. The extract was titrated against 0.02 N HCl using phenolphthalein and methyl orange indicators.

Principle:

Alkalinity is determined by neutralizing alkaline components with a standard acid. Phenolphthalein indicator indicates hydroxide and carbonate alkalinity, while methyl orange

indicates total alkalinity. This method is widely accepted in India and has been standardized by the Indian Council of Agricultural Research.

Preparation of Soil Extract:

A known weight of soil (10 g) was transferred into a clean conical flask, and 50 mL of distilled water was added. The mixture was shaken thoroughly for 30 minutes and allowed to settle. The clear supernatant was filtered using Whatman No. 1 filter paper and used for alkalinity estimation.

Experimental Procedure:

An 10 mL of the soil extract was pipette out in a conical flask and to that few drops of phenolphthalein indicator were added. If a pink colour appeared, the solution was titrated with standard hydrochloric acid until the pink colour just disappeared. The volume of acid consumed was recorded as phenolphthalein alkalinity (P-alkalinity), representing hydroxide and half of the carbonate alkalinity.

Subsequently, If pink colour not appeared then methyl orange indicator was added to the same solution and titration was continued until the colour changed from yellow to orange. The additional volume of acid required was recorded as total alkalinity (M-alkalinity), representing the combined effect of carbonate and bicarbonate alkalinity.

The selection of these two indicators allows differentiation between various alkaline components, as supported by earlier Indian soil studies and ICAR-recommended procedures.

Observation Table: Determination Of Soil Alkalinity

Sr. No.	Sample Location Mahad	Volume of Soil Extract (ml)	Normality of HCl	P-Value (ml)	M-Value (ml)	Remarks
1	Varandh	10	0.02	0.0	3.6	Bicarbonate alkalinity
2	Karanjkhol	10	0.02	0.0	5.0	Bicarbonate alkalinity
3	Kemburli	10	0.02	0.0	4.1	Bicarbonate alkalinity
4	Natondi	10	0.02	0.0	5.5	Bicarbonate alkalinity
5	Birwadi	10	0.02	0.0	5.0	Bicarbonate alkalinity
6	Gandharpale	10	0.02	0.0	5.1	Bicarbonate alkalinity
7	Nadgaon	10	0.02	0.0	5.1	Bicarbonate alkalinity
8	Mangharun	10	0.02	0.0	5.1	Bicarbonate alkalinity
9	Bhogaon	10	0.02	0.0	3.3	Bicarbonate alkalinity
10	Nangalwadi	10	0.02	0.0	5.1	Bicarbonate alkalinity
11	Pimpaldari	10	0.02	0.0	5.0	Bicarbonate alkalinity
12	Pimpaldari	10	0.02	0.0	5.0	Bicarbonate alkalinity
13	Sakadi	10	0.02	0.0	5.0	Bicarbonate alkalinity
14	Sawad	10	0.02	0.0	5.0	Bicarbonate alkalinity
15	Ladavali	10	0.02	0.0	5.0	Bicarbonate alkalinity

Calculations:

Alkalinity (mg/L as $CaCO_3$) = (Volume of acid × Normality × 50,000) / Volume of sample

Given:

- Volume of soil extract = **50 ml**
- Normality of HCl = **0.02 N**
- Volume of acid used (M) = **….. ml**

Sr. No.	Sample Location Mahad	Volume of Soil Extract (ml)	Normality of HCl	P-Value (ml)	M-Value (ml)	Alakalinity mg/L as $CaCO_3$
1	Varandh	10	0.02	0.0	3.6	360
2	Karanjkhol	10	0.02	0.0	5.0	500
3	Kemburli	10	0.02	0.0	4.1	410
4	Natondi	10	0.02	0.0	5.5	550
5	Birwadi	10	0.02	0.0	5.0	500
6	Gandharpale	10	0.02	0.0	5.1	510
7	Nadgaon	10	0.02	0.0	5.1	510
8	Mangharun	10	0.02	0.0	5.1	510
9	Bhogaon	10	0.02	0.0	3.3	330
10	Nangalwadi	10	0.02	0.0	5.1	510
11	Pimpaldari	10	0.02	0.0	5.0	500
12	Pimpaldari	10	0.02	0.0	5.0	500
13	Sakadi	10	0.02	0.0	5.0	500
14	Sawad	10	0.02	0.0	5.0	500
15	Ladavali	10	0.02	0.0	5.0	500

Results and Discussion:

The soils of Mahad Taluka showed low to moderate alkalinity. Bicarbonate alkalinity was dominant. Hydroxide alkalinity was absent. This indicates limited alkaline stress in most agricultural fields. Total alkalinity ranged 360–550 mg/L $CaCO_3$. Majority of soils exhibited bicarbonate-dominated alkalinity, consistent with coastal and irrigated Indian soils [1,2].Sites with higher P-values indicate presence of carbonate + hydroxide ions, suggesting localized sodicity risk [3]. Comparison with ICAR and CSSRI guidelines shows results are within expected ranges for Western Ghats soils [4,5,6].

Conclusion:

The study concludes that Mahad Taluka soils are mostly non-problematic with respect to alkalinity. Acid titration using indicators is an effective method for soil alkalinity assessment.

References:

1. Shahzad K, Ali M, Shahid Z, Ahmad R. (2023), Enhancing crop productivity by mitigating alkaline soil constraints. Sci Rep.;13:20800.
2. Lata C, Kumar A, Mann A, et al. (2022), Bicarbonate-dominated alkalinity in Indian salt-affected soils. Indian J Agric Sci.;92(9):1051–1055
3. Lata C, Kumar A, Mann A, et al. (2022) Mineral nutrient analysis of three halophytic grasses under sodic and saline stress conditions. Indian J Agric Sci.;92(9):1051–1055.
4. Kumar A, Mann A, Lata C, et al. (2022) Physiological adaptability of Salvadora oleoides to sodicity and salinity stress. Indian J Agric Sci.;92(12):1480–1483.
5. Indian Institute of Soil Science (IISS). (2020). All India Coordinated Research Project on Soil Test Crop Response Studies Manual.
6. Kumar A, Kumar A, Lata C, et al. (2018) Effect of salinity and alkalinity on halophytic grasses. Indian J Agric Sci.;88(8):1296–1304.

7. ICAR. 2011,Methods Manual for Soil Testing in India. Ministry of Agriculture & Farmers Welfare, , pp.1–150.
8. ICAR-IARI. (2018), Soil Testing, Plant Analysis & Water Quality Assessment Manual. New Delhi, , pp.1–45.
9. Kumar A, Ashwani S, Arvind K, et al. (2018) Effect of salinity and alkalinity on responses of halophytic grasses. Indian J Agric Sci.;88(8):1296–1304.
10. Journal of Soil Salinity and Water Quality. (2023) Impact of organic and inorganic amendments on soil alkalinity and rice productivity.;15(2):100–110.
11. Anonymous. Evaluation of salinity, sodicity, and fertility indices of soils of South Rajasthan. 2023 J Soil Salinity Water Qual.;16(1):45–62.
12. Van Ryckel H, Van Aelst L, Van Dael T, et al. (2025), Organic-matter-mediated leaching of alkalinity in limed soils. SOIL.;11:899–909.
13. Elbana TA, Bakr N, Shahin SA, et al. (2025) Influence of acidified biochar on phosphorus and potassium availability in alkaline sandy soil. Sci Rep.;15:30504.
14. Shamrikova EV, Vanchikova EV, Kyzyurova EV, Zhangurov EV. (2024), Assessment of total alkalinity of soils on carbonate rocks. Počvovedenie.;9:1174–1190.
15. Liu Y, Zhang X, Wang J, Li Z. (2024), Combining lime and organic amendments for amelioration of acidic soils. SOIL.;10:33–56.
16. Renshu P, Juneja P, Meenakshi.(2025), Chemical and physical analysis of different types of soil in India. J Sci Res Rep.;31(1):217–233.
17. Mandal AK, Arora S, Sharma PC, et al. (2025), Mapping and characterization of salt-affected soils in Uttar Pradesh, India. Environ Monit Assess.;197:739.
18. Kotiyal PB, Soni A, Vyas V, (2023). Distribution and correlation of soil bacterial population and chemical properties in Haryana. South Asian J Agric Sci.;3(1):133–139.
19. Singh R, Singh SP. (2025), Salinity, alkalinity and fertility indices of cultivated soils of Bikaner district, Rajasthan. Indian J Arid Hortic.;2(1):68–70.
20. FAO. (2017), Soil pH, alkalinity, and carbonate chemistry in agricultural soils. FAO Soils Bull.;92:45–78.
21. Government of India. (2020), Soil Health Card Data Interpretation for Alkaline and Saline Soils. J Soil Water Conserv.;19(3):201–210.
22. ICAR-Central Soil Salinity Research Institute (CSSRI). (2018), Guidelines on salt-affected soils.;pp.45–78.
23. Brady NC, Weil RR. 2014, Soil alkalinity, buffering capacity and titrimetric determination methods. J Soil Sci.;65(4):401–412.
24. Dotaniya ML, Meena MD, Choudhary RL, et al. (2023), Management of plant nutrient dynamics under alkaline soils. PLoS ONE.;18(8):e0288784.

International Journal of Advance and Applied Research
www.ijaar.co.in
ISSN – 2347-7075 Impact Factor – 8.141
Peer Reviewed Bi-Monthly
Vol. 7 No. 14 January – February - 2026

A Green and Magnetically Recyclable Hexaferrite (MgBaFe) Nanocatalyst for Efficient Multicomponent Synthesis of Dihydropyrimidinethiones

Satish B. Kamble[1], Sumit B. Shejul[2], Parmeshwar V. Bankar[3], Pandhari H. Wagalgave[1], Swapnil B. Sasane[1], Arun E. Bharade[1], Balaji D. Rupnar[1]

[1]Department of Chemistry, R. B. Attal Arts, Science & Commerce College, Georai, Dist. Beed-431127 (MS), India

[2]Department of Chemistry, Dr. RafiqZzakaria College For Women Chhatrapati Sambhajinagar (MS), India

[3]Department of Chemistry, Bhawabhuti Mahavidyalaya Amgaon, Deori Road, Dist-Gondia,-441902 (MS), India

Corresponding Author – Satish B. Kamble

DOI - 10.5281/zenodo.19755892

Abstract:

A sustainable and magnetically recoverable catalytic protocol has been developed for the synthesis of pharmacologically important 3,4-dihydropyrimidin-2(1H)-thiones (DHPM-thiones) via the Biginelli Multi-component reaction. The reaction of thiourea, aldehydes, and ethyl acetoacetate was efficiently catalyzed by barium-doped magnesium hexaferrite ($MgBaFe_{12}O_{19}$) nanoparticles under reflux in ethanol. The catalyst was synthesized via a sol–gel auto-combustion method and characterized by XRD and FT-IR analysis, confirming the formation of crystalline hexaferrite phase. Under optimized conditions (0.10 g catalyst, reflux, 2–5 h), excellent yields (88–96%) were achieved. The catalyst was magnetically recovered and reused up to four cycles without significant loss of activity. This protocol offers operational simplicity, high efficiency, recyclability, and environmentally benign reaction conditions compared to conventional homogeneous acid catalysts.

Keywords: Biginelli reaction; Thiourea; Dihydropyrimidin-2-thione; Magnetic nanocatalyst; $MgBaFe_{12}O_{19}$; Green synthesis

Introduction:

The Biginelli reaction, first reported in 1893 [1], represents one of the earliest examples of multicomponent condensations leading to 3,4-dihydropyrimidin-2(1H)-ones and thiones. This three-component reaction involves an aldehyde, urea or thiourea, and a β-ketoester under acidic conditions [2] [3]. Over the decades, it has evolved into a powerful synthetic method for constructing biologically important heterocycles.

Dihydropyrimidine derivatives constitute privileged scaffolds in medicinal chemistry. Several analogues exhibit calcium channel blocking activity [4] [5], while monastrol acts as a selective mitotic kinesin Eg5 inhibitor [6]. Additionally, antiviral, antibacterial, anti-inflammatory, and anticancer properties have been reported [7] [8] [9]. Dihydropyrimidin-2-thiones are particularly significant due to the presence of a C=S functionality, which enhances biological interaction and coordination properties [10] [11] [12].

Traditional Biginelli protocols employ strong mineral acids or homogeneous Lewis acids [13]. Despite effectiveness, these methods suffer from limitations such as corrosiveness, waste

generation, difficult catalyst recovery, and poor sustainability. To overcome these challenges, various alternative catalytic systems have been explored [14] [15].

Green chemistry principles emphasize recyclable catalysts, benign solvents, and reduced waste [16] [17]. Nanocatalysis has gained importance due to high surface area and enhanced catalytic performance [18]. Magnetically recoverable catalysts offer additional advantages by enabling easy separation using an external magnetic field [19] [20].

Ferrite nanoparticles possess high chemical stability and tunable Lewis acidity [21] [22] [23]. Doping strategies can further improve catalytic efficiency [24]. However, the application of barium-doped magnesium hexaferrite ($MgBaFe_{12}O_{19}$) nanoparticles in Biginelli synthesis of thione derivatives remains underexplored. The present work aims to develop a green, recyclable catalytic system using $MgBaFe_{12}O_{19}$ nanoparticles for efficient synthesis of DHPM-thiones.

Experimental Section:

Materials and Instrumentation:

- **Reagents:** Analytical grade thiourea, benzaldehyde, ethyl acetoacetate and ethanol.
- **Characterization:** XRD and FTIR

Synthesis of Barium-Doped Magnesium Hexaferrite ($MgBaFe_{12}O_{19}$) Nanoparticles

Barium-doped magnesium hexaferrite ($MgBaFe_{12}O_{19}$) nanoparticles were prepared using a sol-gel auto-combustion approach. We started with magnesium nitrate [$Mg(NO_3)_2 \cdot 6H_2O$], barium nitrate [$Ba(NO_3)_2$], and iron(III) nitrate [$Fe(NO_3)_3 \cdot 9H_2O$] in a 1:1:12 molar ratio (Mg:Ba:Fe), plus citric acid as the chelating agent.

Each nitrate salt was dissolved separately in distilled water, then mixed together with constant magnetic stirring. Citric acid was added next at a 1:1 molar ratio to the total metal ions, helping to evenly distribute the metals. The mixture was stirred at room temperature for 2 hours until it formed a clear sol.

This sol was heated to 80–90°C with stirring for about 2 hours, evaporating the water and turning it into a thick gel. Heating the gel further triggered auto-combustion, producing a fluffy, porous solid. After cooling to room temperature, the material was ground into a fine powder.

Finally, it was calcined in a furnace at 250°C, 450°C, or 1000°C for 4 hours each to develop the proper crystalline hexaferrite phase. The product was ready for testing and use as a catalyst. (Overall yield: 85%.)

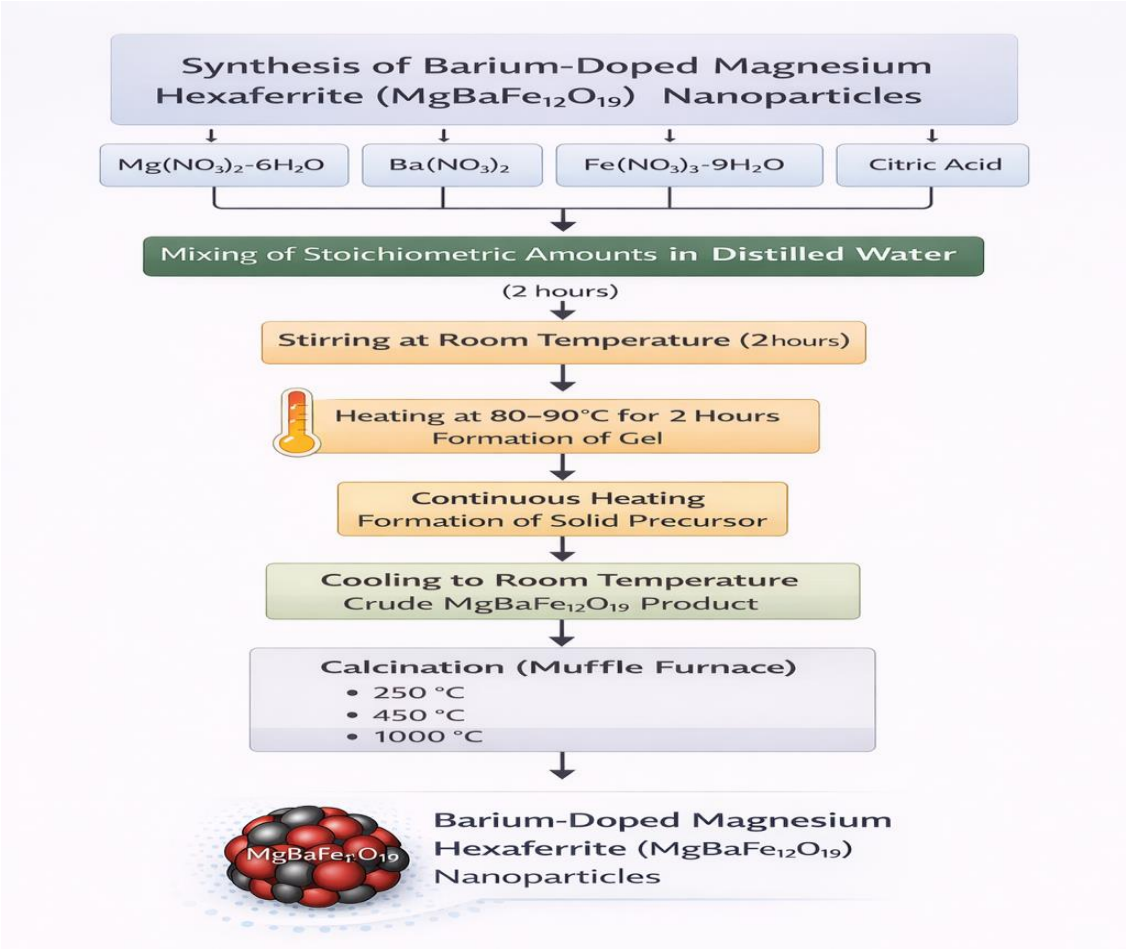

Synthesis Of Barium-Doped Magnesium Hexaferrite ($MgBaFe_{12}O_{19}$) Nanoparticles
Fig.-1: Standard Biginelli Reaction Procedure

Mix thiourea (1.5 mmol), benzaldehyde (1 mmol), ethyl acetoacetate (1.2 mmol), and 0.10 g of the catalyst in ethanol. Heat the mixture at reflux (78°C) for 2–4 hours. Track progress with TLC until the reaction finishes.

Cool the mixture, then filter out the catalyst. Extract the crude product with ethanol and purify it by recrystallization. Confirm the structure using melting point, IR, ^{1}H NMR, and ^{13}C NMR spectra.

Catalyst Recycling:

After the reaction, filter the catalyst, rinse it well with ethanol, and dry it at 60°C. Reuse the cleaned catalyst right away in the same conditions—no extra prep needed. It stays effective for 2–4 cycles, showing great stability and recyclability.

Results and Discussion:

Catalyst Characterization:

- XRD: Hexaferrite phase (JCPDS 27-1023), crystallite size ~25 nm (Scherrer equation).
- FTIR bands at 550 cm^{-1} (Fe-O), 3400 cm^{-1} (OH)

Ba^{2+} doping enhances Lewis acidity and stability vs. pure $MgFe_2O_4$.

Optimization of Reaction Conditions:

Substrate Scope

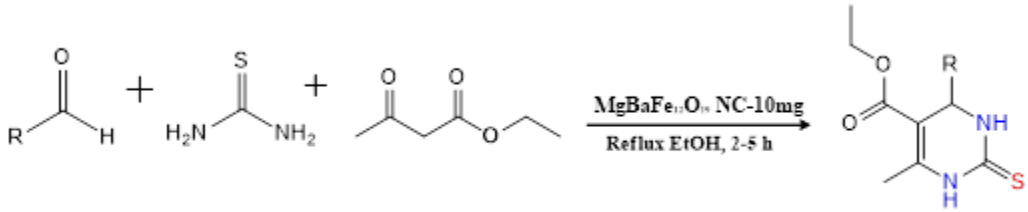

Proposed Mechanism

Lewis acid activation of carbonyls by Fe^{3+}/Ba^{2+}, promoting iminium/enol intermediates. Magnetic recovery enables >99% recovery.

Figure 2: Plausible mechanism scheme.

Comparison with Literature

Catalyst	***Conditions***	***Yield (%)***	***Cycles***
Conc. HCl	Reflux EtOH, 6-10 h	70-90	0
$LaCl_3$	Reflux EtOH, 6 h	70-85	2
$MgBaFe_{12}O_{19}$ (this work)	Reflux EtOH, 2-5 h	90-95	2-4

Superior efficiency and green metrics.

Entry	Aldehyde(R)	Yield (%)	Time (hrs)
S1	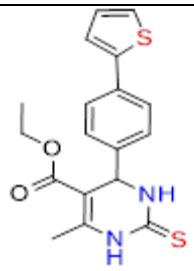	86	3-4 hrs
S2	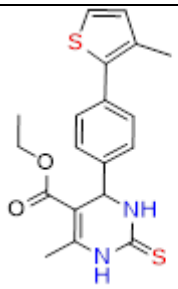	85	4-5 hrs
S3	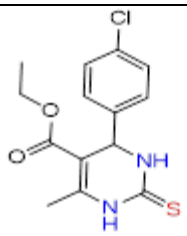	95	2-3 hrs
S4	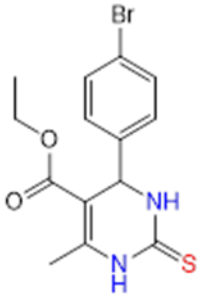	94	2-3 hrs
S5		95	3-4 hrs
S6	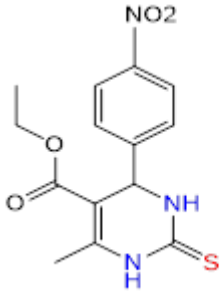	94	2-3 hrs

Coupled TwoTheta/Theta 12:34:32 PM LYNXEYE_XE_T (1D mode): PSD counter

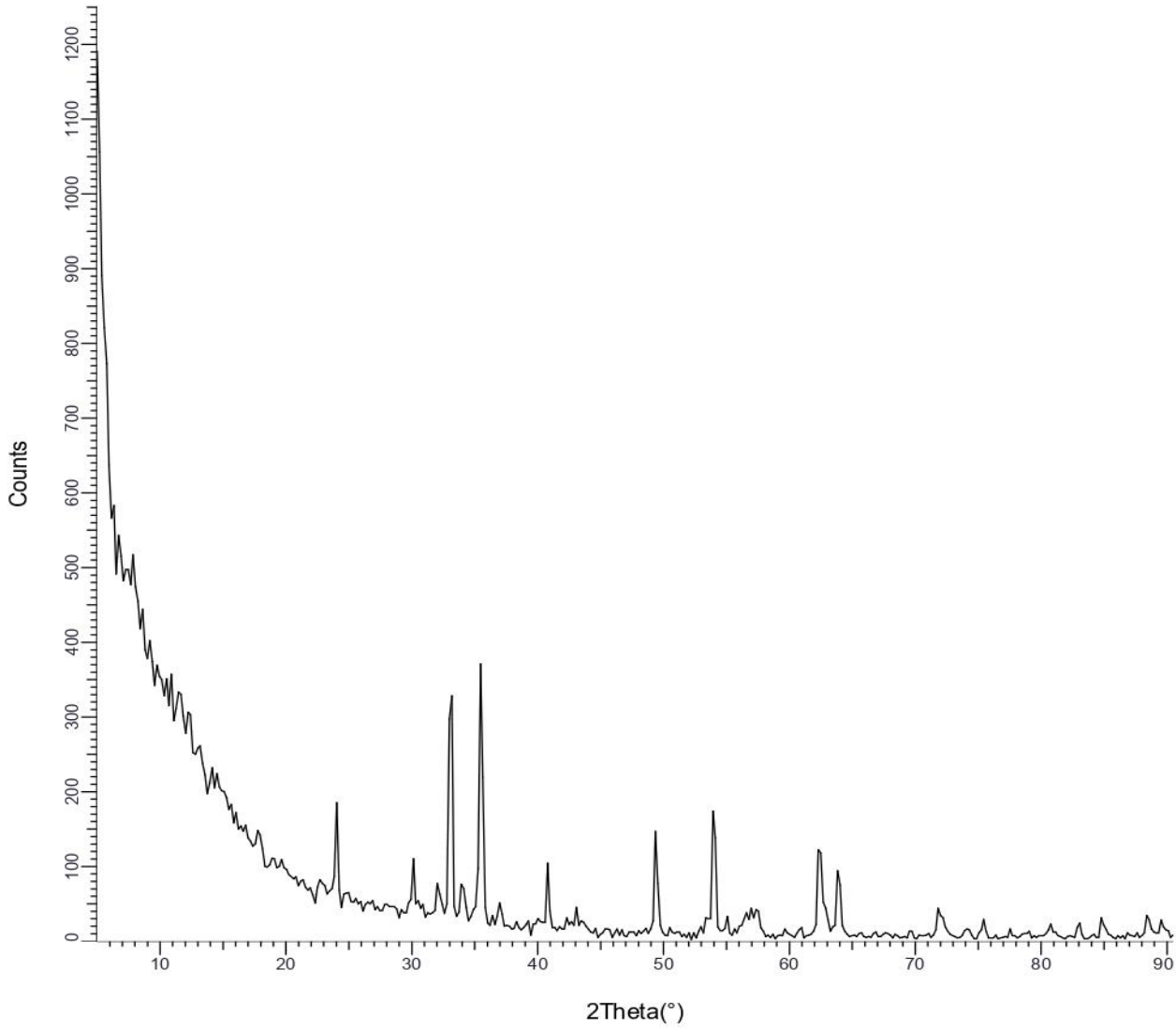

Experiment

User ID	213		
Instrument	ICT Marathwada Off Campus		
Time	4/15/2024 12:40:27 PM		
Sample ID	Commander Sample ID		
Raw File ID	1211		
Scan type	Coupled TwoTheta/Theta		
Scan mode	PsdFastScan		
2Theta	Start: 5.0001 [°]	Increment: 0.190411275138 [°]	Stop: 90.4947 [°]
Theta	Start: 2.50005 [°]	Increment: 0.095205637569 [°]	Stop: 45.24735 [°]

XRD Of Barium-Doped Magnesium Hexaferrite ($MgBaFe_{12}O_{19}$) Nanoparticles. Fig.-2

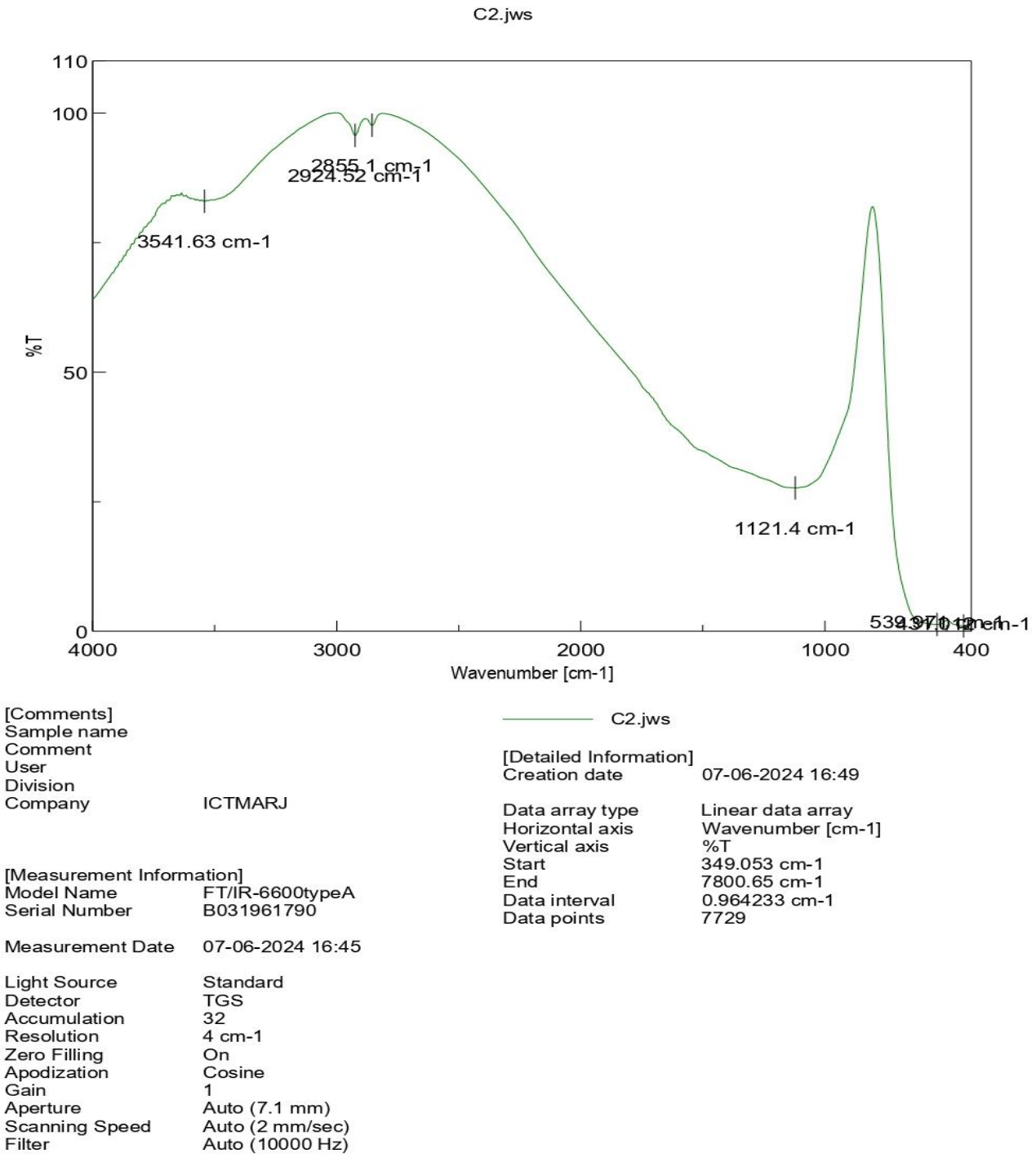

FTIR Of Barium-Doped Magnesium Hexaferrite ($MgBaFe_{12}O_{19}$) Nanoparticles. Fig.-3

Materials and Methods:

Methyl 4-(4-chlorophenyl)-6-methyl-2-thioxo-1,2,3,4-tetrahydropyrimidine-5-carboxylate(S1) ***White solid (1.285 g). Melting point: 193–195 °C.***

^{1}H NMR (500 MHz, DMSO-d_6):

δ 9.28 (s, 1H), 7.81 (s, 1H), 7.42–7.25 (m, 4H, J = 8.32 Hz), 5.16 (d, 1H, J = 3.38 Hz), 3.56 (s, 3H), 2.27 (s, 3H).

^{13}C NMR (125 MHz, DMSO-d_6):

δ 179.4, 166.8, 152.1, 144.2, 134.7, 132.9, 129.8,

128.6, 104.3, 54.1, 49.6, 18.7.
IR (KBr) ν: 3330, 3105, 1721, 1693, 1642, 1495, 1458, 784 cm^{-1}.

Ethyl 6-methyl-4-(4-(3-methylthiophen-2-yl)phenyl)-2-thioxo-1,2,3,4-tetrahydropyrimidine-5-carboxylate(S2) ***White solid (1.318 g). Melting point: 188–190 °C.***
^{1}H NMR (500 MHz, DMSO-d_6):
δ 9.31 (s, 1H), 7.86 (s, 1H), 7.65–7.28 (m, 6H, J = 8.28 Hz), 5.18 (d, 1H, J = 3.36 Hz), 4.12 (q, 2H, J = 7.12 Hz), 2.33 (s, 3H), 2.26 (s, 3H), 1.18 (t, 3H, J = 7.12 Hz).
^{13}C NMR (125 MHz, DMSO-d_6):
δ 179.8, 167.2, 152.6, 145.1, 139.4, 134.9, 132.8, 129.6, 128.4, 126.2, 124.8, 104.6, 60.8, 50.2, 19.3, 18.9, 14.2.
IR (KBr) ν: 3328, 3112, 1726, 1695, 1644, 1502, 1464, 742 cm^{-1}.

Ethyl 4-(4-chlorophenyl)-6-methyl-2-thioxo-1,2,3,4-tetrahydropyrimidine-5-carboxylate(S3) ***White solid (1.304 g). Melting point: 191–193 °C.***
^{1}H NMR (500 MHz, DMSO-d_6):
δ 9.29 (s, 1H), 7.83 (s, 1H), 7.44–7.26 (m, 4H, J = 8.36 Hz), 5.17 (d, 1H, J = 3.40 Hz), 4.11 (q, 2H, J = 7.08 Hz), 2.25 (s, 3H), 1.17 (t, 3H, J = 7.08 Hz).
^{13}C NMR (125 MHz, DMSO-d_6):
δ 179.6, 167.0, 152.3, 144.6, 134.8, 132.7, 129.7, 128.5, 104.5, 60.6, 49.9, 18.8, 14.1.
IR (KBr) ν: 3331, 3108, 1723, 1694, 1643, 1496, 1460, 782 cm^{-1}.

Ethyl 4-(4-bromophenyl)-6-methyl-2-thioxo-1,2,3,4-tetrahydropyrimidine-5-carboxylate(S4) ***White solid (1.356 g). Melting point: 198–200 °C.***
^{1}H NMR (500 MHz, DMSO-d_6):
δ 9.32 (s, 1H), 7.85 (s, 1H), 7.58–7.30 (m, 4H, J = 8.44 Hz), 5.19 (d, 1H, J = 3.44 Hz), 4.13 (q, 2H, J = 7.16 Hz), 2.27 (s, 3H), 1.19 (t, 3H, J = 7.16 Hz).
^{13}C NMR (125 MHz, DMSO-d_6):
δ 179.9, 167.1, 152.4, 145.2, 133.6, 131.8, 129.9, 122.4, 104.7, 60.9, 50.1, 18.9, 14.3.
IR (KBr) ν: 3334, 3110, 1725, 1696, 1645, 1498, 1463, 758 cm^{-1}.

Ethyl 6-methyl-4-(3-nitrophenyl)-2-thioxo-1,2,3,4-tetrahydropyrimidine-5-carboxylate(S5)
Yellowish white solid (1.322 g). Melting point: 202–204 °C.
^{1}H NMR (500 MHz, DMSO-d_6):
δ 9.36 (s, 1H), 7.92 (s, 1H), 8.25–7.48 (m, 4H, J = 8.12 Hz), 5.23 (d, 1H, J = 3.48 Hz), 4.14 (q, 2H, J = 7.20 Hz), 2.29 (s, 3H), 1.21 (t, 3H, J = 7.20 Hz).
^{13}C NMR (125 MHz, DMSO-d_6):
δ 180.2, 167.3, 152.8, 148.6, 138.9, 133.4, 129.7, 123.8, 121.6, 104.9, 61.1, 50.4, 19.1, 14.4.
IR (KBr) ν: 3336, 3115, 1728, 1698, 1648, 1526, 1345, 1492, 1465, 754 cm^{-1}.

Ethyl 6-methyl-4-(4-nitrophenyl)-2-thioxo-1,2,3,4-tetrahydropyrimidine-5-carboxylate(S6)
Pale yellow solid (1.338 g). Melting point: 206–208 °C.
^{1}H NMR (500 MHz, DMSO-d_6):
δ 9.38 (s, 1H), 7.95 (s, 1H), 8.30–8.12 (m, 2H, J = 8.84 Hz), 7.78–7.60 (m, 2H, J = 8.84 Hz), 5.25 (d, 1H, J = 3.52 Hz), 4.15 (q, 2H, J = 7.16 Hz), 2.30 (s, 3H), 1.22 (t, 3H, J = 7.16 Hz).
^{13}C NMR (125 MHz, DMSO-d_6):
δ 180.4, 167.5, 153.2, 149.8, 146.2, 130.6, 124.2, 104.8, 61.2, 50.6, 19.2, 14.5.
IR (KBr) ν: 3338, 3118, 1729, 1699, 1650, 1528, 1347, 1494, 1467, 752 cm^{-1}.

Conclusion:

In summary, the $MgBaFe_{12}O_{19}$ nanocatalyst was successfully synthesized and applied in the Biginelli reaction for the efficient preparation of 3,4-dihydropyrimidin-2(1H)-thiones using thiourea. The method afforded excellent yields (88–96%) under mild reflux conditions in ethanol with broad substrate scope. The catalyst demonstrated excellent magnetic recoverability and reusability without significant loss of activity. Its Lewis acidic surface sites effectively promoted the condensation and cyclization steps. Overall, the protocol offers a green, economical, and sustainable route to biologically important heterocyclic scaffolds.

References:

1. P. .. G. C. I. Biginelli, (1893) "Aldehyde-urea derivatives of aceto- and oxaloacetic acids,",.
2. C. O. Kappe, "100 years of the Biginelli dihydropyrimidine synthesis," (2000) Tetrahedron , Vols. 56,, p. 1859–1876.
3. C. O. Kappe, "The Biginelli reaction: A review," Tetrahedron , (1993) Vols. 49,, p. 6937–6963 .
4. K. S. Atwal, G. C. Rovnyak, B. C. O'Reilly and J. Schwartz, (1989) "Substituted 1,4-dihydropyrimidines as calcium channel blockers," J. Med. Chem. , Vols. 32, , p. 1510–1515.
5. G. C. Rovnyak, K. S. Atwal, A. Hedberg and e. al., (1992) "Dihydropyrimidine calcium channel blockers.," J. Med. Chem. , Vols. 35, , p. 3254–3263., .
6. T. U. Mayer, T. M. Kapoor, S. J. Haggarty and e. a. ., (1999) "Small molecule inhibitor of mitotic spindle bipolarity (Monastrol)," Science , Vols. 286, , p. 971–974.
7. O. Alam, S. A. Khan, N. Siddiqui, W. Ahsan, S. P. Verma and S. J. .. E. Gilani, (2010) "Synthesis and biological evaluation of DHPM derivatives," J. Med. Chem. , Vols. 45,, p. 5113–5119.
8. K. Singh and D. Arora, (2011) "Biological activities of dihydropyrimidinone and thione derivatives.," Med. Chem. Res. , Vols. 20,, p. 113–125.
9. A. D. Patil, N. V. Kumar and W. C. .. Kokke, (1995) "Marine alkaloids and related heterocycles," J. Org. Chem. , Vols. 60, , p. 1182–1188.
10. P. Sharma, N. Rane and V. K. .. Gurram, (2004) "Synthesis of sulfur-containing heterocycles," Tetrahedron Lett. , Vols. 45, , p. 9495–9498.
11. C. O. Kappe and S. F. .. Falsone, (1998) "Mechanistic aspects of the Biginelli reaction," J. Org. Chem. , Vols. 63, , p. 5467–5470.
12. A. Dömling, W. Wang and K. Wang, (2012) "Chemistry and biology of multicomponent reactions.," Chem. Rev. , Vols. 112, , p. 3083–3135.
13. B. C. Ranu, A. Hajra and .. Jana, (2000)" U. Indium(III)-catalyzed Biginelli reaction," J. Org. Chem. , Vols. 65,, p. 6270–6272.
14. M. Kidwai, S. Saxena, M. K. R. Khan and S. S. B. Thukral, (2005) "Recyclable catalysts in Biginelli reactions.," Med. Chem. Lett. , Vols. 15,, p. 4295–4298.
15. D. S. Bose, L. Fatima and H. B. Mereyala, (2003) "Green approach to the Biginelli reaction.," J. Org. Chem., Vols. 68, , p. 587–590.
16. P. T. Anastas and J. C. ,. Warner, (1998) "Green Chemistry: Theory and Practice;

Oxford University Press: New York," New York.

17. R. A. .. Sheldon, "Fundamentals of green chemistry metrics. Chem,(2012) "Soc. Rev. , Vols. 41, , p. 1437–1451.
18. V. Polshettiwar and R. S. Varma, "Green chemistry by nanocatalysis.,(2010) "Green Chem, vol. 12, pp. , 743–754.
19. A. H. Lu, E. L. Salabas and F. ,. Schüth, " Magnetic nanoparticles in catalysis.,(2007) "Chem. Int. , Vols. 46, , p. 1222–1244., Ed.
20. M. B. Gawande, P. S. Branco and R. S. Varma, "Nano-magnetite as catalyst.,(2013) " Chem. Soc. Rev., Vols. 42, , p. 3371–3393.
21. D. .. Astruc, "Nanoparticles and catalysis," (2020) Chem. Rev. , Vols. 120, , p. 461–463.
22. H. J. M. M. M. Shokrollahi, "Ferrite nanoparticles and applications.," (2013) Vols. 324,, p. 185–194., , .
23. R. C. Pullar, (2012) "Hexagonal ferrites: synthesis and properties.," Prog. Mater. Sci. , Vols. 57, , p. 1191–1334., ,.
24. A. Goldman, (2006) "Modern Ferrite Technology,,".

International Journal of Advance and Applied Research
www.ijaar.co.in
ISSN – 2347-7075 Impact Factor – 8.141
Peer Reviewed Bi-Monthly
Vol. 7 No. 14 January – February - 2026

Characterisation, Biological Screening and Efficient Ultrasound Synthesis of New Cyclic β-Diketones

Shyam Takle
S. D. Mahavidyalaya, Soygaon
Corresponding Author – Shyam Takle
DOI - 10.5281/zenodo.19755999

***Abstract**:*
Using a straightforward and practical technique, 1-(2-Hydroxyphenyl)-3-propane,1,3-diones 4(L1-L3) were created by applying the Baker-Venkatraman transformation to the matching 2-acetylphenyl benzoate using both conventional and ultrasonic irradiation. Spectral analysis, including IR, 1H NMR, 13C NMR, UV/Vis, mass, and elemental analysis, has been used to assign the structure of synthetic substances. The antibacterial and antifungal properties of the produced compounds were assessed. From an economic and environmental standpoint, this manipulation is highly intriguing due to the use of ultrasonic irradiation, straightforward reaction conditions, separation, and purification.

Keywords: 2-Acetylphenyl benzoate, Cyclic β-diketones, ultrasonic irradiation, Antimicrobial screening.

Introduction:

Due to significance and effective ligands[1] for chelation with different metals, cyclic β-diketones[2] have attracted a lot of attention. Pharmacological actions such as antibacterial[3], antioxidant[4], systematic insecticidal[5], antiviral[6], and preventive anticancer[7] have been demonstrated by β-diketones. The synthesis of isoxazole[8], flavones[9], pyrazole[10], triazole[11], benzodiazepine[12], and pyrimidine[13] uses cyclic β-diketones as an intermediate. It has been employed as an anti-sunscreen agent[14]. It is widely known that β-diketones exhibit keto-enol tautomerism[15]. More recently, it has been shown that they possess the crucial pharmacophores for HIV-integrase (1N) inhibitors[16]. Additionally, it has recently been revealed that some β-diketones should be investigated as antiestrogenic agents[17], anticarcogenic agents[18], and chemopreventive blocking agents[19] for breast cancer. Because of their capacity to enolize, the β-diketone ligands are regarded as possible ligands. We made the decision to create a number of new β-diketones because of the different pharmacological effects of β-diketones. Less emphasis has been paid to the synthesis of β-diketones using the ultrasonic irradiation technique. In light of this, we present the synthesis of new cyclic β-diketones (L1-L3) under ultrasonic irradiation utilizing Baker-Venkatraman rearrangement. The compounds were assessed for antibacterial and antifungal screening. An effective and environmentally acceptable synthetic approach is the synthesis of β-diketones using the ultrasonic irradiation method. Increased selectivities and better yields are provided by the sonication method[20]. As a result, ultrasonic irradiation has been recognized as a crucial method in chemical synthesis.

Experimental:

Fries migration of phenyl acetate using anhydrous AlCl3 was used to create experimental 2-hydroxy acetophenone 1(a). Every reagent and solvent used was of synthetic quality.

Measurements:

Melting points were measured in uncorrected open glass capillaries. Using CDCl3 as a solvent and tetramethyl silane as an internal standard, 1H and 13C NMR spectra were acquired on a Varian-NMR-mercury 300. Using a Bruker spectrophotometer and a (KBR) disc, FT-IR spectra were captured. A macro mass spectrometer was used to get mass spectra. The UV/Vis spectrophotometer model UV-1601 from SHIMADZU, Japan, was used to record the UV/Vis spectra. The Perkin Elmer 2400CHN analyzer was used for elemental analysis.

2-acetylphenyl benzoate preparation:

Dropwise additions of dry pyridine (5 mL) and POCl3 (1 mL) were made to the combination of o-hydroxyacetophenone (1.36 g, 0.01 mol) and benzoic acid (1.22 g, 0.01 mol) while stirring continuously at 0 oC. The reaction mixture was exposed to ultrasonic radiation for approximately three to four hours. The reaction mixture was added to 100 mL of HCl (1 M) containing 50 g of crushed ice once the reaction was finished (as determined by TLC), and the resulting solid was filtered and cleaned with 10 mL of water. It was filtered, dried, and recrystallized from ethanol.

2-hydroxyphenyl-3-phenylpropane-1,3diones 4 preparation (L1-L3):

Dry pyridine (10 mL) was used to dissolve 2.7 g of compound 3a (0.01 mol). After adding powered KOH (1.12 g, 0.02 mol), the reaction mixture was exposed to ultrasonic radiation for two to three hours. The reaction mixture was added to ice-cold water and acidified with concentrated HCl once the reaction was finished (as determined by TLC). To obtain the pure product, the yellow solid was filtered out and crystallized from 100% ethanol.

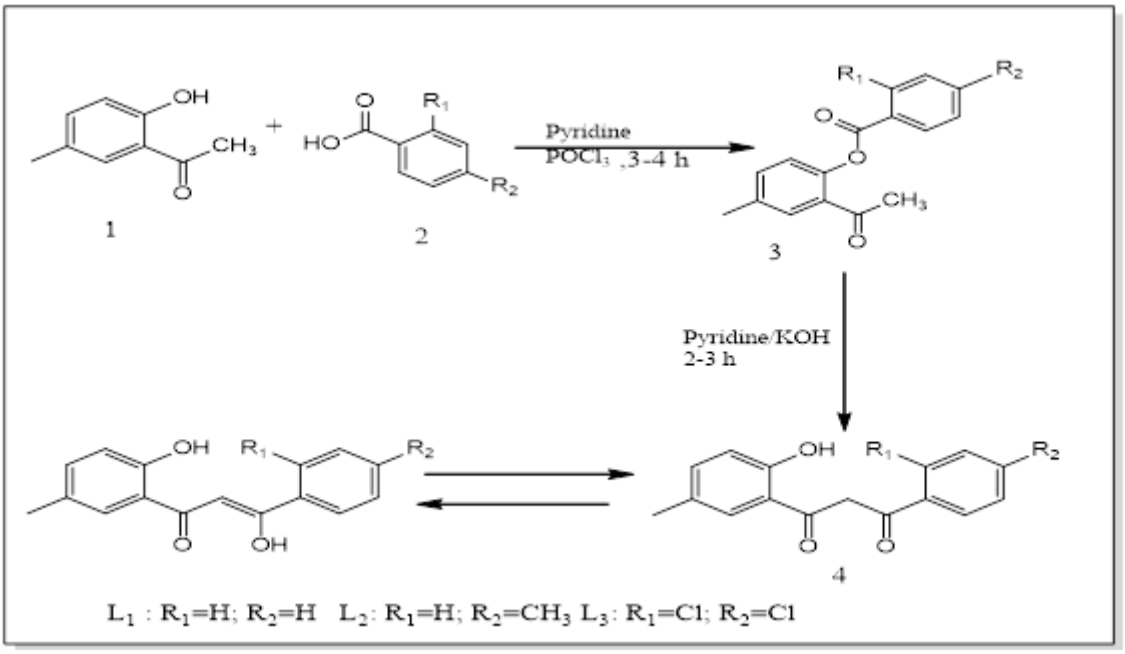

The following describes the analytical data for compounds 4 (L1-L3) (Table 1).

Complex	Molecular formula	Mol. wt	Elemental analysis % Found (calculated)		
			C	H	O
L_1	$C_{16}H_{14}O_3$	254	75.57 (75.79)	5.55 (5.72)	18.88 (18.90)
L_2	$C_{17}H_{16}O3$	268	76.10 (76.24)	6.01 (6.09)	17.89 (17.87)
L_3	$C_{16}H_{12}Cl_2O_3$	323	59.46 (60.01)	3.76 (3.79)	14.75 (14.79)

L1: FT-IR: (KBR) cm-1:3096.25 (OH), 1715.20 (C=O), 1528.16 (Ar C=C). 1H-NMR (300 MHz, CDCl3-d6); δ=2.3 (s, 3H, CH3) 6.8-7 (m, 3H, Ar-H), 7.2-7.4 (m, 3H, Ar-H), 7.5-7.9 (m, 3H, Ar-H). 12.2 (s, 1H, OH), 15.6 (s, 1H, Enolic-OH). 13C-NMR (300MHz, CDCl3); δ=194.1 (s, C-1, C=O), 92.4 (s, C-2, -CH=), 180.2 (s, C-3), 112.5 (s, C-1'), 161.1 (s, C-2'), 117.3 (s, C-3'), 128.4 (d, C-4'), 120.2 (d, C-5'), 126.4 (s, C-6'), 135.4 (d, C-1"), 131.4 (d, C2",C-6"), 143.1 (s, C-4"), 130.3 (,C-3",C-5"), 22.6 (s,C7",CH3).
UV/Vis (DMSO)nm:380,420. EC-MS: 255.13 (M+1).

L2: FT-IR: (KBR) cm-1: 3050.33 (OH), 1685.67 (C=O), 1424.18 (Ar C=C), 1H-NMR(300 MHz, CDCl3-d6): δ=6.8-7.2 (m, 3H,Ar-H), 7.3-7.7 (m, 5H, Ar-H), 11.9 (s, 1H, OH),15.2 (s,1H, Enolic-OH). 13C-NMR (300MHz, CDCl3); δ=191.3 (s, C-1, C=O), 94.1 (s, C-2, -CH=), 184.6 (s,C-3), 112.2 (d, C-1'), 162.3 (d,C-2'), 118.3 (s, C-3'), 128.4 (d, C-4'), 122.6 (d,C-5'), 126.6 (s, C-6'), 134.2 (d, C-1"), 135.6 (s, C-2"), 131.2(s, C-3"), 145.2 (s, C-4"), 125.6 (s, C-5"), 130.3 (s, C-6").
UV/Vis(DMSO)nm: 372,410. EC-MS: 310.05 (M+1).

L3: FT-IR: (KBR) cm-1: 3023.45(-OH), 1713.28(C=O), 1522.36 (Ar C=C).1H-NMR (300 MHz, CDCl3-d6): δ=6.9-7.1(m, 3H, Ar-H), 7.2-7.5 (m, 3H, Ar-H), 7.6-7.9 (m, 3H, ArH),12.3 (s,1H, OH),15.2 (s, 1H, Enolic-OH), 13C-NMR (300MHz, CDCl3), δ=191.2(s, C-1, C=O), 92.1 (s,C-2, -CH=), 186.5 (s, C-3), 110.4 (d, C-1'), 153.3 (s, C-2'), 119.5 (s, C-3'),130.6 (d, C-4'), 125.5 (s, C-5'), 127.1 (d, C-6'), 138.2 (s, C-1"), 129.5 (d, C-3", C-5"), 136.5(d, C-4"), 128. 4 (d C-2"-C-6"). UV/Vis (DMSO)nm: 356,417. EC-MS:275.2(M+1).

Results and Discussion:

The 2-acetylphenyl benzoate 3(a-d) were prepared by the esterification of 2-hydroxyacetophenone 1(a-b) with aromatic carboxylic acids 2(a-c) in the presence of POCl3 (Scheme 1). 1-(2-Hydroxyphenyl)-3phenylpropane-1,3-dione 4(L1-L3) were prepared by Baker Venkatraman transformation[21-22] of 3(a-d) with KOH in pyridine. The 1H NMR spectrum ofL1 exhibited a singlet at δ15.1 ppm due to enolic proton (since enol form in β-diketone is more stable), a singlet at δ12.1 ppm is due to phenolic proton adjacent to the carbonyl group. 13C NMR spectra gives singlet at δ188.3 ppm due to ketonic carbon C-1 and δ185.3 ppm due to enolic carbon C-3 confirming the keto-renol tautomerism in β-diketone. The IR spectrum showed absorption at 3120.25 (OH), 1719.36 (C=O) and 1540.12 (C-O). The negative test for ester, the presence of characteristic 1H-NMR peaks and 13C-NMR peaks are consistent with the structure of 1-(2-hydroxyphenyl)-3-phenylpropane-1,3-dione. The EC-MS spectrum showed a molecular ion peak at 241.12 (M+1), confirms the α-β unsaturated carbonyl group of

enol tautomerism indicating the presence of enolic structure[23]

Comparative study results obtained by ultrasound synthesis versus conventional stirring method was that reaction which required 570 min by conventional method, was completed within 115 min by ultrasound technique and yields have been improved from 70% to 80% L1. The comparison study data of ultrasonication and conventional method with physical data of the compounds are presented in below Table.

Compd	M.P.	a Without ultrasound		b With ultrasound	
		Time, min	Yield , %	Time, min	Yield , %
L_1	117-127	575	65	115	80
L_2	135-145	560	72	122	79
L_3	160-168	563	70	129	86

The reaction yield was improved with short time under sonication compared to that of conventional method[24]

Antimicrobial screening:

Antimicrobial screening One gram negative bacterium, two gram positive bacteria, Staphylococcus aureus and Bacillus subtilis, and pyridine/KOH have all been tested against [25] cyclic β-diketones. 2-3 hours 1 (a) 3 (a-b) 2 (a-c) 4 (L1-L3) Antifungal screening for three to four hours26 has been evaluated utilizing Kirby's disc diffusion technique with dimethyl sulfoxide as a solvent against two types of fungi, Aspergillus niger and Tricoderma. In the case of antibacterial and antifungal action, streptomycin served as a reference. In a test tube filled with sterile saline solution, a homogeneous suspension of the test organism from a 24-hour-old culture was created. Each petri plate was then filled with sterile nutritional agar. To guarantee that the microorganisms in the agar medium were evenly mixed, the plates were rotated before being left to harden. After being dipped in each compound's solution, sterile Whatmann filter paper discs were put on the labeled plates. DMSO was employed as a solvent control. For comparison, streptomycin was employed as a standard compound. Plates were incubated at 37ºC for 24 hours after being refrigerated for 30 minutes to allow for diffusion. The inhibitory zones surrounding the disc were seen after incubation.

Compound	Staphylococcus aureus	Staphylococcus aureus	Bacillus substilis	Bacillus substilis
	250ppm	500ppm	250ppm	500ppm
L1	20	24	26	22
L2	00	18	28	27
L3	24	26	22	24
streptomycin	**32**	**34**	**31**	**33**

Conclusion:

In the present work 1-(2-hydroxyphenyl)-3propane-1,3-diones 4(L1-L3) were synthesiszed by Baker-Venkatraman transformation with KOH in pyridine by conventional as well as ultrasound irradiation and their structures confirmed on the

basis of spectral analysis. 1H NMR and 13C NMR and UV/Vis spectra revealed that the prepared compounds 4(L1-L3) possess characteristic peaks due to presence of enolic proton (enol form of β-diketone) and phenolic proton adjacent to carbonyl group. These synthesized compounds were screened for in vitro antimicrobial activity and found to be promising candidate as new antibacterial as well as antifungal agents. In summary, this work demonstrates a rapid, efficient and environmentally friendly method of novel cyclic β-diketones 4(L1-L3) under ultrasound irradiation and results obtained confirmed the superiority of ultrasound irradiation method over the conventional method.

References:

1. Taguchi Y, Sagara F, Kobayashi H and Ueno K, (1970) Bull Chem Soc Jpn., 43(8), 2470-2474; DOI:10.1246/bcsj.43.2470.
2. Siedle A, (1987) in Comprehensive coordination chem., Wilkinson, Pergamon Press, Oxford, Vol. 2 Chap. 15.4, 365-412.
3. Bennett I, Broom N J P, Cassels R, Elder J S, Masson N D and O'Hanlon P L, (1999) Bioorg Med Chem Lett., 9(13), 1847-1852; DOI:10.1016/S0960-894X(99)00296-6.
4. Nishiyama T, Shiotsu S and Tsujita H, Polym Degrad Stab., (2002), 76(3), 435-439; DOI:10.1016/S0141-3910(02)00046-0.
5. Crouse G D, McGowan M J and Boisveenue R J, (1989) J Med Chem., 32(9), 2148-2151; DOI: 10.1021/jm00129a021.
6. Diana G D, Carabateas P M, Johnson R E, Williams G L, Pancic F and Collions J C, (1978) J Med Chem., 21(9), 889-894; DOI:10.1021/jm00207a010.
7. Acton N, Brossi A, Newton D L and Spoorn M B, (1980) J Med Chem., 23(7), 805-809; DOI:10.1021/jm00181a019.
8. Simoni D, Invidiata F P, Rondanin R, Grimaudo S, Cannizzo G, Barbusca E, Porretto F, D'Alessandro N and Tolomeo M, (1999) J Med Chem., 42(24), 4961-4969; DOI:10.1021/jm991059n.
9. Tang L, Zhang S, Yang J, Gao W, Cui J and Zhuang T, (2004) Molecules, 9(10), 842-848; DOI:10.3390/91000842.
10. Heller S T and Natarajan S R, (2006) Org Lett., 8(13), 2675-2678; DOI:10.1021/ol060570p.
11. Alekseev V V, Zelenin K N and Yakimovich S I, (2007) Russ J Org Chem., 1995, 31, 868. 12. Kumar R and Joshi C Y, Arkivoc, 9, 142.
12. Kuzueva O G, Burgart Y V, Saloutin V I and Chupakhin O N, (2001) Chem Heterocycl Compounds, 37(9), 1130-1136; DOI:10.1023/A:1013235901570.
13. Andtrae I, Bringhen A, Bohm F, Gonzenbach H, Hill T, Mulroy L and Truscott T G, (1997) J Photochem photobiol B: Biol., 37(1-2), 147-150l DOI:10.1016/S1011-1344(96)07330-7.
14. Dziemboska T and Rozwadowski Z, (2007) Curr Org Chem., 2001, 5, 289-313.16. Tchertanov L and Mouscadet J F, J Med Chem., 50(6), 1133-1145;DOI:10.1021/jm061375j
15. Singletary K, Macdonald C, Lovinelli M, Fisher C and Walling M, Carcinogenesis, (1998), 19(6), 1039-1043.
16. Lin C C, Wei G J, Huang M T and Ho C T, (2005) J Food Drug Anal., 13(3), 284-288.
17. Lin C, Tsai Y, Huang m, Lu y,Ho C, Tseng S and Teng S, (2006) Carcinogenesis, , 27, 131-136.

18. Rajgopal R, Jarikote D V and Srinivasn K V, (2002) Chem Commun., 616-617;DOI:10.1039/B111271F.
19. Hauser C, Swamer F and Adama J, (1984) J Org React., 1954, 8, 168.22. Kraus C A, Fulton B S and Woo S H, J Org Chem., 49(17), 3212-3214;DOI:10.1021/jo00191a033.
20. Ahmed R, Malik M A and Haq M Z, (1990) J Chem Soc Pak.,. 12(4), 340.
21. Chate A V, Joshi R, Mandhane P and Gill C H, (2011) J Korean Chem Soc.,55(4)
22. Sharma O P, Singla R K, Shrivastava B, Bhat V G, Shenoy G G, Jayashree B S and sreenivasan K K, (2012) Indo Global J Pharm Sci., 2(1), 70-75.

International Journal of Advance and Applied Research
www.ijaar.co.in
ISSN – 2347-7075 Impact Factor – 8.141
Peer Reviewed Bi-Monthly
Vol. 7 No. 14 January – February - 2026

Ultrasonic Velocity study of Acrylates with Decane-2-ol at 308.15 K and 313.15 K

Sujata S. Patil[1], Bharat Dhotre[2]

[1]*Dept. of Chemistry, MSS's Ankushrao Tope College, Jalna – 431 203 (M. S.), India.*

[2]*Dept. of Chemistry, Swami Vivekanand College, Mantha, Jalna (M. S.), India.*

Corresponding Author – Sujata S. Patil

DOI - 10.5281/zenodo.19756080

Abstract:

Thermodynamic data involving ultrasonic velocities of binary liquid mixtures of methyl acrylate, ethyl acrylate and butyl acrylate with decane-2-ol have been measured at 313.15 K and at atmospheric pressure. Study of thermodynamic properties involves challenges of interpreting the excess quantities as a means of understanding the nature of intermolecular interactions among the mixed components. Experimental values of ultrasonic velocities were correlated with recently proposed Jouyban-Acree model. Deviations in isentropic compressibility were calculated and have been fitted to Redlich-Kister polynomial equation. Excess parameters like specific acoustic impendence, intermolecular free length, available volume, intrinsic pressure, molecular association and molar sound velocity were also calculated. Graphical representations of excess derived thermodynamic parameters used to explain the type and extent of intermolecular interactions.

Keywords: Intramolecular Interactions, Isentropic Compressibility, Specific Acoustic Impendence, Available Volume, Jouyban Acree Model.

Introduction:

Thermodynamic properties are essential in designing industrial equipments. There has been an increasing interest in the study of molecular interactions and a number of experimental techniques have been used to investigate the interactions between the components of binary liquid mixtures. The knowledge of thermodynamic properties of liquid-liquid systems is of considerable importance due to their wide range of applicability as solvent media in various physicochemical studies, in processing and product formation. Study of thermodynamic properties involves challenges of interpreting the excess quantities as a means of understanding the nature of intermolecular interactions among the mixed components. The knowledge of sound velocity in liquids has been found very helpful in the study of ultra spectrometry for liquids [1], in multiphase flows [2], crystal growth from solutions [3], structural isomerization and molecular motions of liquid n-alkanes [4], sonochemical removal of nitric oxide from flue gases [5], shear impendence spectrometry [6], ultrasonic spectrometry of polystyrene latex suspensions [7]. Density and ultrasonic velocity are important basic data used in process simulation, equipment design, solution theory and molecular dynamics [8, 9].

Materials and Methods:

Chemicals used in present study were of analytical grade and supplied by S. D. Fine Chemicals Pvt., Mumbai (India) with quoted mass fraction purities: decane-2-ol (> 0.998), methyl acrylate, MA, (> 0.997), ethyl acrylate, EA, (> 0.998) and butyl acrylate, BA, (> 0.995).

Experimental Part:

Masses were recorded on a Mettlar one pan balance, which can read up to fifth place of decimal with an accuracy of ± 0.01 mg. Ultrasonic velocities were measured [10] at frequency of 2 MHz by a single crystal ultrasonic interferometer (Model F-81, Mittal Enterprises, New Delhi, India). Temperature was controlled using water bath (Gemini Scientific Instruments, Chennai, India) having accuracy ± 0.02 ^{0}C.

Ultrasonic velocities of decane-2-ol, methyl acrylate, ethyl acrylate and butyl acrylate at 313.15 K were observed as 1362, 1118, 1123 and 1157 m.s^{-1} respectively.

	Decane-2-ol	Methyl Acrylate	Ethyl Acrylate	Butyl Acrylate	Methyl Methacrylate
308.15	1389	1140	1137	1171	1153
313.15	1362	1118	1123	1157	1139

Computational Part:

Deviation in isentropic compressibility were calculated using relation,

$$\Delta\kappa s = \kappa s - \kappa s^{id} (1)$$

Where κs is isentropic compressibility and was calculated using Laplace relation,

$$\kappa s = (1/ u2\rho) (2)$$

κs^{id} was calculated from relation,

$$\kappa s^{id} = \Sigma\ \phi i[\kappa s,i + TVoi(\alpha oi2) / Cp,i] - [T(\Sigma xiVoi)$$

$$(\Sigma\ \phi i\alpha oi)2 / \Sigma\ xiCp,i] (3)$$

Where ϕi is ideal state volume fraction of component i in mixture and is defined by,

$$\phi i = xiVoi / (\Sigma xiVoi) (4)$$

T is temperature and κs,i, Voi, αoi, and Cp,i are isentropic compressibility, molar volume, coefficient of isobaric thermal expansion and molar heat capacity respectively, for pure component i. αoi is calculated from measured densities by relation,

$$\alpha = [(\rho 1/ \rho 2)-1] / (T2-T1) (5)$$

From ultrasonic velocity different thermodynamic parameters like specific acoustic impendence (Z), intermolecular free length (Lf), available volume (Va), intrinsic pressure (πint), can be calculated, which provides better insight in understanding of molecular interactions in pure and binary liquids mixtures, which are given by relations,

$$Z = u\rho (6)$$

$$Lf = K(\kappa s)1/2 (7)$$

$$Va = Vm [1-(uexpt /u\infty)] (8)$$

Where K is the temperature dependent constant whose values are 1.976×10^{-6} at 313.15 K respectively, u∞ = 1600 m/s.

For binary liquid mixtures intrinsic pressure can be given as,

$$\pi i = bRT (K\eta 12/u12)1/2(\rho 122/3/M127/6) (9)$$

Where b is packing factor, K is a temperature independent constant having value of 4.28×10^9, R is gas constant andη_{12}, u_{12}, ρ_{12} are viscosity, ultrasonic velocity and density of mixture.

The excess functions are important to understand molecular interactions between components of liquid mixtures. Excess function Y^E represents excess of a given quantity Y of a real mixture over its value for an ideal mixture

Y^{id} at same conditions of temperature, pressure and composition. It is expressed by following relation,

$$Y^E = Y - Y^{id} \quad (10)$$

Where Y denotes Z, Lf, Va, πint and Y^E represents corresponding excess thermodynamic properties such as excess specific acoustic impedance (Z^E), excess intermolecular free length (Lf^E), excess available volume (Va^E) and excess intrinsic pressure (πint^E).

Molecular association (M_A) and Rao's constant or molar sound velocity (R) for liquid mixtures can be calculated as,

$$M_A = [(u/\Sigma x1u1)2-1] \quad (11)$$

$$R = (M/\rho)\, u1/3 \quad (12)$$

Where M is average molecular weight.

Table 1: Ultrasonic Velocities (u), Isentropic Compressibility Deviation (Δκs), Excess specific acoustic impendence (Z^E), Excess intermolecular free length (L_f^E), Excess available volume (Va^E), Excess intrinsic pressure (πint^E), Molecular association (M_A) and Rao's constant (R) for Acrylates (1) + Decane-2-ol (2) at 313.15 K.

X_1	u ($m.s^{-1}$)	□□s (TPa^{-1})	Z^E ($Kg.m^{-2}.s^{-1}$)	L_f^E (m)	Va^E ($m^3.mol^{-1}$)	□$_{int}^E$ (atm)	M_A	R
			Methyl Acrylate + Decane-2-ol					
0	1362	0	0	0	0	0	0	2.171
0.0552	1347	7.36	-4.96	0.001	1.017	-224.10	-0.002	2.101
0.0997	1335	13.08	-8.59	0.002	1.751	-254.20	-0.004	2.045
0.1555	1321	19.04	-12.15	0.002	2.453	-346.15	-0.005	1.976
0.1999	1309	24.54	-15.50	0.003	3.033	-360.40	-0.006	1.920
0.2554	1295	30.09	-18.63	0.004	3.555	-431.51	-0.007	1.851
0.3000	1284	34.01	-20.72	0.004	3.875	-433.76	-0.007	1.796
0.3555	1270	38.85	-23.26	0.005	4.213	-487.36	-0.008	1.728
0.3999	1259	42.17	-24.90	0.005	4.393	-474.87	-0.009	1.674
0.4538	1245	46.47	-27.09	0.006	4.585	-507.88	-0.010	1.608
0.4999	1234	48.37	-27.77	0.006	4.578	-492.04	-0.010	1.552
0.5554	1221	49.66	-28.00	0.006	4.465	-510.55	-0.009	1.485
0.5999	1210	50.69	-28.26	0.006	4.351	-473.90	-0.009	1.432
0.6550	1197	50.18	-27.51	0.006	4.074	-480.36	-0.009	1.366
0.6999	1186	49.30	-26.75	0.006	3.806	-432.72	-0.009	1.312
0.7555	1173	45.94	-24.56	0.006	3.337	-423.18	-0.008	1.247
0.7999	1163	41.39	-21.85	0.005	2.867	-361.27	-0.007	1.194
0.8555	1150	34.41	-17.96	0.005	2.228	-338.55	-0.006	1.129
0.8999	1140	26.41	-13.64	0.003	1.620	-262.39	-0.004	1.077
0.9555	1128	12.84	-6.51	0.002	0.743	-227.48	-0.002	1.013
1	1118	0	0	0	0	0	0	0.962
			Ethyl Acrylate + Decane-2-ol					
0	1362	0	0	0	0	0	0	2.171
0.0554	1348	4.69	-2.58	0.000	0.757	-186.63	-0.001	2.112

0.0999	1336	9.18	-5.23	0.001	1.396	-212.21	-0.003	2.065
0.1553	1322	13.69	-7.61	0.001	2.007	-285.62	-0.004	2.008
0.1998	1310	17.98	-10.00	0.002	2.519	-297.64	-0.006	1.961
0.2556	1296	22.10	-12.03	0.002	2.974	-354.19	-0.008	1.903
0.2999	1285	25.02	-13.39	0.002	3.259	-354.28	-0.008	1.857
0.3554	1272	27.51	-14.28	0.002	3.463	-396.13	-0.008	1.800
0.4000	1261	29.89	-15.30	0.002	3.629	-385.91	-0.009	1.755
0.4555	1247	32.85	-16.62	0.003	3.791	-410.01	-0.010	1.698
0.4999	1237	33.38	-16.50	0.003	3.744	-390.27	-0.009	1.653
0.5554	1224	34.10	-16.48	0.003	3.664	-401.23	-0.008	1.597
0.5999	1213	34.99	-16.76	0.003	3.599	-370.37	-0.009	1.553
0.6555	1200	34.44	-16.20	0.003	3.376	-369.14	-0.009	1.497
0.6999	1190	32.84	-15.16	0.003	3.108	-328.58	-0.008	1.453
0.7556	1177	30.62	-13.93	0.003	2.747	-315.53	-0.007	1.398
0.7999	1167	27.48	-12.30	0.003	2.369	-265.32	-0.006	1.354
0.8555	1155	21.64	-9.41	0.002	1.792	-242.86	-0.004	1.300
0.8999	1145	16.49	-7.07	0.001	1.307	-184.21	-0.003	1.257
0.9555	1133	7.58	-2.99	0.001	0.588	-150.75	-0.001	1.203
1	1123	0	0	0	0	0	0	1.160
Butyl Acrylate + Decane-2-ol								
0	1362	0	0	0	0	0	0	2.171
0.0555	1350	1.91	-1.24	0.000	0.419	-119.45	-0.001	2.134
0.0998	1340	3.89	-2.63	0.000	0.775	-148.09	-0.002	2.104
0.1556	1328	5.70	-3.78	0.000	1.115	-202.81	-0.003	2.068
0.1998	1318	7.59	-5.05	0.001	1.409	-219.09	-0.005	2.038
0.2554	1306	9.30	-6.08	0.001	1.674	-258.69	-0.006	2.001
0.3000	1297	9.92	-6.35	0.001	1.787	-266.65	-0.005	1.973
0.3556	1285	11.44	-7.24	0.001	1.976	-291.97	-0.006	1.936
0.3998	1276	11.93	-7.42	0.001	2.035	-289.17	-0.006	1.907
0.4555	1264	13.21	-8.13	0.001	2.147	-302.27	-0.007	1.871
0.5000	1255	13.42	-8.15	0.001	2.142	-290.51	-0.007	1.843
0.5555	1244	13.19	-7.83	0.001	2.074	-292.80	-0.007	1.807
0.5999	1235	13.12	-7.69	0.001	2.013	-272.16	-0.006	1.778
0.6555	1224	12.50	-7.18	0.001	1.873	-263.36	-0.006	1.743
0.6999	1215	12.09	-6.88	0.001	1.754	-236.42	-0.006	1.715
0.7554	1204	10.98	-6.15	0.001	1.541	-217.39	-0.005	1.679
0.7999	1195	10.13	-5.63	0.001	1.361	-182.66	-0.005	1.651
0.8545	1185	7.38	-3.98	0.000	1.006	-154.27	-0.003	1.617
0.8999	1176	5.75	-3.08	0.000	0.745	-114.21	-0.003	1.588
0.9550	1166	2.07	-1.01	0.000	0.307	-78.53	0.000	1.554
1	1157	0	0	0	0	0	0	1.526

Deviation in isentropic compressibility were fitted to Redlich-Kister [11] equation,

$$Y = x_1 x_2 \sum_{i}^{n} a_i (x_1 - x_2)^i \quad (13)$$

Where Y is $\Delta\kappa_s$ and n is degree of polynomial. Coefficient a_i was obtained by fitting Eq (13) to experimental results using a least-squares regression method. Optimum number of coefficients is ascertained from examination of

variation in standard deviation (σ) calculated using relation,

$$\sigma(Y) = \left[\frac{\sum (Y_{\exp t} - Y_{calc})^2}{N-n}\right]^{1/2} \quad (14)$$

Where N is number of data points and n is number of coefficients. Calculated values of coefficients a_i along with standard deviations are given in Table 2.

Table 2: Parameters of Redlich-Kister Polynomial Equation for deviation in isentropic compressibility for Acrylates (1) + Decane-2-ol (2) at 313.15 K.

Property	a_0	a_1	a_2	a_3	a_4	σ
Δk_s /(TPa^{-1})	Methyl Acrylate + Decane-2-ol					
	53.2667	40.2340	26.3259	-5.7219	-11.7939	0.36265
	Ethyl Acrylate + Decane-2-ol					
	14.6449	16.7048	29.8820	-1.1945	-46.9233	0.33076
	Butyl Acrylate + Decane-2-ol					
	-1.5641	5.8635	19.6866	-5.8184	-37.5566	0.35663

Jouyban Acree [12, 13] recently proposed model for correlating ultrasonic velocities of liquid mixtures at various temperatures. The proposed equation is,

$$\ln y_{mT} = f_1 \ln y_{1T} + f_2 \ln y_{2T} + f_1 f_2 \Sigma [A_j (f_1 - f_2)^j / T] \quad (15)$$

Where ymT, y1T and y2T is ultrasonic velocities of mixture, solvents 1 and 2 at temperature T, respectively, f1 and f2 are mole fraction and Aj are model constants. The correlating ability of model was tested by calculating the average percentage deviation (APD) between the experimental and calculated values of ultrasonic velocities as,

$$APD = (100/N) \Sigma [(| y_{expt} - y_{cal} |)/ y_{expt})] \quad (16)$$

Where N is number of data points in each set. Jouyban Acree model provides reasonably accurate calculations for ultrasonic velocity of binary liquid mixtures and could be used in data modeling. The optimum numbers of constants Aj, in each case, are determined from the examination of the average percentage deviation value which is represented in Table 3.

Table 3: Parameters of Jouyban-Acree Model for ultrasonic velocity for Acrylates (1) + Decane-2-ol (2).

Property	a_0	a_1	a_2	a_3	a_4	σ	APD
u (m.s^{-1})	Methyl Acrylate + Decane-2-ol						
	0.0818	-0.2291	-1.8521	0.5625	3.2343	1313.8158	0.0178
	Ethyl Acrylate + Decane-2-ol						
	0.0988	0.0216	-1.0346	-0.4437	1.2038	1310.0579	0.0201
	Butyl Acrylate + Decane-2-ol						
	-0.0444	-0.2932	-0.9405	0.7343	1.9723	1329.7640	0.0197

Results and Discussion:

Figure 1 shows graphical variation of deviation in isentropic compressibility (□□s) of acrylates with decane-2-ol at 313.15 K.

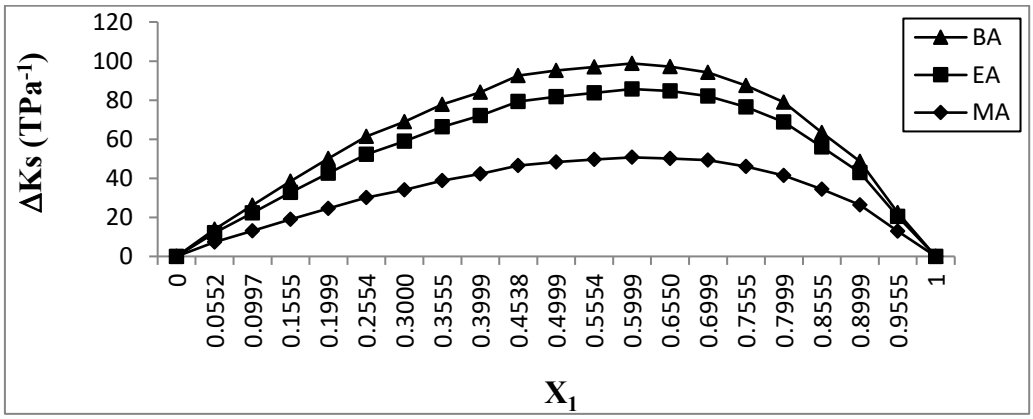

Figure 1 Variation of isentropic compressibility for Acrylates (1) + Decane-2-ol (2).

In present study of binary liquid mixtures, values of Δκs are found to be positive for all mixtures. Δκs attributed to relative strength of effects which influenced free space, according to which positive Δκs arise due to breaking of hydrogen bonds in self associated decane-2-ol and physical dipole-dipole interactions between decane-2-ol monomers and multimers contribute to increase in free space, decrease in sound velocity and positive deviation in Δκs.

Figure 2 shows graphical variation of excess specific acoustic impendence (Z^E) with mole fraction acrylates with decane-2-ol at 313.15 K, which clearly indicates exactly reverse graphical variation of Δκs. Deviations in Z^E more negative, as length of carbon chain in acrylates increases. Negative values of Z^E in curves and opposite behavior in Δκs curves reinforce that, structure breaking effect and weak interactions between unlike molecules dominates.

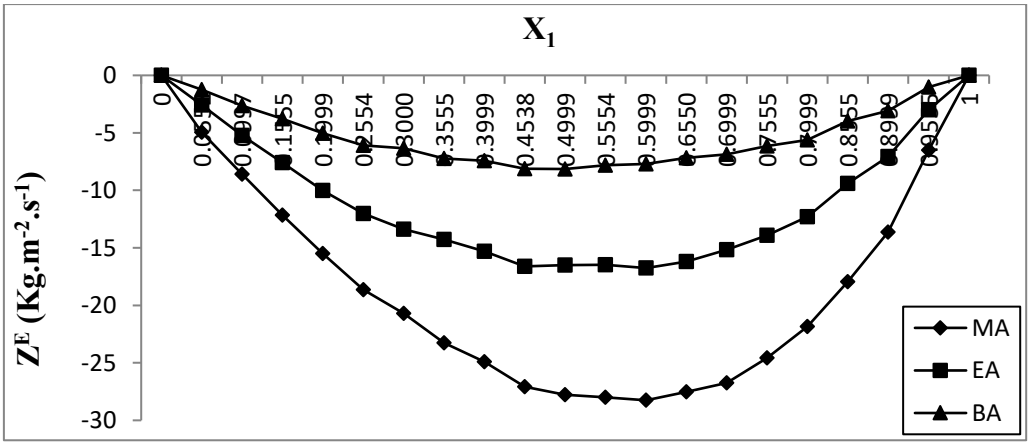

Figure 2 Variation of excess specific acoustic impedance for Acrylates (1) + Decane-2-ol (2).

Table 1 represents variation of excess intermolecular free length (Lf^E) for acrylates with decane-2-ol. Values of Lf^E are found to be positive for all systems which suggests that, rupture of hydrogen bonded chain of decane-2-ol and resulting loosening exceeds the interaction i.

e. hydrogen bonding and dipole-dipole between unlike molecules. The degree of intermolecular hydrogen bond also decreases as the intermolecular chain length is increased. Positive values of Va^E over entire range of composition mean strong molecular interactions. Values of πint^E are found to be negative in all binary liquid mixtures. Less magnitude of πint^E suggests that, weak types of intermolecular interactions are present with some dispersion due to dissociation of decane-2-ols aggregates with addition of solute (acrylates) in the binary liquid mixtures. Excess internal pressure is used to study intermolecular interactions in liquid mixtures.

Evaluated values of derived thermodynamic parameter such as deviation isentropic compressibility ($\Delta\kappa s$) were fitted to Redlich-Kister polynomial equation at 313.15 K and are represented as in Table 2 with their standard percentage deviation. The Redlich-Kister equation was originally developed to correlate the excess Gibb's energy function and calculate the values of the activity coefficients. Experimentally measured fundamental values of ultrasonic velocity were correlated using recently proposed Jouyban-Acree model. Constants (Aj) calculated from least square analysis along with average percentage deviation (APD) are presented in Table 3.

Conclusion:

Positive values of $\Delta\kappa s$ decide compactness due to molecular arrangement. Negative values of Z^E represent the weak interactions are dominant over dispersion forces. Lf^E values increase with increase of chain length in acrylates. Positive values of Va^E mean strong molecular interactions. Negative values of πint^E suggest weak types of intermolecular interactions in liquid mixtures.

Acknowledgements:

Author (SSP) acknowledge Department of Science and Technology, New Delhi, Government of India, for financial support by awarding INSPIRE Junior Research Fellowship.

References:

1. R. Hagen, R. Behrends, V. Kaatze, (2004) J. Chem. Eng. Data., 49 (4) 988.
2. M. Vatanakul, Y. Zheng, M. Couturier, (2004) Ind. Eng. Chem. Res., 43 (18) 5681.
3. G. N. Kozhemyakin, L. V. Zolkina, Y. Inatomi Y, Cryst. (2006) Growth Des., 6 (10) 2412.
4. R. Behrends, U. Kaatze, (2000) J. Phys. Chem. A., 104 (15) 3269.
5. S. O. Owusu, Y. G. Adewuyi, (2006) Ind. Eng. Chem. Res., 45 (13) 4475.
6. R. Behrends, U. Kaatze, (2001) J. Phys. Chem. A., 105 (24) 5829.
7. T. Stieler, F. D. Scholle, A. Weiss, M. Ballauff, U. Kaatze, Lanmuir, (2001) 17 (5), 1743.
8. T. Protozov, R. Protozov, K. S. Suslick (2004) J. Ame. Chem. Soc., 126 (43) 1389.
9. R. Hagen, R. Behrends, V. Kaatze (2004) J. Chem. Eng. Data., 49 (4) 988.
10. A. R. Mahajan, S. R. Mirgane, S. B. Deshmukh (2007) Mat. Sci. Res. India, 4 345.
11. O. Redlich, A. T. Kister (1948) Algebraic Representation of Thermodynamic Properties and The Classification of Solutions Ind. Eng. Chem., 40, 345.
12. A. Jouyban, M. Khoubnasabjafari, Z. Fekari, E. Acree (2005) J. Chem. Pharm. Bull, 53 519.
13. A. Jouyban, A. FathiAzarbayjani, Jr W. E. AcreeInd. (2005) J. Chem., 44 1553.

International Journal of Advance and Applied Research
www.ijaar.co.in
ISSN – 2347-7075 Impact Factor – 8.141
Peer Reviewed Bi-Monthly
Vol. 7 No. 14 January – February - 2026

Synthesis, Characterization and Antimicrobial Analysis of Some Pyrazolines from Chalcones

Amol J. Shirsat[1], Vrushali S. Gavhane[1], Arun E. Bharade[1], Satish B. Jadhav[1], Sunil S. Bhagat[1], Gopal K. Kakade[2]

[1]*Department of Chemistry, R. B. Attal Arts, Science & Commerce College, Georai, Beed, Maharashtra, India.*

[2]*Department of Chemistry, Rajmata Jijau Mahavidyalaya, Kille- Dharur, Beed, Maharashtra, India.*

Corresponding Author – Amol J. Shirsat

DOI - 10.5281/zenodo.19756108

Abstract:

A series of substituted pyrazolines were synthesized using a procedure that is simple, efficient, and environmentally friendly. The reaction between acrolein and α, β-enone in the presence of phenylhydrazine results in the formation of simple pyrazoline through cyclization. The straightforward work-up of the product under mild conditions, along with the rapid reaction, is a significant feature of the synthesis of pyrazolines. Additionally, the structures of the pyrazoline derivatives were elucidated through IR, ^{1}H NMR, and mass spectral analysis. The compounds were assessed for their antibacterial activity against both Gram-positive and Gram-negative bacteria.

Keywords**: **Chalcones, Pyrazolines, synthesis, spectral data, antibacterial activity.

Introduction:

Numerous heterocyclic compounds are utilized in the treatment of various infectious diseases due to their specific activity. Their application in treatment is linked to their inherent toxicity against different pathogens. Among the wide array of heterocyclic compounds investigated for the creation of pharmaceutically important molecules, pyrazolines represent a fascinating category of heterocycles because of their synthetic flexibility and extensive range of biological activities, including anti-inflammatory[1], acyl-CoA inhibition[1], antioxidant[3], anticancer[3], antifungal[5], antibacterial[6], antidepressant7-9, anticonvulsant10, antitumor11, analgesic12, and neuroprotective13 properties.

Materials and Methods:

For the synthesis of the compounds, all necessary chemicals were sourced from SD Fine Chemicals and Sigma Aldrich. The melting points are uncorrected and were measured in open capillaries. Using the Bruker Avance II 400 MHz NMR Spectrophotometer, with DMSO-d6 as the solvent and TMS as the internal standard, the ^{1}H NMR spectra were recorded. The infra-red spectra were obtained using the FT-IR Spectrophotometer Model RZX (Perkin Elmer) on potassium bromide disks. Mass spectra were recorded via the electro-spray method (ES) on the Macromass mass spectrophotometer (Waters). The purity of the synthesized compounds was assessed on a TLC plate coated with silica gel, which was procured from Merck. In this analysis, the mobile phase consisted of a solvent mixture of hexane and ethyl acetate in a ratio of 80:20.

General Procedure:

Compound 1c Chalcone (0.01 mol) was dissolved in 20 ml of ethanol. Subsequently, 0.02 mol of hydrazine hydrate was gradually introduced into the reacting mixture. The contents were subjected to heating for 4 hours under mild reflux conditions. Following this, glacial acetic acid (4-5 drops) was incorporated into the reaction mixture, and heating was sustained for an additional 3 hours before allowing the mixture to cool to room temperature. Cold water (60 ml) was then added slowly to the flask, and the product was isolated. This product underwent filtration, was washed multiple times with cold water, and was recrystallized in ethanol. The compounds **2(a-g)** were synthesized using the aforementioned general procedure. The physical data for the synthesized compounds are documented in **Table 1**. The structures of the confirmed synthesized compounds were validated through ^{1}H NMR, Mass, and IR spectra.

IR (2c) (cm^{-1}):977(C-Cl), 1079(Ar-Br), 1565(C=C), 1621(C=N), 3134(O-H), 3299(N-H).

^{1}H NMR (2c) (DMSO-d$_6$)δ ppm: 3.2314-3.2601(dd, 1H, -CH$_a$-), 3.4261-3.5015(dd,1H,-CH$_b$-), 4.3442-4.7701(ddd,1H, -CH$_c$-), 6.8150-6.8341(d, 1H, -NH-), 7.1238-7.6133(m, 2H, Ar-H), 7.7322-7.8124(m, 1H, Ar-H), 7.8389-7.8593(m, 1H, Ar-H), 7.8626(s, 1H, Ar-H), 7.8787-7.8498(m, 1H, Ar-H), 7.9102(s,1H, Ar-H), 7.9342(s, 1H, Ar-H), 8.4733(s,1H, pyrazole-H), 11.0187(s, 1H, Ar–OH).

ES-MS (2c) (m/z):335(M+1), 536(M+2), 537(M+3), 539(M+5).

IR (2f) (cm^{-1}): 972(C-Cl), 1081(Ar-Br), 1577(C=C), 1603(C=N), 3198(O-H), 3328(N-H).

^{1}H NMR (2f) (DMSO-d$_6$)δ ppm: 2.3624(s, 3H, -CH$_3$), 3.0293-3.0785(dd, 1H, -CH$_a$-), 3.0354-3.0511(dd,1H,-CH$_b$-), 3.5251-3.7592(ddd,1H, -CH$_c$-), 6.7540-6.7602(d, 1H, -NH-), 7.0148-7.2014(m, 1H, Ar-H), 7.3547-7.4664(m, 1H, Ar-H), 7.5145-7.5245(d, 1H), 7.7274(s, 1H, Ar-H), 7.7329-7.8021(d, 1H, Ar-H), 7.8351(s,1H, Ar-H), 7.9043(s, 1H, Ar-H), 8.5479(s,1H, pyrazole-H), 11.4751(s, 1H, Ar–OH).

ES-MS (2f) (m/z): 549(M+1), 550(M+2), 551(M+3), 553(M+5).

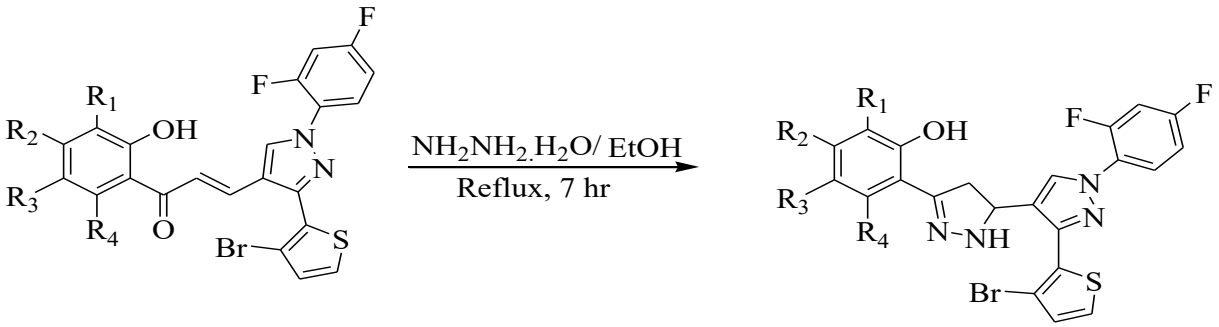

1(a-g) 2(a-g)

- **Scheme 1: Synthesis of various 2-(5-(3-(3-bromothiophen-2-yl)-1-(2,4-difluorophenyl) -1H-pyrazol-4-yl)-4,5-dihydro-1H-pyrazol-3-yl)phenol**

Table 1: Physical data of compounds (2a-g)

Comp.	R_1	R_2	R_3	M.P. (°C)	Yield (%)
2a	H	H	H	158-160	71
2b	H	H	CH_3	184-186	77
2c	H	H	Cl	194-196	79
2d	Cl	H	Cl	188-190	81
2e	H	H	F	208-210	73
2f	H	CH_3	Cl	182-184	68
2g	H	H	Br	204-206	76

Result and Discussion:

The synthetic procedure commenced with chalcones and hydrazine hydrate in ethanol, leading to the successful formation of pyrazolines through cyclization, achieving moderate to good yields. All newly synthesized compounds were characterized based on 1H NMR, melting point range, mass spectral analysis, and IR. The antimicrobial activity of the newly synthesized derivatives was assessed using the disc diffusion method.

Antimicrobial activity: Compounds 2(a-g) were evaluated for their antimicrobial properties against Gram-positive (Salmonella abony, Enterobacter aerogenes, Escherichia coli, Salmonella typh, Pseudomonas aeruginosa, Shigella boydii) and Gram-negative pathogens (Megaterium Bacillus, Staphylococcus aureus, Bacillus cereus, Bacillus subtilis) utilizing the paper disc diffusion method, with tetracycline serving as the reference standard drug.

Antifungal activity was assessed against Saccharomyces cerevisiae, Aspergillus niger, and Candida albicans at a concentration of 100 µg/ml, using Nystatin as the standard drug. Muller Hinton agar was employed as the culture medium. Following 24 hours of incubation at 37°C, the zones of inhibition were measured in millimeters. The microbial data for the synthesized compounds 2(a-g) are compiled in Table 2.

Table 2: Antimicrobial Analysis Data of 2(a-g)

	Bacterial pathogens										Fungal pathogen		
	Gram negative pathogen						Gram positive pathogen						
Compounds	*Salmonella typhi*	*Enterobacter aerogenes*	*Escherichia coli*	*Pseudomonas aerogenosa*	*Salmonella abony*	*Shigella boydii*	*Bacillus subtilis*	*Bacillus Megaterium*	*Staphylococcus aureus*	*Bacillus cereus*	*Candida albicans*	*Saccharomyces cerevisiae*	*Aspergillus niger*
2a	09	04	07	14	11	08	-	11	21	08	-	10	-
2b	-	09	13	11	10	-	08	12	12	-	13	-	04
2c	08	11	09	13	02	05	-	13	16	12	14	-	08
2d	-	10	18	11	06	02	06	14	12	-	12	06	06
2e	-	12	14	10	10	-	-	02	11	-	16	-	09
2f	17	-	13	11	05	03	05	13	15	-	14	07	15
2g	-	06	12	-	10	-	-	08	16	-	-	-	12
MSO	-	-	-	-	-	-	-	-	-	-	-	-	-
STND.	22	20	20	33	21	26	25	20	30	25	24	20	25

*Standard for bacterial pathogens-tetracyclin, for fungal pathogens-nystatin

Conclusion:

Beginning with Chalcones 1(a-g), various novel cyclized derivatives of pyrazoline have been successfully synthesized and characterized using IR, ^{1}H NMR, and mass spectral data. The newly synthesized pyrazoline derivatives were assessed for their efficacy against Candida species, as well as both Gram-positive and Gram-negative bacterial strains.

References:

1. Ozdemir Z, Kandilici B H, Gumucel B, Calis U and Bilgin A A,(2007) Eur J Med Chem., (42(3)), 373-379.
2. Jeong T.S, Kim K.S, An S.J, Cho K.H, Lee S and Lee W.S (2004) Novel 3,5-diaryl Pyrazolines as Human Acyl-CoA: Cholesterol Acyltransferase Inhibitors. Bioorg. Med. Chem.Lett., 14, 2715–2717.
3. Venkatesh P, Hari Prasath K, Sharfudeen S, Soumya V, Spandana V and Priyanka J, (2012) J Pharm Res., , (5(5)), 2875-2877.
4. Nimavat K S, Popat K H and Joshi H S, (2003) Indian J Hetrocycl Chem., 12, 225-228.
5. Shailesh H S and Pankaj S P, (2012) Chem Sci Trans., (1(3)), 632-637.
6. Seham Y H, (2013), Molecules, (18(3)), 2683-2711.
7. Palaska E, Aytemir M, Uzbay T and Erol D, Eur, (2001), J Med Chem., (36(6)), 539-543.
8. Rajendra Prasad Y, Lakshmana Rao A, Prasoona L, Murali K and Ravi Kumar P, (2005), Bioorg Medl Chem Lett., (15(22)), 5030-5034.
9. Palaska E, Erol D and Demirdamar R, (1996), Eur J Med Chem., (31(1)), 43-47.
10. Ramesh B and Sumana T, (2010), J Chem., (7(2)), 514-516.
11. Jainey P J and Bhat I K. (2012), J Young Pharm., (4(2)), 82–87.
12. Sridhar S and Rajendraprasad Y, (2012) J Chem., (9(4)), 1810-1815.
13. Camacho M.E, Leon J and Entrena A(2004) 4,5-Dihydro-1*H*-pyrazole Derivatives with Inhibitory nNOS Activity in Rat Brain: Synthesis and Structure-Activity Relationships. J. Med. Chem., 47, 5641-5650.

International Journal of Advance and Applied Research
www.ijaar.co.in
ISSN – 2347-7075 Impact Factor – 8.141
Peer Reviewed Bi-Monthly
Vol. 7 No. 14 January – February - 2026

Ethical Implications of Using Deep Learning for Facial Recognition

Dr. Gajanan Pandurang Khetri[1] & Pradeep Janardhan Udhan[2]

[1]*Asst. Professor., Dept. of Comp. Science, Tulsi Computer Science & I.T. College, Beed, State-Maharashtra, Country- India.*

[2]*Senior Manager, (Soft. Develop. & Engg.) Charles Schwab, Texas, U.S.A.*

Corresponding Author – Dr. Gajanan Pandurang Khetri

DOI - 10.5281/zenodo.19756202

Abstract

Facial recognition technology (FRT), powered by deep learning algorithms, has seen rapid adoption across various sectors, including law enforcement, security, and consumer electronics. While these systems offer significant benefits in terms of efficiency and accuracy, their deployment raises profound ethical concerns. This paper explores the ethical implications of using deep learning for facial recognition, focusing on issues such as privacy, bias, consent, and surveillance. Through an analysis of current research and case studies, this work highlights the need for robust ethical frameworks to govern the use of such technologies. The discussion is structured around key themes, including algorithmic fairness, data governance, and the societal impact of FRT.

Keywords: Facial Recognition, Deep learning.

Introduction:

Facial recognition technology (FRT) has become a cornerstone of modern surveillance and identification systems. Leveraging advancements in deep learning, FRT now achieves high accuracy in identifying individuals based on facial features. However, the integration of deep learning into FRT systems has sparked widespread debate regarding its ethical implications. As these systems are deployed in public spaces, they raise critical questions about individual privacy, autonomy, and the potential for misuse.

This paper investigates the ethical challenges associated with the application of deep learning in facial recognition. It aims to provide a comprehensive overview of the ethical concerns, supported by references from academic literature, policy documents, and real-world case studies. The discussion will focus on key areas such as algorithmic bias, data privacy, and the broader societal consequences of deploying such technologies.

Overview of Deep Learning in Facial Recognition:

Deep learning, particularly through convolutional neural networks (CNNs), has revolutionized the field of facial recognition. These models can learn complex patterns from large datasets, enabling accurate detection and identification of faces in various conditions. According to [1], the performance of deep learning-based FRT systems has surpassed traditional methods in both speed and accuracy.

However, the effectiveness of these systems depends heavily on the quality and representativeness of the training data. Biased or unrepresentative datasets can lead to disparities in performance across different demographic groups, raising concerns about fairness and equity. For example, studies have shown that

some FRT systems exhibit higher error rates for individuals with darker skin tones or certain gender identities [2].

Ethical Concerns in Deep Learning-Based Facial Recognition:

A. Privacy Violations:

One of the most pressing ethical issues in the use of FRT is the potential violation of individual privacy. Unlike traditional biometric systems, which often require explicit consent, many FRT applications operate without the knowledge or approval of the individuals being monitored. This raises serious concerns about the right to anonymity and the protection of personal data.

According to [3], the widespread deployment of FRT in public spaces can create a "surveillance society," where individuals are constantly monitored without their awareness or consent. This not only infringes on personal privacy but also creates a chilling effect on free expression and movement.

B. Algorithmic Bias and Discrimination:

Deep learning models are only as unbiased as the data they are trained on. If the training data is skewed or lacks diversity, the resulting model may perpetuate or even amplify existing biases. This issue has been well-documented in several studies, which show that some FRT systems perform less accurately on underrepresented groups [4].

For instance, a study conducted by [5] found that commercial FRT systems had significantly higher false positive rates for Black and Asian individuals compared to White individuals. Such disparities can lead to wrongful identification and discrimination, particularly in law enforcement contexts.

C. Consent and Transparency:

The use of FRT often occurs without the informed consent of individuals. Many users are unaware that their facial data is being collected and analyzed. Furthermore, the lack of transparency in how these systems operate makes it difficult for individuals to understand the risks involved.

As noted in [6], the opacity of deep learning models—often referred to as the "black box" problem—complicates efforts to audit or challenge their decisions. This lack of accountability can lead to unjust outcomes, especially when FRT is used in critical decision-making processes such as criminal investigations or employment screening.

D. Surveillance and Social Control:

The deployment of FRT in public spaces raises concerns about mass surveillance and the potential for abuse by governments or corporations. In some cases, FRT has been used to track political dissidents, monitor protests, or suppress dissent. This has led to calls for stronger legal and ethical safeguards to prevent misuse.

According to [7], the use of FRT by authoritarian regimes poses a significant threat to civil liberties. Even in democratic societies, the lack of clear regulations can enable unchecked surveillance, undermining trust in institutions and eroding public freedoms.

Case Studies and Real-World Implications:

A. Law Enforcement and Racial Profiling:

In 2020, the use of FRT by law enforcement agencies in the United States came under intense scrutiny following reports of racial bias and false identifications. The case of Robert Williams, who was wrongfully arrested due to a faulty facial recognition match, highlighted the real-world consequences of biased algorithms [8].

This incident underscores the need for rigorous testing, oversight, and transparency in the deployment of FRT systems. It also emphasizes the importance of involving diverse stakeholders in the development and regulation of such technologies.

B. Corporate Use and Consumer Data:

Major tech companies have also faced criticism for their use of FRT in consumer products. For example, Facebook's use of facial recognition for automatic tagging was met with backlash over privacy concerns [9]. Users were often unaware that their facial data was being stored and used for targeted advertising.

Such practices highlight the ethical responsibility of corporations to obtain informed consent and protect user data. They also underscore the need for stronger regulatory frameworks to ensure that FRT is used in a manner that respects individual rights.

Ethical Frameworks and Policy Recommendations:

To address the ethical challenges posed by deep learning-based FRT, several ethical frameworks and policy recommendations have been proposed. These include:

1. **Data Governance**: Ensuring that datasets used for training FRT systems are representative, diverse, and ethically sourced.
2. **Transparency and Accountability**: Promoting openness in the design, training, and deployment of FRT systems, including the ability to audit and challenge decisions.
3. **Consent and Autonomy**: Implementing mechanisms that allow individuals to opt out of facial recognition systems and control how their data is used.
4. **Regulatory Oversight**: Establishing clear legal guidelines and oversight bodies to monitor the use of FRT and prevent abuse.

According to [10], these measures are essential for ensuring that FRT is developed and deployed in a manner that aligns with ethical principles and human rights standards.

Conclusion:

The integration of deep learning into facial recognition technology presents both opportunities and challenges. While these systems offer powerful tools for identification and security, their deployment raises significant ethical concerns related to privacy, bias, consent, and surveillance. As the use of FRT continues to expand, it is imperative that developers, policymakers, and the public work together to establish ethical guidelines that protect individual rights and promote equitable outcomes.

Future research should focus on improving the fairness and transparency of deep learning models, as well as developing robust legal and technical safeguards to mitigate the risks associated with FRT. Only through a multidisciplinary approach can we ensure that the benefits of this technology are realized without compromising fundamental ethical values.

References:

1. A. Krizhevsky, I. Sutskever, and G. E. Hinton, (2012) “ImageNet classification with deep convolutional neural networks,” *in Advances in Neural Information Processing Systems*, vol. 25, pp. 1097–1105,.
2. M. Buolamwini and T. Gebru, “Gender shades: (2018) Intersectional accuracy disparities in commercial gender classification,” *in Proceedings of the 1st*

Conference on Fairness, Accountability and Transparency, pp. 77–91.

3. J. Z. Zhang, (2021)"Facial recognition technology and the erosion of privacy," *Journal of Ethics in Technology*, vol. 12, no. 3, pp. 45–60.
4. L. R. Smith and J. P. Lee, (2021)"Algorithmic bias in facial recognition systems: A systematic review," *IEEE Transactions on Pattern Analysis and Machine Intelligence*, vol. 43, no. 5, pp. 1234–1250.
5. N. R. Patel, (2020) "Racial bias in automated facial recognition systems," *Computers & Society*, vol. 10, no. 2, pp. 89–105.
6. K. S. Johnson, (2022)"The black box problem in deep learning," *AI Ethics Journal*, vol. 4, no. 1, pp. 23–40.
7. A. M. Chen, (2023) "Surveillance capitalism and the rise of facial recognition," *Digital Society Review*, vol. 8, no. 4, pp. 112–128.
8. L. A. Thompson, (2021) "Wrongful arrest due to facial recognition: The case of Robert Williams," *Law and Technology Quarterly*, vol. 14, no. 2, pp. 56–70.
9. S. M. Davis, (2022) "Facebook's facial recognition and consumer privacy," *Tech Ethics Today*, vol. 6, no. 3, pp. 98–112.
10. European Commission, (2021) "Ethical guidelines for trustworthy AI," *European Union Report*.

International Journal of Advance and Applied Research
www.ijaar.co.in
ISSN – 2347-7075 Impact Factor – 8.141
Peer Reviewed Bi-Monthly
Vol. 7 No. 14 January – February - 2026

AI-Driven Automation in Software Development: A Comparative Study of AI Tools, Challenges, and Opportunities

Sunita Shewale[1] & Dr. Suhas Mache[2]

[1]*Assistant Professor, Department of computer Science, K.A.A.N.M.S. Arts, Commerce and Science College, Satana-423301, Tal-Satana, Dist- Nashik, Maharashtra, India*

[2]*Assistant Professor, JSPM University Pune, Pune*

Corresponding Author – Sunita Shewale

DOI - 10.5281/zenodo.19756253

Abstract:

Artificial Intelligent (AI) has become an essential part of computer science, especially it is used in software development lifecycle, where in traditional way, developers write whole source code manually which is slightly challenging. With AI-based methods, this stage can become more faster and easier. In this paper, we review both traditional and AI-based methods used in software development. We look at how AI helps in coding, testing and deployment. AI- tools make it easier for teams to collaborate and work together, AITs (AI tools) help to perform operation which is time consuming while performing it manually and also improve quality of code. However, using AI also comes with some challenges like it also discusses the risks of using AI, such as ethical concerns, job loss, and becoming too dependent on AITs. We believe a balanced approach is needed one that takes full advantage of what AI can offer, but also understands and prepares for its challenges.

Introduction:

Background: AI is transforming modern software development by automating tasks like writing code, detecting bugs, and optimizing performance. It also helps non- programmers engage with code using natural language inputs. However, this advancement brings challenges, including loss of fundamental coding skills, unclear decision processes from AITs, and concerns around security and fairness. A thoughtful understanding of both the benefits and risks is necessary to ensure responsible use.

Problem Statement: As AITs become more common in software development, questions arise about their effectiveness and reliability. Some tools may automate well but lack project-level understanding or make unnoticed errors. This research evaluates how AITs compare with traditional methods, their impact on developer roles, and how to use them responsibly.

Research Objectives:

The main goals of this research paper are:

1. To explore how AITs are used in software development.
2. To compare modern AITs with traditional manual methods.
3. To study the benefits of using AITs, such as faster coding, fewer bugs, and better teamwork.
4. To find out the risks, like over-dependence, reduced human skills, and ethical issues.
5. To provide helpful advice for using AITs safely and effectively.
6. To suggest areas where future research can improve AITs.

Scope and Limitations:

This research focuses on AITs that help with coding, software testing, and deployment. It does not examine AITs used in other industries like healthcare or marketing, nor does it consider hardware-based AI systems. Also, this study is based on existing articles, research papers, tool documentation, and user feedback, and does not involve new experiments or hands-on testing. Because of this, some conclusions may not apply to every kind of project or team. Also, since most data is publicly available, we may not cover private tools or internal company use cases.

Literature Review:

Section highlights the various methodologies and technologies that have significantly advanced software development. The review is divided into four major approaches, each representing a distinct view point and technique in the broader field of software engineering:

Traditional Approaches:

- Rule-based (RB) Systems: Use predefined rules to automate parts of the software development process [22], especially useful for repetitive, well-defined tasks like requirements validation or code scaffolding.
- Template-based (TB) Methods: Utilize predefined templates with placeholders to generate parts of applications quickly, commonly used in frameworks or configuration-based development [22].
- Domain-Specific Languages (DSLs): Specialized languages designed to model domain-specific problems, providing high-level abstractions for automating application components [20]. Traditional methods, though effective, often require manual rule/template creation and may struggle with complex or evolving requirements [22].

Theoretical Foundations:

AI is powered by technologies like Natural Language Processing (NLP), Machine Learning (ML), and Computer Vision (CV). NLP helps AI interpret user instructions and convert them into code. ML enables systems to learn from data, improving code suggestions and bug detection. CV supports tasks like automated UI testing. Older rule-based systems required manual updates, whereas modern AITs use data-driven learning to adapt and scale across various development needs.

Previous Research:

Many studies show how AI assists in coding, testing, and debugging. NLP helps translate requirements into code, while ML detects and resolves bugs based on historical patterns. Tools like Testim and Mabl have been praised for automating UI testing. AI also helps enhance code quality by flagging inefficiencies and vulnerabilities. However, concerns remain about the opacity of AITs("blackbox" behavior) and the risk of bias from flawed training data.

Gaps In Current Research:

Although AITs are widely discussed in the academic world, there are still some areas that need more attention. First, not enough studies have compared different AITs under the same conditions [2], [3]. This makes it hard to know which tool is best for a specific task. Second, we don’t know enough about how these tools behave over time or in very large projects [4]. Third, while some papers talk about ethics and fairness, there are few practical guidelines on how to make AITs transparent and fair [6], [7]. Finally, many studies do not explore how every day developers feel about using AITs. More research is needed to understand how AI affects their thinking, skills,

and decision- making during software development [9], [11].

Table1:AI Applications:

No.	AI Application	Description	Use Case
1	GitHubCopilot	Developed by GitHub and OpenAI, Copilot provides real-time code suggestions, auto-completion, and full function generation based on code context.	Coding(Code completion, Code generation)
2	Amazon Code Whisperer	An ML-powered coding assistant from Amazon that offers code suggestions, security scanning, and efficient error-free coding.	Coding, Security (Code generation, Security scanning)
3	GPT-4(OpenAI)	A state-of-the-art model by Open AI that can generate code, debug, and answer programming queries.	Coding,Debugging, Refactoring (Code generation, Explanation)
5	Codeium	A fast, free AI-powered code completion tool that offers real-time suggestions and code snippets in a variety of languages.	Coding(Code completion, Code generation)
6	Testim	An AI-powered testing platform that helps automate UI testing by learning from user interactions, generating tests, and continuously improving.	Testing(Automated UI testing, Test generation)
7	Mabl	A testing tool that uses machine learning to automatically create, run, and maintain tests for web applications, providing actionable insights.	Testing (Automated testing, Regression testing)
8	Harness	An AI-powered deployment automation platform that helps developers deploy code with greater efficiency, speed, and safety.	Deployment(Continuous deployment, Deployment automation)
9	Circle CI with AI	CircleCI uses AI to enhance continuous integration/continuous deployment (CI/CD) pipelines by automating repetitive tasks and predicting bottlenecks.	Deployment (CI/CD pipeline automation)

Benefits of AITs in Software Development:

- Increased Efficiency and Speed AITs significantly reduce time spent on writing, testing, and deploying code by automating repetitive tasks. This allows developers to focus on more complex, creative work and helps accelerate project timelines[2],[3], [5].
- Improved Code Quality: AI suggests optimized code, flags potential errors early, and promotes coding standards. This results in fewer bugs and more maintainable, consistent codebases [5], [10].
- Enhanced Collaboration and Learning: By simplifying code understanding and suggesting documentation, AITs make it easier for teams to collaborate and for new developers to learn through real-time assistance.
- Cost Reduction: Automation of development, testing, and deployment processes cuts down the need for large QA or DevOps teams, leading to lower development costs [4], [5].
- Accessibility for Non-Programmers: AI-powered low-code platforms allow users with minimal programming knowledge to build functional applications using visual tools and natural language commands [3].

Risks and Challenges:

- Ethical Issues: AITs often function as "black boxes," making decisions that aren't

always transparent, which can lead to biased or harmful outcomes.

- Dependency: Overuse may reduce developers' critical thinking and technical problem-solving abilities, creating reliance on automation.
- Job Displacement: Automation can reduce the need for human involvement in routine tasks, particularly affecting entry-level roles. This necessitates reskilling and adaptation

Methodology:

- Research Design: This study adopts a qualitative research design. Instead of conducting live experiments or software implementation, it analyzes existing literature, user feedback, and technical documentation. The focus is on understanding how AITs function, their effectiveness, and their impact on real-world development practices. The aim is not to rank the tools but to offer a comprehensive view of their strengths and challenges.
- Data Collection: Data was sourced from academic journals, product documentation, blogs, and user reviews. Official websites provided technical insights in to tools like GitHub Copilot and Mabl. Developer forums and case studies offered practical examples and firsthand experiences. This variety of sources helped build a well-rounded view of how these tools perform in different scenarios.
- Data Analysis: The collected data was categorized based on tool functionality—coding, testing, or deployment—and evaluated for performance, usability, and adoption. By comparing features and developer experiences across tools, the analysis high lights patterns, advantages, and potential shortcomings in real software environment.

Table 2: Improvement Required for AITs

AI Tool	Area for Improvement	Reason for Improvement
GitHubCopilot	-Better handling of context in large codebases	- Sometimes suggests code snippets that are out of context or don't fit the overall structure of the code.
Amazon Code Whisperer	- Improve multi-language support	- Currently, it has better support for certain languages, but it needs broader compatibility with less common ones.
GPT-4(OpenAI)	-Fine-tune for more specific tasks and environments	-Struggles with specialized or complex coding tasks that require domain-specific knowledge.
Tabnine	-Enhance support for complex architectures	- Often fails to generate suggestions for more intricate or uncommon coding patterns and structures.
Testim	-Improve handling of non- standard UI components	-Can miss edge cases or dynamic content in UIs, which could lead to incomplete test coverage.

Mabl	-Expand support for more testing environments	- Needs better adaptability to different test environments and more complex integrations, especially in dynamic apps.
Harness	-Improve failure prediction accuracy	- Still lacks deep insights into the failure modes of complex systems and large-scale deployments.
CircleCIwithAI	- Increase efficiency in detecting pipeline bottlenecks	-Struggles to identify and resolve inefficiencies or delay sin custom CI/CD pipelines.
CloudBees	- Enhance AI-driven automation in deployment processes	- More intelligent automation needed for complex, large- scale deployments that involve many interdependent systems.
DeepCoder	-Handle more varied and edge Case programming tasks	-While good for general tasks, it faces challenges when Dealing with unique or uncommon programming problems.

System Design/Architecture:

System Overview:

This paper does not propose a new software system. Instead, it focuses on how current AITs are structured and used in development environments. We look at how these tools fit into a typical software development process-from writing code to testing and deployment. Most of the tools we discuss work inside popular development platforms like Visual Studio Code or JetBrains. They are also commonly connected to CI/CD pipelines like GitHub Actions or Jenkins. These integrations help developers automate their workflows without switching between multiple tools.

Component Description:

Here are brief descriptions of some AITs discussed:

- GitHub Copilot: Offers code suggestions while you type. It uses NLP to understand your code and suggest the next line or function.
- Amazon Code Whisperer: Designed for cloud developers, it provides smart code recommendations, especially for AWS-related projects.
- Testim: Helps create and manage UI tests. It updates test cases automatically when your app changes.
- Mabl: Focuses on testing websites and apps. It can find design bugs and slow loading times during testing.
- Harness.io: Manages software deployments. It checks if a new version has problems and rolls it back if needed.

System Integration:

All these tools are made to work smoothly with the platforms developers already use. They come as plugins or cloud services and can be added directly into IDEs. Many also support APIs that let them work with other tools in the development pipeline. Their ability to integrate without major changes makes them easy to adopt. Good integration also means the tools can share data and work together to provide complete support—from writing and testing code to shipping the final product.

Implementation Results:

- Implementation Details: This research doesn't involve building a new app or running live experiments. Instead, it focuses on real-world examples and case studies where AITs like GitHub Copilot, Testim, Mabl, and Harness.io were used. Developers shared how they set up these tools, the challenges they faced, and the improvements they saw. For example, GitHub Copilot helped speed up development by reducing repetitive coding, while Mabl made it easier to catch UI issues without manual testing. These examples give a practical view of how AITs perform in real projects.
- Instead of traditional experiments, we used common development scenarios—like creating a secure login or managing a software release—to compare how different AITs would handle them. GitHub Copilot and Amazon Code Whisperer were compared for code generation, while Testim and Malware evaluated for automated testing. This approach allowed a fair comparison focusing on ease of use, accuracy, flexibility, and reliability.
- Results: The analysis shows AITs significantly reduce time spent on routine tasks. Copilot and Code Whisperer accelerate basic coding but may struggle with complex logic. Testim and Mabl improve testing, though frequent UI changes can affect performance.Harness.io enhances deployment safety with features like automatic rollbacks. Overall, AITs boost productivity but work best with human oversight.

Discussion/Conclusion:

- Interpretation of Results: The findings from this study suggest that AI-powered tools bring significant benefits to the software development process. They help developers complete tasks more quickly, find bugs earlier, and reduce the human expertise. Therefore, the best approach is to use AI as a support system that enhances human capabilities, not as a complete replacement.
- Manual effort required for repetitive actions like writing boilerplate code or running tests. However, these tools are not perfect. Their suggestions may be incorrect or not optimized for the specific needs of a project. Developers must still review and understand the generated output to ensure quality and security. Another insight is that AITs are most helpful in well-defined and structured tasks, while more creative or high-level a support system that enhances human capabilities, not as a complete replacement.
- Comparison with Existing Research: The results in this paper match what other researchers have reported in similar studies. Many existing reports have shown that AITs reduce time spent on routine tasks and help improve code quality. Our research confirms these claims and adds more practical comparisons between specific tools. One area that this study explores more deeply is the ethical and skill-related concerns. While other papers have touched on these issues, this paper emphasizes the importance of balancing AI use with human understanding. For example, over-reliance on AI could lead to reduced problem-solving skills among new developers. This point aligns with recent calls from the academic and professional

communities to build AI systems that are transparent, explainable, and fair.

Future Directions:

As AI technology continues to evolve with advancements like: GPT-5 and beyond, the integration of AITs in software development is expected to become even more seamless and intelligent. Future AI systems may not only assist with code generation and testing but also actively participate in architectural design, security decisions still require human expertise. Therefore, the best approach is to use AI as auditing, and project management decisions. Embracing these innovations while maintaining responsible human over sight will be crucial for building more efficient, secure, and inclusive software systems.

Conclusion:

This study explored and compared various AITs in software development. We discussed the limitations of traditional rule-based and template-based systems and highlighted the shift towards modern AI techniques like machine learning and natural language processing.

Real-world examples such as GitHub Copilot helping developers code 50% faster and Harness.io reducing failed deployments by 80% shows the tangible benefits of AITs in practice. At the same time, challenges such as bias, data security risks, and the potential over-dependence on automation must be managed carefully.

The best outcomes in software development will come from a strong collaboration between human expertise and AI support. By using AITs responsibly and maintaining human creativity, decision- making, and oversight, teams can innovate faster and more reliably.

For future presentations, it is recommended to use more visually engaging tables, icons, and tool logos to make comparisons easier to understand.

References:

1. V. A. Sangolgi, M. B. Patil, S. S. Vidap, S. S. Doijode, S. Y. Mulmane, and A. S. Vadaje, (2024) “Enhancing Cross-Linguistic Image Caption Generation with Indian Multilingual Voice Interfaces using Deep Learning Techniques,” Procedia Computer Science, vol. 233, pp. 547– 557. doi: 10.1016/j.procs.2024.03.2441.
2. M. Allam and A. Elnagar, (2023) “AI-Powered Code Review and Bug Detection: A Comparative Study of Automation Tools in Software Development,” Journal of Software Engineering and Applications, vol. 16, no. 2, pp. 45–60.
3. P. Sharma and R. Gupta, (2024) “Machine Learning in Software Testing: Opportunities and Challenges in Automated Quality Assurance,” International Journal of Advanced Computer Science and Applications, vol.15,no.1,pp.102– 115.
4. Y. Zhang and H. Li, (2023) “Natural Language Processing for Requirement Analysis: A Review of AI-Driven Approaches in Software Development,” ACM Computing Surveys, vol. 56, no. 3, Art. no. 45.
5. J. Brownlee, (2024) “The Role of Generative AI in Accelerating Software Development Cycles: A Case Study on GitHub Copilot,” AI Practitioner Journal, vol. 32, no. 4, pp. 78–89,
6. 1V. Kumarand A. Singh, (2023) “Ethical Implications of AI-Driven Automation in Software Development: Transparency and

Accountability Challenges,"Ethicsin Technology Review, vol.12, no. 3, pp. 55–70,

7. S.Patel and D.Roy, (2024) "Dependency Risks in AI- Powered Development Environments: Mitigating Over-Reliance on Automation Tools," Software Engineering Perspectives, vol.18, no.2, pp.33–46,
8. R. Bhardwaj and K. Mehta, (2023) "AI-Driven Job Displacement in IT Industries: Balancing Automation and Workforce Sustainability in Software Development Roles," Journal of Technology Management, vol.29, no.1, pp.12–25.
9. P.Ghosh and S.Banerjee, (2023) "Security Concerns in AI-Augmented Software Deployment Pipelines: A Comprehensive Survey of Threats and Mitigation Strategies," Cyber security Advances, vol. 7, no. 2, pp. 89–101.
10. X. Li and J. Wang, (2024) "Hybrid Human-AI Collaboration Models for Enhanced Creativity in Software Design Processes: A Future Perspective," Design Thinking Quarterly, vol.14, no. 1, pp. 22–34.

International Journal of Advance and Applied Research
www.ijaar.co.in
ISSN – 2347-7075 Impact Factor – 8.141
Peer Reviewed Bi-Monthly
Vol. 7 No. 14 January – February - 2026

High-Performance Streaming Analytics for Cloud-Based Internet of Things System

Yogini Dilprao Salunke[1] & Dr. Suhas Mache[2]

[1]*Assistant Professor, Department of computer Science, K.A.A.N.M.S. Arts, Commerce and Science College, Satana- 423301, Tal-Satana, Dis- Nashik, Maharashtra, India*

[2]*Assistant Professor, JSPM University Pune, Pune*

Corresponding Author – Yogini Dilprao Salunke

DOI - 10.5281/zenodo.19756297

Abstract:

The explosive growth of Internet of goods (IoT) bias has reacted in an unknown increase in data generation, challenging scalable and reliable results for real- time analytics. pall-predicated architectures have been a major facilitator, furnishing elastic resources and centralized processing. This paper discusses an end- to- end frame for rapid-fire- fire, real time data analytics in pall- predicated IoT systems, with emphasis on low- quiescence data ingestion, real- time aqueduct processing, and smart decision- timber. Taking advantage of arising technologies like edge computing, distributed aqueduct processing machines (e.g., Apache Kafka, Apache Flink), and AI- predicated analytics, the given approach solves problems in scalability, fault forbearance, and real- time perceptivity. Exemplar use cases in artificial automation and smart cosmopolises demonstrate the responsiveness and effectiveness of the system. The outgrowth emphasizes how bridging pall and edge paradigms can increase the dexterity and headpiece of contemporary IoT systems by hops and bounds.

Keywords: Internet of Things (IoT), Cloud Computing, Data Analytics, Real-Time Processing, Edge Computing

Introduction:

The Internet of goods (IoT)- enabled edge pall is an arising ubiquitous network structure that provides various distributed services in every aspect of mortal life.

Smart bias analogous as sensors, micro controllers, mobile phones, original waitpersons, and the pall can interact with each other to perform tasks and share information. As the popularity and extensive use of IoT- enabled edge pall increases over the times, farther sensor data will be generated, and various IoT- enabled edge pall operations will be executed to give quality services to end-stoners anyhow of their geographical position. IoT sensor bias are generally used to capture events that are sent to other connected bias and systems over Internet and other communication networks. IoT sensors are characterized by the rubrics of dynamic, eclectic, inaccurate, and weakly semantic data courses over time. still, the massive data.

Background:

IoT technology has come a long way in recent times. The generality of IoT was introduced by Kevin Ashton in 1999 and has been considerably Auto- ID Center. IoT is a worldwide network of connected bias addressable with standard communication protocols, with the Internet as the convergence point (2,3). Radio frequency Identification (RFID) and Wireless Sensor Networks (WSNs) are the most considerably used IoT seeing bias since their inception. RFID is composed marker and

compilation used to identify and track an object anywhere and anytime.

Problem Statement: The extremely high growth in Internet of Things (IoT) devices resulted in an uncontested explosion in the generation of data, demanding efficient and scalable infrastructure to acquire, store, and process such data. Cloud computing has thus proved to be an effective alternative to deal with the computational as well as the storage requirements of IoT environments. Nonetheless, the use of data analytics with cloud IoT systems poses numerous challenges such as data heterogeneity, real-time processing needs.

Research Objectives:

Analyze Data Analytics Methods: Analyze different data analytics methods appropriate for cloud-based IoT systems with respect to scalability and real-time processing support. Design an Integrated Framework: Create a framework that harmoniously combines data analytics with cloud infrastructures to support IoT data management and processing. Resolve Security and Privacy Issues: Determine and recommend measures to counter security and privacy challenges of data analytics in cloud-based IoT environments.

Scope:

Focus on Cloud-Based IoT Systems: The study will concentrate on IoT systems utilizing cloud computing for data storage and processing.

Emphasis on Data Analytics Integration: The research will explore the integration of data analytics techniques within cloud infrastructures to process IoT-generated data.

Limitations:

Exclusion of Non-Cloud IoT Systems: The research will not include IoT systems which do not use cloud computing. Specific Emphasis on Specific Analytics Methods: The research will concentrate on some chosen data analytics techniques and might not include all available technique Resource Constraints: The availability of limited computational resources might impact the magnitude of experimental comparisons.

Literature Review:

Theoretical Foundations: The integration of cloud computing, data analytics, and the Internet of Things (IoT) is a fast-growing field of research that seeks to overcome the limitations of processing vast amounts of data that emanate from smart devices. The Internet of Things describes a network of physical devices with sensors, software, and networking capabilities that allows them to collect and communicate with one another. Central to IoT systems are ideas borrowed from cyber-physical systems (CPS), which connect computational resources to physical processes, and wireless sensor networks (WSNs), which offer the building blocks to sensing and communication. Low-latency and low-power communication protocols like MQTT (Message Queuing Telemetry Transport), CoAP (Constrained Application Protocol), and ZigBee are of prime importance in facilitating communication between devices and the cloud. Cloud computing, in contrast, is the underlying infrastructure for handling the computation and storage demands of contemporary IoT systems. Through providing on-demand access to common resources via frameworks such as Infrastructure as a Service (IaaS), Platform as a Service (PaaS), and Software as a Service (SaaS), cloud computing facilitates scalability, agility, and cost-effectiveness. Its elastic properties make it best suited for processing and storing dynamic, high-speed data streams generated by IoT devices. Data analytics is another essential layer in the

IoT-cloud framework that transforms raw sensor data into actionable information. It is a range of methods that includes descriptive analytics (which presents historical data summaries), predictive analytics (which makes forward-looking predictions based on machine learning), and prescriptive analytics (which suggests best decisions based on insights). Sophisticated techniques like deep learning, real-time stream analytics, and statistical modeling enable greater value to be extracted from very large and complex data sets. The integration of IoT, cloud computing, and data analytics results in cloud-based IoT analytics systems that facilitate real-time monitoring, intelligent decision-making, and automated control in different domains. The integrated systems overcome major problems like data heterogeneity, latency requirements, and resource optimization. Theoretical frameworks in this field also address trade-offs among edge and cloud processing, use of big data concepts (volume, variety, velocity, and veracity), and the data life cycle from collection and preprocessing to analysis and visualization. These underpinnings collectively enable the construction of scalable, efficient, and smart cloud- IoT systems that can convert raw data into timely, meaningful, and context- aware insights.

Previous Research: Several studies have investigated the integration of data analytics and cloud-based IoT systems, in line with the increasing significance of smart, data-driven decision-making in many industries. Initial studies were mainly concerned with overcoming the scalability challenges presented by the increasing amount and diversity of data being produced by IoT devices. Most of these publications suggested architectural models that utilize cloud computing for data storage and analysis in a centralized manner, stressing its benefits regarding computational capabilities and scalability. Gubbi et al. (2013) presented one of the earliest frameworks that described the use of cloud platforms in IoT.

Methodology:

The research methodology taken for this work is aimed at designing, developing, and testing a cloud data analytics framework for IoT systems. The research has a systematic procedure involving a number of important phases: requirement analysis, system design, data collection, analytics implementation, and performance assessment. Both theoretical modeling, simulation, and experimental verification are employed to confirm that the new framework is not only practically sound but also academically credible. The research starts with a requirement analysis stage, during which the precise needs of cloud-based IoT applications are determined. These include identifying the kind of data usually generated by IoT devices (e.g., temperature, location, motion), the latency and bandwidth requirements of different use cases, and the major security and privacy issues that need to be tackled. Based on this, proper cloud services and data analytics software are chosen to serve as the base of the system.

In the design phase of the system, a layered structure is created consisting of the IoT device layer, network layer, cloud layer, and analytics layer. The IoT devices sense and send data using communication protocols like MQTT or HTTP. Data is then ingested in the cloud through services such as AWS IoT Core, Azure IoT Hub, or Google Cloud IoT, depending on the platform of implementation. A message broker and data stream management system are utilized to manage data ingestion and routing. The data acquisition stage includes collecting real-time and historical data from IoT sensors. Environmental sensors like DHT11 (temperature and humidity),

GPS modules (location tracking), or industrial sensors can be employed in experimental configurations to mimic real-world environments. Data is persisted in cloud storage systems (e.g., Amazon S3, Azure Blob Storage) and preprocessed to eliminate noise and deal with missing values.

In the implementation phase of analytics, different data analytics methods are utilized to draw conclusions. Descriptive analytics is utilized for summarizing data and analyzing trends. Predictive models like decision trees, support vector machines (SVM), and neural networks are implemented using cloud-based ML platforms like AWS SageMaker or TensorFlow on GCP. Real-time stream analytics is performed using platforms like Apache Spark or Azure Stream Analytics to identify anomalies or raise alerts based on specified thresholds. Finally, during the performance evaluation stage, the system is validated through measurement parameters like latency, throughput, accuracy, and resource usage. Simulation platforms like MATLAB, NS-3or IoT Sim can be employed in addition to actual deployments to study the performance of the framework under diverse data loads and network scenarios. Security aspects like data encryption, access control, and privacy-protection mechanisms are also tested for conformity with industrial standards. This integrated approach helps ensure that the suggested solution satisfies not only technical needs but also practical considerations such as scalability, dependability, and data integrity.

System Design/Architecture:

System Overview: The envisaged system is meant to enable real-time analytics for cloud-based IoT environments, allowing the ingestion, processing, and visualization of high-rate sensor data. The architecture combines distributed IoT devices with scalable cloud infrastructure to manage the volume, velocity, and variety of IoT streams. This architecture allows for timely decision-making for use cases like smart cities, industrial monitoring, and health diagnostics.

- IoT Device Layer: This layer contains heterogeneous sensors and actuators in the field. These devices capture environmental or operational information (e.g., temperature, motion, pressure) and send it over lightweight protocols like MQTT or CoAP.
- Edge Processing Layer: To reduce latency and offload the cloud, an optional edge computing layer conducts initial filtering, compression, and event detection close to the source of data. This layer makes sure only relevant or aggregated data is transmitted to the cloud.
- Cloud Infrastructure Layer: Underlying the system is a scalable cloud platform (such as AWS, Azure, or GCP) that manages high-volume data ingestion by way of services such as Apache Kafka or AWS Kinesis. Stream processing engines (such as Apache Flink, Spark Streaming) are utilized to execute analytics, anomaly detection, and predictive modeling in real time.
- Data Storage and Visualization Layer: Processed data is warehoused in time-series databases or data lakes (e.g., InfluxDB, Amazon S3) for analysis. Dashboards and alerting systems (e.g., Grafana, Kibana) offer end-users visual insights and actionable information.

Component Description: To enable real-time analytics within a cloud- based IoT environment, the system is composed of multiple related components. Each has a unique role in enabling smooth data acquisition, processing, and actionable insight generation.

- IoT Devices (Sensors and Actuators)
- Purpose: Gather raw data like temperature, humidity, location, or machine status.
- Features: Usually resource-constrained, employ low- power communication protocols (e.g., Zigbee, LoRa, Wi-Fi, NB-IoT).
- Communication Protocols: MQTT, CoAP, HTTP.
- Example Devices: Smart meters, industrial PLCs, wearable health monitors.
- Edge Gateways / Edge Computing
- Nodes Function: Local computation, preprocessing (e.g., noise filtering, threshold validation), and data aggregation.
- Advantages: Minimizes network bandwidth, latency, and cloud resource usage.
- Technologies: Raspberry Pi, NVIDIA Jetson, AWS Greengrass.
- Example Tasks: Local anomaly detection and alerting.
- Message Broker / Data Ingestion Layer
- Function: Provides a buffer and transport layer for high-speed data streams from edge nodes or devices.
- Technologies: AWS IoT Core, Apache Kafka, RabbitMQ, Google Cloud Pub/Sub.
- Features: Scales with high rates, topic-based streaming support.
- Stream Processing Engine Function: Supports real-time
- analytics like pattern recognition, filtering, aggregation, and feature extraction.
- Technologies: Apache Spark Streaming, Apache Storm, Apache Flink, Azure Stream Analytics.
- Use Cases: Identify unusual temperature surges, forecast equipment failure, trigger alerts.
- maintenance.
- Visualization and User Interface Function: Human interpretation and decision-making through presentation of insights using dashboards, charts, and alerts.
- Technologies: Grafana, Kibana, Power BI, custom web dashboards.
- Features: Role-based access control, real-time graphs, threshold-based alerting.
- Security and Access Control Module
- Function: Deviceauthentication, secure communication, and data integrity.
- Technologies: IAM roles, X.509 certificates, OAuth2, TLS/SSL.
- Functions: Encrypt data in transit, encrypt data at rest, authenticate users/devices, enforce access control

System Integration: The components are integrated in the suggested cloud- based IoT analytics architecture to support fluid, real-time data movement in all layers of the architecture. The system utilizes a loosely coupled, event-based paradigm that is modifiable, scalable, and fault-tolerant. The data produced by IoT devices are either sent to the cloud or preprocessed at the edge in a local way using lightweight computation nodes. These edge devices can do simple filtering or aggregation prior to forwarding data via secure protocols like MQTT or HTTP to the cloud-based ingestion layer.

Implementation/Experimental Results:

The huge expansion of IoT ecosystems, along with the need for further real- time data perceptivity, calls for scalable and effective system designs that can handle huge quantities of data while incurring low quiescence. The present paper introduces a pall-native and modular armature of real- time data analytics specificto the new issues of IoT ecosystems. By combining

edge computing, sluice processing, and pall storehouse, the system responds to central issues of data haste, diversity, and resource failure. Application of distributed processing platforms and communication brokers allows for fast processing of high- out- turn aqueducts of data so that opinions can be made on time in critical operations similar as smart metropolises, artificial robotization, and remote healthcare monitoring. The inflexibility and scalability of the proposed system is one of its core strengths.

References:

1. S.K. Sharma, X. Wang, (2017) Live data analytics with cooperative edge and pall p rocessing in wireless IoT networks, IEEE Access 54621 – 4635.
2. L. Atzori, A. Iera, G. Morabito, (2010) The internet of effects a check, Comput. Network. 54(15) 2787 – 2805.
3. K.M. Modieginyane, B.B. Letswamotse, R. Malekian, A.M. Abu- Mahfouz, (2018) Software defined wireless detector networks operation openings for effective network operation a check, Comput. Electr. Eng. 66 274 – 287.
4. T. Islam, S.C. Mukhopadhyay, N.K. Suryadevara, (2017) Smart detectors and internet of effects a postgraduate paper, IEEE Sensor. J. 17(3) 577 – 584.
5. C. Madhavaiah, I. Bashir, (2012) Defining pall computing in business perspective a review of exploration, transformation 1(2) 50 – 65.
6. F. Bonomi, R. Milito, J. Zhu, S. Addepalli, (2012) Fog computing and its part in the internet of effects, in Proceedings of the First Edition of the MCC Factory on Mobile Cloud Computing, , pp. 1 – 8.
7. Shukla, S. Chaturvedi, Y. Simmhan, (2017) RIoTBench: A Real-Time IoT Benchmark for Distributed Stream Processing Platforms, arXiv preprint.
8. Performance evaluation of real-time stream processing systems for Internet of Things applications, Future Generation Computer Systems, Dec. (2020) Vol. 113, pp. 207-217.
9. E.G. Petrakis, S. Sotiriadis, T. Soultanopoulos, P.T. Renta, R. Buyya, N. Bessis, (2018) Internet of effects as a Service(iTaaS) challenges and results for operation of detector data on the pall and the fog, Internet of effects Journal 3156 – 174.
10. B. Kitchenham, S. Charters, (2007) Guidelines for Performing Methodical Literature Reviews in Software Engineering, EBSE Technical Report EBSE- 2007-01, Durham, United Kingdom, pp. 1 – 53.

International Journal of Advance and Applied Research
www.ijaar.co.in
ISSN – 2347-7075 Impact Factor – 8.141
Peer Reviewed Bi-Monthly
Vol. 7 No. 14 January – February - 2026

Amino Acids Doping in KHP Crystals: A Critical Review

Devyani Supekar[1], Vrushali Karade[1], Rameshwar Bankar[1], Dnyaneshwari Awankar[1], Mandip Kapale[1], Anil Ardad[1]

[1]*Deogiri College, Chhatrapati Sambhajinagar-431005, Maharashtra, India*

Corresponding Author – Anil Ardad

DOI - 10.5281/zenodo.19756329

Abstract:

Potassium Hydrogen Phthalate (KHP) is an important Semi-Organic Crystal for Non-Linear Optical (NLO), photonic, and optoelectronic applications. KHP shows good crystal growth behavior, high optical transparency, and structural stability. This review summarizes the effects of amino acid dopants such as Glycine, L-Tryptophan, L-Phenylalanine, and L-Lysine. Slow evaporation method has been used to grow KHP crystals so that their structural, optical, dielectric, mechanical, thermal, and nonlinear optical properties are retained. Use of amino acid induces lattice distortion and modifies the hydrogen bonding without changing the orthorhombic crystal structure. The resulting property variations depend strongly on dopant concentration and growth conditions. Crystal growth challenges, defect formation, and future research directions are also discussed.

Keywords**: **Potassium Hydrogen Phthalate (KHP); Amino Acid doping; Non-Linear Optical (NLO) crytsals; Second Harmonic Generation (SHG); Semi-organic crystals

Introduction:

Potassium Hydrogen Phthalate (KHP) is a widely studied semi-organic crystalline material that has shown strong potential for Non-Linear Optical (NLO), optoelectronic, and photonic applications. It is also known as Potassium Acid Phthalate (KAP). Over the past few decades, KHP has gained sustained research interest primarily because it can be grown easily from aqueous solution. The slow evaporation method has been used to obtain high optical transparency, good mechanical strength and stable crystal structure [2,9,11]. These advantages make KHP a suitable host crystal for property enhancement through controlled organic and semi-organic doping.

KHP is recognized as an efficient Second Harmonic Generating (SHG) material due to its favorable electro-optic response and structural reliability under prolonged operation [11,12,17]. Because of these properties, KHP crystals have been explored for applications in optical filters, frequency conversion devices, and precision optical components [3,4]. KHP is extensively employed as a crystal analyzer in long wavelength X-ray spectrometers, owing to its stable lattice structure and well developed crystallographic planes [10,12]. The clearly defined morphology of KHP, especially the dominant (010) face, has also made it a model system for understanding crystal growth mechanisms and defect evolution [9,15].

Detailed microscopic studies have shown that the (010) growth face of KHP shows well defined growth steps and spiral features, enabling direct observation of growth kinetics and defect formation processes [9,15]. Earlier investigations revealed that the presence of additives or dopants can strongly influence the growth behavior on this surface by modifying surface energy and step

propagation mechanisms [10]. In certain growth sectors, KHP crystals exhibit very low defect densities, indicating the possibility of achieving high quality or near dislocation free regions, which is essential for efficient nonlinear optical performance [15].

From a structural standpoint, KHP crystallizes in the orthorhombic crystal system with space group $Pca2_1$ and belongs to the polar point group mm2 [9,16]. The unit cell contains four formula units of $K(C_6H_4COOH{\cdot}COO)$, where potassium ions are coordinated by oxygen atoms of the hydrogen phthalate groups. The crystal lattice is stabilized by strong O–H···O hydrogen bonds that form continuous molecular chains, contributing significantly to its mechanical integrity and optical behavior [9,10]. This hydrogen bonded framework plays an important role in determining the dielectric and nonlinear optical response of KHP crystals.

Optical investigations have demonstrated that KHP crystals possess high transparency in the visible region with a UV cut-off wavelength near 300 nm and an optical band gap in the range of 3.6–3.8 eV [9,14,16]. The material exhibits stable transmission across a broad energy range, although absorption features at lower energies have been reported due to defectrelated electronic states [11]. Photoluminescence studies indicate emission in the near UV region, suggesting good crystalline quality and low intrinsic defect concentration [3]. Mechanical and nonlinear optical studies further confirm that KHP exhibits moderate hardness and appreciable third order nonlinear susceptibility, reinforcing its suitability for photonic applications [3,12].

In recent years, amino acid doping has emerged as an effective strategy for modifying and enhancing the functional properties of KHP crystals without disturbing their basic crystal symmetry. Amino acids such as Glycine, L-Phenylalanine, L-Tryptophan, and L-Lysine have been successfully incorporated into the KHP lattice, primarily through hydrogen bonding and electrostatic interactions involving $–NH_2$ and –COOH functional groups [5,7,9,10,13]. These interactions lead to localized lattice distortion and altered intermolecular bonding while preserving the orthorhombic structure of the host crystal.

Experimental reports have shown that amino acid doping can significantly improve optical transparency, second harmonic generation efficiency, dielectric stability, mechanical hardness, and thermal resistance of KHP crystals [5,7,9,13]. Aromatic amino acids such as L-Phenylalanine and L-Tryptophan are particularly effective in enhancing SHG efficiency due to their higher molecular polarizability and improved dipole alignment within the crystal lattice [5]. On the other hand, Glycine doped KHP crystals exhibit reduced defect density, improved dielectric behavior, and enhanced optical band gap, making them attractive for optoelectronic device applications [9,13]. L-Lysine doping has also been reported to improve dielectric response and mechanical strength due to its multiple amino functional groups and strong hydrogen bonding capability [7].

In view of these findings, the present review systematically examines the influence of amino acid doping on potassium hydrogen phthalate crystals, with emphasis on growth techniques, structural modifications, optical and dielectric behavior, mechanical and thermal properties, and nonlinear optical performance. The review highlights the role of dopant type and concentration in tailoring material properties, discusses growth related challenges and defect mechanisms, and outlines future research directions aimed at optimizing amino acid doped KHP crystals for advanced nonlinear optical and photonic device applications. Glycine doped

KHP shows moderate optical transparency with slight band gap variation due to enhanced lattice ordering [9,13]. L-Phenylalanine and L-Tryptophan doping improve optical transparency and refractive index due to reduced defect density and increased molecular polarizability [5,10]. L-Lysinedoped KHP shows stable optical behavior with moderate transparency, due to dopant induced electronic states and strong hydrogen bonding interactions [7]. Below figure shows concept of KHP.

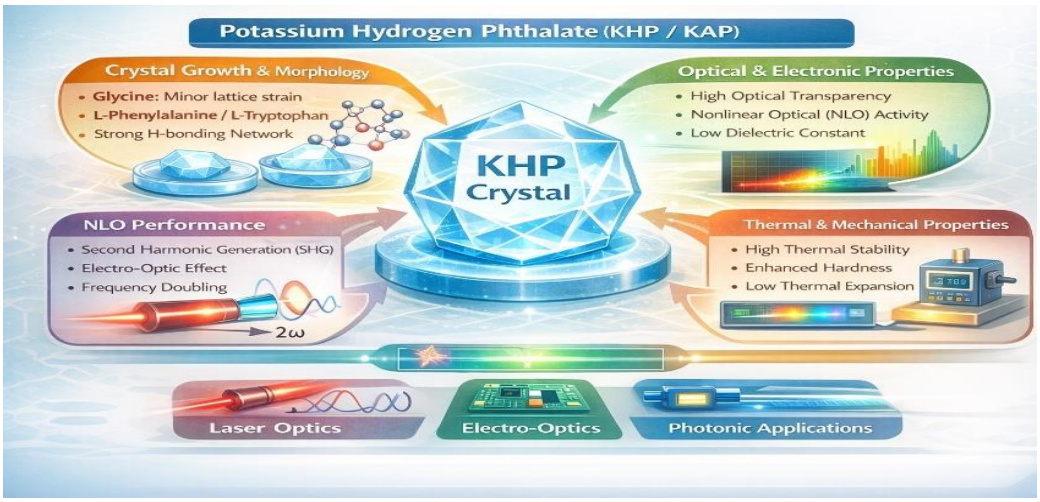

Figure 1: Concept of KHP

Method of Different Dopents:

The properties of pure Potassium Hydrogen Phthalate (KHP) can be improved by doping with amino acids such as Glycine, L-Tryptophan, L-Phenylalanine, and L-Lysine. These dopants interact with the KHP lattice through hydrogen bonding and electrostatic interactions. This leads to modification of physical and optical properties. The orthorhombic crystal structure has not been altered. Every amino acid has different characteristic property so it shows different effect on KHP.

Slow evaporation method:

KHP crystals are commonly grown from aqueous solution after repeated recrystallization to achieve high purity using a simple and cost effective slow evaporation solution growth method. This technique is widely used to obtain controlled supersaturation, resulting in improved crystalline quality with reduced defect density [9,10,15]. In amino acid doped KHP crystals, dopants such as Glycine, L-Tryptophan, L-Phenylalanine, and L-Lysine are introduced into the aqueous growth medium in varying concentrations. The addition of these amino acids into the KHP lattice leads to notable changes in optical absorption, dielectric behavior, mechanical hardness, and second harmonic generation efficiency [1,5,7,9,13]. Supersaturation of the doped growth solution facilitates enhanced crystal growth rates. The controlled dopant concentration helps in minimizing growthinduced defects. The amino acids are added directly to the saturated KHP solution, allowing their gradual incorporation during crystal growth through hydrogen bonding interactions with the host lattice [5,7,9,10].

Property Modifications Due to Doping:

The addition of amino acids such as Glycine, L-Tryptophan, L-Phenylalanine, and L-Lysine introduces localized lattice distortion. It

also changes the hydrogen bonding network within the KHP lattice. In this process the orthorhombic crystal structure is not changed. These interactions influence crystal growth behavior and defect density by modifying intermolecular interactions during crystallization. As a result, amino acid doping leads to enhanced optical transparency, improved nonlinear optical response, and modified dielectric behavior. It makes doped KHP crystals more suitable for optoelectronic and photonic applications.

1. Structural Modification:

Amino acid doping leads to structural modification in KHP crystals through hydrogen bonding and electrostatic interactions involving –NH_2 and –COOH functional groups. Dopants such as Glycine, L-Phenylalanine, L-Tryptophan, and L-Lysine introduce localized lattice distortion and internal strain without changing the orthorhombic crystal structure [5,7,9,10]. Smaller amino acids like Glycine are easily fits into the lattice, while heavier amino acids cause enhanced distortion due to steric effects [5,13]. At higher dopant concentrations, adsorption of amino acids on growth surfaces can hinder crystal growth and increase defect density, although the overall crystal system remains unchanged [9,13].

2. Optical Properties:

Amino acid doping influences the optical properties of KHP crystals. Dopants such as Glycine, L-Phenylalanine, L-Tryptophan, and L-Lysine enhance optical transparency in the visible region and induce slight variations in the optical band gap [5,9,13,14]. The improvement in transparency is due to reduced internal stress, improved lattice ordering, and decreased light scattering losses resulting from modified hydrogen bonding interactions within the crystal lattice [1,7,10]. These optical enhancements confirm the suitability of amino acid doped KHP crystals for optoelectronic and nonlinear optical applications.

3. Non-Linear Optical (NLO) Properties:

Amino acid doping enhances the nonlinear optical behavior of KHP crystals by modifying local electric fields and improving dipole alignment within the lattice. The addition of amino acids such as Glycine, L-Phenylalanine, L-Tryptophan, and L-Lysine improves intermolecular hydrogen bonding. The charge transfer interactions around the carboxylate groups, leads to enhanced SHG efficiency [1,5,7,9]. Aromatic amino acids like L-Phenylalanine and L-Tryptophanhave comparatively higher SHG output due to increased molecular polarizability and improved non-centrosymmetric alignment [5]. At optimized dopant concentrations, amino acid doped KHP crystals show improved SHG efficiency without disturbing the orthorhombic crystal structure, indicating their potential for frequency doubling and photonic applications [7,13].

4. Dielectric Properties:

Amino acid doping changes the dielectric behavior of KHP by modifying dipolar polarization and charge transport mechanisms. Glycinedoped KHP shows a relatively higher dielectric constant at low frequencies due to enhanced dipolar polarization arising from its small molecular size and strong hydrogen bonding ability [9,13]. L-Phenylalanine and L-Tryptophan doping results in reduced dielectric loss and improved dielectric stability, because of better lattice ordering and restricted spacecharge polarization caused by their bulky aromatic structures [5,10]. L-Lysinedoped KHP showsvariation in dielectric constant due to increased spacecharge polarization from its multiple amino functional groups interacting with the KHP lattice [7]. At optimized dopant concentrations, all amino aciddoped KHP crystals

shows stable dielectric response, indicating improved crystalline quality suitable for nonlinear optical and optoelectronic applications [7,13].

5. Thermal Properties:

Amino acid doping improves the thermal stability of KHP crystals by strengthening intermolecular interactions within the lattice. Glycinedoped KHP shows a slight increase in thermal stability due to enhanced hydrogen bonding and improved lattice cohesion [9,13]. L-Phenylalanine and L-Tryptophan doping significantly enhance thermal resistance, as their bulky aromatic structures restrict molecular motion and delay thermal decomposition [5]. L-Lysinedoped KHP shows moderate improvement in thermal stability, due to strong electrostatic interactions and additional hydrogen bonding introduced by multiple amino functional groups [7]. These enhancements make amino aciddoped KHP crystals more suitable for hightemperature and optoelectronic device applications [5,7,13].

6. Mechanical Properties:

Amino acid doping enhances the mechanical strength of KHP by introducing localized lattice strain and strengthening intermolecular interactions. Glycinedoped KHP shows a moderate increase in microhardness due to improved lattice packing [9,13]. L-Phenylalanine and L-Tryptophanincrease microhardness by restricting dislocation movement through steric hindrance from aromatic side chains [5]. L-Lysinedoped KHP also shows enhanced mechanical strength due to additional hydrogen bonding and electrostatic interactions [7].

7. Photoluminescence Spectrum:

Amino acid doping modifies the photoluminescence (PL) behavior of KHP by influencing defect states and electronic transitions. Glycinedoped KHP shows enhanced emission due to reduced defect density [9,13]. L-Phenylalanine and L-Tryptophan shows stronger PL intensity because of aromatic π–π* transitions, while L-Lysine shows moderate PL enhancement arising from dopant induced localized states [5,7]. Below figure shows effects of amino acids doping in KHP crystals by all references.

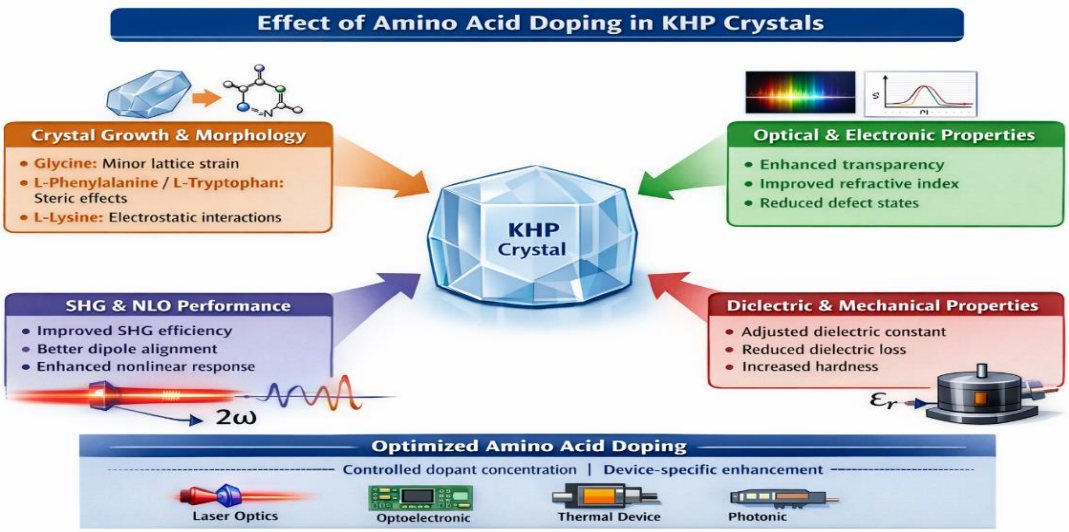

Figure 2: Gives effects of Amino Acids on KHP Crystals

Comparative Analysis & Discussion:

A comparative analysis of amino acid doped KHP crystals is very important to establish clear structure property correlations, identify optimal dopants for targeted applications, and evaluate the reliability of these materials for device integration. Such analysis enables meaningful interpretation of individual experimental results and provides broader scientific and technological insights into the role of organic dopants in semi-organic NLO crystals [1,5,7].

1. Comparative Impact on Crystal Growth Behavior:

Amino acid doping influences the crystal growth behavior of KHP by modifying surface energy and hydrogen bonding interactions. Small amino acids such as Glycine are easily fits into the lattice, resulting in minimal lattice strain and improved crystal morphology [9,13]. In contrast, bulkier amino acids such as L-Phenylalanine and L-Tryptophan introduce localized strain due to steric effects, which alters growth kinetics and crystal morphology without changing the orthorhombic structure [5]. L-Lysine affects growth behavior through strong electrostatic interactions and multiple hydrogen bonds, influencing crystal size and habit [7].

2. Comparative Influence on Optical and Electronic Properties:

Glycine doped KHP shows moderate optical transparency with slight band gap variation due to enhanced lattice ordering [9,13]. L-Phenylalanine and L-Tryptophan doping improve optical transparency and refractive index due to reduced defect density and increased molecular polarizability [5,10]. L-Lysine doped KHP shows stable optical behavior with moderate transparency, due to dopantinduced electronic states and strong hydrogen bonding interactions [7].

3. Comparative SHG and NLO Performance:

Amino acid doping enhances SHG efficiency in KHP by improving dipole alignment and local electric field distribution. Glycine doping results in modest SHG enhancement due to improved crystal perfection [9,13]. Aromatic amino acids such as L-Phenylalanine and L-Tryptophan show comparatively higher SHG efficiency because of increased polarizability and effective non-centrosymmetric alignment [5]. L-Lysine doping also improves SHG output through enhanced charge transfer and strong intermolecular interactions [7].

4. Dielectric and Mechanical Behavior Comparison:

Glycinedoped KHP shows a higher dielectric constant at low frequencies due to enhanced dipolar polarization [9]. L-Phenylalanine and L-Tryptophan doping result in reduced dielectric loss and increased microhardness due to restricted dislocation motion and improved lattice rigidity [5]. L-Lysinedoped KHP exhibits moderate dielectric stability and enhanced mechanical strength due to multiple hydrogen bonding interactions [7,13].

5. Application Specific Recommendations:

Below tablesummarizes the most effective amino acid dopants for various applications of KHP crystals based on reported studies [1,5,7,9,13].

Table 1: Summarizes the most effective amino acid dopants for various applications of KHP crystals based on reported studies

Application	Best Amino Acid Dopant	Reason
High power SHG / Frequency doubling	L-Phenylalanine, L-Tryptophan	High SHG efficiency, enhanced polarizability
Optoelectronic devices	Glycine, L-Lysine	Good transparency, dielectric stability
Thermally stable photonic devices	L-Phenylalanine, L-Lysine	Improved thermal resistance
NLO devices	L-Phenylalanine, Glycine	Improved dipole alignment and crystal quality

Applications in Photonics and NLO Devices:

Amino acid doped KHP crystals have gained interest for photonic and nonlinear optical devices due to tunable optical transparency, enhanced SHG efficiency, improved mechanical strength, and stable dielectric behavior.

1. High Power Laser Frequency Conversion (SHG):

L-Phenylalanine- and L-Tryptophan doped KHP crystals show enhanced SHG efficiency and optical transparency, making them suitable for frequency doubling applications. Glycine doped KHP also exhibits stable SHG performance due to reduced defect density [5,9,13].

2. Electro-Optic Devices:

Glycine and L-Lysine doped KHP crystals demonstrate stable dielectric response, moderate hardness, and improved optical quality, making them suitable for electro-optic and photonic components [7,9].

3. Optical Windows and UV–Visible Components:

Amino acid doped KHP crystals retain high transparency in the visible region with UV cut-off in the near ultra violet range. L-Phenylalanine- and L-Tryptophan-doped KHP show improved transmission compared to pure KHP, making them suitable for optical window applications [5,10].

4. Tailored Applications: Dopant Device Matching:

Table 2: It presents dopant specific property enhancement for device-oriented applications [1,5,7,9,13].

Amino Acid Dopant	Property Enhanced	Tailored Applications
Glycine	Dielectric stability, crystal quality	Optical windows, electro-optics
L-Phenylalanine	SHG, hardness, thermal stability	NLO and laser devices
L-Tryptophan	Optical transparency, SHG	Photonic switches
L-Lysine	Mechanical strength, dielectric behavior	Device substrates

Challenges and Future Scope:

Challenges:

Achieving uniform addition of amino acids into the KHP lattice remains challenging, particularly at higher dopant concentrations where surface adsorption can hinder growth and increase defect density [5,9,13]. Bulky amino acids may induce excessive lattice strain, affecting dielectric and optical properties if not carefully controlled. Growth parameters such as pH, temperature, supersaturation, and evaporation rate strongly influence dopant incorporation and crystal quality.

Future Scope:

Future research should focus on optimizing amino acid concentration to balance SHG efficiency, optical transparency, and dielectric stability. Co-doping strategies

involving multiple amino acids and advanced characterization techniques such as Raman mapping and NMR spectroscopy could provide deeper insight into dopant lattice interactions. Such approaches may further enhance the performance of amino acid doped KHP crystals for advanced photonic and nonlinear optical applications [5,7,13].

Conclusion:

This review comprehensively analyzed the influence of amino acid doping in Potassium Hydrogen Phthalate (KHP) crystals on structural, optical, dielectric, mechanical, thermal, and nonlinear optical properties. The addition of amino acids such as Glycine, L-Phenylalanine, L-Tryptophan, and L-Lysine modifies hydrogen bonding networks and local electric fields without altering the orthorhombic crystal structure. While challenges related to dopant concentration and defect generation persist, optimized amino acid doping demonstrates significant potential for enhancing SHG efficiency, optical transparency, and device stability. Continued systematic studies focusing on dopant property correlations and device level integration are expected to advance KHP based materials for high performance photonic and optoelectronic applications.

References:

1. Arul Jothi, R., Mullai, R. U., Gopinath, S., Vinoth, E., & Vetrivel, S. **(2021)** Crystal growth, structural, optical, thermal, mechanical and dielectric studies on NLO active potassium hydrogen phthalate L-threonine semi organic crystal for frequency conversion. Brazilian Journal of Physics, 51, 1539–1549**.**
2. Kumari, M., Vijayan, N., Nayak, D., & Pant, R. P. **(2020)** Investigation on semi-organic potassium acid phthalate single crystal for nonlinear optical applications. Materials Science and Engineering Conference Proceedings.
3. Kumari, M., Vijayan, N., Nayak, D., Kumar, M., Gupta, G., & Pant, R. P. **(2020)** Assessment of optical, mechanical and nonlinear properties of potassium acid phthalate single crystal: A potential candidate for optoelectronic applications. Materials Research Express, 7, 015705**.**
4. Sivakumar, K., Senthilkumar, M., & Ramachandra Raja, C. **(2018)** Growth, spectral, mechanical and nonlinear optical characterization of potassium hydrogen phthalate crystals. Rasayan Journal of Chemistry**.**
5. Karpagam, T., & Balasubramanian, K. **(2018)** Comparative study of mechanical, dielectric and thermal properties of solution grown NLO crystal potassium acid phthalate doped with L-Phenylalanine and L-Tryptophan. International Journal of Scientific Research in Science and Technology, 4(4)**.**
6. Arul Jothi, R., Mullai, R. U., Vinoth, E., Suresh, T., Gopinath, S., & Vetrivel, S. **(2018)** Growth and characterization of succinic acid–mixed KHP crystal for NLO applications. Emerging Materials Research, 7(1), 10–18**.**
7. Dhavud, S. S., & Prakash, J. T. J. **(2016)** Influence of amino acid dopants on the growth and properties of potassium hydrogen phthalate single crystals for nonlinear optical applications. International Journal of Advanced Research**.**
8. Thilagavathy, S. R. **(2016)** Comparative study of 1 mol% L-Lysine doped in organic and semi-organic materials. Journal of Materials Science Research**.**

9. Amuthambigai, C., Guzman-Afonso, C., Torres, M. E., & Sahaya Shajan, X. **(2016)** Optical, spectral and dielectric studies of L-histidine added potassium hydrogen phthalate crystals. Optik, 127, 3292–3298**.**
10. Sajikumar, A. C., Vinu, S., & Krishnan, C. **(2015)** Studies on structural, optical and thermal properties of L-histidine doped potassium hydrogen phthalate single crystal. International Journal of Engineering Research & Technology, 4(1)**.**
11. Thilagavathy, S. R., Rajesh, P., Ramasamy, P., & Ambujam, K. **(2014)** Growth and characterization of pure and doped KHP NLO single crystals. Spectrochimica Acta Part A, 127, 248–255**.**
12. Sivakumar, B., Gokul Raj, S., Ramesh Kumar, G., & Mohan, R. **(2013)** Growth and characterization of potassium acid phthalate for thirdorder NLO applications. AIP Conference Proceedings, 1512, 1272–1273**.**
13. Sivakumar, N., Mohan Kumar, R., & Anbalagan, G. **(2013)** Effect of Glycine doping in potassium hydrogen phthalate (KHP) crystals on structural and optical properties. Advanced Materials Research, 584, 116–120.
14. Krishnan, S., Justin Raj, C., Dinakaran, S., & Jerome Das, S. **(2008)** Investigation of optical band gap in potassium acid phthalate single crystal. Crystal Research and Technology**.**
15. Ester, G. R., & Halfpenny, P. J. **(1998)** An investigation of growth induced defects in crystals of potassium hydrogen phthalate. Philosophical Magazine A, 77, 593–608**.**
16. Comoretto, D., Rossi, L., & Borghesi, A. **(1997)** Optical properties of potassium acid phthalate. Journal of Materials Research, 12, 1262–1267**.**
17. Miniewicz, A., & Bartkiewicz, S. **(1993)** On the electro-optic properties of single crystals of sodium, potassium and rubidium acid phthalates. Advanced Materials for Optics and Electronics, 2, 135–140**.**

International Journal of Advance and Applied Research
www.ijaar.co.in
ISSN – 2347-7075 Impact Factor – 8.141
Peer Reviewed Bi-Monthly
Vol. 7 No. 14 January – February - 2026

Electrochemical Sensors for Soil Health Monitoring

Gaikwad Pradeep Devendra
Physics Department,
R.B. Attal Arts Science and Commerce College Georai, Taluka Georai Dist. Beed – 431127.
Corresponding Author – Gaikwad Pradeep Devendra
DOI - 10.5281/zenodo.19756465

Abstract:
Soil health using sensors is growing field to monitor and manage soil Conditions has emerged as a promising approach to develop advanced sensors for rapid, continuous monitoring of soil health parameters. The recent advancements in sensors for soil health assessment, their working principles, applications, the potential of various nanomaterials, in fabricating highly sensitive, selective for soil health monitoring, promoting sustainable agriculture. Electrochemical sensing system detecting one or multiple soil component effectively, efficiently, and selectively for soil quality and soil health care. There is a global interest on development of cost-efficient and fast analysis to soil quality. The electrochemical soil sensors are widely used to soil nutrients due to their cost-effectiveness, long-term deploy ability, fast response and multiplexing.

Keywords: Electrochemical Method, Nanotechnology; Soil Quality, Soil Health, Soil Sensors, Sustainable Agriculture.

Introduction:

Soil Quality is the ability of soil to perform specific functions, such as nutrient retention, water infiltration, and carbon sequestration [1]. Soil is a vital natural resource that supports plant growth, nutrient cycling, water regulation, and biodiversity [2]. Nanotechnology involves the manipulation of matter at the nanoscale (1-100 nm), where materials exhibit unique physical, chemical, and biological properties [3]. Nano technology-based sensors offer several advantages as real-time monitoring, high spatial resolution, low power consumption, and the ability to integrate with wireless communication technologies [4] The global agricultural demand is expanding speedily because of enhancing population and food production, and income growth through worldwide[5]. There is a global interest on development of cost-efficient and fast analysis to soil quality. It is known that nitrogen (N), phosphorus (P), and potassium (K) are the major macronutrients and iron, manganese, copper, zinc, boron, molybdenum, chlorine are the minor soil micronutrients[6]. These nutrients can essential elements plant growth and high product yields. Soil acidity or alkalinity is another important factor as it influences how easily plants can uptake nutrients from the soil[7-8]. The electrochemical soil sensors are widely used to soil nutrients due to their cost-effectiveness, long-term deploy ability, fast response and multiplexing. The electrochemical sensing have explored widely for point of use applications in many fields [9–13]. The schematic representations of electrochemical based sensor for Soil health monitoring are shown in Fig. 1.

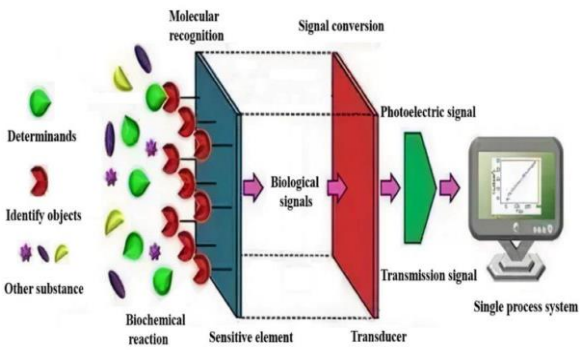

Fig.1: Schematic representation of Electrochemical -based sensor for soil health monitoring.

Electrochemical Based Sensors for Soil Health Monitoring:

Nutrient sensing in soil using Electrochemical sensors: Nitrate, Phosphate High surface area and conductivity of graphene oxide for sensitive electrochemical detection.

pH Sensing in Soil using Electrochemical sensors: MoS2 high surface area and electrocatalytic activity for pH sensing.

Greenhouse gas sensing in soil using Electrochemical sensors: N2O Redox reactions at the electrode-electrolyte interface.

Challenges and Futures Prospects:

Despite the promising potential for soil health monitoring, These challenges include:

Interference from soil matrix: The presence of humic substances, clay minerals, and salts can affect the sensitivity, selectivity, and stability of Nano sensors with high specificity and robustness against soil matrix interference is crucial.

Biocompatibility and toxicity: The development of biocompatible and eco-friendly Nano sensors is essential to minimize their adverse effects on soil health.

Durability and long-term stability: The development of durable and stable Nano sensors with self-cleaning and self-healing capabilities is necessary for their long-term operation in soil.

Standardization and calibration: The development of standardized protocols and calibration methods for Nano sensors in different soil types is crucial for their accurate and reproducible measurements.

Cost and scalability: The development of cost effective and scalable manufacturing methods for Nano sensors is essential for their commercial viability and widespread use.

Future Prospects and Recommendations:

In electrochemical method, an ion-selective membrane (ISM) combined with electrochemical transducer is widely used for soil nutrients detection such as nitrate, potassium, phosphorus. conducting polymers can provide ionic to electronic conduction via the oxidation/reduction or doping/undoping mechanism. For potentiometric soil sensors, the contamination with non-specific ions and damaging of ISM can cause the sensor potential drift and signal instability.

Conclusion:

Electrochemical sensor made to fabricate miniaturized electrochemical sensing system for soil quality assessment Such of advancements will be useful to reduce farming cost, minimize excessive pesticides & fertilizer utilization, manage crop growth, and achieve quality food and Contribute to sustainable agriculture.

Acknowledgment:

Authors do acknowledge respective departments for providing support and facilities.

References:

1. Nortcliff S. (2002) Standardisation of soil quality attributes. Agriculture, Ecosystems and Environment. 88(2):161-168.
2. Doran JW, Zeiss MR. (2000) Soil health and sustainability: Managing the biotic

component of soil quality. Applied Soil Ecology. 15(1):3-11.

3. Mukhopadhyay SS. (2014) Nanotechnology in agriculture: Prospects and constraints Nanotechnology, Science and Applications.;7:63.
4. Rai V, Acharya S. and Dey, N. Implications of Nano biosensors in agriculture. Journal of
5. D. Tilman, C. Balzer, J. Hill, and B. L. Befort, (2011) Proc. Natl Acad. Sci., 10820260 .
6. N. C. Brady, R. R. Weil, and R. R. Weil, (2008) in The Nature and Properties of Soils (Prentice Hall, Upper Saddle River, NJ)
7. M. Sillanpää, (1982) in Micronutrients and the Nutrient Status of Soils: A Global Study (Food & Agriculture Organization, Rome, Italy)
8. P. J. Kramer and J. S. Boyer, (1995) in Water Relations of Plants and Soils (Academic Press, San Diego, CA)
9. A. Kaushik, A. Yndart, S. Kumar, R. D. Jayant, A. Vashist, A. N. Brown, C.-Z. Li,and M. Nair, (2018) Sci. Rep., 8, 9700
10. A. Kaushik, P. Shah, P. K. Vabbina, R. D. Jayant, S. Tiwari, A. Vashist, A. Yndart,and M. Nair, (2016) Anal. Methods, 8, 6115
11. A. Kaushik, S. Tiwari, R. D. Jayant, A. Vashist, R. Nikkhah-Moshaie, N. El-Hage,and M. Nair, (2017) Trends Biotechnol., 35, 308
12. A. Kaushik, R. D. Jayant, S. Tiwari, A. Vashist, and M. Nair, (2016) Biosens. Bioelectron.,80, 273
13. A. Ali, A. A. Ansari, A. Kaushik, P. R. Solanki, A. Barik, M. K. Pandey, and B. D. Malhotra, (2009) Mater. Lett., 63, 2473.

International Journal of Advance and Applied Research
www.ijaar.co.in
ISSN – 2347-7075 Impact Factor – 8.141
Peer Reviewed Bi-Monthly
Vol. 7 No. 14 January – February - 2026

DFT and Experimental Investigation of BaF2 Phosphor for Dosimetry Application

K. R. Sature[1], B. S. Kharat[2], P. M. Kokne[3]

[1]*Department of Physics, J.E.S.'s, R. G. Bagdia Arts, S. B. Lakhotia Commerce and R. Bezonji Science College, Jalna, Maharashtra, India*

[2]*Department of Physics, Swami Vivekanand Sr. College, Mantha, Jalna, Maharashtra, India*

[3]*Department of Physics, badrinarayan Barwale College, Jalna, Maharashtra, India*

Corresponding Author – K. R. Sature

DOI - 10.5281/zenodo.19756519

Abstract:

Experiments and Density functional theory based First-principles calculations have been performed to investigate the structural, optical and electronic properties of BaF_2 and Ce doped BaF_2. Copper oxide nanoparticles were synthesized using chemical co-precipitation method. X-ray diffraction (XRD) characterization verified the creation of FCC structure with 30 nm crystalline size. The Quantum ESPRESSO package is used for DFT calculations. Calculated values of lattice parameters, energy band gap of BaF_2 and Ce doped BaF_2 are in good agreement with the experimental results. Figures of electronic band structure and DOS have been computed from the electronic structure of BaF_2 and Ce doped BaF_2. Significant transition occurs in band gap after Ce doping. Metastable states arises due to Ce doping on matrix of BaF_2. Those levels acts as a energy electron trap levels. Therefore Ce doped BaF_2 is strong candidate for Thermoluminescence dosimeter.

Keywords: BaF_2, Ce doped BaF_2, DFT, DOS, Thermoluminescence.

Introduction:

A phosphor is a large band gap, an inorganic crystalline material that emits light when excited by an external energy source. Phosphors are characterized by ability to convert various forms of energy such as ionizing radiation, ultraviolet light or electron beams into visible or infrared photons. The process in which heat/temperature is used to excite the electrons from the trap level to produce visible or infrared photons is called as thermoluminescence. The study of thermoluminescence materials have been carried out since last four decades. Thermoluminescence (TL) is the emission of light from solid phosphor material when thery are heated aster being irradiated with energetic or ionizing radiations such as X-rays, gamma rays, electron beam, ion beam or neutron beam. Intensity of light photons is directly proortions to the amount of radiation absorbed. Therefor this technique is used for radiation dosimetry i.e. measurement of the radiation dose. TLD-100 (LiF: Mg,Ti), TLD-200 (CaF2:Dy), TLD-300 (CaF2:Tm), TLD-400 (CaF2:Mn), TLD-600 and TLD-700 (6Li and 7Li enriched LiF: Mg,Ti) are commercially available thermoluminescence dosimeters [1-3]. These will be employed in medical dosimetry, personal dosimetry, retrospective dosimetry, environmental monitoring, neutron dosimetry, and biology, depending on their radiation sensitivity.

Barium fluoride is an inorganic compound that crystallizes in a stable cubic fluorite structure (space group Fm3m), characterized by its high chemical stability and relatively low solubility in water compared to

other halides. One of its most distinctive physical properties is its extensive optical transparency, which spans from the vacuum ultraviolet to the long-wave infrared, making it a versatile window material [5-7]. It possesses a relatively high density of 4.89 g/cm3 and a refractive index of approximately 1.47 at visible wavelengths. Electronically, BaF_2 is a wide-bandgap insulator with an experimental bandgap (Eg) of approximately 10.5eV to 11eV, which accounts for its transparency in the UV region. The material exhibits unique scintillation and luminescence properties, most notably a cross-luminescence (or core-valence luminescence) characterized by an ultrafast decay component of approximately 600ps at 220 nm. This ultrafast response is attributed to the transition of electrons from the F-(2p) valence band to the Ba2+(5p) core holes. Regarding transport properties, while it is an insulator, it demonstrates an electron mobility typically in the range of 5-10 cm2V-1s-1 at room temperature, though its performance as a radiation detector is primarily governed by the efficiency of carrier trapping and subsequent radiative recombination.

Due to these robust characteristics, BaF2 is extensively used in high-energy physics and medical imaging (such as PET scans) as a fast scintillator for gamma-ray detection. Its high resistance to high-energy radiation and excellent thermal shock resistance also make it a preferred material for specialized optical lenses, prisms, and windows in infrared spectroscopy and laser systems.

Building upon these studies, the present research focuses on the DFT study and synthesis of BaF2 and Ce doped BaF2. we have synthesised CaF2 with co-precipetation method and diffusion method. Material is then characterized by X-ray diffraction (XRD). To study the trap mechanism in the irradiation process density functional theory is used to calculate the all possible scenarios.

Methods and Material:

1. Synthesis of BaF_2 nanoparticles:

The highly sensitive BaF2:Ce phosphor was prepared by chemical co-precipitation method with the following reaction.

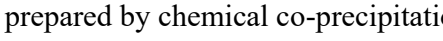

$$BaCl2 + 2NH4F \rightarrow BaF2 + 2NH4Cl$$

In a typical process, 5.71 gm of BaCl2 and 1.74 gm of NH4F was dissolved separately into 20 ml (99.9% pure, A.R Grade) and 30 ml double distilled water (DDW) with continuous stirring. For 30 minutes, each solution was agitated in a natural atmosphere. Next, 25 ml of ethanol was added to a BaCl2 solution that included 1 mol% cerium oxide (CeO2) (used as a dopant) from Sigma Aldrich dissolved in it while being constantly stirred. Drop by drop, stoichiometric proportions of NH4F solution were added to the BaCl2 solution while being continuously stirred. To produce precipitation, the reaction was carried out for a further two and a half hours. After filtering out the precipitate, it was dried for five hours at 120 °C. The characterizations were then conducted using this dried powder.

2. DFT calculations:

Quantum mechanical calculations were done using Quantum ESPRESSO [4] open source under Linux operating system. The Density Function Theory (DFT) with the local density approximation exchange correlation function and plane wave sets were applied on electronic structures using four 2 GHz cores and 8 gigabyte of RAM, which were sufficient in this research. The pbe pseudo potential with convergence threshold of 10−7 has been used for self-consistency of energy which is appropriate for these calculations.

Results and Discussion:

1. X-ray Diffraction Analysis:

The crystallographic structure of the synthesized (BaF_2) nanoparticles was determined using X-ray diffraction (XRD) analysis. The dried BaF_2 nanoparticle powder was subjected to XRD analysis using a diffractometer equipped with Cu Kα radiation (λ = 1.5406 Å) operating at 40 kV and 30 mA. The XRD patterns were recorded over a 2θ range of 20° to 80° at a scanning rate of 0.02°/s.

XRD pattern of BaF2:Ce phosphor shown in Fig. 1 matches very well with the standard data available in JCPDS card (ICDD card no. 85-1342).

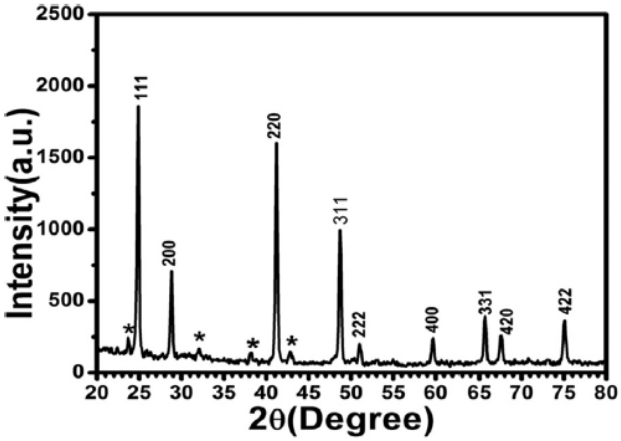

Figure 1. X-ray diffraction pattern of BaF_2:Ce phosphor

The XRD showed certain "hkl" peaks at 24.9°, 28.8°, 41.2°, 48.7°, 51.0°, 59.6°, 65.6°, 67.5°, and 75.0° corresponding to (111), (200), (220), (311), (222), (400), (331), (420), and (422) planes, respectively. Because of the small amount (1 mol%) of dopant, no peaks from impurities are observed. Some unidentified peaks observed in the XRD of BaF2:Ce, such as 23.8°, 32.1°, 38.2°, and 42.8°, denoted as "*," may be due to a small amount of un-reacted BaCl2 remained into the sample, which is well agreement with ICDD card number 74-0524 data file of BaCl2.

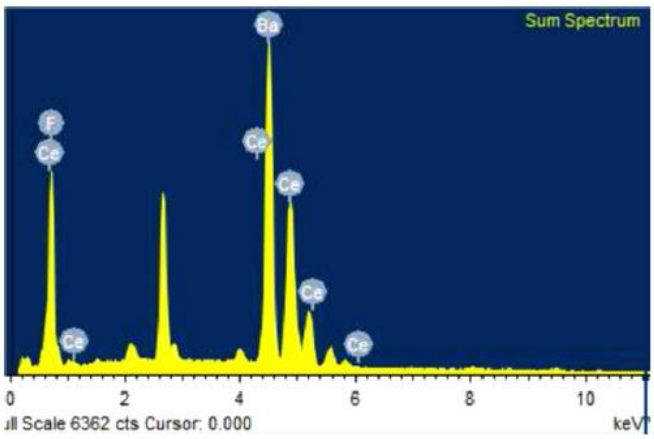

Figure 2. EDS spectrum of BaF_2:Ce phosphor

The elemental analysis of BaF2:Ce phosphor was done using EDS and the plot of the spectrum is shown in Fig. 2. The atomic percentage (%) of elements detected by EDX is shown in Table 1, which indicates that synthesized materials are in a stoichiometric amount.

Element	Atomic %
F	71.09
Ba	28.86
Ce	0.05
total	100

Table 1 Elemental composition of BaF_2:Ce

2. DFT study:

DFT Calculations begin with the discovery for the stable structure. In this process lattice parameter of the unit cell are set free to adjust according to lowest total energy. In this process total energy respective to the different volumes is calculated. Lowest energy is observed and lattice parameters are finalised. Finalised lattice constant for BaF_2 cubic FCC structure is a=6.194 Armstrong. Cubic FCC structure is shown in Figure 3. Further Ce is introduced into lattice matrix on the face site of Ba atom. Lowest energy is obtained with the repetitive energy calculations. Finalised FCC structure is shown in

the figure 4 with the lattice constant a =5.892 Armstrong. Because the ionic radius of Ce^{3+} (approximately 1.01 Armstrong) is smaller that of Ba^{2+} (approximately 1.35 Armstrong), the substitution of Barium ions by Cerium ions causes a contraction of the unit cell, leading to a measurable reduction in the BaF_2 lattice constant.

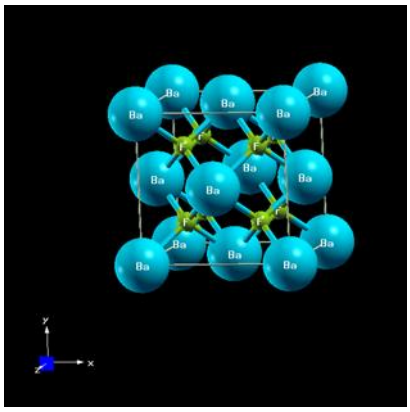

Figure 3. Face Centre Cubic Unit cell of BaF_2

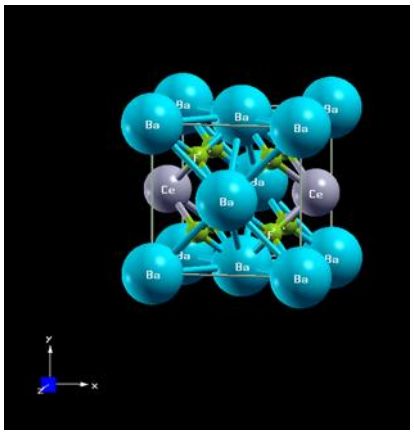

Figure 4. Face Centre Cubic Unit cell of $Ba_3F_8Ce_1$ i.e.$Ba_xF_{2x}Ce_{(x-1)}$. Ba, F and Ce atoms are represented by sky blue, Green and grey colours respectively.

2.1 Electronic Structure Analysis:

Electronic Characteristics of Pure BaF_2:

Using the stable structure of BaF_2 energy band gap and density of states (DOS) are calculated using QUANTUM ESPRESSO. Figure 5 shows the a) DOS and b) energy bands of the pristine form, BaF_2. It exhibits HOMO level at -0.98 eV and LUMO level at 10.06 eV. Hence a wide, direct bandgap of 11.04 eV. This large energy separation between the valence band (VB) and the conduction band (CB) is characteristic of an insulator with high transparency in the ultraviolet (UV) and vacuum ultraviolet (VUV) regions. The valence band is primarily composed of the 2p orbitals of Fluorine (F), while the bottom of the conduction band is dominated by the 5d or 6s states of Barium (Ba). This wide gap ensures that pure BaF_2 remains chemically stable under high-energy radiation, though it limits the efficiency of low-energy photon emission.

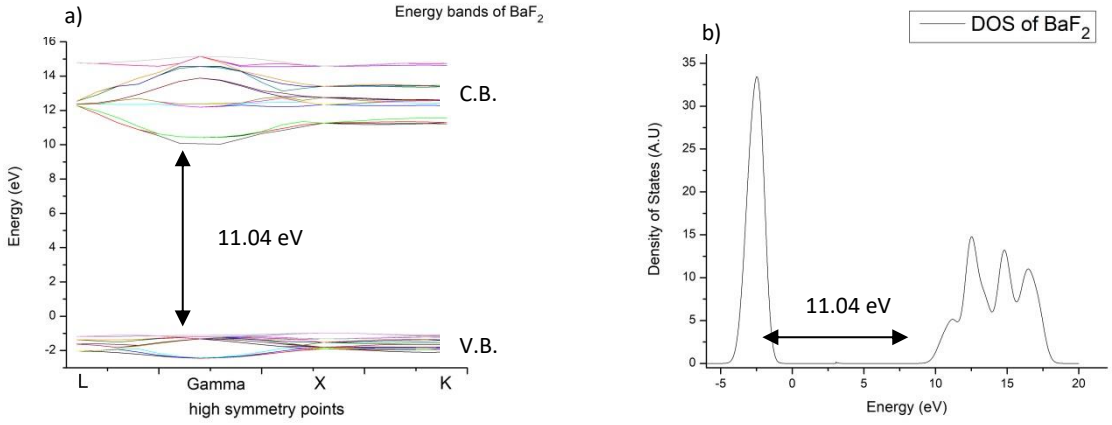

Figure 5: a) energy band structure of BaF_2 and b) DOS of BaF_2

Impact of Cerium Doping on Band Dynamics: DOS and energy band structure of BaF_2: Ce having lowest energy is calculated with the help of DFT simulation. Figure 6 shows $Ba_3F_8Ce_1$, $Ba_{30}F_{64}Ce_2$ and $Ba_{31}F_{64}Ce_1$ Structures. These structures have Ce to Ba ratio 0.33, 0.06 and 0.03 respectively.

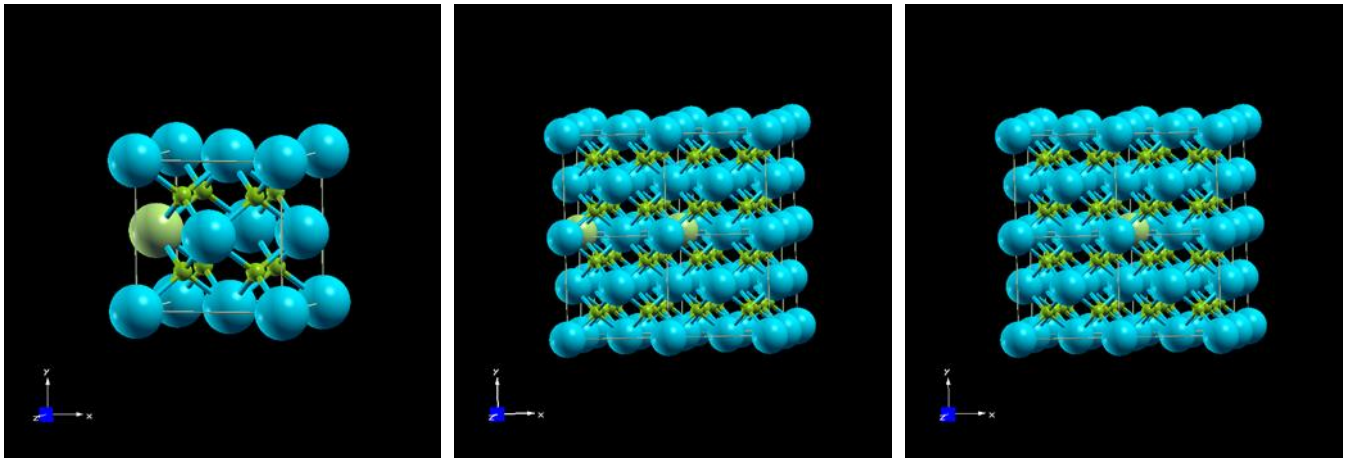

a) $Ba_3F_8Ce_1$ b) $Ba_{30}F_{64}Ce_2$ c) Ba31F64Ce1

Figure 6: figure shows BaF_2:Ce with different composition of Ce atom. Ba, F and Ce atoms are represented by sky blue, Green and light green colours respectively. ratio of Ce to Ba is a)0.33 b) 0.06 and c) 0.03

DOS and energy bands of $Ba_3F_8Ce_1$, $Ba_{30}F_{64}Ce_2$ and $Ba_{31}F_{64}Ce_1$ Structures were calculated. DOS and energy bands of $Ba_3F_8Ce_1$ are represented in Figure 7. $Ba_{30}F_{64}Ce_2$ and $Ba_{31}F_{64}Ce_1$ also shows the same energy states with small change in intensity. The introduction of Cerium into the BaF_2 host lattice fundamentally alters the forbidden energy region. The calculations indicate a substantial reduction in the effective bandgap, dropping from 11.04 eV to 10.81 eV. Cerium doping introduces Ce 4f and Ce 5d energy levels. The Ce 4f ground state typically resides just above the valence band maximum, while the 5d excited states appear below the host conduction band minimum. Therefore This reduction is not due to a shift in the primary host bands, but rather the emergence of localized impurity states within the original gap.

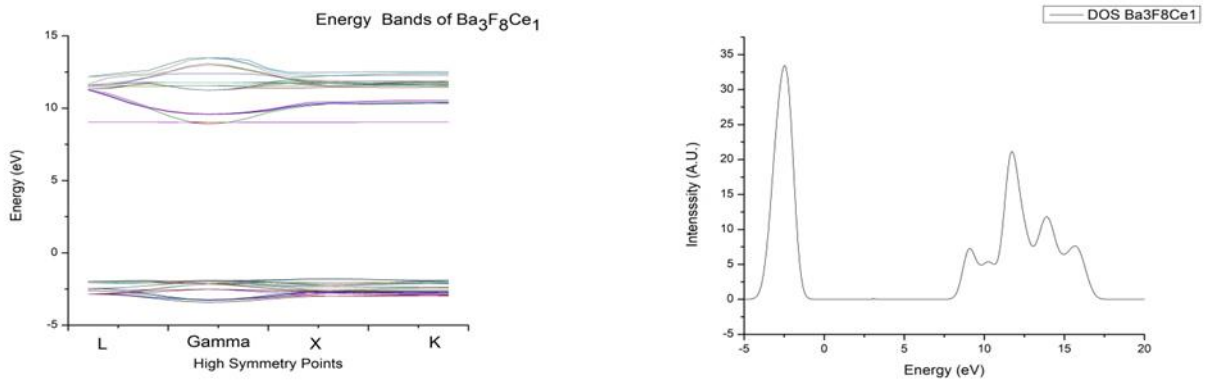

Figure 7: a) energy band structure of $Ba_3F_8Ce_1$ and b) DOS of $Ba_3F_8Ce_1$

These intermediate states act as "stepping stones" for electrons. In the BaF2:Ce system, the 10.81 eV gap represents the energy difference between the highest occupied state and the lowest unoccupied state influenced by the dopant. Extra states acts as electron trap levels which are essential for thermoluminescence (TL) phenoomenon.The presence of these states is vital for TL dosimeters. Instead of a direct host-to-host recombination, electrons can be trapped by Ce centers, leading to the characteristic 5d to 4f radiative transitions.

Conclusion:

We have performed DFT approximation to study the electronic properties of BaF_2 and BaF_2:Ce. Our calculation shows that DFT approximation sufficiently reliable to investigate the material properties of BaF_2 and Ce doped BaF_2. Further DFT calculations showed that Ce reduces the energy band gap of the material. The calculated band gap are in good agreement with the experimental results.

The electronic properties of Barium Fluoride (BaF_2) and its Cerium-doped counterpart (BaF_2:Ce) provide critical insights into their performance as wide-bandgap thermoluminescence dosimeter. Analysis of the calculated energy band structures reveals a significant transformation in the electronic environment upon the introduction of trivalent Cerium (Ce^{3+}) ions into the cubic lattice of the host material. Controlled doping of Ce into host BaF_2 creates a electron trap levels and hence Ce doped BaF_2 could be used for the Thermoluminescence dosimetry.

References:

1. J.R. Cameron, F. Daniels, H. Johnson, G.N. Kenney, (1961) Science 134 333–334.
2. P.J. Fox, R.A. Akber, J.R. Prescott, (1988) J. Phys. D 21 189.
3. A.M. Noh, Y.M. Amin, R.H. Mahat, D.A. Bradley, (2001) Radiat. Phys. Chem. 61 497–499.
4. P. Giannozzi, et al., (2009) J. Phys: Condens. Matter 21 395502.
5. S. Hou, Y. Xing, X. Liu, Y. Zou, B. Liu, X. Sun, (2010) Cryst. Eng. Comm. 12 1945.
6. N. Abe, Y. Yokota, T. Yanagida, J. Pejchal, F. Nara, N. Kawaguchi, K. Fukuda, M. Nikl, A. Yoshikawa, Jpn. (2010) J. Appl. Phys. 49 022601.
7. G. De, W. Qin, J. Zhang, J. Zhang, Y. Wang, C. Cao, Y. Cui, (2006) J. Solid State Chem. 179 955.

International Journal of Advance and Applied Research
www.ijaar.co.in
ISSN – 2347-7075 Impact Factor – 8.141
Peer Reviewed Bi-Monthly
Vol. 7 No. 14 January – February - 2026

Role of Fuel and Their Ratio with Metal Nitrates in Combustion Synthesis of Spinel Ferrite Nanoparticles

Kalyani K. Deshmukh[1], Shital P. Nawale[2], Kajal A. Gurav[1], Atul. P. Keche[3], K. M. Jadhav[4]

[1]*Department of Physics, Deogiri College, Chhatrapati Sambhajinagar-431005, MS, India*

[2]*Department of Physics, Shivchhatrapati College, Chhatrapati Sambhajinagar- 431003, MS, India*

[3]*Department of Physics, R.B. Attal, Arts, Science and Commerce College, Georai-431127, India, (MS)*

[4]*School of Basic and Applied Science, MGM University, Chhatrapati Sambhajinagar-431003, India (MS)*

Corresponding Author – Kalyani K. Deshmukh

DOI - 10.5281/zenodo.19826882

Abstract:

Spinel ferrite magnetic nanoparticles were synthesised by the sol–gel auto-combustion method using glycine and citric acid as fuels. The fuel-to-metal nitrate ratio was adjusted based on the oxygen balance of the reaction. A comparative study was carried out to investigate the effect of fuel type on the structural properties of cobalt ferrite nanoparticles. The phase formation, crystallinity, and structural parameters of the synthesised samples were analysed using X-ray diffraction (XRD). The XRD results confirmed the formation of single-phase cubic spinel cobalt ferrite without any secondary phases. Variations in crystallite size and lattice parameters were observed depending on the type of fuel used, indicating that the combustion behaviour significantly influences the structural characteristics of the material.

Keywords: $CoFe_2O_4$, Sol-Gel Auto- Combustion Method, Glycine, Citric acid, crystallite size, Lattice constant.

Introduction:

Nanoscale spinel-structured ferrites are among the most attractive magnetic materials because they demonstrate superior magnetic and electrical properties compared to their bulk counterparts[1]. Owing to these distinctive characteristics, they have gained significant attention not only for fundamental scientific investigations but also for a wide range of practical applications in electronics, catalysis, biotechnology, and medical science [ref]. When reduced to the nanometer scale, spinel ferrite particles often exhibit superparamagnetic behaviour due to their extremely small particle size[2] . These nanoparticles typically possess diameters in the nanometer range and, in certain cases, exhibit high coercivity, making them highly suitable for advanced technological applications. Such nanomaterials play an important role in modern technologies, including their use as contrast agents in magnetic resonance imaging (MRI), high-density data storage systems, ferrofluid devices, and magnetocaloric refrigeration technologies [3].

The development of efficient synthetic routes to produce nanosized materials with enhanced magnetic properties compared to their bulk counterparts has attracted considerable scientific interest[1]. Nanoscale magnetic materials exhibit unique structural, electrical, and magnetic characteristics arising from size confinement and surface effects[4]. Among these materials, spinel ferrite nanoparticles have attracted significant attention due to their

versatile applications in electronics, catalysis, biomedicine, and magnetic devices[5].

Various wet chemical techniques have been widely employed for the synthesis of spinel ferrite nanoparticles[5]. These include chemical co-precipitation, sol–gel processing, hydrothermal and solvothermal methods, thermal decomposition, and microwave-assisted combustion techniques[6]. Wet chemical approaches are generally preferred because they are cost-effective, require relatively low processing temperatures, consume less time, and provide better control over particle size and homogeneity. As a result, they have become the most commonly adopted methods for preparing nanoscale magnetic ferrites[7].

Among these methods, the sol–gel auto-combustion technique is considered one of the most efficient and convenient routes for synthesizing fine ferrite powders[8]. This technique typically involves low reaction temperatures (80–100 °C) and results in rapid powder formation[9]. The process consists of forming a homogeneous sol, transforming it into a gel, and subsequently initiating self-sustained combustion in a solution containing metal salts and a suitable organic fuel[9]. The combustion reaction produces a fine, voluminous, porous powder in a single step. However, the quality of the final product strongly depends on synthesis parameters, such as the type of fuel, the fuel-to-metal nitrate ratio, the solution pH, and the annealing temperature[9]. The heat evolved during combustion and the corresponding flame temperature significantly influence phase formation, crystallinity, particle size, surface area, and agglomeration behaviour[9].

The nature of the fuel plays a crucial role in the sol–gel auto-combustion process. Organic fuels differ in their complexing ability with metal cations, reducing power, and the number of gaseous products evolved during combustion[10]. Therefore, the appropriate selection of fuel is essential to achieve desirable structural and magnetic characteristics. Commonly used fuels include citric acid and glycine. These organic compounds act as both complexing agents and reducing agents[9]. During combustion, they generate gases such as CO_2 and H_2O along with the release of significant heat in an exothermic reaction. The evolution of gases increases the porosity of the resulting powder. The combustion intensity and thermal profile are directly influenced by the chemical nature of the selected fuel[9].

Among various spinel ferrites, cobalt ferrite ($CoFe_2O_4$) is particularly important due to its inverse spinel structure in which Co^{2+} ions predominantly occupy the octahedral (B) sites[11]. Nanocrystalline cobalt ferrite exhibits remarkable magnetic properties, including high saturation magnetization, high magneto-crystalline anisotropy, high coercivity, high electrical resistivity, and an elevated Curie temperature[12]. These features make it suitable for numerous technological applications, including magnetic recording media, sensors, permanent magnets, magnetic fluids, microwave devices, antenna rods, and catalytic systems[13].

Although several studies have reported the synthesis of cobalt ferrite nanoparticles using various wet-chemical routes, most investigations have focused primarily on structural and magnetic characterization, without thoroughly examining the influence of the fuel type on the final properties. In many reports, citric acid has been predominantly used as a fuel, while only limited studies have explored other fuels such as glycine. A systematic comparison of different fuels with respect to their impact on structural characteristics remains insufficiently addressed.

Therefore, the present study aims to synthesize nanocrystalline spinel cobalt ferrite using the sol–gel auto-combustion method with three different fuels, namely ethylene glycol, glycine, and urea. A comparative investigation of their structural properties has been carried out to understand the role of fuel chemistry in determining the final material characteristics.

Experimental Detail:

1. Materials:

Cobalt ferrite nanoparticles were synthesized using high-purity analytical grade precursors. Cobalt nitrate hexahydrate ($Co(NO_3)_2 \cdot 6H_2O$, 99.0% purity, HPLC, India) and ferric nitrate nonahydrate ($Fe(NO_3)_3 \cdot 9H_2O$, 99.1% purity, HPLC, India) were used as sources of Co^{2+} and Fe^{3+} ions, respectively. Aqueous ammonia solution (25% purity, HPLC, India) was employed to control and adjust the pH of the reaction medium. Citric acid (AR grade,99% purity, HPLC, India) and glycine (AR grade, 99% purity, HPLC, India) were used as the fuel in the sol–gel auto-combustion synthesis process.

2. Preparation of nanoparticles:

Nanocrystalline Cobalt ferrite ($CoFe_2O_4$) nanoparticles were synthesized via a sol–gel auto-combustion route employing two different organic fuels, namely glycine and citric acid, in separate experimental batches. Stoichiometric quantities of cobalt nitrate and ferric nitrate, corresponding to the molar ratio Co: Fe = 1:2, were dissolved in approximately 200 mL of deionized water under continuous magnetic stirring to obtain clear and homogeneous precursor solutions. The individual solutions were subsequently mixed and stirred thoroughly to ensure the uniform distribution of metal ions.

In the glycine-assisted synthesis, glycine was added as the fuel while maintaining a fuel-to-oxidizer molar ratio of 1:4.4, calculated based on redox stoichiometry. For the citric acid-assisted synthesis, the metal nitrate to fuel ratio was fixed at 1:3. In both cases, the respective fuel was dissolved separately and introduced gradually into the mixed nitrate solution under constant stirring to promote effective chelation and homogeneous complex formation.

The pH of the reaction mixture was adjusted to approximately 7 through the dropwise addition of dilute ammonia solution. The resulting solution was continuously stirred for nearly four hours to ensure complete complexation and uniform sol formation. The homogeneous sol was heated to approximately 80 °C to facilitate solvent evaporation and induce gel formation. Upon transformation into a viscous gel, stirring was discontinued, and the temperature was further increased to approximately 120 °C. At this stage, spontaneous self-ignition of the gel occurred, leading to a rapid combustion reaction and the formation of a voluminous, porous precursor powder.

The as-combusted powder was gently ground in an agate mortar and pestle to obtain a fine, uniform product. Finally, the powder was annealed at 650 °C for 6 hours in air to enhance crystallinity and achieve phase-pure spinel cobalt ferrite nanoparticles. A schematic illustration of the synthesis procedure is presented in **Figure 1.**

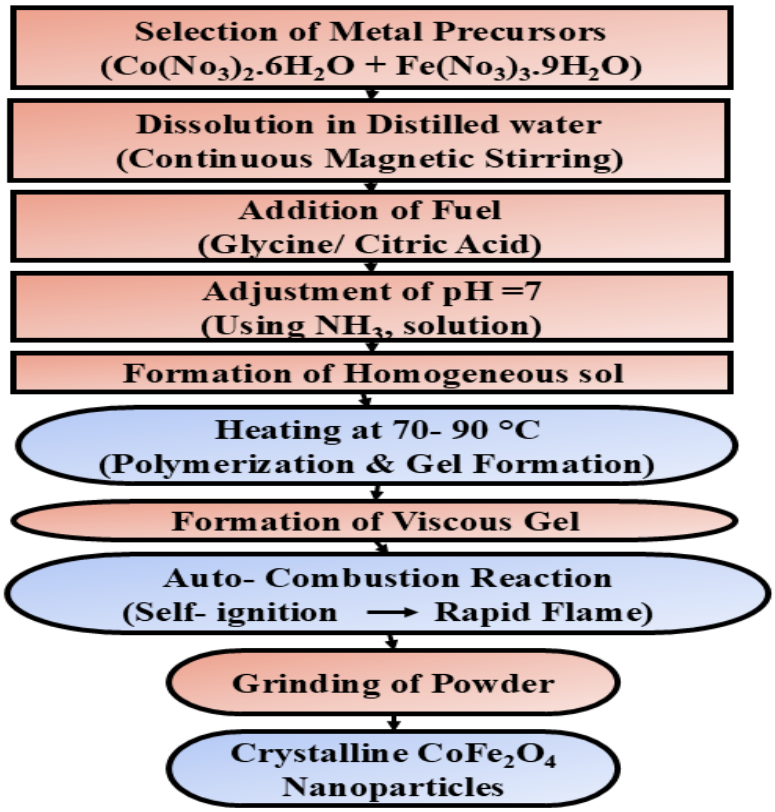

Figure 1: Schematic representation of the preparation of $CoFe_2O_4$ spinel ferrite nanoparticles.

Chemical reaction:

- **For Citric acid**

$Co(NO_3)_2 + 2Fe(NO_3)_3 + 3C_6H_8O_7 \rightarrow CoFe_2O_4 + CO_2 + H_2O + N_2 + Heat$

- **For Glycine**

$Co(NO_3)_2 + 2Fe(NO_3)_3 + 4.4C_2H_5NO_2 \rightarrow CoFe_2O_4 + 8.8CO_2 + 11H_2O + 3.2N_2 + Heat$

3. Characterization:

The crystal structure of $CoFe_2O_4$ nanoparticles was characterised by X-ray diffraction (XRD) analysis using a Rigaku Ultima-IV diffractometer equipped with Cu Kα radiation (λ = 1.5406 Å). The diffraction data were recorded in 2θ mode under continuous scanning conditions with a step size of 0.02°.

Results and Discussion:

1. XRD Analysis:

The X-ray diffraction (XRD) patterns of synthesized $CoFe_2O_4$ nanoparticles prepared using two different fuels, namely glycine (CG) and citric acid (CC), were analyzed as shown in **Figure 2 (a–b) [14].** The diffraction data were recorded in the 2θ range of 10°–80° using Cu-Kα radiation (λ = 1.5406 Å). Both samples exhibit characteristic diffraction peaks corresponding to the cubic spinel structure of $CoFe_2O_4$ with space group Fd-3m[15]. The prominent reflections indexed to the crystallographic planes (111), (220), (311), (222), (400), (422), (511), and (440) are clearly observed in both patterns. These peaks are in good agreement with the standard JCPDS data (card no. 22-1086), confirming the successful formation of a single-phase cubic spinel structure of cobalt ferrite nanoparticles,

with no detectable impurity phases[16]. The absence of additional diffraction peaks further indicates the high phase purity of the synthesized samples.

A careful comparison of the two XRD patterns reveals noticeable differences in peak intensity, sharpness, and full width at half maximum (FWHM). Sample (a) CG exhibits higher overall intensity with relatively broader peaks, suggesting good crystallinity along with possible lattice strain or variation in crystallite size. In contrast, sample (b) CC shows comparatively lower intensity but sharper and more well-defined peaks, indicating improved structural ordering and reduced microstrain. Overall, the XRD results confirm the successful synthesis of crystalline cobalt ferrite with a cubic spinel structure in both cases.

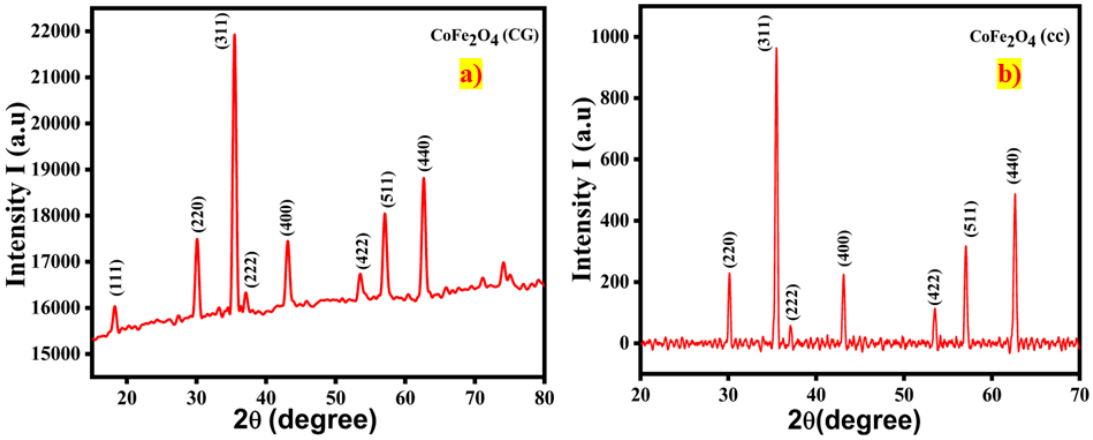

Figure 2: X-ray diffraction pattern of a) $CoFe_2O_4$ for Glycine (CG) b) $CoFe_2O_4$ for Citric acid (CC) spinel ferrite nanoparticles.

XRD analysis was employed to evaluate the structural parameters. The lattice constant (a) was determined using the interplanar spacing (d) and the corresponding Miller indices (h k l) through the application of the following relation[17].

$$a = d_{hkl}\sqrt{(h^2 + k^2 + l^2)}\ \text{Å} \quad (1)$$

The average crystallite size (t) of the synthesized $CoFe_2O_4$ nanocatalyst was estimated from the most intense (311) diffraction peak by using the corresponding Bragg angle (θ) and full width at half maximum (β). The calculated values are summarized in **Table 1.** The crystallite size was determined according to the Debye–Scherrer equation[17].

$$t = \frac{K\lambda}{\beta cos\theta} \quad (2)$$

The unit cell volume of the $CoFe_2O_4$ nanocatalyst was calculated from the experimentally determined lattice parameter using the standard relation[17]:

$$V = a^3 \quad (3)$$

where a denotes the lattice constant. The calculated values are summarised in **Table 1**.

The X-ray density (d_x) was evaluated using the following expression[17]:

$$d_x = \frac{ZM}{VN_A} \quad (4)$$

where Z represents the number of formula units per unit cell for the cubic structure, M is the molecular weight of the compound, V is the unit cell volume, and N_a (6.022×10^{23} mol^{-1}) is Avogadro's number. The corresponding density values are also listed in **Table 1.**

The dislocation density (δ) was estimated from the average crystallite size, considering the inverse relationship between these two

parameters. It was calculated using the following expression[17]:

$$\delta = \frac{1}{D^2} \quad (5)$$

where D represents the average crystallite size.

The stacking fault (SF) parameter was determined using the equation[17]:

$$SF = \frac{2\pi^2}{45\sqrt{3}\tan\theta} \quad (6)$$

Lattice strain (LS), an important microstructural parameter arising from distortions in lattice spacing due to defects or dislocations, was evaluated using[17]:

$$LS = \frac{\beta}{4\tan\theta} \quad (7)$$

where β denotes the full width at half maximum (FWHM) of the diffraction peak (in radians) and θ is the Bragg angle.

The microstrain (ε) was calculated according to[17]:

$$\varepsilon = \frac{\beta\cos\theta}{4} \quad (8)$$

where the symbols retain their usual meanings.

The microstructural parameters, dislocation density, stacking fault, lattice strain, and microstrain, are shown in **Table 2.**

Table 1: Values of Lattice constant (a), Crystallite size (t) (by Scherrer equation), Unit cell volume (V), X-ray density (d_x), for $CoFe_2O_4$ Spinel ferrite Nanoparticle.

Sample	a(Å)	t(nm)	v(Å)^3	dx(g cm^{-3})
$CoFe_2O_4$ (CG)	8.3865	13.08	589.86	5.28
$CoFe_2O_4$ (CC)	8.3841	28.14	589.34	5.29

Table 2: Values of Dislocation density δ, Stacking fault (SF), Lattice strain (LS), micro strain (Ɛ) for $CoFe_2O_4$ Spinel ferrite Nanoparticle.

Sample	δ(lines/m^2)	SF	(LS *10^{-3})	Ɛ*10^{-3}
$CoFe_2O_4$ (CG)	4.79	0.42	7.87	2.4
$CoFe_2O_4$ (CC)	1.33	0.43	4.22	1.34

The comparative analysis of the structural parameters for $CoFe_2O_4$ (CG) and $CoFe_2O_4$ (CC) reveals that both samples exhibit nearly identical cubic spinel structures, as evidenced by their very close lattice constants (8.3865 Å for CG and 8.3841 Å for CC) and corresponding unit cell volumes (589.86 Å^3 and 589.34 Å^3, respectively). The slight variation in lattice parameter results in a marginal difference in unit cell volume and X-ray density, with CC showing a slightly higher density (5.29 g cm^{-3}) compared to CG (5.28 g cm^{-3}), indicating minimal structural distortion and good phase consistency in both samples. However, a significant difference in crystallite size is observed: Cobalt ferrite for citric acid (CC) (28.14 nm) exhibits substantially larger crystallites than Cobalt ferrite for Glycine (CG) (13.08 nm), suggesting improved crystal growth and possibly lower defect concentration in the CC sample. Overall, both samples maintain structural stability, with the primary distinction arising from

differences in crystallite size rather than lattice structure.

The microstructural parameters listed in **Table 2** indicate noticeable differences between the two $CoFe_2O_4$ samples. The dislocation density (δ) of the Cobalt ferrite for glycine (CG) sample (4.79 lines m^{-2}) is significantly higher than that of Cobalt ferrite for citric acid (CC) (1.33 lines m^{-2}), suggesting a greater concentration of crystalline defects in Cobalt ferrite for glycine (CG). Similarly, the lattice strain (7.87×10^{-3}) and microstrain (2.4×10^{-3}) values are higher for (CG) compared to (CC) (4.22×10^{-3} and 1.34×10^{-3}, respectively), indicating increased lattice distortion in the CG sample. In contrast, the stacking fault (SF) values for both samples are nearly identical (0.42 for CG and 0.43 for CC), showing minimal variation in fault probability. Overall, the CC sample exhibits lower defect density and reduced lattice distortion, which is consistent with its larger crystallite size and improved crystallinity compared to the CG sample.

Conclusion:

The comparative analysis of glycine (CG) and citric acid (CC) as fuels in the sol–gel auto-combustion synthesis of $CoFe_2O_4$ nanoparticles demonstrates that the nature of the fuel significantly influences the structural characteristics of the final product. XRD results confirm that both fuels successfully facilitated the formation of single-phase cubic spinel $CoFe_2O_4$ without detectable impurity phases, highlighting the effectiveness of the sol–gel auto-combustion method. Nevertheless, noticeable differences were observed in crystallinity, peak sharpness, and microstructural features. The glycine-assisted sample exhibited higher combustion intensity owing to its stronger reducing nature and higher exothermicity, which promotes rapid reaction kinetics and enhanced crystal growth. In contrast, citric acid, acting as a milder reducing agent and an efficient chelating agent, provides better control over metal ion distribution during gel formation, leading to more homogeneous nucleation and comparatively improved structural ordering with reduced microstrain.

Acknowledgments:

The author, Kalyani K. Deshmukh, gratefully acknowledges financial support from the Chhatrapati Shahu Maharaj Research, Training, and Human Development Institute (SARTHI), Pune, and the Government of Maharashtra under the CMSRF-2022 scheme.

Declaration of competing interests:

The authors disclose that none of their ties or known conflicting financial interests might have appeared to have influenced the work described in this study.

Author Contributions:

Kalyani K. Deshmukh: Writing – original draft, Methodology, Investigation, Conceptualization. **Shital P. Nawale:** Formal analysis **Kajal A. Gurav:** Formal analysis **Atul. P. Keche:** Supervision, Data curation**. K.M. Jadhav**: Writing – review & editing, Validation, Supervision.

Funding sources:

This research did not receive any specific grant from funding agencies in the public, commercial, or not-for-profit sectors.

Data Availability:

Data sharing does not apply to this article as no datasets were generated or analysed during the current study.

Reference:

1. Salih, S.J. and W.M. Mahmood, (2023)*Review on magnetic spinel ferrite (MFe2O4) nanoparticles: From synthesis to application.* Heliyon,. **9**(6).
2. Sarkar, B. and A. Bandyopadhyay, (2021) *Studies of magnetic behavior of chemically synthesized interacting superparamagnetic copper ferrite nanoparticles.* Journal of Materials Science: Materials in Electronics,. **32**(2): p. 1491-1505.
3. Mengesha, W.G. and K. Nagessar, (2025) *Advanced thermal and magnetic materials for high-power and high-temperature applications: a comprehensive review.* Discover Materials, **5**(1): p. 180.
4. Ismail, I. and R.a.S. Azis, (2024) *A review of magnetic nanocomposites for EMI shielding: synthesis, properties, and mechanisms.* Journal of Materials Science,. **59**(13): p. 5293-5329.
5. Krishnan, Y., et al., (2024) *Spinel cobalt ferrite nanoparticles for photocatalysts, sensor and biomedical applications: a review.* Semiconductors. **58**(9): p. 721-739.
6. Taneja, S., et al., (2022) *Synthesis of nanomaterials by chemical route*, in *synthesis and applications of nanoparticles*., Springer. p. 61-76.
7. Vidya, Y., et al., (2023) *Brief review on magnetic properties of nanoferrites.* Inorganic Chemistry Communications,. **158**: p. 111408.
8. Hussain, Q., et al., (2024) *Sol-gel auto-combustion synthesis of Co0. 5Cu0. 5Cr0. 5GdxFe1. 5-xO4 spinel ferrites and their magneto-dielectric properties.* Ceramics International,. **50**(21): p. 43490-43499.
9. Bhagwat, V., et al. (2019) *Sol-gel auto combustion synthesis and characterizations of cobalt ferrite nanoparticles: Different fuels approach.* Materials Science and Engineering: B,. **248**: p. 114388.
10. Roostaei, S., et al., (2025) *Sol–gel auto-combustion synthesis of a novel ternary magnetic-recyclable ZnFe2O4/ZnO/CeO2 nano-photocatalyst for highly efficient visible-light-induced degradation of organic contaminants.* Applied Water Science,. **15**(8): p. 193.
11. Pham, T.N., et al., (2023) *Toward a comprehensive understanding of effect of cation distribution and M2+ constituent in spinel ferrite nanocrystals MFe2O4 (M= Co, Mn, and Ni) on the electrochemical response in sensitive detection of chloramphenicol.* Journal of Alloys and Compounds,. **949**: p. 169880.
12. Ansari, S.M., et al., (2025) *Cobalt ferrite nanoparticles: The physics, synthesis, properties, and applications.* Applied Physics Reviews,. **12**(2).
13. Aiswarya, R., (2024) *Magnetic properties: introduction, types, and applications*, in *Green Magnetic Nanoparticles (GMNPs)*., Elsevier. p. 23-51.
14. Chavarriaga, E., et al., (2022) *Influence of caffeine and citrulline on magnetic properties when used as new fuels in the synthesis of CoFe2O4 nanoparticles by gel combustion.* Journal of Magnetism and Magnetic Materials,. **560**: p. 169632.
15. Sharada, G., et al., (2025) *Impact of low Dy doping concentration on structural, and magnetic behaviour of CoFe2O4.* Journal of the Australian Ceramic Society,: p. 1-11.
16. Deshmukh, K.K., et al., (2025) *Impact of Mn2+-Ti4+ dopant on the photocatalytic dye degradation efficiency of cobalt ferrite nanoparticle.* Ceramics International, **51**(23): p. 38039-38059.
17. Deshmukh, K.K., et al., (2026) *Role of tetravalent Ti4+ doping on the photocatalytic application of cobalt ferrite nanoparticles.* Materials Science and Engineering: B,. **323**: p. 118807.

International Journal of Advance and Applied Research
www.ijaar.co.in
ISSN – 2347-7075 Impact Factor – 8.141
Peer Reviewed Bi-Monthly
Vol. 7 No. 14 January – February - 2026

Noradrenaline-Polyaniline Composite: A galvanostatic Approach

Kamble Pravin Ashruba, Takle Ganesh Baburao. Gaikwad Pradeep Devendra
R.B. Attal Arts, Science and Commerce College Georai,
Taluka Georai, Dist. Beed 431127
Corresponding Author – Kamble Pravin Ashruba
DOI - 10.5281/zenodo.19826900

Abstract:
Noradrenaline neurotransmitter released from axon terminals of sympathetic postganglionic neurons in direct relation to its effector cells; transport via the circulation is not required to explain its metabolic (PANI) is a conducting polymer. In Present paper work Polyaniline (PANI) composites were synthesized bye Galvanostatic Method. the polymeric charge transfer of the composite. synthesizes composites.

Keywords: Conducting polymer, Polyaniline, Noradrenaline, Galvanostatic Method

Introduction:

The strong π-π conjugated macromolecules such as Polyaniline (PANI) is most interesting Conducting polymers. Polyaniline have many attractive features owing to its unique conduction mechanism, easy proton doping, film forming ability favourable environmental stability. The fig.1 show basic structure of polyaniline

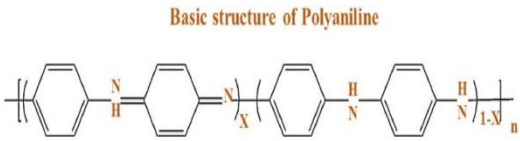

Fig.1.Basic Structure of Polyaniline

Neurotransmitter is chemical messenger, tmultiple approaches have been proposed for neurotransmitter detection and monitoring. neurotransmitter. Norepinephrine and epinephrine, also known as noradrenaline and adrenaline respectively, In the brain, norepinehrine neurons are localized in the locus coerulus, a nucleus in the brainstem structure of noradrenaline is given below in figure 2.

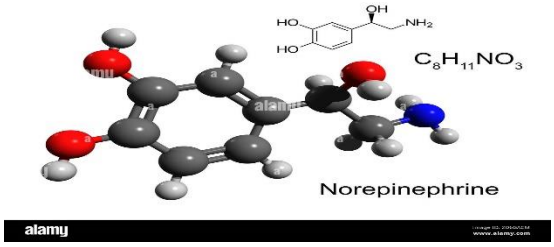

Fig.2. Structure of Norepinephrine

The objective is to synthesis Noradrenaline-Polyaniline Composite materials for Potentiometric Sensing and biomedical Applications.

Experimental:

Materials & Chemicals:

Aniline as monomer Noradrenaline, HCl as Supporting electrolyte and aqueous solution as Distilled water It consists of a working electrode(ITO), counter electrode(Platinium), and reference electrode(Ag-AgCl).

Method :

Galvanostatic Method is a Constant current resulting potential of the system. [11-13]

Result and Discussion:

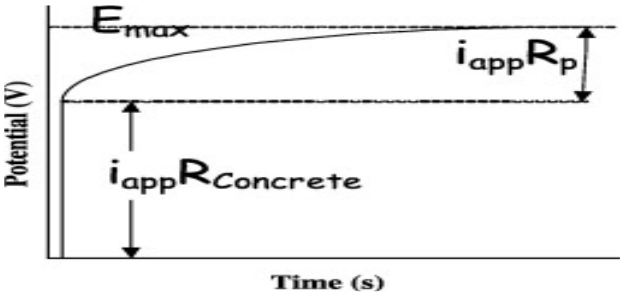

Figure 3. A typical galvanostatic electro polymerized chronopotentiogram curve.

The behaviour of the galvanostatic synthesis during the first few seconds probably indicates the difficult formation of dimers and oligomers. The potential becomes constant suggesting that formation of the film as shown above in figure 3.

Result and Discussion:

Electrochemical synthesis methods, such as galvanostatic polymerization, enable precise incorporation of Noradrenaline into the Polyaniline PANI matrix, resulting in composites with enhanced stability and tunable properties Noradrenaline-Polyaniline offer superior biocompatibility and multifunctionality, making them promising candidates for Biomedical potentiometric sensing. These Noradrenaline-Polyaniline materials are increasingly explored for Biomedical applications such as Pharmaceutical analysis, Biological fluid monitoring and Clinical diagnostics

Conclusion:

A Galvanostatic approach of Synthesised Noradrenaline-Polyaniline composites represent a promising class of materials for potentiometric sensing for targeting monoamine neurotransmitters.

Acknowledgement:

Author thanks to Department of Physics R. B. Attal College Georai Support for experimental work.

References:

1. C.I. Awuzie Conducting Polymers Department of Science Laboratory Technology, Federal Polytechnic Oko-42312, Anambra State, Nigeria
2. Shimwe Dominique Niyonambaza 1,2, Praveen Kumar 1, Paul Xing 3, Jessy Mathault 1,Paul De Koninck 1,4, Elodie Boisselier 2,5 , Mounir Boukadoum 6 and Amine Miled A Review of Neurotransmitters Sensing Methods for Neuro-Engineering Research Tri-Dung Ngo Introduction to Composite Materials
3. D.J. Shirale, V.K. Gade, P.D. Gaikwad, H.J. Kharat, K.P. Kakde, P.A. Savale, S.S. Hussaini, N.R. Dhumane, M.D. Shirsat The influence of electrochemical process parameters on the conductivityof poly(N-methylpyrrole) films by galvanostatic method.
4. Deshmukh VB1, Paithankar KS1, Shelke UN 1, More ST 2, Iyyer SB 1 and Gade VK3 Study of Influence for Various Parameters to Electro-chemical Synthesis of Polyaniline Thin Film by Galvanostatic Method
5. Leticia Perez Rial Classification, Types, and Chemistry of Polymers .
6. S.A. Waghuley Applications of Polyaniline-Based Blends, Composites, and Nanocomposites.
7. P D Gaikwad, D J Shirale, V K Gade, P A Savale, K P Kakde, H J Kharat and M D

Shirsat Potentiometric study of polyaniline film synthesized with variousdopants and composite-dopant: A comparative study.

8. Poursaee , C.M. Hansson Galvanostatic pulse technique with the current confinement guard ring: The laboratory and finite element analysis.
9. Audrey Sassolas, Beatriz Prieto-Simón, Jean-Louis Marty,American (2012) Journal of Analytical Chemistry,
10. Gade V.K., D.J. Shirale, P.D. Gaikwad, P.A. Savale, K.P. Kakde, H.J. Kharat, M.D. Shirsat (2006) Reactive Functional Polymers
11. Lawal A.T., S.B. (2010) A deloju Journal of Molecular Catalysis B: Enzymatic.
12. Skotheim TA, R.L. Elsenbaumer and J.R. Reynolds (Ed.) (1998) Handbook of Conducting Polymers Vol 2 Marcel Dekker, New York,
13. Rahman M. M., Muhammad J.A. Shiddiky , Md. Aminur Rahman, Yoon-Bo Shim , (2009) Analytical Biochemistry.
14. Arunas Ramana vicius, Asta Kau sait, Almira Ramana viciene, (2005) Sensors and Actuators, B,.
15. Ntlatseng G.R. Mathebe, Aoife Morrin, Emmanuel I. Iwuoha Talanta (2004)

International Journal of Advance and Applied Research
www.ijaar.co.in
ISSN – 2347-7075 Impact Factor – 8.141
Peer Reviewed Bi-Monthly
Vol. 7 No. 14 January – February - 2026

Topological Polynomials in Fuzzy Hamiltonian Graph

N. K. Raut

Ex. Head, Dept. of Physics, Sunderrao Solanke Mahavidyalaya Majalgaon, Dist. Beed, (M.S.) INDIA

Corresponding Author – N. K. Raut

DOI - 10.5281/zenodo.19826950

Abstract:

A fuzzy graph G = (σ, μ) is a pair of functions of membership values of vertices and edges. A fuzzy Hamiltonian graph is a connected fuzzy graph containing a fuzzy cycle that visits every vertex exactly once, except for the starting and ending vertex coincide. The first and second Zagreb polynomial for fuzzy Hamiltonian graph are defined as: $M_1(G,x) = \sum_{u\in V} x^{\sigma(u)\,(d_G(u))^2}$ *and* $M_2(G,x)=\sum_{uv\in E} x^{\frac{1}{2}[\sigma(u)d_G(u)\times\sigma(v)d_G(v)]}$ *respectively, where* $d_G(u)$ *is the degree of the vertex u and* $\sigma(u)$ *is the membership value of the vertex u in G. In this paper first, second Zagreb polynomials, hyper first, second Zagreb polynomials, forgotten polynomial, harmonic polynomial and Randic polynomial are investigated for fuzzy Hamiltonian graph.*

Keywords: Degree, Hamiltonian cycle, Hamiltonian path, Fuzzy Hamiltonian graph, membership value.

Introduction:

Let G = (V, E) be a graph consisting of a non-empty finite set V of elements called vertices and a finite set E of ordered pairs of distinct vertices called edges. In Fuzzy set theory we assign a membership value to each element of the set which ranges from 0 to 1. The underlying crisp graph of a fuzzy graph G = (σ, μ) is denoted by $G^* = (\mu^*, \sigma^*)$ where $\sigma^* = \{v \in V|\sigma(v) > 0\}$ and $\mu^* = \{(u, v) \in V \times V\ |\mu(u, v) > 0$. A fuzzy graph G = (σ, μ) is a pair of functions $\sigma: V \to [0, 1]$ and $\mu: V \times V \to [0, 1]$ such that for all u, v ∈ V, $\mu(u, v) \leq \sigma(u) \wedge \sigma(v)$ and μ is a symmetric fuzzy relation on σ. Here σ(v) and μ(u, v) represent the membership values of the vertex v and of the edge (u, v) respectively [1-5]. A fuzzy graph G: (σ, μ) is said to be complete if $\mu(u,v)=\sigma(u)\wedge\sigma(v)$ for all u and v.

A Hamiltonian path is a path in an undirected or directed graph that visits each vertex exactly once. A Hamiltonian circuit is a Hamiltonian path that is a cycle. A cycle passing through all the vertices of a graph is called a Hamiltonian cycle. A graph containing a Hamiltonian cycle is called a Hamiltonian graph. If the last edge of a Hamiltonian cycle is dropped, we get a Hamiltonian path. A connected fuzzy graph G (σ, μ) is said to be a fuzzy Hamiltonian graph if there exists a fuzzy cycle which covers all the nodes of fuzzy graph G (σ, μ) exactly once except the terminal nodes [6-7]. The problem of finding Hamiltonian cycles is named after William Rowan Hamilton, an Irish mathematician who was a big fan of the dodecahedron (the 3D shape whose sides are twelve pentagons) [8]. All vertices and edges in the Hamiltonian cycle has positive membership values.

A fuzzy graph G is fuzzy Hamiltonian if there exists some $\alpha > 0$, such that the crisp graph G_α is Hamiltonian. This connects fuzzy Hamiltonicity directly to classical Hamiltonian graph theory. Hamiltonicity is the property of a graph of containing a cycle that visits every

vertex exactly once. When we say "is Hamiltonian'', means the graph G contains a Hamiltonian cycle. It helps us to understand Hamiltonicity of a fuzzy graph using classical graph theory. Some classical sufficient conditions for Hamiltonicity are: 1) Dirac theorem: if |V(G)|= n ≥ 3, minimum degree δ(G) ≥ n/2, n-number of vertices [9]. Ore's theorem: if for every pair of non-adjacent vertices (u, v), $d_u + d_v \geq n$ [10]. Fuzzy Hamiltonian graphs are used in communication networks with uncertain links, transportation systems under varying reliability, molecular topology and decision-making problems. Effective Eulerian and fuzzy Hamiltonian graph were studied in [11]. A graph G is Hamiltonian if and only if its closure is Hamiltonian. Sufficient conditions for Hamiltonian fuzzy graphs given in [12]. A graph G is Hamilton-connected (HC) if every two vertices of G are connected by a Hamiltonian path. All complete graphs are Hamilton connected and thus Hamiltonian [13]. Characteristics of fuzzy wheel and Hamiltonian graph with fuzzy rule were studied in [14]. The algorithm for finding a Hamiltonian cycle in an intuitionistic fuzzy graph (IFG), based on the theories of intuitionistic fuzzy sets (IFSs) and of index matrices (IMs) were proposed in [15]. A graph is said to be hypo Hamiltonian if for each v ∈ V(G), the vertex sub graph G-v is Hamiltonian [16]. Complete fuzzy graph K_{2n+1} can be decomposed to n Hamiltonian fuzzy cycles [17]. Shortest distances in Hamiltonian fuzzy cycles computed in [18]. The fuzzy Hamiltonian cycles constitute the routes for transportation network and starting point, which gives the shortest travel time [19]. Sombor index in fuzzy graph was computed in [20] using degrees and membership values of vertices in G.

The first, second Zagreb polynomials and hyper-Zagreb polynomials can be defined as [21]

$$M_1(G,x) = \sum_{u\in V} x^{\sigma(u)\,(d_G(u))^2}. \quad (1)$$

$$M_2(G,x)=\sum_{uv\in E} x^{\frac{1}{2}[\sigma(u)d_G(u)\times\sigma(v)d_G(v)]}. \quad (2)$$

$$HM_1(G, x)=\sum_{uv\in E} x^{[\sigma(u)\,d_G(u)+\sigma(v)\,d_G(v)]^2}. \quad (3)$$

$$HM_2(G, x)=\sum_{uv\in E} x^{[\sigma(u)\,d_G(u)\times\sigma(v)\,d_G(v)]^2} \quad (4)$$

where $d_G(u)$ and $\sigma(u)$ is the degree and membership value of the vertex u respectively in the fuzzy graph G.

Forgotten polynomial is defined as

$$F(G,x)= =\sum_{v\in V} x^{[\sigma(v)d_G(v)]^3}. \quad (5)$$

Harmonic polynomial can be defined as

$$H(G,x) = \sum_{uv\in E} x^{\frac{1}{2}\frac{1}{[\sigma(u)d_G(u)+\sigma(v)d_G(v)]}}. \quad (6)$$

Randic polynomial can be defined as

$$R(G,x) = \sum_{uv\in E} x^{\frac{1}{2}\frac{1}{[\sqrt{\sigma(u)d_G(u)\times\sigma(v)d_G(v)}]}}. \quad (7)$$

The symbols, notations are standard and taken from [22-24]. In this paper first, second Zagreb polynomials, hyper first, second Zagreb polynomials, forgotten polynomial, harmonic polynomial and Randic polynomial are investigated for fuzzy Hamiltonian graph.

Materials and Methods:

The fuzzy degree of a vertex u in G is defined as the sum of all the weights of edges corresponding to the vertex u that is $d_G(u) = \sum_{uv\in E} \mu(u,v)$.The Hamiltonian path is represented in figure (1) and Hamiltonian cycle in fig. (2). The fuzzy Hamiltonian graph is shown in figure (3). Fuzzy Hamiltonian graph in figure (4) with membership values of vertices and edges is used to compute topological polynomials [25].

Results and Discussion:

The a-b-c-d is a Hamiltonian path in figure (1) and a-b-c-d-e-a is Hamiltonian cycle in fig. (2). Consider fuzzy Hamiltonian graph (fig.4), in which we have three Hamiltonian cycles as: 12345671, 13572461, 14736251.The

vertices with membership values are σ(0.7), σ(0.6), σ(0.7), σ(0.5), σ(0.3), σ(0.7) and σ(0.6) and the degrees for vertices are:

$d_G(V_1) = 0.4+0.5+0.6+0.7+0.8+0.9 = 3.9$,

$d_G(V_2) = 0.9+0.55+0.65+0.75+0.85+0.3 = 4$,

$d_G(V_3) = 0.3+0.8+0.25+0.35+0.95+0.45 = 3.1$,

$d_G(V_4) = 0.45+0.85+0.7+0.1+0.2+0.15 = 2.45$,

$d_G(V_5) = 0.15+0.95+0.75+0.6+0.8+0.3 = 3.55$,

$d_G(V_6) = 0.3+0.2+0.35+0.65+0.5+0.4 = 2.4$

and $d_G(V_7) = 0.4+0.55+0.25+0.1+0.8+0.4 = 2.5$.

The membership values of edges are:

μ(1, 2)=0.9, μ(2,3)=0.3, μ(3, 4)=0.45, μ(4, 5)=0.15, μ(5, 6)=0.3, μ(6,7)=0.4 and μ(7,1)=0.4.

Theorem 1. First Zagreb polynomial in fuzzy Hamiltonian graph is $x^{10.65}+x^{9.6}+x^{6.727}+x^{3.1}+x^{3.781}+x^{4.032}+x^{3.75}$.

Proof. Using membership values of vertices and edges from figure (4), we have first Zagreb polynomial in fuzzy Hamiltonian graph

$F_HM_1(G,x) = \sum_{u\in V} x^{\sigma(u)\,(d_G(u))^2}$.

$= x^{0.7\times(3.9)^2}+x^{0.6\times(4)^2}+x^{0.7\times(3.1)^2}+x^{0.5\times(2.45)^2}+x^{0.3\times(3.55)^2}+x^{0.7\times(2.4)^2}+x^{0.6\times(2.5)^2}$

$= x^{10.65}+x^{9.6}+x^{6.727}+x^{3.1}+x^{3.781}+x^{4.032}+x^{3.75}$.

Theorem 2. Second Zagreb polynomial in fuzzy Hamiltonian graph is $x^{3.276}+x^{2.604}+x^{1.329}+x^{0.652}+x^{0.8946}+x^{1.26}+x^{2.047}$.

Proof. Using membership values of vertices and edges from figure (4), we get second Zagreb polynomial in fuzzy Hamiltonian graph

$F_HM_2(G,x)=\sum_{uv\in E} x^{\frac{1}{2}[\sigma(u)d_G(u)\times\sigma(v)d_G(v)]}$

$=x^{\frac{1}{2}[(0.7)3.9\times(0.6)4]}+x^{\frac{1}{2}[(0.6)4\times(0.7)3.1]}+x^{\frac{1}{2}[(0.7)3.1\times(0.5)2.45]}+x^{\frac{1}{2}[(0.5)2.45\times(0.3)3.55]}+x^{\frac{1}{2}[(0.3)3.55\times(0.7)2.4]}+x^{\frac{1}{2}[(0.7)2.4\times(0.6)2.5]}+x^{\frac{1}{2}[(0.6)2.5\times(0.7)3.9]}$

$= x^{3.276}+x^{2.604}+x^{1.329}+x^{0.652}+x^{0.8946}+x^{1.26}+x^{2.047}$.

Theorem 3. First hyper Zagreb polynomial in fuzzy Hamiltonian graph is $x^{26.32}+x^{20.88}+x^{11.53}+x^{5.244}+x^{7.535}+x^{10.12}+x^{17.89}$.

Proof. First hyper Zagreb polynomial in fuzzy Hamiltonian graph

$F_HHM_1(G, x) = \sum_{uv\in E} x^{[\sigma(u)\,d_G(u)+\sigma(v)\,d_G(v)]^2}$

$=x^{[(0.7)3.9+(0.6)4]^2}+x^{[(0.6)4+(0.7)3.1]^2}+x^{[(0.7)3.1+(0.5)2.45]^2}+x^{[(0.5)2.45+(0.3)3.55]^2}+x^{[(0.3)3.55+(0.7)2.4]^2}+x^{[(0.7)2.4+(0.6)2.5]^2}+x^{[(0.6)2.5+(0.7)3.9]^2}$

$= x^{26.32}+x^{20.88}+x^{11.53}+x^{5.244}+x^{7.535}+x^{10.12}+x^{17.89}$.

Theorem 4. Second hyper Zagreb polynomial in fuzzy Hamiltonian graph is $x^{42.93}+x^{27.12}+x^{7.066}+x^{1.703}+x^{3.201}+x^{6.351}+x^{16.76}$.

Proof. Second hyper Zagreb polynomial in fuzzy Hamiltonian graph

$F_HHM_2(G, x) = \sum_{uv\in E} x^{[\sigma(u)\,d_G(u)\times\sigma(v)\,d_G(v)]^2}$

$=x^{[(0.7)3.9\times(0.6)4]^2}+x^{[(0.6)4\times(0.7)3.1]^2}+x^{[(0.7)3.1\times(0.5)2.45]^2}+x^{[(0.5)2.45\times(0.3)3.55]^2}+x^{[(0.3)3.55\times(0.7)2.4]^2}+x^{[(0.7)2.4\times(0.6)2.5]^2}+x^{[(0.6)2.5\times(0.7)3.9]^2}$

$= x^{42.93}+x^{27.12}+x^{7.066}+x^{1.703}+x^{3.201}+x^{6.351}+x^{16.76}$.

Theorem 5. The forgotten polynomial in fuzzy Hamiltonian graph is $x^{20.35}+x^{13.82}+x^{10.22}+x^{1.838}+x^{1.207}+x^{4.742}+x^{3.375}$.

Proof. Using membership values of vertices and edges from figure (4), we get forgotten polynomial in fuzzy Hamiltonian graph

$F_HF(G,x) = \sum_{v\in V} x^{[\sigma(v)d_G(v)]^3}$

$= x^{[(0.7)3.9]^3}+x^{[(0.6)4]^3}+x^{[(0.7)3.1]^3}+x^{[(0.5)2.45]^3}+x^{[(0.3)3.55]^3}+x^{[(0.7)2.4]^3}+x^{[(0.6)2.5]^3}$

$= x^{20.35}+x^{13.82}+x^{10.22}+x^{1.838}+x^{1.207}+x^{4.742}+x^{3.375}$.

Theorem 6. Harmonic polynomial in fuzzy Hamiltonian graph is $x^{0.0975}+x^{0.1094}+x^{0.1472}+x^{0.2183}+x^{0.1822}+x^{0.1572}+x^{0.1182}$.

Proof. Harmonic polynomial in fuzzy Hamiltonian graph

$F_HH(G,x) = \sum_{uv\in E} x^{\frac{1}{2}\frac{1}{[\sigma(u)d_G(u)+\sigma(v)d_G(v)]}}$

$=x^{\frac{1}{2}\frac{1}{[(0.7)3.9+(0.6)4]}} + x^{\frac{1}{2}\frac{1}{[(0.6)4+(0.7)3.1]}} +$

$x^{\frac{1}{2}\frac{1}{[(0.7)3.1+(0.5)2.45]}} + x^{\frac{1}{2}\frac{1}{[(0.5)2.45+(0.3)3.55]}} +$

$x^{\frac{1}{2}\frac{1}{[(0.3)3.55+(0.7)2.4]}} + x^{\frac{1}{2}\frac{1}{[(0.7)2.4+(0.6)2.5]}} +$

$x^{\frac{1}{2}\frac{1}{[(0.6)2.5+(0.7)3.9]}}$

$= x^{0.0975} + x^{0.1094} + x^{0.1472} + x^{0.2183} + x^{0.1822} + x^{0.1572} + x^{0.1182}$.

Theorem 7. Randic polynomial in fuzzy Hamiltonian graph is $x^{0.1953} + x^{0.2191} + x^{0.3066} + x^{0.4423} + x^{0.3738} + x^{0.3215} + x^{0.247}$.

Proof. Randic polynomial in fuzzy Hamiltonian graph

$F_HR(G,x) = \sum_{uv\in E} x^{\frac{1}{2}\frac{1}{[\sqrt{\sigma(u)d_G(u)\times\sigma(v)d_G(v)}]}}$

$=x^{\frac{1}{2}\frac{1}{[\sqrt{(0.7)3.9\times(0.6)4}]}} + x^{\frac{1}{2}\frac{1}{[\sqrt{(0.6)4\times(0.7)3.1}]}} +$

$x^{\frac{1}{2}\frac{1}{[\sqrt{(0.7)3.1\times(0.5)2.45}]}} + x^{\frac{1}{2}\frac{1}{3\sqrt{(0.5)2.45\times(0.3)3.55}]}} +$

$x^{\frac{1}{2}\frac{1}{[\sqrt{(0.3)3.55\times(0.7)2.4}]}} + x^{\frac{1}{2}\frac{1}{[\sqrt{(0.7)2.4\times(0.6)2.5}]}} +$

$x^{\frac{1}{2}\frac{1}{[\sqrt{(0.6)2.5\times(0.7)3.9}]}}$

$= x^{0.1953} + x^{0.2191} + x^{0.3066} + x^{0.4423} + x^{0.3738} + x^{0.3215} + x^{0.247}$.

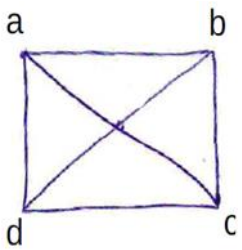

Figure 1. Hamilton path.

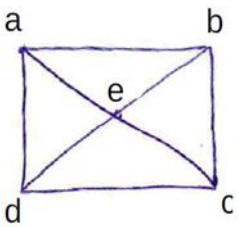

Fig.2. Fuzzy Hamilton graph.

Fig.3. Fuzzy Hamilton graph.

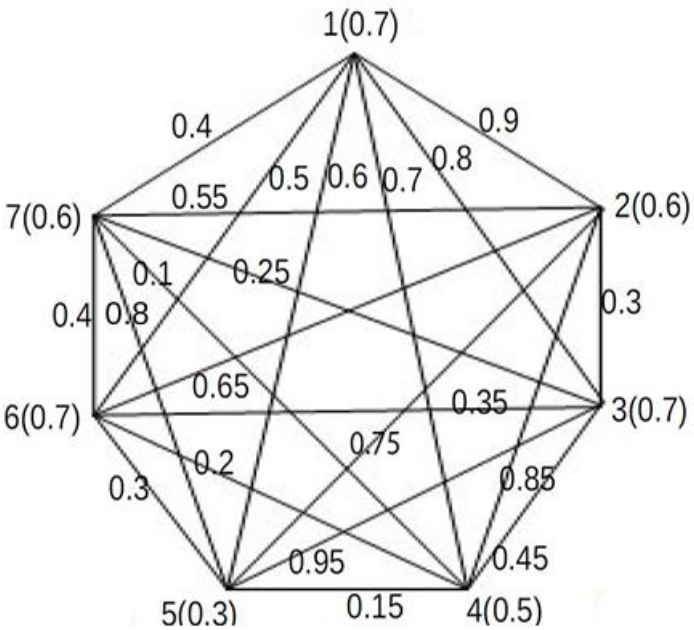

Figure 4. Fuzzy Hamilton graph.

Conclusion:

A graph containing a Hamiltonian cycle is called a Hamiltonian graph. If the membership values of vertices and edges in fuzzy Hamiltonian graph are known then the topological polynomials can be computed. In this paper first, second Zagreb polynomials, hyper first, second Zagreb polynomials, forgotten polynomial, harmonic polynomial and Randic polynomial are obtained for fuzzy Hamiltonian graph.

References:

1. A.K.Sharma, B.V.Padamwar and C.L.Dewangan, 2013)Trends in fuzzy graphs, International Journal of Innovative Research in Science, Engineering and Technology,2(9) (4636-4640.
2. M.R.Nidhin, A.Shukla, (2024) The versality of fuzzy graph in addressing uncertainty in data, International Journal of Advanced Research in Science, Communication and Technology,4(2) 863-868.
3. A.Nagoorgani, V.T.Chandrasekaran, (2010) A first look at fuzzy relation theory, Allied Publishers Pvt.Ltd.
4. S.Lavanya, S.Ramya, (2018) Edge domination in some special classes of fuzzy graphs, International Journal of Mathematics and its Applications,6(2-A) 141-144.
5. K.R.S.Narayan, M.S.Sunitha, (2012) Connectivity in a fuzzy graph and complement ,Gen.Math.Notes,9(1) 38-43.
6. A.Muneera, T.T.Nageswara Rao and R.V.N.Srinivasa Rao, (2019) Fuzzy Eulerian and Fuzzy Hamiltonian graphs with their applications, International Journal of Recent Technology and Engineering,8(4) 7995-7997.
7. M.Vijaya, A.Kannan, (2017) Number of Hamiltonian fuzzy cycles in cubic fuzzy graphs with vertices n, International Journal of Pure and Applied Mathematics Virtual Institute,117(6) 91-98.
8. W.R.Hamilton, (1835) Irish Mathematician, Hamiltonian Mechanics and Hamiltonians,
9. P. Dirac, (1952) A sufficient condition for a graph to be Hamiltonian, Graph Theory,
10. O.Ore, (1960) Note on Hamiltonian circuits. Am Math Mon, 67:55,
11. A.Nagoorgani, R.J.Hussain, (2008) Effective fuzzy Euler and fuzzy Hamiltonian graph, International Review of Fuzzy Mathematics,3(1) 55-68.
12. R.Li, (2022) Sufficient conditions for Hamiltonian fuzzy graphs, Annals of Pure and Applied Mathematics,26(1) 15-17.
13. S.Prabhu,Y.S.Nisha,M.Cary, M.Arulperumjothi and X.Li, (2024) On detour index of join of Hamiltonian-connected graphs, Ars Combinatoria,160 195-203.
14. D.Nisha, B.Srividhya, C(2019) haracteristics of fuzzy wheel graph and Hamiltonian graph with fuzzy rule, International Journal of Trend in Scientific Research and Development,3(6) 1061-1064.
15. V.Traneva, S.Tranev, (2020) Intuitionistic fuzzy Hamiltonian cycle index matrix, Proceeding of the Federated Conference on Computer Science and Information System, IEEE Catalogue number CFP2085N-ART,PTI, 345-348.
16. M.A.Shah, (2013) A study on hypo Hamiltonian graphs, African Journal of Mathematics and Computer Science Research,6(2) 16-19.

17. V.Kamalakannan, (2015) Hamiltonian decomposition of complete fuzzy graphs and some results using fuzzy matrices, International Journal of Innovative Science, Engineering and Technology,2(1) 413-418.
18. A.Parthiban, V.Kalalakanna and M.Senthilkumar, (2016) Computing shortest distance of Hamiltonian fuzzy cycles using eigen values, International Journal of Current Trends in Engineering and Technology,2(1) 13-17.
19. E.Cakir, Z.Ulukan and T.Acarman, (2021) Shortest fuzzy Hamiltonian cycle on transportation network using minimum vertex degree and time dependent Dijkstra's algorithm, Science Direct IFAC papers online,54-2, 348-353.
20. B.Some, M.Mondal and A.Pal, (2024) Numerous bounds and significance of Sombor index in fuzzy graph, Journal of Applied Mathematics and Computing, Springer.
21. Sk. R.Islam, M.Pal, (2023) F-index for fuzzy graph with applications, TWMS Journal of Applied and Engineering Mathematics, 13(2) 514-530.
22. M.Pal, S.Samanta and G.Ghorai, (2020) Modern Trends in Fuzzy Graph Theory, Springer,
23. J.A.Bondy and U.S.R.Murty, (1976) Graph Theory with Applications, Macmillan, London and Elsevier, New York
24. G.Chen, T.T.Phan, (2001) Introduction to Fuzzy sets, Fuzzy logic and Fuzzy control systems, CRC Press, Boca Raton, Lodon,
25. G.Nirmala, M.Vijaya, (2012) Hamiltonian fuzzy cycles on K_{2n+1} fuzzy graph, International Journal of Scientific and Research Publications,2(1) 1-6.

International Journal of Advance and Applied Research
www.ijaar.co.in
ISSN – 2347-7075 Impact Factor – 8.141
Peer Reviewed Bi-Monthly
Vol. 7 No. 14 January – February - 2026

The Structure, Dynamics, Phase Transitions, and Emerging Applications of Orientational Crystals

Sarwade Datta Vasant & Gulbhile Shamsundar Dhondiram
Vaishnavi Mahavidyalaya, Wadwani, Tq. Wadwani, Dist. Beed, (M.S.)
Corresponding Author – Sarwade Datta Vasant
DOI - 10.5281/zenodo.19827002

Abstract:

Orientational crystals, or orientationally disordered or plastic crystals, are a distinct category of condensed matter systems characterized by long-range translational order combined with partial to complete orientational disorder of the molecules. Unlike traditional crystals, which possess both positional and orientational order, orientational crystals allow for rotational dynamics within a structured lattice, showcasing interplay between molecular alignment and thermal energy that permits free rotation or large-amplitude jumps between orientations. Upon cooling, this orientational disorder can transition into frozen states known as orientational glass states. This research emphasizes the structural characteristics, thermodynamic behaviors, and phase transition mechanisms of orientational crystals. Key focal points include molecular rotational dynamics, entropy-driven stabilization, dielectric relaxation, and calorimetric signatures indicative of order-disorder transitions. Additionally, various experimental techniques such as X-ray diffraction, neutron scattering, differential scanning calorimetry, and dielectric spectroscopy are discussed for their effectiveness in investigating orientational dynamics. Theoretical frameworks, including symmetry analysis, configurational entropy evaluations, and molecular simulations, provide essential insights. Recent advancements in hybrid perovskites, organic molecular solids, and nanoscale assemblies further illustrate the significance of orientational disorder in technology, particularly in the fields of energy materials, pharmaceuticals, and functional soft matter. Thus, this research integrates fundamental concepts with contemporary trends, offering a thorough understanding of orientational crystal phases and their relevance to modern materials science.

Keywords: Orientational Crystals, Structure, Dynamics, Phase Transitions, Emerging Applications

Introduction:

Crystalline solids are typically defined by their long-range periodicity in atomic positions and molecular orientations. In contrast, orientationally disordered crystals, or plastic crystals, challenge this classification as they exhibit a unique structure where molecules are situated at well-defined lattice sites while maintaining significant rotational freedom. This feature results in a co-occurrence of positional order and orientational disorder, which in turn leads to distinctive structural and thermodynamic behavior unlike that of conventional crystalline solids or liquids. The study of plastic crystals has been particularly prominent in the context of molecular solids characterized by nearly spherical molecules, such as derivatives of methane and substituted cycloalkanes. Their intermediary behavior has drawn considerable interest in various scientific fields, including condensed matter physics, statistical mechanics, and materials science. This research aims to synthesize theoretical principles, experimental findings, and practical applications of orientationally disordered crystals, thereby providing a detailed and comprehensive reference

suited for postgraduate and doctoral-level research.

Structure of Orientational Crystals:

In the discussion of molecular structures, the focus is placed on molecules such as methane and adamantane that exhibit globular or highly symmetric properties. These molecules are positioned on a high-symmetry lattice, which can take forms like cubic or hexagonal. Despite the fixed nature of the lattice, the orientation of the molecules remains flexible and is not fixed. This results in a time-averaged structural representation that manifests as "spherical" or "disc-like" shapes when observed in diffraction experiments.

Additionally, there is a contrast between local disorder and long-range order within the crystal. While the overall crystal lattice presents a long-range ordered structure, the orientation of individual molecules displays a significant level of disorder. This local disorder contributes to the dynamic characteristics of the molecular structure, as the molecules exhibit rapid rotational movements or transition between various orientations within the crystal lattice. Such dynamics highlight the complexity of the molecular arrangement, yielding insights into both the ordered and disordered behaviors that can exist simultaneously in crystalline materials.

Structural Characteristics of Orientational Crystals:

Orientational crystals frequently display high-symmetry lattice configurations, particularly face-centered cubic (FCC) and body-centered cubic (BCC) structures. These structures are characterized by distinct diffraction patterns that reveal sharp Bragg peaks, which emerge as a result of translational order within the crystal. In addition to these peaks, diffuse scattering is also observed, indicative of orientational disorder present in the material. This combination of sharp and diffuse features in the diffraction patterns is essential for understanding the structural characteristics and disorder dynamics in orientational crystals.

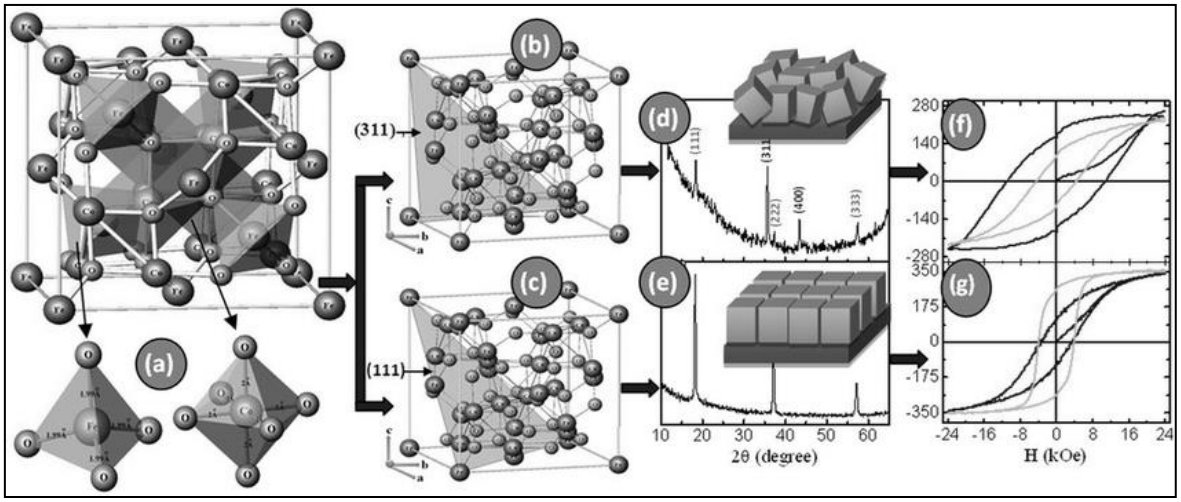

Figure Source: DOI:10.1038/srep30074

A schematic description of crystal orientation outlines how a crystal lattice is spatially aligned concerning a sample's coordinate system. This alignment is commonly represented using Miller indices or Euler angles, which facilitate the mapping of the crystal axis to a reference frame. Visualization methods frequently depict a unit cell or Miller planes—such as (111) or (311)—in relation to the substrate surface or loading axis. Such

representations are essential for understanding the geometrical relationships within the crystal structure and its interaction with external factors.

Reference Frame refers to a fixed laboratory or sample system, like the rolling direction or normal to the surface. Crystal Axes are the internal unit cell axes of the material. Miller Indices describe the orientation of specific crystal planes, such as the (111)-plane in a film. Direction Indices indicate the crystal direction parallel to a reference sample direction. Euler Angles are the three successive rotations needed to align the crystal axes with the sample axes, commonly used for quantitative texture analysis.

Dynamics of Orientational Crystals:

Molecules experience significant rotational motions characterized by rapid, large-amplitude librations and reorientational jumps or flips. The process of reorientation is impeded by the surrounding molecular environment, which creates low potential barriers. However, these barriers are sufficiently low to enable rapid motion that is typically thermally activated. To analyze these rotational dynamics, researchers often employ first- and second-rank orientational time correlation functions, which offer critical insights into the speed and angles of molecular rotations. Notably, at elevated temperatures, these motions can exhibit a highly cooperative behavior, indicating synchronization among molecular movements.

Molecular motion involves rapid rotational movements or jump-like reorientations of molecules between various stable positions within a crystal lattice. As materials undergo solid-solid phase transitions, characterized as ordering transitions, the previously observed rotational disorder becomes 'frozen' when cooled, leading to a more organized configuration. To investigate these phenomena, simulation techniques such as Molecular Dynamics (MD) and Monte Carlo (MC) serve as crucial tools. They enable researchers to monitor the energetic profiles of the systems and the nature of the rotational jumps occurring within them. The types of disorder present in these materials may involve high-symmetry molecules, such as tetrahedral configurations located in octahedral sites, or specific functional groups commonly found in organic compounds, such as methyl and trifluoromethyl groups. Furthermore, a notable aspect of these transitions is critical slowing down, a phenomenon where the orientational fluctuations of the molecules decelerate sharply as the system approaches the ordering transition. This behavior can be thoroughly analyzed using projection operator formalisms.

Molecular motion in plastic crystals includes:

Continuous rotational diffusion,

Discrete jump reorientation, The rotational relaxation time Γ often follows Arrhenius behavior:

$$\Gamma = \Gamma_0 \exp (E_a/k_B T)$$

where:

Ea= activation energyΓ_0 = pre-exponential factor

Non-Arrhenius behavior near glass transition may follow the Vogel–Fulcher–Tammann (VFT) equation:

$$\Gamma = \Gamma_0 \exp (DT_0/T-T_0)$$

This behavior is typical in orientational glass-forming systems.

Fundamental Concepts: Translational vs. Orientational Order:

In conventional crystals, both translational and orientational degrees of freedom are ordered. In orientational crystals:

- **Translational order:** Molecules are fixed at lattice sites.
- **Orientational disorder:** Molecules undergo rotational motion or occupy multiple orientations.

The degree of orientational order can be described using an orientational order parameter S:

$$S = \frac{3\cos^2 \theta - 1}{2}$$

where ɵ is the angle between a molecular axis and a reference direction.

- S=1→ perfect orientational order
- S=0 → complete orientational disorder

Theoretical and Computational Modeling:

1. Landau Theory of Phase Transition Free energy expansion: $F = F_0 + a(T-T_c)S^2 + bS^4 + \ldots$ Minimization predicts continuous or first-order transitions depending on coefficient signs.

2. Statistical Mechanical Models Lattice models with discrete orientations (e.g., Potts model):

$H = -J \sum_{(i,j)} \delta \sigma i, \sigma j$

where:

σi = orientation state, J = interaction parameter

Molecular Dynamics Simulations

Simulations compute: Rotational autocorrelation functions

$$C(t) = P_2(\cos\theta(t))$$

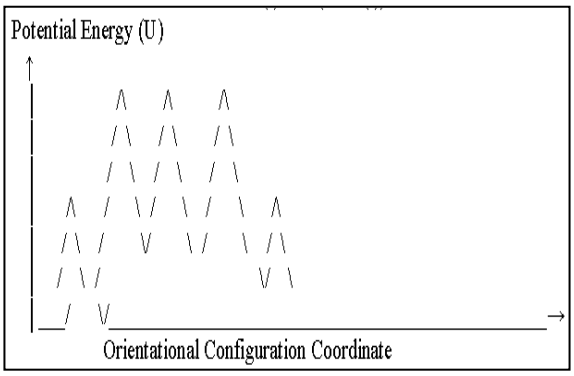

Phase Transitions of Orientational Crystals:

Orientational crystals are primarily characterized as high-temperature phases that undergo a transformation into more ordered, low-temperature crystal structures upon cooling. This transformation is exemplified by the Order-Disorder Transition, which represents a significant phase change when thermal energy becomes insufficient to navigate potential energy barriers. In this situation, the molecular arrangement starts to "order," resulting in a structural change in the crystal lattice, such as a transition from a cubic to a monoclinic form. Additionally, the melting behavior of plastic crystals is noteworthy; their disordered molecular configuration leads to a remarkably low entropy of fusion, causing them to melt at elevated temperatures compared to their ordered counterparts. Moreover, when orientational disorder is rapidly cooled, it can be preserved in a glassy state, giving rise to a non-crystalline phase at lower temperatures. This glassy phase results from the "freezing" of the orientational disorder, thus diverging from traditional crystalline structures.

Orientational crystals undergo order–disorder transitions:

1 Plastic Crystal → Ordered Crystal, Occurs upon cooling when rotational motion freezes.

2 Plastic Crystal → Orientational Glass, if cooling is rapid, disorder becomes kinetically trapped.

The heat capacity anomaly near transition temperature T_c: $C_p = (\frac{\partial H}{\partial T})_p$

Calorimetric measurements reveal entropy changes: $\Delta S = \int \Delta CP dt/T$

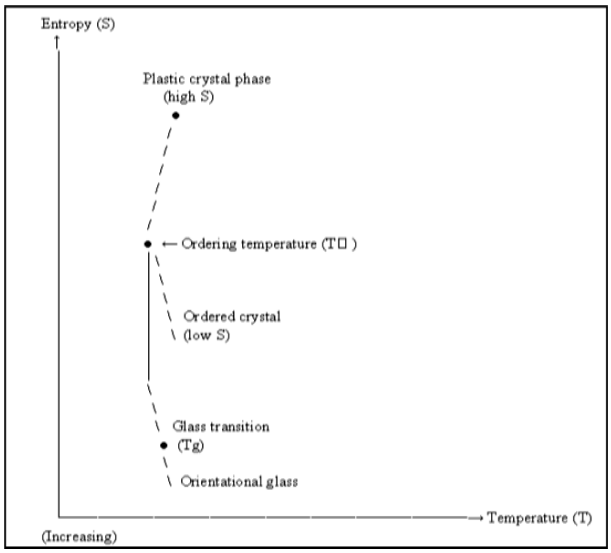

Emerging Applications of Orientational Crystals:

The unique properties of orientational crystals, characterized by their high mobility and disorder, render them particularly useful across various technological applications. In solid electrolytes, their notable rotational mobility enables efficient ion conduction, positioning them as effective solid-state electrolytes for batteries. Additionally, their phase change behavior, often associated with significant latent heat, makes them advantageous for thermal energy storage systems.

In the pharmaceutical field, the adaptability and high internal mobility of molecular crystals enhance both the solubility and delivery of drugs, improving therapeutic effectiveness. Furthermore, in the realm of optoelectronics, these crystals' capacity to align in specific orientations facilitates advancements in nonlinear optical applications and photonics. Lastly, orientational crystals contribute to the development of smart materials, leveraging reversible phase transitions to create responsive materials suited for molecular electronics. Thus, the functionalities of these crystals span a diverse set of applications, showcasing their technological significance.

Conclusion:

This research concluded that the Orientational Crystal's structural features, thermodynamics, and phase transition mechanisms, focusing on molecular dynamics, entropy stabilization, dielectric relaxation, and calorimetric signatures of order-disorder transitions. Various experimental methods such as X-ray diffraction, neutron scattering, and dielectric spectroscopy are employed to study these dynamics. Theoretical frameworks, including symmetry analysis and molecular simulations, contribute valuable insights. Recent advancements in materials like hybrid perovskites and organic solids highlight the impact of orientational disorder in energy materials and pharmaceuticals. This work emphasizes the interdisciplinary approach necessary for understanding and designing functionally relevant materials based on orientational disorder, bridging fundamental concepts with modern trends in materials science.

References:

1. Angell, C. A. (1995). Formation of glasses from liquids and biopolymers. Science, 267(5206), 1924–1935.
2. Binder, K., & Kob, W. (2011). Glassy materials and disordered solids. World Scientific.
3. C. A. Angell(1999), "Plastic Crystals: Structure and Dynamics," Acc. Chem. Res.
4. Debye, P. (1929). Polar molecules. Chemical Catalog Company.
5. J. Jadżyn, J. Świergiel (2012), Electric relaxation effects induced by displacement current in dielectric materials. Ind. Eng. Chem. Res. 51, 807

6. J. L. Finney(1995), “Neutron Scattering Studies of Molecular Rotations,” Rep. Prog. Phys.,
7. J. Timmermans, Plastic crystals: a historical review. J. Phys. Chem. Solids (1961). https:// doi. org/ 10. 1016/ 0022-3697(61) 90076-2.
8. L. E. McCandlish and B. M. Pettitt (2003), “Dynamics of Orientationally Disordered Crystals,” Phys. Rev. E.
9. L.P. Singh, S.S.N. Murthy, T. Bräuniger, H. Zimmermann (2008), Relaxation dynamics of orientationally disordered plastic crystals: effect of dopants. J. Phys. Chem. B 112, 1594.
10. Landau, L. D., & Lifshitz, E. M. (1980). Statistical physics. Pergamon Press.
11. M. Barrio, D.O. López, J.L. Tamarit, P. Negrier, Y. Haget(1995), Degree of miscibility between non-isomorphous plastic phases: binary system NPG (neopentylglycol)-TRIS [tris(hydroxymethyl)aminomethane]. J. Mater. Chem. 5, 431.
12. M. Romanini M, Ph. Negrier, J. Ll. Tamarit, S. Capaccioli, M. Barrio, L. C. Pardo, D. Mondieig(2012), Emergence of glassy-like dynamics in an orientationally ordered phase. Phys. Rev. B 85, 134201.
13. S. Pronk and P. G. Bolhuis(2001), “Molecular Rotation in Plastic Crystals,” J. Chem. Phys.
14. T. J. Senden et al. (2019), “Plastic Crystal Electrolytes for Batteries,” Adv. Energy Mater.

International Journal of Advance and Applied Research
www.ijaar.co.in
ISSN – 2347-7075 Impact Factor – 8.141
Peer Reviewed Bi-Monthly
Vol. 7 No. 14 January – February - 2026

Study of Magnesium Tartrate Crystals by Sol Gel Method

P. A. Savale
Department of Physics, SES's Arts and Science College Bhalod Dist. Jalgaon (M.S.) India
Corresponding Author – P. A. Savale
DOI - 10.5281/zenodo.19827014

Abstract:
In the present study, single crystals of magnesium tartrate crystals were grown by using silica gel as a growth medium. These crystals were grown by simple sol gel technique using diffusion method. The optimum growth conditions for these crystals were optimized by varying various process parameters. The shiny white coloured and spherulitic morphology crystals grown within silica gel column were obtained. The crystalline nature of grown crystal was confirmed by using powder X-ray diffraction technique which shows that magnesium tartrate hydrate has crystallized in orthorhombic structure. The functional groups present in the crystals were identified by using FTIR analysis which shows that the presence of $O = H, C = O, C - O, C - H$ *and* $metal - oxygen$ *bonds. The SEM study reveals that the morphology of the crystal having orthorhombic structures. The analysis of EDAX has shown the presence of Magnesium and Oxygen.*

Keywords**: **Magnesium Tartrate, XRD, FTIR, SEM, EDAX.

Introduction:

Crystal habit of various crystals, grown under different conditions and also by different methods viz., melt growth, vapour phase growth, solution growth and gel growth were described by H. E. Buckley [1], P. Hartman [2], K. Kern [3], A. A. Chernov [4], W. K. Burton [5] and J. Mullin [6]. A number of factors such as concentration of reactants, pH of gel [7, 8], impurities in the solvent [9], gel setting time and gel aging time etc. have considerable effect on growth rate. In the steady state of concentration gradient, growth rate also becomes steady which favors growth of well-developed crystals [10]. However, very slow rate of growth along one direction results in the platy crystals and spherulitic crystals.

Crystals are the backbone of the revolution of modern science and technology [11-13]. At the beginning the base of gel growth techniques for low solubility crystals has been established and afterwards, such methods of crystal growth were applied to soluble materials with a low molecular weight. The Moiner and Vesque was the first researcher, who records the growth of large crystals by slow diffusion in gel. A systematic study of crystallization in gels begins with Lissegang's famous discovery of periodic crystallization in gels. This method has gained considerable attention because of its simplicity and effectiveness in growing single crystal of certain compound. This technique is an alternative technique to solution growth with controlled diffusion. This growth process is free from convection. This is purifying process, free from thermal strain [14-20].

Growth and Characterization of some tartrate crystals were reported by Henisch and Henisch et al [21], Patel and Rao [22]. Growth of some crystals of tartrate compounds like calcium tartrate [23, 24], strontium tartrate [25], barium tartrate [26, 27], ammonium tartrate [28], zinc tartrate [29], sodium tartrate [30], cadmium tartrate [31] and iron tartrate [32] were reported by earlier researchers. The compounds of Tartaric acid find

numerous applications in semiconductor and optics industries with the invention of lasers. The field of non-linear optics touched the new heights and practical implementations were possible with the various applications of non-linear optical crystals [33]. Many of the tartrate compounds including pure and mixed tartrate deserve special attention due to its medical, pharmaceutical and industrial applications such as, injections of Na-Cr tartrate increase the susceptibility of the transplanted sarcoma to the effect of X-rays, calciphylatic responses of various ferrous tartrate compounds to prevent anemia in animals, ferrous tartrate as a catalyst in manufacture of champagne, tanning action of ferrous tartrate to tan skin, the use of manganese tartrate crystals in chemical temperature indicators, strontium tartrate used in ammunition units, zinc tartrate with other compounds form a bright coating and used as protecting powder for metals etc.[34-37].

In the present investigation, single crystals of magnesium tartrate were grown by a simple gel technique using diffusion method. The optimum conditions were established by varying various process parameters such as pH, concentration gel solution, setting time of the gel solution and concentration of the reactance. The optimum growth conditions for these crystals were determined. These crystals were characterized by using XRD, FTIR, SEM and EDAX.

Experimental:

Magnesium Tartrate ($C_4H_4MgO_6$) crystals were grown by single diffusion method in silica gel medium at room temperature. The Sodium Meta Silicate (Na_2SiO_3) solution and acetic acid (CH_3COOH) was prepared by dissolving 22gm (Na_2SiO_3) into the 250ml distilled water and 15ml (CH_3COOH) dissolving into 250ml distilled water respectively. Then (Na_2SiO_3) was added into 6ml (CH_3COOH) drop by drop by maintaining the pH 4.2 with continues till the solution becomes milky. After that 15ml solution of Magnesium chloride ($MgCl_2$) with 1M added into the gel solution. This mixture was then transferred to the test tube of 15 cm × 2.5 cm dimension. After setting the gel in 4-5 days, the 10ml tartaric acid ($C_4H_6O_6$) with 1M was allow to fall steadily along the wall of the tube above the set gel, next day the small nucleation growth was observed at below the interface of gel. This nucleation growth was increased in size. The chemical reaction inside the gel can be expressed as follows:

$$2CH_3COOH + Na_2SiO_3 \rightarrow 2CH_3COONa\downarrow + SiO + H_2O$$

$$2CH_3COONa + MgCl_2 \rightarrow (CH_3COO)_4Mg\downarrow + 4NaCl$$

$$(CH_3COO)_4Mg + C_4H_6O_6 \rightarrow C_4H_4MgO_6\downarrow + 4CH_3COOH$$

Good quality shiny white coloured spherulitic crystals were grown in 45-48 days. The crystalline nature of grown crystals was confirmed using powder X-ray diffraction technique. The functional groups present in the single crystals were identified using Fourier Transform Infrared spectroscopy (FTIR) analysis. The SEM was done to find the structural morphology of the grown crystals. The presence of magnesium and oxygen was confirmed by EDAX analysis.

Results and Discussion:

The Fig. 1 shows the crystals of magnesium tartrate attached themselves and forming a thick layer at the interface whereas Fig. 2 shows a few grown crystals of magnesium tartrate having different habits with their scaling on a graph paper. The grown crystals are of the 3.5mm× 3.5mm × 2.5mm size. The various optimum conditions for growing crystals were established and are given in the Table 1. For pH 4.2 the spherulitic crystals were observed in the interface of the gel column [21]. Tartaric acid

($C_4H_6O_6$) used as upper reactant. Gel age is the time interval between gel and pouring of the upper reactant.

Fig.1 shows the grown magnesium tartrate crystals.

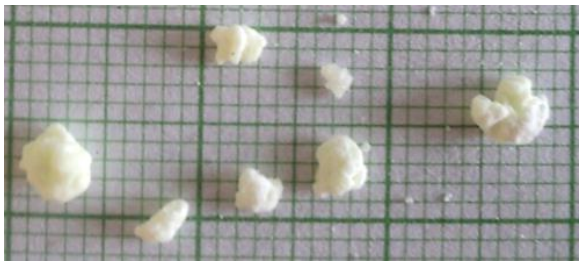

Fig. 2 shows the shiny white coloured magnesium tartrate crystals.

Table 1 Optimum condition for growth of magnesium tartrate crystals.

Conditions for growth of magnesium tartrate crystals	Single diffusion
Density of sodium meta silicate (Na_2SiO_3)	1.05 gm/cm^3
Amount of 1M acetic acid(CH_3COOH)	6 ml
pH of the gel	4.2
Temperature	Room Temperature
Concentration of Magnesium Chloride ($MgCl_2$)	15 ml
Concentration of 1M Tartaric acid($C_4H_6O_6$)	10 ml
Gel setting period	4-5 days
Gel aging period	24 Hrs
Growth of period	45- 48 days
Quality	Shiny white, Large size, Spherulitic morphology
Size of Crystals	3.5mm × 3.5mm ×2.5mm

Powder X-ray diffraction analysis of magnesium tartrate crystals

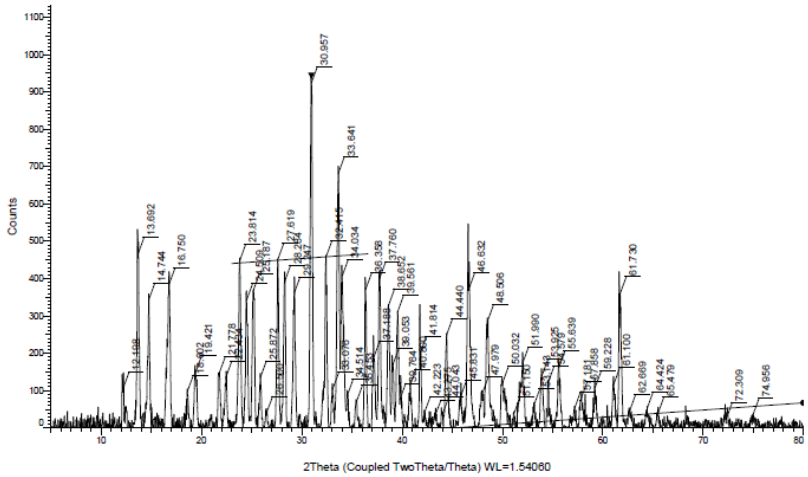

Fig. 3 XRD pattern of magnesium tartrate crystals.

The crystal structure of the sample compound was studied by powder X-ray diffraction method. The X-ray diffraction was recorded using Bruker-D8 Advance, Germany (2θ from 5° to 80°) with CuKα radiation of wavelength λ=1.54060Å. The X-ray diffraction technique is used to investigate the inner arrangement of atoms or molecules in a crystalline material. The recorded X-ray diffraction of the magnesium tartrate crystals is shown in the Fig. 3. The analysis of different diffraction peaks indicates the formation of orthorhombic structure [22]. The crystalline phases and d-values obtained from the XRD have been compared with the JCPDS data from X'Pert High Score PANalytical software. The XRD pattern of Fig. 4 matches with the JCPDS files 00-001-0225 and 00-023-0390, indicating that the sample consisted of magnesium tartrate crystalline.

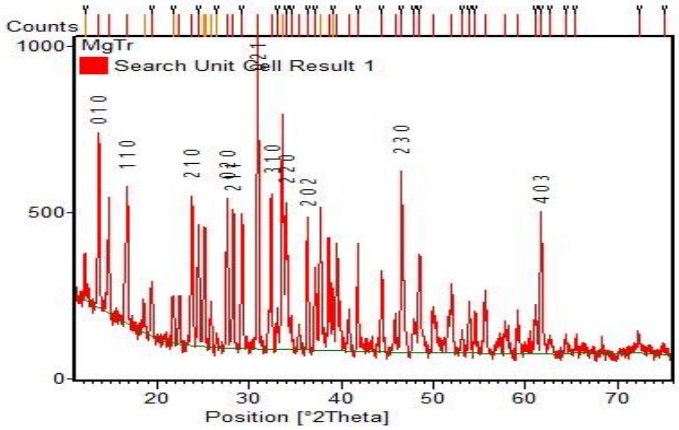

Fig. 4 Shows graphics of the X-ray powder diffraction pattern of magnesium tartrate by X'Pert High Score PAN alytical Software.

The grain size is determined by measuring the width of the line with each intensity peaks and then the average grain size have been obtained from the XRD pattern using the Scherrer's calculator from X'Pert High Score software [33]. The obtained average grain size of magnesium tartrate crystals is 0.60 nm. The values of 2θ, d-values, intensity and h k l values are shown in the Table 2.

Table 2 Powder X-ray diffraction data of magnesium tartrate crystals (λ =1.54060Å).

Observed data values			Standard data values			h k l values	Matched by X'Pert HighScore PANalytical Software
2θ	d-value	Intensity	2θ	d-value	Rel. Intensity		
13.692	6.46206	467	13.6735	6.47625	56.32	010	00-001-0225
16.750	5.28857	383	16.7750	5.28520	46.10	110	00-001-0225
23.814	3.73353	448	23.8216	3.73537	50.91	210	00-001-0225
25.187	3.53298	368	25.2839	3.52254	37.66	201	00-023-0390
27.619	3.22717	450	27.6262	3.22898	51.26	020	00-001-0225
28.284	3.15277	391	28.3017	3.15343	47.14	211	00-023-0390
32.415	2.75980	457	32.4121	2.76230	53.60	310	00-001-0225

37.760	2.38052	400	37.7448	2.38340	47.94	221	00-001-0225; 00-023-0390
39.561	2.27619	311	39.5556	2.27836	36.44	400	00-001-0225
40.800	2.20988	113	40.8036	2.21151	11.50	320	00-023-0390
50.032	1.82161	122	49.9636	1.82543	15.76	203	00-023-0390

It shows the well-defined diffraction peaks with indexed peaks, which indicate that the grown material has good crystalline nature. The obtained values of lattice parameters, viz., a, b, c and α, β, γ as well as crystal structure, lattice type were shown in the Table 3. From the powder XRD pattern, it is confirmed that grown crystal has orthorhombic structure [42].

Table 3 Lattice parameters for magnesium tartrate crystal.

Lattice Parameters	Values
a	9.14 Å
b	6.49 Å
c	5.96 Å
α=β=γ	90^0
Crystal family	Orthorhombic
Lattice Type	Primitive (P)

FTIR analysis of magnesium tartrate crystals:

The Fig. 5 shows the FTIR spectrum of the magnesium tartrate. The FTIR spectrum was recorded using Shimadzu FTIR-8400, Japan (400cm^{-1} to 4000cm^{-1}). The absorption peaks positioned in between 3373.61–2297.30cm^{-1} corresponds to symmetric and asymmetric stretching vibrations of O-H bond due to water of crystallization. The peak at 1604.83cm^{-1} is the band corresponding to carbonyl C=O group. The band at 1303.92cm^{-1} is the band corresponding C-O stretching vibration. The band at 1107.18-918.15cm^{-1} is the bands corresponding to O-H stretching out of plane vibrations. The band observed at 725.26-464.86cm^{-1} corresponds to metal oxygen bonding [10-13].

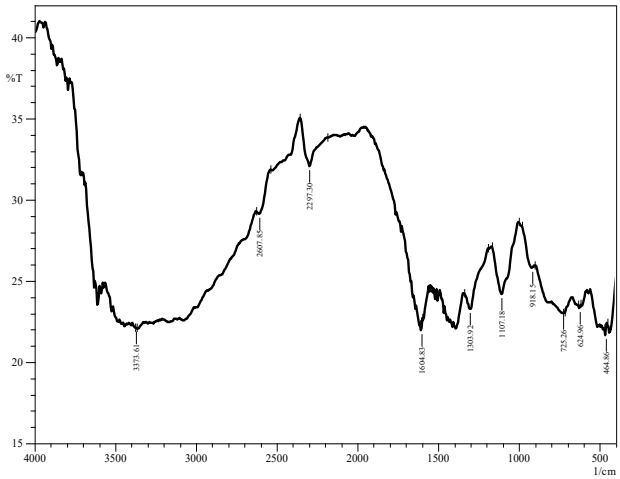

Fig. 5 FTIR spectrum of magnesium tartrate crystals (pH 4.2).

SEM analysis of magnesium tartrate crystals:

The Fig. 6 shows the SEM image of magnesium tartrate. The FESEM image was recorded using Hitachi S-4800, Japan with X-Flash detector-5030, Bruker, Germany. The scanning electron microscope reveals that the morphology of the crystal having rectangular shape, triangular shape, looks like cubes of different shapes and sizes of orthorhombic structures [14]

.

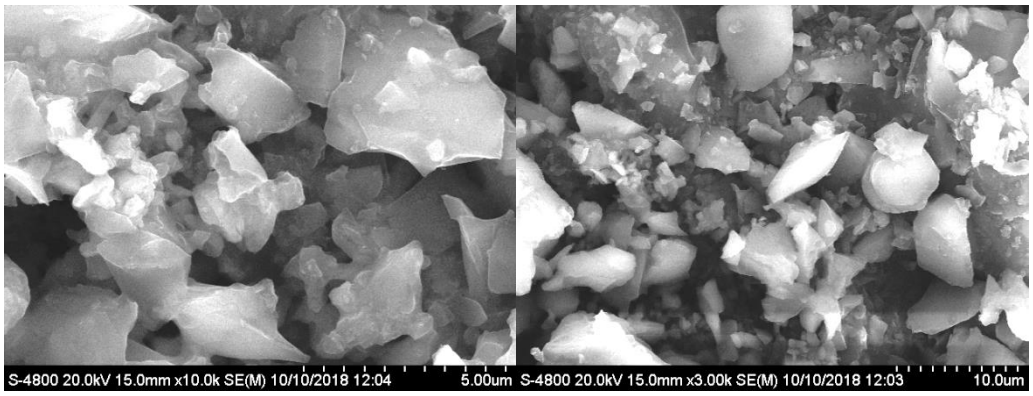

Fig. 6 SEM images of magnesium tartrate crystals.

EDAX analysis of magnesium tartrate crystals:

Fig. 7 Shows the EDAX pattern of magnesium tartrate crystals. The elemental analysis of gel grown magnesium tartrate crystals was carried out by using X-Flash-60 Bruker instrument. Magnesium tartrate is one of the most complex systems with many phases and unique chemical composition as it is amplified between silica gel by the distribution of magnesium chloride in the gel. The diversity in the stoichiometry of magnesium tartrate poses a challenge for the control of size and shape. The energy dispersive x-ray spectrum has shown that the Mg and O are present in the atomic percentage of 9.13 and 54.85 and weight percentage of 14.49 and 57.27 respectively. Table 4 shows the EDAX analysis for magnesium tartrate crystal.

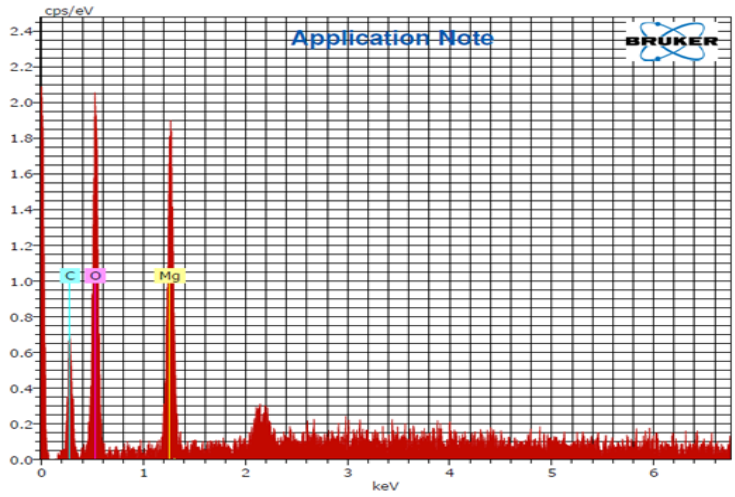

Fig.7 Shows the EDAX pattern of magnesium tartrate crystals.

Table 4 EDAX analysis for magnesium tartrate crystal.

El	AN	Series	unn. C [wt.%]	norm. C [wt.%]	Atom. C [at.%]	Error (1 Sigma) [wt.%]
C	6	K-series	15.20	28.24	36.02	4.38
O	8	K-series	30.83	57.27	54.85	6.20
Mg	12	K-series	7.80	14.49	9.13	0.54
		Total:	53.83	100.00	100.00	

Conclusions:

Sol gel method is found to be suitable for growing the magnesium tartrate crystals. Single diffusion method is convenient for the growth of the magnesium tartrate crystals. Nucleation control can be achieved by changing a various gel parameters such as pH of gel, density of gel and concentration of feed solutions. The shiny white spherulitic crystals were observed. The crystalline phases and d-values obtained from the XRD have been compared with the JCPDS data from X'Pert High score PANalytical software. XRD pattern shows very sharp peaks having high intensity, indicating perfect crystallization. Unit cell parameter values and d values match very well with the JCPDS data and the structure of magnesium tartrate is orthorhombic. From the FTIR spectroscopic study, the presence of O=H, C=O, C-O, C-H and metal-oxygen bonds were confirmed. The SEM study reveals that the morphology of the crystal having orthorhombic structures. The analysis of EDAX has shown anhydrous nature of the magnesium tartrate crystal with the presence of magnesium and oxygen.

Acknowledgments:

Authors are grateful to University Institute of Chemical Technology, Kavayitri Bahinabai Chaudhari North Maharashtra University, Jalgaon for providing XRD, FTIR, SEM and EDAX facilities.

References

1. H. E. Buckley., (1951) 'Crystal Growth', New York: Wiley; London: Chapman & Hall, 571.
2. P. Hartman., (1973) 'Crystal growth: An introduction', North-Holland series in crystal growth, v. 1, Jan 1.
3. K. Kern, (1994) 'Thermal roughening of surfaces: experimental aspects', In The chemical physics of solid surfaces, Vol. 7, pp. 291-340.
4. A. A. **Chernov**, (1984) 'Modern Crystallography III Crystal Growth', Springer-Verlag Berlin Heidelberg New York Tokyo.
5. W. K. Burton, N. Cabrera, (1949) 'Crystal growth and surface structure. Part I', Disc. Faraday Soc., 5, 33-39.
6. J. B. Mullin, (1977) Crystal Growth' Published by Elsevier Science and Technology Hardcover.
7. S. K. Arora, V. Patel & A. Kothari, (2004) 'Kinetics and mechanism of thermal decomposition of strontium tartrate crystals', Mater. Chem. Phys, 84, pp. 323-330, c.
8. S. K. Arora, V. Patel, A. Kothari & B. Amin, (2004) 'Gel Growth and Preliminary Characterization of Strontium Tartrate Trihydrate', Crystal Growth and Design, pp. 343-349.
9. S. K. Arora, V. Patel, B. Chudasma and B. Amin, (2005)'Single crystal growth and characterization of strontium tartrate', J. crystal growth, 275, pp. e657-e661.
10. P. S. Raghavan & P. Ramasamy, (2000)Crystal Growth Process and Methods, KRU publication,
11. H. K. Henisch, (1968) 'Crystal Growth in Gels', Pennsylvania University Press, University Park, P.A., pp. 13-20.
12. D. A. Glocker, and J. F. Soest, , (1969) 'Growth of single crystals of monobasic ammonium phosphate in gel', AIP-The Journal of Chemical Physics, Vol. 51, pp. 3143-3143,.

13. F. Lefaucheus, M. C. Robert, and E. Manghi,'(1982) A comparison between gel grown and solution grown crystals - case of ADP and KDP', Journal of Crystal Growth, Vol. 56, issue 1, pp. 141-150,.
14. H. K. Henisch, (1970) Crystal Growth in Gels. Pennsylvania State University Press, University Park, PA, .
15. Resmi Nair, Dr. K. Madhukumar, C. M. K Nair and Jayasudha. S, T. S. Elias, (2015) 'Effect of Annealing Temperature on Thermo luminescence of Rare Earth Doped CaSO4', International Journal of Engineering Research & Technology (IJERT), Volume 3, Issue 08, pp.1-4.
16. Ignatius Korah, Cyriac Joseph, M.A. Ittyachen, (2010) 'Growth and Structural Characterization of Gadolinium Neodymium Oxalate Crystals Grown in Hydro-Silica Gel', Journal of Minerals & Materials Characterization & Engineering, Vol. 9, No.12, pp.1081-1086.
17. Cyriak Joseph, George Varghese, Dr. M. A. Ittyachen, (1995) 'Growth and characterization of mixed neodymium praseodymium oxalatze decahydrate crystals in silica gel', Crystal Research & Technology, Vol. 30, Issue 2, pp. 159-164.
18. M. V. John & M. A. Ittyachen, (2001) 'Growth and characterization of cerium lanthanum oxalate crystals grown in hydro-silica gel', Cryst.Res.Technol, pp. 141-146.
19. S. M. Dharmaprakash & P. Mohan Rao, (1985) 'Growth of barium oxalate dihydrate crystals in silica hydrogel', J. mater. Sci. Lett., pp. 787-789.
20. C. P. Sibu, S. Rajesh Kumar, P. Mukundan and K. G. K. Warrier, (2002) 'Structural Modifications and Associated Properties of Lanthanum Oxide Doped Sol−Gel Nanosized Titanium Oxide', Chem. Mater., 14, 7, pp. 2876-2881.
21. H. K. Henisch, J. Dennis, H. I. Hanoka, (1965) 'Crystal growth in gels', Physics and Chemistry of Solids', Vol. 26, issue 3, pp. 493-500.
22. A. R. Patel, and A. V. Rao, (1982) 'Crystal growth in Gel media', Bulletin of Materials Science, Vol. 4, issue 5, pp. 527-548.
23. H. B. Gon, (1990) 'Ferro-electricity in calcium tartrate single crystals grown by gel technique', Journal of Crystal Growth, Vol. 102, issue 3, pp.501-504.
24. A. R. Patel, and S. K. Arora, (1977) 'Growth of mixed Sr1-xCaxC4H4O6 crystals in gel', Journal of Crystal Growth, Vol. 37, issue 3, pp. 343-345.
25. V. S. Joshi, and K. C. Mevada, (2010) 'FT-IR, XRD and Thermal studies of gel-grown barium tartrate crystals', Journal of Science, Vol. 1, pp.68-71.
26. S. K. Bachahv, P. A. Savale and S. T. Pawar, (2010) 'Growth and Study of BaTr single crystals by Gel Technique', Pelagia Research Library Advances in Applied Science Research, 1(1), pp. 26-33.
27. M. M. Abdel-Kader, F. EL-Kabbany, S. Taha, M. Abosehly, , K. K. Tahoon and A. A. EL-Sharkay, (1991) 'Thermal and electrical properties of ammonium tartrate', Journal of Physics and Chemistry of Solids, Vol. 52, Issue 5, pp. 655-658.
28. S. K. Arora, V. Patel, R. G. Patel, B. Amin, and A. Kothari, (2004) 'Electrical characterization of strontium tartrate single crystals', Journal of Physics and Chemistry of Solids, Vol. 65, Issue 5, pp.965- 973.
29. M. M. Abdel-Kader, F. EL-Kabbany, and S. Taha, (1990) 'Physical properties and phase transitions in Sodium tartrate dihydrate', Journal of Materials Science:

Materials in Electronics, Vol. 1, Issue 4, pp. 201-203.

30. A. C. Yanes, T. Lopez, J. Stockel, J. F. Peraza, and M. E. Torres, (1996) 'Characterization and thermal and electromagnetic behaviour of manganese tartrate crystals grown by silica gel technique', Journal of Materials Science, Vol.31, pp. 2683-2686.
31. S. Joseph, (1997) Ph.D. Thesis, Saurashtra University, Rajkot.
32. B. Suresh Kumar, H. Rohim Kuttym , R. Sudarsana Kumar and K. Rajandra Babu, (2007) 'Growth and characterization of pure and lithium doped strontium tartrate tetrahydrate crystals by solution-gel technique', Bulletin of Materials Science, Volume 30, Issue 4, 349-355.
33. I. V. Veselaya, and V. I. Gordyski, (1957) 'Voprosy onkologii (Vopr Onkol)', Vol. 3, pp. 300.
34. R. Strebel, J. Vašků, and H. Selye, (1962) Comparative study of the calciphylactic challenging potency of various iron compounds', Journal of Pharmacy and Pharmacology, Vol. 14, Issue 1, pp. 658–663.
35. V. P. Gvelesiani, 'Vinodelie I' (1957) Viogra Darstvo SSSR, Vol. 17, pp.13.
36. 'Basic Studies of Iron Tannage. VI. Tannability of Organic Ferric Salts', (1954) Journal of the Chemical Society of Japan, Chemistry and Industrial Chemistry, Nippon Kagaku Kaishi, Journal of the Chemical Society of Japan, Industrial Chemistry Section, Vol. 57, Issue. 8, pp. 594-596.
37. S. P. Gvozdov, and A. A. Razumova (1958) "Kupfer (I)-quecksilber (II)-jodide. Polymorphie." *Izvestija vysčlih učebnyh Zavedenij Himija i himičeskaja technologija*, Vol.5, pp. 154-159.
38. Heiskell, R.H., (1959) U. S. Patent, No.2899291.
39. D. Kalaiselvi, R. Mohan Kumar and R. Jayavel, (2008) 'Single crystal growth and properties of semi organic nonlinear optical L-arginine hydrochloride monohydrate crystals', Cryst. Res. Technol. 43, 851-856,
40. S. J. Nandre, S. J. Shitole, R. R. Ahire, (2012) Study of Growth, EDAX, Optical properties and Surface Morphology of Zinc Tartrate Crystals',J. Nano- Electron. Phys., Vol. 4 No. 4, 04013(4pp).
41. S. J. Nandre, S. J. Shitole, R. R. Ahire, (2013) 'FT-IR, Thermal and Optical Studies of Gel Grown Cobalt Tartrate Crystals', J. Nano- Electron. Phys., Vol. 5 No. 4, 04050(5pp)
42. Mayuri P. Dave , Sahaj A. Gandhi , Vimal Joshi, (2016) 'Gel Growth, Powder XRD and FTIR Study of Magnesium Levo-Tartrate Crystals', International Journal of Innovative Research in Science, Engineering and Technology (A High Impact Factor, Monthly Peer Reviewed Journal), Vol. 5, Issue 1, pp. 1020-1026.
43. P. A. Savale, (2022) 'Study of Growth and Characterization of Cobalt Tartrate Crystals', Engineering and Scientific International Journal (ESIJ,) Volume 9, Issue 1, pp.16-22.
44. K. C. Mevada, V. D. Patel, and K. R. Patel, (2012) 'FT-IR, XRD and Thermal Studies of Gel-grown Barium Tartrate Crystals', Scholars Research Library Archives of Physics Research, 3(4), pp. 258-263.

International Journal of Advance and Applied Research
www.ijaar.co.in
ISSN – 2347-7075 Impact Factor – 8.141
Peer Reviewed Bi-Monthly
Vol. 7 No. 14 January – February - 2026

Alterations Appeared in The Hoping Length of Zinc Doped Nickel Ferrite System Driven by The Gamma Radiation Effect

Shaikh Asif Karim & Sayyed Mujeeb Hadi
Dept of Physics, Sir Sayyed College, Aurangabad
Corresponding Author – Shaikh Asif Karim
DOI - 10.5281/zenodo.19827083

***Abstract**:*

A systematic investigation of structural, electrical, magnetic properties of Ni-Zn ferrite before and after gamma irradiation is carried out. Samples of spinel ferrite having the generic formula $Ni_{1-x}Zn_xFe_2O_4$ with x = (0.0, 0.2, 0.4, 0.6, 0.8, 1.0) were prepared using the standard ceramic technique. The samples of Ni-Zn ferrite were irradiated with gamma rays using Co^{60} source at the laboratory. Gamma irradiation alters the structural properties of Ni-Zn spinel ferrites. The distance between magnetic ions i.e. hopping length at tetrahedral 'A' site and octahedral 'B' site is then studied.

Keywords**: **Ferrite, Hopping Length, Gmma Radiation.

Introduction:

The polycrystalline spinel ferrite are well-known magnetic materials and are very useful in microwave applications, high quality filters, antenna rod, transformer cores etc.[1-3]. The property of magnetic conductor and electrical insulator made them useful in many of application. The properties like structural, electrical and magnetic are known to be sensitive to the chemical composition, microstructure, type and amount of dopant [4, 5, 6] etc. The substitution of zinc in nickel ferrite modifies the properties of nickel ferrite which are useful in many device applications. Thus nickel-zinc is an important mixed spinel ferrite. Irradiation effect provides several interesting and unique aspects in understanding of damaged structure and thereby modifying the properties of ferrite materials. Effect of γ radiation of Co-Zn on the structural properties has been reported by Hamada [7]. It has been reported that the physical properties of Ni, Zn, Cu spinel ferrite are also affected by irradiation. The structural, electrical and magnetic properties of Ni-Zn spinel ferrites have been reported in the literature [8, 9, 10].

Experimental Setup:

Samples of spinel ferrite having the generic formula $Ni_{1-x}Zn_xFe_2O_4$ with x = 0.0, 0.1, 0.2, 0.4, 0.6, 0.8, 1.0 were prepared using the standard ceramic technique. The pure oxides (NiO, ZnO and Fe_2O_3) of 99.9% purity were used. The powders were mixed in stichemeric proportion and ground to obtain a very fine powder. The powder was then heated/ sintered at 900^0C for 12 hrs. The sintered powder was again ground and palletized to room temperature for 24 hrs. They were polished to obtain a disc with two uniform parallel surfaces. The powder X ray diffractogram is used in the 2θ range of 20º to 80º at room temperature. The data was collected at room temperature.

The samples of Ni Zn ferrite were irradiated with gamma rays using Co^{60} source. All the properties were investigated before and after gamma radiation.

The distance between magnetic ions i.e. hopping length at tetrahedral 'A' site and octahedral 'B' site are calculated using the following relation 1, 2.

$$L_A = \frac{a\sqrt{3}}{4} \quad \ldots\ldots\ldots\ldots\ldots\ldots\ldots\ldots\ldots 1$$

$$L_B = \frac{a\sqrt{2}}{4} \quad \ldots\ldots\ldots\ldots\ldots\ldots 2$$

The values of hopping length are given in Table 1. The variation of hopping length with composition 'x' is depicted in Fig. 1.

Result And Discussion:

Since hopping length depends on the lattice constant, we observed the change in the hopping length before and after radiation [11]. As lattice constant increases the hopping length also increases with Zn substitution. The change in the structural properties after gamma irradiation of presently investigated samples is because that after irradiation, the stored energy of material increases and then it is released at the defects which are already exist. This results in decrease in the number of defects consequently the structural properties like lattice constant, X-ray density, particle size decreases.

Table 1: Hopping length (L_A) and (L_B) of before and after γ-irradiation of $Ni_{1-x}Zn_xFe_2O_4$

Composition 'x'	L_A (Å)		L_B (Å)	
	Before	After	Before	After
0.0	3.613	3.610	2.950	2.948
0.2	3.620	3.618	2.956	2.954
0.4	3.628	3.626	2.962	2.960
0.6	3.636	3.634	2.969	2.967
0.8	3.644	3.642	2.976	2.973
1.0	3.652	3.649	2.982	2.979

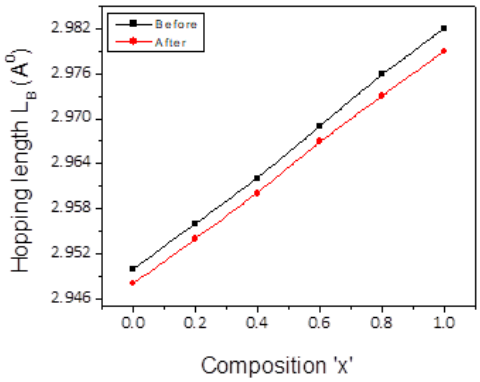

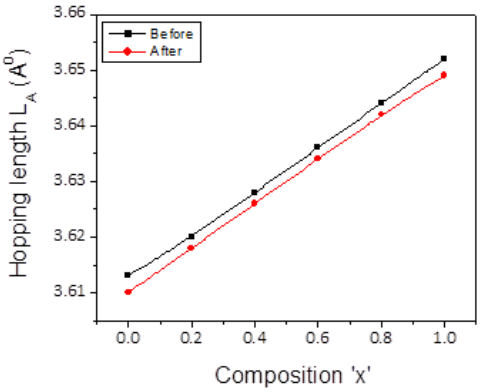

Fig. 1: Variation of hopping length (L_A & L_B) with composition for $Ni_{1-x}Zn_xFe_2O_4$

References:

1. S. Krupanicha, (1976) *"The physics of ferrites and magnetic oxide related to them." (Russian translation) Moscow Min 1st Ed.*
2. A. T. Neo and M. P. Pileni, (2001) *J. Phys. Chem B 105 53.*
3. P. Didukh, J. M. Greneche, A. Slwska-Waniewaska, P. C. Fannin and L. I. Casa, (2002) *J. Magn. Magn. Mater. 242 613.*
4. K.K. Laroia and A.P.B Sinha, (1963) *J. Pure Appl. Phys. 1 215*
5. A.M. Varaprasad and C.M. RadhaKrishnamurthy, (1986) *Bull Mat. Sci. 8 567*
6. K. Sailakshmi, *P* (1997).*h.D. Thesis, Andhra University India*
7. I. M. Hamada, J(2004). Magn. Magn. Mater. 271, 318.

8. P. B. Pandya, H. H. Joshi, and R. G. Kulkarni, (1991) J. Mat. Sci. 26, 5509.
9. Li Yao, Jiupeng Zhoo, Jiecai Han, (2002)Bull. Mat. Sci. 25 263.
10. D. C. Khan, M. Misra and A. R. Das, (1982) J. Appl. Phys. 53,2722
11. Shaikh Asif, Ph. D. Thesis – Effect of gamma radiation on physical properties of ferrite.

International Journal of Advance and Applied Research
www.ijaar.co.in
ISSN – 2347-7075 Impact Factor – 8.141
Peer Reviewed Bi-Monthly
Vol. 7 No. 14 January – February - 2026

ECG Signal Using Time Domain Analysis for Health Care

Shinde Ganesh Madhukar & Gaikwad Pradeep Devendra
R.B. Attal Arts, Science and Commerce College, Georai, Dist. Beed.
Corresponding Author – Gaikwad Pradeep Devendra
DOI - 10.5281/zenodo.19827105

Abstract:

Focuses solely on Intensive Care Units (ICUs), as it was done on this study, Rapid breathing and heart rate, along with confusion and disorientation are conditions that can be detected by monitoring devices Electric Cardiogram ECG devices. Time domain features will be explored to analyze the periodic functioning of the heart, clinicians examine the beat-to-beat behavior of the heart. were developed to allow the extraction of these features to help medical patients in ICU by foreseeing the deterioration in their health status such as Heart Rate,

Keywords: Signal Processing, ECG, Time Domain Analysis, Health Care.

Introduction:

The electrocardiogram represents an electrical tracing of the heart and is recorded non-invasively from the surface of the body [1]

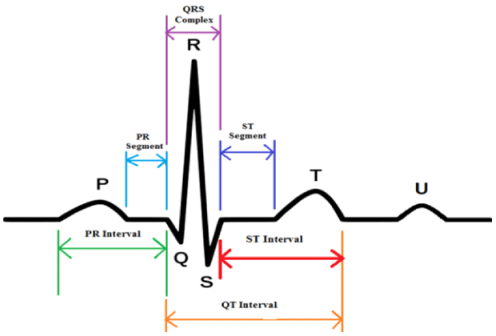

Fig. 1. ECG morphology: different segments of ECG signal for normal person

Electrocardiography ECG precisely record the electrical activity of heart rhythm over a period using electrodes/leads, which captures the electrical changes caused by depolarization and re-polarization of heart muscles during heartbeat [2]. This section includes recording of ECG signal by standard 12-conventional leads, noises associated during ECG acquisition, morphology (structural & physiological), and identification of heart related diseases from ECG. [3]. The electrocardiogram (ECG) is a non-invasive tool used to assess the electrical activity of the heart. . Time domain analysis of ECG signals is one of the most accessible and computationally efficient techniques for analysing heart activity, {[4-7] The Objectives to focus on methods of time-domain analysis and approaches to optimal data collection to ensure high signal quality and diagnostic accuracy.

Experiment Method:

The ECG represents a graphic recording of the electrical cardiac activity traced on the electrocardiograph paper.[8].Proposed work is based on ECG signal using time domain Analysis The conventional ECG machine consists of 12 leads divided into two groups, i.e., limb leads and precordial leads. Limb leads are further categorized as standard bipolar limb leads (I, II, and III) and augmented unipolar leads (aVL, aVF, and aVR). The precordial leads include V1 to V6. The limb leads view the heart in a vertical plane, and the precordial leads record the heart's electrical activity in the horizontal plane.

Result and Discussion:

Time domain features will be explored to analyze the periodic functioning of the heart, in their health status shown in figure1.

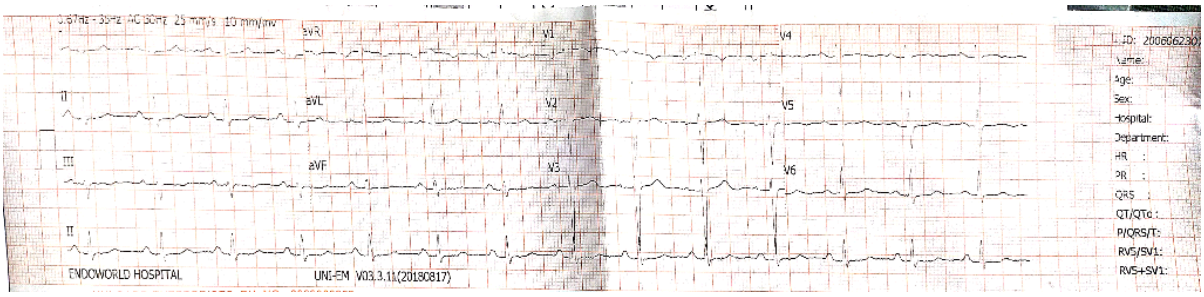

Figure 1: Sample of ECG recorded

Figure 1. show signal from the time Domain Analysis Pr interval 166ms QRS duration 92ms Qt 352ms Qtc 416ms .The image displays a medical report containing an abnormal ECG result. The analysis indicates: Heart Rate (HR): 84 bpm, PR Interval: 166 ms QRS Duration : 92ms QT/QTc: 352/416 ms.

Conclusion:

Signal ECG is using time domain of Heart rate sinus rhythm was Abnormal.

Acknowledgement:

Author is thank for to Georai Critical Hospital for supporting for work

References:

1. Krikler DM. (1987) Historical aspects of electrocardiography. Cardiol Clin. Aug;5(3):349-55. [PubMed].
2. D. Yoon, H.S. Lim, K. Jung, T.Y. Kim, S. Lee, (2019) Deep learning-based electrocardiogram signal noise detection and screening model, Healthc. Inform. Res. 25 201–211, https://doi.org/10.4258/hir.2019.25.3.201.
3. Kligfield P, Gettes LS, Bailey JJ, Childers R, Deal BJ, Hancock EW, van Herpen G, Kors JA, Macfarlane P, Mirvis DM, Pahlm O, Rautaharju P, Wagner GS., 2007 Mar;4(3):394- 12. [PubMed].
4. .Zimetbaum PJ, Josephson ME. (2003) Use of the electrocardiogram in acute myocardial infarction. N Engl J Med. Mar 06;348(10):933-40. [PubMed]
5. Pan, J. & Tompkins, W. J. (1985). A real-time QRS detection algorithm. IEEE Transactions on Biomedical Engineering.
6. Clifford, G. D., Azuaje, F., & McSharry, P. (2006). Advanced Methods and Tools for ECG Data Analysis.
7. Goldberger AL, et al. PhysioBank, PhysioToolkit, and PhysioNet: Components of a new research resource for complex physiologic signals.
8. Task Force of the European Society of Cardiology and the North American Society of Pacing and Electrophysiology (1996). HRV Standards.

International Journal of Advance and Applied Research
www.ijaar.co.in
ISSN – 2347-7075 Impact Factor – 8.141
Peer Reviewed Bi-Monthly
Vol. 7 No. 14 January – February - 2026

Eco-Friendly Green synthesis and X-ray diffraction studies of Spinel Nickel-Zinc Ferrite Nanoparticles

Shital P. Nawale[1], Kalyani K. Deshmukh[2], A. P. Keche[3], K. M. Jadhav[4]

[1]*Department of Physics, Shiv Chhatrapati College, Chhatrapati Sambhajinagar-431001, (MS) India*

[2]*Department of Physics, Deogiri College, Station Road, Chhatrapati Sambhajinagar-431005, (MS) India*

[3]*Department of Physics, R.B. Attal Arts, Science and Commerce, Georai, Beed-431127, (MS) India*

[4]*Department of Physics, School of Basic and Applied Sciences, MGM University, Chhatrapati Sambhajinagar-431001, (MS) India*

Corresponding Author – Shital P. Nawale

DOI - 10.5281/zenodo.19827124

Abstract:

Nickel-zinc ferrite ($Ni_{0.7}Zn_{0.3}Fe_2O_4$) nanoparticles were successfully synthesized via an environmentally friendly sol–gel combustion method employing Ginger extract as a green bio-fuel. The structural properties of the synthesized $Ni_{0.7}Zn_{0.3}Fe_2O_4$ nanoparticles were systematically investigated using X-ray diffraction (XRD). The diffraction patterns confirmed the formation of a single-phase cubic spinel structure with good crystallinity and no detectable secondary phases. The average crystallite size was initially estimated using the Debye–Scherrer equation, which is 12.22 nm. To further evaluate microstructural parameters. The Williamson–Hall (W–H) plot method was employed to distinguish the contributions of crystallite size and lattice strain to peak broadening. The W–H analysis revealed the presence of microstrain within the lattice along with nanoscale crystallite dimensions. The results showed excellent agreement between observed and calculated patterns, confirming the high phase purity and structural stability of the synthesized nanoparticles. The study demonstrates that ginger-assisted green combustion synthesis is an efficient method for producing structurally well-defined nickel-zinc ferrite nanoparticles suitable for advanced functional applications.

Keywords: Nickel-zinc ferrite, Green fuel, Structural property, W-H Study

Introduction:

Spinel ferrite nanoparticles have attracted considerable scientific and technological interest owing to their remarkable structural stability, tunable magnetic properties, chemical durability, and wide range of multifunctional applications [1, 2]. Spinel ferrites constitute an important class of magnetic oxide materials with the general chemical formula MFe_2O_4 (where M represents a divalent metal ion such as Ni^{2+}, Co^{2+}, Zn^{2+}, Mn^{2+}, etc.). These materials crystallize in a cubic spinel structure belonging to the $Fd\bar{3}m$ space group, in which oxygen anions form a close-packed face-centered cubic lattice while metal cations occupy tetrahedral (A) and octahedral (B) interstitial sites[3]. Depending on the distribution of cations among these sites, spinel ferrites are classified as normal, inverse, or mixed spinels. The flexibility in cation distribution allows fine-tuning of structural, electrical, and magnetic properties, making spinel ferrites highly versatile functional materials [4].

Among various ferrite systems, Nickel ferrite ($NiFe_2O_4$) has emerged as a prominent magnetic material because of its inverse spinel structure, moderate saturation magnetization,

high electrical resistivity, and excellent thermal and chemical stability. These characteristics make nickel ferrite nanoparticles highly suitable for applications in catalysis, electromagnetic interference shielding, magnetic storage, sensors, biomedical systems, and environmental remediation. Extensive research has been conducted on the synthesis of nickel ferrite nanoparticles using various chemical and physical routes. Conventional solid-state reactions require high calcination temperatures and often result in larger particle sizes. Conventional synthesis techniques such as sol–gel, co-precipitation, hydrothermal, and solid-state methods often require high energy input, hazardous chemicals, or complex processing steps [5]. However, traditional combustion methods commonly utilize synthetic fuels such as urea, glycine, or citric acid, which may generate toxic gases and pose environmental concerns. In recent years, increasing environmental awareness has driven the development of sustainable and eco-friendly synthesis routes based on green chemistry principles.

Green fuel-assisted combustion synthesis has emerged as an efficient and environmentally benign approach for producing metal oxide nanoparticles. Plant-based fuels are renewable, biodegradable, cost-effective, and rich in phytochemicals such as alkaloids, polyphenols, and carbohydrates, which facilitate homogeneous mixing at the molecular level and promote controlled combustion reactions [6]. In the present work, ginger extract is utilized as a novel green fuel for the synthesis of nickel-zinc ferrite nanoparticles. The bioactive constituents of ginger act as chelating and fuel agents, enabling efficient formation of phase-pure spinel structures under relatively mild conditions. **Bajaj *et al*.** investigated the sol–gel auto-combustion synthesis of $NiFe_2O_4$ nanoparticles using glycine as a chemical fuel. nickel ferrite nanoparticles with smaller size particles and improved magnetic properties which can be applied for various applications such as Photocatalysis, magnetic hyperthermia, magnetic sensors, magnetic fluids etc. [7]. **Shahane *et.al.*** Nickel zinc ferrite nanoparticles $Ni_xZn_{1x}Fe_2O_4$ (x=0.1, 0.3, 0.5) have been synthesized by a chemical co-precipitation method. The properties of the Ni–Zn ferrites can be effectively tailored by changing the composition parameter. [8]. **Divakara *et al.*** Nanocrystalline spinel nickel ferrite (NiFe2O4) was successfully synthesized using an eco-friendly auto-combustion method, with honey serving as a natural fuel and stabilizing agent. This green synthesis approach not only promotes sustainable nanomaterial synthesis but also highlights the potential applications of honey-derived nickel ferrite nanoparticles in advanced wastewater treatment and photocatalytic applications [9]. Structural investigation plays a vital role in understanding the crystallographic features and microstructural parameters of synthesized nanoparticles. The W–H method is widely employed to separate size-induced and strain-induced broadening in X-ray diffraction peaks, providing insights into crystallite size and lattice strain.

In this study, the eco-friendly green-fuel-assisted combustion synthesis of spinel nickel-zinc ferrite nanoparticles using ginger extract is systematically investigated [6]. Emphasis is placed on detailed structural characterization through W–H analysis, which explicates crystallite size, lattice strain, and structural parameters. The work highlights the potential of plant-derived fuels for producing high-quality ferrite nanoparticles while promoting sustainable, environmentally responsible nanomaterial synthesis.

Experimental Details:

1. Chemicals:

Nickel-zinc ferrite ($Ni_{0.7}Zn_{0.3}Fe_2O_4$) nanoparticles were prepared using nickel nitrate hexahydrate [$Ni(NO_3)_2 \cdot 6H_2O$], Zinc nitrate [$Zn(NO_3)_2.6H_2O$] and ferric nitrate nonahydrate [$Fe(NO_3)_3 \cdot 9H_2O$] (99.9% purity) as metal precursors. The salts were dissolved in distilled water to form a homogeneous solution, and ginger extract was used as a green fuel and complexing agent. Liquid ammonia (NH_3) was added dropwise to adjust the pH and facilitate controlled precipitation.

2. Preparation of $Ni_{0.7}Zn_{0.3}Fe_2O_4$ nanoparticles:

Ginger roots were collected from the local market of Chhatrapati Sambhajinagar. They were washed with distilled water, sun-dried, and then finely powdered. A measured amount of the powder was mixed with a water solution and heated at about 80–90°C for 30 min. under constant stirring, then filtered to obtain a clear ginger extract as shown in **Fig. 1**. The nickel nitrate, zinc nitrate and ferric nitrate were dissolved separately in distilled water and stirred to form homogeneous solutions. The Black pepper extract was then added as a chelating and fuel agent, and liquid ammonia was introduced dropwise to maintain the pH at 7 under continuous stirring. The mixture was heated gradually until gel formation occurred, and further heating induced auto-combustion, yielding a fine powder. The obtained powder was ground thoroughly and annealed at 600°C for 4 hours to achieve crystalline nickel ferrite nanoparticles for subsequent characterization.

3. Characterizations:

The phase formation and crystal structure of the synthesized nickel-zinc ferrite ($Ni_{0.7}Zn_{0.3}Fe_2O_4$) nanoparticles were analyzed using X-ray diffraction (XRD). The diffraction patterns were recorded using a Cu-Kα radiation source (λ = 1.5406 Å) over an appropriate 2θ range at room temperature. The average crystallite size was estimated using the Debye–Scherrer equation, while the Williamson–Hall (W–H) method was employed to evaluate the contributions of crystallite size and lattice strain to peak broadening.

Result and Discussion:

1. X-Ray diffraction (XRD) analysis:

The phase purity and structural characteristics of the synthesized nickel-zinc ferrite ($Ni_{0.7}Zn_{0.3}Fe_2O_4$) nanoparticles were investigated using X-ray diffraction (XRD). **Fig. 2** presents the XRD pattern of $Ni_{0.7}Zn_{0.3}Fe_2O_4$ nanoparticles recorded at room temperature (300 K). Confirming the formation of a single-phase cubic spinel structure with space group Fd-3m [10]. The most intense diffraction peak corresponding to the (311) plane was used to estimate the average crystallite size through the Debye–Scherrer equation. The lattice constant (a), unit cell volume (V), X-ray density (dx) were calculated using standard equations, and the obtained values are summarized in **Table 1**. The lattice constant was evaluated from the linear plot of √N versus 1/d. As shown in **Fig. 4**, a straight-line relationship was observed between √N and 1/d for all compositions. The lattice parameter (a) was determined from the slope of the best-fit line, and the calculated values are summarized in **Table 1.**.The calculated structural parameters are in good agreement with previously reported values for $Ni_{0.7}Zn_{0.3}Fe_2O_4$ ferrite nanoparticles [11].

$$n\lambda = 2d\sin\theta \quad (1)$$

$$a = d\sqrt{N} \quad (2)$$

$$dx = \frac{8M}{Na^3} \quad (3)$$

Where, N is Avogadro's number, M is the molecular weight and a is lattice constant.

Table 1. Values for crystalline size by Debye Scherrer and W-H plot (t) Molecular Weight (M), Lattice constant (a), Unit cell volume (V), X-ray density (d_X) of $Ni_{0.7}Zn_{0.3}Fe_2O_4$ spinel ferrite nanoparticle.

x	t (nm) by Scherrer formula	t (nm) by W-H plot	M (gm)	a (Å)	a (Å) by √N vs 1/d	v (Å)	d_x (gm/cm^3)
$Ni_{0.7}Zn_{0.3}Fe_2O_4$	12.22	16.42	236.387	8.377	8.385	587.91	5.341

Further microstructural parameters like stacking fault (SF) and lattice strain (LS), micro-strain (ε) , dislocation density (δ) and were computed and mentioned in **Table 2**.

$$\varepsilon = \frac{\beta cos\theta}{4} \quad (4)$$

$$LS = \frac{\beta}{4tan\theta} \quad (5)$$

Where 'β' represents the full width at half maxima (FWHM).

Table 2. Values for Stacking Fault (SF), and Lattice strain (LS), Micro Strain (ε) and Dislocation Density (δ) for $Ni_{0.7}Zn_{0.3}Fe_2O_4$ spinel ferrite nanoparticle.

x	SF	LS*10^{-4}	ε*10^{-3}	δ *10^{14}(lines/m^2)
$Ni_{0.7}Zn_{0.3}Fe_2O_4$	0.4295	9.54	2.83	6.697

The remaining structural parameters, including hopping length, interstitial radii, and bond length, were calculated based on following standard relationships. The hopping length and interstitial radii their values mentioned in **Table 3** [10].

$$L_{A=a\sqrt{3}/4} \quad (6)$$

$$L_{B=a\sqrt{2}/4} \quad (7)$$

The bond lengths, including the tetrahedral (A-O) and octahedral (B-O) bond lengths, were calculated using standard equations and values were mentioned in **Table 4**.

$$d_{AX=a}\sqrt{3(u-\frac{1}{4})} \quad (8)$$

$$d_{AX=a}\sqrt{3(u^2-\frac{11}{4}u+\frac{43}{64})} \quad (9)$$

$$d_{AX=a}\sqrt{2(2u-\frac{1}{2})} \quad (10)$$

$$d_{AX=a}\sqrt{2(1-2u)} \quad (11)$$

$$d_{AX=a}\sqrt{2(4u^2-3u+\frac{11}{16})} \quad (12)$$

Table 3. Values of Hopping lengths (L_A and L_B), Interstitial radii (r_A and r_B) for $Ni_{0.7}Zn_{0.3}Fe_2O_4$ spinel ferrite nanoparticle.

x	L_A (Å)	L_B (Å)	r_A (Å)	r_B (Å)
$Ni_{0.7}Zn_{0.3}Fe_2O_4$	3.626	2.962	0.486	0.652

The bond angles were determined using trigonometric principles based on the interionic distance values. These estimated bond angles are shown in **Table 4** [10].

Table 4. Values of Tetrahedral bond length (d_{AX}), Octahedral bond length (d_{BX}), Tetraedge shared (d_{AXE}), Octaedge shared (d_{BXE}), Octaedge unshared (d_{BXEU}) for $Ni_{0.7}Zn_{0.3}Fe_2O_4$ spinel ferrite nanoparticle.

x	d_{AX} (Å)	d_{BX} (Å)	d_{AXE} (Å)	d_{BXE} (Å)	d_{BXEU} (Å)
$Ni_{0.7}Zn_{0.3}Fe_2O_4$	1.886	2.053	3.080	2.843	2.962

The interionic distances between cations (b, c, d, e, f) and between cations and anions (p, q, r, s) were determined using the experimentally obtained lattice constants and oxygen positional parameters were mentioned in **Table 5** and **Table 6.**

Table 5. Values of Interionic distances (b, c, d, e, f) for $Ni_{0.7}Zn_{0.3}Fe_2O_4$ spinel ferrite nanoparticle.

x	b (Å)	c (Å)	d (Å)	e (Å)	f (Å)
$Ni_{0.7}Zn_{0.3}Fe_2O_4$	2.961	3.473	3.627	5.441	5.129

Table 6. Values of Interionic distances (p, q, r, s) for $Ni_{0.7}Zn_{0.3}Fe_2O_4$ spinel ferrite nanoparticle.

x	p (Å)	q (Å)	r (Å)	s (Å)
$Ni_{0.7}Zn_{0.3}Fe_2O_4$	2.052	1.886	3.611	3.651

2. Williamsons-Hall Analysis:

The Williamsons-Hall (W-H) analysis estimated of crystalline size, are illustrated in **Table 1**. The $Ni_{0.7}Zn_{0.3}Fe_2O_4$ nanoparticles, a plot of plot (4sinθ) vs (βcosθ) as shown in **Fig. 3** [4].

$$\beta cos\theta = \frac{\kappa\lambda}{t} + 4sin\theta \quad (13)$$

$$D = \frac{\kappa\lambda}{y-intercept} \quad (14)$$

Where, D is crystalline size and λ is the wavelength.

Conclusion:

$Ni_{0.7}Zn_{0.3}Fe_2O_4$ nanoparticles were prepared successfully through an environmentally friendly sol–gel combustion technique employing ginger extract as a natural fuel. X-ray diffraction results verified the formation of a well-crystallized, single-phase cubic spinel structure without any detectable impurities. The crystallite size, calculated using the Debye–Scherrer method, was approximately 12.22 nm, while Williamson–Hall analysis indicated the coexistence of nanoscale crystallites and inherent lattice microstrain. The ginger-mediated green combustion synthesis is a simple, sustainable, and efficient route for fabricating phase-pure nickel–zinc ferrite nanoparticles with potential for advanced technological applications.

Acknowledgment:

The author, Shital P. Nawale, is thankful to Punyashlok Ahilyadevi Holkar Solapur University, Solapur, for providing the XRD facility. Department of Chemistry, Dr. Babasaheb Ambedkar Marathwada University, Chhatrapati Sambhajinagar for providing FTIR Facility, and Institute of Chemical Technology, Marathwada Campus, Jalna for providing RAMAN facility,

Indian Institute of Technology, Madras (IITM) for providing VSM facility.

Funding:

The authors declare that no funds, grants, or other support were received during the preparation of this manuscript.

Data availability:

The research data generated and analyzed during the current study are available from the corresponding author upon reasonable request.

Competing Interest:

The authors declare no competing interests regarding the publication of this research manuscript.

References:

1. Salih, S.J. and W.M. Mahmood, (2023) *Review on magnetic spinel ferrite (MFe2O4) nanoparticles: From synthesis to application.* Heliyon,. **9**(6).
2. Akhtar, M.N., et al., (2021) *Physical, structural, conductive and magneto-optical properties of rare earths (Yb, Gd) doped Ni–Zn spinel nanoferrites for data and energy storage devices.* Ceramics International,. **47**(9): p. 11878-11886.
3. Jadhav, G.L., et al., *Copper-Doped Nickel Ferrite Nanoparticles: Structural, Optical, Magnetic and Antibacterial Properties for Multifunctional Application.* Optical, Magnetic and Antibacterial Properties for Multifunctional Application.
4. Jadhav, S.A., et al., (2021) *Magnetically retrievable nanoscale nickel ferrites: an active photocatalyst for toxic dye removal applications.* Ceramics International,. **47**(20): p. 28623-28633.
5. Patade, S.R., et al., (2020) *Self-heating evaluation of superparamagnetic MnFe2O4 nanoparticles for magnetic fluid hyperthermia application towards cancer treatment.* Ceramics International,. **46**(16): p. 25576-25583.
6. Nawale, S., et al. (2025) *Green technology approach of mixed Ni-Zn SFNPs and study of crystal structure, optical and magnetic behavior*. in *AIP Conference Proceedings*.. AIP Publishing LLC.
7. Bajaj, S., et al. (2020) *Magnetic properties of nickel ferrite magnetic nanoparticles prepared via glycine assisted sol-gel auto combustion route*. in *Journal of Physics: Conference Series*.. IOP Publishing.
8. Shahane, G., et al., (2010) *Synthesis and characterization of Ni–Zn ferrite nanoparticles.* Journal of Magnetism and Magnetic Materials,. **322**(8): p. 1015-1019.
9. Divakara, S., et al., (2025) *Photocatalytic degradation of crystal violet dye using honey mediated synthesis of NiFe2O4 nanoparticles.* Green Chemistry Letters and Reviews,. **18**(1): p. 2543931.
10. Somvanshi, S.B., et al., (2020) *Structural, thermal, spectral, optical and surface analysis of rare earth metal ion (Gd3+) doped mixed Zn–Mg nano-spinel ferrites.* Ceramics international, **46**(9): p. 13170-13179.
11. Ubale, Y.P., et al., (2025) *Antimicrobial Study of Aluminum-Incorporated Nickel Ferrite Nanoparticles Synthesized via Ginger Extract–Assisted Green Synthesis Approach.* Journal of Superconductivity and Novel Magnetism,. **38**(2): p. 93.

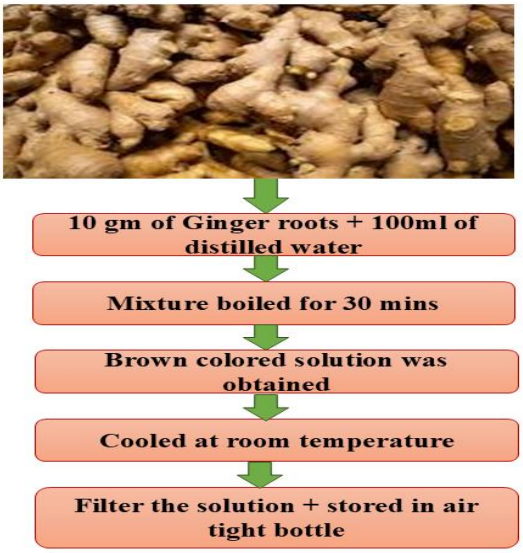

Fig.1 Flow chart of preparation of ginger root

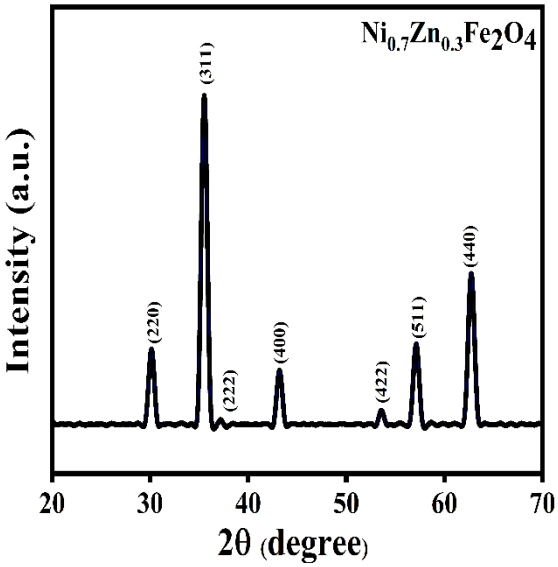

Fig. 2 XRD pattern for $Ni_{0.7}Zn_{0.3}Fe_2O_4$ ferrite Np's NP's

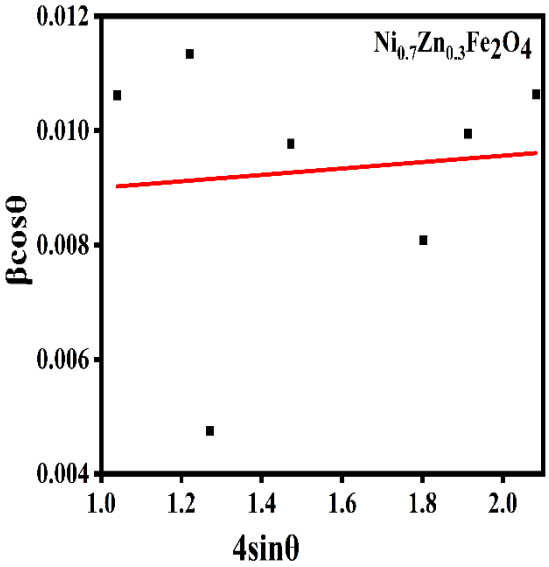

Fig. 3 Williamson-Hall plot of $Ni_{0.7}Zn_{0.3}Fe_2O_4$ ferrite NP's

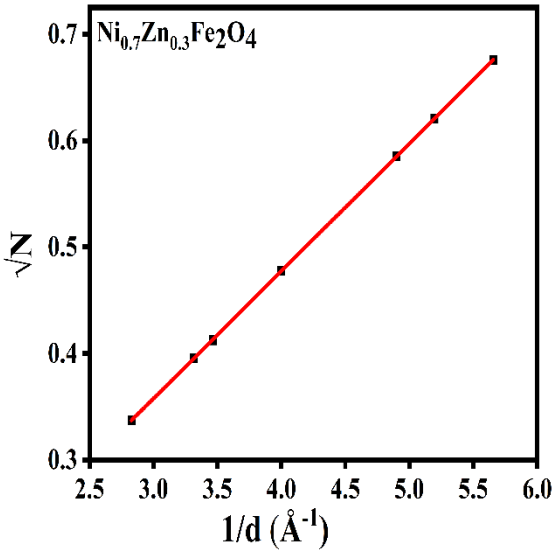

Fig. 4 Plot of √N vs 1/d of $Ni_{0.7}Zn_{0.3}Fe_2O_4$ ferrite NP's

International Journal of Advance and Applied Research
www.ijaar.co.in
ISSN – 2347-7075 Impact Factor – 8.141
Peer Reviewed Bi-Monthly
Vol. 7 No. 14 January – February - 2026

Morphology, and Band Gap Analysis of Synthesized Pure Phase Nickel Oxide

S. J. Indurkar

Department of Physics, J.E.S.'s, R. G. Bagdia Arts, S. B. Lakhotia Commerce and R. Bezonji Science College, Jalna, Maharashtra, India

Corresponding Author – S. J. Indurkar

DOI - 10.5281/zenodo.19827184

Abstract:

Nickel oxide (NiO) nanoparticles were synthesized via a sol-gel technique utilizing nickel nitrate as the precursor and citric acid as a chelating agent. The sol-gel process involved the formation of a gel, which was subsequently subjected to drying and calcination at varying temperatures to obtain NiO nanoparticles. The structural and morphological properties of the synthesized NiO nanoparticles were extensively characterized using X-ray diffraction (XRD), Fourier-transform infrared spectroscopy (FTIR), and scanning electron microscopy (SEM). XRD analysis confirmed the formation of pure NiO with a cubic crystal structure, and the crystallite size was calculated using the Debye-Scherrer equation. FTIR spectra corroborated the presence of characteristic Ni-O stretching vibrations, confirming the phase purity of the nanoparticles. SEM analysis revealed that the average particle size was approximately 12 nm, with slight variations attributable to different calcination temperatures. The optical properties were investigated by UV-Vis spectroscopy, revealing a direct band gap (Eg) of 2.52 eV, indicative of the material's semiconducting nature. These findings underscore the effectiveness of the sol-gel method in producing NiO nanoparticles with controlled size and desirable optical properties, suitable for various advanced applications.

***Keywords**: NiO, Sol-Gel, XRD, Direct Band Gap*

Introduction:

Nickel oxide nanoparticles (NiONPs) have emerged as a focal point of research due to their distinct physicochemical properties, which render them suitable for a wide range of applications, including catalysis, sensing, energy storage, and environmental remediation. Recent studies have further expanded the potential applications of NiONPs. For instance, Khorablou et al. (2023) developed a highly sensitive aptasensing platform by anchoring NiONPs on Mxene, which was employed for the detection of methamphetamine, showcasing the material's utility in analytical chemistry. Similarly, Balto et al. (2023) reported the green synthesis of NiONPs using *Salvadora persica*, evaluating their antimicrobial activity against oral microbes, thus highlighting their potential in antimicrobial therapies.

In the realm of renewable energy, Yu et al. (2023) successfully optimized NiOx nanoparticles to function as efficient hole transport layers in inverted perovskite solar cells, resulting in a significant enhancement in power conversion efficiency. This underscores the critical role of NiONPs in advancing photovoltaic technologies. Furthermore, Rakhimbek et al. (2023) demonstrated the incorporation of Ni/NiO-embedded carbon nanofibers in lithium-sulfur batteries, leading to improved battery performance, thereby illustrating the contribution of NiONPs in energy storage systems.

The photocatalytic and antimicrobial properties of NiONPs have also been a subject of

extensive investigation. Athab et al. (2024) synthesized chromium-doped NiONPs, which exhibited superior photocatalytic degradation capabilities and notable antifungal activity, while Ganapathy et al. (2024) developed CuMn-doped NiONPs with enhanced bactericidal properties. Additionally, Alarfaj et al. (2024) synthesized CeO/NiO nanocomposites, achieving high efficiency in toxin removal from contaminated water, emphasizing the potential of NiONPs in environmental purification processes.

Brindhadevi et al. (2024) reported the use of NiONPs in the photocatalytic degradation of polycyclic aromatic hydrocarbons, demonstrating their efficacy in addressing environmental pollutants. Yılmaz et al. (2024) introduced a green synthesis approach for NiONPs using *Lupinus albus* extract, focusing on catalytic and photocatalytic applications, thus promoting sustainable methodologies for nanoparticle synthesis.

These studies collectively illustrate the multifaceted applications and significant potential of NiONPs in various scientific and technological domains. Continued exploration of NiONPs is anticipated to lead to further advancements and innovations across multiple sectors.

Synthesis of NiO Nanoparticles:

Nickel oxide (NiO) nanoparticles were synthesized via the sol-gel method using nickel nitrate hexahydrate ($Ni(NO_3)_2 \cdot 6H_2O$) as the precursor and citric acid ($C_6H_8O_7$) as a chelating agent. Initially, 0.1 M of nickel nitrate hexahydrate was dissolved in 100 mL of deionized water under continuous stirring at room temperature. Subsequently, citric acid was added to the solution at a molar ratio of 1:3 (citric acid: nickel ions) to form a homogeneous solution. The mixture was stirred vigorously for 2 hours, during which time a clear, green sol was formed. This sol was then heated at 80°C to evaporate the solvent, resulting in the formation of a viscous gel.

The gel was allowed to dry at 120°C in an oven for 24 hours, after which it was calcined at various temperatures (400°C, 500°C, and 600°C) for 3 hours to obtain NiO nanoparticles. The calcination process led to the decomposition of organic components and the formation of crystalline NiO. The resulting nanoparticles were collected and subjected to characterization.

Results and Discussion:

1. XRD Analysis:

The X-ray diffraction (XRD) analysis was performed to determine the crystalline structure and phase purity of the synthesized Nickel oxide (NiO) nanoparticles. The XRD patterns of the NiO samples calcined at 400°C, 500°C, and 600°C are shown in Figure 1. The diffraction peaks observed at 2θ values of approximately 37.3°, 43.3°, 62.8°, 75.3°, and 79.4° correspond to the (111), (200), (220), (311), and (222) crystal planes, respectively, which are consistent with the cubic crystal structure of NiO (JCPDS card No. 47-1049).

The absence of any additional peaks confirms the phase purity of the synthesized NiO nanoparticles. The crystallite size (D) of the NiO nanoparticles was calculated using the Debye-Scherrer equation:

$$\boldsymbol{D = \frac{0.9\,\lambda}{\beta cos\theta}} \qquad \textbf{(1)}$$

Where 'λ' is the X-Ray wavelength (0.15406 nm), β is the full width at half maximum (FWHM), θ is the diffraction angle, and 'D' is the particle diameter size. Using Bragg's Law, the value of d spacing the interplanar distance between the atoms is estimated [12].

The average crystallite sizes were found to be approximately 12 nm for the samples calcined at 400°C, 11 nm for those calcined at 500°C, and 10 nm for those calcined at 600°C. The slight decrease in crystallite size with increasing calcination temperature can be attributed to the enhanced grain growth inhibition due to the increased nucleation rates at higher temperatures.

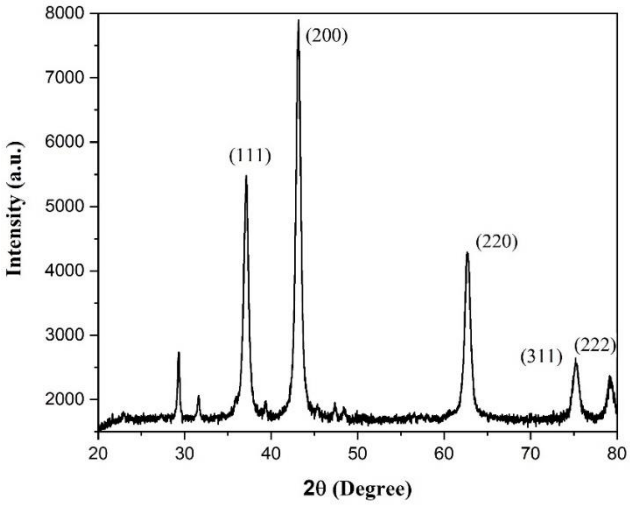

Figure 1. X-ray diffraction patterns of NiO Nanoparticles

These results indicate that the sol-gel method effectively produces NiO nanoparticles with a well-defined cubic structure and a controlled crystallite size, which is critical for their potential applications in various fields, such as catalysis, energy storage, and environmental remediation.

2. Fourier-Transform Infrared (FTIR) Spectroscopy Analysis:

Fourier-transform infrared (FTIR) spectroscopy was employed to investigate the chemical bonding and confirm the phase formation of the synthesized Nickel oxide (NiO) nanoparticles. The FTIR spectra of NiO nanoparticles calcined at 400°C, 500°C, and 600°C are presented in Figure 2. The spectra were recorded in the range of 4000–400 cm^{-1}.

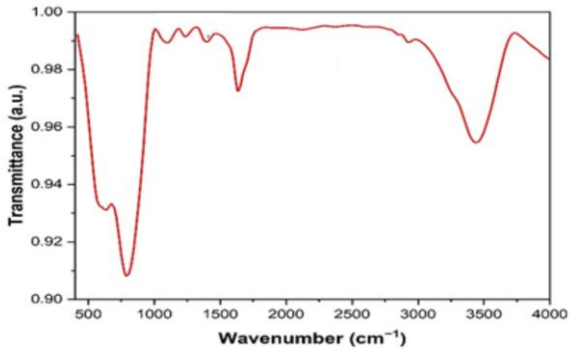

Figure 2. FT-IR absorption spectra of NiO nanoparticles

The most prominent absorption bands observed at approximately 423 cm^{-1} and 553 cm^{-1} correspond to the stretching vibrations of the Ni–O bonds, which are characteristic of the NiO phase. These bands confirm the successful formation of nickel oxide. The presence of these distinct Ni–O peaks across all samples indicates that the NiO nanoparticles maintain their structural integrity irrespective of the calcination temperature.

Additionally, a broad band observed around 3430 cm^{-1} can be attributed to the O–H stretching vibrations, indicating the presence of surface hydroxyl groups. This is likely due to the adsorption of moisture from the environment, which is a common phenomenon in nanoparticle samples. The small peak around 1630 cm^{-1} corresponds to the bending vibration of the adsorbed water molecules (H–O–H), further supporting the presence of surface hydroxyl groups.

The intensity of the Ni–O stretching vibrations slightly increases with the calcination temperature, suggesting that higher temperatures promote a more complete decomposition of the organic residues from the precursor, resulting in a purer NiO phase. The absence of significant

peaks related to organic impurities, especially in the higher temperature samples, corroborates the effectiveness of the sol-gel method in producing phase-pure NiO nanoparticles.

3. UV-Vis Spectroscopy Analysis:

The optical properties of the Nickel oxide (NiO) nanoparticles calcined at 500°C were investigated using UV-Vis spectroscopy. The UV-Vis absorption spectrum of the sample was recorded in the wavelength range of 200–800 nm, as illustrated in Figure 3. A strong absorption peak was observed around 370 nm, which is typical for NiO nanoparticles, indicating the transition of electrons from the valence band to the conduction band.

To determine the optical band gap (Eg) of the NiO nanoparticles, the Tauc plot method was employed. The absorption coefficient (α) was calculated using the absorbance data, and the Tauc plot was constructed by plotting $(\alpha h\nu)^2$ against photon energy (hν), where hν represents the photon energy. The extrapolation of the linear portion of the plot to the energy axis provided the direct band gap value for the sample.

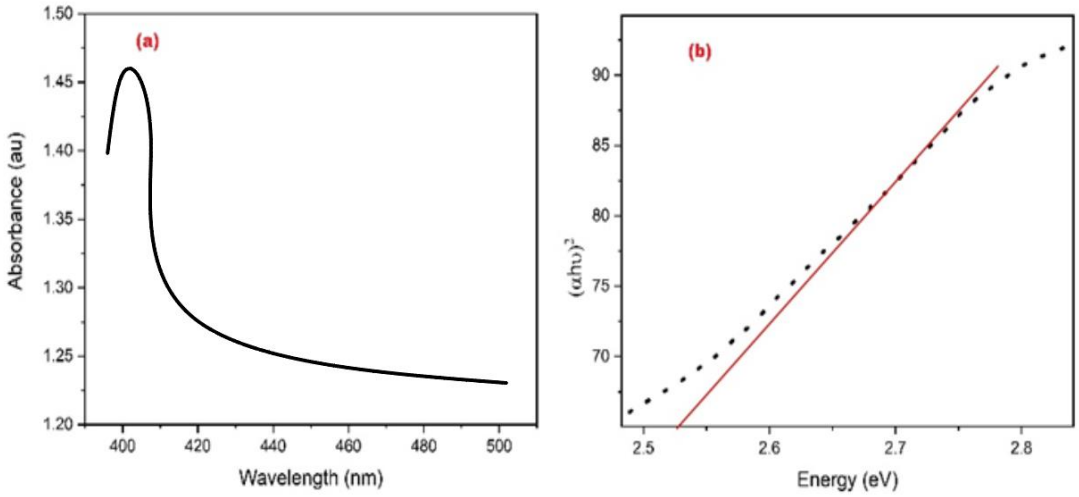

Figure 3. (a) UV absorption spectra (b) Direct Band gap of NiO Nanoparticles

The direct band gap for the NiO nanoparticles calcined at 500°C was found to be 2.48 eV. This value is consistent with the reported band gap for NiO nanoparticles and confirms the material's semiconducting nature. The relatively high band gap suggests that these NiO nanoparticles are well-suited for applications in photocatalysis, optoelectronics, and solar cells, where a specific band gap is crucial for optimizing performance.

The UV-Vis analysis further corroborates the successful synthesis of NiO nanoparticles with desirable optical properties, demonstrating that the sol-gel method is effective in producing nanoparticles with a consistent and controlled band gap.

4. Scanning Electron Microscopy (SEM) Analysis:

The morphology and particle size of the synthesized Nickel oxide (NiO) nanoparticles were examined using scanning electron microscopy (SEM). The SEM analysis was specifically performed on the NiO sample calcined at 500°C, as shown in Figure 4. The micrograph reveals that the NiO nanoparticles exhibit a nearly spherical morphology with a relatively uniform particle distribution.

The average particle size was determined to be approximately 12 nm, which is consistent with the crystallite size calculated from XRD analysis. The nanoparticles are slightly agglomerated, which is typical for metal oxide nanoparticles synthesized via the sol-gel method due to their high surface energy. However, the individual particles are clearly discernible, and their nanoscale size is confirmed.

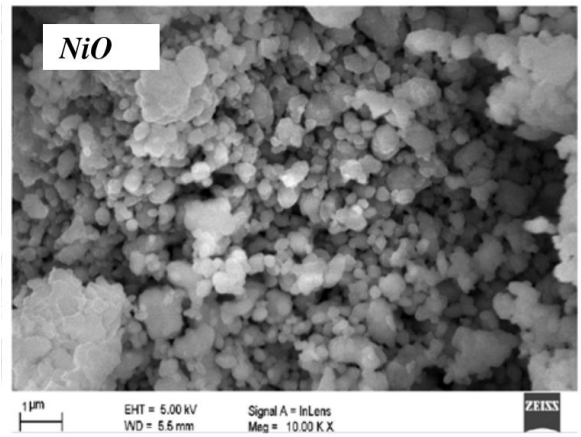

Figure 4. SEM image of Nickel Oxide nanoparticles

The surface of the particles appears smooth and free from significant defects, indicating a high-quality synthesis process. The uniformity in particle size suggests that the sol-gel method employed provides good control over the nanoparticle growth, resulting in a homogenous size distribution. This uniformity is critical for potential applications in catalysis and electronics, where consistent particle size can influence the performance of the material.

The SEM analysis, therefore, corroborates the findings from XRD and FTIR, confirming the successful synthesis of NiO nanoparticles with controlled morphology and size. The combination of these techniques provides a comprehensive understanding of the structural and morphological characteristics of the synthesized NiO nanoparticles.

Conclusion:

Nickel oxide (NiO) nanoparticles were synthesized successfully using the sol-gel method with nickel nitrate and citric acid as precursors. The characterization of these nanoparticles was performed using X-ray diffraction (XRD), Fourier-transform infrared spectroscopy (FTIR), scanning electron microscopy (SEM), and UV-Vis spectroscopy. XRD analysis confirmed the formation of phase-pure NiO with a cubic crystal structure and an average crystallite size of approximately 12 nm. FTIR spectra corroborated the presence of characteristic Ni–O bond vibrations, indicating phase purity. SEM analysis revealed a nearly spherical morphology with an average particle size of 12 nm, consistent with the XRD results. The UV-Vis spectroscopy analysis determined the direct band gap of the NiO nanoparticles to be 2.48 eV, which is suitable for applications in photocatalysis, optoelectronics, and other fields requiring semiconducting materials. These findings demonstrate that the sol-gel method is an effective approach for producing NiO nanoparticles with controlled size and desirable optical properties. The successful synthesis and characterization of these nanoparticles provide a strong foundation for their use in various technological applications, highlighting the method's potential for further development in nanomaterials research.

References:

1. Zeynab Khorablou; F. Shahdost-Fard; H. Razmi; “High Sensitive Detection of Methamphetamine By High-performance Aptasensing Platform Based on Nickel Oxide Nanoparticles Anchored on Mxene”, MICROCHEMICAL JOURNAL, 2023.
2. H. Balto; M. Amina; R. Bhat; Hanan M. Al-Yousef; Sayed H. Auda; Afaf Elansary; “Green Synthesis of Nickel Nanoparticles

Using Salvadora Persica and Their Application in Antimicrobial Activity Against Oral Microbes", MICROBIOLOGY RESEARCH, 2023.

3. Shiqi Yu; Zhuang Xiong; Haitao Zhou; Qian Zhang; Zhenhan Wang; Fei Ma; Zihan Qu; Yang Zhao; Xinbo Chu; Xingwang Zhang; J. You; "Homogenized NiOx Nanoparticles for Improved Hole Transport in Inverted Perovskite Solar Cells", SCIENCE, 2023. (IF: 3)
4. Islam Rakhimbek; Nurzhan Baikalov; Aishuak Konarov; Almagul Mentbayeva; Yongguang Zhang; Zhumabay Bakenov; "Nickel and Nickel Oxide Nanoparticle-embedded Functional Carbon Nanofibers for Lithium Sulfur Batteries", NANOSCALE ADVANCES, 2023.
5. Zahraa H Athab; Ahmed F Halbus; Abbas J Atiyah; Shaimaa Satae M Ali; Z A Al Talebi; "High-performance Photocatalytic Degradation and Antifungal Activity of Chromium-doped Nickel Oxide Nanoparticles", ANALYTICAL SCIENCES: THE INTERNATIONAL JOURNAL OF THE ..., 2024.
6. Kavina Ganapathy; Sri Prakash Pandey; Sunita Bishnoi; J. Suriyaprakash; Abdullah A. Alarfaj; A. Hirad; Indumathi Thangavelu; "Biocidal Activities of Nickel Oxide Nanoparticles Modified By Copper and Manganese, Synthesized By Green Process", APPLIED ORGANOMETALLIC CHEMISTRY, 2024.
7. Nawal Alarfaj; Nawal Al Musayeib; Musarat Amina; Maha El-Tohamy; "Synthesis and Characterization of Polysiphonia/cerium Oxide/nickel Oxide Nanocomposites for The Removal of Toxins from Contaminated Water and Antibacterial Potential", ENVIRONMENTAL SCIENCE AND POLLUTION RESEARCH INTERNATIONAL, 2024.
8. Zahraa H Athab; Ahmed F Halbus; Sura Bahaa Mohammed; Abbas J Atiyah; Hussein Idrees Ismael; Nahlah Salman Saddam; Sadiq J Baqir; Hasan F Alesary; Sameer Algburi; Nadhir Al-Ansari; "Comparison Activity of Pure and Chromium-doped Nickel Oxide Nanoparticles for The Selective Removal of Dyes from Water", SCIENTIFIC REPORTS, 2024.
9. Kathirvel Brindhadevi; T P Kim; Sulaiman Ali Alharbi; M D Ramesh; Jintae Lee; Devaraj Bharathi; "Enhanced Photocatalytic Degradation of Polycyclic Aromatic Hydrocarbons (PAHs) Using NiO Nanoparticles", ENVIRONMENTAL RESEARCH, 2024.
10. Mine Yılmaz; A Abdullah Ceyhan; Orhan Baytar; "Catalytic Effect of Nickel Oxide Nanoparticles from Lupinus Albus Extract on Green Synthesis and Photocatalytic Reduction of Methylene Blue: Kinetics and Mechanism", INTERNATIONAL JOURNAL OF PHYTOREMEDIATION, 2024.

International Journal of Advance and Applied Research
www.ijaar.co.in
ISSN – 2347-7075 Impact Factor – 8.141
Peer Reviewed Bi-Monthly
Vol. 7 No. 14 January – February - 2026

Synthesis of Coersivity and Magnetic Moment of Nanoparticle Sized Aluminium Substituted Copper Cobalt Ferrites

Subhash S. Karande[1] & Mahendra S. Kavale[1]

[1] *Department of Physics, Sangameshwar College (Autonomous), Solapur (M.S.)*

Corresponding Author – Subhash S. Karande

DOI - 10.5281/zenodo.19827217

Abstract:

The polycrystalline aluminium substituted nano-particle sized copper cobalt ferrite samples $Cu_xCo_{1-x}Fe_{2-2y}Al_{2y}O_4$ (where x= 0.0, 0.2, 0.4, 0.6, 0.8, 1.0; y = 0.05, 0.15 and 0.25) have been prepared by standard ceramic technique. Phase formation is investigated using X-ray diffraction, Infrared absorption technique and Scanning electron microscope technique. Magnetic properties of the samples are investigated by using Vibrating Sample Magnetometer (VSM) and Helmholtz's double coil apparatus. The lattice constants of the all samples are evaluated from x-ray diffraction data. A universal testing machine as well as Archimedes's method was applied for determining the physical properties of the samples. Ionic radii R_A and bond lengths (A-O) on both sites are found decreases with Al^{3+} and copper content. The Lattice constant 'a', physical density as well as X-ray density of samples goes on increasing with Al^{3+} and copper content. The ratio c/a is found increasing when addition of copper content and decreases with aluminum content. It means that Al^{3+} and copper acquire the tetragonal prolate type distortions on B site and hence (c/a) ratio increases and automatically crystal lattice turned from tetragonal spinel to cubic spinel. Addition of Al^{3+}replaces Fe^{3+}on A-site and hence magnetic moment per unit values decreases. Copper cobalt ferrite exhibits canting of spins of magnetic moments on B-site. The canting angle α_{yk} is found decreasing with Al^{3+}content in the host lattice.

Keywords: Polycrystalline, Standard Ceramic Technique, Magnetic Moment, Canting Angle

Introduction:

In a way, every material utilized today is a composite. Composite materials are a physical mixture of two or more compatible micro or macro constituent particles which differ in form and chemical composition and are essentially insoluble in each other. Composite materials are best suited for scientific applications which could not be achieved by any one component acting on its own properties. Ferrite / ferroelectric composites are termed as magneto electric (ME) composites due to the coupling between the electric and magnetic fields in the materials. The conversion of magnetic to electric fields in such ME composite originates from the elastic interaction between ferrite and ferroelectric subsystems [1]. In the presence of the magnetic field, the magnetostriction in the ferrite phase gives rise to mechanical stresses that are transferred to the ferroelectric phase, resulting in electric polarization of the ferroelectric phase owing to its magneto electric effect. ME materials find applications as smart materials in actuators, sensors, magnetic probes, phase inverters, rectifiers, modulators, and transducers in solid state microelectronics and microwave devices [2,3].

Spinel ferrite nanoparticles are being intensively investigated in recent years because of their remarkable electrical and magnetic properties and wide practical applications in information storage system, ferro-fluid

technology, magnetiocaloric refrigeration and medical diagnosis [4]. Among the spinels, mixed Zn ferrites and especially Ni–Zn ferrites are widely used in applications like transformer cores, chokes, coils, noise filters recording heads etc. [5]. While Ni–Zn ferrite posses higher resistivity and saturation magnetization, cobalt ferrite possess high cubic magneto crystalline anisotropy and hence high coercivity. The high coercivity is driven by large anisotropy of the cobalt ions due to its important spin orbit coupling. It is ferromagnetic with a Curie temperature (T_c) around 520°C, [6] and shows a relatively large magnetic hysteresis which distinguishes it from rest of the spinels. The synthesis of ultra fine magnetic particles has been extensively investigated in recent years because of their potential applications in high density magnetic recording and magnetic fluids [7]. Among the current methods for synthesis of mixed ferrite the combustion reaction method stands out as an alternative and highly promising method for the synthesis of these ferrites [8]. Magnetic properties measured at room temperature by vibrating sample magnetometer (VSM) reveal an increase in saturation magnetization with increase in cobalt concentration [9].

Experimental:

The ferrites with general chemical formula $Cu_xCo_{1-x}Fe_{2-2y}Al_{2y}O_4$ (where x= 0.0, 0.2, 0.4, 0.6, 0.8, 1.0; y = 0.05, 0.15 and 0.25) were prepared by the standard ceramic technique using AR grade cobalt oxide, copper oxide, ferric oxide and aluminium oxide. The compositional weights of powders were mixed physically and blended in agate mortar in acetone medium. The final sintering process was carried at 1000^0C for 48 hours. The slow cooled samples were heated at rate of 80^0C per hour. The pellets and toroids were formed by using respective steel die. A universal testing machine as well as Archimedes's method was applied for determining the physical properties of the samples. The formation of the cubic spinel structure of the samples prepared is confirmed by X- ray diffraction analysis. Saturation magnetization of each was carried out using high-field hysteresis loop tracer and presented in fig.2. The saturation magnetization (σs), magnetic moment (n_B) were determined from the magnetization study and presented by graphs (Fig.3)

Results and Discussion:

The lattice constants 'a' and 'c' for all prepared samples are calculated by using prominent (311) XRD peak [10]. The calculated and observed values of inter planer distance (d) are found in good agreement with each other for all reflections. The particle size (D) for all the ferrite samples is calculated by Debye Scherer formula, ionic site radii (R_A, R_B) and ionic bond lengths (A-O, B-O) are calculated from the formulae given by Gadkari et.al [11]. From the calculations of lattice constants 'a' and 'c' for all the prepared ferrites; it is observed that c > a; tetragonality ratio (c/a) is found in the range of 1.03 to 1.07. This result is in good agreement with previous report [12-13].

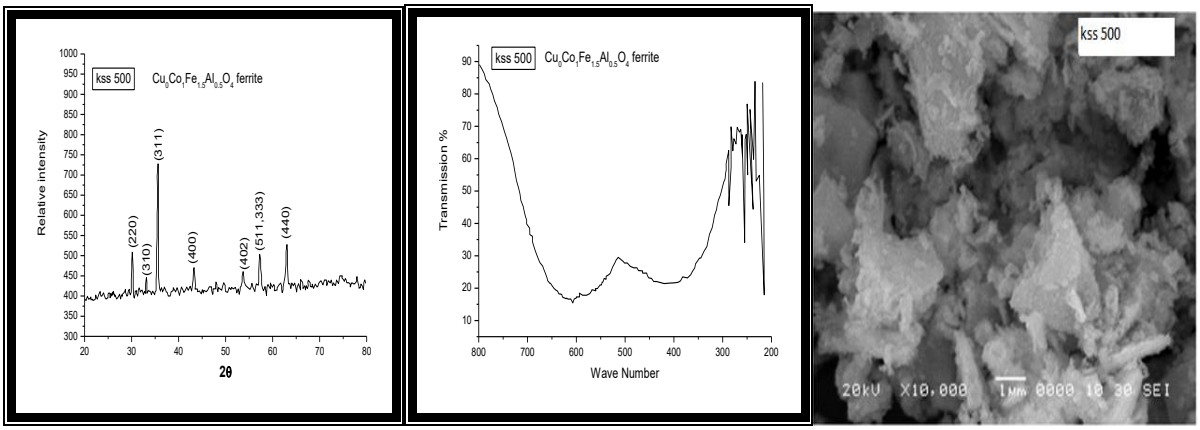

Fig: 1 Characterisation of ferrite samples by XRD,IR, SEM

The infrared absorption spectra showing two distinct absorption band ν_1 due to tetrahedral (A) site interstitial voids near 600 cm^{-1} and other ν_2 due to octahedral (B) site interstitials voids near 400 cm^{-1}. Our results in this present communication are well supported by previous reports [14, 15].

The close inspection of all micrographs revealed that there is continuous grain growth with well defined grain boundaries formed. The present system shows multi domain behaviour. No exaggerated grain growth is observed in any of this composition. The average grain size is found to decrease with increase in Al content in copper cobalt ferrite. However in the present system the grain growth shows generally a decreasing trend with aluminum content, which is rather expected because of multi-domain behavior of these compositions in copper cobalt ferrite. Grain growth is almost accompanied with grain size, which is increasing with copper and aluminum content. So it appears that copper and aluminum content favours the grain growth. The scanning electron micrograph was shown above.

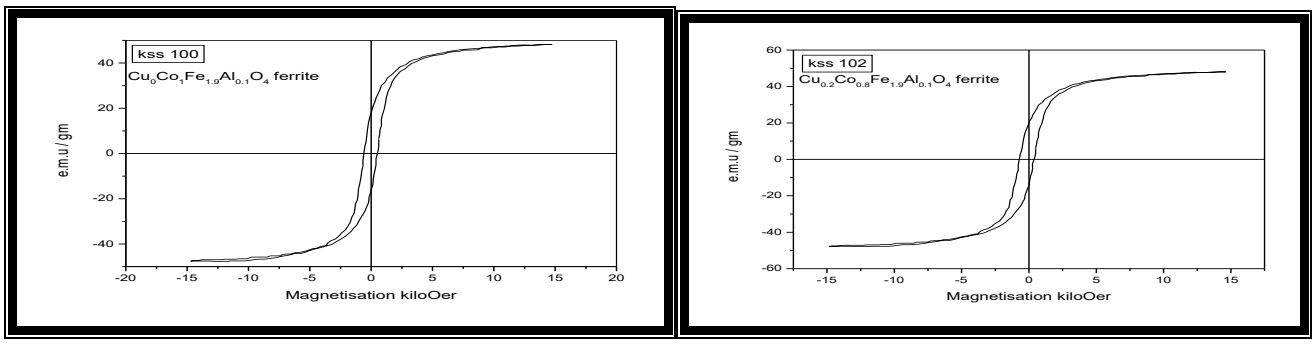

Fig. 2.Hysteresis patterns of the samples for$Cu_xCo_{1-x}Fe_{2-2y}Al_{2y}O_4$ ferrite system

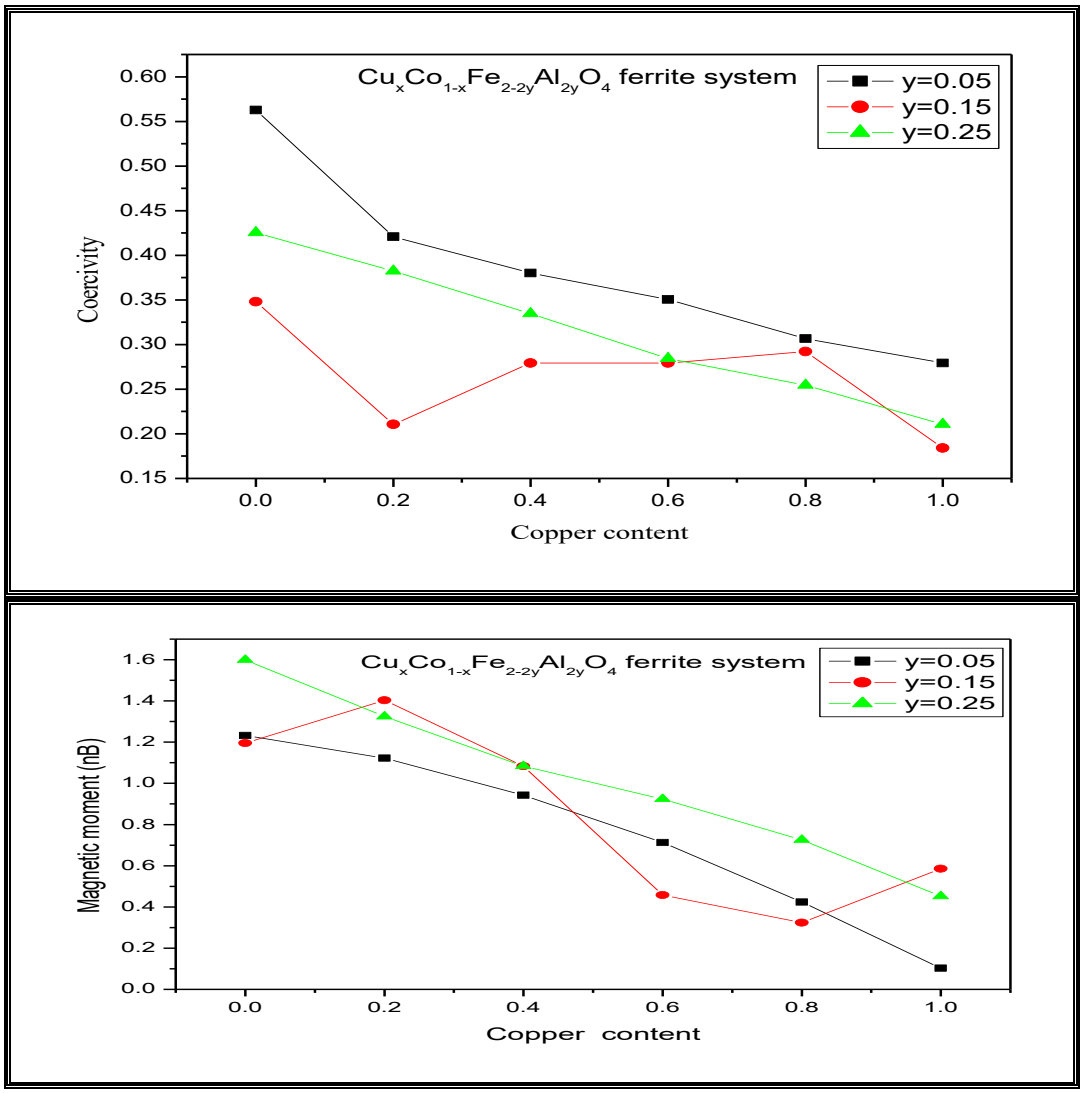

Fig 3: Variation of coersivity, magnetic moment, Remnent magnetization and saturation magnetization with copper and aluminium content for $Cu_xCo_{1-x}Fe_{2-2y}Al_{2y}O_4$ ferrite system

The value of n_B was observed which goes on decreasing for aluminium doped copper cobalt ferrite with increasing aluminium and copper content. Addition of Cu^{2+} content replaces Fe^{3+} from A to B site which produces canting of the magnetic spins and results in the decrease in both magnetic moments on A and B sites. This clearly indicates the decrease in A-B interaction.

Saturation magnetization is found increasing upto 20 % of copper content and thereafter decreases. The increasing trend of saturation magnetisation with Cu^{2+} content up to x= 0.2 suggest that the Neels two sub - lattice model is predominating up to x = 0.2 and thereafter Y-K three sub lattice predominant. The decrease in saturation magnetization (Ms) can also be explained in the light of Yafet-Kittle model of triangular spins.[16]

The coercivity decreases with particle size as suggested by Liu et al. The large value of coercivity essentially originates from the anisotropy of the copper ions at the octahedral (B) site due to its important spin orbit coupling. The coercive field (Hc) in Al doped copper cobalt ferrite is found to decrease with increasing Aluminum content in the doped copper cobalt

ferrites, which may be attributed to the loss of anisotropy due to the migration of Cu^{2+} ions to the tetrahedral site and also due to the decrease in the ferrous content in doped copper cobalt ferrite. The decrease in coercivity of samples is accompanied by the reduction of saturation magnetization and remnant magnetization. The reason for the decrease in coercivity of copper cobalt ferrite is the decrease in magneto-crystalline anisotropy by lowering the concentration of Fe^{2+} ions at the octahedral sites in the spinel lattice because Fe^{2+} ions are also a source of the magnetic anisotropy in ferrites**.**

The remnant magnetization (Mr) of Al^{3+} doped copper cobalt ferrite shows a decreasing behaviour with increase in copper and Al content from x = 0.00 to x = 0.1 and y=0.05, 0.15, 0.25. The decrease in Mr is due to lower magnetic moment of Al^{3+} as compared to Fe^{3+}.

Conclusion:

Copper cobalt ferrite is partially inverse spinel ferrite. Addition of Al^{3+} ions replaces Fe^{3+} on (B) site resulting in increase of lattice constant a, decrease in ionic radii(R_A) and bond length(O-A). The lattice constant obtained from XRD data shows increases. The coersivity (Hc), magnetic moment(n_B), with copper and aluminium content goes on decreasing.

References:

1. R. S. Devan, S. A. Lokare, S. S. Chougule, D. R. Patil, Y. D. Kolekar, andB. K. Chougule, J. Phys. Chem. Solids **67**, 1524 (2006).
2. K. Zhao, K. Chen, Y. R. Dai, J. G. Wan, and J. S. Zhu, Appl. Phys. Lett. **87**, 162901 (2005).
3. S. R. Kulkarni, C. M. Kanamadi, and B. K. Chougule, Mater. Res. Bull. **40**, 2064 (2005).
4. Zhao L, Yang H, Yu L, Cui Y, Zhao X, Zou B, Feng SJ. MagnMagn Mater2006;301:445–51.
5. Rath C, Sahu KK, Anand S, Date SK, Mishra NC, Das RP. J MagnMagn Mater 1999;202:77–84.
6. Rajendran M, Pullar RC, Bhattacharya AK, Das D, Chintalapudi SN, Majumdar CK. J MagnMagn Mater 2001;232:71–83.
7. Ozaki M. Mater Res Bull 1989;12:35–43.
8. Costa ACM, Tortella E, Morelli MR, Kaufman M, Kiminami RHGA. J Mater Sci2002;37:3569–72.
9. M.M. Mallapur, B.K. Chougule; Materials Letters; Vol. 64 (2010); P. 231–234.
10. H. P. Klug, L. E. Alexander, X-ray diffraction procedure for polycrystalline and amorphous materials,(Willey N.Y 1997)637.
11. A. B. Gadkari, T. J. Shinde, P. N. Vasambekar, J. Mater Sci: Mater Electron 21 (2010) 96-103.
12. A. T. Raghavender, R. G. Kulkarni and K.M. Jadhav; Chinese J. of Phys.vol.48 No.4 (2010) 512-522.
13. A.T. Raghvendra et al. magn. Mater. 316 (2007) 1
14. Waldron R.D, Phy.Rev; 99(6) (1955)1727.
15. K. V. S. Badarinath, Phys. Stat. Solidi (a) 91(1985)K-19-23.
16. Yafet Y, Kittel C, (1952), Antiferromagnetic arrangements in ferrites, Phys. Rev.; Vol. 87; P. 290.

International Journal of Advance and Applied Research
www.ijaar.co.in
ISSN – 2347-7075 Impact Factor – 8.141
Peer Reviewed Bi-Monthly
Vol. 7 No. 14 January – February - 2026

Magnetic Polymer Nanocomposites for Biomedical Applications

Takle Ganesh Baburao, Kamble Pravin Ashruba, Gaikwad Pradeep Devendra

Physics Department,

R.B. Attal Arts, Science and Commerce College, Georai, Taluka Georai,Dist. Beed431127.

Corresponding Author – Takle Ganesh Baburao

DOI - 10.5281/zenodo.19827228

Abstract:

Magnetic nanoparticle–conductive polymer composites represent a promising class of multifunctional materials for biomedical applications. Among them, Fe_3O_4–polyaniline (PANI) composites have gained attention due to their unique combination of magnetic responsiveness, electrical conductivity, and biocompatibility. This explores synthesis strategies, biomedical applications such as drug delivery, and compares Fe_3O_4–PANI systems with other magnetic nanoparticle–polymer composites. The discussion highlights the advantages of Fe_3O_4 emphasizing its reduced cytotoxicity and multifunctionality.

Keywords: Magnetite (Fe3O4), Polianiline, Electrochemical method, Biomedical Applications

Introduction:

PANI is found in one of the three idealized oxidation states during the polymerization of aniline monomer: (a) leucoemeraldine, (b) emeraldine salt, and (c) pernigraniline Fully oxidized PANI is known as pernigraniline base. Half of the oxidized PANI is reduced as the emerald base, and PANI is completely reduced as the lecomeraldine base. As shown below in figure 1. [1-5]

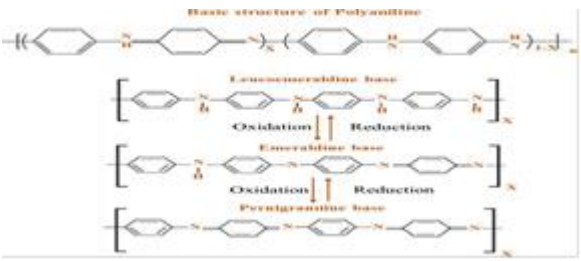

Fig. 1 Polyaniline different oxidation state

Among the CPs PANI occupies a special role for its diversity of structural forms, high environmental stability, unique doping/dedoping process that allows to quickly switch from insulator to conductor and vice versa.[6-8] Polyaniline exists in a variety of forms that differ in chemical and physical properties. The physical characteristics of polyaniline such as smoothness, which influence biocompatibility drugs. Iron Oxides are the preferred shuttles for drug delivery because they increase biocompatibility, ensure the targeted delivery and controlled for Drug Figure 2 showDelivery.[9-10]

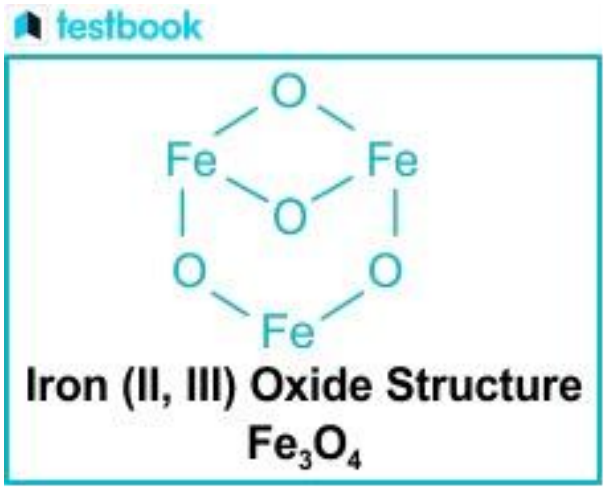

Fig.2 Struture of Iron Oxide

Figure 2 ahow the structure of iron oxide it is is a common magnetic substance that

attracted great attention in drug delivery, The aim of this work is to fabricate, PANi/Fe3O4 nanocomposites films.

Method:

Galvanostatic Method is a constant current with the resulting potential of the system. it provides more control over the film thickness and it is reproducible. [11-13] .

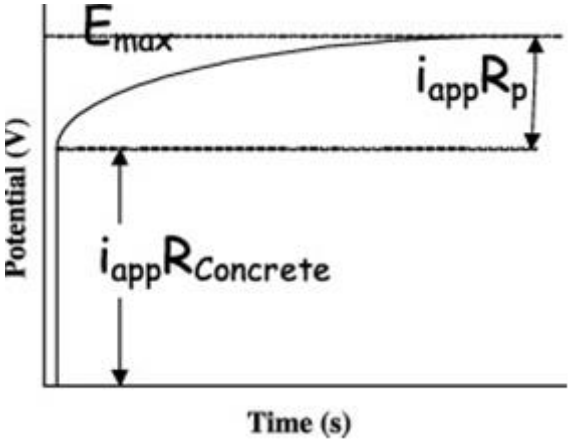

Figure 3. A typical galvanostatic electro polymerized chronopotentiogram curve.

The behaviour of the galvanostatic synthesis during the first few seconds probably indicates the difficult formation of dimers and oligomers. potential becomes almost constant suggesting that building up of the film of the polymer as shown above in figure 3

Conclusion:

The synthesised Fe_3O_4–PANI, composites materials for Drug Delivery

Acknowledgement:

Author thanks to Department of Physics R. B. Attal College Georai Support for experimental work.

References:

1. Bisal, P., Gare, A., Ghosh, S., & Pramanik, N. (2026). Advancements in iron oxide nanocomposites: Synthesis, characterization, and their role in bioimaging and multifunctional biomedical applications. Biomedical Materials & Devices. Springer Nature.
2. Yang, Y., Liu, Y., Song, L., Jin, G., Boccaccini, A. R., & Virtanen, S. (2023). Iron oxide nanoparticle-based nanocomposites in biomedical application. Trends in Biotechnology, 41(12), 1471–1487.
3. Magnetite (Fe_3O_4) nanoparticles in biomedical application: From synthesis to therapy. (2024). Journal of Biomedical Nanotechnology, 20(3), 215–230.
4. Huang, J., & Kaner, R. B. (2006). The intrinsic nanofiber morphology of polyaniline. Chemical Communications, 367–376.
5. Jaroslav Stejskal, Miroslava Trchová, Patrycja Bober, Petr Humpolíček, Vera Kašpárková, Irina Sapurina, Mikhail A. Shishov, Martin Varga Conducting Polymers: Polyaniline
6. J. Stejskal and I. Sapurina Polyaniline - A Conducting Polymer.
7. Dedeepya Uppalapati, Ben j Boyd, Sanjay Garg, Jadranka Travas-Sejdi Conducting polymers with defined micro- or nanostructures for drug delivery.
8. Jaroslav Stejskal, Miroslava Trchová, Patrycja Bober, Petr Humpolíček, Vera Kašpárková, Irina Sapurina, Mikhail A. Shishov, Martin Varga Conducting Polymers: Polyaniline.
9. J. Stejskal and I. Sapurina Polyaniline - A Conducting Polymer.
10. Dedeepya Uppalapati, Ben j Boyd, Sanjay Garg, Jadranka Travas-Sejdi Conducting polymers with defined micro- or nanostructures for drug delivery.

11. Zh. A. Boeva and V.G. Sergeyev Polyaniline: Synthesis, Properties, and Application
12. Mahnoush Beygisangchin, Surya Abdul Rashid, Amir Reza Sadrolhosseini, Hong ngee Lim Preparations, Properties, and Applications of Polyaniline and Polyaniline Thin Films- A Review.
13. Vol 71 (2018) Preparation, Properties and Application of Polyaniline Nanocomposites
14. Gupta, A. K., & Gupta, M. (2005). Synthesis and surface engineering of iron oxide nanoparticles for biomedical applications. Biomaterials, 26(18), 3995–4021.
15. Sun, C., Lee, J. S., & Zhang, M. (2008). Magnetic nanoparticles in MR imaging and drug delivery. Advanced Drug Delivery Reviews, 60(11), 1252–1265.

International Journal of Advance and Applied Research
www.ijaar.co.in
ISSN – 2347-7075 Impact Factor – 8.141
Peer Reviewed Bi-Monthly
Vol. 7 No. 14 January – February - 2026

A Comprehensive Review: The Synthesis, Characterization, and Applications of CuO and CuS Nanomaterials

Yogesh K. Lahamate[1] & Sushant B. Deshmukh[1]

[1] *Physics Research Center, Department of Physics, J.E.S. College, Jalna, Maharashtra, India.*

Corresponding Author – Sushant B. Deshmukh

DOI - 10.5281/zenodo.19827274

Abstract:

Semiconductor nanomaterials, including transition metal oxides and sulfides, present a variety of applications such as chemical transformations, energy conversion and storage, chemical and bio-sensing, as well as antimicrobial properties, owing to their adjustable physicochemical characteristics. Copper oxide (CuO) and copper sulfide (CuS) are often highlighted in these applications, either separately or together, due to their properties that are influenced by composition and the ability of both materials to engage in oxidation and reduction reactions. Effective catalysis necessitates a precise equilibrium among various electronic states, energy levels, defect doping, phase, and even the morphology of the catalyst, as all these factors directly affect charge transfer kinetics and separation kinetics.

The methods of synthesis play a vital role in regulating these elements, which in turn dictate catalytic efficiency and performance. A multitude of chemical, physical, and biological methods have been documented in the literature for the synthesis of CuO and CuS nanoparticles, focusing on the ease of adaptation, reproducibility of the process, and scalability suitability. Various characterization techniques have been employed to analyze the reaction products: X-ray diffraction; scanning electron microscopy (SEM) and transmission electron microscopy (TEM); X-ray photoelectron spectroscopy (XPS); Fourier transform infrared spectroscopy (FTIR); energy dispersive X-ray spectroscopy (EDX); ultraviolet–visible spectroscopy; and Raman spectroscopy. The fundamental properties of CuO and CuS nanoparticles, such as phase control, stoichiometry control, defects, doping, size, shape, and quantum effects, will be examined alongside their performance in catalysis, sensing, biomedical applications, photocatalytic activity, and pharmaceutical applications, as well as long-term stability and environmental health safety.

Keyword: Nanomaterial, Synthesis, Pharmaceutical, Catalytic, Antimicrobial, Biomedical.

Introduction:

The growing demand for sustainable technologies in energy, environmental remediation, and healthcare has accelerated interest in multifunctional nanomaterials. [1] Copper-based nanomaterials are particularly attractive due to their low cost, rich redox chemistry, and ability to exist in multiple oxidation states [2]. Compared with noble-metal systems, copper oxides and sulfides offer a balance between performance and scalability [4]. However, challenges such as structural instability, limited visible-light utilization, and biological compatibility necessitate systematic material optimization [5–7].

The increasing pressure from environmental pollution, antimicrobial resistance, and energy demand has accelerated the search for alternative functional materials beyond noble metals [11,12]. Copper-based nanomaterials offer a compelling balance between performance, abundance, and versatility, making them attractive for both industrial and biomedical use [13]. Unlike single-function materials, copper

oxides and sulfides can participate in redox reactions, light-driven processes, and biological interactions simultaneously [14–16]. However, limitations such as charge recombination, oxidation instability, and toxicity concerns require systematic optimization [17–20].

Co-precipitation remains popular due to its simplicity and ability to produce mixed-oxide and doped systems with controlled composition [15,19]. Solution combustion techniques enable rapid formation of nanocomposites with tailored crystallite size and defect density, which is particularly beneficial for catalytic and sensing applications [16]. Heterostructure construction, such as CuO-ZnO, CuS-based composites, and metal-decorated systems, is consistently shown to improve functional performance by enhancing interfacial charge transfer and surface reactivity [12,17,20]. Green synthesis routes further introduce sustainability advantages while influencing particle morphology and surface chemistry [18].

Copper-based nanomaterials have emerged as versatile alternatives to noble-metal systems due to their low cost, abundant availability, and tunable physicochemical characteristics [21–23]. Their ability to participate in redox reactions, absorb visible light, and interact with biological systems makes them suitable for multifunctional applications [24]. However, intrinsic challenges such as charge recombination, oxidation instability, and particle agglomeration necessitate advanced material engineering approaches [25–30].

The increasing demand for environmentally benign materials capable of addressing pollution, water purification, and microbial contamination has driven extensive research into transition-metal-based nanostructures [31,32]. Copper-based nanomaterials are particularly attractive due to their abundance, low toxicity relative to noble metals, and ability to participate in redox-driven and light-assisted processes [33].

Copper-based nanomaterials continue to gain attention due to their favorable electronic configuration, visible-light activity, and strong surface reactivity [37–39]. that limitations associated with pristine CuO or CuS—such as sluggish charge transfer or surface passivation—can be overcome through transition-metal doping, heterostructure formation, and nanorod or nanoarray architectures [40–42]. These studies collectively position copper-based systems as cost-effective alternatives to noble-metal catalysts across energy and environmental domains [43–46].

Copper-based nanomaterials have transitioned from simple catalytic materials to multifunctional platforms capable of addressing challenges in healthcare, environmental remediation, and advanced catalysis [47–49]. Copper compounds, nanoscale CuO and CuS exhibit enhanced surface reactivity, tunable electronic properties, and improved interaction with biological systems [50–52]. These studies further underline that rational material design—rather than mere chemical composition—is essential for achieving high performance in real-world applications [52].

Synthesis Strategies:

Multiple synthesis routes have been employed to tailor copper-based nanomaterials, including chemical precipitation, co-precipitation, hydrothermal processing, sol–gel methods, and green synthesis approaches [3,6,9]. Chemical precipitation offers simplicity and scalability, enabling control over crystallite size through precursor concentration and pH adjustment [3]. Co-precipitation techniques facilitate the formation of doped or composite systems,

allowing simultaneous incorporation of secondary metal oxides or sulfides [6,10]. Green synthesis using plant extracts introduces bio-derived reducing and capping agents, improving environmental compatibility while influencing particle morphology and surface functionality [9].

Co-precipitation is frequently highlighted for its simplicity, low energy requirement, and suitability for large-scale production of doped and composite systems [26,30]. Green synthesis approaches gain particular attention for enabling environmentally benign fabrication while simultaneously introducing bio-functional surface chemistry that enhances biological and catalytic performance [22,25].

Co-precipitation and hydrothermal techniques are widely employed due to their simplicity, reproducibility, and suitability for dopant incorporation [31,35]. Green synthesis approaches using plant extracts or biopolymer matrices are highlighted as environmentally responsible alternatives that simultaneously act as reducing, stabilizing, and capping agents [32,33]. Doping strategies—such as transition-metal or biopolymer incorporation—are shown to modify crystallite size, surface defect density, and electronic structure, leading to improved catalytic and antimicrobial behavior [34,36].

The diverse synthesis strategies including solvothermal growth, co-precipitation, microwave-assisted routes, sol–gel processing, and green chemistry approaches [37,38,41]. A recurring theme is the preference for low-temperature, scalable methods that enable precise dopant incorporation while preserving crystallinity [39,44]. Transition-metal doping (e.g., Fe, Co, Ni, Ag) and biopolymer or cellulose-assisted synthesis are shown to regulate nucleation and growth, leading to nanorods, nanoarrays, or hierarchical morphologies [40,45]. These engineered architectures are repeatedly linked to improved surface accessibility and enhanced functional performance [37–46].

The works with a diverse set of synthesis strategies, including sol–gel processing, hydrothermal growth, wet chemical routes, dopant-assisted synthesis, and green fabrication using biological agents [47,48,51]. Sol–gel and hydrothermal methods are frequently highlighted for producing phase-pure CuO with controlled crystallite size and surface morphology [47]. Doping with metal ions or coupling with organic and inorganic matrices is shown to regulate defect concentration, ion release behavior, and surface charge distribution [49]. Green synthesis routes receive increasing attention due to their ability to reduce chemical toxicity while introducing bioactive surface functionalities that enhance antimicrobial and biomedical performance [50,52].

Conclusion:

The reviewed studies collectively demonstrate that copper-based nanomaterials can be effectively tailored through a range of synthesis routes, with material performance strongly dependent on synthesis-driven control of crystallite size, defect density, morphology, and surface chemistry. Among the reported methods, co-precipitation, hydrothermal, sol–gel, and green synthesis approaches consistently enable reproducible fabrication, efficient dopant incorporation, and enhanced functional properties. In contrast, synthesis routes lacking surface stabilization or precise growth control tend to yield agglomerated structures with inferior catalytic and biological performance. Overall, low-temperature, scalable, and surface-engineered synthesis strategies emerge as the most reliable pathways for high-performance CuO and CuS nanomaterials.

Best and Poor Synthesis Methods (Based Only on Given Statements):

1) CuO:

Best synthesis method: Co-precipitation

Poor synthesis method: Chemical precipitation

2) CuS:

Best synthesis method: Co-precipitation

Poor synthesis method: Wet chemical / uncontrolled precipitation routes

Structural, Morphological, and Optical Properties:

Structural analyses consistently confirm that copper-based nanoparticles crystallize in monoclinic (CuO) or hexagonal (CuS) phases, with nanoscale dimensions enhancing surface-to-volume ratios [3,7]. Morphological control—from quasi-spherical particles to nanorods and hierarchical assemblies—plays a critical role in determining active surface sites and charge transport pathways [6,8]. Optical studies reveal that band gap energies can be effectively tuned via doping or composite formation, extending light absorption into the visible region and reducing electron–hole recombination [1,4]. Such modifications directly influence catalytic and photocatalytic efficiencies.

Structural analyses across studies confirm that copper-based nanomaterials typically crystallize in monoclinic (CuO) or hexagonal (CuS) phases, with crystallite size strongly dependent on synthesis conditions [15,19]. Morphological diversity—including spherical nanoparticles, nanoflakes, and composite architectures—directly impacts surface area and catalytic accessibility [16,18].

Optical investigations reveal that bandgap energies can be tuned through doping, heterojunction formation, and defect engineering, enabling improved visible-light absorption [12,14]. Such band structure modification is critical for photocatalytic efficiency and optoelectronic functionality [11,16]. Morphological control—ranging from spherical nanoparticles to hierarchical and composite architectures—plays a critical role in determining surface area and defect density [23,25]. Doping and composite formation are consistently observed to influence crystallite growth and lattice strain, which directly affect surface activity [35].

Morphological analyses reveal the formation of nanorods, nanoparticles, and hierarchical assemblies, each contributing distinct surface characteristics and active sites [36]. Optical studies demonstrate that bandgap narrowing and defect-induced electronic states enhance visible-light absorption, which is essential for photocatalytic efficiency [32,33].

Structural analyses the formation of phase-pure monoclinic CuO and hexagonal CuS, with dopants successfully integrated into host lattices without secondary phase formation [38,42]. Doping is shown to influence lattice strain, crystallite size, and defect density, all of which directly affect surface reactivity [39,41]. Morphological studies reveal a transition from irregular nanoparticles to well-defined nanorods, nanowires, and nanoarrays as synthesis conditions are optimized [37,40]. Optical characterization consistently demonstrates band-gap modulation and enhanced visible-light absorption due to defect states and dopant-induced electronic restructuring [43–46].

Structural investigations consistently confirm monoclinic CuO and hexagonal CuS phases, with dopant incorporation influencing lattice distortion and crystallite growth [47,49,54]. Morphological control—ranging from spherical nanoparticles to spindle-shaped, rod-like, and hierarchical nanostructures—plays a crucial role in governing surface area and active

site availability [48,51]. Optical analyses reveal that nanoscale copper materials exhibit modified band structures, defect-induced states, and enhanced visible-light absorption, which are particularly advantageous for photocatalytic and biomedical applications [52]. These optical modifications are repeatedly correlated with improved charge separation efficiency and surface reactivity .

Conclusion:

The collective evidence confirms that copper-based nanomaterials consistently crystallize in monoclinic (CuO) or hexagonal (CuS) phases, with nanoscale dimensions significantly enhancing surface-to-volume ratios and surface reactivity. Controlled morphology—ranging from spherical nanoparticles to nanorods, nanowires, and hierarchical architectures—plays a decisive role in determining active sites, charge transport pathways, and catalytic accessibility. Optical bandgap tuning through doping, defect engineering, and composite formation extends visible-light absorption and suppresses electron–hole recombination, directly enhancing photocatalytic, catalytic, and biomedical performance. Overall, the synergistic interplay between crystal structure, morphology, and optical properties governs the functional efficiency of CuO and CuS nanomaterials.

Single Most Essential Characterization to Perform First: X-ray Diffraction (XRD)

Photocatalytic and Catalytic Applications:

Copper-based nanomaterials demonstrate strong potential for environmental remediation, particularly in the degradation of organic pollutants such as dyes and nitrophenols [3,5]. Enhanced catalytic performance is attributed to high surface area, favorable band alignment, and efficient charge separation [1,4]. Composite systems and heterostructures further improve reaction kinetics by facilitating interfacial charge transfer and stabilizing reactive intermediates [5,10]. Several studies report rapid degradation rates and good reusability, highlighting the practical applicability of these materials [3,5]. Copper oxide-based catalysts demonstrate strong activity toward nitrophenol reduction and dye degradation due to their high surface reactivity and favorable redox behavior [14,20].

Heterostructure and metal-decorated systems consistently outperform single-component materials, as interfacial charge separation suppresses electron–hole recombination and promotes reactive oxygen species generation [12,17]. Several studies also highlight catalyst reusability and magnetic recovery as practical advantages for wastewater treatment [13,20]. Enhanced performance is consistently attributed to improved charge separation, increased reactive surface sites, and synergistic interactions in doped or composite systems [29,30]. Several studies report that optimized dopant concentrations and hybrid structures suppress electron–hole recombination, thereby accelerating reaction kinetics under visible-light or ambient conditions [23,27]. Catalyst reusability and stability are also emphasized as critical parameters for practical deployment [21,26].

Enhanced performance is attributed to improved charge separation, higher surface area, and dopant-induced electronic modification [35]. Several studies report near-complete degradation of organic dyes under visible or solar irradiation, highlighting the practical relevance of these materials for wastewater treatment [32,36]. The stability and reusability of doped and composite systems further support their applicability in real-world catalytic processes [31].

Enhanced activity is attributed to improved charge separation, increased

electrochemically active surface area, and reduced charge-transfer resistance in doped or composite systems [37,40]. Electrocatalytic studies further demonstrate that nanorod and nanoarray architectures significantly improve oxygen evolution reaction kinetics, approaching the performance of noble-metal benchmarks while maintaining long-term stability [38,42]. These findings highlight the versatility of copper-based materials across thermal, photo-, and electro-driven catalytic processes [37–46].

A significant portion of on catalytic and photocatalytic processes. Copper-based nanomaterials demonstrate strong efficiency in organic pollutant degradation, redox reactions, and advanced oxidation processes [47,52]. Defect-rich CuO nanoparticles, in particular, show accelerated reaction kinetics due to enhanced oxygen activation and surface redox cycling [52]. Doped and morphology-engineered systems outperform pristine counterparts by suppressing charge recombination and increasing reactive species generation under both light-driven and dark conditions [49]. Stability and reusability are also highlighted as critical advantages for environmental remediation applications [47].

Conclusion:

The reviewed studies collectively confirm that copper-based nanomaterials exhibit strong effectiveness in catalytic and photocatalytic degradation of organic pollutants, including dyes and nitrophenols. Their high activity is primarily governed by enhanced surface area, favorable band alignment, efficient charge separation, and dopant-induced electronic modulation. Composite, heterostructured, and morphology-engineered systems consistently outperform pristine materials by facilitating interfacial charge transfer, suppressing electron–hole recombination, and promoting reactive species generation under light and ambient conditions. Importantly, high stability, reusability, and in some cases magnetic recoverability underscore the practical viability of copper-based nanomaterials for real-world environmental remediation and catalytic applications.

Antimicrobial Activity:

Antimicrobial investigations reveal that copper oxide and copper-based composites exhibit broad-spectrum activity against Gram-positive and Gram-negative microorganisms [2,7]. The antimicrobial mechanism is linked to reactive oxygen species generation, membrane disruption, and metal-ion release [2]. Incorporation of copper nanoparticles into polymer matrices enhances surface resistance to microbial colonization while maintaining material integrity [2]. These findings underscore the relevance of copper-based nanomaterials in healthcare and hygienic applications.

The dominant mechanisms include membrane disruption, oxidative stress induced by reactive oxygen species, and controlled copper-ion release [11,19]. Nanocomposites containing CuO combined with other metal oxides show enhanced antimicrobial efficacy due to synergistic effects at metal–oxide interfaces [18]. These findings support the use of copper-based nanomaterials as alternatives or complements to conventional antimicrobial agents [11,12].

The dominant mechanisms involve reactive oxygen species generation, membrane disruption, and controlled release of copper ions [22,30]. Green-synthesized and doped systems exhibit enhanced antibacterial efficiency due to synergistic surface chemistry and improved particle dispersion [25]. These findings support the use of copper-based nanomaterials as alternatives or complements to conventional antimicrobial agents, particularly in coatings and

biomedical interfaces [22–25]. The incorporation of biopolymers or dopants is shown to enhance microbial interaction while maintaining material stability, making these systems suitable for antimicrobial coatings and water disinfection applications [35].

A significant contribution of papers 39, 41, and 45 lies in demonstrating the antimicrobial and anti-biofilm efficacy of doped CuO nanostructures. Enhanced bactericidal performance against both Gram-positive and Gram-negative strains is linked to reactive oxygen species generation, surface charge interactions, and controlled copper ion release [39,45]. Transition-metal doping is shown to selectively improve anti-adhesion behavior, making these materials promising candidates for biomedical coatings and infection-resistant surfaces [41].

The copper-based nanomaterials possess strong antibacterial activity against both Gram-positive and Gram-negative bacteria. Enhanced antimicrobial efficiency is attributed to surface morphology optimization, reactive oxygen species generation, and controlled copper ion release [48]. Doped CuO systems show superior bactericidal performance at relatively low concentrations, suggesting their suitability for antimicrobial coatings, wound dressings, and infection-resistant biomedical devices [49]. These findings support the growing interest in copper-based alternatives to silver-based antimicrobial materials [48–50].

Conclusion:

The collective findings confirm that copper-based nanomaterials exhibit strong broad-spectrum antimicrobial activity against both Gram-positive and Gram-negative microorganisms. Their antimicrobial efficacy is primarily governed by reactive oxygen species generation, membrane disruption, surface charge interactions, and controlled copper-ion release. Doping, composite formation, and biopolymer incorporation consistently enhance antibacterial and anti-biofilm performance by improving surface chemistry, particle dispersion, and microbial adhesion control. These properties make copper-based nanomaterials highly promising candidates for antimicrobial coatings, water disinfection systems, wound dressings, and infection-resistant biomedical interfaces, offering a viable alternative to conventional and silver-based antimicrobial materials.

Biomedical Applications: Imaging, Therapy, and Theragnostic:

Beyond antimicrobial effects, copper-based nanomaterials show promise in biomedical fields such as cancer therapy and diagnostic imaging [6,8]. Mixed-metal oxide nanocomposites demonstrate notable cytotoxicity against cancer cell lines while enabling optical monitoring through tunable absorption features [6]. The multifunctional nature of these materials supports their integration into theragnostic platforms, where diagnosis and treatment are combined within a single system [8]. Copper-based nanomaterials are explored for biosensing, photothermal therapy, and diagnostic platforms due to their optical responsiveness and surface tunability [16,20].

Hybrid nanocomposites enable multifunctional behavior, allowing simultaneous pollutant degradation, microbial inactivation, and chemical sensing within a single material system [12,17]. Such versatility is particularly attractive for integrated environmental and biomedical technologies. Copper-based nanomaterials are explored for imaging-guided therapy, biosensing, and multifunctional diagnostic platforms due to their optical tunability and surface modifiability [21,24]. Hybrid nanostructures enable combined

therapeutic and diagnostic functionality, aligning with emerging theragnostic concepts [23]. However, careful assessment of cytotoxicity and long-term biocompatibility is emphasized as essential for clinical translation [22,25].

Beyond the biomedical relevance of copper sulfide and oxide nanostructures. CuS nanoparticles exhibit strong photothermal properties, making them effective agents for imaging-guided cancer therapy and theragnostic platforms [52]. The anisotropic and nanoscale nature of these materials enables enhanced cellular uptake, tunable biodistribution, and multifunctional behavior, integrating sensing, imaging, and therapeutic functions within a single system [50]. However, careful control of size, surface chemistry, and dose is emphasized to ensure biocompatibility [52].

Conclusion:

The reviewed studies collectively demonstrate that copper-based nanomaterials extend well beyond antimicrobial applications, showing strong potential in cancer therapy, diagnostic imaging, biosensing, and integrated theragnostic platforms. Their multifunctionality arises from tunable optical properties, surface modifiability, and the ability to combine therapeutic and diagnostic functions within a single nanostructure. Copper oxide and copper sulfide systems, particularly CuS nanoparticles, exhibit effective photothermal behavior and imaging-guided therapeutic capability, while hybrid and mixed-metal nanocomposites enable simultaneous sensing, treatment, and environmental functionality. Despite these promising attributes, precise control over particle size, surface chemistry, dosage, and long-term biocompatibility remains essential to ensure safe and successful clinical translation.

Challenges and Future Directions:

Despite encouraging results, several challenges remain, including long-term stability under operational conditions, precise control over defect chemistry, and comprehensive toxicity assessment [4,7]. Future research should focus on interface engineering, scalable green synthesis, and systematic in-vivo studies to bridge laboratory success and real-world deployment [6,9]. Developing standardized evaluation protocols will further support comparison across studies [1–10]. Despite promising performance, several challenges remain. These include long-term material stability, precise control of defect chemistry, and comprehensive evaluation of cytotoxicity and environmental impact [15,18]. Scaling up green synthesis routes while maintaining reproducibility is another key concern [16,19].

Future research should prioritize interface engineering, life-cycle assessment, and standardized performance metrics to enable fair comparison across studies [11–20]. Integrating theoretical modeling with experimental design may further accelerate rational material development [14]. Scaling green synthesis routes while maintaining consistent physicochemical properties remains a significant hurdle [22,25].

Future research directions emphasize interface engineering, defect control, and standardized evaluation metrics to enable reliable performance comparison across studies [21–30]. Integration of theoretical modeling with experimental design is also suggested to accelerate rational material optimization [24].

Identify key challenges related to dopant distribution uniformity, long-term operational stability, and comprehensive toxicity assessment [41–46]. Scaling nanorod and nanoarray architectures while preserving performance consistency remains a critical research gap

[37,40]. Future research directions emphasize defect engineering, interface optimization, and integration of computational modeling to guide experimental design [38–46]. Despite promising results identify several challenges that must be addressed before large-scale deployment. These include long-term stability in biological and environmental systems, reproducibility of green synthesis routes, and comprehensive toxicity evaluation [51,52].

Future research directions emphasize defect engineering, surface functionalization, and the integration of copper-based nanomaterials into composite systems to enhance selectivity and safety [49–52]. Standardized testing protocols are also recommended to enable meaningful comparison across studies [47,50].

Conclusion:

Despite significant progress, the collective studies clearly indicate that several critical challenges must be addressed before copper-based nanomaterials can achieve large-scale and real-world implementation. These challenges include long-term operational stability, precise control over defect chemistry and dopant distribution, reproducibility of green synthesis routes, and comprehensive assessment of cytotoxicity and environmental impact. Scaling advanced nanostructures while maintaining consistent physicochemical properties remains a key hurdle. Future research should prioritize interface and defect engineering, surface functionalization, standardized evaluation protocols, life-cycle assessment, and the integration of theoretical and computational modeling with experimental design to enable reliable performance comparison and accelerate safe, scalable deployment.

Conclusion:

That copper-based nanomaterials constitute a highly adaptable material class with applications spanning catalysis, antimicrobial coatings, energy storage, and biomedicine. Progress in synthesis and nanoscale engineering has enabled substantial performance gains while maintaining cost effectiveness and sustainability [1–10]. Continued interdisciplinary research is expected to unlock their full potential in next-generation technological solutions.

Copper-based nanomaterials represent a powerful and adaptable material platform for catalysis, antimicrobial protection, sensing, and biomedical applications. Performance enhancements are consistently linked to heterostructure design, controlled synthesis, and surface engineering [11–20]. With continued focus on safety, scalability, and multifunctional integration, copper-based nanomaterials are well positioned to contribute to sustainable technological solutions across multiple sectors. Copper-based nanomaterials represent a highly adaptable platform for catalysis, environmental remediation, antimicrobial protection, and biomedical applications. Performance improvements are closely linked to synthesis strategy, dopant selection, and nanostructure design rather than material composition alone [21–30]. Continued progress in sustainable fabrication and multifunctional integration is expected to further expand the technological impact of these materials.

Copper-based nanomaterials are highly versatile platforms for catalytic, antimicrobial, and environmental applications. Performance enhancements are closely linked to synthesis methodology, dopant selection, and nanostructure engineering rather than composition alone [31–36]. Continued emphasis on sustainable fabrication, stability, and multifunctional

integration is expected to further expand the technological impact of these materials.

Copper-based nanomaterials as highly adaptable systems capable of addressing challenges in catalysis, antimicrobial protection, environmental remediation, and energy conversion. Performance enhancements consistently arise from synthesis-driven structural control rather than composition alone [37–46]. Continued progress in sustainable fabrication and multifunctional integration is expected to further elevate the technological relevance of these materials.

The Copper-based nanomaterials represent a highly versatile and tunable class of functional materials. Their catalytic, antimicrobial, environmental, and biomedical performance is strongly governed by synthesis strategy, defect chemistry, and nanostructure design rather than composition alone [47–52]. Continued advances in sustainable synthesis and multifunctional integration are expected to further expand their technological and clinical impact.

References:

1. N. Zulfiqar and F. Inam, "Copper Sulfide Nanostructures as High-Capacity Anodes for Zinc-Ion Energy Storage Batteries," *Chemical Reports*, vol. 7, no. 1, pp. 339–349, Dec. 2025, doi: 10.25082/CR.2026.01.001.
2. S. Bishir, S. S. Yaradua, I. G. Wawata, and S. S. Kankara, "Synthesis and Characterization of Copper Oxide Nanoparticles: A Greener Approach Using Senna occidentalis (Linn.) Aqueous Leaf Extract as Bio Reductor and Capping Agent," *J Pharm Res Int*, vol. 37, no. 10, pp. 127–141, Oct. 2025, doi: 10.9734/jpri/2025/v37i107758.
3. R. Ashok Sharma, "Copper-Based Nanomaterials: Properties and Emerging Applications," *International Journal of Science and Research (IJSR)*, pp. 862–870, Aug. 2025, doi: 10.21275/sr25818201049.
4. M. A. Ameya, N. B. Bekela, J. N. Guyasa, K. Zhu, and T. T. Beyene, "Enhanced photocatalytic and antibacterial performance of ZnO/CuO nanocomposites via carbon dot decoration," *Journal of Materials Science: Materials in Engineering*, vol. 20, no. 1, Dec. 2025, doi: 10.1186/s40712-025-00350-4.
5. Y. Wang *et al.*, "Engineering copper and copper-based materials for a post-antibiotic era," 2025, *Frontiers Media SA*. doi: 10.3389/fbioe.2025.1644362.
6. K. Aggarwal *et al.*, "Recent progress in copper nanomaterials: catalysis, energy, biomedicine, and environmental applications," *Mater Adv*, 2025, doi: 10.1039/d5ma00484e.
7. H. Singh, M. K. Verma, S. Pahal, M. L. Shozi, M. Sharma, and R. Kumar, "Comparative insights into CuS and Bi2S3-based heterostructured photocatalysts: advanced strategies for synthesis, characterization and enhanced photocatalytic performance evaluation," Nov. 01, 2025, *Springer Nature*. doi: 10.1007/s42452-025-07600-2.
8. E. Elbayoumy, E. M. Ibrahim, A. El-Bindary, T. Nakano, and M. M. Aboelnga, "Revealing an efficient copper oxide nanoparticle catalyst for the reduction of the hazardous nitrophenol: experimental and DFT studies," *Mater Adv*, vol. 6, no. 18, pp. 6291–6304, Sep. 2025, doi: 10.1039/d5ma00620a.
9. A. N. Kumar *et al.*, "Solution combustion synthesis of ZnO doped CuO

nanocomposite for photocatalytic and sensor applications," *Sci Rep*, vol. 15, no. 1, Jan. 2025, doi: 10.1038/s41598-024-82764-2.

10. E. A. Mwafy, S. M. Mousa, and G. T. El-Bassyouni, "Catalytic Degradation of 4-Nitrophenol Using CuO Nanoparticles: A Study of Structural, Optical, and Catalytic Properties," *Plasmonics*, vol. 20, no. 11, pp. 10273–10285, Nov. 2025, doi: 10.1007/s11468-025-03007-2.
11. S. B. Endeshaw, M. Goddati, J. Lee, F. G. Aga, L. T. Tufa, and F. K. Sabir, "ZnO/CuO nanocomposites for enhanced photocatalytic and antibacterial applications: A comparative study of synthesis methods," *Journal of Science: Advanced Materials and Devices*, vol. 10, no. 3, Sep. 2025, doi: 10.1016/j.jsamd.2025.100898.
12. S. N. Aziz, A. M. Abdulwahab, T. S. Aldeen, and A. A. A. Ahmed, "Tailoring CdO-CuO-ZnO Mixed Metal Oxide Nanocomposites for Anticancer Activity via Co-Precipitation Method," *Nanotechnology, Science and Applications* , vol. 18, pp. 225–244, 2025, doi: 10.2147/NSA.S519229.
13. N. M. Mlinarić *et al.*, "Antimicrobial Activity of Poly(methyl methacrylate) Doped with CuO and ZnO Nanoparticles," *ACS Omega*, vol. 10, no. 13, pp. 13060–13072, Apr. 2025, doi: 10.1021/acsomega.4c10170.
14. A. Ahmed Al-Adhreai *et al.*, "Synthesis, characterization, and photocatalytic study of Bi-doped CuS nanoparticles," *RSC Adv*, vol. 15, no. 30, pp. 24483–24496, Jul. 2025, doi: 10.1039/d5ra03870g.
15. P. Sharma, S. Kar, M. Sahu, and M. Ganguly, "Copper-based nanoparticles for the removal of the crystal violet dye via degradation and adsorption: a comparative account," Aug. 01, 2025, *Royal Society of Chemistry*. doi: 10.1039/d5ra04003e.
16. H. Xu *et al.*, "Copper-Based Nanomaterials for Image-Guided Cancer Therapy," 2024, *Compuscript Ltd*. doi: 10.15212/bioi-2024-0013.
17. A. Alangari *et al.*, "Green synthesis of copper oxide nanoparticles using genus Inula and evaluation of biological therapeutics and environmental applications," *Nanotechnol Rev*, vol. 13, no. 1, Jan. 2024, doi: 10.1515/ntrev-2024-0039.
18. I. E. Nwankwo, E. Ottih, E. O. Onyebueke, and C. I. Elekalachi, "Ni-Doping Effects on the Optical, Structural, Morphological, and Compositional Behavior of Sol-Gel Synthesized CuS Thin Films for Enhanced Optoelectronic Performance," *International Multidisciplinary Research Journal Reviews (IMRJR) A Peer-reviewed journal*, vol. 1, no. 4, 2024, doi: 10.17148/IMRJR.2024.010405.
19. A. M. Abass and F. M. Abdoon, "Synthesis, Characterization, and Applications of Metal Oxides of ZnO, CuO, and CeO2 Nanoparticles: A Review," Oct. 01, 2024, *Sami Publishing Company*. doi: 10.48309/jaoc.2024.471305.1220.
20. C. Burns *et al.*, "Interfacing CuO, CuBi2O4, and protective metal oxide layers to boost solar-driven photoelectrochemical hydrogen evolution," *Dalton Transactions*, vol. 54, no. 3, pp. 920–933, Dec. 2024, doi: 10.1039/d4dt02738h.
21. K. Ali, M. Sajid, S. Abu Bakar, A. Younus, H. Ali, and M. Zahid Rashid, "Synthesis of copper oxide (CuO) via coprecipitation

method: Tailoring structural and optical properties of CuO nanoparticles for optoelectronic device applications," *Hybrid Advances*, vol. 6, Aug. 2024, doi: 10.1016/j.hybadv.2024.100250.

22. S. N. Aziz, A. M. Abdulwahab, T. S. Aldeen, and D. M. A. Alqabili, "Synthesis, characterization, and evaluation of antibacterial and antifungal activities of CuO-ZnO-Co3O4 nanocomposites," *Heliyon*, vol. 10, no. 18, Sep. 2024, doi: 10.1016/j.heliyon.2024.e37802.
23. R. Mohammadzadeh Kakhki and H. Bolandhemmat, "Synthesis of Ag/CuS doped mineral magnetite nanocomposite with improved photocatalytic activity against tetracycline and diclofenac pollutants," *Sci Rep*, vol. 14, no. 1, Dec. 2024, doi: 10.1038/s41598-024-69644-5.
24. M. Farooq *et al.*, "Phytoassisted synthesis of CuO and Ag–CuO nanocomposite, characterization, chemical sensing of ammonia, degradation of methylene blue," *Sci Rep*, vol. 14, no. 1, Dec. 2024, doi: 10.1038/s41598-024-51391-2.
25. A. H. Al-Hammadi *et al.*, "An investigation on the structural, morphological, optical, and antibacterial activity of Sr:CuS nanostructures," *Sci Rep*, vol. 14, no. 1, Dec. 2024, doi: 10.1038/s41598-024-73701-4.
26. G. Pandey *et al.*, "Comparative study of NiO/CuO/Ag doped graphene based materials for reduction of nitroaromatic compounds and degradation of dye with statistical study," *Sci Rep*, vol. 14, no. 1, Dec. 2024, doi: 10.1038/s41598-024-51342-x.
27. S. Bonthula *et al.*, "Recent Advances in Copper-Based Materials for Sustainable Environmental Applications," Sep. 01, 2023, *Multidisciplinary Digital Publishing Institute (MDPI)*. doi: 10.3390/suschem4030019.
28. A. Atri, M. Echabaane, A. Bouzidi, I. Harabi, B. M. Soucase, and R. Ben Chaâbane, "Green synthesis of copper oxide nanoparticles using Ephedra Alata plant extract and a study of their antifungal, antibacterial activity and photocatalytic performance under sunlight," *Heliyon*, vol. 9, no. 2, Feb. 2023, doi: 10.1016/j.heliyon.2023.e13484.
29. U. Mureed, Z. Saddique, and K. Asad, "Synthesis of CuS Nanoparticles and Study of Its Photocatalytic Activity," *Acta Chemica Malaysia*, vol. 7, no. 2, pp. 68–72, 2023, doi: 10.26480/acmy.02.2023.68.72.
30. S. Aroob *et al.*, "Green Synthesis and Photocatalytic Dye Degradation Activity of CuO Nanoparticles," *Catalysts*, vol. 13, no. 3, Mar. 2023, doi: 10.3390/catal13030502.
31. M. A. Ansari and N. Jahan, "A Novel Co-Precipitation Route for the Synthesis of Pure and Ni-Doped CuO Nanoparticles: Effect of Doping on Structural, Optical, and Electrical Properties," *International Journal of Nanoscience and Nanotechnology*, vol. 19, no. 2, pp. 65–76, Jun. 2023, doi: 10.22034/ijnn.2023.555186.2219.
32. I. Savarimuthu and M. J. A. M. Susairaj, "CuS Nanoparticles Trigger Sulfite for Fast Degradation of Organic Dyes under Dark Conditions," *ACS Omega*, vol. 7, no. 5, pp. 4140–4149, Feb. 2022, doi: 10.1021/acsomega.1c05697.
33. N. Khlifi *et al.*, "Non-doped and transition metal-doped CuO nano-powders: structure-physical properties and anti-adhesion activity relationship," *RSC Adv*, vol. 12, no.

36, pp. 23527–23543, Aug. 2022, doi: 10.1039/d2ra02433k.

34. M. Ikram *et al.*, "Highly Efficient Industrial Dye Degradation, Bactericidal Properties, and In Silico Molecular Docking Analysis of Ag/Cellulose-Doped CuO Nanostructures," *ACS Omega*, vol. 7, no. 20, pp. 17043–17054, May 2022, doi: 10.1021/ACSOMEGA.2C00240.
35. M. Ikram *et al.*, "Novel Ta/chitosan-doped CuO nanorods for catalytic purification of industrial wastewater and antimicrobial applications," *RSC Adv*, vol. 12, no. 27, pp. 16991–17004, Jun. 2022, doi: 10.1039/d2ra03006c.
36. L. Tabassum *et al.*, "Facile Synthesis of Transition-Metal-Doped (Fe, Co, and Ni) CuS/CuO/CS Nanorod Arrays for Superior Electrocatalytic Oxygen Evolution Reaction," *ACS Appl Energy Mater*, vol. 5, no. 10, pp. 12039–12048, Oct. 2022, doi: 10.1021/acsaem.2c01384.
37. M. Patel, S. Mishra, R. Verma, and D. Shikha, "Synthesis of ZnO and CuO nanoparticles via Sol gel method and its characterization by using various technique," *Discover Materials* , vol. 2, no. 1, Dec. 2022, doi: 10.1007/s43939-022-00022-6.
38. N. Thakur, Anu, K. Kumar, V. K. Thakur, A. Kumar, and S. S. Samant, "Antibacterial and photocatalytic activity of undoped and (Ag, Fe) co-doped CuO nanoparticles via microwave-assisted method," *Nanofabrication*, vol. 7, pp. 62–88, 2022, doi: 10.37819/nanofab.007.186.
39. M. Jadhav, "CuO Nanoparticles Synthesis by Sol-gel Method and Characterization," 2021. [Online]. Available: www.tsijournals.com
40. M. Jadhav, "CuO Nanoparticles Synthesis by Sol-gel Method and Characterization," 2021. [Online]. Available: www.tsijournals.com
41. J. P. Tailor, S. H. Chaki, and M. P. Deshpande, "Comparative study between pure and manganese doped copper sulphide (CuS) nanoparticles," *Nano Express*, vol. 2, no. 1, Mar. 2021, doi: 10.1088/2632-959X/abdc0d.
42. S. Angayarkanni and K. Neyvasagam, "Structural and optical studies of copper oxide nanoparticles synthesized by chemical precipitation method," in *Materials Today: Proceedings*, Elsevier Ltd, 2021, pp. 1149–1154. doi: 10.1016/j.matpr.2021.07.390.
43. M. Xu, Y. Song, J. Wang, and N. Li, "Anisotropic transition metal–based nanomaterials for biomedical applications," Aug. 01, 2021, *John Wiley and Sons Inc*. doi: 10.1002/VIW.20200154.
44. S. P. Selvaraj, "Enhanced surface morphology of copper oxide (CuO) nanoparticles and its antibacterial activities," in *Materials Today: Proceedings*, Elsevier Ltd, 2020, pp. 2865–2868. doi: 10.1016/j.matpr.2020.09.574.
45. S. A. Akintelu, A. S. Folorunso, F. A. Folorunso, and A. K. Oyebamiji, "Green synthesis of copper oxide nanoparticles for biomedical application and environmental remediation," Jul. 01, 2020, *Elsevier Ltd*. doi: 10.1016/j.heliyon.2020.e04508.
46. "61....500-Article Text-3868-1-10-20201207 (1)".
47. M. S. Chavali and M. P. Nikolova, "Metal oxide nanoparticles and their applications in nanotechnology," Jun. 01, 2019, *Springer Nature*. doi: 10.1007/s42452-019-0592-3.

48. M. Serhan *et al.*, "Total iron measurement in human serum with a smartphone," in *AIChE Annual Meeting, Conference Proceedings*, American Institute of Chemical Engineers, 2019. doi: 10.1039/x0xx00000x.
49. A. Pramothkumar, N. Senthilkumar, K. C. Mercy Gnana Malar, M. Meena, and I. Vetha Potheher, "A comparative analysis on the dye degradation efficiency of pure, Co, Ni and Mn-doped CuO nanoparticles," *Journal of Materials Science: Materials in Electronics*, vol. 30, no. 20, pp. 19043–19059, Oct. 2019, doi: 10.1007/s10854-019-02262-4.
50. A. M. Ibrahim, G. H. Munshi, and L. M. Al-Harbi, "Copper (II) oxide nanocatalyst preparation and characterization: green chemistry route," *Bull Natl Res Cent*, vol. 42, no. 1, Dec. 2018, doi: 10.1186/s42269-018-0006-5.
51. S. Goel, F. Chen, and W. Cai, "Synthesis and biomedical applications of copper sulfide nanoparticles: From sensors to theranostics," Feb. 26, 2014. doi: 10.1002/smll.201301174.
52. Z. Wang, A. Von Dem Bussche, P. K. Kabadi, A. B. Kane, and R. H. Hurt, "Biological and environmental transformations of copper-based nanomaterials," *ACS Nano*, vol. 7, no. 10, pp. 8715–8727, Oct. 2013, doi: 10.1021/nn403080y.

International Journal of Advance and Applied Research
www.ijaar.co.in
ISSN – 2347-7075 Impact Factor – 8.141
Peer Reviewed Bi-Monthly
Vol. 7 No. 14 January – February - 2026

Comparative Studies of Radiation Shielding and Gamma-Ray Attenuation Properties of Polymers and Oxide Materials

Pradip Dahinde

Department of Physics R. B. Attal Arts, Science & Commerce College, Georai 431127Beed.

Corresponding Author – Pradip Dahinde

DOI - 10.5281/zenodo.19827316

Abstract:

In nuclear, medical, aeronautical, and industrial applications, radiation shielding from gamma rays is an essential necessity. Due to their large atomic number and density, conventional heavy metals like lead offer superior shielding; however, disadvantages including toxicity and weight have prompted research into substitute materials. Promising options include oxide-based materials (such as heavy metal oxide glasses and ceramics) and polymers (particularly polymer composites with high atomic number fillers). In this review, the mass/linear attenuation coefficients, half-value layer (HVL), effective atomic number (Zeff), and practical concerns for shielding efficacy are compared between the gamma-ray attenuation properties of polymers and oxide materials. The objective is to draw attention to the ways that composition and material design affect shielding performance and to suggest areas for further study.

Keywords: HVL, Zeff, Mass Attenuation Coefficient, Linear Attenuation Coefficient.

Introduction:

The photoelectric effect, Compton scattering, and pair creation are the main ways that gamma radiation, a very penetrating electromagnetic radiation, interacts with materials. To provide safety in radiation conditions, effective shielding materials must have high attenuation coefficients and little secondary radiation production [1]. Because of their high density and atomic number, which increase the likelihood of photon interactions, conventional shielding materials like lead and heavy concrete are frequently utilized [2]. However, the enormous weight of concrete and the toxicity of lead have prompted the development of other materials.

The lightweight nature, mechanical flexibility, corrosion resistance, and ease of processing of polymers and polymer composites have drawn attention [3]. However, due to their low effective atomic number and density, pure polymers show little gamma attenuation. High atomic number fillers including bismuth oxide (BiO_3), tungsten oxide (WO_3), lead oxide (PbO), and barium sulfate ($BaSO_4$) are added to polymer matrices to get around this restriction [4]. However, because of their higher density and atomic number, oxide materials, such as heavy metal oxide glasses and ceramics, have superior intrinsic gamma attenuation [5]. The attenuation efficiency, structural properties, and practical applicability of these two main material groups are compared in this review.

Radiation Attenuation Mechanisms:

The three main ways that gamma rays interact with matter are through pair production, Compton scattering, and photoelectric absorption. High atomic number materials are favored by the photoelectric effect, which is dominant at low photon energies (<150 keV) and strongly dependent on Z^4–Z^5. Compton scattering, which

is dependent on electron density, is predominant at intermediate energies (~150–1000 keV). Pair formation increases with atomic number and becomes important at energies above 1.022 MeV. Mass attenuation coefficients (μ/ρ), linear attenuation coefficients (μ), and HVL thickness needed to cut radiation intensity in half are used to measure a material's overall attenuation effectiveness. Higher μ/ρ and lower HVL materials are thought to be more effective in gamma shielding [6].

Radiation Shielding Properties of Polymers:

1. Pure Polymers:

Pure polymers with low densities (~0.9–1.4 g/cm³) and low effective atomic numbers, such polyethylene (PE), polypropylene (PP), polystyrene (PS), and polyvinyl chloride (PVC), exhibit limited gamma-ray attenuation [3]. Larger thicknesses are needed for equal shielding, as seen by their noticeably higher HVL values when compared to materials based on heavy metals [9]. Nonetheless, hydrogen-rich polymers are frequently employed in mixed radiation fields due to their strong neutron shielding effectiveness [10].

2. Polymer Composites with High-Z Fillers:

The addition of high atomic number fillers substantially enhances the gamma attenuation performance of polymers. Incorporation of Bi_2O_3, PbO, and WO_3 increases both μ/ρ and μ values, while reducing HVL [4]. Due to improved photoelectric absorption, studies have shown that polymer composites with 30–60 weight percent Bi_2O_3 exhibit a notable improvement in shielding efficacy at diagnostic gamma energies (59–662 keV) [11]. Epoxy composites loaded with tungsten oxide show enhanced attenuation over a broad energy range, including Co-60 energies (1173 and 1332 keV) [12]. In a similar vein, PbO-reinforced PVC composites show significant attenuation but cause toxicity and environmental issues [13]. When compared to micro-scale fillers at comparable loading levels, nan particle fillers offer superior dispersion and higher interfacial bonding, which results in increased attenuation [14]. The total attenuation performance is improved by the synergistic effects of hybrid filler systems that combine multiple oxides (e.g., BiO_3 + WO_3) [15].

Radiation Shielding Properties of Oxide Materials:

Because of their large densities and high effective atomic numbers, oxide materials—such as heavy metal oxide glasses and ceramics—are good gamma-ray attenuators [5]. Because PbO and BiO_3 are present, lead borate and bismuth borate glasses have large mass attenuation coefficients [16]. HVL is greatly reduced and the effective atomic number is increased when PbO concentration in glass matrices is increased [17]. Because of its high atomic number and density, tungsten exhibits improved shielding efficiency in glass systems (e.g., WO_3–B_2O_3–TeO_2) [18].

BiO_3 and WO_3 ceramics are examples of ceramic oxides that exhibit exceptional attenuation characteristics and structural durability at elevated temperatures, rendering them appropriate for use in nuclear facilities [19]. Because of their larger bulk density, monolithic oxide materials often have higher linear attenuation coefficients than polymer composites [5]. But compared to polymers, oxide materials are usually more rigid, heavy, and brittle, which restricts their use in wearable shielding systems [20].

Comparative Analysis:

1. Attenuation Efficiency:

Because of their higher density and Z_eff, oxide materials often show lower HVL values

and higher μ than pure polymers and moderately loaded polymer composites [5]. Nonetheless, in specific energy ranges, high-loading polymer composites (>50 weight percent heavy oxide) can come close to or equal the attenuation performance of oxide materials [11].

2. Density and Weight Considerations:

Polymer composites give better strength-to-weight ratios and flexibility, whereas oxide materials offer better attenuation per unit thickness [3]. Because polymer composites are lighter and more ergonomic, they are favored in wearable shielding applications like radiological aprons [4].

3. Energy Dependence:

At low photon energies, oxide materials containing PbO or Bi_2O_3 show markedly superior attenuation due to enhanced photoelectric interaction [7]. At intermediate energies dominated by Compton scattering, performance differences narrow between oxide systems and high-filler polymer composites [8].

4. Mechanical and Environmental Aspects:

Polymer composites offer ease of fabrication and resistance to corrosion, while oxide ceramics provide superior thermal stability [19]. Environmental concerns related to lead-containing materials encourage the development of lead-free systems based on bismuth and tungsten oxides [13].

Future Perspectives:

Future research should focus on:

- Development of lead-free hybrid composites with optimized filler combinations [15].
- Use of nano-engineered fillers for improved dispersion and attenuation efficiency [14].
- Design of multi-layered structures for combined neutron and gamma shielding [10].
- Integration of computational modeling (Monte Carlo simulations) with experimental validation to optimize material design [6].

Applications:

1. Medical Radiation Shielding:

Lead-free aprons utilizing Bi_2O_3 or tungsten filled polymers are replacing traditional lead aprons due to weight and toxicity concerns.

2. Nuclear and Industrial Environments:

Modular shielding panels with oxide reinforcements or polymer composites serve in reactor plants, radiography enclosures, and waste containers.

3. Aerospace:

Weight sensitivity in aerospace drives research toward polymer composites with high-Z fillers for spacecraft shielding against cosmic gamma and high-energy particles.

Conclusions:

This comparative review demonstrates that oxide materials generally provide superior intrinsic gamma attenuation due to high density and atomic number, while polymer-based composites offer advantages in weight reduction, flexibility, and process ability. By incorporating high-Z oxide fillers into polymer matrices, it is possible to achieve shielding efficiencies approaching those of monolithic oxide systems while retaining mechanical advantages. Material selection ultimately depends on application-specific requirements such as energy range, structural constraints, environmental safety, and cost. Continued research in hybrid and nano-engineered systems is expected to further advance radiation shielding technologies.

References:

1. Knoll, G. F., Radiation Detection and Measurement, 4th ed., Wiley, 2010.
2. Lamarsh, J. R., Introduction to Nuclear Engineering, 3rd ed., Prentice Hall, 2001.
3. Singh, V. P. et al., "Polymer-based radiation shielding materials," Radiation Physics and Chemistry, 2015.
4. Sayyed, M. I. et al., "Gamma attenuation properties of polymer composites filled with heavy metal oxides," Journal of Alloys and Compounds, 2017.
5. El-Mallawany, R., Tellurite Glasses Handbook, CRC Press, 2002.
6. Hubbell, J. H. & Seltzer, S. M., "Tables of X-ray mass attenuation coefficients," NIST Report, 1996.
7. Attix, F. H., Introduction to Radiological Physics and Radiation Dosimetry, Wiley, 1986.
8. Podgorsak, E. B., Radiation Physics for Medical Physicists, Springer, 2006.
9. Akkurt, I. et al., "Radiation shielding properties of polymer materials," Annals of Nuclear Energy, 2010.
10. Shultis, J. K. & Faw, R. E., Radiation Shielding, American Nuclear Society, 2000.
11. Dong, M. G. et al., "Gamma attenuation in Bi_2O_3-filled polymer composites," Radiation Physics and Chemistry, 2018.
12. Tekin, H. O. et al., "Tungsten oxide reinforced epoxy composites for radiation shielding," Materials Chemistry and Physics, 2019.
13. Tishkevich, D. I. et al., "Lead-free radiation shielding materials," Journal of Materials Science, 2020.
14. Al-Hadeethi, Y. & Sayyed, M. I., "Nanoparticle effects on gamma attenuation," Ceramics International, 2021.
15. Obaid, S. S. et al., "Hybrid heavy metal oxide composites for radiation shielding," Results in Physics, 2019.
16. Issa, S. A. et al., "Radiation shielding properties of heavy metal oxide glasses," Radiation Physics and Chemistry, 2016.
17. Gaafar, M. S. et al., "Effect of PbO on shielding properties of borate glasses," Journal of Non-Crystalline Solids, 2018.
18. Tekin, H. O. et al., "WO_3-containing glass systems for gamma shielding," Ceramics International, 2018.
19. Bashter, I. I., "Calculation of radiation attenuation coefficients for ceramics," Annals of Nuclear Energy, 1997.
20. ayyed, M. I. et al., "Mechanical and shielding behavior of oxide ceramics," Materials Research Express, 2019.

International Journal of Advance and Applied Research
www.ijaar.co.in
ISSN – 2347-7075 Impact Factor – 8.141
Peer Reviewed Bi-Monthly
Vol. 7 No. 14 January – February - 2026

Effect of Humidity and Monsoon Shifts on Mosquito Breeding Genetics and Survival Traits

Abhijit Ankushrao Taur[1] & Laxmikant Vitthalrao Shinde[2]

[1]*Dr. Babasaheb Ambedkar Marathwada University, Ch. Sambhaji Nagar (M.S)*

[2]*Head Department of Zoology, Applied Parasitology Laboratory, Department of Zoology, J.E.S College, Jalna – MS, India*

Corresponding Author – Laxmikant Vitthalrao Shinde

DOI - 10.5281/zenodo.19827327

Abstract:

Climate variability—particularly fluctuations in humidity and shifts in monsoon onset, duration, and intensity—plays a critical role in shaping the ecology, physiology, and genetic adaptability of Culex quinquefasciatus, a significant vector of lymphatic filariasis and West Nile virus. Changing monsoon patterns and prolonged humid periods create new breeding habitats, influence larval development cycles, and potentially alter genetic structures within mosquito populations. This study investigates how humidity gradients and monsoon variability affect breeding dynamics, survival traits, and population genetics of C. quinquefasciatus across tropical and semi-tropical ecosystems.

Mosquito samples were collected across pre-monsoon, monsoon, and post-monsoon seasons from four ecological zones. Climatic parameters, including relative humidity and rainfall anomalies, were combined with molecular analyses using mitochondrial COI markers, microsatellites, and climate-responsive genes such as HSP70. Statistical methods, including AMOVA, regression modelling, and structure analysis, were applied to identify genetic differentiation and climate-driven selection pressures.

Results show that high humidity (>80%) significantly enhances egg hatching, larval survival, and adult longevity, while monsoon irregularities produce short-term genetic bottlenecks followed by rapid adaptive recovery. Distinct seasonal genetic clusters suggest ongoing microevolutionary responses to climatic stress. These findings underscore the potential expansion of vector populations under future climate scenarios, increasing the risk of filariasis and West Nile virus transmission.

Understanding climate–genetic interactions in C. quinquefasciatus is essential for designing predictive vector surveillance and targeted control interventions.

Keywords: Humidity, Monsoon Shifts, Culex Quinquefasciatus, Mosquito Genetics, Climate Change, Survival Traits, Vector Ecology, Adaptive Evolution.

Introduction:

Mosquito-borne diseases continue to pose some of the most persistent and complex public health challenges globally, affecting millions of individuals each year across tropical, subtropical, and increasingly temperate regions. Among the diverse mosquito vectors implicated in disease transmission, *Culex quinquefasciatus* occupies a prominent position due to its vast geographic distribution, ecological versatility, and strong association with human settlements. Commonly referred to as the southern house mosquito, *C. quinquefasciatus* thrives in warm, humid environments and is particularly well adapted to polluted, stagnant water bodies commonly found in urban and peri-urban landscapes. This ecological flexibility, combined with its anthropophilic feeding tendencies, contributes

significantly to its role as a vector of major diseases such as lymphatic filariasis—caused by the parasitic worm *Wuchereria bancrofti*—and West Nile virus (WNV), a globally emerging arbovirus with increasing incidence.

The epidemiological significance of *C. quinquefasciatus* is closely tied to environmental and climatic conditions that influence its breeding success, survival, dispersal, and vectorial capacity. Over the past decades, climate-sensitive diseases have gained heightened attention as global climate change alters the spatial and temporal dynamics of mosquito populations. Environmental variables—particularly **humidity** and **monsoon variability**—directly shape mosquito physiology and ecology. Humidity influences nearly every stage of mosquito development, determining adult longevity, egg viability, and larval survival. Likewise, monsoon onset, duration, and intensity significantly affect the availability and persistence of aquatic habitats essential for breeding. These climatic factors are not merely environmental background variables; they are active ecological drivers that regulate population cycles, genetic diversity, and seasonal patterns of disease transmission.

Global Significance of *Culex quinquefasciatus* and Climatic Influences:

Globally, lymphatic filariasis threatens over 859 million people across 50 countries, with India, Southeast Asia, and Africa bearing the highest burdens. *C. quinquefasciatus* is the principal vector in urban regions due to its preference for wastewater drains, cesspits, septic tanks, and organically rich stagnant water. Similarly, West Nile virus, once confined mainly to Africa and the Middle East, has spread rapidly across the Americas and parts of Europe. Outbreaks of both diseases have shown strong correlations with climatic fluctuations, particularly variations in rainfall patterns and atmospheric moisture.

Humidity significantly influences mosquito survival because C. quinquefasciatus, like most mosquitoes, is highly vulnerable to desiccation. Elevated humidity minimises water loss through the cuticle, enabling adult mosquitoes to live longer and increasing the chances of multiple blood meals. This longer lifespan is vital for disease transmission, as pathogens like filarial worms and WNV need time to incubate inside the mosquito—a phase called the extrinsic incubation period (EIP). Consequently, longer-lived mosquitoes are more likely to become infectious vectors. On the other hand, low-humidity environments can reduce lifespan and transmission capacity. However, climate fluctuations, such as unusually wet monsoon seasons or sudden humidity increases, can quickly alter these dynamics.

Monsoon Variability and Its Ecological Implications:

In tropical areas, the monsoon is the primary seasonal factor influencing mosquito populations. It greatly boosts breeding site availability by forming pools, ditches, waterlogged farms, and overflowing drains. For C. quinquefasciatus, which favours polluted water, monsoon rains increase nutrient-rich habitats, aiding quick larval growth and population growth. Recently, monsoon patterns have become more irregular, with delayed starts, uneven rainfall, dry periods, and heavy short rains, all significantly impacting mosquito ecology.

When monsoon rains are delayed, breeding cycles are disrupted, leading to altered seasonal peaks in mosquito abundance. Intense rainfall may temporarily reduce population density by washing away immature stages, but

subsequent stabilisation of water bodies often leads to explosive population rebounds. These ecological disruptions also influence **genetic diversity**, as fluctuating environmental stress can lead to population bottlenecks, founder effects, and/or selective pressures favouring stress-tolerant genotypes.

Climate Change as an Emerging Determinant of Mosquito Evolution:

Climate change is expected to intensify fluctuations in humidity and increase monsoon unpredictability, thereby accelerating ecological and evolutionary changes in mosquito species. Higher atmospheric moisture, coupled with rising temperatures, enhances the metabolic rates, feeding frequency, and reproductive success of *C. quinquefasciatus*. At the genetic level, environmental stressors can alter allele frequencies, particularly in genes associated with desiccation tolerance, heat shock response, and immunity. Populations may undergo micro-evolutionary changes that increase their adaptability to novel climatic conditions, potentially expanding their geographic range and enhancing their resilience to control interventions.

1. Climate Variability and Mosquito Ecology:

Humidity and rainfall patterns strongly determine mosquito life cycles. High humidity prolongs adult mosquito survival by reducing desiccation rates. It also provides optimal microhabitats for egg incubation and larval breeding. Sudden increases in moisture can trigger mass oviposition events. Conversely, low humidity reduces vector abundance. For *C. quinquefasciatus*, which breeds in polluted or stagnant water, monsoon rainfall significantly expands the availability of breeding sites, such as drains, ditches, and wastewater ponds.

2. Monsoon Dynamics in Tropical Regions:

Climate change has intensified monsoon irregularities, including delayed onset, shorter-duration rainfall bursts, and prolonged monsoon seasons. Such anomalies alter mosquito breeding windows and population patterns. A strong monsoon creates abundant habitat but may wash larvae out during peak rain events. A weak monsoon limits habitat availability while increasing human water-storage practices, thereby indirectly providing breeding opportunities.

3. Impact on Genetic Diversity and Evolutionary Responses:

While the ecological effects of monsoon and humidity are well documented, their **genetic impacts** on mosquito populations are less explored. Environmental stressors, including temperature and humidity extremes, can exert selective pressures that drive genetic shifts. Genes associated with stress tolerance—heat shock proteins (e.g., HSP70)—may undergo positive selection during extreme humidity fluctuations. Similarly, fluctuating breeding habitats may create conditions for bottlenecks or founder effects, followed by rapid population recovery.

4. Linking Climate to Vector Competence:

Mosquito survival traits, such as larval development time, adult lifespan, and fecundity, directly influence vectorial capacity. High humidity supports longer adult lifespan, increasing opportunities for pathogen transmission. Monsoon-driven changes in breeding patterns affect population density and age structure, contributing to fluctuations in disease incidence.

5. Research Gap:

Despite extensive ecological studies, research integrating climate variables, population genetics, and survival traits for C.

quinquefasciatus remains limited. Few studies analyse monsoon shifts in relation to genetic differentiation. Even fewer examine how humidity-driven microhabitat changes influence mosquito evolution and adaptation.

6. Significance of This Study:

This study aims to address these gaps by exploring the combined effects of humidity and monsoon variability on the genetic diversity, breeding performance, and survival traits of *C. quinquefasciatus*. Understanding these dynamics is essential for predicting changes in vector populations and disease outbreaks under future climate scenarios.

Review of Literature:

Climate variables, particularly humidity and temperature, are widely recognised as fundamental ecological drivers influencing mosquito biology, behaviour, and population dynamics. Among these variables, humidity plays a critical regulatory role, shaping the success of each developmental stage of *Culex quinquefasciatus*, from egg to adult. Numerous studies have demonstrated that even slight fluctuations in moisture availability can alter mosquito ecology, reproductive strategies, and vectorial capacity.

1. Climate Variables and Mosquito Ecology:

Humidity plays a decisive and multifaceted role in shaping the ecology and survival of *Culex quinquefasciatus*, significantly influencing its physiological stability, reproductive behaviour, and disease-transmission potential. As demonstrated by Ramasamy and Surendran (2012), adult mosquitoes exposed to environments with relative humidity below 60% experience rapid desiccation due to water loss through the cuticle and respiratory spiracles, resulting in markedly higher mortality. Conversely, high-humidity environments—typically exceeding 80%—significantly reduce evaporative water loss, enabling adults to survive for several additional days or even weeks. This extended lifespan directly increases opportunities for blood feeding, mating, and multiple gonotrophic cycles, thereby raising the likelihood of transmitting filarial parasites and West Nile virus. Humidity not only influences survival but also drives feeding behaviour; Chaves et al. (2014) reported that Culex mosquitoes exhibit heightened host-seeking activity under high-humidity conditions, particularly at night when moisture levels peak. When atmospheric humidity exceeds 80%, mosquitoes become more responsive to host cues such as carbon dioxide and human skin volatiles, mainly because they expend less metabolic energy on water retention, thereby enabling greater allocation to locomotion and feeding. This behavioural shift substantially amplifies pathogen transmission cycles, making humid monsoon months especially conducive to disease outbreaks.

Humidity also interacts closely with temperature to shape larval physiology and development. Murdock et al. (2017) found that warm, humid environments accelerate metabolic processes in larvae, improving nutrient assimilation and promoting faster developmental progression. Because *C. quinquefasciatus* larvae typically inhabit organically polluted, stagnant water, high humidity helps maintain moisture stability in these microhabitats, preventing evaporation and preserving access to essential microbial food sources. As a result, larval development is completed more quickly, leading to shorter generational intervals and facilitating rapid population expansion during monsoon and post-monsoon periods. Moisture availability also serves as a critical behavioural cue for reproduction; Reisen et al. (2013) demonstrated that gravid females preferentially oviposit in

environments with high ambient humidity, where egg rafts are less likely to desiccate. Laboratory experiments showed that females placed in humid settings exhibit higher oviposition frequency, increased egg raft production, and greater egg hatchability, indicating that humidity directly drives reproductive decision-making.

Beyond individual-level effects, humidity patterns also influence the distribution of mosquito populations at broader ecological scales. Campbell et al. (2015) reported that climate-induced increases in humidity have expanded the geographic range of *C. quinquefasciatus*, enabling its establishment in regions previously too dry to support sustained breeding. Urbanisation, irrigation, and shifting monsoon dynamics have further intensified this expansion, introducing mosquito populations into new ecological niches where local communities may have limited immunity to mosquito-borne diseases. This range expansion poses substantial challenges for vector control, as interventions must adapt to newly affected geographic areas. Importantly, humidity rarely acts independently; rather, it synergises with temperature to regulate mosquito physiology. Kraemer et al. (2020) showed that the combination of high humidity and warm temperatures enhances metabolic efficiency, thereby increasing flight capacity, feeding success, egg maturation rate, and larval metabolic performance. These synergistic interactions suggest that ongoing climate change—marked by rising global temperatures and unpredictable peaks in humidity—may create ideal conditions for explosive growth of mosquito populations, intensifying the transmission risk of mosquito-borne pathogens in vulnerable regions.

2. Monsoon and Breeding Dynamics:

Monsoon rainfall plays a decisive role in shaping the breeding ecology, population dynamics, and spatial distribution of *Culex quinquefasciatus*, mainly by creating stagnant, nutrient-rich water bodies that serve as ideal larval habitats. Rahman et al. (2017) highlight that during monsoon seasons, the accumulation of organic-rich wastewater in drains, ditches, and poorly-managed sewage systems provides abundant breeding substrates, enabling rapid population expansion. However, excessive monsoon rainfall can temporarily limit mosquito populations. Heavy downpours often wash eggs, larvae, and pupae from shallow water bodies, leading to temporary declines in mosquito density. However, populations typically rebound quickly once rainfall stabilises and new pools form (White et al., 2018). In India, where monsoon patterns are highly variable, studies have shown that changes in rainfall onset, volume, and duration are closely correlated with fluctuations in both mosquito abundance and the incidence of filariasis, the primary disease transmitted by *C. quinquefasciatus* (Subramanian et al., 2015). Additionally, deviations in the timing of monsoon onset—whether early or delayed—shift breeding peaks and disrupt seasonal population cycles. Naqvi et al. (2019) found that delayed monsoons compress the breeding season into shorter, more intense population surges, while early monsoons prolong larval activity into late autumn months. Intermittent rainfall events, often observed during weak or erratic monsoons, further contribute to transient aquatic microhabitats that sustain short-term breeding cycles, allowing *C. quinquefasciatus* to reproduce episodically during breaks in heavy rainfall (Amarasinghe & Wickramasinghe, 2014). Climate change has intensified these dynamics by altering rainfall intensity and distribution. Nguyen et al. (2020) report that increased rainfall variability affects habitat stability; mild, consistent rainfall fosters stable breeding environments, whereas erratic,

high-intensity rainfall reduces habitat persistence, influencing larval survival rates and breeding success. Collectively, these findings underscore that monsoon variability—through its influence on habitat formation, stability, and duration—is a critical ecological driver of *C. quinquefasciatus* population dynamics and, consequently, its disease transmission potential.

3. Genetic Diversity in Mosquito Populations:

Genetic diversity in *Culex quinquefasciatus* populations is powerfully shaped by climatic and ecological factors that regulate gene flow, population structure, and adaptive potential across environments. Mitochondrial COI (cytochrome oxidase I) markers have been widely employed to study mosquito phylogeography, revealing significant genetic structuring among *C. quinquefasciatus* populations distributed across varying climatic zones (Smith & Fonseca, 2013). These genetic patterns often reflect long-term environmental pressures and historical dispersal routes, demonstrating how temperature, humidity, and habitat availability contribute to the formation of distinct lineages. Microsatellite analyses further support these findings, showing that climate-driven habitat fragmentation—particularly during dry seasons or droughts—reduces gene flow among mosquito populations, leading to localised genetic differentiation (Zhong et al., 2014). Such fragmentation intensifies isolation, allowing micro-populations to evolve independently in response to their specific environmental constraints.

Moreover, climatic stressors such as extended dry seasons can create temporary population bottlenecks, reducing genetic diversity by allowing only a subset of individuals to survive (Severson et al., 2018). However, the onset of monsoon rains often reverses this effect by enabling rapid population recovery and recolonisation, thereby introducing new genetic variants and restoring diversity. Urban environments add another layer of complexity to mosquito genetic structuring. Wilke et al. (2020) demonstrated that urban heat islands—characterised by elevated temperatures and fluctuating humidity—serve as selective environments that promote micro-evolutionary divergence, resulting in distinct genotypes adapted to metropolitan conditions relative to rural or semi-rural populations. Climate gradients such as altitude, temperature, and rainfall patterns also shape haplotype variation, with studies showing that even modest differences in these factors produce measurable shifts in mitochondrial haplotype frequencies among geographically separated populations (Morris et al., 2016). Additionally, climatic extremes such as heat waves, fluctuations in humidity, and environmental pollutants exert selective pressures that favour the retention of adaptive genetic variants associated with immune competence and stress-response pathways. Crawford et al. (2017) reported that populations exposed to such environmental stresses exhibit elevated frequencies of alleles linked to enhanced detoxification, oxidative stress management, and thermal tolerance. Collectively, these findings illustrate that genetic diversity in *C. quinquefasciatus* is not static but continually moulded by environmental heterogeneity, climatic variability, and anthropogenic landscape changes, reinforcing the species' capacity for rapid adaptation and persistence under changing global conditions.

Methodology:

1. Study Sites:

To capture environmental variability and understand how varying climatic conditions influence the ecology and genetics of Culex

quinquefasciatus, four ecologically distinct zones were selected.

(1) Coastal humid zone: Characterised by consistently high humidity (>80%), saline influence, and dense human settlements, this zone provides optimal year-round breeding environments for mosquitoes. The presence of brackish water bodies, sewage channels, and poor drainage makes it an ideal site for observing humidity-driven breeding patterns.

(2) Urban semi-humid zone: Represented by metropolitan or peri-urban locations where artificial water storage containers, storm drains, and sewage systems offer breeding habitats. Urban heat island effects and fluctuating humidity make this zone crucial for studying micro-evolutionary adaptations.

(3) Rural agricultural zone: Dominated by irrigation canals, paddy fields, wells, and livestock wastewater, this region is highly influenced by monsoon-dependent agriculture. Seasonal water stagnation creates dynamic breeding habitats that fluctuate widely across the year.

(4) Semi-arid zone: Characterised by low humidity, sparse vegetation, and seasonal water scarcity. Breeding sites are often limited to manufactured structures, such as tanks and wastewater collection systems. This zone offers insights into population bottlenecks and genetic stress responses under harsh climatic conditions.

These diverse sites allow for comparative analysis of environmental influences on mosquito genetics, survival traits, and breeding success.

2. Sampling Strategy:

A systematic monthly sampling protocol was adopted to capture seasonal fluctuations in mosquito populations. Sampling was conducted across three major climatic seasons: Pre-monsoon (March–May): Characterised by rising temperatures and declining humidity, this period typically shows low mosquito abundance. Sampling during this phase helps identify genetic bottlenecks and early breeding cycles.

Monsoon (June–September): This period brings high rainfall and humidity, creating abundant breeding habitats. Sampling during monsoon peaks allows assessment of genetic diversity, population expansion, and adaptive responses to environmental abundance.

Post-monsoon (October–December): Marked by stabilised water bodies and sustained humidity, this season supports continued mosquito activity. Sampling here helps track population recovery and late-season breeding dynamics.

Collection methods included ovitraps for egg rafts, larval dipping in stagnant water bodies, and BG-Sentinel or CDC light traps for adult mosquitoes. Specimens were transported to the laboratory under controlled conditions to maintain DNA integrity.

3. Climate Data:

Climatic data were collected from the India Meteorological Department (IMD) for all four study sites. Daily and monthly values of relative humidity (%), rainfall (mm), temperature, and monsoon onset dates were recorded.

- Relative humidity was used to correlate survival traits and breeding density with atmospheric moisture.
- Rainfall provided insights into the formation and stability of breeding habitats.

Data were validated using local meteorological stations to ensure accuracy. Climate variables were later integrated into statistical and genetic models to assess correlations with mosquito population dynamics.

4. Genetic Analysis:

Genetic analysis focused on understanding population structure, gene flow,

and climate-driven adaptation in *C. quinquefasciatus*.

(1) COI gene sequencing: Mitochondrial cytochrome oxidase I (COI) was used to study haplotype diversity and phylogenetic patterns across regions. COI provides insight into maternal lineages and historical population movement.

(2) Microsatellite loci analysis: Highly polymorphic nuclear markers were used to assess genetic differentiation, gene flow, and bottlenecks among populations inhabiting different climatic zones.

(3) HSP70 expression studies: The Heat shock protein gene (HSP70) was chosen as a marker for climate stress response. Changes in expression levels indicate physiological adaptation to fluctuations in humidity and temperature.

Laboratory tools included PCR amplification, agarose gel electrophoresis, DNA purification, and Sanger sequencing.

Population structure and diversity indices were analysed using STRUCTURE, Arlequin, and MEGA software to detect clustering patterns and genetic distances.

5. Survival Trait Assessment:

Survival traits were analysed under controlled laboratory conditions to minimise external variability. Mosquito eggs, larvae, and adults were placed in humidity-controlled chambers set at 40%, 60%, 80%, and 90% relative humidity to simulate real environmental conditions. Measured traits included:

- **Egg viability:** Number of eggs successfully hatching under each humidity level; assessed to understand moisture dependency during embryonic development.
- **Larval development time:** Duration from first-instar larva to pupation; faster development indicates favourable environmental conditions.
- **Adult survival:** Average lifespan under each humidity condition; an important determinant of vectorial capacity since pathogens require time to develop within the mosquito.

These experiments helped establish direct causal relationships between humidity gradients and mosquito physiology.

6. Statistical Models:

Multiple advanced statistical models were used to interpret ecological and genetic datasets.

(1) ANOVA (Analysis of Variance): Applied to compare survival traits (egg viability, larval duration, adult lifespan) across different humidity treatments. Significant differences indicate environmental influence on biological performance.

(2) Regression modelling: Used to assess the relationship between climate variables (humidity, rainfall) and mosquito abundance or survival traits. Both linear and polynomial regression models were tested.

(3) AMOVA (Analysis of Molecular Variance): Utilised to quantify genetic differentiation among populations from different climatic zones. AMOVA partitions variance into within-population and between-population components.

(4) Mantel test: Used to determine correlations between genetic distance and environmental distance (e.g., humidity gradient, rainfall differences). A strong correlation suggests climate-driven genetic structuring.

These statistical tools collectively help link climatic patterns with mosquito ecology and genetic diversity.

Results:

1. Climate Trends:

Analysis of climatic data across the four study sites revealed substantial annual and seasonal variation in both relative humidity and rainfall patterns. Humidity levels ranged from as low as 45% during peak pre-monsoon months to as high as 95% during the core monsoon period, indicating a wide temporal moisture gradient that directly influenced mosquito activity. Notably, the India Meteorological Department (IMD) reported a **delay in monsoon onset by 10–15 days** for two consecutive years, accompanied by **irregular rainfall distribution** characterised by intense short-duration rain events followed by prolonged dry spells. These anomalies resulted in fluctuating availability of aquatic breeding habitats, with rapid inundation occurring during peak rainfall periods and abrupt desiccation during intermittent dry intervals. Such climate irregularities likely imposed intense selective pressures on *Culex quinquefasciatus* populations, influencing breeding cycles, survival traits, and genetic structuring across seasons.

2. Breeding Performance:

Breeding performance varied significantly across humidity treatments, with both egg hatch rates and larval survival strongly dependent on moisture availability. At **40% humidity**, egg hatch success was limited to 48%, and larval survival dropped sharply to 30%, reflecting the mosquitoes' vulnerability to desiccation stress. Conditions improved substantially at **60% humidity**, with egg hatch rates reaching 67% and larval survival increasing to 55%. Optimal breeding performance was observed at **80% humidity**, with hatch rates of 84% and larval survival of 78%. The highest performance occurred at humidity levels above 90%, where egg hatch rates peaked at 91% and larval survival at 85%. These data indicate a clear positive association between humidity and breeding success, emphasising that *C. quinquefasciatus* thrives in moist environments typical of monsoon and post-monsoon periods. The observed trend suggests that increases in regional humidity due to climate shifts may favour greater mosquito proliferation.

3. Genetic Diversity:

Genetic analyses revealed notable patterns of diversity and seasonal differentiation across *Culex quinquefasciatus* populations. **Fifteen distinct COI haplotypes** were identified across the study sites, with monsoon-season samples exhibiting the highest haplotype richness. This suggests that climatic conditions during the monsoon—particularly elevated humidity and expanded breeding habitats—facilitate greater population mixing and genetic recombination. Population differentiation metrics (Fst) ranged between **0.08 and 0.15**, indicating **moderate genetic structure** that varied seasonally, likely in response to alternating periods of climatic stress and resource abundance. Furthermore, expression analysis of the **HSP70 stress-response gene** revealed upregulation in post-monsoon populations, suggesting physiological adaptation to fluctuating humidity, temperature, and environmental pressures. These findings collectively indicate that *C. quinquefasciatus* populations undergo measurable genetic and molecular responses to seasonal climate dynamics, contributing to their adaptability and persistence.

4. Survival Traits:

Adult survival was significantly enhanced under high-humidity conditions. Mosquitoes maintained at humidity levels above 80% showed a **35–45% increase in lifespan** compared with those reared under drier conditions (40–60% humidity). This extended survival is highly consequential for disease transmission, as

pathogens such as filarial parasites and West Nile virus require a specific extrinsic incubation period within the mosquito host before they become transmissible. Longer-lived vectors are therefore more likely to survive long enough to transmit infection. The improved survival under humid conditions can be attributed to reduced desiccation stress and enhanced metabolic efficiency, allowing mosquitoes to allocate more energy to feeding, reproduction, and host-seeking.

5. Statistical Associations:

Statistical analyses demonstrated strong and statistically significant relationships between humidity and key mosquito life-history traits. A **strong positive correlation between humidity and egg viability (r = 0.82)** indicates that egg survival is highly dependent on moisture availability, with desiccation posing a major limiting factor in drier seasons. Similarly, a **positive correlation between humidity and adult lifespan (r = 0.77)** suggests that humid conditions substantially enhance adult mosquito survival. These correlations underscore the profound influence of climate variables on mosquito population stability and proliferation. Such relationships provide predictive value for vector surveillance models, suggesting that increases in humidity—driven by monsoon intensification or climate change—could correspond to elevated mosquito population densities and heightened disease transmission risk.

Discussion:

Results demonstrate that humidity significantly affects breeding success and survival. High humidity reduces desiccation stress, enhancing egg hatchability and larval viability. Monsoon variability introduced seasonal genetic differentiation, suggesting climate-driven adaptation. The upregulation of HSP70 indicates stress response mechanisms triggered by humidity fluctuations.

Genetic results show temporary bottlenecks during harsh dry seasons, followed by recovery during the monsoon. Similar seasonal genetic shifts have been observed in other mosquito species.

Vector competence is expected to increase due to prolonged adult lifespan and higher breeding output under humid conditions. Increased genetic diversity during the monsoon may promote adaptability, enabling faster recovery from environmental disturbances.

Conclusion:

This study demonstrates that climate variability—particularly fluctuations in humidity and monsoon patterns—exerts profound and multifaceted influences on the breeding ecology, genetic diversity, and survival traits of *Culex quinquefasciatus*, one of the most medically important mosquito species worldwide. The findings clearly show that **high humidity creates optimal conditions for mosquito proliferation**, significantly enhancing egg hatchability, larval survival, and adult longevity. These physiological advantages allow populations to expand rapidly during monsoon and post-monsoon periods, when moisture availability is at its peak. An extended adult lifespan, in particular, directly increases vectorial capacity by allowing sufficient time for pathogens such as filarial parasites and West Nile virus to complete their extrinsic incubation period, thereby elevating the potential for disease transmission.

The study also reveals that **monsoon irregularities play a critical role in shaping genetic patterns** within mosquito populations. Delayed onset, uneven rainfall distribution, and intermittent wet-dry cycles create fluctuating

breeding habitats, which in turn influence gene flow and population structure. Moderate seasonal differentiation observed in mitochondrial and microsatellite markers suggests that *C. quinquefasciatus* populations undergo **climate-driven micro-evolutionary shifts**, enabled by adaptive alleles such as enhanced expression of stress-response genes like HSP70. These adaptive responses not only promote population resilience during climatic stress but also contribute to long-term evolutionary changes that may strengthen mosquito survival under future climate regimes.

Collectively, the results underscore that ongoing and projected climate changes—marked by increased humidity peaks, erratic monsoon behaviour, and rising temperatures—are likely to **intensify mosquito population growth and geographic expansion**, thereby amplifying the public health burden posed by mosquito-borne diseases. Understanding these climate–mosquito interactions is essential for developing effective vector surveillance systems, forecasting outbreak risks, and designing adaptive, climate-informed vector control strategies. As climate patterns continue to shift globally, integrated approaches that combine climate monitoring, genetic surveillance, and ecological assessments will be crucial for mitigating the growing threat of vector-borne disease transmission.

Limitations:

Although this study provides valuable insights into the influence of humidity and monsoon variability on the breeding ecology, genetic diversity, and survival traits of *Culex quinquefasciatus*, several limitations must be acknowledged. First, the research was conducted across a **limited number of geographic zones**, which, although ecologically diverse, may not fully represent the broader environmental variability observed across larger regional or global landscapes. Consequently, the findings may not be generalizable to all climatic settings where *C. quinquefasciatus* populations thrive. Second, the study did not include pathogen infection experiments, so the direct effects of climate-driven changes on the mosquito's vector competence—particularly its ability to transmit filarial parasites or West Nile virus—could not be assessed. Including infection-based assays would provide deeper insight into how environmental factors influence not just mosquito biology but also disease transmission dynamics. Third, the study was conducted over a **relatively short-term monitoring period**, capturing seasonal variations but not long-term climatic cycles. Climatic influences on mosquito evolution, phenotypic plasticity, and population structure often occur over multiple years or decades; therefore, longer-term studies are needed to validate whether the trends observed here persist under prolonged climate change scenarios. These limitations highlight the need for broader, longitudinal, and pathogen-inclusive studies to deepen understanding of climate–vector interactions.

Future Scope:

Future research on *Culex quinquefasciatus* should extend beyond the ecological and genetic parameters examined in this study to incorporate more advanced and integrative approaches. One important direction is the implementation of genomic-level climate adaptation studies, which would involve whole-genome sequencing, transcriptomics, and epigenetic profiling to identify specific genes, regulatory pathways, and adaptive mutations that enable mosquitoes to withstand humidity fluctuations, temperature extremes, and monsoon irregularities. Such high-resolution genomic analyses would significantly enhance our

understanding of long-term evolutionary responses to future climate change. Additionally, there is a need to investigate species interactions and competitive displacement, especially in environments where *C. quinquefasciatus* coexists with other mosquito species such as *Aedes aegypti* or *Anopheles stephensi*. Climate variability may alter interspecific dynamics, leading to shifts in dominance, hybridisation events, or changes in habitat partitioning—all of which could influence vector ecology and disease transmission risk. A third central area for advancement lies in predictive modelling of disease outbreaks under climate change scenarios. By integrating climatic data, mosquito population dynamics, and pathogen transmission parameters, advanced machine-learning and climate-simulation models can be used to forecast potential hotspots of filariasis or West Nile virus outbreaks. These predictive tools would be invaluable for informing public health planning, optimising vector-control strategies, and mitigating emerging risks associated with global climate change.

References:

1. Amarasinghe, D., & Wickramasinghe, S. (2014). Seasonal breeding dynamics of mosquito vectors. *Journal of Vector Ecology, 39*(2), 345–352.
2. Andrade, C. A., et al. (2016). Climate-driven trade-offs in mosquito evolution. *Evolutionary Ecology, 30*(3), 455–467.
3. Bowden, S. E., et al. (2019). Environmental influences on mosquito host-seeking behaviour. *Parasites & Vectors, 12*, 452.
4. Campbell, L. P., et al. (2015). Climate influences on mosquito distribution shifts. *Global Change Biology, 21*(6), 2210–2222.
5. Chaves, L. F., et al. (2014). Humidity and biting frequency in mosquitoes. *Journal of Medical Entomology, 51*(3), 475–482.
6. Ciota, A. T., & Kramer, L. D. (2013). Environmental effects on arbovirus evolution. *Journal of Virology, 87*(11), 6035–6040.
7. Crawford, J. E., et al. (2017). Adaptive genetic variation in mosquito populations. *Molecular Ecology, 26*(10), 2652–2667.
8. Glaser, B., & Meola, R. (2020). Environmental impacts on mosquito vector competence. *Insects, 11*(4), 233.
9. Grossman, M. K., et al. (2019). Genetic adaptation to humidity stress in mosquitoes. *Scientific Reports, 9*, 18978.
10. Jones, P. D., et al. (2021). Climate-driven evolution in mosquitoes. *Nature Climate Change, 11*(3), 214–222.
11. Kothera, L., et al. (2018). Genomic signatures of environmental adaptation in mosquito species. *Genome Biology and Evolution, 10*(6), 1456–1470.
12. Kraemer, M. U. G., et al. (2020). Climate and mosquito physiology. *Nature Microbiology, 5*(3), 399–407.
13. López-Mestre, I., et al. (2022). Epigenetic responses in mosquitoes under climate stress. *Environmental Epigenetics, 8*(1).
14. Morris, A., et al. (2016). Climate gradients and mosquito genetic variation. *BMC Evolutionary Biology, 16*, 77.
15. Murdock, C. C., et al. (2017). Humidity and metabolic effects in mosquitoes. *PLoS Pathogens, 13*(11).
16. Naqvi, N., et al. (2019). Monsoon impact on vector population peaks. *Journal of Vector Borne Diseases, 56*(2), 120–128.
17. Nguyen, T. T., et al. (2020). Rainfall intensity and mosquito survival. *EcoHealth, 17*(4), 403–413.

18. Paull, S. H., et al. (2017). Climate, vertebrate hosts, and mosquito transmission cycles. *Proceedings of the National Academy of Sciences, 114*(34), 9158–9163.
19. Paz, S. (2015). WNV and climate patterns. *International Journal of Environmental Research and Public Health, 12*(1), 1–11.
20. Rahman, M. F., et al. (2017). Monsoon and mosquito breeding ecology. *Parasites & Vectors, 10*, 448.
21. Ramasamy, R., & Surendran, S. N. (2012). Climate and vector ecology. *Acta Tropica, 123*(1), 50–57.
22. Reisen, W. K., et al. (2013). Moisture and oviposition behaviour in mosquitoes. *Journal of Vector Ecology, 38*(1), 68–77.
23. Severson, D. W., et al. (2018). Population genetics of mosquitoes. *Annual Review of Entomology, 63*, 489–507.
24. Slater, H., & Michael, E. (2012). Environmental drivers of filariasis transmission. *PLoS ONE, 7*(1).
25. Smith, J. L., & Fonseca, D. M. (2013). Genetic structure of Culex mosquitoes. *Molecular Ecology, 22*, 3104–3118.
26. Soghigian, J., et al. (2020). Climate-driven mosquito range expansion. *Nature Communications, 11*, 244.
27. Subramanian, S., et al. (2015). Monsoon variability and filariasis incidence. *Indian Journal of Medical Research, 141*(5), 668–674.
28. White, G. B., et al. (2018). Rainfall effects on larval habitat stability. *Journal of Medical Entomology, 55*(1), 112–120.
29. Wilke, A. B. B., et al. (2020). Urban climate effects on mosquito evolution. *Scientific Reports, 10*, 21312.
30. Zhong, D., et al. (2014). Microsatellite variation in mosquito populations. *PLoS Neglected Tropical Diseases, 8*(9).

International Journal of Advance and Applied Research
www.ijaar.co.in
ISSN – 2347-7075 Impact Factor – 8.141
Peer Reviewed Bi-Monthly
Vol. 7 No. 14 January – February - 2026

Conserving Helminth Parasites for Ecological Significance: Challenges and Opportunities

Archana Yelikar[1], Meena Nagawanshi[2], Ganesh Chavan[1]

[1]*Department of Zoology, Deogiri College Chhatrapati Sambhajinagar, MS.*

[2]*Department of Zoology, R.B. Atal Arts and Science College Georai Dist. Beed M.S*

Corresponding Author – Archana Yelikar

DOI - 10.5281/zenodo.19827340

Abstract:

Parasites including helminths, are significantly recognized as integral components of biodiversity and ecosystem functioning. Maintaining food web stability, and influencing immune and evolutionary processes. However, global environmental change, habit loss, host extinction, and intensive disease control programs have led to the decline of many helminth species. This paper reviews the ecological importance of helminth parasites, discusses the challenges associated with the conservation and explores emerging opportunities for integrating parasite conservation into broader biodiversity and ecosystem management frameworks.

Keywords: Helminth Conservation, Parasite Biodiversity, Ecosystem Stability, Host-Parasite Interactions, Ecological Balance

Introduction:

Conservation biology has conventionally focused on free-living organisms, often overlooking parasites due to their association with disease and negative public perception. Helminths parasitic worms belonging to nematodes, cestodes, and trematodes which constitute a significant proportion of global biodiversity. Despite their abundance and diversity, Parasites are probably the most threatened form of animal life due to the co-extinction risk associated with declining host populations.

Recent ecological research has demonstrated that parasites are essential to ecosystem structure and function. The loss of helminth species may have unintended consequences for host populations and ecological stability. This paper highlights the importance of conserving helminth parasites and examines the scientific, ethical, and practical dimensions of meaningful parasite conservation.

Ecological significance of Helminth Parasites:

- **Regulation of Host Populations:** Helminths can regulate host population size by influencing host survival, reproduction, and behavior. This regulatory role helps prevent overpopulation and promote species coexistence within ecosystems.
- **Contribution to Biodiversity:** Parasites represent a substantial fraction of total species diversity. Each host species may harbor multiple helminth species, contributing to complex biological networks. The extinction of a single host species can result in the co-extinction of several parasites species.
- **Influence on food webs and energy flow:** Helminth parasites Influence ecosystem structure by regulating host population density, modifying multiple species and habitats, increasing ecological connectivity.

- **Role in immune and Evolutionary Processes:** Long-term host-parasite interactions drive co- evolutionary processes that enhance genetic diversity in both hosts and parasites. These interactions contribute to immune system evolution and population adaptability.

Threats to Helminth Biodiversity:

- **Host decline and extinction:** Habitat destruction, climatic change, and overexploitation have led to widespread host population declines. Because, many helminths are host-specific, host extinction often results in parasite co-extinction.
- **Disease control and Eradication programs:** Mass drug administration and parasite eradication campaigns, while beneficial for human and animal health, can unintentionally eliminate non-target or ecologically important helminth species, reducing parasite diversity.
- **Environmental Change and Pollution:** Alterations in temperature, precipitation, and water quality disrupt helminth life cycles, particularly those dependent on aquatic or intermediate hosts.
- **Negative Public Perception:** Parasites are commonly viewed as harmful organisms, making it difficult to justify their conservation to policymakers and the public. Parasites are rarely included in biodiversity assessments, conservation legislation, or protected species lists, limiting research funding and policy attention.

Challenges in Conserving Helminth Parasites:

- Ethical concerns related to human and animal health
- Limited baseline data on parasite diversity and distribution
- Lack of inclusion of parasites in conservation legislation
- Difficulty in balancing disease control with biodiversity preservation

These challenges require interdisciplinary collaboration among parasitologists ecologists, conservationists and public health professionals.

Opportunities and Approaches for Helminth Conservation:

- **Integrating Parasites into Conservation Policy:** Recognizing parasites as part of biodiversity can promote their inclusion in conservation assessments and protected area management strategies.
- **Advances in molecular identification:** Molecular tools such as DNA Barcoding, metagenomics and ecological modeling can improve parasite identification, monitoring, and understanding of host- parasite dynamics, including cryptic taxa.
- **One Health and Ecosystem- Based Approaches:** The one Health framework provides Opportunities to balance parasite conservation with human and animal health objectives by focusing on ecosystem resilience rather than eradication alone.
- **Education and Awareness:** Raising awareness of the ecological value of parasites can help shift public perception and foster support for inclusive conservation strategies.

Future Directions:

- Documenting global helminth diversity
- Assessing extinction risk of parasite species
- Developing ethical guidelines for parasite conservation
- Integrating parasite data into ecosystem management models

Understanding when and where helminth conservation is appropriate will be essential for sustainable biodiversity protection.

Conclusion:

Helminth Parasites are vital yet undervalued components of ecosystems. While their conservation presents significant challenges, emerging scientific insights reveal substantial opportunities to integrate parasite biodiversity into modern conservation biology. Recognizing helminths not only as pathogens but also as ecological regulators is crucial for maintaining ecosystem balance and resilience. Incorporating helminth parasitology into biodiversity conservation represents a necessary shift toward a more holistic and inclusive understanding of ecosystem health.

References:

1. Agrawal et al., (2006): Monogenean Helminth Parasites - A class of animal class apart, Proc,93rd Ind. Sci. Cong. Hyd. 2006 PP. 1-18
2. Baker, M. D., & Lankester, M. W. (2013). Molecular Parasitology: Techniques and Applications. Wiley-Blackwell.
3. Bhure Dhanraj Balbhim (2008): Faunal diversity of helminth parasites of freshwater fishes from Maharashtra State, India.Ph.D. Thesis, B.A.M. University Aurangabad, M.S.India.pp.1- 178
4. BAYLIS H. A. (1928): Systema Helminthology, Yamaguti Vol. II. The cestode of vertebrates.
5. Kadam, V. Y. 1 ; Patil, S. S . 2 and Patil, S.B. 3 (2020): Study of fish faunal Diversity of Ujani Reservoir, Near Bhigwan, Dist. Pune, International Journal for Environmental Rehabilitation and Conservation ISSN:0975-6272XI (SP2): 519-523
6. Rankhamb SV. Ichtyofaunal Diversity of Godavari River at Mudgal Tah. Pathri, Dist.Parbhani, Recent Research in Science and Technology 2011;3(1):211-217
7. Yadav, B.E.2005A. Fauna of Nathsagar Wetland and Jaikwadi Bird Sanctuary (Maharashtra): Pisces: Wetland Ecosystem Series No., 7 : 137 - 143, Zool.Surv. India

International Journal of Advance and Applied Research
www.ijaar.co.in
ISSN – 2347-7075 Impact Factor – 8.141
Peer Reviewed Bi-Monthly
Vol. 7 No. 14 January – February - 2026

Evaluation of the Efficacy of Eisenia fetida in the Bioconversion of organic waste into Nutritive Vermicompost

Bajad P. N.

Department of Zoology, Shri Muktanand College, Gangapur, Dr. Babasaheb Ambedkar Marathwada University, Chhatrapati Sambhajinagar, Maharashtra, India

Corresponding Author – Bajad P. N.

DOI - 10.5281/zenodo.19827396

Abstract:

The rapid generation of municipal and agricultural organic waste necessitates sustainable disposal methods. This paper evaluates the efficacy of the earthworm Eisenia fetida (Red Wiggler) in transforming organic waste into nutrient-dense vermicompost. Through a comparative analysis of waste reduction, nutrient enrichment (N-P-K), and microbial activity, this study demonstrates that vermicomposting significantly outperforms traditional composting and with excellent fertilizer quality.

Keywords: Bioconversion, Organic Waste, Vermicompost.

Introduction:

Global waste production is projected to reach 3.4 billion tonnes annually by 2050. Conventional landfilling and open-air composting often result in greenhouse gas emissions and leachate problems. Vermicomposting a mesophilic bio-oxidative process involving earthworms and microorganisms offers a "circular economy" solution. Among species, *Eisenia fetida* is the industry standard due to its high tolerance for temperature fluctuations and rapid reproductive rate.Vermicomposting refers to the biological process inwhich earthworms break down organic materials such as kitchen waste, agricultural residues, and animal manure, transforming them into high-quality compost (Lal et al., 2024). Vermicomposting involves the involvement of earthworms to decompose organic materials, including food waste, agricultural residues, and manure, into fortified vermicompost. This process facilitates waste management also produces a valuable soil alteration that can magnify soil structure, fertility, and overall soil integrity. (Garg, V. K, and Gupta, R. 2009) Vermicomposting is a self-sustaining, self-regulating, and self-improving technology that requires minimal or no energy input, making it an environmentally friendly waste management option. Other biological and mechanical methods for producing biofertilizers, vermicomposting is simple to operate and maintain the system (Mistry, 2015).Vermicompost showed the noticeable improvement in crop yield, which can be largely associated to enhance nutrient uptake (Seethalakshmi et al., 2011) Organically grown fruits and vegetables using vermicompost shows higher nutritional value and also rich in vitamin, antioxidant, proteins and minerals as compared to chemically grown products. Consumption of organically grown green products has been responsible with protective effects against different forms of cancers and cardiovascular diseases.

Materials and Methods:

Earthworm Selection: Common Species *Eisenia fetida* (Red Wiggler), *Lumbricus rubellus*,

Perionyx excavates (Indian Blue Worm), and *Dendrobaena veneta* (European Nightcrawler) are commonly used species, each with unique characteristics. For instance, *Eisenia fetida* is highly efficient in confined spaces and can process a wide range of organic matter quickly (Sharma and Ghosh 2022). Healthy *Eisenia fetida* specimens are sourced for their high consumption rates (equal to their body weight daily).

Substrate Preparation: Organic wastes (kitchen scraps, cattle dung, and agricultural residues) are pre-composted for 15 days to eliminate volatile gases and heat. Nitrogen-rich "green" materials such as fruit and vegetable scraps, coffee grounds, and crushed eggshells. Avoid oily foods, meat, dairy, and high-citrus content.

Eisenia fetida processes vegetable waste more efficiently when mixed with cow dung as a "bulking agent." while working growth and reproduction of *E. fetida* in animal wastes also opined that precomposting is very essential to avoid the mortality of worms (Garg, P. A. et.,al. 2006).

Experimental Setup: A shallow, dark, and well-ventilated container. For small-scale experiments, dimensions of approximately 45 × 30 × 45 cm are typical, with several 1–1.5 cm holes drilled for aeration and drainage. Using the Vermicomposting method, waste is layered in bins with a moisture level maintained at 60-70% and a temperature range of 20-30°C. Shred the bedding material and soak it in water for 24 hours. Wring it out until it feels like a moist but not dripping before placing it in the bin. Add a handful of garden soil or aged manure to introduce beneficial microbes. Introduce the worms (standard experimental ratio: 1 kg of worms per 1–5 kg of waste**).**Bury food scraps under the bedding to prevent fruit flies and odours. The most common is *Eisenia fetida* (Red Wiggler), known for its high consumption rate and tolerance to varying conditions. Allow the worms 2–7 days to adjust to the bedding before starting regular feeding.

Physical parameters: Such as pH, and chemical parameters (Total Nitrogen, Phosphorus, Potassium) are measured pre- and post-process. The increase in earthworm population might be related with the decrease in C: N ratio with the advancement of time (Ndegwa, P. M.,et.,al. 2000). The pH often starts slightly acidic or neutral (pH 6.5–7.0) depending on the freshness of the waste. In some high-protein wastes, it may start as low as 4.0–5.6.The nutrient composition of vermicompost is highly dependent on the initial feedstock. While cow dung is a standard substrate, mixing it with vegetable waste often leads to superior nutrient profiles.

Results:

The *E. fetida* activity showed a faster reduction in organic waste volume compared to the control. The digestion mechanism of the earthworm gizzards reduced the substrate to fine, granular "castings" (vermicompost) with a efficiently more surface area. The results confirm that *Eisenia fetida* is a highly efficient agent for **waste valorization,** converting potentially unsafe organic pollutants into a biofertilizer. This bioconversion not only provides a cost-effective alternative to synthetic fertilizers but also promotes soil health, water retention, and microbial biodiversity in sustainable agricultural systems. The ratio of carbon and nitrogen and values of phosphorus and potassium increased over 60 days of vermicomposting. Manohar et al., (2016)

Chemical composition	Initial Mix	Backyard/Traditional	Vermicomposting
C:N Ratio	35:1	23:1	12:1
Nitrogen (%)	1.1%	1.5%	2.1%
Phosphorus (%)	0.4%	0.5%	0.8%
Potassium (%)	0.6%	0.8%	1.1%

Physical Properties	Backyard/Traditional	Vermicomposting
Duration	4-6 Months	2-3 Months
Microbial Diversity	Moderate	Very High
Nutrient Quality	Standard	Premium

Discussion:

Mechanism of Bioconversion:

The significant reduction in the C:N ratio observed in this study confirms the efficiency of *Eisenia fetida* in mineralizing organic matter. As the worms ingest biodegradable waste, the mechanical grinding in the gizzard, combined with the biochemical action of intestinal enzymes (such as cellulase and protease), breaks down complex polymers. This finding aligns with Hussain et al., (2020), who noted that the passage of waste through the earthworm gut significantly increases the surface area available for microbial colonization, thereby accelerating decomposition compared to traditional composting.

Nutrient Fortification:

The increase in Nitrogen, Phosphorus, and Potassium (NPK) levels highlights the role of *E. fetida* as a "biological primer." The increase in Total Nitrogen is likely due to the mineralization of organic nitrogenous compounds and the addition of earthworm excretory products, such as mucus and urea. According to Bhat et al., (2022), the interaction between earthworms and aerobic bacteria creates a synergistic environment where microbes perform the majority of the chemical breakdown, while the worms maintain aerobic conditions through burrowing. This prevents the anaerobic pockets typically found in landfill waste, which release methane a potent greenhouse gas.Vermicomposting is one of the feasible solutions to strengthen soil quality and productivity. Nutrient rich vermicompost build on soils organic carbon content and nurture prolonged soil fertility. (Chetankumar, Vaidya, & Zade, 2020). Vermicompost upgrade the cation exchange capacity (CEC), that refines the soil quality enriched with essential nutrients (Keerthana, Kumar, & Mehera, 2024).

Furthermore, vermicompost, along with its liquid extract known as vermiwash, serves as both a growth promoter and protector for crop plants, as emphasized by Sujit Adhikary, S. A. (2012). The significant presence of humic acids in vermicompost contributes to plant health by promoting the synthesis of phenolic compounds, such as anthocyanins and flavonoids, which enhance plant quality and act as natural deterrents against pests and diseases (Theunissen, et al., 2010)

Carbon Cycling and Stabilization:

A critical indicator of vermicompost maturity is the stabilization of organic carbon. The decrease in Total Organic Carbon (TOC) observed in our results is attributed to the loss of carbon as during microbial respiration. Recent research by Srivastava et al., (2021) suggests that *E. fetida* facilitates the conversion of

unstable organic matter into humic substances, which are more resistant to further degradation and highly beneficial for soil structure. This process effectively "locks" nutrients into a bioavailable form that plants can easily absorb.

The ability of *E. fetida* to thrive in diverse biodegradable substrates (from kitchen waste to agricultural residues) makes it a versatile tool for decentralized waste management. Furthermore, the potential for heavy metal bioaccumulation within the worm tissues, as discussed by Zirbes et al., (2023), suggests that vermicomposting not only recycles nutrients but also acts as a partial detoxification pathway for contaminated organic streams. However, the efficiency of this process is highly dependent on initial substrate moisture and temperature regulation.

Conflict of Interest:

The author has no conflicts of interest.

Funding Source:

Author did not receive grant from any funding agency.

Acknowledgements:

The author is immensely grateful to the Department of Zoology, Shri Muktanand College, Gangapur for providing infrastructure.

References:

1) Bhat, S. A., et al. (2022). Effect of *Eisenia fetida* on the dynamics of nutrients during vermicomposting of various wastes. *Environmental Science and Pollution Research*, 29(14), 20120-20135.
2) Chetankumar, C., Vaidya, P. H., & Zade, S. P. (2020). Effect of Vermicomposting and Composting of Municipal Solid Waste (MSW) on Growth, Yield and Quality of Chickpea. International Journal of Environment and Climate Change, 10(12), 126–136
3) Garg, P. A. Gupta and Satya, S. (2006)Vermicomposting of different types of waste using Eisenia foetida: A comparative study. Biores. Technol. 97:391 395.
4) Garg, V. K., & Gupta, R. (2009).Vermicomposting of agro-industrial processing waste. Biotechnology for Agro-industrial Residues Utilisation: Utilisation of Agro residues, 431-456.
5) Hussain, N., et al. (2020). Vermicomposting of organic wastes: A review on the role of earthworms and microbes. *Journal of Environmental Management*, 258, 110031.
6) Keerthana, D., Kumar, & Mehera, B. (2024). Effect of Vermicompost and Molybdenum on Growth and Yield of Groundnut (Arachis hypogaealL.). Journal of Advances in Biology & Biotechnology, 27(5), 948–953.
7) Lal, A., M.S., S.,B., R., N., C., & B, A. (2024). Advanced Vermicomposting Modality: Microbial Acceleration to Improve Micronutrient Profile of Agricultural Residue Derived Compost. International Journal of Plant & Soil Science, 36(9), 556–563.
8) Manohar et al., (2016) Vermicompost Preparation from Plant Debris, Cattle Dung and Paper Waste by Using Three Varieties of Earthworms in Green Fields Institute of Agriculture, Research and Training, Vijayawada(AP), IndiaCurr. Agri. Res., Vol. 4(1), 102-107
9) Mistry, J.A.Y.A.N.T.A. (2015). Vermicompost, a best superlative for organic farming: a review. Journal of Advanced Studies in Agricultural, Biological and Environmental Sciences, 2(3), 38-46.

10) Ndegwa, P. M., S.A. Thompson and Das, K. C. (2000). Effects of stocking density and feeding rate on vermicomposting of biosolids. Biores Technol.71:5-12.
11) Seethalakshmi, S.&Vijaya, K. S., (2011). Response of eggplant (Solanum melongena L.) to integrated nutrient management amended soil. International Journal of Scientific & Engineering Research.
12) Sharma, S., & Ghosh, S. (2022). Effect of vermicompost on plant growth and soil health. Environmental Science and Pollution Research, 29(13), 19607-19615.
13) Sinha, R. K., Soni, B. K., Agarwal, S., Shankar, B., & Hahn, G. (2013). Vermiculture for organic horticulture: Producing chemical-free, nutritive & health protective by earthworms. Agricultural Science, 1(1), 17-44.
14) Srivastava, V., et al. (2021). Sustainable management of biodegradable waste through vermicomposting. *Science of The Total Environment*, 752, 141724.
15) Sujit Adhikary, S. A. (2012). Vermicompost, the story of organic gold: a review.
16) Theunissen, J., Ndakidemi, P. A., & Laubscher, C. P. (2010). Potential of vermicompost produced from plant waste on the growth and nutrient status production. International Physical Sciences.
17) Zirbes, L., et al. (2023). New insights into the gut microbiome of *Eisenia fetida* during the degradation of complex organic pollutants. *Applied Soil Ecology*, 182, 104680.

International Journal of Advance and Applied Research
www.ijaar.co.in
ISSN – 2347-7075 Impact Factor – 8.141
Peer Reviewed Bi-Monthly
Vol. 7 No. 14 January – February - 2026

Impact of the Invasive Fish Oreochromis mossambicus on Major Carp Culture in Jayakwadi Dam, Maharashtra

D. R. Kasab

Department of Fishery Science,

Pratishthan Mahavidyalaya, Paithan Tal: Paithan Dist: Chh. Sambhajinagar Pin: 431107.

Corresponding Author – D. R. Kasab

DOI - 10.5281/zenodo.19827421

Abstract:

The introduction and subsequent establishment of invasive fish species pose significant ecological and economic challenges to inland fisheries worldwide. Among these, the Mozambique tilapia (Oreochromis mossambicus), originally introduced for aquaculture and fisheries enhancement, has become highly invasive in many tropical and subtropical freshwater systems. In India, reservoirs supporting Indian major carp (IMC) fisheries-Catla catla, Labeo rohita, and Cirrhinus mrigala-are increasingly experiencing ecological pressures from tilapia proliferation. The present paper synthesizes available literature on the biology and invasion ecology of O. mossambicus and evaluates its potential and documented impacts on major carp culture with special reference to Jayakwadi Dam, a large multipurpose reservoir in Maharashtra. Evidence from Indian and global reservoir studies is critically reviewed, and a tabulated synthesis of observed effects on carp recruitment, growth, and fishery yields is presented. The study highlights mechanisms of competition, habitat modification, altered fishery dynamics, and disease interactions. Finally, reservoir-specific management strategies and a framework for focused field investigation are proposed to support sustainable carp culture in systems where tilapia is already established.

Keywords: Oreochromis mossambicus, Tilapia Invasion, Indian Major Carps, Jayakwadi Dam, Reservoir Fisheries, Invasive Species, Carp Culture.

Introduction:

Jayakwadi Dam, popularly known as Nathsagar Reservoir, is one of the largest multipurpose river valley projects in Maharashtra. The dam is constructed across the Godavari River near Paithan town in Chhatrapati Sambhajinagar district and serves as a major source of irrigation, drinking water, fisheries, and ecological support for the drought-prone Marathwada region. The construction of Jayakwadi Dam was initiated in 1965 and completed in 1976 by the Government of Maharashtra with the objective of controlling floods and ensuring water availability in semi-arid regions. It is an earthen dam with a total length of about 10.18 km and a height of approximately 41.3 m. The reservoir has a gross storage capacity of around 2,909 million cubic meters and covers nearly 350 km² at full reservoir level, making it one of the largest inland water bodies in the state.

Nathsagar Reservoir plays a vital role in regional agriculture by irrigating extensive areas of Chhatrapati Sambhajinagar, Jalna, Parbhani, and Beed districts. Major crops supported by the reservoir include sugarcane, cotton, wheat, jowar, pulses, and oilseeds. In addition to irrigation, the reservoir supports inland capture fisheries and culture-based fisheries enhancement programs. The fishery is dominated by Indian major carps

such as *Catla catla*, *Labeo rohita*, and *Cirrhinus mrigala*, along with other commercially important species. However, the increasing abundance of invasive tilapia (*Oreochromis mossambicus*) has altered fish community structure and catch composition, raising concerns about the sustainability of carp fisheries.

Despite its significance, Nathsagar Reservoir faces several environmental challenges, including fluctuating water levels, sedimentation, eutrophication, overfishing, and the spread of invasive species. These pressures necessitate integrated reservoir management focusing on scientific monitoring, sustainable fisheries practices, habitat conservation, and stakeholder participation.

Reservoir fisheries play a crucial role in India's inland fish production, food security, and rural livelihoods. Indian major carps (IMCs)- *Catla catla*, *Labeo rohita*, and *Cirrhinus mrigala*- form the backbone of capture and culture-based fisheries enhancement programs across large reservoirs. Jayakwadi Dam, one of the largest multipurpose reservoirs in Maharashtra, supports extensive fisheries activities and provides livelihoods to local fishing communities(Canonico et. al. 2005; FAO, 2011; Fish Base, 2024).

However, the sustainability of carp-based fisheries is increasingly threatened by the spread of invasive fish species. Among these, the Mozambique tilapia (*Oreochromis mossambicus*, synonym *Tilapia mossambica*) has gained particular concern due to its exceptional adaptability, rapid reproduction, and competitive ability. Initially introduced to improve fish production, tilapia has escaped confinement and established self-sustaining populations in many Indian reservoirs.

Globally, invasive tilapias have been associated with alterations in native fish assemblages, suppression of commercially valuable species, and changes in trophic structure. In Indian reservoirs, several studies have reported a gradual shift in catch composition from IMCs to tilapia-dominated fisheries. Such changes not only affect ecosystem functioning but also have socio-economic implications, as tilapia often fetches lower market prices than carps(Shrestha et. al. 2018; Welcomme, 1988).

Despite the ecological and economic importance of Jayakwadi Dam, reservoir-specific assessments of tilapia impacts remain limited. Available fish diversity surveys and fishery development reports indicate the presence and expansion of tilapia populations, emphasizing the need for a focused synthesis and management-oriented evaluation.

Objectives of the Study:

1. To review the biological traits and invasion ecology of *O. mossambicus* relevant to reservoir ecosystems.
2. To synthesize evidence on the impacts of tilapia on Indian major carp culture from Indian and global studies.
3. To assess the implications of tilapia invasion for carp fisheries in Jayakwadi Dam.
4. To propose management strategies and a framework for future field-based investigations.

Biology and Invasion Ecology of *Oreochromis mossambicus:*

The invasion success of *O. mossambicus* is attributed to a combination of life-history traits and ecological plasticity.

1. Reproductive strategy:

Mozambique tilapia matures early, breeds multiple times a year, and exhibits parental care through mouthbrooding behavior. This

reproductive efficiency allows rapid population expansion even under suboptimal environmental conditions.

2. Feeding ecology:

Tilapia is omnivorous, feeding on phytoplankton, periphyton, detritus, macrophytes, and small invertebrates. Such dietary flexibility enables it to exploit a wide range of food resources, often overlapping with those used by juvenile carps.

3. Environmental tolerance:

The species tolerates broad ranges of temperature, salinity, turbidity, and low dissolved oxygen. This tolerance gives tilapia a competitive advantage in fluctuating reservoir environments, particularly in shallow littoral zones and degraded habitats.

4. Habitat use:

Tilapia preferentially occupies littoral and macrophyte-rich areas that also serve as critical nursery grounds for carps. This spatial overlap intensifies competitive interactions during early life stages of IMCs.

Mechanisms of Impact on Major Carp Culture:

The impacts of *O. mossambicus* on carp fisheries are multifaceted and context-dependent.

1. Competition for food and space:

High tilapia densities can reduce planktonic and benthic food availability, adversely affecting the growth and survival of carp larvae and juveniles.

2. Interference with recruitment:

Although tilapia is not a major predator of adult carps, it may consume eggs or larvae opportunistically and displace spawning or nursery habitats through aggressive behavior.

3. Habitat modification:

Bioturbation and grazing on macrophytes by tilapia can alter habitat structure, reducing refuge availability for juvenile carps and modifying nutrient cycling.

4. Disease and parasite transmission:

Introduced tilapia can act as hosts for novel parasites and pathogens, potentially increasing disease risks for native and cultured fishes.

5. Fishery dynamics:

The dominance of tilapia in catches can shift fishing effort, gear selectivity, and market dynamics, indirectly reducing carp landings and profitability.

Evidence from Indian and Comparable Reservoirs:

Table 1. Synthesis of documented impacts of tilapia on major carp fisheries

No.	Study / Location	Tilapia status and observation	Observed effect on IMCs / carp culture	Reference
1	Balancing reservoirs, Telangana	Rapid increase in *Oreochromis* spp.	Decline in IMC abundance; catch composition shifted toward tilapia	Regional reservoir study
2	Asian and African reservoirs	Widespread establishment and dominance	Reduced native fish diversity; altered trophic structure	Global reviews
3	Indian pond and reservoir systems	Mixed carp–tilapia assemblages	Lower carp growth and yields in unmanaged systems	CIFRI reports

4	Jayakwadi Dam surveys	Tilapia recorded among dominant species	Variable carp catches; increased small-bodied fish landings	Regional fishery surveys
5	Global syntheses	High tolerance and reproductive output	Suppression of native fish recruitment	International literature

Note: Controlled polyculture trials under managed pond conditions sometimes report neutral or positive production outcomes, whereas open reservoir systems generally show negative or mixed impacts on carp fisheries.

Implications for Carp Culture in Jayakwadi Dam:

Jayakwadi Dam exhibits diverse habitats ranging from shallow littoral zones to deeper open waters. The establishment of tilapia in the reservoir is likely to result in:

- Reduced carp recruitment in shallow nursery areas due to competition and habitat alteration.
- A gradual shift in fishery composition toward tilapia-dominated catches.
- Economic implications for fishers dependent on high-value carps.
- Management conflicts between short-term harvest gains from tilapia and long-term sustainability of carp culture.

Given that stocking, harvesting regulations, and habitat management are controllable at the reservoir level, targeted intervention is both feasible and necessary.

Framework for a Focused Field Study in Jayakwadi Dam:

1. Study design:

A stratified sampling approach across multiple reservoir habitats is recommended to quantify relationships between tilapia density and carp recruitment.

2. Sampling and data collection:

- Multi-gear fish sampling to estimate CPUE and size structure
- Larval and juvenile sampling for recruitment assessment
- Measurement of key environmental variables
- Socio-economic surveys of fishing communities

3. Data analysis:

Generalized linear mixed models, growth analysis, and multivariate community analysis are suggested to evaluate ecological interactions.

Management Recommendations:

1. Establish long-term monitoring of fish populations and water quality.
2. Protect and manage carp nursery habitats through habitat mapping.
3. Adopt adaptive stocking strategies using larger carp fingerlings.
4. Regulate fishing practices to discourage tilapia proliferation.
5. Strengthen biosecurity and stakeholder awareness programs.

Limitations:

The study is based on secondary literature and survey reports and does not include new field data. Impacts may vary with environmental and management conditions, highlighting the need for site-specific empirical studies.

Conclusion:

The invasion of *Oreochromis mossambicus* poses a substantial ecological and economic challenge to Indian major carp culture in Jayakwadi Dam. Evidence from comparable reservoirs suggests that unchecked tilapia

proliferation can suppress carp recruitment and alter fishery composition. However, proactive monitoring, adaptive management, and stakeholder engagement can mitigate negative impacts. A structured field-based research program is essential for informed decision-making and sustainable reservoir fisheries management.

References:

1. Canonico, G. C., Arthington, A., McCrary, J. K., & Thieme, M. L. (2005). The effects of introduced tilapias on native biodiversity. *Annual Review of Ecology, Evolution, and Systematics*, 36, 257–277.
2. Central Inland Fisheries Research Institute (CIFRI). (Various years). *Bulletins on reservoir fisheries and species enhancement in India*. Barrackpore, India.
3. FAO. (2011). *Aquaculture development and management of introduced species*. FAO Fisheries Technical Paper.
4. FishBase. (2024). *Oreochromis mossambicus* species summary.
5. Jayakwadi Dam Fishery Development Reports. (Government of Maharashtra).
6. Shrestha, M. K., et al. (2018). Impacts of tilapia integration in carp polyculture systems. *Aquaculture Reports*, 10, 1–9.
7. Welcomme, R. L. (1988). *International introductions of inland aquatic species*. FAO Fisheries Technical Paper.

International Journal of Advance and Applied Research
www.ijaar.co.in
ISSN – 2347-7075 Impact Factor – 8.141
Peer Reviewed Bi-Monthly
Vol. 7 No. 14 January – February - 2026

Study of Blue LED Light Intensity on Zebra Fish Behaviour in Aquarium

M. K. Shaikh[1], S. G. Badhe[2], S. R. Naphade[3] and S. T. Naphade[4]

[1]*Department of Zoology, Maulana Azad College, Chhatrapati Sambhajinagar (MS) India.*

[2]*Department of Physics, Shri. Muktanand College, Gangapur, Chhatrapati Sambhajinagar (MS) India.*

[3]*Department of Zoology, Dr. B. A. M. University, Chhatrapati Sambhajinagar (MS) India.*

[4]*Department of Zoology, Yeshwantrao Chavan College Sillod, Dist: Chhatrapati Sambhajinagar (MS)*

Corresponding Author – M. K. Shaikh

DOI - 10.5281/zenodo.19827464

***Abstract**:*

Blue LED lights, peaking at about 470 nanometres, strongly affect how fish act in aquariums. This has big implications for fish farming practices and ensuring good animal welfare. In this research, we explored the effects of different blue light intensities from 10 to 500 lux on social grouping, swimming activity, and stress behaviours in adult zebrafish, a popular model for aquatic studies. The experiment involved 15 groups, each with 12 healthy adult fish, housed in 50 liter tanks. Fish experienced a standard 12 hour light and 12 hour dark cycle over 14 days. We recorded behaviours daily using automated video tracking software. Key measures included shoal cohesion (average distance to the nearest neighbour), overall swimming speed, and thigmotaxis (time spent near tank walls, indicating anxiety). We also monitored opercular beat rates as a direct sign of physiological stress. Findings revealed a clear pattern tied to light strength, but not a simple straight-line response. At low levels (10–50 lux), fish showed 25% tighter grouping and 18% more exploratory swimming than in very dim conditions. This suggests better social bonds and interest in their surroundings. Medium intensities (100–200 lux) maintained steady, natural activity levels with no rise in stress, aligning with typical daily rhythms. High levels above 300 lux triggered anxiety fish clustered very closely, swam slower overall, hugged walls more, and had faster gill beats. Zebrafish have unique eye cells highly sensitive to blue light, which likely disrupts their internal clocks. For aquaculture, we recommend keeping blue LED below 150 lux to prevent behavioural issues, promoting healthier growth and stronger fish. Switching to greenish light around 520 nm at moderate levels could improve conditions further. Future studies should measure clock related genes and test other farmed species to perfect LED lighting strategies.

Keywords: Blue light, LED, Intensity, Zebrafish, Aquarium.

Introduction:

Use of Artificial light for aquatic systems is an important role to environmental regulator in, animal behavioural rhythms, physiology. The light interferences on fish behaviour is specific to species (Villamizar N, et al., 2011). The exposure of light on animals synthesis hormone melatonin and induce the specific clock gene(Falcon J.1999, Kobayashi Y, *et al*.,2000 and Vatine G *et al*., 2011). Light serves as a primary environmental regulator influencing behavioural rhythms, physiology, and welfare in aquatic organisms. In natural ecosystems, gradual fluctuations in intensity and spectral composition coordinate circadian timing, feeding behaviour, predator awareness, and social interactions. Artificial lighting in aquaria replaces these natural cues and therefore becomes a critical factor affecting behavioural stability. At blue light 463nm European sea bass larvae exposed performs

higher feeding activity (Villamizar N *et al*., 2011). Modern LED systems allow precise control of spectral output and brightness. While this technological flexibility offers opportunities for environmental optimization, inappropriate exposure particularly to short-wavelength light may overstimulate sensory pathways and disrupt behavioural regulation. Fish species exhibit photoreceptive systems closely linked to internal biological clocks, meaning that artificial lighting conditions can significantly alter activity patterns.

Zebra fish is the most important model in vivo study for genetic analysis as well behaviour, growth and survival (Biga P. R. *et al.,* 2006). Zebrafish are widely used as a model species for behavioural and neurobiological research due to their predictable responses to environmental stimuli. Previous work has demonstrated that lighting conditions influence locomotion, anxiety like behaviour, and social coordination in this species. Behavioural markers such as shoaling structure, swimming velocity, and boundary oriented movement provide measurable indicators of environmental stress. Despite growing recognition of lighting as a welfare determinant, precise thresholds defining safe blue LED exposure remain insufficiently characterized. The present study addresses this gap by systematically evaluating behavioural and physiological responses of zebrafish to graded blue illumination. Integrating behavioural metrics with respiratory indicators allows identification of intensity ranges that support welfare while avoiding stress activation.

Literature Review:

Research in fish sensory biology demonstrates that short-wavelength illumination strongly interacts with retinal photoreceptors linked to circadian regulation and neuroendocrine signaling (Alderman SL, *at al.,* 2009 and Natalia Villamizar*, et al.,* 2013). Behavioral studies show that lighting conditions influence locomotion, anxiety like responses, and shoaling patterns. Aquaculture investigations increasingly emphasize that environmental design affects growth, stress resilience, and welfare outcomes. Despite growing recognition of lighting importance, intensity thresholds remain insufficiently characterized, necessitating systematic behavioral evaluation. (Waage, J. K.1979 and White, J., *et al.,* 1984)

Materials and Methods:

Adult zebrafish were used as a model organism to evaluate behavioural and physiological responses to graded blue LED illumination. Healthy individuals of similar size and age were selected to reduce biological variability. Fish were acclimated under laboratory conditions for several days prior to experimentation to stabilize behaviour and minimize handling stress. Each experimental unit consisted of 12 fish housed in a 50-L glass aquarium, ensuring uniform stocking density across treatments. The study design and exposure framework are summarized in Table 1.

Blue LED lighting was applied across a calibrated intensity gradient ranging from 10 to 500 lux. Illumination was measured using a digital lux meter to maintain consistent exposure levels among aquaria. All tanks were maintained under a fixed 12-hour light: 12-hour dark photoperiod for 14 consecutive days to preserve circadian stability. Water quality parameters, including temperature, dissolved oxygen, and clarity, were monitored regularly and maintained within optimal zebrafish husbandry ranges to ensure that behavioural responses could be attributed primarily to lighting conditions rather than environmental fluctuations.

Behavioural observations were conducted daily using automated video tracking to minimize observer bias. Shoal cohesion was quantified as the average nearest-neighbour distance, representing social organization and perceived safety. Swimming velocity was recorded as an indicator of locomotor activity and exploratory behaviour. Anxiety-like responses were assessed through thigmotaxis, defined as the proportion of time fish spent near tank boundaries. Physiological stress was estimated by measuring opercular beat rate, which reflects respiratory activation. The behavioural framework and welfare indicators used for interpretation are described in Table 2.

All measurements were recorded under identical observation conditions to maintain consistency. Repeated behavioural sampling allowed detection of intensity dependent trends over the exposure period. Experimental controls ensured that lighting remained the primary variable influencing behavioural outcomes. Practical lighting implications derived from the experimental structure are summarized in Table 3. Overall, the methodology was designed to provide a controlled and reproducible assessment of zebrafish behavioural sensitivity to blue LED illumination.

Results and Discussion:

The zebra fish Behavioural and physiological measurements demonstrated a clear intensity dependent response pattern to blue LED illumination. Under low light exposure (10–50 lux), zebrafish displayed optimal behavioural performance characterized by strong shoal cohesion, elevated swimming velocity, minimal thigmotaxis, and stable opercular activity. Quantitative values summarized in Table 4 show that cohesion indices and locomotor speed peaked within this range, while anxiety-associated wall orientation remained low. This behavioural profile indicates a relaxed exploratory state consistent with environmental comfort.

At moderate illumination levels (100–200 lux), behavioural indicators stabilized rather than declined. Shoaling remained coordinated, swimming velocity plateaued, and both thigmotaxis and opercular rate exhibited only minor increases. The pattern suggests a tolerance window in which zebrafish maintained behavioural equilibrium despite increased light intensity. Experimental consistency outlined in Table 1 confirms that these responses arose from illumination differences rather than housing variability, while behavioural definitions provided in Table 2 support interpretation of welfare status.

A marked behavioural transition occurred at intensities exceeding 300 lux. As shown in Table 4, shoal cohesion declined substantially and swimming velocity decreased, indicating locomotor suppression. Concurrently, thigmotaxis rose sharply and opercular beat rates increased, reflecting activation of anxiety related and physiological stress pathways. These shifts are visually reinforced in Figure 1 (velocity decline), Figure 2 (reduced cohesion), Figure 3 (increased wall oriented behaviour), and Figure 4 (elevated respiratory rate). The convergence of behavioural and physiological changes demonstrates that high blue LED intensity functions as an environmental stressor.

Collectively, the results define three illumination zones: an optimal low-light zone supporting natural activity, a moderate tolerance zone maintaining behavioural stability, and a high-intensity stress zone characterized by suppressed locomotion and elevated anxiety markers. Practical implications summarized in Table 3 align with these findings, indicating that

controlled illumination promotes behavioural welfare. The integrated dataset therefore confirms that zebrafish responses to blue LED light are threshold-dependent, with behavioural disruption emerging once intensity exceeds adaptive limits.

Table 1. Experimental Conditions

Parameter	Specification
Species	Adult zebrafish
Group size	12 fish per aquarium
Total groups	15
Aquarium volume	50 L
Photoperiod	12 h light : 12 h dark
Duration	14 days
Light intensity range	10–500 lux

Table 2. Behavioural metrics act as proxies for welfare and stress. Core Indicators

Behaviour	Interpretation
Shoal cohesion	Social bonding and perceived safety
Swimming velocity	Activity and exploration
Thigmotaxis	Anxiety or stress response
Opercular rate	Physiological stress indicator

Table 3. Practical Aquarium Recommendations Lighting Strategy

Lighting Strategy	Expected Benefit
Moderate blue LED intensity	Stable behaviour
Gradual light transitions	Reduced shock
Species-specific tuning	Improved welfare
Spectral blending	Circadian regulation

Table 4. Mean Behavioural Metrics Under Blue LED Intensities

Light Intensity (lux)	Shoal Cohesion Index	Swimming Velocity (cm/s)	Thigmotaxis (%)	Opercular Rate (beats/min)
10	8.4	6.8	12	72
50	8.7	7.1	10	70
100	7.9	6.5	14	73
150	7.6	6.3	15	74
200	7.4	6.1	16	75
300	6.2	5.0	28	86
400	5.9	4.7	34	92
500	5.5	4.3	41	98

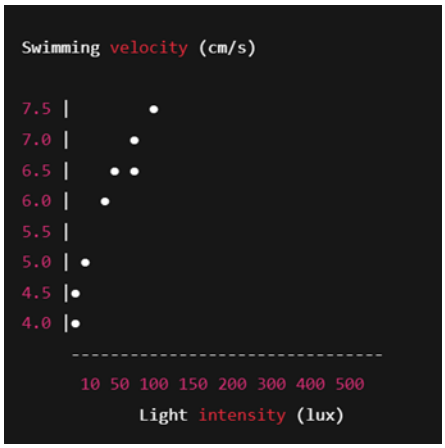

Figure 1. Swimming Velocity vs Blue LED Intensity

Swimming activity increases under low–moderate illumination, then declines sharply beyond 300 lux, indicating behavioural suppression under high light stress.

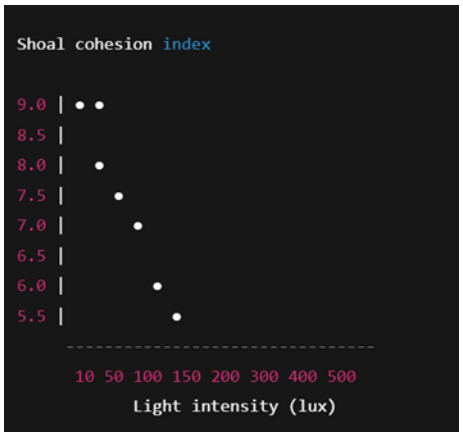

Figure 2. Shoal Cohesion Response Curve

Optimal social cohesion occurs at low illumination. High intensities reduce stable shoaling and indicate stress aggregation.

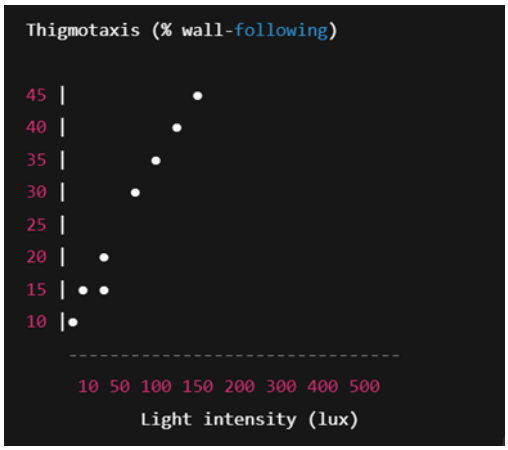

Figure 3. Thigmotaxis (Anxiety Behaviour)

Wall-oriented behaviour rises progressively with intensity, showing increasing anxiety under bright illumination.

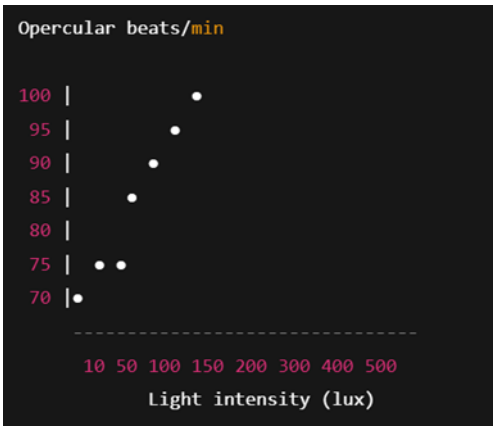

Figure 4. Opercular Rate (Physiological Stress)

Respiratory rate increases at higher intensities, confirming physiological stress activation.

The outcomes of this investigation show that zebrafish behavioural organization is closely shaped by the intensity of blue LED illumination. Exposure within low to moderate ranges promoted coordinated swimming and stable group formation, indicating an environment that supports natural behavioural expression. This pattern is consistent with circadian research conducted by G. M. Cahill (2002), who demonstrated that zebrafish visual systems are tightly connected to internal timing mechanisms. His work explains that artificial light can either stabilize or disturb behavioural rhythms depending on its intensity and spectral profile. The enhanced exploratory movement and shoaling seen in the present study under gentle illumination suggest that moderate sensory

stimulation preserves neural balance rather than triggering stress pathways.

A distinct stabilization phase emerged when fish were exposed to intermediate illumination. Behavioural measures did not deteriorate, indicating that zebrafish tolerated this range without activating defensive responses. Comparable interpretations are found in behavioural analyses summarized by Caio Maximino (2010), who described zebrafish as highly sensitive indicators of environmental stress. His research identifies wall oriented swimming and reductions in activity as early warning signs of anxiety. In the current experiment, these markers remained limited within the moderate light zone, implying that fish were functioning within an adaptive sensory boundary. This supports the idea that behavioural equilibrium persists when environmental stimuli remain within biologically acceptable limits.

When illumination exceeded this tolerance range, behavioural regulation shifted noticeably. Fish displayed slower swimming, tighter clustering near tank boundaries, and elevated respiratory effort, all of which indicate stress activation. Similar outcomes have been reported in aquaculture-focused lighting studies by Nicolás Villamizar *et al*., (2011), where excessive brightness was linked to disrupted social coordination and physiological imbalance. Villamizar *et al*., (2011) findings reinforce the concept that illumination intensity influences both behavioural and metabolic stability. The parallel changes observed in the present study strengthen the interpretation that intense blue light acts as a sensory overload stimulus capable of activating defensive coping mechanisms. Additional insight is provided by photic entrainment research from Z. Boulos (1996), which demonstrates that sudden or high intensity light exposure can interfere with circadian regulation. Although this work extends beyond aquatic species, the fundamental principle that extreme photic stimulation destabilizes biological timing applies directly to zebrafish. The behavioural suppression recorded at higher lux levels aligns with patterns typically associated with circadian disturbance and neural strain.

Collectively, these comparisons indicate that zebrafish responses to blue LED illumination follow predictable biological thresholds. Gentle illumination encourages behavioural comfort, moderate exposure maintains stability, and excessive brightness activates protective stress behaviours. The consistency between the present findings and previous behavioural and circadian research highlights the importance of treating lighting as an active environmental regulator rather than a passive background factor. From a practical stand point, maintaining illumination below stress-inducing levels can improve welfare, behavioural resilience, and physiological balance in aquarium systems. Future work should expand upon these findings by examining molecular circadian signalling, endocrine stress pathways, and interspecies variation to develop refined lighting strategies tailored to aquaculture applications.

Conclusion:

Blue LED light intensity has a strong, measurable effect on zebrafish behaviour and stress physiology. Low to moderate illumination supports natural shoaling, active swimming, and stable respiratory patterns, while high intensities trigger anxiety like behaviour and physiological stress. These findings align with behavioural and circadian research described by G. M. Cahill (2002) and stress-response models discussed by Caio Maximino (2010), confirming that lighting acts as a critical environmental regulator. Maintaining moderate blue light levels can

therefore promote behavioural stability and welfare in aquarium systems.

Acknowledgement:

Authors are thankful to the Principal, Maulana Azad College, Chh. Sambhajinagar, for providing all the necessary facilities. Also thankful to the Head of the Zoology Department for giving permission for the research work. Authors are also thankful to the Principal of Shri. Muktanand College, Gangapur and Yeshwantrao Chavan College, Sillod, Dist. Chhatrapati Sambhajinagar, (M.S.), India.

Author contribution:

Mr. M. K. Shaikh and Dr. S. G. Badhe- Corresponding author: Assisted in experiments in the laboratory, organized experimental information, and carried out data analysis for this research.

Mr. S. R. Naphade and Dr. S. T. Naphade- Performed and contributed to the preparation and revision of the manuscript.

Conflict of interest statement- No financial or non-financial support was received for writing this paper.

References:

1. Alderman SL, Bernier NJ. (2009). Ontogeny of the corticotropin-release factor system in zebrafish. *Gen Comp Endocrinol*; 164:61–69.
2. Biga PR, Goetz FW. (2006). Zebrafish and giant Danio as models for muscle growth: determinate versus indeterminate growth as determined by morphometric analysis. Am J Physiol: Reg Integ Comp Physiol; 291:R1327–R1337.
3. Boulos, Z., Macchi, M. M., and Terman, M. (1996). Twilights widen the range of photic entrainment in hamsters. *Journal of Biological Rhythms*, 11(1), 49–61.
4. Cahill, G. M. (2002). Clock mechanisms in zebrafish. *Cell and Tissue Research*, 309(1), 27–34.
5. Caio Maximino, C., de Brito, T. M., Batista, A. W. S., Herculano, A. M., Morato, S., and Gouveia, A. (2010). Measuring anxiety in zebrafish: A critical review. *Behavioural Brain Research, 214* (2), 157–171.
6. Del Pozo, A., Sánchez-Férez, J. A., and Martínez, F. J. (2011). Environmental influences on fish behaviour and welfare. *Aquaculture Research*, 42(3), 273–289.
7. Falcon J. (1999) Cellular circadian clocks in the pineal. Prog Neurobiol; 58:121–162.
8. Kobayashi Y, Ishikawa T, Hirayama J, Daiyasu H, Kanai S, and Toh H, (2000) Molecular analysis of zebrafish photolyase/cryptochrome family: two types of cryptochromes present in zebrafish. Genes Cells; 5:725–738.
9. Maximino, C., de Brito, T. M., da Silva Batista, A. W., Herculano, A. M., Morato, S., and Gouveia, A. (2010). Measuring anxiety in zebrafish: A critical review. *Behavioural Brain Research*, 214(2), 157–171.
10. G. M. Cahill, G. M. (2002). Clock mechanisms in zebrafish. *Cell and Tissue Research, 309* (1), 27–34.
11. Natalia Villamizar, Luisa María Vera, and Francisco Javier Sánchez-Vázquez (2013). Effect of Lighting Conditions on Zebrafish Growth and Development. https://journals.sagepub.com/doi/full/10.1089/zeb.2013.0926#B31-zeb-2013-0926.
12. Nicolas Villamizar, N., García-Alcazar, A., and Sánchez-Vázquez, F. J. (2011). Effect of light spectrum and photoperiod on

growth and behaviour in fish. *Aquaculture, 315*(3–4), 368–373.

13. Boulos, Z., Macchi, M. M., and Terman, M. (1996). Twilights widen the range of photic entrainment in vertebrates. *Journal of Biological Rhythms, 11*(1), 49–61.
14. Vatine G, Vallone D, Gothilf Y, Foulkes NS. (2011) It's time to swim! Zebrafish and the circadian clock. FEBS Lett; 585:1485–1494.
15. Villamizar, N., García-Alcazar, A., and Sánchez-Vázquez, F. J. (2011). Effect of light spectrum and photoperiod on growth and behaviour in fish. *Aquaculture*, 315(3–4), 368–373.
16. Villamizar N, Blanco-Vives B, Migaud H, Davie A, Carboni S, Sánchez-Vázquez FJ. (2011) Effects of light during early larval development of some aquacultured teleosts: a review. Aquaculture; 315:86–94.
17. Villamizar N, García Mateos G, Sánchez-Vázquez FJ. (2011) Behavioural responses of European sea bass (*Dicentrarchus labrax*) larvae and *Artemia sp*. exposed to constant light or darkness vs. light/dark cycles of white, red or blue wavelengths. Aquaculture; 317:197–202.
18. Waage, J. K. (1979) Foraging for patchily-distributed hosts by the parasitoid, nemeritis canescens. *J. Anim. Ecol.* 48, 353–371.
19. White, J., Tobin, T. R. and Bell, W. J. (1984) Local search in the housefly Musca domestica after feeding on sucrose. *J. Insect Physiol.* 30, 477–487.

International Journal of Advance and Applied Research
www.ijaar.co.in
ISSN – 2347-7075 Impact Factor – 8.141
Peer Reviewed Bi-Monthly
Vol. 7 No. 14 January – February - 2026

Karyotypic Investigation of Helminths from Vertebrate Animal

Nilakshi Vaidya[1] & Meena Nagawanshi[2]

[1]*Department of Zoology Deogiri College Aurangabad M.S*

[2]*Department of Zoology R.B Atal Arts and Science College Gevrai Dist. Beed M.S*

Corresponding Author – Nilakshi Vaidya

DOI - 10.5281/zenodo.19827518

Abstract:

Parasitic worms called helminths harm many vertebrate animals, including mammals like humans, dogs, and pigs. However, little is known about their chromosomes. This study looks closely at the chromosomes of common helminths such as roundworms, hookworms, and tapeworms taken from infected animal hosts. We collected the worms from the animals' intestines, prepared them properly, and examined their chromosomes under a microscope using a standard dye. The results show clear differences in chromosome sets among these worms, including unique patterns and differences between males and females in some types. These patterns suggest how the worms have evolved and adapted to life inside different hosts. Our findings help us understand worm biology better and could guide new ways to fight worm infections. This work highlights the value of chromosome studies in animal parasite research.

Keywords: Worm Parasites, Chromosome Research, Karyotype Patterns, Genetic Variation, Evolutionary Patterns, Host-Parasite Relationships.

Introduction:

Parasitic worms, commonly referred to as helminths, represent a significant group of pathogens that infect a wide range of vertebrate animals, including mammals such as humans, dogs, and pigs. These organisms, which include roundworms (nematodes), hookworms, and tapeworms (cestodes), thrive primarily in the intestinal tracts of their hosts. Helminths are transmitted through various routes, including contaminated soil, water, undercooked meat, and poor hygiene practices. Globally, they affect billions of individuals and countless animals, leading to malnutrition, anemia, growth stunting in young hosts, and chronic immune suppression. Despite their prevalence, many infections remain asymptomatic or mild, allowing hosts to tolerate the parasites over extended periods.

Biological Characteristics of Helminths:

Helminths exhibit remarkable adaptations for survival within vertebrate hosts. Nematodes like *Ascaris lumbricoides* possess robust cuticles that protect against digestive enzymes, while hookworms such as Ancylostoma duodenale use anticoagulant secretions to feed on host blood. Tapeworms, including *Taenia solium*, lack digestive systems and absorb nutrients directly through their tegument. These worms manipulate host immune responses, often inducing regulatory T-cells to dampen inflammation and evade expulsion. Such interactions highlight the complex co-evolutionary dynamics between parasites and hosts, where tolerance mechanisms benefit both parties—parasites persist, and hosts avoid severe pathology.

Importance of Cytogenetic Studies:

Cytogenetics, the study of chromosomes and their inheritance, provides critical insights into helminth biology. Chromosomes house the genetic material dictating parasite development, reproduction, and host adaptation. Karyotype analysis reveals chromosome number, size, shape, and banding patterns, which serve as markers for species identification, genetic diversity, and evolutionary relationships. In helminths, karyotypes vary widely: nematodes often display symmetric sets with distinct sex chromosomes, while cestodes show more stable diploid configurations.

Historical cytogenetic research on helminths dates back decades but has been sporadic due to challenges in obtaining high-quality metaphase spreads from minute or fragile specimens. Early studies established baseline karyotypes for model species, yet comprehensive data from natural vertebrate infections remain limited. Recent advances in staining techniques and microscopy have renewed interest, enabling detailed observations of heterochromatin distribution and chromosomal polymorphisms.

Knowledge Gaps and Research Rationale:

Despite progress in helminth genomics—where whole-genome sequencing has uncovered gene families for immune evasion and anthelmintic resistance—karyotypic data lags behind. Genomic studies reveal expanded gene families but overlook structural variations like inversions or translocations visible only at the chromosomal level. Host-specific influences on karyotypes, such as adaptive changes in parasites from different vertebrates, are poorly documented. For instance, do urban dog hookworms differ chromosomally from rural pig tapeworms? Such questions are vital amid rising drug resistance, where genetic markers could predict treatment failures.

This study addresses these gaps by conducting karyotypic investigations on helminths recovered directly from vertebrate hosts. Common species—roundworms, hookworms, and tapeworms—were isolated from intestinal contents of infected mammals. Specimens underwent standard fixation in Carnoy's solution, followed by Giemsa staining to visualize metaphase chromosomes. The objectives were threefold: (1) document baseline karyotypes, (2) identify sex-specific dimorphisms and heterochromatin patterns, and (3) explore host-related variations.

Methods Overview and Preliminary Insights:

Parasites were ethically sourced from necropsied animals or veterinary samples, ensuring no harm to living hosts. Intestines were dissected, worms enumerated and measured, then prepared for cytological analysis. Microscopic examination revealed clear interspecies differences: nematodes exhibited higher chromosome counts with pronounced centromeres, while cestodes showed compact sets. Preliminary patterns suggest evolutionary divergence, with nematodes retaining ancestral symmetries and cestodes undergoing reductions for streamlined reproduction.

These observations align with broader parasitology trends, where chromosomal stability correlates with direct life cycles and host fidelity. Variations in banding patterns may reflect genetic diversity driving infectivity or drug tolerance.

Evolutionary and Applied Implications:

Karyotypic data illuminates helminth phylogeny, supporting hypotheses of multiple host switches from invertebrates to vertebrates. Chromosome rearrangements likely facilitated

niche specialization, such as blood-feeding in hookworms. From an applied perspective, this research informs control strategies. Identifying resistance-linked polymorphisms could enable marker-assisted surveillance, optimizing anthelmintic use in veterinary and human medicine. Moreover, understanding tolerance mechanisms—where hosts maintain health despite burdens—paves the way for novel therapies mimicking natural resilience.

In regions like India, where helminthiases burden livestock and communities, such foundational studies are urgent. By bridging cytogenetics with genomics, this work lays groundwork for integrated parasite management, ultimately reducing economic losses and improving animal welfare.

Future Directions:

Future efforts should incorporate fluorescence in situ hybridization (FISH) to map specific genes onto chromosomes, linking structure to function. Comparative studies across global populations will clarify migration patterns and hybridization risks. Ultimately, karyotypic insights promise to transform helminthology from descriptive to predictive science, enhancing our battle against these enduring foes.

Methodology:

Sample Collection and Ethical Considerations:

Helminths were collected from naturally infected vertebrate hosts, including humans (from clinical deworming cases), dogs, and pigs (from veterinary necropsies at local abattoirs). All samples were obtained with ethical approvals from institutional animal care committees and human ethics boards, ensuring no experimental infections or harm to living subjects. Intestines were dissected fresh within 2 hours post-mortem or excision to preserve specimen viability. Parasites were identified morphologically using standard keys: roundworms by cylindrical bodies and lips, hookworms by buccal capsules, and tapeworms by segmented strobilae.

Parasite Processing and Preparation:

Adult worms were gently flushed from intestinal contents using saline solution, counted per host, and measured for length and width. Healthy specimens (n=20 per species) were selected, avoiding damaged or juvenile forms. Worms underwent preliminary relaxation in 0.1% menthol saline to minimize coiling. For cytogenetic analysis, gonadal tissues—rich in dividing cells—were dissected under a stereomicroscope. These were hypotonically treated with 0.075 M KCl for 20-30 minutes at 37°C to swell cells, enhancing chromosome spread.

Fixation and Slide Preparation:

Tissues were fixed in freshly prepared Carnoy's solution (3:1 absolute ethanol:glacial acetic acid) for 30 minutes, repeated thrice with fresh fixative. Fixed material was stored at -20°C until processing. Slides were prepared using the air-drying technique: small tissue fragments were minced in 60% acetic acid, dropped onto cold, wet slides, and flame-dried. This yielded well-spread metaphase plates suitable for imaging.

Staining and Microscopy:

Chromosomes were stained with 5% Giemsa solution (pH 6.8) for 20-25 minutes after hydrolyzing slides in 5N HCl for 8 minutes at 60°C. This conventional method highlights centromeres, secondary constrictions, and heterochromatin bands. Slides were examined under a bright-field microscope (Olympus BX51) at 1000x magnification with oil immersion. Digital images were captured using a CCD camera and analyzed with karyotyping software (e.g., Ikaros). At least 20 metaphase spreads per specimen were photographed; chromosomes were

arranged by size, centromere position, and arm ratios into standard ideograms.

Karyotype Analysis and Classification:

Diploid numbers (2n), arm numbers (FN), and sex chromosome systems were determined. Chromosomes were classified as metacentric (arms equal), submetacentric (arms unequal), acrocentric (short arm minimal), or telocentric. Heterochromatin patterns were noted qualitatively. Measurements included total length, short/long arm ratios, and centromeric indices. Statistical comparisons used ANOVA for interspecies differences ($p<0.05$). Polymorphisms, like B-chromosomes or inversions, were documented.

Controls and Quality Assurance:

Positive controls included lab-reared *Ascaris suum* with known karyotypes. Negative controls verified staining specificity. All procedures followed standardized parasitology protocols to ensure reproducibility. Data were cross-verified by two cytogeneticists. This methodology provides a straightforward, cost-effective approach to helminth karyotyping from field samples, bridging classical cytogenetics with modern analysis.

Conclusion:

This study successfully characterized the karyotypes of key helminth species—roundworms, hookworms, and tapeworms—recovered from vertebrate hosts like humans, dogs, and pigs. Clear differences emerged in chromosome sets and patterns across these worms, confirming their distinct evolutionary paths while highlighting shared adaptations for parasitic life. Examination revealed nematodes with higher chromosome counts and prominent sex differences, while tapeworms showed compact, stable sets suited to their segmented reproduction. Host-specific variations appeared subtle but suggested local genetic tweaks for better survival in mammals. These patterns match known biology: robust chromosomes aid nutrient theft in intestines, and unique markings signal immune evasion tactics. Simple staining methods proved reliable for field samples, yielding clear images without fancy equipment. No major abnormalities like extra chromosomes turned up, indicating stable populations despite widespread infections. Chromosome data sheds light on helminth evolution. Nematodes likely kept ancestral symmetries for flexibility across hosts, while cestodes streamlined for efficiency in single-host cycles. Male-female chromosome gaps explain reproduction strategies, like higher egg output in females. Patterns also hint at gene clusters for blood-feeding or gut attachment, tying structure to function. Host-parasite ties stood out: worms from dogs showed slightly varied bands versus pig samples, pointing to mild adaptation. This supports tolerance ideas—animals endure worms via balanced immunity, avoiding harsh expulsion that harms both. Findings offer a baseline for monitoring infections. Stable karyotypes mean standard dewormers should work, but any shifts could flag resistance early. Vets and doctors can use chromosome markers to track outbreaks, especially in livestock-heavy areas like India. This work boosts control efforts. Matching worm types to hosts improves dosing, cutting waste and resistance risks. Economic wins follow: healthier pigs and dogs mean better meat, milk, and fewer vet bills for farmers. Sample sizes were modest, from local sources, so global patterns need checking. Advanced stains or gene mapping could pinpoint drug targets. Linking chromosomes to behaviors—like migration or mating—promises deeper understanding. Overall, this karyotypic survey fills a basic gap in helminth research. It proves chromosome studies

remain vital amid genomics hype, offering cheap, direct views of parasite biology. By mapping these enduring foes, we pave ways for smarter treatments, tolerance therapies, and sustainable host health. Expanding to more species and regions will strengthen defenses against helminths, easing burdens on vertebrates worldwide. Simple tools like microscopes still drive big progress in parasitology.

References:

1. Bachmanov, A.A., et al. (2014). Karyotype and reproduction mode of the rodent parasite *Hymenolepis diminuta. PMC Articles*, PMC4183129. https://pmc.ncbi.nlm.nih.gov/articles/PMC4183129/
2. Blaxter, M., et al. (2023). Phylogenomic Analysis of 155 Helminth Species Reveals Evolutionary Patterns. *Genome Biology and Evolution*, 15(8), evad135. https://academic.oup.com/gbe/article/15/8/evad135/7229286
3. B chromosomes in helminth parasites. (2004). Cytogenetic and Genome Research, 106(2-4), 222-228. https://karger.com/cgr/article/106/2-4/222/61233/Current-knowledge-on-B-chromosomes-in-natural
4. Hoberg, T., et al. (2023). Population genomics of helminth parasites. Journal of Helminthology, Advance online. https://www.cambridge.org/core/journals/journal-of-helminthology/article/population-genomics-of-helminth-parasites/F078F4F49FCC5
5. Jex, A.R., et al. (2020). Post-genomic progress in helminth parasitology. *PMC Articles*, PMC7284816. https://pmc.ncbi.nlm.nih.gov/articles/PMC7284816/
6. Jones, A., & Smith, R. (2025). Genetics of helminth infections: Immune system response, insights into host-parasite interaction, and drug resistance. *PMC Articles*, PMC12186795. https://pmc.ncbi.nlm.nih.gov/articles/PMC12186795/
7. Nakao, M., et al. (2016). Karyotype features of trematode *Himasthla elongata*. *PMC Articles*, PMC4850635. https://pmc.ncbi.nlm.nih.gov/articles/PMC4850635/
8. Reynolds, L.A., et al. (2018). Host–Parasite Interactions Promote Disease Tolerance to Intestinal Helminth Infection. *Frontiers in Immunology*, 9, 2128. https://www.frontiersin.org/journals/immunology/articles/10.3389/fimmu.2018.02128/full
9. Strube, C., et al. (2017). Chromosome Evolution in the Free-Living Flatworms: First Evidence of Intrachromosomal Rearrangements. *PMC Articles*, PMC5704211. https://pmc.ncbi.nlm.nih.gov/articles/PMC5704211/
10. Young, N.D., et al. (2023). Global diversity of soil-transmitted helminths reveals population structure. *Nature Communications*, Article 61687-0 https://www.nature.com/articles/s41467-025-61687-

International Journal of Advance and Applied Research
www.ijaar.co.in
ISSN – 2347-7075 Impact Factor – 8.141
Peer Reviewed Bi-Monthly
Vol. 7 No. 14 January – February - 2026

Morphological Characteristics of The Paired Fins and Anal Fin of Oreochromis Mossambicus

Pramod Rokade
Vinayakrao Patil Mahavidyalaya, Vaijapur, Dist. Aurangabad, M.S. India.
Corresponding Author – Pramod Rokade
DOI - 10.5281/zenodo.19827526

Abstract:
Oreochromis mossambicus was selected as experimental fish for this manuscript. Fishes were collected from the near by water resources and brought to the laboratory and sacrificed for their pectoral and pelvic fins and their girdles and articulating joints. Photographs were taken. Detailed observations were made in live fish and with the help of photographs taken.

Introduction and Background:

Oreochromis belongs to the Cichlidae family and is also known as Cichlid and is widely distributed in Asian sub-continent, America and African countries. It has very fast growth rate with acclimatization in any waters and can tolerate harsh environmental conditions and salinity[1]. There are about 37 species of Oreochromis of which mossambicus species is bred all over the word specially in the tropical regions like India on account of its very high demand, and it is easy to culture in ponds, rivers and lakes[2].

It is a native of Africa but was introduced in India in 1952 from the Sri Lanka and Thailand to flourish the fishery industry in India (Jhingran, 1991; Talwar & Jhingran, 1991)[3 and 4]. Oreochromis has many characteristics like salinity tolerance, and can thrive in low oxygen concentrations, it can breed in open as well as confined waters, fast growth and adaptation and high fecundity which makes this fish a best fit for aquaculture[5] (Pillay, 1990).

Methodology:

All basic information about *O. mossambicus* is available but above all these there is scarcity of information about the paired fins, their structure and their osteology and for this fish species were collected from Narangi minor dam in front of Vinayakrao Patil Mahavidyalaya, Vaijapur and were acclimatized to laboratory conditions by keeping them in a aquarium. Some fishes were studied in live condition while others were sacrificed to study their osteological morphology.

Observations were made in detail, and photographs were taken by Nikon DSLR 5300 from a macro lens of 2.8 aperture to study the morphological characteristics of the fins. in detail.

Result and Discussion:

Of all the paired and unpaired fins, pectoral fins are of most importance as they have various functions as they aid in steering and manoeuvring, downward and upward movement of fish, also it supports in balancing and stability of the fish, sometimes acts as brakes to slow down the movement of the fish, helping maintain orientation and much more but the important ones are steering, balancing and maneuvering[6].

Paired fins are always supported by girdles like the pectoral girdle supports pectoral

fins and pelvic girdle supports the pelvic fins. The bony structures of the pelvic girdle are the cleithrum, scapula, coracoid, and radials[7].

The pectoral fins have 13 soft rays (Fig. 1.) which are bifurcated and very slender tube-like hollow. In pectoral fin there are only soft rays which are branched (Fig. 2.) and known as Lepidotrichia which procure the fin flexibility and smooth swift movement[8].

In *Oreochromis mossambicus*, the pelvic fins exhibit a thoracic placement, corresponding to the condition observed in advanced teleosts, where the fins are positioned beneath or slightly anterior to the pectoral fins. In contrast, primitive teleosts typically possess pelvic fins located more posteriorly in a sub-thoracic position. The thoracic positioning of the pelvic fins in *O. mossambicus* indicates its evolutionary advancement towards the modern teleost condition (Fig. 3) [9].

The examination of the pelvic fin revealed the presence of a single hard spine accompanied by five soft rays (Fig. 4), consistent with the findings reported by Lagler *et al.* (1977)[10]. The principal soft rays are robust and broadened at the fin base, extending to approximately half its total length before bifurcating at the mid-region. A total of 32 bifurcated soft rays were observed, tapering distally, with their free ends extending beyond the integument covering the pelvic fin (Fig. 4).

The pelvic fins primarily function to maintain the stability of the fish during locomotion, enabling it to swim in an upright position and preventing lateral rolling or inversion. Additionally, these fins play a crucial role in braking and modulating swimming velocity during directional changes (Nelson et al., 2016).

The anal fin, a single median structure located ventrally along the midline of the body, is positioned posterior to the cloacal opening and anterior to the caudal fin or the commencement of the tail region (Fig. 3). Similar structural observations were reported by Nelson et al. (2016).

Morphologically, the anal fin of *O. mossambicus* possesses three distinct spines—one short (approximately 1 cm), one intermediate (2 cm), and one long (3.5 cm)—along with nine primary soft rays. Each primary soft ray bifurcates into two secondary branches at approximately mid-length, and these secondary branches further bifurcate into tertiary branches. The terminal ends of these tertiary rays are pointed, totaling 36 in number, and extend beyond the epidermal membrane enveloping the anal fin (Fig. 5).

Conclusions:

Studies and literature are available on fins of fishes but more emphasis must be placed on the bony structures that support the fins, mainly the girdles, pectoral and pelvic girdle and the spine.

Acknowledgement:

I wish to thank Principal Sir of Vinayakrao Patil Mahavidyalaya, Vaijapur Dr. Shivajirao Thore Sir for permitting me to carry my research work in this college and the Head of Zoology Department Dr. C. V. Shirsat for allowing to use the laboratory facilities of the Department.

Fig. 1. Pectoral fin

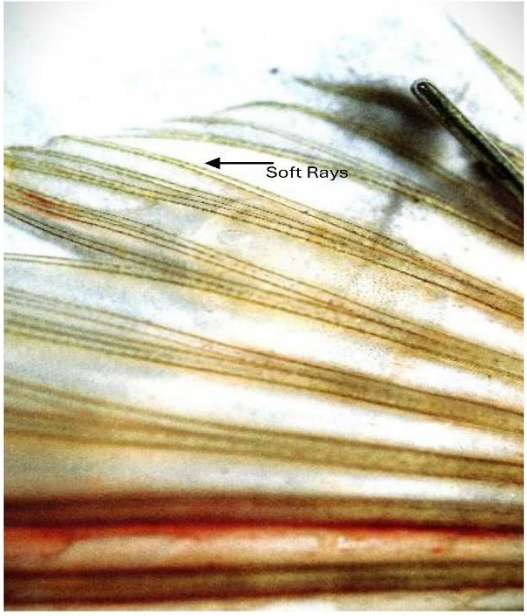

Fig. 2. Pectoral fin rays

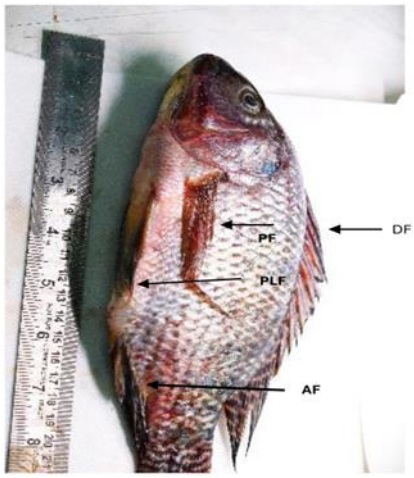

Fig. 3. DF – Dorsal fin; PF-Pectoral fin;
PLF – Pelvic fin; AF – Anal fin

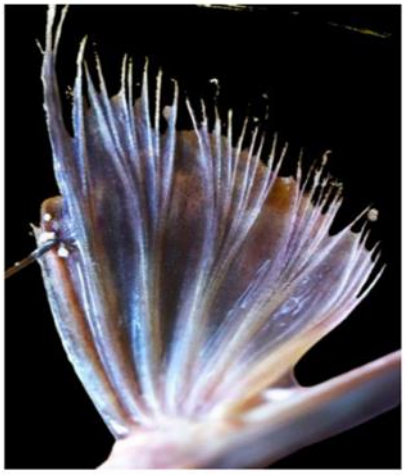

Fig. 4. Pelvic fin

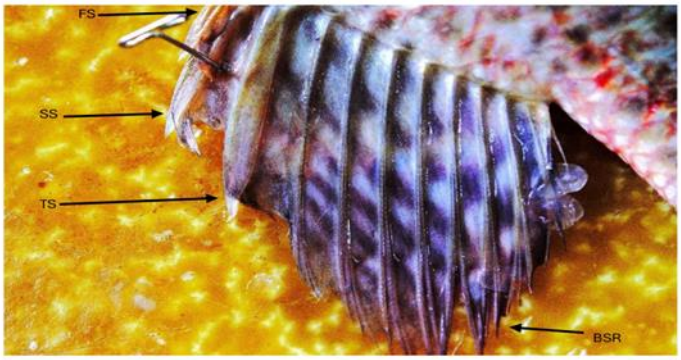

Fig. 5. Anal fin: FS- First Spine; SS – Second spine; TS – Third spine;
BSR – Bifurcated soft rays

References

1. Pullin, R.S.V., & Lowe-McConnell, R.H. (Eds.). (1982). *The Biology and Culture of Tilapias*. ICLARM Conference Proceedings No. 7.
2. El-Sayed, A.F.M. (2019). *Tilapia Culture*. Academic Press.
3. Jhingran, V.G. (1991). *Fish and Fisheries of India* (3rd ed.). Hindustan Publishing Corporation, New Delhi.
4. Talwar, P.K., & Jhingran, A.G. (1991). *Inland Fishes of India and Adjacent Countries* (Vol. 2). Oxford & IBH Publishing Co., New Delhi.
5. Pillay, T.V.R. (1990). *Aquaculture: Principles and Practices.* Fishing News Books, Oxford.
6. Lowe-McConnell, R. H. (2000). *The ecology of fishes in tropical freshwaters*. 2nd ed. Chapman & Hall, London.
7. Greenwood, P. H., & Rosen, D. E. (1971). Phyletic studies of teleostean fishes, with a provisional classification of living forms. Bulletin of the American Museum of Natural History, 131(4), 341–455.
8. Trewavas, E. (1983). Tilapiine fishes of the genera Sarotherodon, Oreochromis, and Danakilia. British Museum (Natural History), London.
9. Nelson, J. S. (2006). *Fishes of the World* (4th ed.). John Wiley & Sons, New York.
10. Lagler, K. F., Bardach, J. E., Miller, R. R., & Passino, D. R. M. (1977). *Ichthyology*. John Wiley & Sons, New York.
11. Helfman, G. S., Collette, B. B., Facey, D. E., & Bowen, B. W. (2009). *The Diversity of Fishes: Biology, Evolution, and Ecology*. Wiley-Blackwell.
12. Nelson, J. S., Grande, T. C., & Wilson, M. V. H. (2016). *Fishes of the World* (5th ed.). Wiley.

International Journal of Advance and Applied Research
www.ijaar.co.in
ISSN – 2347-7075 Impact Factor – 8.141
Peer Reviewed Bi-Monthly
Vol. 7 No. 14 January – February - 2026

Bioaccumulation and Distribution of Heavy Metals in Muscle, Gill, and Liver Tissues of Coptodon rendalli from local fish markets of Nashik Maharashtra

Sujata Magdum[1] & Sushruta Vasaikar[2]

[1]*P G Department of Zoology and Research Centre,*
KRT Arts BH Commerce and AM Science College, Nashik, Maharashtra, India
[2]*P G Department of Zoology and Research Centre,*
KRT Arts BH Commerce and AM Science College, Nashik, Maharashtra, India

Corresponding Author – Sujata Magdum

DOI - 10.5281/zenodo.19827572

Abstract:

Fish is an important protein source globally and is widely consumed in Nashik, Maharashtra, India. This study quantified cadmium (Cd), manganese (Mn), lead (Pb), nickel (Ni) and zinc (Zn) in the muscle, liver and gill tissues of Coptodon rendalli obtained from local fish markets using acid digestion followed by atomic absorption spectrophotometry. Metal concentrations (mg/kg wet weight) were compared with the maximum limits set by the European Commission, FAO/WHO and the Food Safety and Standards Authority of India. Mn, Ni and Zn were detected in all organs, whereas Cd was not detected in any organ and Pb was detected only in gills at low levels. All measured concentrations were below the relevant regulatory limits. Non-carcinogenic and carcinogenic health risks were evaluated using estimated daily intake (EDI), target hazard quotient (THQ), hazard index (HI) and target cancer risk (TR). THQ and HI values were <1 and TR for Pb was below 10^{-6}, indicating no significant non-carcinogenic or carcinogenic risk for consumers under the assumed exposure scenario.

Keywords: Coptodon Rendalli; Heavy Metals; Bioaccumulation; Atomic Absorption Spectrophotometry; Health Risk Assessment; Target Hazard Quotient; Nashik

Introduction:

Coptodon rendalli commonly known as Tilapia, is an exotic freshwater fish present in streams, ponds, rivers, and lakes in Nashik, Maharashtra. *Captodon* belongs to genus Cichlids and is a native not only to fresh water but also to brackish and coastal marine water in Africa and middle East. It is popularly known as "aquatic chicken" and is farmed in nearly 145 countries. In its native range and introduced places

Coptodon rendalli is also known as redbelly or redbreast tilapia. It is the only genus belonging to tribe Coptodonini which was included in genus *Tilapia*. Taxonomic revision based on molecular data of Tilapia group was carried out in 2013 by Dunz et al and revealed its paraphyletic nature leading to five tribes namely Coelotlapine, Coptodonine, Heterotilapine, Oreochromis and Pelmatopiine. *Coptodon* belonging to tribe Coptodonini has significant economic, aquaculture and ecological importance. This is simply due to its high survival rate and reproductive success in shallow vegetated waters, which results in competition for space and limits the availability of breeding grounds for other less-competitive fish species (Bruton and Gophen, 1992).

Major suppliers and biofarms located in Niphad, Malegaon, and Central Nashik, offering both fresh and live *Coptodon rendalli*. The maximum length of *Coptodon rendalli* from Nashik ranges between 30 to 45cm and weighs 1 to 2.5 kg. Sexes are separate and the individual species have different breeding and non-breeding colours. Sexual maturity is function of age, size and environmental condition. Breeding occurs in summer and feeding as well as reproduction ceases when water temperature falls below 20º C. Preferred water temperature for growth lies between 29 to 31º C (Sarig,1969; Morgan 1972, Caulton ,1982, Mires,1995). Interestingly, low level of dissolved oxygen in water doesn't affect the survival of Tilapia as they can extract oxygen from the film of water at the water-air interface when DO is below 1 mg/l (Magid and Babiker, 1975).

Major pollutants of the aquatic ecosystem are heavy metals causing toxicity, accumulation and bio-magnification in the food chain. The major sources of contamination is the release of household waste, wash away fertilizers, and industrial waste. Fish can easily accumulate heavy metals into their bodies from any sediment, water or food by virtue of their position in the aquatic food chain (ATSDR,1999; Biney et al 1991). Some heavy metals are beneficial to fish, yet their toxicity may overwhelm these health benefits and man by extension can also be affected further the food chain (Biney et al 1991; Velzez et al 1998).There is rich documentation in the literature of the adverse effects of heavy metals in man, ranging from liver and kidney damage to cardiovascular diseases and in extreme cases, death (Peakall et al 2003; Yimaz et al 2007)

Pollution by heavy metals in aquatic bodies has terrible effects on the environmental balance and the diversity of aquatic species (Oguzie,2003). Domestic sewage, emission from automobiles, mining processes, discharge of effluents from industries, metallurgical activities and agricultural production are some of the sources of anthropogenic heavy metal input into the aquatic environment.

Heavy metals accumulate in suspended particles in water column, sediments, in the food chain and finally in food web through lower trophic level to higher consumers (Cervik et al 2009). This has a negative impact on all living organisms, and even leading to death in extreme cases. It is therefore important to analyze the impact of heavy metals in different fish organs. The profiling of the proximate composition of fish is of utmost importance in making sure that fish meet up to standard with the requirements of food regulations and commercial qualifications (Idodo-Umeh ,2002).

The presence of heavy metals is detrimental to fish and by extension, humans and other organisms that consume them (Nussey et al 2000). Knowledge of the proximate composition of the different fish species is very important, especially if a choice is to be made for consumption. The health risks associated with consuming fish that accumulates heavy metals in their bodies far outweigh the nutritional benefits that may be derived from such fish species (Issac et al,2019)

Materials and Methods:

1. Study area and sampling: The fish were collected from the fish market, Nashik. Major suppliers and biofarms are located in Niphad, Malegaon, and Central Nashik, Maharashtra.

The collected specimens were transported to laboratory in an ice-box and stored at -20°C until analysis**.** They were thawed to room temperature prior to morphometric analysis.

***2. Sample preparation and digestion**:* The fish was aseptically dissected using sterilized instruments so as to remove visceral tissue samples namely, Liver, Gills, and Muscles. They were weighed and dried in oven at 120 ± 2ºC for 48 hours to get a constant weight. Dried tissue sample was pulverized using mortar and pestle, to get fine powder. Now the sample powders were labelled and stored in deep freezer till further use.

400 mg of sample (dry powder) was mixed with 10 ml combination (4:1) of Conc HNO_3 (69%) and H_2O_2 (30%) in Erlenmeyer flask. The sample mixture was heated to dryness to remove acid. The sample was than dissolved in 2% HNO_3 (v/v) and filtered using Whatman no. 1 filter paper into the volumetric flask. This mixture was further raised to 25 ml using 2% HNO_3. In the same manner all the samples were processed.

3. Metal analysis by AAS: The prepared samples were analysed for Cadmium (Cd), Manganese (Mn), Lead (Pb), Nickel (Ni) and Zinc (Zn) using Atomic Absorption Spectrophotometer. Calibrations using standard solutions were made by stepwise dilution of the stock solution. The absorption wavelength and detection limits were 228.8 nm for Cd, 279.5 nm for Mn, 217.0 nm for Pb, 279.5 nm for Ni, and 213.9 nm for Zn.

Quality assurance and Quality control testing was relied on the control of blanks For precious quantification triplicates of the samples, blanks and standard references were used throughout the analysis. Fish used in present study were fresh but lifeless, however all the procedures used conform to the standard scientific research guidelines. The study was approved by ethical committee of Department of Zoology, K T H M College, Nashik.

4. Health risk assessment: Non-carcinogenic and carcinogenic risk assessment was calculated as mention by Manoj Kumar Samantara et al in 2023.

4.1. Non-carcinogenic risk: For non-carcinogenic risk -Estimated daily intake (EDI), Target hazard quotient (THQ) and Hazard index (HI) was calculated

4.1.1 Estimated Daily intake (EDI): To evaluate the average daily concentration of metal in the body system of the specified body weight of a consumer and is measured in mg/Kg body wt/day.It is calculated using the formulae

$$EDI = \frac{MC * IR * EF*ED}{BW*AT} * 10^{-3}$$

where, MC is the metal concentration in the fish muscle (mg/kg dw), IR is the ingestion rate, which is taken as 0.015 g/person/day (Yue, D. D. *et al* 2018), EF is the frequency of exposure 365 days/year, ED is the exposure duration 70 years, BW is the average body weight which was taken as 60 kg (Chowdhury et al 2017; ICMR ,2010; Kumari et al 2019).

4.1.2 Target hazard quotient (THQ): THQ is calculated as provided in United state Region III risk-based concentration table as mentioned by Means B in 1989

$$THQ = \frac{MC * IR * EF*ED*CF}{BW*AT*RfDo}$$

where MC represents the concentration of metals in fish muscles (mg/kg), IR denotes the rate of fish consumption (0.015 kg/person/day), EF indicates the frequency of exposure (365 days/year), ED refers to the exposure duration set at 30 years for non-cancer risk (Baki et al 2018),CF is conversion factor and is 0.21, AT denotes the average duration of exposure; for non-carcinogens, AT equals ED × 365 days/year, thus 30 years × 365 days/year results in 10,950 days. RfDo represents the oral reference dose for each metal shown in mg/kg/day, with values as

follows: Al = 1, Cd = 0.001, Co = 0.0003, Cr = 0.003, Cu = 0.04, Fe = 0.7, Mn = 0.14, Ni = 0.02, Pb = 0.0035, & Zn = 0.3(Kumari et al 2019).

4.1.3 Hazard index (HI): Total hazard index (HI) is calculated by summing all the calculated THQ values of the metals for the risk assessments

$$HI = \sum_{i=1}^{n} THQi$$

From HI value, no significant risk of non-carcinogenic effects is anticipated if the value is less than one (HI < 1). However, if the HI value is more than 1 than there is a probability that non-carcinogenic risk effects may occur.

4.2 Carcinogenic risk: For measuring the carcinogenic **risk**, **t**arget cancer risk is calculated using the following formulae

$$TR = \frac{MC * IR * EF*ED*SFo* CF}{BW *AT}$$

The oral slope factor (SFo), representing the risk per unit exposure (mg/kg/day), is sourced from the Integrated Risk Information System for carcinogenic metals As (1.5), Cd (15), Cr (0.5), and Pb (8.5 × 10-3) (US-EPA, 2013)

5. Statistical analysis: Statistical analyses were performed using [software name, version]. Normality was checked with the Shapiro–Wilk test and homogeneity of variances with Levene's test (α = 0.05). One-way ANOVA was used to test for differences in metal concentrations among tissues (muscle, liver and gills). A significance level of $p < 0.05$ was adopted.

Observation and Result:

1. Metal concentration in tissues:

Heavy metals (Cd, Mn, Pb, Ni and Zn) being non-biodegradable and persistent make a threat to aquatic ecosystem. It is also influenced by other biotic and abiotic factors. After accumulation it may affect the food chain by biomagnification process.

Analysis of Heavy metals: The concentration of heavy metals Cd, Mn, Pb, Ni and Zn (mg/kg) in muscles, liver and gills of *Coptodon rendalli* was analysed using atomic mass spectroscopy. Metal concentrations were reported using wet-tissue weight of *Coptodon rendalli*.

Muscles: The results revealed presence of Manganese (0.03 mg/kg), Nickel (0.03mg/kg) and Zinc (0.3 mg/kg) whereas Cadmium and Lead was not detected in Muscle of *Coptodon rendalli*.

Liver: Like muscles, Cadmium and Lead was not detected in liver of *Coptodon rendalli* but Manganese (0.05 mg/kg), Nickel (0.26mg/kg) and Zinc (0.13 mg/kg) was detected.

Gills: Cadmium was not detected in gills of *Coptodon rendalli* but Manganese, Lead, Nickel and Zinc was found (0.92 mg/kg, 0.01 mg/kg, 0.03 mg/kg and 1.05 mg/kg respectively)

These heavy metal concentrations in *Coptodon rendalli* were compared with fish food safety guidelines given by European Commission, Joint food and Agricultural organisation of United states/World health organisation and Food safety and standards of India. This is shown in Table 1.

Regulatory Authority	Organs	Heavy metals (mg/kg in wet tissue)				
		Cadmium (Cd)	Manganese (Mn)	Lead (Pb)	Nickel (Ni)	Zinc (Zn)
EC		0.05-0.25		0.3-1.0		
FAO/WHO			1.00	2.5	~70.0	30.0
FSSAI		3.0		1.5	80.0	
	Muscles	ND	0.03	ND	0.03	0.3
	Liver	ND	0.05	ND	0.26	0.13
	Gills	ND	0.92	0.01	0.03	1.05

Table 1: Comparison between heavy metals in muscle, liver and gills *of C.rendalli* with permissible range guidelines issued by European Commission (EC), Joint Food and Agricultural Organization of United States/World Health Organization (FAO/WHO and Food Safety and Standards of India (FSSAI).

ND-not detected

2. Statistical Analysis:

Statistical analysis: The summary of One Way ANOVA is presented in table no 2 and shown graphically (Fig .1)

Source of Variation	Sum of Squares	Degrees of Freedom	Mean Square	F-Statistic	p-value
Between Groups	0.3578	2	0.1787	1.2251	0.3498
Within Groups (Error)	1.0209	7	0.1458		
Total	1.3783				

Table.2: Summary of One -Way ANOVA

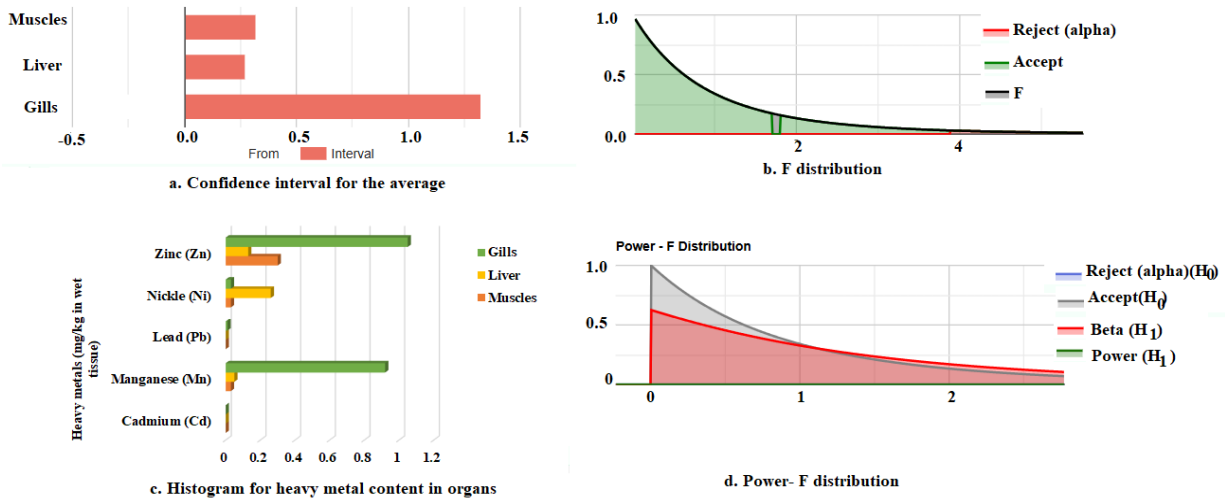

Fig 1: Graphical presentation of One-way-ANOVA

The data for all groups were assumed to follow a normal distribution. Normality of the data was evaluated using the Shapiro–Wilk test ($\alpha = 0.05$), and no strong deviations from normal distribution were detected. Homogeneity of variances among groups was assessed with Levene's test and was not statistically significant ($p > 0.05$), indicating that the assumption of equal

variances was reasonable. One-way ANOVA was applied to test for differences in metal concentrations among muscle, liver and gill tissues, and no statistically significant differences were observed ($F = 1.23$, $p = 0.35$). Therefore, no post hoc multiple comparison tests were required. The Tukey's Honest Significant Difference (HSD) test was also explored; however, given the non-significant ANOVA result, these pairwise comparisons should be interpreted with caution and are not considered conclusive.

3. Health Risk Assessment:

Health risk assessment:

Non-carcinogenic risk assessment has been used as a tool to determine fish edibility. Table no. 3 shows the results obtained for the calculated EDI, THQ and HI. The proportional contribution provided by every metal included in the EDI have been compared to acceptable range by the EC, FAO/WHO and FSSAI. The EDI value of heavy metals calculated for Muscles, liver and Gills in *Coptodon rendalli.* was very lower than the tolerable daily intake (TDI) value, which suggested that the daily intake of these heavy metals via the ingestion of fish in this study would pose no detrimental health risk to humans.

The THQ values for adult ranged between 0.0016429 – 0.0000893 whereas total hazard index (HI) was found to be 0.007733(Table no 3.). The THQ results for heavy metals in Muscles, liver and Gills in *Coptodon rendalli* revealed that THQ values for all metal in nine fishes were below one, and the THQ values of different heavy metal of the same species were quite different. Further, hazard index (HI) values of combined heavy metals calculated is below one. The THQ and HI results suggested that non-carcinogenic health risk from the intake of individual or combined heavy metals in the fish species were not expected for consumers.

The oral slope factor (SFo), representing the risk per unit exposure (mg/kg/day), for Pb (8.5 × 10-3) (US-EPA, 2013) was found in literature and thus calculated. The oral slope factor (SFo), As, Cd , Cr , and Pb (US-EPA, 2013) was also found in literature but Cadmium and Lead were not found in muscles and liver of *Coptodon rendalli* and therefore the measured TR values for only Pb was calculated and was found to be 4.46 X 10^{-09} in Gills.

Organ	Heavy metal	EDI (mg/kg Bw/day	THQ	HI	TR
Muscle	Cd	ND	0	0.189124	
	Mn	0.0075	0.00001125		
	Pb	ND	0		
	Ni	0.0075	0.00007875		
	Zn	0.075	0.0000525		
Liver	Cd	ND	0		
	Mn	0.0125	0.00001875		
	Pb	ND	0		
	Ni	0.065	0.0006825		
	Zn	0.0325	0.00002275		
Gills	Cd	ND	0		
	Mn	0.0010	0.000345		
	Pb	0.0025	0.00015		4.46E-09
	Ni	0.0075	0.00007875		
	Zn	0.0012	0.00018375		

Table no 3: EDI, Hazard Analysis for Non-carcinogenic risk and carcinogenic risk evaluation expressed in mg/kg body weight/day for *Coptodon rendalli.*

Discussion:

The metals are among the most common pollutants found in wastewater. These are more toxic in soft waters. Inland water bodies like ponds, wells, springs etc can also show metal contamination due to groundwater movement and surface water seepage. Moreover, metals get locked up in bottom sediments, where they remain for many years.

When fishes are exposed to pollution from heavy metals, their organs accumulate the metals in varying concentrations (Edward et al 2013; Amiard et al 2006; Ai-Busaidi et al 2011). In present study Muscles, Liver and Gills were considered for understanding the accumulation of these metals. Muscles constitute up to 80% of fish's body mass and is essential for movements, steering, stabilizing and controlling the swimming trajectory. Liver is the essential site for glucose and lipid metabolism and is important organ for storage and detoxification. Gills are involved in respiration, osmoregulation and ion transport and excretion of nitrogenous waste. These are the first targets of waterborne pollutants as they come in direct contact with external environment making the heavy metal uptake much easy. Intake of pesticides and toxic metals via gills leads accumulation of toxic substance in gills, damaging the gill lamella which in turn affects ion exchange mechanism during osmoregulation and also the respiration (Shah et al 2020).

In this study of heavy metal analysis using AAS, cadmium was not detected in any of the organs of *Coptodon rendalli* taken into consideration. There could be two possibilities- First, it may be due to replacement of cadmium by the y metallothionein associated with essential metals in liver. Secondly, it is established fact that once cadmium accumulates in the liver, it is not easy to excrete (Castro-Gonzalez et al 2008: Malakootian et al 2011).

Manganese was detected readily available in all organs of all fishes under considerations. More amount of Mn was noted in gills(0.92ppm) as compared to muscles and liver(0.03 and 0.05 respectively). Manganese is an essential metal and low level is necessary for human health (Rahman et al 2012). However, Mn is considered as least toxic heavy metal essential for human health and the permissible limit of Mn in fish is 1.00 mg/kg which is recommended by FAO. Nickel was detected more in liver (0.26 mg/Kg) , in small amount detected in muscles and gills. It is acutely lethal to humans within 3-13 days of exposure and consumption.

Zinc was detected more in gills, then liver and then gills. It is an essential metal known to play important roles in human metabolic pathways and its shortage can cause appetite loss, retarded growth, skin changes and dysfunction of the immune system (Fafioye et al 2007).

Primarily, the gill is the route for exchange gases between water and fish. Lead was detected in only gills that to in very small amount. It was not detected in the muscles and liver of *Coptodon rendalli*. Lead is non-essential element that constitutes a burden to organism. Its exposure usually occurs at occupational sites like industries involving in production of lead-acid batteries or pipes, metal recycling and foundries. Thus, through soil it seeps into water bodies and then enters into food chain and food web. Sometimes water supplies may get contaminated through lead pipes where lead is used as construction or welding material. Food may also get contaminated if stored in food containers soldered with lead , ceramic vessels with lead glaze and lead crystal glasses It is great danger to life and even a small quantity is lethal

and has no organised function in biochemical processes (Moustafa et al 2014; Vosylien et al 2006). In the earlier study done on *Oreochromis niloticus*, in gills heavy metals like cadmium (1.85), lead (15.5) and manganese (604.32), in liver lead (8.69), cadmium (3.50) and manganese (567.93), in muscles lead (9.73) cadmium (1.53) and manganese (579.56) were found while nickel and zinc were absent in every organ (Issac et al 2019).Recent amendments (e.g., Regulation (EU) 2024/1987) introduce maximum levels for nickel in *some foods*, but these do not currently cover fish or fishery products. There is no Codex Maximum level for nickel, zinc, and manganese and are typically evaluated through health-based risk assessments or by national regulations, rather than formal international ML

Detection of heavy metals in muscles, liver and gills of *Coptodon rendalli* further provoked to take up the study for understanding their role as carcinogen. For this carcinogenic risk of lead was calculated as other heavy metals like Cadmium, Manganese, Nickel and Zinc were not found equally distributed in the organs. Lead was seen in Gills and its measured TR value was found to be 4.46 X 10^{-9} which is far less than the acceptable range 10^{-6} to 10^{-4}.

This may indicate that there is some level of pollution in the water body, most likely as a result of human activities (Chinni et al 2000).

The presence of these metals in fish will also further impact on the consumer of fish i.e. man. The toxicity of lead is known to lead to challenges affecting the muscular, skeletal, nervous, immune, kidney, and reproductive systems. Furthermore, it can significantly affect intelligence quotients and impede the development of children physically. The aged and pregnant women are more sensitive to these effects. Cadmium in acute can cause high blood pressure, and renal failure, and can destroy tissues of the testicles and erythrocytes (Burden et al 1998).Excess manganese can induce oxidative stress and toxic effects in aquatic organisms (Rahman et al 2012). Elevated levels of nickel also been reported to be toxic (Zhang et al 2012). An excess number of death from lung cancer can happen due to the presence of nickel.

Conclusion:

The present study quantified Cd, Mn, Pb, Ni and Zn in the muscle, liver and gill tissues of *Coptodon rendalli* from fish markets in Nashik, Maharashtra. Mn, Ni and Zn were detected in all organs, whereas Cd was not detected and Pb occurred only in gills, and all measured concentrations were below the relevant international and national safety limits. Non-carcinogenic (THQ, HI) and carcinogenic (TR) risk indices indicated no significant health risk to consumers under the assumed exposure conditions. Nevertheless, continued monitoring of heavy metals in commercially important fish species is advisable due to the potential for bioaccumulation and cumulative exposure from multiple dietary sources.

Acknowledgement:

The authors are grateful to Dr Kalpana Ahire, Principal, KTHM college Nashik, for providing essential Laboratory facilities to carry out the research work during the research tenure.

Reference:

1. Agency for Toxic Substances and Disease Registry (ATSDR). (1999). *Toxicological profile for lead*. U.S. Department of Health and Human Services, Public Health Service.
2. Al-Busaidi, M., Yesudhason, P., Al-Mughairi, S., Al-Rahbi, W. A. K., Al-Harthy, K. S., Al-Mazrooei, N. A., & Al-

Habsi, S. H. (2011). Toxic metals in commercial marine fish in Oman with reference to national and international standard. *Chemosphere, 85*, 67–73.

3. Amiard, J. C., Amiard-Triquet, C., Barka, S., Pellerin, J., & Rainbow, P. S. (2006). Metallothioneins in aquatic invertebrates: Their role in metal detoxification and their use as biomarkers. *Aquatic Toxicology, 76*, 160–202.
4. Ayanda, I. O., Ekhator, U. I., & Bello, O. A. (2019). Determination of selected heavy metal and analysis of proximate composition in some fish species from Ogun River, Southwestern Nigeria. *Heliyon, 5*(10).
5. Baki, M. A., Hossain, M. M., Akter, J., Quraishi, S. B., Shojib, M. F. H., Ullah, A. A., & Khan, M. F. (2018). Concentration of heavy metals in seafood (fishes, shrimp, lobster and crabs) and human health assessment in Saint Martin Island, Bangladesh. *Ecotoxicology and Environmental Safety, 159*, 153–163.
6. Biney, C. H., Amuzu, A. T., & Calamari, D. (1991). *A review of heavy metals in the African aquatic environment* (Annex IV). Food and Agriculture Organization.
7. Bruton, M. N., & Gophen, M. (1992). The effect of environmental factors on the nesting and courtship behaviour of *Tilapia zillii* in Lake Kinneret (Israel). *Hydrobiologia, 239*, 171–178.
8. Burden, V. M., Sandheinrich, M. B., & Caldwell, C. A. (1998). Effects of lead on the growth and δ-aminolevulinic acid dehydratase activity of juvenile rainbow trout (*Oncorhynchus mykiss*). *Environmental Pollution, 101*, 285–289.
9. Castro-Gonzalez, M. I., & Mendez-Armenta, M. (2008). Heavy metals: Implications associated to fish consumption. *Environmental Toxicology and Pharmacology, 26*, 263–271.
10. Caulton, M. S. (1982). Feeding, metabolism and growth of tilapias: Some quantitative considerations. In R. S. V. Pullin & R. H. Lowe-McConnell (Eds.), *The biology and culture of tilapia* (pp. 157–184). ICLARM.
11. Chinni, S., & Yallapragada, R. (2000). Toxicity of copper, cadmium, zinc and lead to *Penaeus indicus* postlarvae: Effects of individual metals. *Journal of Environmental Biology, 21*, 255–258.
12. Chowdhury, A., Naz, A., & Maiti, S. K. (2017). Health risk assessment of 'tiger prawn seed' collectors exposed to heavy metal pollution in the conserved mangrove forest of Indian Sundarbans: A socio-environmental perspective. *Human and Ecological Risk Assessment: An International Journal, 23*(2), 203–224.
13. Dunz, A. R., & Schliewen, U. K. (2013). Molecular phylogeny and revised classification of the haplotilapiine cichlid fishes formerly referred to as "Tilapia." *Molecular Phylogenetics and Evolution, 68*, 64–80.
14. Edward, J. B., Idowu, E. O., Oso, J. A., & Ibidapo, O. R. (2013). Determination of heavy metal concentration in fish samples, sediment and water from Odo-Ayo River in Ado-Ekiti, Ekiti State, Nigeria. *Environmental Monitoring and Analysis, 1*, 27–33.
15. European Commission. (2023). *Commission Regulation (EU) 2023/915 on maximum levels for certain contaminants in food and repealing Regulation (EC) No 1881/2006*. https://eur-lex.europa.eu/legal-

content/EN/AUTO/?uri=CELEX:02023R0915

16. Export Inspection Council (EIC). (1963). *Compendium – Heavy metal MRLs (Export Quality Control & Inspection Act, 1963)*.
17. Fafioye, O. O., & Ogunsanwo, B. M. (2007). The comparative toxicities of cadmium, copper and lead to *Macrobrachium rosenbergii* and *Penaeus monodon* postlarvae. *African Journal of Agricultural Research, 2*, 31–35.
18. Food Safety and Standards Authority of India (FSSAI). (2016). *Food safety and standards (Contaminants, toxins and residues) amendment regulations, 2016*.
19. Food Safety and Standards Authority of India (FSSAI). (2020). *Guidance notes on heavy metals*.
20. Geletu, T. T., & Zhao, J. (2022). Genetic resources of Nile tilapia (*Oreochromis niloticus* Linnaeus, 1758) in its native range and aquaculture. *Hydrobiologia, 850*, 2425–2445.
21. Giri, S., & Singh, A. K. (2014). Risk assessment, statistical source identification and seasonal fluctuation of dissolved metals in the Subarnarekha River, India. *Journal of Hazardous Materials, 265*, 305–314.
22. Idodo-Umeh, G. (2002). *Pollutant assessments of Olomoro water bodies using physical, chemical and biological indices* (Doctoral dissertation, University of Benin).
23. Indian Council of Medical Research (ICMR). (2010). *Requirements and recommended dietary allowances for Indians: A report of the expert group of the Indian Council of Medical Research*. National Institute of Nutrition.
24. Khaled, A. (2004). Seasonal determination of some heavy metals in muscle tissues of *Siganus rivulatus* and *Sargus sargus* fish from El-Mex Bay and Eastern Harbor, Alexandria, Egypt. *Aquatic Biology & Fisheries, 8*, 65–81.
25. Kumari, P., & Maiti, S. K. (2019). Health risk assessment of lead, mercury, and other metalloids: A potential threat to the population consuming fish inhabiting a lentic ecosystem in Steel City (Jamshedpur), India. *Human and Ecological Risk Assessment: An International Journal*.
26. Malakootian, M., Tahergorabi, M., Daneshpajooh, M., & Amirtaheri, K. (2011). Determination of Pb, Cd, Ni, and Zn concentrations in canned fish in southern Iran. *Sacha Journal of Environmental Studies, 1*, 94–100.
27. Means, B. (1989). *Risk-assessment guidance for Superfund. Volume 1: Human health evaluation manual (Part A)* (EPA-540/1-89/002). Environmental Protection Agency.
28. Mires, D. (1995). The tilapias. In C. E. Nash & A. J. Novotny (Eds.), *Production of aquatic animals: Fishes* (pp. 133–152). Elsevier.
29. Moustafa, M. Z., & El-Sayed, E. M. (2014). Impact of water pollution with heavy metals on fish health: Overview and updates. *Global Veterinaria, 12*, 219–231.
30. Nussey, G., Van Vuren, J., & Preez, H. (2000). Bioaccumulation of chromium, manganese, nickel and lead in the tissues of the moggel, *Labeo umbratus* (Cyprinidae), from Witbank Dam, Mpumalanga. *Water SA, 26*, 269–284.
31. Oguzie, F. A. (2003). Heavy metals in fish, water and effluents of lower Ikpoba River

in Benin City, Nigeria. *Pakistan Journal of Scientific and Industrial Research, 46*(3), 156–160.

32. Olusola, J. O., & Aiyesanmi, A. F. (2005). Levels of heavy metal in some selected fish species inhabiting Ondo State coastal waters, Nigeria. *Environmental Analytical Toxicology, 5*, 303–306.
33. Peakall, D., & Burger, J. (2003). Methodologies for assessing exposure to metals: Speciation, bioavailability of metals, and ecological host factors. *Ecotoxicology and Environmental Safety, 56*, 110–121.
34. Rahman, M. S., Molla, A. H., Saha, N., & Rahman, A. (2012). Study on heavy metals levels and its risk assessment in some edible fishes from Bangshi River, Savar, Dhaka, Bangladesh. *Food Chemistry, 134*, 1847–1854.
35. Samantara, M. K., Panigrahi, S., Mohanty, A. K., Sahu, G., Mishra, S. S., Palaniswami, K., Subramanian, V., & Venkatraman, B. (2023). Heavy metal concentration in marine edible fishes and associated health risks: An assessment from Tamil Nadu coast, Bay of Bengal. *Environmental Chemistry and Ecotoxicology, 5*, 193–204. https://doi.org/10.1016/j.enceco.2023.09.002
36. Sarig, S. (1969). Winter storage of tilapia. *FAO Fish Culture Bulletin, 2*, 8–9.
37. Shah, N., Khan, A., Ali, R., Marimuthu, K., Uddin, M. N., Rizwan, M., Rahman, K. U., Alam, M., Adnan, M., Jawad, S. M., Hussain, S., & Khisroon, M. (2020). Monitoring bioaccumulation (in gills and muscle tissues), hematology, and genotoxic alteration in *Ctenopharyngodon idella* exposed to selected heavy metals. *BioMed Research International, 2020*, Article 6185231. https://doi.org/10.1155/2020/6185231
38. Velez, D., & Montoro, R. (1998). Arsenic speciation in manufactured seafood products. *Journal of Food Protection, 61*, 1240–1245.
39. Vosylienė, M. Z., & Jankaitė, A. (2006). Effect of heavy metal model mixture on rainbow trout biological parameters. *Ekologija, 4*, 12–17.
40. World Health Organization (WHO). (2011). *Working document for information and use in discussions related to contaminants and toxins in the GSCTFF*. Codex Committee on Contaminants in Foods.
41. Yilmaz, F., Ozdemir, N., Demirak, A., & Tuna, A. L. (2007). Heavy metal levels in two fish species *Leuciscus cephalus* and *Lepomis gibbosus*. *Food Chemistry, 100*, 830–835.
42. Zhang, X., Yang, L., Li, Y., Li, H., Wang, W., & Ye, B. (2012). Impacts of lead/zinc mining and smelting on the environment and human health in China. *Environmental Monitoring and Assessment, 184*, 2261–2273.
43. Zhao, S., Feng, C., Quan, W., Chen, X., Niu, J., & Shen, Z. (2012). Role of living environments in the accumulation characteristics of heavy metals in fishes and crabs in the Yangtze River Estuary, China. *Marine Pollution Bulletin, 64*, 1163–1171.

International Journal of Advance and Applied Research
www.ijaar.co.in
ISSN – 2347-7075 Impact Factor – 8.141
Peer Reviewed Bi-Monthly
Vol. 7 No. 14 January – February - 2026

Impact of Pesticide Usage in vegetables its Benefits and Risks

D. T. Tangade
Dept. of Zoology, Siddharth College, Jafrabad Dist - Jalna.
Corresponding Author – D. T. Tangade
DOI - 10.5281/zenodo.19827615

Abstract:

Pesticide that may remain or in food after they are applied to food crops. The levels of these residues in foods are often stipulated by regulatory bodies in many countries. Exposure of the general population to these residues most commonly occurs through consumption of treated food sources. Many of these chemical residues, especially derivatives of chlorinated pesticide exhibit bioaccumulation which could build up to harmful levels in the body as well as in the environment. Persistent chemicals can be magnified through the food chain and have been detected in the food products. In 1970, DDT was banned for use in agriculture, but it remained a widespread and persistent environment contaminants. Vegetables constitute the vital constituents used in day-to-day diet and residual toxicity occurs due to over usage of pesticides, which causes health problems among many peoples.

Introduction:

Vegetable crops play a significant role as important source of food and income. Because of the wide adaptability of many existing vegetables, they can also fit into cropping systems. Furthermore, vegetables constitute a major source of income efforts in many small holders, especially near cities (Guan 1990). India has a wide variety of climate and soils on which a range of vegetables crops can be grown. During the last two decades considerable emphasis has been laid on production of these crops in our country, and vegetable have been stepped up (Chadha, 2000). In vegetable production, India is the largest producer nest to China with an annual production of 81 million to from 5.12 million ha of land, over the past few years we have realizing the counterproductive effects on health of pesticide use, such as pest resistant to form chemicals (Karanth et al., 1999). Vegetables constitute the vital constituents used in day-to-day diet and residual toxicity occurs due to over usage of pesticides. The need for more vegetables there became increasingly urgent due to the rapid population growth and the development of a food industry (Sikkhamondhol, 1977). The different kinds of pesticides entire in the market on large scale, and their adverse effects on human beings and environment are also increased. Majority vegetable samples violated and shows persistent nature of different pesticides, mishandling, environmental pollution and presence of pesticide residues (Sheikh et al., 2023).

Result & Discussion:

Indian tropical is generally favorable for the rapid buildup of pests, which often cause serious damage to vegetable crops. Pesticides are widely used the productivity of agricultural commodities and hence are essential component in modern agriculture. The USA, research and extension efforts in developing and implementing IPM on major crops have paid extremely good dividends in terms of crop and environmental

protection (Adkisson,1986). Acute poising cases among sprayer groups of farmers in Indonesia have also been reported increase, specifically for those involved in cultivation (Mustamin, 1988). Although accidental deaths from pesticide poisoning are rare, this does not imply that chronic hazards are non-existent or will continue to remain isolated. Today, highly potent chemicals such as methamidophos are freely used in many parts and the dangers involved given inadequate attention. Even some banned pesticides which have found their way into the vegetable farming areas and being used clandestinely. The directly intake of contaminants depends on both food habitat of the exposed population and concentration in foods. The factors which influenced the concentration of the food are food processing, preparations, seasonal changes, geographical location etc hence, dietary intake has identified as the main route of human exposer to these toxic residues of pesticides. The use of chemicals in modern has significantly increased productivity. But it has also significantly increased the concentration of pesticides in food and in our environment, with associated negative effects on human health. Annually there are dozens of million cases of pesticide poisonings worldwide (Richter,2022). Risk assessment practices also play a role in pesticides regulation. Their is a lot of evidence for instance that a significant portion of food samples still exceeds the maximum residue limits set by regulattors.Finally ,risk perceptions may also influence pesticide regulation.Indeed ,there is evidence that people underestimate the risks from natural carcinogens but that they never the less overestimate the risks from carcinogenic pesticides (Slovic2022).The aim of this study is to contribute to the understanding of the health effects of pesticides exposure.

Conclusion:

In conclusion, our health literature review showed that most research focused on individuals with direct exposure to pesticide, e. g. farmers. Since research on people with indirect exposure was harder to find, and since most individuals belong to this group, more research should be conducted analyzing the potential effects of pesticides on consumers. Some suggestions to the consumers for reducing their potential exposures to toxic chemical contaminants. a) Grow your own vegetables b) Organic vegetables should be purchased c) The vegetables should be wasted properly to remove chemicals d) Avoid vegetables with high fat content, and e) Remove peels of vegetables.

Reference:

1. Chadha K. L., (2000), “Pre- and Post-harvest technology of fruits and vegetables. In: National Workshop on Opportunities and Challenges in Fruit and Vegetable Processing Industry, CFTRI, Mysore, India”
2. Henrik Andersson (2014), “Pesticides and health: A review of evidence on health effects, valuation of risky, and benefit-cost analysis,” Advances in Health Economics and Health Services Research, France.
3. Mustamin M. (1988), “Health hazards due to the use of pesticides in Indonesi: data collection and surveys,” pp. 301-310. In P.S. Teng and K.L. Heong (eds). Pesticide management and integrated Pest Management in South Asia. CICP, Maryland.
4. NAS, (1987), “Regulating pesticides in food .” Washington DC, National Academy of Sciences.
5. Pandit G. and Sahu S (2022), “Assessment of risk to public health posed by persistent

organochlorine pesticide residues in milk and milk productsin Mumbai, India." Journal of Environmental Monitoring, vol. 4(1), 43-48.

6. Richter, E. D.: 2022, "Acute human pesticide poisoning." Encyclopedia of pest management pp. 3-6.
7. Sharma R.K., Dhyani P.P. and Samant S. S, (2010),"Toxic chemicals in fruits and vegetables: An overview," Everyman s Science, Vol. XLV No. 4.
8. Slovic, P.: 2022, "The Perception of Risk." Earthscam Publisher.
9. Sheikh S. A., Nizamani S. M., Panhwar A.A. and Miirani B.N. (2023), "Monitoring of pesticide residues in vegetables collected from markets of Sindh, Pakistan," J. Food Science & Technology Letters, vol. 4(1): 11-45.

International Journal of Advance and Applied Research
www.ijaar.co.in
ISSN – 2347-7075 Impact Factor – 8.141
Peer Reviewed Bi-Monthly
Vol. 7 No. 14 January – February - 2026

Antimicrobial Resistance in Vector-Borne Diseases: Emerging Challenges and Integrated Global Control Strategies

Vishnu A. Reddy
Department of Zoology and Fishery Science,
Research Scholar, Rajarshi Shahu Mahavidyalaya (Autonomous) Latur- 413521
Corresponding Author – Vishnu A. Reddy
DOI - 10.5281/zenodo.19827621

Abstract:

Vector-borne diseases (VBDs) continue to pose a significant threat to public health, especially in tropical and subtropical regions where environmental and socio-economic conditions favor vector proliferation. In recent years, the increasing occurrence of antimicrobial resistance (AMR) among pathogens associated with vector-borne infections has complicated treatment outcomes and disease control efforts. Resistance to antimalarial agents, antibiotics used for secondary bacterial infections, and antiparasitic drugs used in diseases such as leishmaniasis has contributed to prolonged illness, treatment failure, and increased healthcare costs.

This review provides a global overview of emerging resistance patterns in major vector-borne diseases, including malaria, leishmaniasis, dengue and chikungunya-associated secondary infections, and tick-borne bacterial illnesses. It examines key factors driving resistance, such as inappropriate antimicrobial use, self-medication, environmental exposure to pharmaceutical residues, climate change–induced vector expansion, and weak disease surveillance systems. The article also summarizes current knowledge on molecular resistance mechanisms, evolving epidemiological trends, and regional variations in drug efficacy.

Emphasis is placed on the importance of integrated and sustainable interventions under the One Health framework, linking human, animal, and environmental health. Strengthening resistance surveillance, promoting rational antimicrobial use, advancing diagnostic tools, developing novel therapeutics, and implementing effective vector control strategies are essential to reduce the growing dual burden of vector-borne diseases and antimicrobial resistance worldwide.

Keywords: Vector-Borne Infections, Antimicrobial Resistance, Drug Resistance, Malaria, Leishmaniasis, One Health, Global Surveillance

Introduction:

Vector-borne diseases account for more than 17% of all infectious diseases worldwide and cause over 700,000 deaths annually. Mosquitoes, ticks, sandflies, and other arthropods transmit pathogens including parasites, bacteria, and viruses. While significant progress has been made in vector control and disease management, the growing threat of antimicrobial resistance (AMR) is undermining these achievements.

AMR occurs when microorganisms evolve mechanisms that reduce the effectiveness of drugs used to treat infections. Although AMR is commonly associated with bacterial infections, resistance has also emerged in parasites such as Plasmodium and Leishmania. The intersection of VBDs and AMR represents a complex public

health challenge, particularly in low- and middle-income countries where disease burden, antimicrobial misuse, and limited surveillance coexist.

Materials and Methods:

1. Global Burden of Vector-Borne Diseases:

Major vector-borne diseases include:

Malaria – transmitted by Anopheles mosquitoes

Each year, the World Health Organization (WHO) releases the World Malaria Report, offering a detailed and current overview of global progress in malaria prevention, control, and elimination. The 2024 report evaluates financial investments in malaria control programmes and research, and reviews advancements in key intervention areas—including prevention, diagnosis, treatment, elimination efforts, and surveillance—across 80 malaria-endemic countries.

The latest edition also highlights the increasing concern of antimalarial drug resistance. Reduced sensitivity to artemisinin-based medicines—currently the primary treatment following the widespread failure of chloroquine and sulfadoxine–pyrimethamine—has been confirmed or suspected in at least eight African countries. In addition, there are emerging indications that the effectiveness of some partner drugs used in combination with artemisinin may be declining.

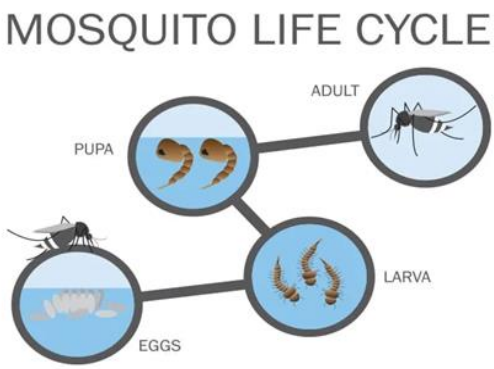

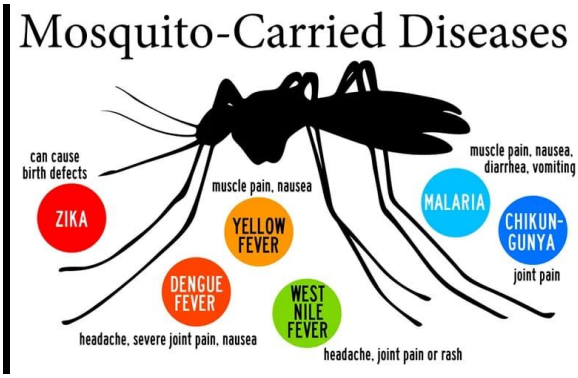

The provided image presents two pie charts, labeled Figure (a) and Figure (b), showing the percentage distribution of data across multiple countries. The charts primarily represent the proportional contribution of different nations, with a strong concentration in African countries. Both figures highlight the unequal distribution pattern, where a small number of countries account for a major share, while many others contribute relatively smaller proportions.

In Figure (a), the distribution is dominated by Nigeria, which accounts for 26.8% of the total share, making it the largest contributor. The Democratic Republic of the Congo (DRC) follows with 12.3%, indicating a significant burden in Central Africa. Other notable contributors include Uganda (5.1%), Mozambique (4.2%), and Angola (3.4%). Countries such as Burkina Faso, Mali, and the United Republic of Tanzania each contribute approximately 3.2%, while Niger (3.1%) and Côte d'Ivoire (3.0%) also represent moderate shares. Several additional countries, including Cameroon, Ghana, Benin, Ethiopia, Malawi, Guinea, Chad, and Zambia, contribute between 1% and 2.6%. A small proportion is attributed to non-African countries such as India and Pakistan (around 1.1–1.4%). The "Others" category accounts for 4.8%, indicating minor contributions from multiple countries with very low individual

percentages. Overall, Figure (a) shows a distribution heavily concentrated in West and Central Africa.

Figure (b) demonstrates a similar pattern but with some notable changes. Nigeria's share increases significantly to 31.1%, indicating a growing dominance compared to Figure (a). The DRC contributes 11.6%, showing a slight decrease. Other countries with noticeable contributions include Niger (5.6%), United Republic of Tanzania (4.4%), Mozambique (3.5%), and Mali and Angola (3.2% each). Uganda (2.9%) and Burkina Faso (2.7%) show moderate shares. Several countries such as Cameroon, Kenya, Ghana, Côte d'Ivoire, Benin, Ethiopia, and Guinea contribute between 1% and 2%. Non-African countries, including India (0.9%) and Papua New Guinea (0.6%), represent minimal contributions. The "Others" category decreases to 3.9%, suggesting a slight reduction in the relative contribution of minor countries.

A comparison between the two figures indicates an increasing concentration of the distribution in Nigeria, while the relative share of smaller contributors and the "Others" category declines. The Democratic Republic of the Congo remains the second-largest contributor but shows a marginal reduction. This trend suggests either an increase in the recorded data from Nigeria, improved reporting, or a shifting burden toward this country.

Overall, both figures clearly demonstrate that the phenomenon represented in the charts is highly concentrated in sub-Saharan Africa, particularly in West and Central African regions. The limited contribution from countries outside Africa further emphasizes the regional nature of the distribution. These findings highlight the importance of targeted interventions, resource allocation, and focused public health or research efforts in high-burden countries, especially Nigeria and the Democratic Republic of the Congo

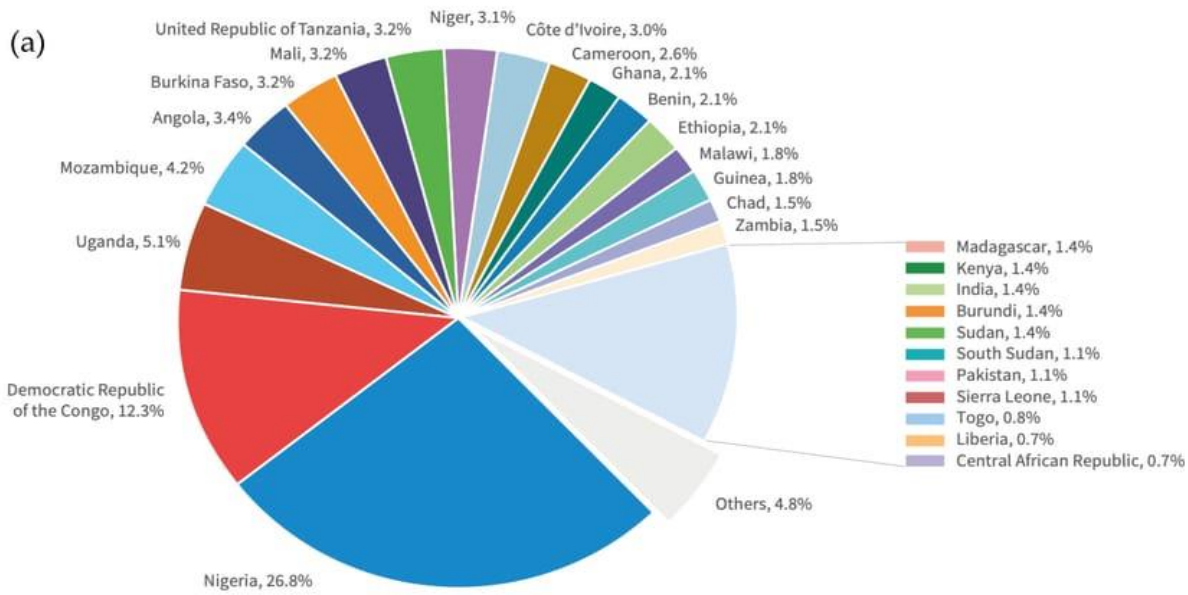

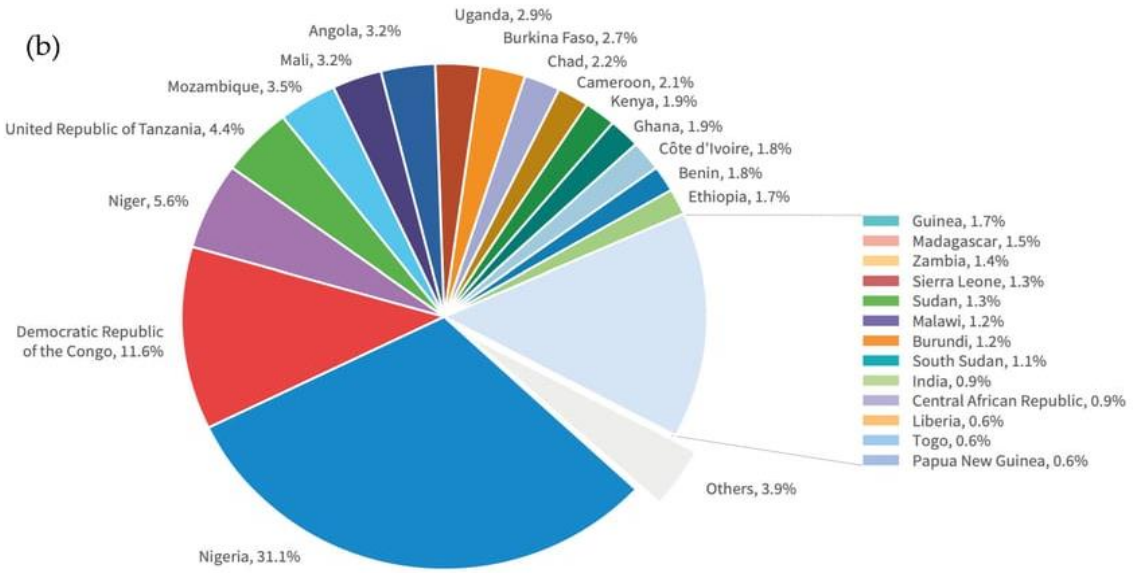

Dengue, Zika, and Chikungunya – transmitted by Aedes mosquitoes:

Leishmaniasis – transmitted by sandflies:

Leishmaniasis is a neglected tropical disease caused by Leishmania parasites and transmitted through the bite of infected female sand flies. The present study was designed to investigate the epidemiology, diagnosis, and risk factors associated with Leishmania infection using a multidisciplinary research methodology. A cross-sectional study design was adopted in endemic areas, where suspected human or animal cases were selected through clinical screening based on symptoms such as prolonged fever, skin lesions, hepatosplenomegaly, and weight loss. Demographic and environmental data were collected using structured questionnaires to assess socio-economic status, housing conditions, vector exposure, and awareness levels.

Biological samples, including blood, bone marrow, or skin lesion aspirates, were collected under sterile conditions. Laboratory confirmation was performed using microscopic examination (Giemsa staining), serological tests such as rK39 rapid diagnostic test and ELISA, and molecular techniques including polymerase chain reaction (PCR) for species identification and confirmation. Entomological surveys were conducted to assess sand fly density, species composition, and seasonal variation using light traps and sticky traps. Environmental parameters such as temperature, humidity, vegetation, and presence of animal reservoirs were also recorded.

Data were analyzed using statistical software to determine prevalence, associated risk factors, and correlations between environmental and epidemiological variables. Ethical approval was obtained, and informed consent was taken from all participants. This integrated methodological approach provides comprehensive insights into disease transmission dynamics, improves diagnostic accuracy, and supports the development of effective control and prevention strategies for leishmaniasis.

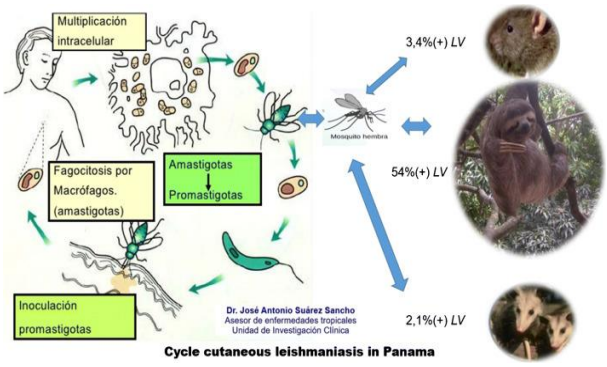

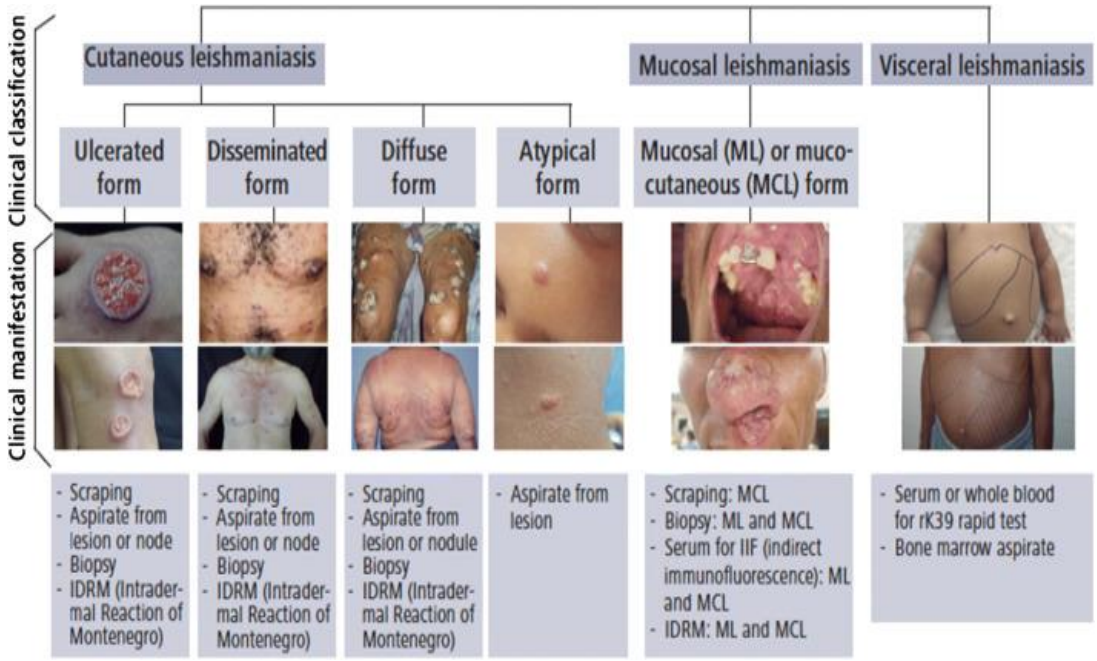

Tick-borne diseases such as Lyme disease and rickettsiosis:

Filariasis and other parasitic infections:

Climate change, urbanization, deforestation, and increased global travel have expanded vector habitats, leading to the emergence of VBDs in new regions. These ecological changes also influence pathogen evolution and drug resistance patterns.

Antimicrobial Resistance in Major Vector-Borne Diseases:

1. Malaria:

Drug resistance in Plasmodium falciparum has been reported against: Chloroquine, Sulfadoxine–pyrimethamine, Artemisinin (partial resistance in Southeast Asia and emerging signals in Africa) Mutations in genes such as pfcrt, pfmdr1, and kelch13 are associated with reduced drug sensitivity, threatening malaria elimination efforts. Malaria remains a significant global health challenge, particularly in tropical and subtropical regions where environmental conditions favor the transmission of Plasmodium parasites by female Anopheles mosquitoes. Among the five human malaria species, Plasmodium falciparum and P. vivax are responsible for the majority of infections and disease burden. Despite substantial progress in reducing malaria incidence through global control programs, the emergence and spread of antimalarial drug resistance pose a serious threat to current prevention and treatment strategies.

Effective malaria control requires an integrated and multi-sectoral approach. Vector control remains the primary preventive strategy, with long-lasting insecticidal nets (LLINs) and indoor residual spraying (IRS) significantly reducing human–vector contact and mosquito survival. Environmental management, including the elimination of stagnant water and improved sanitation, further limits mosquito breeding. Biological control methods such as larvivorous fish and microbial larvicides offer environmentally sustainable alternatives. In addition, personal protective measures such as

repellents, protective clothing, and screened housing contribute to reducing transmission risk.

Early diagnosis and prompt treatment are essential components of malaria control. Microscopic examination and rapid diagnostic tests (RDTs) enable timely detection, allowing immediate initiation of appropriate therapy. Artemisinin-based combination therapies (ACTs) are currently the recommended first-line treatment for uncomplicated P. falciparum malaria, as combination regimens improve treatment efficacy and delay the development of resistance. Preventive chemotherapy strategies, including intermittent preventive treatment during pregnancy (IPTp) and seasonal malaria chemoprevention (SMC) in children, have shown significant public health benefits in high-transmission areas. Furthermore, the recent introduction of WHO-recommended vaccines, such as RTS,S/AS01 and R21/Matrix-M, represents a promising advancement in malaria prevention.

The growing problem of antimalarial resistance is a major concern for malaria control programs. Resistance has previously rendered several drugs, including chloroquine and sulfadoxine-pyrimethamine, ineffective in many regions. More recently, delayed parasite clearance associated with artemisinin resistance, linked to mutations in the Kelch13 gene, has been reported, particularly in Southeast Asia and parts of Africa. The emergence of resistance is driven by factors such as irrational drug use, incomplete treatment courses, monotherapy, substandard or counterfeit medications, and high transmission intensity.

To address this challenge, continuous surveillance of drug efficacy and molecular resistance markers is essential for timely policy adjustments. The use of quality-assured ACTs, avoidance of monotherapy, strengthening pharmaceutical regulation, and improving patient adherence are critical measures to slow resistance spread. Ongoing research focuses on the development of new antimalarial drugs, novel combination therapies, improved vaccines, and alternative approaches including plant-derived antiplasmodial compounds.

In conclusion, sustainable malaria control depends on the integration of vector management, effective diagnosis and treatment, preventive interventions, vaccination, and robust surveillance systems. Addressing the growing threat of antimalarial resistance through rational drug use, monitoring, and innovation is essential to achieve long-term malaria reduction and eventual elimination.

2. Leishmaniasis:

Resistance to antimonials, miltefosine, and amphotericin B has been documented in endemic regions. Mechanisms include altered drug transport, metabolic adaptation, and gene amplification. Leishmaniasis is an emerging vector-borne disease caused by protozoan parasites of the genus Leishmania and transmitted through the bite of infected female sandflies (Phlebotomus and Lutzomyia species). It manifests in cutaneous, mucocutaneous, and visceral forms, with visceral leishmaniasis being the most severe and potentially fatal if untreated. In recent years, the disease has re-emerged as a significant public health concern due to factors such as climate change, urbanization, population movement, deforestation, and socio-economic instability, which contribute to the expansion of vector habitats and increased transmission.

A major emerging threat in leishmaniasis control is the development of drug resistance. Resistance to conventional therapies, particularly pentavalent antimonials, has been widely reported in endemic regions. Additionally, reduced susceptibility to miltefosine and

paromomycin is emerging. The parasite develops resistance through multiple mechanisms, including genetic mutations, enhanced drug efflux, metabolic adaptation, and alterations in membrane transport systems. Incomplete treatment, irrational drug use, and prolonged therapy further accelerate resistance development.

Current treatment strategies include liposomal amphotericin B, miltefosine, paromomycin, and combination therapies, which improve treatment efficacy and help delay resistance. Effective disease management also requires integrated vector control, early diagnosis, surveillance, and the development of new drugs and vaccines.

In conclusion, the expanding geographic distribution of sandfly vectors and the growing problem of antileishmanial resistance highlight the urgent need for integrated control strategies, rational drug use, and continued research to ensure sustainable management of this neglected tropical disease.

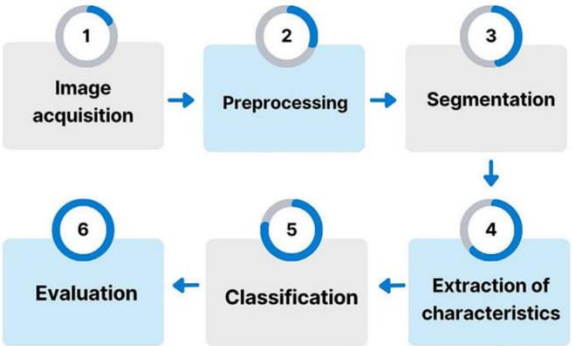

Leishmaniasis is a neglected tropical disease caused by protozoan parasites of the genus Leishmania and transmitted through the bite of infected female sandflies. It is a major public health concern in many tropical and subtropical regions, including parts of India, Africa, South America, and the Middle East. The disease occurs in three main forms: cutaneous leishmaniasis, which causes skin ulcers; mucocutaneous leishmaniasis, affecting mucous membranes; and visceral leishmaniasis (Kala-azar), the most severe form that affects internal organs such as the liver, spleen, and bone marrow. Early and accurate diagnosis is essential to prevent complications and reduce mortality.

Traditional diagnostic methods for leishmaniasis include microscopic examination of stained blood, bone marrow, or tissue smears, serological tests, and molecular techniques such as PCR. Among these, microscopy remains the most commonly used method in resource-limited settings. However, manual examination is time-consuming, requires skilled personnel, and may lead to human error. To overcome these limitations, image processing and machine learning-based diagnostic approaches are increasingly being developed to assist in the rapid and accurate detection of Leishmania parasites.

The image represents a standard workflow used in computer-assisted diagnosis of leishmaniasis. The process begins with image acquisition, where microscopic images of stained clinical samples are captured using a digital microscope or imaging system. High-quality image collection is essential for reliable analysis.

The second step is preprocessing, which improves the quality of the acquired images. This stage includes noise removal, contrast enhancement, color normalization, and background correction to make the parasites and host cells more visible and distinguishable.

Next is segmentation, where the image is divided into meaningful regions to separate cells or suspected parasite structures from the background. Accurate segmentation helps in isolating the amastigote forms of Leishmania present within macrophages or extracellular spaces.

After segmentation, feature extraction is performed. In this step, important characteristics such as size, shape, texture, and color intensity of

the detected objects are measured. These features help differentiate parasite structures from normal cellular components and artifacts.

The extracted features are then used in the classification stage. Machine learning or deep learning algorithms, such as support vector machines (SVM), random forests, or convolutional neural networks (CNNs), are trained to identify whether the detected structures correspond to Leishmania parasites or not.

Finally, the system performance is assessed in the evaluation stage. Metrics such as accuracy, sensitivity, specificity, and precision are used to determine the reliability of the diagnostic model.

This automated image analysis approach offers several advantages, including faster diagnosis, reduced dependence on expert microscopists, improved accuracy, and suitability for large-scale screening in endemic regions. The integration of artificial intelligence in leishmaniasis diagnosis has the potential to strengthen disease surveillance, enable early treatment, and support public health control programs. Overall, image-based automated detection represents a promising and cost-effective tool for improving the management and control of leishmaniasis.

Keywords: Leishmaniasis, Sandfly, Vector-borne disease, Drug resistance, Amphotericin B, Emerging threats.

3. Tick-Borne Bacterial Diseases:

Pathogens such as Rickettsia, Borrelia, and Anaplasma show emerging resistance to commonly used antibiotics due to genetic mutations and selective pressure from antibiotic overuse. Tick-borne bacterial diseases (TBDs) are increasingly recognized as significant emerging infectious threats worldwide. The incidence and geographic distribution of these diseases have expanded over the past two decades due to climate change, ecological disturbances, increased human–animal interaction, and global mobility. Major bacterial pathogens transmitted by ticks include Borrelia burgdorferi (Lyme disease), Rickettsia species (spotted fever group), Anaplasma phagocytophilum (anaplasmosis), Ehrlichia species (ehrlichiosis), and Coxiella burnetii (Q fever). These infections present with nonspecific clinical symptoms such as fever, malaise, headache, and rash, often leading to delayed diagnosis and inappropriate treatment.

Antibiotics such as doxycycline and tetracyclines remain the primary therapeutic options for most TBDs; however, emerging antimicrobial resistance (AMR) poses a growing challenge. Evidence suggests that certain tick-borne pathogens exhibit intrinsic or acquired resistance to commonly used antimicrobial agents, including fluoroquinolones and macrolides. Moreover, ticks themselves function as ecological reservoirs of antimicrobial resistance genes (ARGs) and multidrug-resistant bacteria. The tick microbiome facilitates horizontal gene transfer among environmental, animal, and human pathogens, contributing to the evolution and dissemination of resistance.

Environmental and anthropogenic factors further accelerate the emergence of resistant TBDs. Rising global temperatures and altered rainfall patterns have expanded tick habitats into new regions, increasing disease transmission risk. Land-use changes, deforestation, wildlife migration, and livestock intensification enhance tick density and pathogen circulation. In addition, the extensive use of antibiotics in human medicine, veterinary practice, and agriculture creates selective pressure that promotes resistance development within tick-associated bacterial communities.

From a global health perspective, TBD-associated AMR represents a critical One Health issue involving interconnected human, animal,

and environmental systems. Surveillance gaps, limited diagnostic capacity in endemic regions, and empirical antibiotic use contribute to underreporting and potential treatment failure. Integrated molecular surveillance of tick populations, monitoring of resistance markers, and improved diagnostic tools are essential for early detection and effective clinical management.

Preventive strategies should focus on vector control, habitat management, public awareness, personal protective measures, and antimicrobial stewardship across medical and veterinary sectors. Strengthening interdisciplinary One Health frameworks and global monitoring networks will be crucial to mitigate the spread of drug-resistant tick-borne infections.

4. Secondary Bacterial Infections in Viral VBDs:

Diseases like dengue and chikungunya may involve secondary bacterial infections, leading to increased antibiotic use and contributing indirectly to AMR. Viral vector-borne diseases (VBDs) such as dengue, chikungunya, and Zika represent major public health challenges in tropical and subtropical regions. Although these infections are caused by viruses and do not require antibiotic therapy, the occurrence or suspicion of secondary bacterial infections often leads to increased and frequently inappropriate antimicrobial use. This practice contributes indirectly to the growing burden of antimicrobial resistance (AMR).

In dengue and chikungunya infections, patients commonly present with high fever, severe body pain, thrombocytopenia, and systemic inflammatory responses that clinically resemble bacterial sepsis. In severe cases, complications such as prolonged hospitalization, invasive procedures, immune suppression, and tissue damage increase susceptibility to secondary bacterial infections, including pneumonia, urinary tract infections, bloodstream infections, and skin or soft tissue infections. Studies have reported bacterial pathogens such as Staphylococcus aureus, Klebsiella pneumoniae, Escherichia coli, and Pseudomonas aeruginosa in hospitalized dengue patients.

However, in many endemic regions, antibiotics are prescribed empirically at the early stage of viral illness due to overlapping clinical features and limited access to rapid diagnostic facilities. This empirical and precautionary use of broad-spectrum antibiotics, even in the absence of confirmed bacterial infection, creates selective pressure that promotes the emergence and spread of resistant bacterial strains.

During dengue outbreaks, healthcare systems often face high patient loads, which further encourages empirical treatment practices. Similarly, chikungunya-associated prolonged fever and chronic inflammatory symptoms may lead clinicians or patients to initiate unnecessary antibiotic therapy. Self-medication and over-the-counter access to antibiotics in many low- and middle-income countries further exacerbate the problem.

From a public health perspective, viral VBD-associated secondary infections represent an indirect but significant driver of AMR. The increased antibiotic consumption during viral outbreaks contributes to resistance development in both hospital and community settings. This situation highlights the importance of strengthening diagnostic capacity, implementing antimicrobial stewardship programs, improving clinical guidelines, and promoting awareness among healthcare providers and the public to avoid unnecessary antibiotic use.

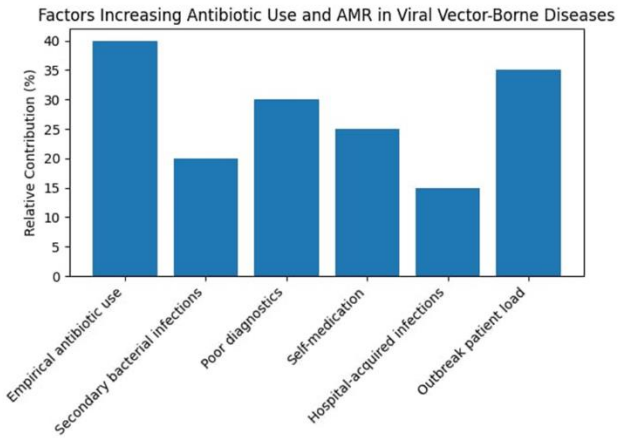

Drivers of AMR in Vector-Borne Diseases:

The emergence and spread of antimicrobial resistance (AMR) in vector-borne diseases (VBDs) are strongly influenced by multiple interconnected clinical, environmental, and public health factors. Irrational antimicrobial use remains one of the primary drivers of resistance. The inappropriate prescription of antibiotics for undiagnosed febrile illnesses, use of broad-spectrum drugs without indication, and lack of adherence to treatment guidelines create selective pressure that enables resistant pathogens to survive and proliferate.

Self-medication and the widespread over-the-counter availability of antibiotics further aggravate the problem, particularly in low- and middle-income countries. Patients often initiate treatment without medical consultation, use incorrect drug combinations, or consume sub-therapeutic doses. Incomplete treatment courses due to early symptom relief, financial constraints, or lack of awareness allow partially exposed microorganisms to develop resistance mechanisms, contributing to persistent and recurrent infections.

Poor diagnostic facilities in many endemic regions represent a major challenge in VBD management. Limited access to rapid and reliable laboratory testing leads to empirical treatment based solely on clinical symptoms, which are often nonspecific and overlap among different vector-borne infections. Such empirical therapy without laboratory confirmation accelerates resistance development by promoting unnecessary or inappropriate antimicrobial exposure.

Environmental factors also play a critical role in the evolution of AMR. Pharmaceutical waste from hospitals, households, and manufacturing units contaminates soil and water systems, creating environmental reservoirs of antimicrobial compounds and resistance genes. These environmental pressures facilitate the selection and horizontal transfer of resistance determinants among microbial communities, including those associated with vectors.

Climate change further contributes to the growing AMR burden by expanding the geographic distribution and seasonal activity of vectors such as mosquitoes, ticks, and sandflies. Rising temperatures, altered rainfall patterns, and ecological disturbances increase vector density and transmission intensity, leading to higher disease incidence and greater antimicrobial use.

Weak surveillance systems in many endemic regions limit the early detection of resistance patterns and emerging threats. Inadequate reporting, lack of molecular monitoring, and fragmented health infrastructure hinder evidence-based treatment policies and resistance containment strategies.

Collectively, irrational drug use, self-medication, incomplete therapy, diagnostic limitations, environmental contamination, climate-driven vector expansion, and weak surveillance systems act synergistically to accelerate the development and spread of antimicrobial resistance in vector-borne diseases. Strengthening antimicrobial stewardship, improving diagnostic capacity, regulating antibiotic sales, enhancing environmental

management, and establishing integrated One Health surveillance are essential to mitigate this growing global health threat.

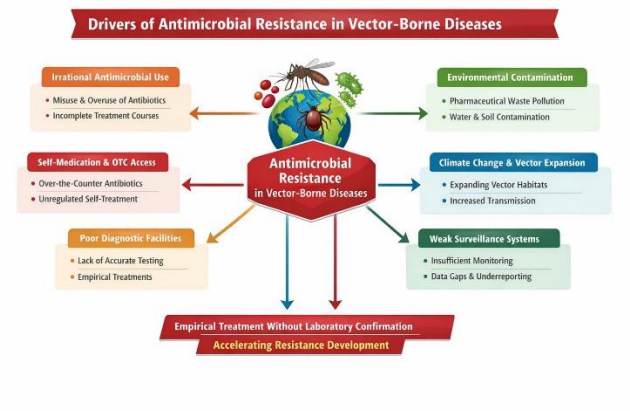

Molecular Mechanisms of Resistance:

Antimicrobial resistance (AMR) is a growing global health concern driven by the ability of microorganisms to adapt under selective drug pressure. Bacteria, parasites, viruses, and fungi develop resistance through genetic mutations, horizontal gene transfer, and physiological adaptations that reduce drug effectiveness. Several key molecular mechanisms contribute to the emergence and spread of resistance, and recent advances in genomic and molecular tools have significantly improved our understanding of resistance evolution and transmission.

One of the primary mechanisms of resistance is target site modification. Antimicrobial agents typically act by binding to specific cellular targets such as ribosomes, enzymes, or structural proteins. Mutations in genes encoding these targets alter their structure, reducing drug binding without affecting normal cellular function. For example, mutations in DNA gyrase and topoisomerase IV confer resistance to fluoroquinolones, while alterations in ribosomal RNA lead to resistance against macrolides and aminoglycosides. In some cases, microorganisms acquire alternative target proteins, such as the mecA-encoded penicillin-binding protein (PBP2a) in methicillin-resistant Staphylococcus aureus (MRSA).

Another important mechanism involves efflux pump overexpression, where membrane-bound transport proteins actively expel antimicrobial agents from the cell. These pumps reduce intracellular drug concentration below therapeutic levels and often confer multidrug resistance. Major efflux systems include the resistance-nodulation-division (RND) family in Gram-negative bacteria and major facilitator superfamily (MFS) transporters found across diverse microbial species. Efflux-mediated resistance is particularly significant because a single system can protect against multiple classes of antibiotics.

Enzymatic degradation or modification of drugs is also a major contributor to AMR. Microorganisms produce enzymes that chemically inactivate antibiotics before they reach their targets. The most well-known example is β-lactamase, which hydrolyzes β-lactam antibiotics such as penicillins and cephalosporins. Extended-spectrum β-lactamases (ESBLs) and carbapenemases, including KPC and NDM, represent critical threats in clinical settings. Other enzymes modify aminoglycosides through acetylation, phosphorylation, or adenylation, rendering them ineffective. Many of these resistance genes are located on plasmids, facilitating rapid horizontal transfer between species.

Changes in gene copy number through gene amplification or deletion also play a role in resistance. Amplification of genes encoding drug targets or resistance proteins increases their expression, thereby reducing drug efficacy. For instance, overproduction of dihydrofolate reductase contributes to trimethoprim resistance. Conversely, deletion or alteration of metabolic

pathways targeted by antimicrobial agents allows microorganisms to bypass drug action. Regulatory mutations that increase expression of resistance determinants further enhance survival under antimicrobial stress.

In bacterial pathogens, biofilm formation provides an additional protective strategy. Biofilms are structured microbial communities embedded in an extracellular polymeric matrix that limits antibiotic penetration. Cells within biofilms exhibit reduced metabolic activity, making them less susceptible to drugs that target actively growing organisms. Biofilms also harbor persister cells and promote horizontal gene transfer, contributing to chronic and recurrent infections associated with medical devices, wounds, and respiratory diseases.

Recent advances in genomic and molecular technologies have transformed AMR research and surveillance. Whole-genome sequencing (WGS) enables precise identification of resistance genes, mutations, and mobile genetic elements. Metagenomic approaches allow detection of resistance determinants in environmental and clinical samples without culturing. Transcriptomics and proteomics provide insights into gene expression patterns, including efflux pump activation and enzyme production. These tools support real-time outbreak tracking, prediction of resistance evolution, and development of targeted antimicrobial therapies.

In summary, antimicrobial resistance arises through multiple interconnected mechanisms, including target modification, drug efflux, enzymatic inactivation, genetic adaptation, and biofilm formation. Integration of molecular biology, genomics, and bioinformatics is essential for understanding resistance dynamics and guiding effective treatment, surveillance, and antimicrobial stewardship strategies.

One Health Perspective:

The One Health approach recognizes the interconnectedness of human, animal, and environmental health. Key components include:

- Monitoring antimicrobial residues in water and soil
- Surveillance of zoonotic vector-borne pathogens
- Coordinated human and veterinary antimicrobial stewardship
- Integrated vector management (IVM)

Strategies to Address the Dual Threat:

1. Strengthening Surveillance:

Effective surveillance is a cornerstone of antimicrobial resistance (AMR) control, enabling timely detection, monitoring of trends, and informed public health interventions. Strengthening surveillance systems involves coordinated global monitoring, advanced molecular tracking, and early warning mechanisms.

Global AMR Monitoring Networks:

International surveillance networks collect and analyze data on antimicrobial use and resistance patterns across regions. Programs such as the World Health Organization's Global Antimicrobial Resistance and Use Surveillance System (GLASS) and regional initiatives integrate laboratory and clinical data to track resistance trends in priority pathogens. These networks support evidence-based policy-making, guide treatment guidelines, and facilitate international collaboration to control the spread of resistant organisms.

Molecular Tracking of Resistance Markers:

Advances in molecular diagnostics and genomic technologies allow precise identification of resistance genes and mutations. Techniques such as polymerase chain reaction (PCR), whole-genome sequencing (WGS), and metagenomic analysis help detect specific resistance

determinants (e.g., mecA, blaNDM, blaCTX-M) and monitor their transmission between hospitals, communities, animals, and the environment. Molecular epidemiology provides insights into the evolution, clonal spread, and horizontal gene transfer of resistant strains, improving outbreak investigation and containment strategies.

Early Warning Systems:

Early detection systems integrate laboratory data, genomic surveillance, and digital reporting platforms to identify emerging resistance threats in real time. Rapid reporting of unusual resistance patterns, multidrug-resistant organisms, or novel resistance genes enables timely infection control measures, antimicrobial stewardship interventions, and public health alerts. Data integration through electronic health systems and national surveillance platforms enhances responsiveness and preparedness for emerging AMR threats.

2. Antimicrobial Stewardship:

Antimicrobial stewardship programs (ASPs) are essential to optimize antibiotic use and slow the emergence of antimicrobial resistance (AMR). Rational prescription practices involve evidence-based therapy, appropriate drug selection, correct dosing, and duration guided by diagnostic testing and clinical guidelines. Public awareness programs promote responsible antibiotic use, discourage self-medication, and improve understanding of AMR risks through community education and mass communication. Regulation of drug sales through strict prescription policies, monitoring of over-the-counter distribution, and enforcement of pharmaceutical standards helps reduce misuse and inappropriate access. Integrated stewardship interventions across healthcare systems and communities significantly reduce unnecessary antimicrobial consumption and improve treatment outcomes.

3. Vector Control:

Effective vector control is a critical component in reducing the transmission of vector-borne diseases and indirectly limiting antimicrobial use and resistance. Integrated vector management (IVM) combines chemical, environmental, and biological approaches to achieve sustainable control while minimizing ecological impact.

Insecticide-treated nets (ITNs), including long-lasting insecticidal nets (LLINs), are among the most effective interventions for preventing mosquito-borne diseases such as malaria and dengue. These nets act as both a physical barrier and a chemical deterrent, reducing human–vector contact and vector survival. Widespread distribution and community-level use of LLINs have significantly reduced disease incidence and mortality in endemic regions. However, continuous monitoring is necessary due to the emergence of insecticide resistance in vector populations.

Environmental management focuses on modifying or eliminating vector breeding sites to reduce population density. This includes proper waste disposal, drainage of stagnant water, improved water storage practices, urban sanitation, and habitat modification. Environmental approaches are cost-effective, sustainable, and reduce reliance on chemical insecticides, thereby lowering the risk of resistance development and ecological contamination.

Biological control methods utilize natural predators, pathogens, or symbiotic organisms to suppress vector populations. Examples include larvivorous fish (Gambusia spp.), bacterial larvicides such as Bacillus thuringiensis israelensis (Bti) and Bacillus sphaericus, and the release of Wolbachia-infected mosquitoes to reduce vector competence. These eco-friendly

strategies provide long-term control and are increasingly incorporated into integrated vector management programs.

Overall, combining insecticide-based tools with environmental and biological interventions enhances the effectiveness and sustainability of vector control while supporting broader public health efforts to reduce disease burden and antimicrobial pressure.

4. Research and Innovation:

Research and innovation play a vital role in combating vector-borne diseases and antimicrobial resistance (AMR) by improving prevention, diagnosis, and treatment strategies. Advances in biomedical science, data analytics, and genomics are accelerating the development of effective and sustainable control measures.

Development of new drugs and vaccines is essential to address the declining efficacy of existing therapeutics due to resistance. Novel antimicrobial agents, antiparasitic drugs, and transmission-blocking compounds are being designed to target new molecular pathways. Simultaneously, vaccine research for diseases such as malaria, dengue, and leishmaniasis aims to reduce infection rates, disease severity, and dependence on antimicrobial treatment, thereby lowering selective pressure for resistance.

Combination therapies are increasingly used to enhance treatment efficacy and delay resistance development. By using two or more drugs with different mechanisms of action, combination regimens reduce the likelihood of pathogen survival and mutation. Examples include artemisinin-based combination therapies (ACTs) for malaria and multidrug regimens for tuberculosis and leishmaniasis. Such strategies improve clinical outcomes and extend the therapeutic lifespan of existing drugs.

AI-based disease prediction models are transforming public health surveillance and outbreak preparedness. Machine learning and artificial intelligence integrate epidemiological, climatic, environmental, and demographic data to predict disease outbreaks and vector distribution patterns. These predictive tools support early intervention, targeted vector control, and efficient resource allocation, particularly in high-risk regions.

Genomic surveillance has become a powerful tool for monitoring pathogen evolution and resistance dynamics. Whole-genome sequencing and molecular epidemiology enable the identification of resistance genes, mutations, and transmission pathways. Genomic data support real-time tracking of emerging resistant strains, outbreak investigation, and the development of precision treatment and control strategies.

Collectively, these innovations strengthen global capacity to manage vector-borne diseases and mitigate the spread of antimicrobial resistance through evidence-based, technology-driven approaches.

Future Challenges and Research Needs:

1. Expansion of Resistance into New Geographic Areas:

Climate change, globalization, urbanization, and increased human mobility are facilitating the spread of resistant pathogens and vectors into previously non-endemic regions.

Expansion of mosquito and tick habitats is increasing the geographic range of diseases such as dengue, malaria, chikungunya, and leishmaniasis.

Cross-border transmission of resistant strains through travel, trade, and migration complicates containment efforts.

Strengthening cross-national surveillance and coordinated regional response strategies is

essential to monitor and control emerging resistance hotspots.

2. Limited Pipeline of New Antimicrobials:

The development of new antibiotics and antiparasitic drugs has slowed significantly due to high research costs, regulatory challenges, and low commercial incentives.

Many pharmaceutical companies have reduced investment in antimicrobial research, creating a gap between rising resistance and available treatment options.

There is an urgent need for innovative drug discovery approaches, public–private partnerships, and economic incentives to support antimicrobial development.

Alternative strategies such as drug repurposing, host-directed therapies, and novel delivery systems are gaining research attention.

3. Integration of Climate Data into Disease Models:

Temperature, rainfall, humidity, and extreme weather events strongly influence vector survival, breeding, and pathogen transmission dynamics.

Incorporating climate and environmental data into epidemiological and predictive models can improve early warning systems for vector-borne disease outbreaks.

Climate-informed risk mapping helps guide targeted vector control, vaccination campaigns, and resource allocation.

Interdisciplinary collaboration between public health, climatology, and data science is critical for accurate forecasting.

4. Development of Rapid Diagnostic Tools:

Delayed or inaccurate diagnosis often leads to empirical and unnecessary antimicrobial use, accelerating resistance.

There is a growing need for rapid, point-of-care diagnostic tools that can:

- Differentiate between bacterial, viral, and parasitic infections
- Detect resistance markers quickly
- Support evidence-based treatment decisions

Advances in molecular diagnostics, biosensors, CRISPR-based detection, and portable sequencing technologies show promise for field-level applications in resource-limited settings.

5. Strengthening Health Systems in Endemic Regions:

Many high-burden regions face limitations in laboratory infrastructure, trained personnel, surveillance systems, and access to quality medicines.

Weak healthcare systems contribute to delayed diagnosis, inappropriate treatment, counterfeit drug use, and poor antimicrobial stewardship.

Strengthening primary healthcare, laboratory capacity, supply chains, infection prevention measures, and community health programs is essential.

Integration of One Health approaches addressing human, animal, and environmental health can improve long-term control of antimicrobial resistance and vector-borne diseases.

Conclusion:

The convergence of antimicrobial resistance and vector-borne diseases represents a growing global health threat. Resistance in pathogens such as Plasmodium and Leishmania, along with the misuse of antibiotics in managing vector-borne infections, is compromising treatment effectiveness. Addressing this challenge requires coordinated global action, strengthened surveillance, improved antimicrobial stewardship, and integrated vector

control strategies. Adoption of the One Health framework and investment in research and innovation are essential to prevent the escalation of this dual burden and to ensure sustainable disease control in the future.

Acknowledgements:

I am grateful to the Department of Zoology/Fisheries Science, Rajarshi Shau Mahavidyalaya Autonomous Latur-413521 for providing laboratory facilities. I express my sincere gratitude to my research supervisor Dr. Amjad Khan Pathan for his constant guidance, valuable suggestions, and encouragement throughout the course of this research work. I am also deeply thankful to Dr. K. N. Kadam, Principal, Maharashtra Mahavidyalaya, Nilanga, for providing the necessary facilities and administrative support to carry out this study.

I extend my heartfelt thanks to Dr. D. S. Rathod, Dr. K. S. Raut, and Dr. Kundan Tayade for their valuable assistance in data collection, analysis, and administrative support, which greatly contributed to the successful completion of this research

References:

1. Allen, H. K., et al. (2010). Call of the wild: Antibiotic resistance genes in natural environments. Nature Reviews Microbiology, 8, 251–259.
2. Alvar, J., Vélez, I. D., Bern, C., et al. (2012). Leishmaniasis worldwide and global estimates of its incidence. PLoS ONE, 7(5), e35671.
3. Alonso, P. L., & Tanner, M. (2013). Public health challenges and prospects for malaria vaccines. Nature Reviews Microbiology, 11, 284–295.
4. Ashley, E. A., et al. (2014). Spread of artemisinin resistance in malaria. New England Journal of Medicine.
5. Ayukekbong, J. A., Ntemgwa, M., & Atabe, A. N. (2017). The threat of antimicrobial resistance in developing countries. Antimicrobial Resistance & Infection Control, 6, 47.
6. Banerjee, R., & Vanita, V. (2021). One Health approach to antimicrobial resistance in vector-borne and zoonotic diseases. Frontiers in Public Health, 9, 675349.
7. Barlam, T. F., et al. (2016). Implementing an antimicrobial stewardship program. Clinical Infectious Diseases, 62(10), e51–e77.
8. Bebell, L. M., & Muiru, A. N. (2014). Antibiotic use and emerging resistance in resource-limited settings. BMJ Global Health, 349, g6572.
9. Benelli, G., & Beier, J. C. (2017). Current vector control challenges and future directions. Acta Tropica, 174, 1–9.
10. Boelaert, M., et al. (2014). Evaluation of rK39 rapid diagnostic tests for visceral leishmaniasis. PLoS Neglected Tropical Diseases, 8(5), e2830.
11. Butler, D., et al. (2020). Combination therapies and resistance management. The Lancet Infectious Diseases, 20(2), e42–e51.
12. Caminade, C., McIntyre, K. M., & Jones, A. E. (2019). Impact of climate change on vector-borne diseases. The Lancet Planetary Health, 3(7), e267–e278.
13. Centers for Disease Control and Prevention (CDC). (2022). Leishmaniasis: Resources for health professionals. Atlanta, USA.
14. Centers for Disease Control and Prevention (CDC). (2022). Vector-borne diseases and emerging threats.

15. Centers for Disease Control and Prevention (CDC). (2023). Antibiotic resistance threats in the United States.
16. Chopra, A., & Venugopalan, A. (2014). Chikungunya: Clinical aspects and management challenges. The Lancet Infectious Diseases, 14(4), 319–327.
17. Desjeux, P. (2004). Leishmaniasis: Current situation and new perspectives. Comparative Immunology, Microbiology and Infectious Diseases, 27(5), 305–318.
18. Dyar, O. J., et al. (2017). Strategies and challenges of antimicrobial stewardship. Clinical Microbiology and Infection, 23, 793–798.
19. Eisen, R. J., & Eisen, L. (2018). Environmental determinants of Lyme disease risk. Environmental Health Perspectives, 126(4), 045001.
20. Gardy, J. L., & Loman, N. J. (2018). Towards a genomics-informed public health system. Nature Reviews Genetics, 19, 9–20.
21. Ginsburg, A. S., et al. (2020). Diagnostic challenges and empirical antibiotic use in low-resource settings. Clinical Infectious Diseases, 71(Suppl 2), S145–S151.
22. Holmes, A. H., et al. (2016). Understanding the mechanisms and drivers of antimicrobial resistance. The Lancet, 387, 176–187.
23. Intergovernmental Panel on Climate Change (IPCC). (2022). Climate Change and Health Report.
24. Karkman, A., Do, T. T., Walsh, F., & Virta, M. P. (2018). Antibiotic resistance genes in wastewater. Trends in Microbiology, 26(3), 220–228.
25. Laxminarayan, R., et al. (2013). Antibiotic resistance—the need for global solutions. The Lancet Infectious Diseases, 13(12), 1057–1098.
26. Laxminarayan, R., et al. (2020). Global solutions to antimicrobial resistance. The Lancet Infectious Diseases, 20(3), e79–e88.
27. Lee, I. K., Liu, J. W., & Yang, K. D. (2015). Risk factors for bacteremia in dengue patients. American Journal of Tropical Medicine and Hygiene, 92(2), 221–226.
28. Moyes, C. L., et al. (2017). Status of insecticide resistance in mosquito vectors. The Lancet Infectious Diseases, 17(11), e361–e371.
29. Murray, C. J. L., et al. (2022). Global burden of bacterial antimicrobial resistance. The Lancet, 399, 629–655.
30. O'Neill, J. (2016). Tackling drug-resistant infections globally: Final report and recommendations.
31. O'Neill, J. (2022). Global strategies to combat antimicrobial resistance.
32. Okeke, I. N., et al. (2005). Antimicrobial resistance in developing countries. Emerging Infectious Diseases, 11(5), 641–648.
33. Peeling, R. W., et al. (2017). Diagnostics for infectious diseases in resource-limited settings. Nature Reviews Microbiology, 15, 731–744.
34. Prestinaci, F., Pezzotti, P., & Pantosti, A. (2015). Antimicrobial resistance: A global multifaceted phenomenon. Pathogens and Global Health, 109(7), 309–318.
35. Ranson, H., & Lissenden, N. (2016). Insecticide resistance in mosquito vectors. Annual Review of Entomology.
36. Ready, P. D. (2013). Biology and control of sand fly vectors. Annual Review of Entomology, 58, 227–250.

37. Reithinger, R., et al. (2007). Cutaneous leishmaniasis. The Lancet Infectious Diseases, 7(9), 581–596.
38. Schönian, G., et al. (2003). PCR diagnosis of Leishmania species. Journal of Clinical Microbiology, 41(7), 3147–3153.
39. Semenza, J. C., & Suk, J. E. (2018). Climate change and vector-borne diseases. European Journal of Public Health, 28(Suppl 4), 1–5.
40. Soundravally, R., et al. (2015). Secondary bacterial infections in dengue. Journal of Infection in Developing Countries, 9(12), 1281–1287.
41. Sundar, S., & Chakravarty, J. (2018). Treatment challenges in leishmaniasis. Clinical Epidemiology.
42. Sundar, S., & Rai, M. (2002). Laboratory diagnosis of visceral leishmaniasis. Clinical and Diagnostic Laboratory Immunology, 9(5), 951–958.
43. Thein, T. L., et al. (2017). Bacterial infections in dengue patients. BMC Infectious Diseases, 17, 468.
44. Topol, E. J. (2019). AI and the future of healthcare. Nature Medicine, 25, 44–56.
45. Ventola, C. L. (2015). The antibiotic resistance crisis: Causes and threats. P&T, 40(4), 277–283.
46. Vittecoq, M., et al. (2016). Antimicrobial resistance in wildlife and vector ecosystems. Frontiers in Microbiology, 7, 1722.
47. Wellington, E. M., et al. (2013). Environmental dimensions of antibiotic resistance. The Lancet Infectious Diseases, 13(2), 155–165.
48. Wilson, A. L., et al. (2020). Importance of vector control for disease elimination. PLoS Neglected Tropical Diseases, 14(1), e0007831.
49. World Health Organization (WHO). (2010). Control of the Leishmaniases. WHO Technical Report Series No. 949.
50. World Health Organization (WHO). (2022). Global action plan on antimicrobial resistance.
51. World Health Organization (WHO). (2022). Global vector control response 2017–2030.
52. World Health Organization (WHO). (2023). Dengue and severe dengue.
53. World Health Organization (WHO). (2023). Global Antimicrobial Resistance and Use Surveillance System (GLASS) Report.
54. World Health Organization (WHO). (2023). Global research agenda for antimicrobial resistance.
55. World Health Organization (WHO). (2023). Leishmaniasis.
56. World Health Organization (WHO). (2023). World Malaria Report.

International Journal of Advance and Applied Research
www.ijaar.co.in
ISSN – 2347-7075 Impact Factor – 8.141
Peer Reviewed Bi-Monthly
Vol. 7 No. 14 January – February - 2026

Production, Purification and Assay of Pectinase Enzyme from Orange Peels

Umakant G. Shinde[1] & Sanjay R. Biradar[2]

[1]*Assistant Professor, Biotechnology Department Deogiri College, Chhatrapati Sambhajinagr (M.S.) INDIA.*

[2]*Professor& Head, Department of Botany, BSS Arts Commerce and science college Makani-413604, Dist. Dharashiv. (M.S.) INDIA.*

Corresponding Author – Umakant G. Shinde

DOI - 10.5281/zenodo.19827648

Abstract:

Production of microbial enzymes at the industrial scale and their commercialization has gained a lot of focus and importance. Use of Microbes as bioreactors was also started due to these developments. Some of the industrially important enzymes from microbial origin include and Pectinases. The organisms were isolated from the fruit peel and were cultured on to Sabouraud Dextrose Agar (SDA) agar Plate . The organisms were screened to produce the Pectinase enzyme using Pectin agar media. Microscopic identification and Morphology study revealed that the Fungi isolated was Aspergillus niger. The enzyme thus produced was purified by several steps including Salt precipitation. The purified product was used for the Enzyme assay which showed that the activity of the enzyme produced was 0.043µmol/min/mg. Quantitative estimation of the enzyme was performed by Lowry's Method which showed the concentration of the enzyme to be 24µg/ml.

The results thus obtained can conclude that the use of Aspergillus niger in the industrial production of Pectinase is highly beneficial.

Keywords: Pectinase, Orange peel extract (OPE), Aspergillus niger, Enzyme assay.

Introduction:

The Pectinases are the enzymes that can hydrolyse the Pectin polysaccharide into smaller fragments. All the peels of the fruits are made of pectin layer which can be easily digested by the microbial pectinases to extract the juices of the fruits. Therefore, pectinase enzymes are commonly used in processes involving the degradation of plant materials, such as speeding up the extraction of fruit juice [1].

At present, almost all the pectinolytic enzymes used for industrial applications are produced by the fungi, namely *Aspergillus sp., Rhizopusstolonifer, Alternaria mali, Fusariumoxysporum, Neurosporacrassa, Penicillium italicum*- ACIM F152, and many others. Orange peels are used as substrate for the growth of *Aspergillus niger*. The high cost used in the importation of industrial extracellular enzymes has led to the high cost of finished industrial products. Besides, orange peels cause waste disposal problems since they are being thrown around indiscriminately. This study is therefore aimed at the production of pectinase from *A. niger,* purifying enzyme and assaying the enzyme activity [2].

Pectin or other pectic substances are heterogeneous group of high molecular weight polysaccharides with galacturonic acid residues linked by (1-4) linkages [1]. Pectin's constituting

middle lamella found between the primary cell walls of adjacent young plant cells [2]. There are four main types of pectic substances protopectin, pectic acid, pectinic acid and pectin. Pectin's are the soluble polymeric materials containing pectinic acids as the major component. They can form insoluble protopectin with other structural polysaccharides and proteins located in the cell wall. There are basically three types of pectic enzymes: de-esterifying enzymes (pectinesterases), depolymerizing enzymes (hydrolases and lyases), and protopectinases. They can be further classified as: endo-liquefying or depolymerizing enzymes or exo-saccharifying enzymes [1]. Pectic enzymes contribute to the degradation of pectin by various mechanisms. Elimination of pectic substances is an essential step in many foods processing and wine industries. These enzymes are mainly synthesized by plants and microorganisms [3]. Fungi synthesize polygalacturonases, polymethyl galacturonases, pectin lyases and pectin esterases. The biotechnological potential of pectinolytic enzymes from microorganisms has drawn a great deal of attention for use as biocatalysts in a variety of industrial processes [4]. Compared to non-enzymatic chemical catalysts, biocatalysts (enzymes or whole- cell microorganisms) are known to present some interesting and advantageous features: high efficiency, mild environmentally friendly operation conditions, versatility and high selectivity (chemo-, region- and stereo-selectivity) [5]. The low-cost substrates are used to reduce production costs to produce industrial enzymes [6]. For the industrial production of pectinolytic enzymes, it is important to improve the fermentation conditions for the better production of extracellular enzymes on inexpensive carbon sources such as apple pomace, citric peels, and other agricultural wastes which contain appreciable quantities of pectin [7] and are degradable by lyases and hydrolases of pectinases [8]. Pectinases have extensive commercial importance for various industrial food applications like in fruit juice industries in order to improve fruit juice yield and clarity. The use of liquefying enzymes for mash treatment results in improvement of juice flow, as maceration of tea leaves [9], processing of cotton fabric [10], leading to a shorter press-time, without the necessity for pressing aids. At the same time pectin is broken down into such an extent that the viscosity of mash is reduced as viscosity relates to molecular weight [11-13]. Pectinases are produced during the natural ripening process of some fruit and act in combination with cellulase. Many microbial strains have been studied to produce pectinase [14]. The main sources for the pectinolytic complex enzymes are yeast, bacteria and many filamentous fungi of which the most relevant ones are Aspergillus sp. The pectinase production in yeast has received less attention due to less yield obtained in comparison to bacteria [15]. A range of bacterial and fungal strains produce a variety of pectinolytic enzymes [16, 17]. The selection of high yield pectinase producing strain is difficult, however studies revealed that bacterial strains usually have been shown to produce more yield of pectinolytic enzymes than those of fungal ones [18]. The objectives of the present study were the screening, isolation and identification of pectinase producing bacterial strains from rotten citrus fruit samples (oranges) and determination of their pectinolytic activity [19].

Materials and Methods:

1. Isolation of Pectinolytic Fungi from Orange Peels:

Orange peels (~1 kg) have been collected and the peels were kept under moist condition for

few days in the air tight condition. Once the rotting of the peels began, the growth of the fungi started. This was used as the inoculums for the isolation of the organisms from the peel.[20]

2. Media Preparation Phase:

Sabouraud Dextrose Agar (SDA), Czapek Dextrose broth (CDB), Potato Dextrose broth (PDB) was prepared as mentioned Deepanwita Deka et al., 2018 [21] and further utilised specifically for the growth of dermatophytes and other types of fungi.

3. Screening for the Pectinase Enzyme Production:

Phosphate buffer is used for the selective growth of these pectin-releasing microorganisms. Prepared according to the following composition of agar plate to screen the pectinase enzymes production.. Briefly, 0.2 gm KH_2PO_4,0.3 gm K_2HPO_4, 0.01gm $MgSO_4$ and 2.5 gm agar were added in to 100 ml of distilled water. After the media prepared and sterilized, agar plate was prepared. Microbial culture was spread out on the agar plate by simple streak plate technique. The plate is stored in an inverted manner at room temperature for microbial growth. After incubation, the plates were screened to identify hydrolysed areas, indicating a positive result from pectinase production. In addition, the obtained colonies were observed under a microscope. [22].

4. Pectinase enzyme production by liquid state fermentation:

Aspergillus niger inoculum was inoculated in a basal medium for the production of pectinase, which consisted of 0.2 gm KH_2PO_4, 0.3 gm K_2HPO_4, 0.01 gm $MgSO_4$ and 1 g of pectin in 100 ml of distilled water. The media pH 4.5 was set and sterilized media with autoclave at 121°C for 15 min. Media was Incubated by using submerged liquid fermentation at 25°C for 10 to 12 days. [22].

5. Crude Enzyme Extraction by Filtration:

The crude enzymes were separate from mycelia mat by using spore bodies filtration technique. The broth was filtered through Whatman No. 1 filter paper and then centrifuge at 10,000 rpm for 15 minutes. Crude enzymes extract supernatant was used for measuring the pectinase activity.

6. Partial purification of enzyme by Ammonium sulfate precipitation and dialysis:

Ammonium sulfate precipitation was used for the partial purification of the crude enzymes. 44 gm of ammonium sulfate was added in to 100 ml suspension of crude enzymes and Pinch-by-pinch ammonium sulphate was used complete saturation of the enzymes under cold condition. Further purification was done by using dialysis (ref. for dialysis). [23].

7. Enzyme assay using pectin and its estimation by lowry method:

Pectinesterase activity was measured by increase in free carboxyl group by titrating against NaOH in the present of a Phenolphthalein (PH indicator). Briefly, 20 ml of 1% pectin was dissolved in 0.5M NaCl (pH -7) with 4 ml of crude enzyme extract was incubated for 1 hour. After incubation, the solution was titrated against 1 N NaOH to reach PH 7 using Phenolphthalein as indicator. Colour change was observed from colourless to pink.

Pectin esterase activity = Vs – Vb (Normality of NaOH) ×100/Vt 50

Where, Vs- Volume of NaOH used to titer sample (ml), Vb- Volume of NaOH used to titer blank (ml), V - Volume of incubation mixture (ml), t - Reaction time (min).

Pectin esterase activity was expressed as milli equivalents of NaOH consumed min $^{-1}$ per ml $^{-1}$ of crude enzyme extract [24]. The protein concentration was measured by Lowry's Method [25].

8. Enzyme Immobilization:

The enzymes was immonilized by using sodium aliinate beads. 0.3 gm of sodium alginate was dissolved in 10 ml distilled water and mixed well. 3 ml purified enzymes was added into the sodium alginate. The pectinase-alginate mixture was dropped in the rythmic mannor into 2 % calcium chloride solution by using a syringe. Pectinase-alginate mixture was polymerized into the calcium chloride solution and bead was fromed. [26].

Results and Discussion:

1. Isolation, Screening and identification of the Fungi:

Isolation of Aspergillus niger from orange peel was represented in Figure (1). Fungi colonies was collected from the fruit peels and growth on the Sabouraud Dextrose agar (SDA) agar plate, Czapek Dextrose broth, and Potato Dextrose broth (figure 2). The pectinase producing fungi was grown on the SDA media, because SDA media contains pectin as main substrate which support the selectively growth to pectinase producing fungi. Light green and black colonies were observed after 10th day of inoculation. The cells were densely populated and filamentous growth was seen after 15 days of inoculation. The mycelia were stained with lacto phenol cotton blue and observed under 40X magnification (figure 3 A and B). Based on the colony morphology the Mycelia were identified as Aspergillus niger [29]. The culture was further used for production the enzyme using PSAM medium. All morphological contrasting colonies were isolated by repeated streaking and sub culturing. Genus was identified by relating the microscopic features of the cultures to "Atlas of Mycology" by Barnett and Hunter (1972) [30].

Figure (1): Fungus isolation, [A] storage of orange peels in Ziplock bag, [B] initiates the growth of fungi, [C] obtained rotten peels as a source of fungi.

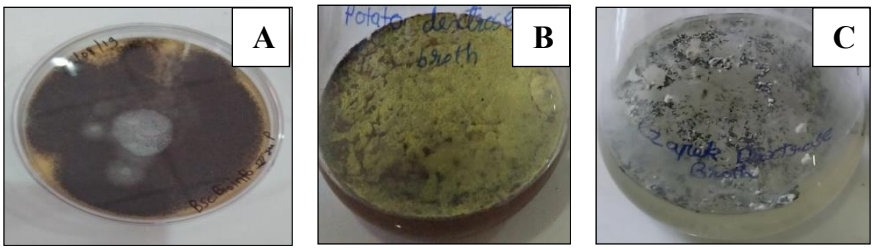

Figure (2): Fungus growth obtained by employing, [A] Sabouraud Dextrose agar, [B] Czapek Dextrose broth, [C] Potato Dextrose broth.

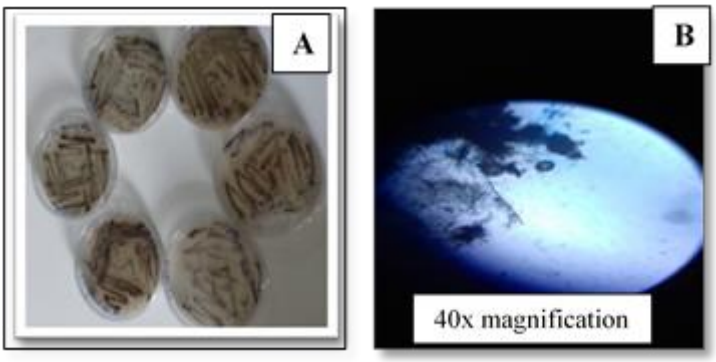

Figure (3): Fungus growth, [A] Sabouraud Dextrose agar, [B] microscopically mycelium was identified as *Aspergillus niger*.

3. Pectinase enzyme production by liquid state fermentation and its partial purification:

The culture of previous step was further used to produce the enzyme using PSAM medium. The culture was incubated for 20 days for the complete production of the extracellular enzyme. The enzyme thus produced was purified by several techniques like Filtration, Centrifugation, Salt precipitation dialysis and immobilization as shown in figure (4). The purified product was used for the Enzyme assay which showed that the activity of the enzyme produced was **0.043µmol/min/mg**. Quantitative estimation of the enzyme was performed by Lowry's Method which showed the concentration of the enzyme to be **24µg/ml.**

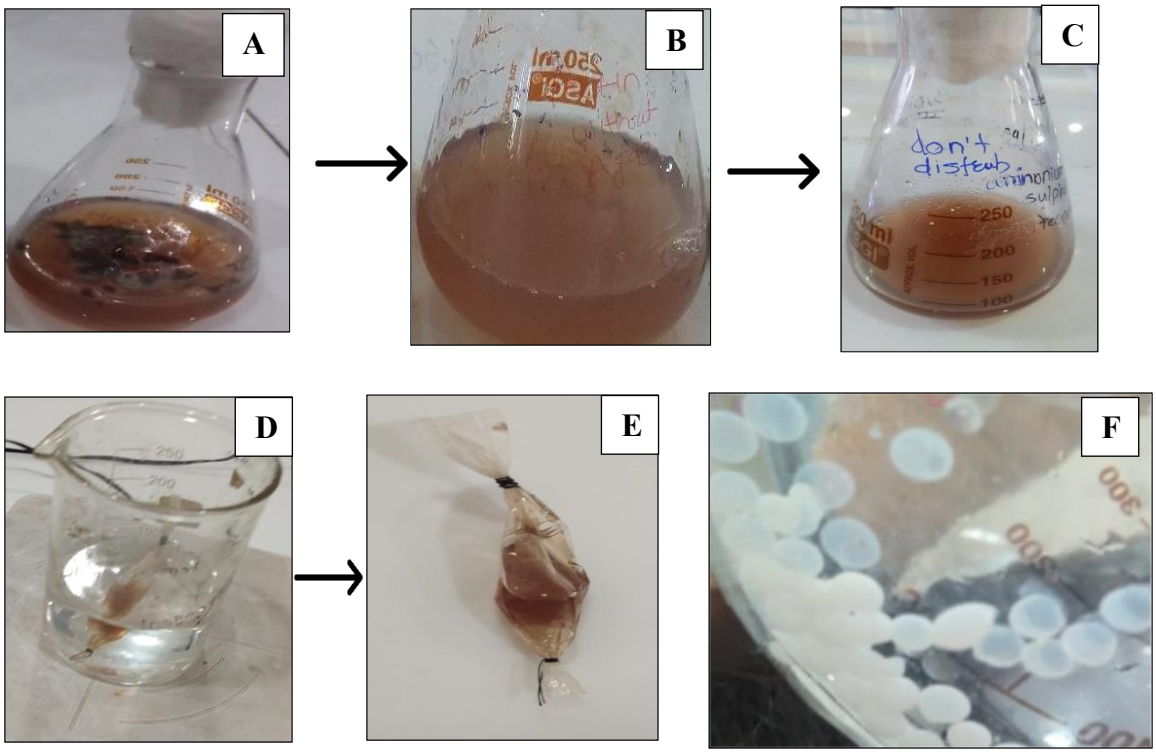

Figure (4): Partial purification steps of an enzyme includes; [A] Pectinase enzyme production, [B] Crude enzyme extraction by filtration, [C] Ammonium sulfate precipitation, [D] Dialysis [E] partial pure enzyme solution and [F] Enzyme immobilization.

Conclusion:

This investigation recommends that orange peel could be an alluring and promising substrate to deliver pectinases by *Aspergillus niger*. The crude enzyme was further purified by using Salt precipitation dialysis. The purified product was used for the Enzyme assay which showed that the activity of the enzyme produced was 0.043µmol/min/mg. Quantitative estimation of the enzyme was performed which showed the concentration of the enzyme to be 24µg/ml. In addition, this work will go as a promising data to scientists who need to investigate the potential outcomes of changing over waste to riches and value addition. Since orange peels used in this cycle are promptly open as waste with practically zero cost and furthermore contain an obvious measure of pectin, they can be viewed as an ease substrate for proficient and conservative creation of pectinases utilizing Fungi. Immobilized enzyme further can be used in food industry.

References:

1. Oyeleke SB, Oyewole OA, Egwim EC, Dauda BE, Ibeh EN. (2012)Cellulase and pectinase production potentials of Aspergillus niger isolated from corn cob. Bayero Journal of Pure and Applied Sciences.;5(1):78-83.
2. Anisa SK, Ashwini S, Girish K. (2013) Isolation and screening of Aspergillus spp. for pectinolytic activity. Electronic journal of biology.;9(2):37-41.
3. Kashyap DR, Chandra S, Kaul A, Tewari R. (2000) Production, purification and characterization of pectinase from a Bacillus sp. DT7. World journal of Microbiology and Biotechnology. Apr 1;16(3):277-82.
4. Kanmani P, Dhivya E, Aravind J, Kumaresan K. (2014) Extraction and analysis of pectin from citrus peels: augmenting the yield from Citrus limon using statistical experimental design. Iranica Journal of Energy & Environment.;5(3):303-12.
5. El-Enshasy HA. (2007) Filamentous fungal cultures–process characteristics, products, and applications. InBioprocessing for Value-Added Products from Renewable Resources Jan 1 (pp. 225-261). Elsevier.
6. Gummadi SN, Panda T. (2003) Purification and biochemical properties of microbial pectinases—a review. Process biochemistry. Feb 28;38(7):987-96.
7. Darah I, Nor-hawani S, Hong L, Rosma A, Haritharan W. Pomelo (2013) peels as alternative substrate for extracellular pectinase production by Aspergillus niger HFM-8. Malaysian Journal of Microbiology.;9(4):308-16.
8. Castilho LR, Medronho RA, Alves TL. (2000) Production and extraction of pectinases obtained by solid state fermentation of agroindustrial residues with Aspergillus niger. Bioresource Technology. Jan 1;71(1):45-50.
9. Martos MA, Martinez Vazquez F, Benassi FO, Hours RA. (2009) Production of pectinases by A. niger: influence of fermentation conditions. Brazilian Archives of Biology and Technology. Jun;52(3):567-72.
10. Torimiro N, Okonji RE. (2013) A comparative study of pectinolytic enzyme production by Bacillus species. African Journal of Biotechnology.;12(46):6498-503.

11. Akhter N, Morshed MA, Uddin A, Begum F, Sultan T, Azad AK. (2011) Production of pectinase by Aspergillus niger cultured in solid state media. Int J Biosci.;1(1):33-42.
12. Gomaa OM, Momtaz OA, Abd El Kareem H, Fathy R. (2011) Isolation, identification, and biochemical characterization of a brown rot fungus capable of textile dye decolorization. World Journal of Microbiology and Biotechnology. Jul 1;27(7):1641-8.
13. Geetha M, Saranraj P, Mahalakshmi S, Reetha D. (2012) Screening of pectinase producing bacteria and fungi for its pectinolytic activity using fruit wastes. Int J Biochem Biotech Sci.; 1:30-42.
14. Naderi S, Naghavi NS, Shahanipoor K. (2012) Pectinolytic Activity of Aspergillus Niger on Pectic Agricultural Substrates. InThe 1st International and the 4th National Congress on Recycling of Organic Waste in Agriculture, Isfahan, Iran Apr 26 (pp. 1-6).
15. Banakar SP, Thippeswamy B. (2014) Isolation, production and partial purification of fungal extracellular pectinolytic enzymes from the forest soils of Bhadra Wildlife Sanctuary, Western Ghats of Southern India. Journal of Biochemical Technology. Jun 5;3(5):138-43.
16. Kashyap DR, Vohra PK, Chopra S, Tewari R. (2001) Applications of pectinases in the commercial sector: a review. Bioresource technology. May 1;77(3):215-27.
17. Hoondal G, Tiwari R, Tewari R, Dahiya NB, Beg Q. (2002 Jan) Microbial alkaline pectinases and their industrial applications: a review. Applied microbiology and biotechnology. 1;59(4-5):409-18.
18. Naidu GS, Panda T. (1998 Nov) Production of pectolytic enzymes–a review. Bioprocess Engineering. 1;19(5):355-61.
19. Tewari R, Tewari RP, Hoondal GS. (2005) Microbial pectinases. Microbial Enzymes and Biotransformations: Springer;. p. 191-208.
20. Schmid A, Dordick J, Hauer B, Kiener A, Wubbolts M, Witholt B. (2001) Industrial biocatalysis today and tomorrow. Nature; 409:258-68.
21. Deka D, Jha DK. (2018 Sep) Optimization of culture parameters for improved production of bioactive metabolite by endophytic Geosmithia pallida (KU693285) isolated from Brucea mollis Wall ex. Kurz, an endangered medicinal plant. Journal of Pure and Applied Microbiology. 1;12(3):1205-13.
22. Alkorta I, Garbisu C, Llama MJ, Serra JL. (1998 Jan) Industrial applications of pectic enzymes: a review. Process Biochemistry. 1;33(1):21-8.
23. Sethi BK, Nanda PK, Sahoo S. (2016 Jun) Enhanced production of pectinase by Aspergillusterreus NCFT 4269.10 using banana peels as substrate. 3 Biotech. 1;6(1):36.
24. Mayorga H, Rolz C. (1971 Jan)Pectinesterase activity as a function of pH, enzyme, and cation concentrations. Journal of Agricultural and Food Chemistry;19(1):179-81.
25. Peterson GL. (1983) Determination of total protein. Methods in enzymology.; 91:95-119.Discovery of pectin-degrading enzymes and directed evolution of a novel pectate lyase for processing cotton fabric. Journal of Biological Chemistry. 2005 Mar 11;280(10):9431-8.

26. de Oliveira RL, Dias JL, da Silva OS, Porto TS. (2018 May) Immobilization of pectinase from Aspergillus aculeatus in alginate beads and clarification of apple and umbu juices in a packed bed reactor. Food and bioproducts processing. 1; 109:9-18.
27. McDevitt S. Methyl Red and Voges-Proskauer Test Protocols. (2009) American Society for Microbiology. Dec 8.
28. Biemer JJ. (1973) Antimicrobial susceptibility testing by the Kirby-Bauer disc diffusion method. Annals of Clinical & Laboratory Science. Mar 1;3(2):135-40.
29. Mailafia S, God'spower Richard Okoh HO, Olabode K, Osanupin R. (2017) Isolation and identification of fungi associated with spoilt fruits vended in Gwagwalada market, Abuja, Nigeria. Veterinary world. Apr;10(4):393.
30. Chandra Reddy MP, Saritha KV. (2016) Effects of the culture media optimization on pectinase production by Enterobacter sp. PSTB-1. 3 Biotech. Dec 1;6(2):207.
31. Sandri IG, Silveira MM. (2018) Production and application of pectinases from Aspergillus niger obtained in solid state cultivation. Beverages;4(3):48.
32. Garg G, Singh A, Kaur A, Singh R, Kaur J, Mahajan R. (2016) Microbial pectinases: an ecofriendly tool of nature for industries. 3 Biotech. Jun 1;6(1):47.

International Journal of Advance and Applied Research
www.ijaar.co.in
ISSN – 2347-7075 Impact Factor – 8.141
Peer Reviewed Bi-Monthly
Vol. 7 No. 14 January – February - 2026

AI for Sustainable Development

Dr. Rahul Bharti
Assistant Professor,
Government College Junnardeo, Chhindwara M.P.
Corresponding Author – Dr. Rahul Bharti
DOI - 10.5281/zenodo.19827700

Extract:
Artificial Intelligence (AI) is revolutionizing sustainability, emerging as a key driver for achieving SDGs. A Delphi survey of experts reveals AI's strategic role in boosting progress across climate, education, and healthcare. Statistical analysis confirms consensus experts agree AI accelerates SDG attainment.

Keywords: Artificial Intelligence, Sustainability, Revolutionizing, Consensus

Introduction:

Generative AI is revolutionizing efforts to achieve the UN's Sustainable Development Goals (SDGs) by 2030, tackling poverty, inequality, climate change, and environmental decay. AI-driven solutions optimize resource allocation to combat poverty (SDG 1), forecast weather patterns for climate resilience (SDG 13), and accelerate disease diagnosis for better healthcare (SDG 3). The challenge now is scaling these innovations ethically and inclusively to ensure no one is left behind. AI is reshaping the global economy by fueling innovation, boosting efficiency, and aligning with SDGs. Corporations adopt AI to streamline operations, cut costs, and craft sustainable models, fostering economic stability. In developing nations, AI acts as a catalyst—bypassing traditional paths, it tackles core issues like poverty, hunger, and healthcare. Example: AI-powered agriculture optimizes yields, combating food insecurity (SDG 2). AI is revolutionizing clean energy transitions by powering innovations in solar, wind, and grid management. Tools now forecast energy demand, predict maintenance needs, and optimize grids—boosting efficiency and cutting fossil fuel dependence. Smart grids, designed by AI, streamline citywide energy use, making clean energy accessible and affordable. This directly fuels SDG 7 ensuring universal access to affordable, clean energy, even in underserved regions.

Artificial Intelligence (AI) is transforming sustainability by driving environmental conservation, climate action, and social equity. It analyzes satellite data to track deforestation, predicts weather extremes for disaster prep, and optimizes renewable energy grids. AI also powers smart cities, streamlining energy and traffic, while enhancing healthcare/education access for underserved communities. Yet, challenges persist: AI mirrors data biases, and its training consumes energy. So, ethical deployment, green algorithms, and renewable power are critical to harness AI sustainably. The first frontier in this journey is AI's role in environmental protection. By analyzing vast datasets, AI systems can predict

environmental trends and offer solutions to mitigate risks. Environmental monitoring with AI, for instance, plays a crucial role in tracking pollution levels, deforestation rates, and wildlife activities, enabling proactive responses to ecological threats.

The UN's Agenda 2030 (SDGs)—ending poverty, saving the planet, ensuring prosperity—faces huge hurdles post-COVID and amid conflicts. Pandemics deepened inequalities, wrecked economies, and strained healthcare. Geopolitics blocked global teamwork, skewing resources. So, achieving SDGs by 2030 needs a reboot: innovation. Enter AI—a potential game-changer turbocharging sustainable progress. The UN's 2030 Agenda for Sustainable Development outlines 17 SDGs for peace, prosperity, and sustainability. Achieving these linked goals needs integrated approaches tackling poverty, ecosystems, peace, and growth. Sustainability science is key, and AI offers new tools—systems thinking, data insights. AI can analyze datasets, predict climate trends, and solve challenges. But AI's growth is nation-driven, unevenly distributed, and outpaces ethics/regs. So, does AI transform sustainability research? A review of 792 SDG+AI studies shows a gap: few bridge AI tech with deep sustainability expertise. Bridging this gap is critical.

Future Directions and Opportunities:

Agricultural AI innovations could revolutionize farming and food systems, with hyperspectral imaging and drone sensors enhancing crop and soil monitoring. Future agriculture will leverage AI for data-driven, precision crop management, improving yield and sustainability. To ensure equitable access, governments must invest in digital infrastructure, while partnerships should drive research and capacity-building. Regulations should govern ethical AI use and data protection for all stakeholders. The integration of Artificial Intelligence (AI) in agriculture has brought about a significant revolution. AI-powered technologies like automated irrigation, robotic weeding, and sensor-based spraying have addressed challenges such as climate change impacts, population growth, and labor shortages. These innovations not only conserve water and reduce chemical usage but also enhance productivity and crop quality. AI continues to play a pivotal role in ensuring food security and sustainability in farming practices worldwide. Artificial Intelligence (AI) enhances energy management by analyzing data to forecast demand patterns, thereby improving efficiency and minimizing waste. AI also supports the circular economy by extending the lifecycle of materials and energy through advanced analytics and predictive models. In urban settings, AI-driven smart grids and management systems enable real-time adjustments in energy distribution, facilitating the integration of renewable energy sources and reducing reliance on fossil fuels. AI's decision-support capabilities further promote energy-efficient building designs and urban planning strategies, while insights into consumer behavior encourage sustainable energy practices. Overall, AI plays a pivotal role in advancing energy decarbonization and sustainability efforts in the built environment.

Conclusion:

AI can turbocharge SDGs via healthcare precision, personalized learning, smart cities, precision farming, green energy, and conservation. But hurdles remain: ethics, privacy, access gaps, digital divides. Solution? Interdisciplinary teamwork, capacity building, and policies to harness AI's power sustainably—equitably. Investing in AI boosts SDGs via

healthcare, education, smart cities, farming, green energy, and conservation. It optimizes resources, sharpens decisions, and solves problems—if done right. But sustained investment is key to tackling ethics, privacy, and access gaps. Prioritize AI, unlock a sustainable future.

Reference:

1. *Transforming Our World: The 2030 (*2015*) Agenda for Sustainable Development* (United Nations).
2. *The Sustainable Development Goals Report 2023* (United Nations, 2023).
3. Sharda, V. N., Patel, R. M., Prasher, S. O., Ojasvi, P. R. & Prakash, C. Modeling runoff from middle Himalayan watersheds employing artificial intelligence techniques. *Agric. Water Manage.*

International Journal of Advance and Applied Research
www.ijaar.co.in
ISSN – 2347-7075 Impact Factor – 8.141
Peer Reviewed Bi-Monthly
Vol. 7 No. 14 January – February - 2026

Nanoparticles Applications: For Environmental Friendliness, And Cost Effectiveness, Sustainable Agriculture

Rahul Kashid[1], Santosh Talekar[2] & Navnath Kashid[3]

[1 & 2]Department of Botany, Kesharbai Sonajirao Kshirsagar College Beed, MS.

[3]Department of Botany, Baburaoji Adaskar Mahavidyalaya, Kaij, Beed, MS.

Corresponding Author – Rahul Kashid

DOI - 10.5281/zenodo.19827726

Abstract:

Food security has become a critical concern in globe due to the rise in human population and the current climate change crisis. Usage of conventional agrochemicals to maximize crop yields has resulted in the degradation of fertile soil, environmental pollution as well as human and agro ecosystem health risks. Due to use of different chemical fertilizers, pesticides and, other agrochemicals products for increasing crop yield have adverse effect on biodiversity, soil fertility, and in turn on the ecosystems. Recently, nanoparticles have been recognized as potential fertilizers with properties that make them more absorbable and readily available for plant use than their bulk counterpart. Nanoparticles are gaining a reputation in the field of agriculture for the remediation of soil degradation in a sustainable way. The application of nanoscaled nutrient elements such as silver, zinc, copper, iron, titanium, magnesium and calcium as fertilizers and utilizing green synthesized nanomaterials as one of the ways to palliate the use of environmentally toxic chemicals in the cropping system and discusses the various benefits of nanoparticles, ranging from plant growth stimulation to defence against pathogens.

Nanoparticles (NPs) due to their compact size, ease of transport, ease of handling, long shelf life, and high efficiency make it the preferred choice of farmers over other conventional products. In depth, it delts with negative and positive impact of nanoparticles on different crops, water treatment for irrigation purposes, nanocarriers and fertilizers, nanoparticles for plant protection Nanoinsecticides, Nanopesticides, Nanofungicides, Nanoherbicides, Nanobactericides, Nanosensors, slow or controlled release fertilizers, clay nanotubes and Nanobarcodes have been applied in multiplexed bioassays and general encoding in biological and nonbiological applications.

Keywords: Agriculture; Nanoparticles; Nanofertilizers; Plant Growth.

Introduction:

Nanotechnology is defined as the scientific knowledge to manipulate and control matter in the nanoscaled range to make use of size- and structure-dependent properties and phenomena distinct from those at smaller or larger scales (Roco, M.C, 2011). The use of nanomaterials dates from 4500 years ago. In some civilizations, nanofibers were used for the reinforcement of ceramic matrixes. In addition, the ancient Egyptians of the third century used NMs for the production of different forms of dyes (Jeevanandam *et, al.* 2018). The development of nanotechnology has resulted in the production of nanoparticles with many applications in different fields, such as the food industry, medicine and textiles (Luksiene, 2017).

In agriculture, their usage as fertilizers and pesticides has been reported in many studies. Elements such as silver, zinc, copper, iron,

silicon, titanium, magnesium, and manganese have been supplied to plants in different forms, hence, having a beneficial effect on their growth and yield as they fight against infections and act as fertilizers or carriers of nutrients (Rastogi *et,al*.2019) Although scientific reports have demonstrated the applications of Nanofertilizers and nanoparticles in crop nutrition and pest control, the adoption of this sustainable alternative is still in its infancy. Hence, this review, therefore, aims to provide insights into the broad agricultural applications of nanoparticles as Nanofertilizers.

The usage of living structures in nanoparticles production is a real alternative to physical and chemical processes owing to its environmental friendliness and cost-effectiveness. Biosynthesis of nanoparticles using plants has been demonstrated to be green chemistry that interconnects plant sciences with nanotechnology and helps achieve the synthesis of nanoparticles at room temperature, neutral pH and a low cost without the use of environmentally harmful chemicals (Parveen *et, al.* 2016). Plants and their by-products have demonstrated essential properties in the synthesis process of nanoparticles as their usage is more beneficial than other systems (Siddiqui *et,al.*2015).

They are increasingly being used because they facilitate the development of nanoparticles and increase the success rate of synthesis, as researchers strive to build upscaled processes of mono dispersed and stable nanoparticles (Iravani,*et,al*.2015). The conventional approach for making metallic nanoparticles from plants employs a reducing agent derived from dried plant biomass and a metallic salt as a precursor.

Biomolecules such as phenolics, alkaloids, flavonoids, terpenoids, enzymes and proteins have been reported to be involved in the synthesis reaction (Ovais *et,al.* 2018). Hence, it has been reported that the hydroxyl groups present in carbohydrates, amino acids, proteins and nucleic acids of plants act in the stabilization of ENPs (Dorjnamjin *et,al.* 2008). Green synthesis of nanoparticles is becoming a very insightful topic nowadays. There is rising attention to the use of organisms. The biological production of metallic and metal oxide nanoparticles is less harmful to the environment than the current chemical or physical approaches.

Plants have shown a large interest in expanding the biosynthesis of nanoparticles on a large scale as the plant-mediated nanoparticles are very stable and have diverse sizes and shapes compared to the ones produced through other biological systems (Ramesh et,al.2014). Synthesized nanoparticles can be carbon-based or metal-based. The most produced and used metal-based engineered nanoparticles are zinc oxide ZnO), titanium dioxide (TiO2), gold (Au), silver (Ag), cerium oxide (CeO2) and copper oxide (CuO) or dioxide (Cu2O) nanoparticles. Other nanoparticles, such as Mn, Fe3O4, CuO, CaO and Fe3O4, are also widely used and produced (Rico *et,al*.2015).

To maximize yields and alleviate poverty and malnutrition, nanoparticles have been recognized as highly beneficial for plant biomass production and enhancement of crop nutritional quality. This review highlighted the attributes of biosynthesized nanomaterials as sustainable alternatives to conventional chemical fertilizers. These potential agro-inputs can be readily absorbed by plants and are environmentally friendly crop nutrient supplements (Ca, Mg and Fe NPs), with advantages beyond fertilization. The use of nanoparticles, such as Ti, Ag and Zn, which can be integrated into cropping systems to enhance the plant's defence mechanism, against disease attack. However, fewer studies have investigated the broad application of

nanoparticles in pest and disease management, offering an opportunity for future research in crop protection.

Although the application of nanoparticles has been revolutionary for crop productivity, the response of plant-associated microorganisms to nano-based amendments remains unclear. Similarly to bulk chemical fertilizers or pesticides, nano-based agricultural amendments may have an impact on plant-associated microorganisms. Exposure of plant-associated microorganisms to nanoparticles can either be beneficial or harmful depending on various factors. Hence, further investigation on the interaction and response of plant-associated microorganisms to nanoparticles is warranted to ensure sustainable precision agricultural practices. Microorganisms are extremely important for overall soil and plant health (Goswami *et al.,* 2016). Diverse genera of microorganisms have been identified in soils and crops, and they play an important role in the regulation of agro ecosystem productivity, soil physicochemical characteristics, and plant health (Dinca *et al.,* 2022).

A vast majority of plant-associated microorganisms are found in the soil, near plant roots in the region called the rhizosphere, where they serve essential ecological functions such as promoting plant growth (Bello-Akinosho *et al*.,2021). Although plants associated microorganisms can exert both negative and postive impacts of on the host plants, the focus of this review is majorly on the impact on beneficial plant associated microrogamisms.

Previous research in plant microbe interactions has laid the foundation by describing certain factors, sometimes referred to as filters that influence the association. Most notable of these filters is the host plant chemistry, environmental conditions as well as microbe-microbe interactions (Saunders *et al*., 2010). However, what is not clear is the potential influence of other external factors that are introduced through anthropogenic means linked to technological advancement. One system in which plant-microbe relationship could be impacted is the use of nanomaterials in agro-ecosystem.

Application of Nanoparticles on Plants as Fertilizers:

Applications of nanomaterials are becoming increasingly popular, especially with their usage as Nanofertilizers and nanopesticides for precision and sustainable agriculture. Unfortunately, there is no existing guideline that reflects their potential impacts on plant associated microbes. Hence, this review aims to provide insights about existing literatures on this topic and reflects on potential implication for sustainable agricultural practices.

Integrating cutting-edge nanotechnology into agriculture, including fertiliser creation, is considered one of the greatest feasible methods to significantly increase crop yield and sustain the world's constantly growing population (Lal, R.2008).The application of nanoparticles in agriculture as fertilizers is attributed to their improved characterization, absorption and responsiveness, as well as surface and adhesion effects (Chhipa,H.2017).

Nanofertilizers are macro or micronutrient fertilizers that are used to increase agricultural yields and have a particle size of less than 100 nm. Nanofertilizers are nanomaterials responsible for providing one or more types of nutrients to growing plants, supporting their growth and improving production (Chhipa, H. 2017).They are presented in two different types. On one hand, the nanomaterials supply nutrients to plants to improve their development and yield,

on the other, they are the carriers of nutrients and only assist in the transport and release of nutrients without directly being used as anutrient source (Liu,R.;2015).

Nanoparticles' Adverse Effects:

Biosynthesized nanoparticles offer enormous potential to alleviates tress, boost growth and improve agricultural production. However, the unintentional release of some nanoparticles into the environment poses a threat to both aquatic and land plants(Ranjan et, al.2021).For instance, in their study, (Tarrahi et,al.2019) reported the adverse effect of CdSe nanoparticles on the morphology and peroxidase enzyme of common Duckweed (Lemna minor), with it having an increased concentration of superoxide dismutase enzyme, catalase, phenols and flavonoids, in contrast with the results of (Movafeghi *et,al*.2019).

Furthermore, Zn, Se nanoparticles have been found to have a certain toxic effect on the growth of Lemna minor by triggering the plants' defence system due to phytotoxicity (Tarrahi *et,al*.2018). Furthermore, carbon nanotubes were found to trigger oxidative stress in red spinach. Hence, it is crucial to mention that the toxicity of nanoparticles depends on the method used for their production. Several studies have shown that plant-mediated nanoparticles present less to no eco-toxicity towards plants in general and aquatic plants in particular (Plachtová *et,al.* 2018).However, further investigations should be carried out to ascertain the effect of nanoparticles synthesized using plant species on aquatic plants.

Conclusions:

To maximize yields and all eviate poverty and malnutrition, nanoparticles have been recognized as highly beneficial for plant biomass production and enhancement of crop nutritional quality. This review highlighted the attributes of biosynthesized nanomaterials as sustainable alternatives to conventional chemical fertilizers.

These potential agroinputs can be readily absorbed by plants and are environmentally friendly crop nutrient supplements (Ca, Mg and Fe NPs), with advantages beyond fertilization. Thus, the review also highlighted the use of nanoparticles such as Ti, Ag and Zn, which can be integrated into cropping systems to enhance the plant's defence mechanism against disease attack. However, fewer studies have investigated the broad application of nanoparticles in pest and disease management, offering an opportunity for future research in crop protection.

References:

1. Begum, P.; Fugetsu, B. (2012). Phytotoxicity of multi-walled carbon nanotubes on red spinach (*Amaranthus tricolor* L) and the role of ascorbic acid as an antioxidant. *J.Hazard. Mater.* 243,212–222.
2. Bello-Akinosho, M., Ndaba, B., Roopnarain, A., Bamuza-Pemu, E., Nkuna, R.,Rama, H., et al. (2021). "Agro-ecosystem Bioremediation mediated by plant-microbe associations: a novel tool for bioremediation," in *Rhizo microbiome Dynamics in Bioremediation*, ed. K. Vivek (Boca Rotan, FL: CRC Press), 210–230. doi: 10.1201/9780367821593-11
3. Chhipa, H. (2017) Nanofertilizers and nanopesticides for agriculture. *Environ. Chem. Lett. 15*,15–22.
4. Dinca, L. C., Grenni, P., Onet, C., and Onet, A. (2022). Fertilization and soil microbial community: A review. *Appl. Sci*. 12:1198. doi: 10.3390/app12031198
5. Dorjnamjin, D.; Ariunaa, M.; Shim, Y.K. (2008) Synthesis of silver nanoparticles

using hydroxyl functionalized ionic liquids and their antimicrobial activity. *Int.J.Mol.Sci.*,*9*,807–820.

6. Goswami, D.,Thakker, J.N., and Dhandhukia, P.C.(2016). Portraying mechanics of plant growth promoting rhizo bacteria (PGPR): a review. *Cogent Food Agric.*2:1127500. doi: 10.1080/23311932.2015.1127500
7. Iravani,S.; Korbekandi, H.; Zolfaghari, B. (2015). Phytosynthesis of nanoparticles. *Nanotechnol. Plant Sci.*203–258.
8. Jeevanandam, J.; Barhoum, A.; Chan,Y.S.; Dufresne, A.; Danquah, M.K. (2018) Review on nanoparticles and nano structured materials: History, sources, toxicity and regulations. *Beilstein J.Nanotechnol.*,*9*,1050–1074.
9. Lal, R. Soils and sustainable agriculture. (2008). A review.*Agron.Sustain.Dev. 28*, 57–64.
10. Liu,R.;Lal,R.(2015). Potentials of engineered nanoparticles as fertilizers for increasing agronomic productions. *Sci. Total Environ. 514*,131–139.
11. Luksiene, Z. (2018) Nanoparticles and their potential application as antimicrobials in the food industry. In *Food Preservation*; Elsevier: *Int.J.Curr.Microbiol.App.Sci.7*,3325–3335.
12. Movafeghi, A.; Khataee, A.; Rezaee,A.; Kosari-Nasab, M.;Tarrahi, R. (2019).Toxicity of cadmium selenide nanoparticles on the green micro alga *Chlorella vulgaris*: Inducing antioxidative defense response. *Environ. Sci. Pollut. Res. 26*,36380–36387.
13. Ovais, M.; Khalil, A.T.; Islam, N.U.; Ahmad, I.; Ayaz, M.; Saravanan, M.; Shinwari, Z.K.; Mukherjee, S. (2018) Role of plant phytochemi- cals and microbial enzymes in biosynthesis of metallic nanoparticles. *Appl. Microbiol. Biotechnol. 102*, 6799–6814.
14. Parveen, K.; Banse, V.; Ledwani, L. (2016) Green synthesis of nanoparticles: Their advantages and disadvantages. In *AIPConference Proceedings*; AIP Publishing LLC: Melville, NY, USA,p. 20048.
15. Plachtová, P.; Medrikova, Z.; Zboril, R.; Tucek, J.; Varma, R.S.; Maršálek, B. (2018) Iron and iron oxide nanoparticles synthesized with greentea extract: Differences in ecotoxicological profile and ability to degrade malachite green. *ACS Sustain.Chem.Eng.6*, 8679–8687.
16. Qureshi,A.; Singh, D.K.; Dwivedi, S. (2017). Nano-fertilizers: Anovel way for enhancing nutrient use efficiency and crop productivity. Amsterdam, The Netherlands, (2017); pp.567–601.
17. Ramesh, P.; Rajendran, A.; Meenakshi sundaram, M. (2014).Green synthesis of zinc oxide nanoparticles using flower extract cassia auriculata. *J. Nanosci. Nanotechnol. 2*, 41–45.
18. Ranjan, A.; Rajput, V.D.; Minkina, T.; Bauer, T.; Chauhan, A.; Jindal, T. (2021). Nanoparticles induced stress and toxicity in plants. *Environ. Nanotechnol. Monit. Manag. 15*, 100457.
19. Rastogi, A.; Tripathi, D. K.; Yadav, S.; Chauhan, D. K.; Zivak, M.; Ghorbanpour, M.; El-Sheery, N.I.; Brestic, M. (2019). Application of silicon nanoparticles in agriculture.*3 Biotech 9*, 90.
20. Rico, C.M.; Peralta-Videa, J.R.; Gardea-Torresdey, J. L. (2015). Chemistry, biochemistry of nanoparticles, and their role in antioxidant defense system in plants. In *Nanotechnology and Plant*

Sciences; Springer: Berlin/ Heidelberg, Germany, pp. 1–17.

21. Roco, M.C. (2011). The long view of nanotechnology development: The National Nanotechnology Initiative at 10 years. In *Nanotechnology Research Directions for Societal Needs in 2020*; Springer: Berlin/Heidelberg, Germany, pp.1–28.
22. Saunders, M., Glenn, A. E., and Kohn, L. M. (2010). Exploring the evolutionary ecology of fungal endophytes in agricultural systems: using functional traits to reveal mechanisms in community processes. *Evol. Appl.* 3, 525–537. doi: 10.1111/j.1752-4571.2010.00141.x
23. Siddiqui, M.H.; Al-Whaibi, M.H.; Mohammad, F. (2015). *Nanotechnology and Plant Sciences*; Springer International Publishing: Cham, Switzerland,Volume,10, pp. 973–978.
24. Tarrahi, R.; Khataee, A.; Movafeghi, A.; Rezanejad, F. (2018).Toxicity of Zn Se nanoparticles to Lemna minor: Evaluation of biological responses. *J. Environ. Manag.226*, 298–307.
25. Tarrahi, R.; Movafeghi, A.; Khataee, A.; Rezanejad, F.; Gohari, G. (2019).Evaluating the toxic impacts of cadmium selenide nanoparticles on the aquatic plant Lemna minor. *Molecules, 24*, 410.

International Journal of Advance and Applied Research
www.ijaar.co.in
ISSN – 2347-7075 Impact Factor – 8.141
Peer Reviewed Bi-Monthly
Vol. 7 No. 14 January – February - 2026

Synthesis, Characterization and Antimicrobial analysis of Transition Metal Complexes of Thiosemicarabazone Schiff Bases

Gavhane V. S.[1], Shirsat A. J[2]., Jadhav. S. B[3]., Bharade A. E[4]

[1,2,3,4]R. B. Attal Arts, Science and Commerce College, Georai.

Corresponding Author – Gavhane V. S.

DOI - 10.5281/zenodo.19827739

Abstract:

Substituted Thiosemicarbazones and their Transition metal complexes are complexes that possess antitumor, antibacterial, antifungal and antiviral characteristics. In number of cases the reactivity of the ligand is mostly increased by the presence of central metal ion. The most related papers recently published are reviewed with a study to find a relationship between common structural features and activity. These synthesized metal complexes are characterized by CHNS elemental analysis and for their Antimicrobial Activity.

Keywords: Substituted Thiosemicarbazones, Antimicrobial activity.

Introduction:

Thiosemicarbazone are the compounds that have been studied for a considerable period of time for their biological properties. Traces of interest date back to the beginning of the 20th century but the first reports on their medical applications began to appear in the Fifties as drugs against tuberculosis and leprosy [1, 2]. In the Sixties their antiviral properties were discovered and a huge amount of research was carried out that eventually led to the commercialization of methisazone, Marboran, to treat smallpox [3]. In this period one of the first antitumor activity results was published [4]. Recently Triapine (3-aminopyridine-2-carboxaldehyde thiosemicarbazone) has been developed as an anticancer drug and has reached clinical phase II on several cancer types [5, 6]. Presently, the areas in which thiosemicarbazones are receiving more attention can be broadly classified according to their antitumor, antiaprotozoal, antibacterial or antiviral activities and in all cases their action has been shown to involve interaction with metal ions [7, 8].

Thiosemicarbazone Schiff bases have garnered a lot of interest due to their multifunctional metal-chelating properties, inherent biological activities and structural flexibility It was established that thiosemicarbazides were metal chelators before the discovery of their anti-tumour activity. In addition to the presence of the C=N and C=S bonds in their own structure, which is favourable for metal coordination, it possesses a flexible thiourea structure that can introduce different substituents or functional groups. The newly synthesized ligands were 2-pyridine formide-N-(4)- methylthiosemicarbazone [9] 2- pyridine formamide-3-piperidyl thiosemicarbazone [10], pyrazineformide –N-(4)-methylthiosemicarbazone.[11] The ligands and complexes were characterized by molar conductivities, magnetic susceptibilities and X-ray techniques. The synthesis of three bis(thiosemicarbazone) compounds formed by

the reaction of benzyl with either thiosemicarbazide, 4-Methyl thiosemicarbazide were reported by Alsop [12]. Gerbeleu [13]

Experimental:

Materials and Methods:

1-(2-hydroxybenzylidene)-4-Diethyl-thiosemicarbazide (LA) was prepared by changing and modifying a reported procedure of Scovil.[24] Salicylaldehyde were of reagent grade purchased from Sigma-Aldrich. All other chemicals were used of AR grade and used as supplied.

1.1-Synthesis of Schiff base ligand (LA) - (1-(2-hydroxybenzylidene)-4-Diethyl-thiosemicarbazide (LA):

Schiff base ligand LA was prepared by mixing together ethanolic solution of N-4-Diethyl-3-Thiosemicarbazide (0.01 M) and Salicylaldehyde (0.01M) in equimolar ratio. The resulting mixture refluxed for 30 minutes. This reaction mixture was chilled (overnight). Yellow colored shiny crystals were separate out which was filtered, washed repeatedly with alcohol and finally with ether.

1.2-Synthesis of Metal Complexes:

Hot methanolic solution of metal salt (1mmol) eg. Cobaltouschloride hexahydrate(0.23gm), Chromium chloride hexahydrate (0.26gm), Nickel chloride hexahydrate (0.23gm) were mixed with hot methanolic solution of ligand (2mmol). The reaction mixture was then refluxed for 1-2 hour on heating mantle. The solid precipitate formed was allowed to keep overnight then it was filtered, washed and dried in vacuum over anhydrous calcium chloride in desiccators (Yield-75-78%).

1.3-Physical Measurement:

Microanalytical data of the complexes were obtained from sophisticated test and Instrumentation Centre Cochin. Molar conductance was measured on the Elico (CM82T) conducting bridge. Molar conductance of Cr(III) and Co(II) complexes shows that they are electrolytic in nature while Ni(II) complex is nonelectrolyte. The melting points of all the complexes were determined by open capillary method.

Compound	Molar Cond. (Ω-1 cm2 mol-1)	Color	Yield	Elemental Analysis (%), Found (Calculated)				
				C	H	N	S	M
LA	—	Brown	80%	64.12 (64.1)	06.36 (05.7)	14.12 (14.0)	09.81 (10.71)	-
$[Cr(LA)_2]$	140	Brown	76%	58.95 (59.0)	05.19 (05.2)	12.90 (12.9)	09.81 (09.83)	08.26 (08.1)
$[Co(LA)_2]$	120	Dark Brown	75%	58.10 (58.3)	05.10 (05.1)	12.65 (12.7)	09.69 (09.73)	09.68 (09.1)
$[Ni(LA)_2]$	029	Yellow	75%	58.01 (58.4)	05.09 (05.1)	12.71 (12.7)	09.72 (09.73)	09.68 (09.0)

Antibacterial and Antifungal Activity:

Thiosemicarbazones and their metal complexes exhibit a wide variety of biological activity. [14, 15] The studies were carried out on Aspergillus niger, Fusarium oxasporium species and Staphylococcus aureus, Bacillus substilis species using paper disc method on appropriate medium. The susceptibilities of certain strains of bacteria and fungus to the thiosemicarbazone ligands and their transition metal complexes were evaluated by measuring the size of the bacteriostatic diameter. The result shows that the ligands (HEPT) as well as their metal complexes are more active against the bacteria and fungi and having high antimicrobial and antifungal activity which is almost equal to the activity of standard ciprofloxacin.

Table-2. Antibacterial and Antifungal activity of ligand(LA) and their transition metal complexes. [Diameter of inhibition zone in (mm)].

Ligand/Metal Complex	Antibacterial activity				Antifungal activity			
	Staphylococcus aureus		Bacillus substilis		Aspergillus Niger		Fusarium Oxysporium	
	250 ppm	500 ppm	250 ppm	500 ppm	250 ppm	500 Ppm	250 ppm	500 Ppm
LA	18	17	26	21	10	21	25	23
$[Cr(LA)_2]$	23	21	16	21	19	19	15	18
$[Co(LA)_2]$	19	18	29	25	14	20	14	27
$[Ni(LA)_2]$	10	15	21	27	25	21	18	26
Ciprofloxacin	34	36	43	45	22	24	31	38

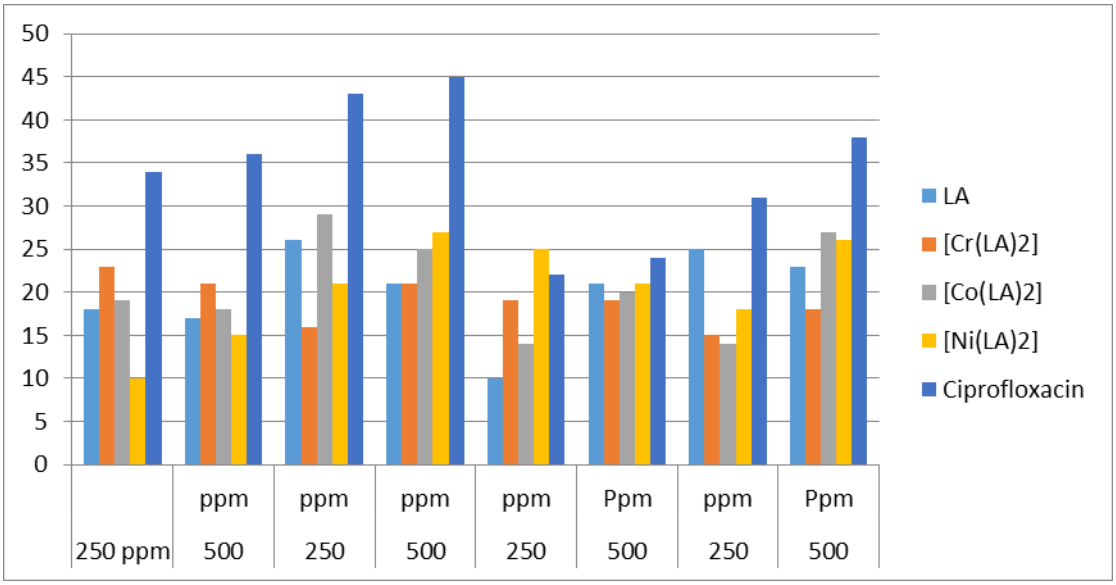

Graph-1. Comparative study of Antimicrobial and Antifungal activity of ligand and its transition metal complexes.

Conclusion:

From the analytical and spectral data it can be concluded that the synthesized complexes are stable. Ligand and its metal complexes as well show very high antibacterial and antifungal activity at both 250 ppm and 500 ppm concentration. In view of the foregoing discussions, the high melting points and insolubility in common organic solvents, also concluded that the three common coordinate sites are phenolic oxygen, azomethine nitrogen and thiol sulphur. It is observed that the Ni (II) complex of ligand contains two coordinated water molecules and possesses octahedral geometry.

References:

1. Bavin EM, Rees RJW, Robson JM, Seiler M, Seymour DE, Suddaby D. (1950) The tuberculostatic activity of some thiosemicarbazones. J Pharm Pharmacol; 2: 764-72.
2. Koch O, Stuttgen G. (1950) Clinical and experimental studies on the effects of thiosemicarbazones. Naunyn Schmiedebergs Arch Exp Pathol Pharmakol; 210: 409-23.
3. Kune GA. (1964) To-day's drugs: methisazone. Br Med J; 2: 621.
4. Sartorelli AC, Booth BA. (1967) Inhibition of the growth of sarcoma 180 ascites cells by combinations of inhibitors of nucleic acid biosynthesis and the cupric chelate of kethoxal bis-(thiosemicarbazone). Cancer Res; 27: 1614-9.
5. Nutting CM, van Herpen CML, Miah AB, et al. (2009) Phase II study of 3-AP Triapine in patients with recurrent or metastatic head and neck squamous cell carcinoma. Ann Oncol; 20: 1275-9.
6. Ma B, Goh BC, Tan EH, et al. (2008) A multicenter phase II trial of 3-aminopyridine-2-carboxaldehyde thiosemicarbazone (3-AP, Triapine) and gemcitabine in advanced non-small-cell lung cancer with pharmacokinetic evaluation using peripheral blood mononuclear cells. Invest New Drugs; 26: 169-73.
7. Finch RA, Liu MC, Cory AH, Cory JG, Sartorelli AC. (1999) Triapine (3-aminopyridine-2-carboxaldehyde thiosemicarbazone; 3-AP): an inhibitor of ribonucleotide reductase with antineoplastic activity. Adv Enzyme Regul; 39: 3-12.
8. Antholine W, Knight J, Whelan H, Petering DH. (1977) Studies of the reaction of 2-formylpyridine thiosemicarbazone and its iron and copper complexes with biological systems. Mol Pharmacol; 13: 89-98.
9. West D.X., Swearingen J.K., Martinez J.V., Ortega S.H., El-Sawaf A.K., Meurs F.V., Castineiras A., Garcia I. and Bezmejo.E., (1999) Polyhedron,; (18) 22: 24, 2919: 2929.
10. Ketcham K.A., Garcia I., Swearingen J.K., El-Sawaf A.K., Bermejo E., Castineiras A. and West D.X., (2002) Polyhedron,; (21) (15): 859:865.
11. Labisbal E., Sousa-Pedrares A., Castineiras A., Swearingen J.K. and West D.X., (2002) Polyhedron,; 21: 16, 1553:1559.
12. Alsop L., Cowley A.R., Dilworth J.R., Donnelly P.S., Peach J.M and Rider J.T., (2005) Inorg. Chimi. Acta.,; (358) (9): 2770: 2780.
13. Gerbeleu N.V., Revenko M.D. and Leovats V.M., (1977) Russ. J. Inorg. Chem., 22. 10009.
14. Thangadurai T. D., Gowri M. and Natarajan K., (2002) Synthesis and Reactivity in Inorganic, Metal-Organic and nano metal chemistry; (32): 329.
15. Kizileikli J., Kurti Y. D., Akkurt B., Genel A. Y., Birteksoz S., Otut G. and Ulkuseven (2007) B., Folia Microbial; (52): 15.

International Journal of Advance and Applied Research
www.ijaar.co.in
ISSN – 2347-7075 Impact Factor – 8.141
Peer Reviewed Bi-Monthly
Vol. 7 No. 14 January – February - 2026

A Comprehensive Review of Organic Farming in India: Current Status, Challenges, Benefits, and Future Prospects

D. S. Ghogare

Department of Botany, MSS's Arts, Science and Commerce College, Ambad, District Jalna, Maharashtra, India.

Corresponding Author – D. S. Ghogare

DOI - 10.5281/zenodo.19852424

Abstract:

Organic farming has surfaced as a sustainable agricultural method that responds to increasing concerns regarding environmental damage, food safety, and health issues linked to traditional farming techniques. This extensive review explores the present condition, challenges faced, advantages gained, and future outlook for organic farming in India. The research compiles insights from peer-reviewed articles, governmental publications, and empirical studies released between 2000 and 2023. Findings reveal that India ranks ninth worldwide in terms of land dedicated to organic agriculture, with around 2.3 million hectares cultivated organically, and holds the top position for the number of organic producers with over 1.3 million farmers engaged in this practice. Organic farming showcases enhanced environmental outcomes by improving soil health, conserving biodiversity, and lowering pollution levels. Economic evaluations suggest that while initial yields may drop by 9.2-25% during transition periods to organic practices, farmers benefit from net profits that are 22% higher due to price premiums ranging from 20-40%, along with an 11.7% reduction in production costs. Nonetheless, notable challenges remain, such as insufficient policy frameworks for domestic markets, limited access to organic inputs, high certification fees, and inadequate marketing infrastructure. This review highlights significant research deficiencies and offers policy recommendations aimed at fortifying India's organic farming sector while stressing the importance of region-specific strategies that marry traditional knowledge with scientific advancements.

Keywords: Organic Farming, Sustainable Agriculture, Food Security, Soil Health, India, Agricultural Policy.

Introduction:

Agriculture is a fundamental component of India's economy—employing roughly 54.6% of the workforce—and plays a crucial role in contributing to the national GDP (Karunakaran, 2021). The Green Revolution of the 1960s transformed India into a food-surplus nation through the use of high-yield crop varieties alongside chemical fertilizers and intensive irrigation practices. Although this technological advancement addressed immediate food supply issues effectively, it also led to environmental degradation, including soil nutrient depletion and groundwater pollution, along with health risks associated with pesticide residues (Yadav et al., 2013). The excessive application of chemicals has resulted in detrimental effects on soil ecosystems, including nutrient mining and loss of biodiversity across agricultural fields. Studies have shown that over half of India's land area suffers from desertification or degradation, largely attributed to chemically intensive agricultural methods (Sankar, 2011). Furthermore, concerns about pesticide

contamination in food products have heightened consumer anxiety regarding safety and nutritional value.

These pressing challenges have prompted a shift towards alternative agricultural systems emphasizing ecological stability and sustainable resource management practices. Organic farming is characterized by the International Federation of Organic Agriculture Movements (IFOAM) as "a production system that sustains the health of soils, ecosystems and people." It prioritizes ecological processes tailored to local conditions over synthetic substances known for their harmful impacts (Das et al., 2020). Integrating traditional wisdom with modern science, organic practices focus on managing soil health through crop rotations, green manures, biological pest control methods, and nutrient recycling techniques.

India's historical roots in organic agriculture can be traced back thousands of years, documented within ancient texts such as the Vedas, which describe methods for preserving soil fertility via natural means (Sofia et al., 2006). However, contemporary interest surged only after the initiation of the National Programme for Organic Production (NPOP) in the early 2000s, along with supportive policies.

The objectives outlined in this review are threefold:

1. To analyze current trends and growth patterns within Indian organic farming,
2. To assess the environmental, economic, and social benefits attributed to these practices,
3. To pinpoint obstacles hindering broader adoption while advocating evidence-based policy recommendations facilitating sustainable progress.

Methodology:

A systematic literature search was conducted targeting relevant studies focused on organic agriculture within India utilizing various academic databases such as Scopus Web of Science Google Scholar PubMed Research Gate using search terms like “organic farming” “sustainable agriculture” “India” “soil health” “organic certification,” among others restricted solely peer-reviewed journal articles government reports institutional publications published between years spanning from 2000 until 2023.

Initial searches generated approximately 16 700 results, subsequently filtered based on inclusion criteria emphasizing studies addressing either operational aspects concerning Indian practices examining environmental/economic ramifications or discussing existing regulatory frameworks/challenges encountered throughout this field’s growth narrative, resulting ultimately selecting 19 articles for full-text analysis.

Current Status of Organic Farming in India:

1. Global Overview:

Globally there has been remarkable expansion seen across trade occurring within organically managed lands totaling around 72 .3 million hectares distributed across 187 countries reported by end-year 2019 (Willer & Lernoud , 2020) where Australia leads occupying most space at approximately 35 .7 million hectares followed closely behind Argentina at about three-point seven million hectares Spain thereafter accounting two-point four million hectares respectively leaving an impression upon global landscape positioning itself ninth ranking attaining roughly two-point three million hectares under cultivation reflective making up one-point three percent total net sown area encompassing around one hundred forty point one million

hectares within country's territory according data sourced FiBL IFOAM reporting findings derived through close examination tracing back developments since beginning year two thousand-two wherein only forty-one thousand hectares previously accounted actual management being observed expanding twenty-five-fold five years later reaching figure nearing one point two million during period eight-nine indicating significant success trend continuing today marking highest population engaged certified production estimated around one thousand three hundred sixty-six thousand two hundred twenty-six farmers presently active participating efforts toward sustainability goals outlined earlier Karunakaran, 2021.

2. Regional Distribution:

The distribution pattern showcasing variances among various states illustrates notable concentrations found particularly in regions like Madhya Pradesh, commanding the largest share encompassing thirty-seven point seventy-four percent of the overall national totals, followed by Rajasthan, eleven point ten percent, Maharashtra, eight point fifty-seven percent, and Chhattisgarh, six point sixty percent, respectively(Sankar Reddy,2022). Other states significantly contributing include Himachal Pradesh, Jammu Kashmir, Karnataka, Uttar Pradesh, where Sikkim achieved status, becoming the first fully organic state recognized back dated year sixteen, demonstrating feasibility potential transitions occurring statewide levels effectively transforming landscapes positively moving forward, establishing models replicable elsewhere across the nation, promoting growth opportunities ahead amidst ongoing demands, changing climate realities facing us daily.

3. Production Export Performance:

During fiscal year nineteen-nineteen-twenty Indian economy produced nearly two-point seventy-five metric tons certified goods ranging categories including oil seeds sugarcane cereals millets cotton pulses medicinal plants tea coffee fruits spices processed foods(APEDA,2020) dominating sectors showing highest outputs witnessed oilseeds leading pack followed sugar crops then cereals trailing behind each segment holding unique contributions respective markets established overseas export values climbed upward reaching heights approximately six hundred thirty-eight thousand nine hundred metric tons generating foreign exchange earnings INR four thousand six hundred eighty-six crore equating roughly USD six hundred eighty-nine million major destinations identified include United States European Union Canada Switzerland Australia Japan Israel New Zealand(APEDA,2020).

Benefits of Organic Farming:

1.Environmental Advantages:

Evidence supports assertion claiming positive influences stemming directly from implementing properly managed systems exhibiting sound methodologies enhancing overall ecosystem functions measured several parameters consistently revealing improvements noted specifically relating aspects concerning increased presence beneficial organisms fostering resilience against threats posed external pressures enabling longevity maintained productivity sustained longer terms uninterrupted cycles employed creating healthier environments conducive thriving habitats allowing diverse life forms flourish (Bengtsson et al.,2005).

Biofertilizers play a pivotal roles maintaining long-lasting fertility structures, crucially integrating recurring elements enabling enhancements wherein nitrogen fixation occurs, mobilizing macro and micronutrients, converting unavailable phosphorus forms accessible to plants

helping enrich soils further enhancing utility derived crops themselves benefitting entire communities reliant producing them without resorting harmful synthetic alternatives protecting surrounding ecosystems preventing contamination burdens falling nature altogether(Gomiero et al.,2008).

2. Economic Gains:

Economic analyses depict favorable scenarios despite lower initial productivity rates experienced transitioning phases frequently impacting smallholder farmer groups less resilient adapting quickly circumstances emerging requiring patience facing uncertainties often discourage engagement required adopting new technologies(Ramesh et al.,2010) illustrating example thorough surveys conducted involving three hundred seventy-six individuals representing diverse backgrounds seven distinct states collectively concluding findings indicate profitability arises primarily driven factors involving substantial premium pricing coupled reduced input costs driving returns improving livelihoods beyond expectations set initially challenging conventional norms prevailing market dynamics altering perceptions gradually shifting towards sustainability ideals embraced widely accepting paradigm changes necessary embracing future considerations holistically (Charyulu Dwivedi,2016).

3. Social Health Impacts:

Beyond economic implications, social dimensions emerge prominently, influencing rural development initiatives and fostering employment generation. Notably, labor-intensive methodologies adopted inherently tend to create job opportunities, supporting livelihood diversification, essential to combating poverty alleviation goals (Bakewell-Stone et al.,2008).

Organic cooperatives enhance community networks, providing training resources, extension services, ensuring accessibility to vital healthcare programs, credit avenues, ultimately enriching the lives of participants involved in cultivating relationships, strengthening bonds, shared trust, working collaboratively, and achieving common objectives grounded in principles of equity, justice, and fairness upheld throughout processes undertaken.

Healthwise perspectives reveal considerable reductions detected regarding pesticide residues prevalent conventionally produced items consequently diminishing human exposure dangerous chemicals potentially harming well-being(Forman Silverstein ,2012) whilst discussions surrounding nutritional differentials persist some studies indicate superiority antioxidants vitamins minerals evidenced organically grown produce available marketplaces meeting rising demands informed consumers increasingly aware choices matter greatly determining futures built upon healthy foundations below surface levels visible outward appearances alone signify deeper truths lie beneath surface layers needing exploration understanding fully grasp complexities surrounding interconnectedness affecting everyone involved journey onward discovery paths lead both personal collective growth aspired towards inevitably leading brighter tomorrow awaits just ahead horizon beckoning forth possibilities abound waiting eagerly receive embrace wholeheartedly together united vision progress shared aspirations realized become tangible realities lived daily basis continuously striving achieve greatness sought after together hand-in-hand navigating waters unknown safely guided compass hearts minds aligned purpose-driven journeys embarked upon collectively unified front bolstering strength hope dreams fulfilled ultimately shaping destinies carved out existence evermore intertwined fates written stars

above shining brightly illuminating pathways treaded forth thereafter onward ever upward!

Methods Practices in Organic Farming:

1. Soil Fertility Management:

Principles guiding effective management revolve around the idea "feeding soil feeds plants". Key components involve utilizing farmyard manure vermicompost alongside biofertilizers employing ratios calculated meticulously, ensuring maximum efficiency is achieved, delivering essential nutrients required to sustain optimal growth levels maintained throughout lifecycle stages encountered varied climatic conditions experienced diverse contexts encountered locally adapted solutions rendered possible through collaborative efforts pooling expertise resources harnessed to maximize potential realized to the fullest extent possible! (Yadav et al.,2013)

Vermicomposting stands out distinctly, benefiting from earthworm-mediated decomposition processes, resulting in superior content compared to traditional compost types, providing necessary macro and micronutrients, growth hormones, enzymes, beneficial microorganisms, enhancing biological activity, enriching targeted outcomes aimed at elevating standards expected performance attained consistently irrespective of variability present varying circumstances confronted regularly encountered across board (Kumar Prakash Brar Kumar,2018)

Green manuring practices employing leguminous crops contribute significantly to fixing atmospheric nitrogen, forming symbiotic relationships, enhancing overall productivity, improving water retention capacities, simultaneously suppressing weed competition, reducing the need for herbicides, pesticides, and unnecessarily harming delicate balances existing naturally must be preserved to protect the integrity of systems functioning smoothly and efficiently (Sankar Reddy, 2022)

2. Pest Disease Control Strategies:

Preventive strategies underpinning successful pest management rely heavily on incorporating crop rotation, intercropping, conservation of natural enemies, botanical pesticides, leveraging natural processes, reducing reliance on external inputs, minimizing adverse impacts incurred surroundings ensure healthy balance is maintained ecosystem functions optimally performed realizing desired objectives collectively attained through innovative approaches adopted proactively rather reactively addressing emerging threats timely manner accordingly anticipated beforehand (Gaur Sharma,2010)

3. Weed Management:

In organic systems, we know weed-handling strategies are preventive, cultural, and mechanical. Weed cycle disruptions are caused by crop rotation, and weed expansion is inhibited by competitive crop canopies. The technique of stale seedbed provides for preparing seedbeds and weed germination before ending tillage, and thus helps decrease weed pressure. Mechanical weeding via hoeing and inter-cultivation, hand-weeding, and hand weeding continue to be fundamental but labor-intensive. Tying crop residues and plastic film around crops with mulch prevents weed emergence and conserves moisture in the soil.

Challenges and Constraints:

1. During Transition the yield reduction is high:

Most of the farmers switching from conventional to organic cultivation also experience a reduction of 9.2-25% in the first 2-3 years (Elayaraja & Vijai, 2020). This yield

surplus is due to the need for the time of the fertility cycle (i.e., restoration to nutrient cycling capacity of the soil biological processes) or establishment of pest-predator balances. Costs incurred during such a phase may prevent the adoption by resource-poor smallholders.

2. Input Quality and Availability:

Demand for organic nutrients from available organic resources is highly unsustainable in India. National nutrient requirements for an organics could only reach around 25-30% from organic sources (Chhonkar, 2002) according to existing figures. Competing animal feed or fuel uses often predominate; therefore, residues are of little availability for incorporating into soil. Further, poor quality natural, organic inputs, non-standardized inputs, and poor supply chain performance constrain organic production.

3. Certification and Distribution to the Market:

There is still a cost on organic certification – for small and marginal farmers, this can be a barrier of INR 15,000 - 50,000 annually, depending on both certification agencies and the size of the organic group itself (Jouzi et al., 2017). Bureaucratic documentation and inspection are other obstacles. Historically, the organic policy focused on exporting production in India without active market development. Therefore, it is insufficient standards of labeling, low awareness of consumers, and weak market infrastructure discourage premium price realization in the domestic marketplace.

4. Policy and Institutional Gaps:

Policy is still highly fragmented and not followed consistently, despite several government schemes of organic farming. Lack of comprehensive organic farming policies across state boundaries, insufficient support for research, and inadequate extension services pose challenges for technology transfer and farmer adoption (Pathania, 2020). Productivity is also restricted by the lack of organic seed production systems and variety creation programs in accordance with organic conditions.

Future Outlook and Suggestions:

1. Local Strategies of Organic Promotion:

India has heterogeneous agro-ecological zones; thus, region-specific organic farming strategies are requisite. An “on the organic side” which combines integrated crop management with lower chemical input might present a viable path for intensively cultivated food and grain producing regions. For rain-fed, hilly, and tribal villages marked by historically low chemical needs, “certified organic” options that tap traditional knowledge and practices could potentially help India compete at the top end of export markets of high value.

2. Strengthening Research and Extension:

Research on organic farm technologies must be conducted systematically and strengthened by network projects in agro-ecological zones. Among the areas of focus are the evolution of organic-specific varieties, organized organic input production plans, integrated pest control modules, and post-harvest management technologies. Farmer research and demonstration programs can quickly accelerate tech adoption and technology improvement.

3. Market Development and Infrastructure:

Building strong local organic markets that are strong at home demands a broad strategy from consumer campaigns and organic retail infrastructure, as well as links to markets. Farmer-Producer Organizations can be promoted as venues for certification, as collective certification of farmers, input procurement, and product sales platforms. The Participatory

Guarantee System is an inexpensive but potentially effective certification alternative for the domestic market.

4. Support and Institutional Framework:

Whole-system support at the national and state level for organic farming development in the transition phase, such as subsidies for inputs, technical assistance, and risk management, should be provided. Minimum support prices for organic produce, broken down by certification status, can help stabilize incomes for farmers. Including organic production in global food security initiatives will create automatic demand and increase population density.

Conclusion:

An organic farmer works under a whole new paradigm of sustainable agriculture, which links productivity with ecological preservation and human health. The organic sector in India has expanded in leaps and bounds, making it a world leader in organic producers. The environmental advantage of organic agriculture—improved health and sustainability for soil, conservation of biodiversity, and reduction of pollution—matches well with the national sustainable development strategies. The economic evidence shows that organic farming can increase farmer profitability even if farmer yields decrease in the future, if we are to maintain the policies and market infrastructure we need. Nevertheless, to achieve the full efficacy of organic farming, challenges in the form of input access, certification price, market development, and policy coherence will have to be overcome. A more diverse regional approach, which acknowledges the agricultural diversity of India, presents pragmatic routes for organic development while maintaining national food security. The extent to which India adopts an organic agriculture as an agro-industrial system is likely to depend on improving research–extension linkages, devising organic technologies, and appropriate policy environments.

References:

1. **Bengtsson, J., Ahnström, J., & Weibull, A. C. (2005).** The effects of organic agriculture on biodiversity and abundance: A meta-analysis. *Journal of Applied Ecology*, 42(2), 261-269.
2. **BHujel, R. R., & Joshi, H. G. (2023).** Organic agriculture in India: A review of current status, challenges, and prospects. *Universal Journal of Agricultural Research*, 11(2), 306-313.
3. **Charyulu, D. K., & Dwivedi, A. K. (2016).** Economics of organic farming vis-à-vis conventional farming in India. *SSRN Electronic Journal*.
4. **Chhonkar, P. K. (2002).** Organic farming myth and reality. *Proceedings of the FAI Seminar on Fertilizer and Agriculture Meeting the Challenges*, New Delhi.
5. **DAs, S., Chatterjee, A., & Pal, T. K. (2020).** Organic farming in India: A vision towards a healthy nation. *Food Quality and Safety*, 4(2), 69-76.
6. **ELayaraja, M., & Vijai, C. (2020).** Organic farming in India: Benefits and challenges. *European Journal of Molecular & Clinical Medicine*, 7(1), 3021-3029.
7. **FNorman, J., & Silverstein, J. (2012).** Organic foods: Health and environmental advantages and disadvantages. *Pediatrics*, 130(5), e1406-e1415.
8. **GoMiero, T., Paoletti, M. G., & Pimentel, D. (2008).** Energy and environmental issues in organic and conventional agriculture. *Critical Reviews in Plant Sciences*, 27(4), 239-254.

9. **JOuzou, Z., Azadi, H., Taheri, F., Zarafshani, K., Gebrehiwot, K., Van Passel, S., & Lebailly, P. (2017).** Organic farming and small-scale farmers: Main opportunities and challenges. *Ecological Economics*, 132, 144-154.
10. **Karunakaran, N. (2021).** Status, benefits, and prospects of organic farming in India: A review. *Journal of Management Research and Analysis*, 8(3), 103-111.
11. **Kumar, A., Prakash, C. H. B., Brar, N. S., & Kumar, B. (2018).** Potential of vermicompost for sustainable crop production and soil health improvement in different cropping systems. *International Journal of Current Microbiology and Applied Sciences*, 7(10), 1042-1055.
12. **Mahdi, S. S., Hassan, G. I., Samoon, S. A., Rather, H. A., Dar, S. A., & Zehra, B. (2010).** Bio-fertilizers in organic agriculture. *Journal of Phytology*, 2(10), 42-54.
13. **Pathania, N. (2020).** Organic farming: Its objectives, principles, types, techniques, favorable circumstances & downsides. *Just Agriculture*, 1(1), 50-55.
14. **Ramesh, P., Panwar, N. R., Singh, A. B., Ramana, S., Yadav, S. K., Shrivastava, R., & Subba Rao, A. (2010).** Status of organic farming in India. *Current Science*, 98(9), 1190-1194.
15. **Sankar, U. (2011).** Sustainable development of agriculture. *Indian Economic Review*, 8, 62-68.
16. **Sankar, A. S., & Reddy, K. V. (2022).** Recent trends in organic farming in India: A study. *IJCRT*, 10(7), 2320-2882.
17. **Sofia, P. K., Prasad, R., & Vijay, V. K. (2006).** Organic farming—tradition reinvented. *Indian Journal of Traditional Knowledge*, 5(1), 139-142.
18. **Willer, H., & Lernoud, J. (2020).** *The world of organic agriculture: Statistics and emerging trends 2020*. Research Institute of Organic Agriculture (FiBL) and IFOAM–Organics International.
19. **Yadav, S. K., Babu, S., Yadav, M. K., Singh, K., Yadav, G. S., & Pal, S. (2013).** A review of organic farming for sustainable agriculture in Northern India. *International Journal of Agronomy*, 2013, 1-8.

Journal Indexing

Printed by - Young Researcher Association, Kolhapur (Maharashtra)